Monitoring of Mesophotic Habitats and Associated Benthic and Fish/Shellfish Communities from Abrir la Sierra, Bajo de Sico, Tourmaline, Isla Desecheo, El Seco and Boya 4, 2018-20 Survey

Jorge R, Garcia-Sais, Stacey Williams, Evan Tuohy, Jorge Sabater-Clavell and Milton Carlo

SEDAR84-RD-02

July 2023

Final Report

Monitoring of Mesophotic Habitats and Associated Benthic and Fish/Shellfish Communities from Abrir la Sierra, Bajo de Sico, Tourmaline, Isla Desecheo, El Seco and Boya 4, 2018-20 Survey

NA17NMF4410270

Jorge R, Garcia-Sais, Stacey Williams, Evan Tuohy, Jorge Sabater-Clavell and Milton Carlo

Reef Research Inc.
P. O. Box 178
Boquerón, PR
<goingdeep49@gmail.com>

December 2020

I. Executive Summary

The 2018-20 monitoring survey of mesophotic habitats and associated benthic and fish/shellfish communities included three seasonally closed fishing areas in the west coast of Puerto Rico (Abrir La Sierra – ALS; Bajo de Sico – BDS; Tourmaline Reef -TOUR), one permanently closed fishing area (Isla Desecheo - DES) in the northwest coast, one known multi-species spawning aggregation site open to fishing year-round (El Seco – SECO) in the east coast, and one reference site (Boya 4 – BOYA) open to fishing year-round located adjacent to the seasonally closed fishing areas of the west coast. A total of 273 transects were surveyed for determinations of the percent reef substrate cover by sessile-benthic categories (abiotic, benthic algae, stony corals, soft corals, black corals, sponges) and the taxonomic composition, density, and size frequency distributions of fishes and shellfishes (queen conch, spiny lobster) following the same habitat/depth stratified sampling design, methodological approach, and station positions within the 25 – 50m range previously established in the baseline surveys at each site. The 2018-20 survey at BOYA represents a baseline characterization for that site. Additional baseline characterizations of marginal sub-mesophotic (22 – 28m) habitats were produced at ALS, TOUR, DES and BOYA to compare with existing baseline data sets from BDS and SECO.

Benthic algae were the dominant sessile-benthic assemblage in terms of reef substrate cover from all sites surveyed during 2018-20. Statistically significant depth/habitat related patterns were detected from some of the main taxonomic algal groups. Turf algae (mixed assemblage) was mostly associated with the colonized pavement reef top (CPRT) habitats that prevailed in the 25 – 30m depth range but declined with depth. Conversely, encrusting fan alga, *Lobophora sp*., and y-twig alga, *Dictyota sp*., increased in cover with depth, associated with rhodolith (Rhodo) beds typically found within the 40 – 50m depth range at most sites. Marked taxonomic phase shifts of benthic algae community structure were noted between baseline and the 2018-20 monitoring survey. Reef substrate cover by *Lobophora sp*., fleshy algae (mostly *Dictyota sp*), and crustose Peyssonnelid red algae (including *Ramicrusta sp*.) increased during the 2018-20 survey from all sites. Corresponding declines of cover by turf algae (mixed assemblage) were measured. The sharp increment of cover by *Ramicrusta sp*. at SECO was associated with a significant decline of cover by stony corals, particularly from the CPRT habitat prevailing in the 22-28m depth range. Increased nutrient availability, contributed by upwelling and/or sediment resuspension driven perhaps by hurricane activity during 2017 are proposed as potential drivers of the increased reef substrate cover by *Lobophora sp*. and fleshy algae. The increased cover by *Ramicrusta sp*. at SECO coincided with the proliferation of this alga throughout the east coast neritic reefs but was facilitated at SECO by the availability of new hard substrates for colonization upon stony coral mortality at the CPRT habitat.

A total of 30 scleractinian corals and one hydrocoral were identified within photo-transects at sites surveyed during 2018-20. Statistically significant habitat/depth related distribution patterns were evident from all sites except BOYA, associated with the higher substrate cover at coral reef habitats within the sub-mesophotic 22 – 28m depth range (e. g. ACR25), compared to other habitats/depths from all sites except SECO, where the BCR and PCR habitats with higher substrate cover by stony corals were distributed deeper within the 30 – 40m depth range. Habitat/depth related distribution patterns were also noted for coral species. Higher cover by the *Orbicella faveolata/franksi* complex was associated with ACR and CPRT habitats in the 22 – 27m depth range, whereas lettuce corals *Agaricia lamarki, A. grahamae, A. undata* prevailed at the Rhodo habitat in the 40 – 50m depth range. Mustard-hill coral (*Porites astreoides*) was ubiquitous throughout the surveyed habitat/depth range. Black corals, particularly the bushy black coral, *Antipathes caribbeana* were mostly associated with the deeper sections of colonized pavement slope (CPSlope) and wall (CPWall) habitats in the 40 – 50m depth range.

Reef substrate cover by stony corals remained stable between the baseline and the 2018-20 monitoring survey at all sites, except at SECO, where statistically significant declines of substrate cover were measured from all habitats/depths. Mechanical damage associated with hurricane activity, coral bleaching, and coral disease outbreak(s) (including SCTLD) are proposed as potentially important drivers of the measured stony coral loss at SECO during 2018-20. Statistically significant reductions of cover by soft corals (gorgonians) were also measured from the CPRT habitat at SECO, perhaps also influenced by hurricane-related mechanical damage, surge and sand abrasion effects.

A total of 132 fish species and two shellfishes (queen conch and spiny lobster) were identified from belt-transects within the 22 – 50m depth range at sites surveyed during 2018-20. The community structure of small demersal fishes, surveyed by 142 – 10m x 3m belt-transects (across all habitats and sites) was characterized by the numerical dominance of a relatively small assemblage of species, many of which exhibited highly aggregated distributions associated with schooling behavior (e.g. *Clepticus parrae, Chromis cyanea, C. multilineata, C. insolata, Coryphopterus personatus, Thalassoma bifasciatum, Schultzea beta, Lutjanus buccanella, L. apodus*), and others with more uniform distributions (e.g. *Stegastes partitus, Centropyge argi, Halichoeres garnoti, Cephalopholis fulva*). Strong habitat/depth related affinities of small demersal fishes were detected and contributed both to community structure similarities within habitats/depths and to dissimilarities between the different habitats/depths surveyed across the 22 – 50m depth gradient. Habitat plasticity across the entire depth range surveyed was exhibited by an assemblage of small demersal fishes, including some numerically dominant species, such as bicolor damselfish (*S. partitus*), bluehead and yellowhead wrasse (*T. bifasciatum, H. garnoti*), coney (*C. fulva*), and red hind (*E. guttatus*). This assemblage contributed to the similarity between habitats/depths from most surveyed sites. Small demersal fish density differences between surveys depended on habitat/depths but were mostly influenced by the high sampling variability introduced by the aggregated distributions of numerically dominant species. Of particular relevance was the statistically significant density decline between surveys of masked goby (*Coryphopterus personatus*), a numerically dominant species from coral reef habitats in baseline surveys. It is suggested that this species was highly vulnerable to the surge and sand abrasion effects of hurricanes and winter storms during 2017-18 and still unable to replenish its populations to the pre-hurricane status.

Large demersal fishes and shellfishes were surveyed by 133 drift belt-transects covering an area of 20.7 ha (207,898 m^2) within the 22 – 50m depth range from the six surveyed sites as part of the 2018-20 monitoring survey. The total assemblage included 7,396 individuals, including 277 queen conch (*Lobatus gigas*), and 40 spiny lobsters (*Panulirus argus*). Differences between habitats/depths for the total large demersal fish/shellfish assemblage during the 2018-20 survey were statistically significant only at SECO (lower densities at Rhod40-50), due to the high sampling variability introduced by the aggregated distributions of numerically dominant species, such as yellowtail, schoolmaster, dog, lane, mutton, and cubera snappers, (*Ocyurus chrysurus, Lutjanus apodus, L. jocu, L. synagris, L. analis, and L. cyanopterus*), and queen conch (*L. gigas*). Species specific habitat/depth related density differences depended on site. Some of the most prominent patterns included higher densities of queen triggerfish (*B. vetula*) from rhodolith habitats at ALS, BDS, and TOUR, higher densities of red hind (*E. guttatus*) from CPRT and rhodolith habitats at ALS and SECO, higher densities of yellowtail snapper (*O. chrysurus*) at ACR25 habitats in DES and TOUR and higher densities of queen conch (*L. gigas*) at ALS and TOUR. Habitat/depth affinities by numerically dominant large demersal fishes/shellfishes appeared to be related to habitat slope and reef morphology. Red hind (*E. guttatus*), coney (*C. fulva*), queen triggerfish (*B. vetula*), and queen conch (*L. gigas*) were mostly distributed on horizontally oriented habitats with scattered coral colonies, sponges, coral rubble, and sand, such as CPRT's and Rhodo beds. Yellowtail, schoolmaster, cubera, and blackfin snappers (*O. chrysurus, L. apodus, L. cyanopterus, L. buccanella*) were mostly associated with vertically oriented habitats, such as colonized pavement slopes (CPSlope) and colonized pavement walls (CPWall). Horizontally oriented, high rugosity habitats with high coral cover, mostly devoid of sandy substrates, such as BCR and ACR appeared to be residential and foraging habitats for coney, red hind, and Nassau groupers (*C. fulva, E. guttatus, E. striatus*), lionfish (*Pterois sp*.), and mahogany, lane, cubera and schoolmaster snappers (*L. mahogoni, L. synagris, L. cyanopterus, L. apodus*). The patch coral reef (PCR) habitat from SECO, previously known as a multi-species fish spawning aggregation site (FSA) was observed to function as the FSA site also for cubera snapper (*L. cyanopterus*) during the 2018-20 survey. Superimposed on the observed habitat preferences, depth appeared to be a significant factor influencing community structure within the 22 – 50m range. Marked depth-related differences were noted for blackfin snapper (*L. buccanella*), and coney (*C. fulva*). Blackfin snappers were mostly observed from CPSlopes and CPWalls at 50m. Although present throughout the 22 – 50m depth range, densities of coneys were consistently higher at the CPRT in the 22 – 30m depths, relative to deeper habitat/depths from most sites.

Analyses of density differences by large demersal fishes/shellfishes between surveys were influenced by the high variability within and between habitats/depth for any given site introduced by the aggregated distributions of numerically dominant populations, including species observed within drift belt-transects in spawning aggregations (e. g. *Lutjanus jocu, L. cyanopterus*), and what appeared to be large feeding aggregations (*O. chrysurus*). Still, increments of the study mean densities (across all habitats/depths) were consistent on all surveyed sites for red hind and Nassau groupers (*Epinephelus guttatus, E. striatus*), queen triggerfish (*Balistes vetula*), and spiny lobster (*Panulirus argus*). Sharp increments of queen conch (*Lobatus gigas*) density were observed from ALS and DES, whereas equivalent declines were observed from TOUR and in less magnitude at BDS. Density increments of red hind, queen triggerfish and spiny lobster appeared to be real and supported both by increments in recruitment and maximum size of individuals. The recuperation of these fish/shellfish populations may be related to a release of fishing effort influenced perhaps, by a reduction of demand associated with the economic slow-down prevailing in PR since 2006, destruction of fishing gear and infrastructure related to impact by hurricanes, and/or increased awareness and compliance by fishermen to seasonal and areal fishing closures.

Broad-scale spatial distribution patterns of large demersal fishes and shellfishes were pronounced even between adjacent sites surveyed in the west coast outer shelf and slope. At such spatial scales, differences appeared related to preferences and/or adaptations of numerically dominant species for habitats with particular slope inclination, morphometry, reef rugosity, and depth. Direct intra-shelf connectivity with nursery habitats appeared to be an important driver of broad-scale spatial distributions of large demersal fishes and shellfishes. Perhaps with the exception of schoolmaster (*Lutjanus apodus*), snappers (Lutjanidae) were more abundant from mesophotic habitats within the main insular shelf and slope (ALS, TOUR, BOYA, SECO) than at DES and BDS, separated from mainland habitats by deep oceanic channels. Conversely, groupers (Serranidae) in general were more abundant at DES and BDS than from mainland sites, perhaps with the exception of red hinds (*Epinephelus guttatus*) at ALS. Groupers are known to undertake offshore larval development and relatively longer pelagic larval duration than snappers. Such extended pelagic larval adaptations may favor recruitment into offshore sites, such as oceanic islands and seamounts.

Table of Contents

II. List of Figures

III. List of Tables

IV. Introduction

Benthic habitats in the 30 – 50m upper mesophotic range are associated In Puerto Rico and the US Virgin Islands (USVI) with outer shelf and shelf-edge reefs, upper sections of insular slopes, and seamount reef tops at the interphase of shelf, slope, and open water oceanic ecosystems. As such, they function as prime residential, foraging, mating, nesting, and seasonal spawning aggregation sites for a wide variety of commercially valuable fishes and shellfishes, including shelf and slope demersal, coastal pelagic, and migratory pelagic populations (Garcia-Sais et al., 2005, 2007, 2010a, b, 2011, 2012, 2013, 2014).

Since the 1950's, but particularly after the 1970's intense fishing effort on fish spawning aggregations (FSA's) within these frontier mesophotic habitats led to a sharp decline of several commercially valuable fish populations throughout the Caribbean, including the Nassau, red hind, yellowfin, and tiger groupers (*Epinephelus striatus*, *E. guttatus*, *Mycteroperca venenosa, M. tigris*), and perhaps other large demersal species for which there is limited (or only anecdotal) data for assessment of the overfishing impact (Olsen and La Place, 1979; Munro, 1983; Bannerot et al. 1987; Sadovy, 1990, 1995; Sadovy and Figuerola, 1992; Beets and Friedlander 1992, 1999; Aguilar-Perera, 2006). In response to the declining grouper fishery trends, shifts in the species composition of commercial landings, and disappearance of several Nassau grouper FSA sites a series of conservation management approaches were established in Puerto Rico, USVI, and throughout the Caribbean, including size limits, catch quotas, gear restrictions/bans, total harvest bans, and seasonal and permanent areal closures for protection of FSA's.

The Caribbean Fishery Management Council (CFMC) in collaborations with government agencies, state universities, and local fishermen associations of Puerto Rico and the USVI established a series of seasonal and permanent fishing closures for protection of known grouper/snapper FSA sites within federally regulated U.S. Exclusive Economic Zones (EEZ). These included the Marine Conservation District (MCD) Hind Bank, and Grammanik Bank off the south coast of St. Thomas, and Lang Bank and Mutton Snapper Bank off the east coast of St. Croix. In Puerto Rico, federally managed seasonal fishing closures were enacted in 1996 for protection of three red hind (*Epinephelus guttatus*) FSA sites off the west coast of Puerto Rico: Tourmaline Reef, Bajo de Sico, and Abrir La Sierra (CFMC 2005). In addition, state managed permanently closed fishing areas were established for sections of Isla Desecheo, Isla de Mona, and Isla de Culebra.

Assessments of the effectiveness of seasonal/permanent fishing area closures in protection of red hind (*Epinephelus guttatus*) populations were initially performed for the Hind Bank MCD (Nemeth, 2005), and Lang Bank (Nemeth et al. 2006) with different results. One decade after the seasonal closures, red hinds from the spawning aggregation at the Hind Bank MCD were significantly larger and nearly nine times more abundant than those from the Lang Bank FSA. Relative to the baseline studies of 1997 (Beets and Friedlander, 1999), seven years after the seasonal closure in 1990, and previous to the permanent closure in 1999 the average size of red hind increased by 10 cm during a period of 12 years, and the average density and biomass of the spawning population increased by over 60% following permanent closure at the Hind Bank MCD. Inappropriate placement of areal closure boundaries and the lack of enforcement at Lang Bank were proposed as possible factors influencing the contrasting results of the seasonal areal closures between the two USVI sites in restoration of the red hind spawning population (Nemeth et al. 2006).

Since 2003, combined management strategies for protection of the Nassau grouper (*Epinephelus striatus*) including seasonal areal fishing closures during the spawning aggregation (December through April) were established in the Cayman Islands. In a period of approximately 15 years, the size of the Nassau grouper population on Little Cayman Island has more than tripled in response to the conservation efforts (Waterhouse et al. 2020). Likewise, the Nassau grouper population has increased by more than 400% and modal size has more than doubled during the last 15 years of seasonal fishing closure at Grammanik Bank (Nemeth and Kadison, 2020).

Evaluations of seasonal fishing closures in Puerto Rico are limited to the assessment by Marshak (2007) on the status of the red hind (*Epinephelus guttatus*) population from three seasonally closed FSA sites off the west coast based on fishery-dependent (commercial landings, port-samplings), and fishery-independent time series data (SEAMAP-C). An initial post-enactment increase of fishery-independent Catch-per-Unit-Effort (CPUE; kg/trip) was observed from all three sites, and within spawning aggregations. Marshak (2007) proposed that increased fishing effort within previously under-targeted shelf regions (open to fishing) led to increases in nominal CPUE within later years but resulted in subsequent reductions of fishery independent CPUE. Increased average length of *E. guttatus* was observed in both fishery-dependent and fishery independent data sets but was related to limited recruitment and proportional contributions of few remaining large females. Although the closure was initially effective in stemming further stock decline, shifts in fishing strategies apparently overrode the potential recovery of red hind (Marshak, 2007).

Baseline characterizations of seasonally and/or permanently closed fishing areas in Puerto Rico included quantitative assessments of reef substrate cover by sessile-benthic categories and determinations of taxonomic composition and density of small demersal fishes from the main benthic habitats in the 30 – 50m depth range at Isla Desecheo (Garcia-Sais et al., 2005), Bajo de Sico (Garcia-Sais et al., 2007), Abrir La Sierra (Garcia-Sais et al., 2010), El Seco (Garcia-Sais et al., 2011), and Tourmaline Reef (Garcia-Sais et al., 2013). Quantitative baseline data on the density and size distributions of the large demersal fishes and shellfishes of commercial value (spiny lobster and queen conch) were acquired in a diver (visual census) fishery independent survey of the main benthic habitats in the 30-50m mesophotic depth range from Isla Desecheo, Abrir La Sierra, and Bajo de Sico (Garcia-Sais et al., 2012).

Since the onset of these baseline characterizations, extreme climatological/oceanographical and biological phenomena have affected marine ecosystems of Puerto Rico and the USVI, including the invasion of exotic species, such as the lionfish (*Pterois sp.*) (Morris and Atkins, 2009; Toledo-Hernandez et al., 2014) and halophila seagrass (*Halophila stipulacea*) (Ruiz et al, 2017), the passing of two category 4-5 hurricanes Irma and Maria in September 2017 (NOAA, 2018), an extraordinary event of wave action brought about by winter storm Riley in March 2018, a regional coral bleaching event that started in October 2019 and extended until February 2020, and the most recent arrival of the Stony Coral Tissue Loss Disease (SCTLD) affecting both neritic and mesophotic coral reefs in PR and the USVI (Weil et al., 2019).

This research represents the first evaluation of temporal changes in the sessile-benthic, and small/large demersal fishes/shellfishes originally surveyed by Garcia-Sais et al. (2005, 2007, 2010, 2011, 2012, 2013), including an additional baseline characterization of a reference, year-round open to fishing site (Boya 4), and of sub-mesophotic habitats in the 25 – 28m depths from all sites. Assessments of the effectiveness of closed fishing areas for the benthic/fish/shellfish multispecies assemblages associated with the different benthic habitats and depths of all surveyed sites is complicated by the natural, yet extreme events affecting mesophotic ecosystems in Puerto Rico and the USVI, and the uncertainty of compliance by commercial and/or recreational fishermen with applicable fishery management regulations in a scenario of limited surveillance and enforcement.

V. Study Objectives

1- Perform a quantitative/qualitative characterization (2018-20 survey) of sessile-benthic and fish/shellfish communities from mesophotic habitats/depths in the 25 – 50m range previously surveyed (baseline characterizations) at Abrir La Sierra (ALS), Bajo de Sico (BDS), Tourmaline (TOUR), Isla Desecheo (DES), and El Seco (SECO).

2- Produce new baseline characterizations of sessile-benthic and fish/shellfish communities from mesophotic habitats in the 25 – 50m depth range at Boya 4 (BOYA) as a reference site open year-round to fishing located within the same west coast shelf/slope as the seasonally closed areas at ALS, BDS, and TOUR.

3- Expand the upper depth limit of quantitative/qualitative baseline characterizations with surveys of the sessile-benthic and fish/shellfish communities in the sub-mesophotic range (25 – 28m) where the main coral reef habitats were detected at TOUR, DES, and ALS.

4- Provide a comparative assessment of temporal change (monitoring) based on quantitative and multivariate analyses of data on percent substrate cover by sessile-benthic taxonomic categories, and the density, taxonomic structure, and size distributions of fish/shellfish between the baseline characterizations and the 2018-20 survey following the same sampling approach and station geographic positions.

5- Construct a georeferenced data base incorporating all the biological and physical information of surveyed sites to allow production of species-habitat-depth-site distributions

6- Produce still digital photo and video documentation of the main benthic habitats and associated mesophotic communities from each site surveyed during 2018-20.

VI. Research Background

Characterizations of mesophotic benthic communities associated with fore-reef and insular slopes in relation to morphological/sedimentary features, species composition/reef zonation, and depth were originally described by Goreau (1959), and Goreau and Goreau (1973) for Jamaican coral reefs, Bak and Luckhurst (1980) in Curacao and Bonaire, and James and Ginsburg (1973), Colin (1974), and Rützler and Macintyre (1982) for Carrie Bow Reef in Belize. These early studies noted contrasting features of higher coral cover and diversity of coral assemblages associated with spur and groove formations at the shelf-edge in the 20 - 25m depth range, and the more scattered and depauperate coral growth along vertically oriented sections of the insular slopes below 30m. Golberg (1983) found higher scleractinian coral cover below 30m at the fore-reef slope of Cay Sal Bank in the Bahamas, relative to shallower shelf zones and related the variation to the less physically driven environment of the deeper insular slope.

Some of the initial quantitative assessments of reef substrate cover by sessile-benthic communities from upper mesophotic reef habitats (30 – 50m) in the U. S. Caribbean (Puerto Rico and the US Virgin Islands) include the autonomous underwater vehicle (AUV) surveys of the La Parguera shelf-edge and insular slope (Singh et al., 2004) and the Hind Bank Marine Conservation District (MCD) coral reef system south of St. Thomas, USVI (Armstrong et al., 2006). The aforementioned studies identified differences of sessile-benthic community structure associated with habitat types and depths but were more methodologically oriented towards validating the effectiveness of an AUV for mesophotic benthic community surveys.

The influence of slope as a key driver of benthic habitat formation and associated community structure in the upper mesophotic depth range was noted by Garcia-Sais et al. (2005, 2007, 2010a, b, 2012, 2013) from technical diving surveys (30 – 50m) at Isla Desecheo, Bajo de Sico, Abrir La Sierra, Isla Desecheo, and El Seco in Puerto Rico, and by Smith et al. (2010, 2015) from the Hind Bank MCD reef system in St. Thomas, USVI. Higher substrate cover by stony corals, mostly *Agaricia spp*. was associated with a gently sloping rhodolith bed in the 45 – 50m depth at Isla Desecheo, whereas steeper shallower slopes surveyed in the 30 – 40m depth range exhibited relatively lower coral cover and higher relative composition by *Orbicella spp*. Differences in the taxonomic composition of benthic algae, sponges, and abiotic categories were also noted between habitats across the depth gradient surveyed at Isla Desecheo (Garcia-Sais et al. 2005, 2010b). Instead of rhodolith beds, geographically extensive coral reef bank habitats of high scleractinian coral cover (> 20%) largely contributed by *Orbicella spp*. have developed on mostly flat terraces at outer shelf sections of the Hind Bank MCD, south of St. Thomas, USVI (Smith et al., 2010, 2015), and El Seco, Isla de Vieques, southeast coast of PR (Garcia-Sais et al., 2011).

Variability of coral (scleractinian, octocoral, antipatharian) development within similar slopes and depths in Caribbean mesophotic reefs appear to be strongly influenced by geomorphological and sedimentary processes. Sherman et al. (2010) found higher scleractinian coral cover associated with topographic highs in the 30 – 90m depth range down the insular slope off La Parguera, suggesting that such topographic anomalies were largely unaffected by sediment transport, allowing for coral settlement and growth. Sand transport was also proposed as a limiting factor for colonization and substrate cover by corals and sponges in the 70 – 120m depth range off Isla Desecheo insular slope, where coral and sponge cover was largely associated with rock outcrops and vertical sections of crevices devoid of sediment (Garcia-Sais et al., 2018). Geomorphological and sedimentary processes also appear to play an important role on the variability of sessile-benthic community structure in horizontally oriented seascapes within mesophotic depths. Rhodolith beds appear to be more commonly associated with gently sloping or flat terraces located at the base of slopes, ridges, or in substrate depressions (Garcia-Sais et al., 2018). In contrast, bank coral reef habitats appear to prevail on outer shelf sections not directly influenced from adjacent shallower slopes.

The taxonomic composition of corals, octocorals, and sponge species has been shown to vary as a function of depth within the 20 – 80m range off the La Parguera insular slope (Appeldoorn et al., 2016). The main pattern for scleractinian corals appears to be the dominance of *Orbicella spp, Colpophyllia spp.* and *Diploria spp*. in shallower areas of the shelf-edge, and the dominance of Agariciidae and *Madracis spp*. on the deeper slope sections surveyed. According to Appeldoorn et al (2016) the connectivity between coral populations within the 20 – 80m depth range of La Parguera insular slope appears to be low, given the sharp differences in the taxonomic composition of corals and coral species richness as a function of depth. These observations are consistent with recent observations by Eckert et al. (2019) of strong contemporary genetic differentiation between shallow (10 – 16m) and relatively deep (25 – 35m) *Montastraea cavernosa* colonies, coinciding with a physiographic transition zone from reef crest to reef slope on the Belize Barrier Reef. Differences of sessile-benthic community associated with depth appear to be magnified when different benthic habitats are found across the depth profile within a given site (Garcia-Sais et al, 2005, 2011, 2012, 2014). For example, colonized pavement reef tops, colonized pavement slopes, bank coral reefs, and rhodolith bed habitats have been reported from different depths at El Seco (Garcia-Sais et al., 2011) and Lang-Bank (Garcia-Sais et al., 2014). Marked variations of sessile-benthic community structure associated with different depths and benthic habitats have also been reported for the MCD Hind Bank Reef by Smith et al. (2010).

Mesophotic reefs have been proposed as refuge habitats for shallow coral populations based on their observed higher resiliency to physical disturbances (e.g., hurricanes), anthropogenic stressors, and thermally induced coral bleaching events (Glynn, 1996; Lesser et al., 2009). The Deep Reef Refugia Hypothesis (DRRH) has been the subject of much attention and debate given the limited amount of "depth-generalists" among Caribbean coral species, brooding reproductive strategies, and vertical symbiont acquisition modes (Bongaerts et al., 2010, 2017; Eckert et al., 2019). Corals in the upper mesophotic range (30 – 50m) have also been shown vulnerable to thermally induced bleaching (Garcia-Sais et al., 2007), and extreme coral disease infections (Menza, 2007; Smith et al., 2010), the most recent being the Stony Coral Loss Disease outbreaks reported both for the Hind Bank MCD (Brant et al, 2020) and El Seco (Williams et al., 2020). More specific research is needed to establish if the large reservoir of corals found at depths of 30 - 40m in the extensive coral bank reef systems of El Seco (Vieques, PR), and the MCD Hind Reef (St. Thomas, USVI) largely unaffected by recent bleaching and/or hurricane events may serve to replenish the massive coral losses documented for shallower reefs in PR since 2006 (Garcia-Sais et al., 2006, Hernandez-Delgado et al., 2006, 2014; Weil, 2009) and the USVI (Smith el al, 2010, 2015).

Long-term monitoring programs of mesophotic benthic communities are rare in the Caribbean. Slope coral communities have been surveyed since 1973 to the present from permanent photo-quadrats at 10, 20, 30 and 40m along a depth gradient over leeward reefs in Curacao and Bonaire (Bak and Luckhurst, 1980; Bak and Nieuwland, 1995; Bak et al., 2005; Bakker et al., 2017). During the first two decades of monitoring reductions in the number of colonies, coral diversity and percent coral cover were noted from all depths but differences were statistically significant only for samples at 10m and 20m, suggesting a more stable and undisturbed environment at the 30m and 40m depths. By 2003, drastic reductions of coral cover and density of coral colonies were reported across the entire depth gradient, particularly at 30m and 40m associated with fluctuating water temperatures and what was described as a low-temperature induced "deep-reef bleaching" (Bak et al., 2005). By 2013, live coral cover had declined by more than 70% and benthic community structure phase shifts were evidenced: from coral (1970's), to turf algae (2000's), to cyanobacterial/fleshy algae dominated systems in 2013 (Bakker et al., 2017).

The Territorial Coral Reef Monitoring Program (TCRMP) in the USVI includes monitoring of nearshore, offshore, and several mesophotic reef sites since 2003. The largest and most significant variations of reef benthic community structure were related to a sharp decline (approx. 50%) of live coral cover measured in most reefs during the 2006 – 2007 period after the regional (Caribbean wide) coral bleaching event of late 2005, followed by a proportional increase of benthic algae colonizing available dead coral substrates (Smith et al., 2015). Nearshore and offshore reefs were the most affected, but impacts on mesophotic reefs were also detected, particularly at Meri Shoal, Hind Bank, and College Shoal. In Puerto Rico, the 2005 coral bleaching event had the most severe impact upon shallow (< 30m) coral reefs in high transparency waters, such those associated with oceanic islands (e. g. Isla de Mona, Desecheo, Vieques). Still, even in the most affected sites (Isla Desecheo, Vieques), a clear trend of declining loss of live coral cover with depth was measured from the few available stations in the Puerto Rico Coral Reef Monitoring Program (PRCRMP) (Garcia-Sais et al. 2017; Garcia-Sais et al., 2019 and references therein). More recently, both the physical and biological structure of borderline mesophotic coral reefs at 30m have changed significantly due to the breakage and overturn of very large coral colonies caused by the extreme wave action impact of Hurricanes Irma/Maria in 2017 and/or winter storm Riley in 2018 (Garcia-Sais et al 2018, 2019).

Cascading effects of the large-scale stony coral loss on other components of the coral reef ecosystem are difficult to ascertain on short time scales, due to the confounding effects of many simultaneously operating factors. Small demersal fish density, for example are driven by fluctuations of numerically dominant species with aggregated (patchy) distributions, and such fluctuations appear to be strongly influenced by density-independent factors, such physical disturbances, including the intense scouring and abrasion effects associated with strong wave action events (Esteves, 2013; Garcia-Sais et al., 2019 and references therein). Some of these small demersal fishes (e. g. Gobiidae, Labridae, Pomacentridae) may be important components of the coral reef food web, with potentially relevant implications for the entire fish community structure.

Characterizations of mesophotic reef fish communities in the Caribbean are scarce, and until recently, mostly available from submersible surveys. Colin (1974; 1976) described the taxonomic composition of reef fishes at depths between 90 – 305m off the coasts of Jamaica, Belize and the Bahamas as a mixed assemblage of shallow reef (< 30 m) and true “deep-reef” species seldom present shallower than 50m. Colin (1974) argued that the vertical distribution of some reef fish species was more related to local environmental conditions (habitat features) than depth, and noted ontogenetic trends in the vertical distribution of "deep-reef" species, where juvenile stages were typically observed at shallower depths than adults. In Puerto Rico, the Seward Johnson-Sea Link submersible survey (Nelson and Appeldoorn, 1985) provided a qualitative characterization of fish assemblages of the insular slope, encompassing depths between 100 – 1,250 m. Despite observations of a "rich and highly complex" reef fish community associated with the upper insular slope (30 – 70 m), these habitats were left virtually undescribed by the Seward Johnson - Sea Link survey.

An ROV survey of mesophotic habitats from the west coast of Puerto Rico, including sections of Isla Desecheo Insular slope, Desecheo Ridge, Corona del Sur, and Bajo de Sico in the 70 - 220m depth range by Garcia-Sais et al. (2018) found decreasing number of fish species with increasing depth, and depth-related variations of fish community structure between 70 – 120m and the 121 – 220m depth sections. The strong depth-related patterns appeared to be associated with the different benthic habitats observed across the depth gradient. The rhodolith habitat that prevailed at 70m served as the residential habitat for an assemblage of small territorial neritic fishes with an extended distribution range down to a depth of approximately 120 m, influencing the marked depth-related differences of fish community structure across the depth gradient. The silk snapper (*L. vivanus*) was the main species driving similarities between the two deeper stratas (121 – 170m and 171- 220m), contributing more than 60% of the similarity. At depths below 120m, slopes were markedly steeper in all sites surveyed and major differences of substrate cover were noted, along with variations of fish taxonomic composition as compared to the community prevailing at the upper slope rhodolith habitat.

Technical closed circuit (mixed gas rebreather) diving applications have facilitated quantitative assessments of the upper mesophotic communities and expanded our knowledge of depth and habitat related patterns of fish community structure in the 30 – 70m range (Pyle 1996, 1999, 2000; Pyle et al. 2016; Grigg et al., 2002; Bejarano et al 2010,) due in part to the presence of small bodied and/or cryptic species that are easily missed by ROVs. Differences of fish community structure have been associated habitat type, depth, slope, and rugosity (Garcia-Sais, 2010b; Bejarano et al.,2010). In general, fish assemblages exhibited a high degree of connectivity between habitats across depth gradients down to 50m, and presence of what appears to be a small group of indicator fish species of upper range mesophotic reefs (Garcia-Sais et al., 2007; Garcia-Sais, 2010b, Bejarano et al., 2010).

From the limited research available on mesophotic reefs of Puerto Rico and the USVI, it is evident that they function as the residential, foraging, mating, nesting, and spawning aggregation habitats for a broad range of commercially exploited reef fishes, particularly large groupers and snappers, sea turtles and queen conch (Nemeth, 2005, Nemeth et al., 2006a, 2006b, Nemeth et al, 2007; Garcia-Sais et al. 2005, 2007, 2010, 2011, 2012, 2014; Biggs and Nemeth, 2014; Kadison et al. 2017). The particularly high abundance of post-settlement juveniles of coneys (*Cephalopholis fulva*), blue chromis (*Chromis cyanea*) and fairy basslet (*Gramma loreto*) reported for Isla Desecheo, Bajo de Sico and Abrir La Sierra (Garcia-Sais et al., 2005, 2007, 2010a) suggest that upper mesophotic reef zones may also function as prime recruitment habitats for these and other reef fish populations that undertake ontogenetic migrations to replenish adjacent shallow (neritic) reef populations.

The most relevant temporal changes of fish community structure from mesophotic habitats in the US Caribbean (PR and the USVI) and elsewhere in the Caribbean relates to the massive losses of large demersal species to fishing mortality during seasonal fish spawning aggregations (FSA's). Since the 1950's, but particularly after the 1970's intense fishing effort on FSA's led to a sharp decline of several commercially valuable fish populations, including the Nassau, red hind, yellowfin, and tiger groupers (*Epinephelus striatus*, *E. guttatus*, *Mycteroperca venenosa, M. tigris*), and perhaps other large demersal species for which there is limited (or only anecdotal) data for assessment of the overfishing impact (Olsen and La Place, 1979; Munro, 1983; Bannerot et al. 1987; Sadovy, 1990, 1995; Sadovy and Figuerola, 1992; Beets and Friedlander 1992, 1999; Sala et al., 2001; Aguilar-Perera, 2006). Some of the earliest numerical estimates of Nassau grouper (*Epinephelus striatus*) individuals in FSA's are reported in the order of 10,000 – 100,000 (Aguilar-Perera, 1994, Aguilar-Perera and Aguilar-Davila, 1996; Sala et al., 2001; Sadovy et al. 2008), and up to 150,000 individuals (Smith, 1972 – as cited in Olsen and La Place, 1979). In a review of the status of the Nassau and jewfish (*E. itajara*) populations, Sadovy and Ecklund (1999), reported that approximately 30% of the 67 known Nassau grouper aggregations in the wider Caribbean had disappeared by 1998, and less than 5% had not shown signs of rapidly declining numbers of spawners.

The impact of disappearing FSA's upon top predator fish populations, such as sharks, and reef-associated mantas (Rhodes et al, 2019) has not been quantitatively established but may be of critical relevance for the sustainability of these populations. Requiem sharks are believed to live in inverted trophic pyramids, where they need to eat much more than is available in any given area. In order to meet their food requirements, they must travel to areas of high food concentrations, such as FSA's to supplement their nutrition needs (Mourier et al., 2016). Therefore, the absence of FSA's in the Caribbean may have had significant impacts on the local occurrence, and perhaps the population status of requiem sharks.

Seasonal and permanent fishing closures, when properly designed and managed, have shown to be effective in re-establishing FSA's and the overall status of overfished populations. Combined management strategies including a closed fishing season during FSA, bag and size limits, and gear bans and restrictions during the open fishing season have contributed to more than triple the Nassau grouper (*Epinephelus striatus*) population at Little Cayman Island, making this site now the largest identified Nassau grouper spawning aggregation with an estimate of over 5,000 individuals (Waterhouse et al., 2020). Another example that spatial and seasonal closures aimed at rebuilding aggregation-based fisheries can foster conservation success is the case of the Hind Bank MCD, south of St. Thomas. This reef was seasonally closed to fishing in 1990 during the red hind (*E. guttatus*) seasonal FSA, and later in 1999 permanently closed to fishing. Compared with studies conducted previous to the permanent closure, the average size of red hind increased 10cm over 12 years, and the average density more than doubled at the spawning aggregation site (Nemeth, 2005). Conversely, the seasonal closure at Lang Bank, east of St. Croix (USVI) was shown to be less effective, with significantly smaller red hinds and nine times less abundant than at Hind Bank (Nemeth et al., 2006).

The spatial and temporal patterns of migration and movement by red hind during its seasonal spawning aggregation at Lang Bank was studied by Nemeth et al. (2007). The aggregation site was located at the edge of a coral spur that projects into a deeper water basin within the outer shelf. The study found that *E. guttatus* migrated 5 – 18 km from an area of about 90 km around St. Croix. Similarities in terms of movement timing, temporal and spatial changes in sex ratios, annual and lunar predictabilities and sexual behavioral responses to environmental cues were similar than those at the Hind Bank, MCD in St. Thomas. With respect to the benthic habitat, Nemeth et al (2007) noted that Lang Bank presented less topographic relief than the MCD at the aggregation site, but that the composition of the reef coral species was similar between sites. Differences in the effectiveness of the fishing closures in reconstruction of the red hind aggregation between sites were associated with inappropriate area closure boundaries and lack of enforcement at Lang Bank (Nemeth et al., 2006).

Evaluations of seasonal fishing closures in Puerto Rico are limited to the assessment by Marshak (2007) on the status of the red hind (*Epinephelus guttatus*) population from three seasonally closed FSA sites off the west coast based on fishery-dependent (commercial landings, port-samplings), and fishery-independent time series data (SEAMAP-C). An initial post-enactment increases of fishery-independent Catch-per-Unit-Effort (CPUE; kg/trip) was observed from all three sites, and within spawning aggregations. Marshak (2007) proposed that increased fishing effort within previously under-targeted shelf regions (open to fishing) led to increases in nominal CPUE within later years but resulted in subsequent reductions of fishery independent CPUE. Increased average length of *E. guttatus* was observed in both data sets but was related to limited recruitment and proportional contributions of few remaining large females. Although the closure was initially effective in stemming further stock decline, shifts in fishing strategies apparently overrode the potential recovery of red hind (Marshak, 2007). Lack of enforcement of the seasonal closures may have also played a significant role in the conservation initiative.

Previous to its No Take Zone (NTZ) designation by the DNER in 2004, Isla de Mona was the focus of an intense fishing effort for sea turtles and large commercially important groupers during their seasonal FSA's (Scharer-Umpierre et al., 2014). The original designation of 1 nautical mile around the island was expanded in 2007 to include spawning aggregation sites of at least 22 coral reef fish species, including threatened red hind, tiger and yellowfin groupers (*Epinephelus guttatus, Mycteroperca tigris, M. venenosa*) that fell outside of the original NTZ boundaries (Scharer, 2010). Based on diver surveys and Geographic Position System (GPS) tracking instruments, Nemeth et al. (2007) determined the spawning times and identified locations with highest densities of red hinds (*E. guttatus*) and yellowfin groupers (M. *venenosa*) during their FSA's in Isla de Mona. Red hinds aggregated at a depth of 20m on a low-relief colonized pavement habitat whereas yellowfin groupers were found at depths of 25 – 30m on the high relief shelf-edge (Nemeth et al., 2007). The reproductive behavior and sound production of yellowfin grouper was studied at a spawning aggregation site off Mona Island by Scharer (2010). The highest abundance was detected in March and April, five to nine days after the full moon. Yellowfin grouper individuals in the size range of 30 – 89 cm were observed in these spawning aggregations (Nemeth et al., 2007).

Olson et al., (2019) evaluated the response of snapper (Lutjanidae) and grouper (Serranidae) populations from Isla de Mona 14 years after its initial 2004 NTZ designation by the DNER. Despite indications of fishing activity within the NTZ, a reserve-effect was evidenced from increasing mean sizes and densities of smaller growing species and mean total fish density 36% higher than 2005. However, the large demersal predators remained in low densities, preventing meaningful analyses of population trends. Recent follow-ups on grouper population stocks from visual and passive acoustic monitoring surveys during spawning aggregations in Isla de Mona support the conclusions by Olson et al. (2019) that populations of red hind (*Epinephelus guttatus*), yellowfin grouper (*Mycteroperca venenosa*), and black grouper (*Mycteroperca bonaci*) were comprised by very low number of individuals. The maximum number of individuals observed per survey were of 67 for *M. venenosa*, six for *M. bonaci* and 14 for *E. guttatus*. Also, a decreasing density trend for *M. venenosa*, an increasing trend for *M. bonaci* and no change of mean density for *E. guttatus* between 2016 and 2017 visual surveys was reported by Ruiz et al. (2018).

The limited research performed in Puerto Rico regarding the recovery of large commercially important groupers after both seasonal and permanent area closures are indicative of no significant progress in the recovery of these populations (Marshak, 2007; Olson et al., 2019). Monitoring programs based on acoustic telemetry (Scharer, 2012) are in place to follow-up the population responses of red hind, Nassau, black, and yellowfin groupers at Isla de Mona and other closed fishing areas in the west coast but strict and effective enforcement strategies need to be in place before conclusions about the effectiveness of closed fishing areas for replenishment of overfished grouper stock can be reached.

VII. Methods

The sampling approach and methodologies of the 2018-20 monitoring survey followed the field protocols designed for the original baseline characterizations of sessile-benthic, fish and shellfish communities from mesophotic habitats in the 30 – 50m depth range at Isla Desecheo (DES), Bajo de Sico (BDS), Abrir la Sierra (ALS), El Seco (SECO), and Tourmaline Reef (TOUR) (García-Sais et al., 2005, 2007, 2010, 2011, 2012, 2013). Maps showing the general location of surveyed sites in the west and east coasts of Puerto Rico are presented as Figures 1 and 2. At least five (5) samples representative of the main benthic habitats originally included in the baseline surveys at each site were re-visited during the 2018-20 monitoring survey for quantitative and qualitative monitoring assessments. Observations and/or measurements of the percent reef substrate cover by sessile-benthic categories, and taxonomic composition, density, and size-frequency distributions per habitat/depth of small demersal and large demersal fishes and shellfishes (queen conch and spiny lobster) were produced for each site. A complete set of benthic and fish baseline characterizations were produced for Boya 4 (BOYA), to serve as a reference site adjacent to seasonally closed sites in the west coast (ALS, TOUR, BDS) that are open to fishing year-round (with exception of applicable island wide species regulations). Geographic coordinates, depths, dates, habitat classifications, and other information of the stations sampled during the 2018-20 monitoring survey are included in Table 1. The baseline and monitoring survey data for all sites was organized in an excel database available in electronic format as Appendix 1.

Sessile-benthic Community Characterizations

Data on the percent reef substrate cover by sessile-benthic categories, including benthic algae, cyanobacteria, stony corals, soft corals, black corals, sponges, and abiotic substrates were produced from 10m long photo-transects of the seafloor at stations previously characterized during baseline surveys at each site. At least five (5) photo-transects were surveyed from each of the main benthic habitats within the 25 – 50m depth range per site. At least 10 non-overlapping photos were taken along transect lines separated by a distance of approximately 0.5m from the substrate using a Nikon 500 camera with an Aquatica housing. The digital images of the seafloor were uploaded and analyzed with Coral Point Count (CPC) software. An array of 25 random points was overlaid on each photo image and the underlying sessile-benthic categories identified to species, or to the lowest taxonomic unit possible. The percent substrate cover was calculated as the fraction of total points overlaid on each species/benthic category divided by the total points overlaid on each transect and multiplied by 100.

Habitat/depth classifications were designed to include descriptions of both the physiographic reef zone (habitat) and the depth range (m) in which it was surveyed. These included:

CPRT – colonized pavement reef tops. Horizontally oriented seascapes variably colonized by reef biota

CPSlope – colonized pavement slope. Vertically oriented insular slope sections variably colonized by reef biota

CPWall – colonized pavement wall. Completely vertical (90 degree) sections of the insular slope variably colonized by reef biota

BCR – bank coral reef. Outer shelf coral reef buildup on mostly horizontally oriented seascape.

PCR – patch coral reef. Coral reef buildup on mostly horizontally oriented seascape surrounded by deep pockets of sand.

ACR – aggregate coral reef. Coral buildup that occurs in various shapes and lacks sand channels

Rhod – rhodolith bed. Extensive deposits of rhodolith nodules (Rhodophyta) forming a bed along mostly flat, horizontally or gently sloping seascapes.

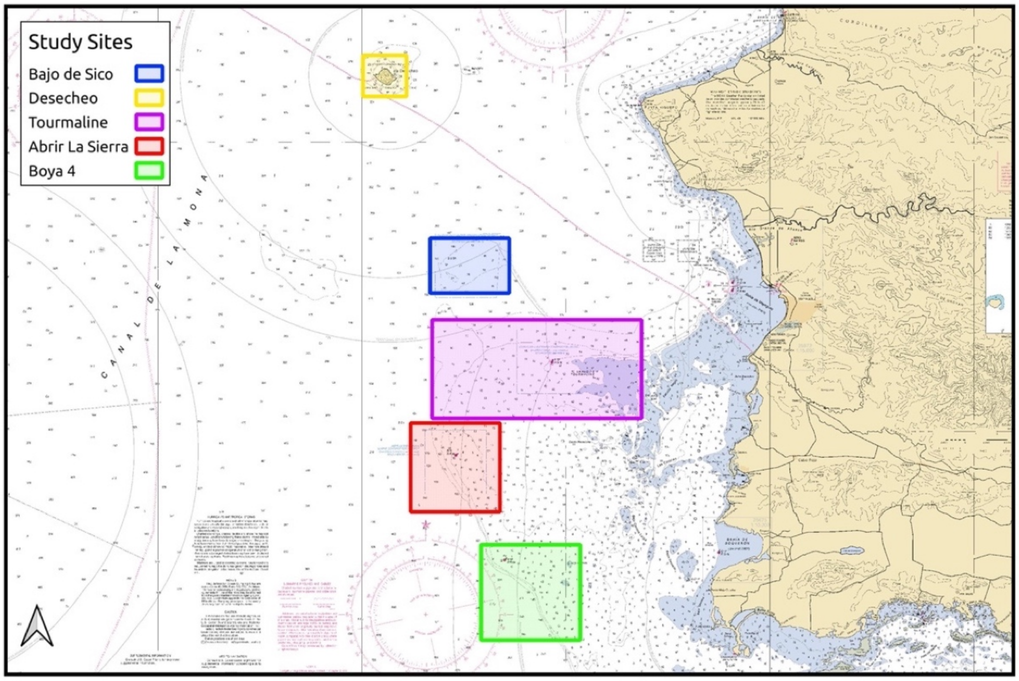

Figure 1 Map of study sites in the west coast of Puerto Rico, Boya 4, Abrir La Sierra, Bajo de Sico, Isla Desecheo

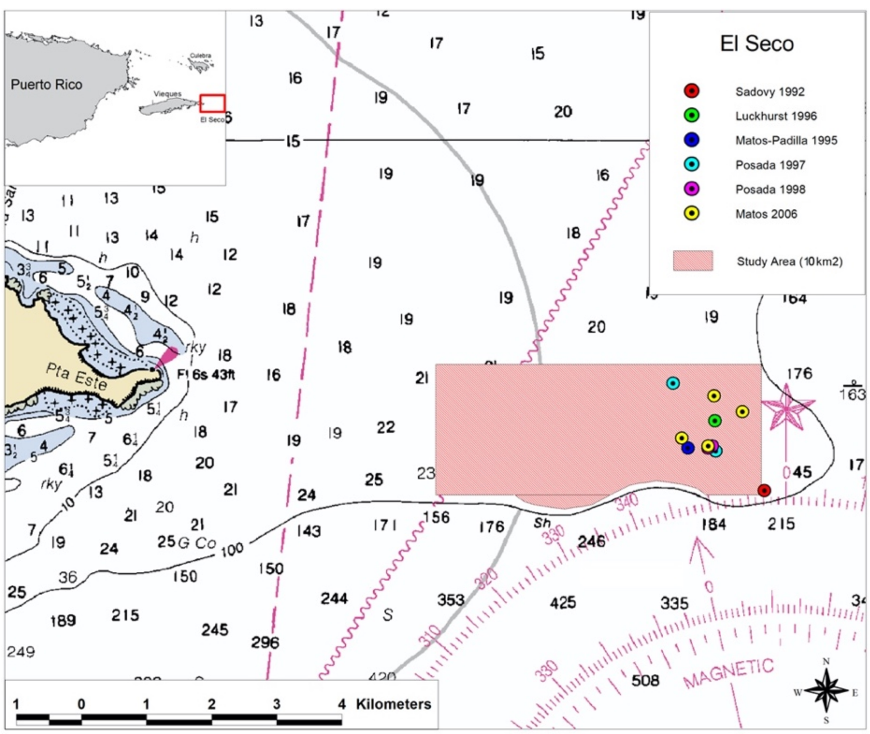

Figure 2. Map of study site at El Seco Reef, east coast of Puerto Rico.

Table 1. Geographic coordinates, depths, survey dates, and benthic habitat classifications for stations sampled during the 2018-20 monitoring survey compatible to those originally sampled during the baseline surveys.

CPRT – Colonized Pavement Reef Top; **CPSlope** – Colonized Pavement Slope; **CPWall** – Colonized Pavement Wall; **Rhod** – Rhodolith bed; **BCR** – Bank Coral Reef; **PCR** – Patch Coral Reef; **ACR** – Aggregate Coral Reef; **DT** – Drift Belt-Transect; **PT** – 3 x 10m Permanent Transect; **LT** – 3 x 10m Line Photo-Transect; **B/F** –Benthic/Fish Survey on 3 x 10m belt-transect; **LDF** - Large Demersal Fishes/Shellfishes

Date	Site	Station	Depth (m)	Benthic Habitat	Latitude Start	Longitude Start	Survey
Abrir La Sierra (ALS)							
10/31/18	ALS	ALS 25-0	22.1	CPRT25	18.0583	67.4127	Photo
10/31/18	ALS	ALS 25-0	22.1	CPRT25	18.0583	67.4127	Photo
10/31/18	ALS	ALS 25-1	22.7	CPRT25	18.0572	67.4121	PT - B/F
10/31/18	ALS	ALS 25-2	21.8	CPRT25	18.0571	67.4120	PT - B/F
10/31/18	ALS	ALS 25-3	20.9	CPRT25	18.0570	67.4119	PT - B/F
10/31/18	ALS	ALS 25-4	22.2	CPRT25	18.0569	67.4119	PT - B/F
10/31/18	ALS	ALS 25-5	23.0	CPRT25	18.0569	67.4119	PT - B/F
1/29/19	ALS	ALS 3	30.3	CPRT30	18.0930	67.4330	LT - B/F
7/2/19	ALS	ALS 11-a	30.9	CPRT30	18.0778	67.4330	LT - B/F
7/2/19	ALS	ALS 11-b	30.9	CPRT30	18.0778	67.4330	LT - B/F
7/2/19	ALS	ALS-3a	30.9	CPRT30	18.0930	67.4330	LT - B/F
7/2/19	ALS	ALS-3b	30.9	CPRT30	18.0930	67.4330	LT - B/F
6/27/19	ALS	ALS 33-a	30.3	CPRT30	18.0673	67.4217	LT - B/F
6/27/19	ALS	ALS 33-b	30.3	CPRT30	18.0673	67.4217	LT - B/F
7/3/19	ALS	ALS 18-a	35.9	CPRT40	18.0919	67.4341	LT - B/F
7/3/19	ALS	ALS 18-b	35.9	CPRT40	18.0919	67.4341	LT - B/F
6/27/19	ALS	ALS 27-a	39.4	CPRT40	18.0837	67.6432	LT - B/F
6/27/19	ALS	ALS 27-b	39.4	CPRT40	18.0837	67.6432	LT - B/F
6/27/19	ALS	ALS 23-a	39.4	CPRT40	18.0642	67.4204	LT - B/F
6/27/19	ALS	ALS 23-b	39.4	CPRT40	18.0642	67.4204	LT - B/F
7/2/19	ALS	ALS 21-a	41.2	CPRT40	18.0645	67.4200	LT - B/F
7/2/19	ALS	ALS 21-b	41.2	CPRT40	18.0645	67.4200	LT - B/F
6/7/20	ALS	ALS 54-a	36.1	Rhodo40	18.0001	67.4326	LT - B/F
6/7/20	ALS	ALS 54-b	36.1	Rhodo40	18.0001	67.4326	LT - B/F
6/7/20	ALS	ALS 10-a	36.1	Rhodo40	18.0940	67.4301	LT - B/F
6/7/20	ALS	ALS 10-b	36.1	Rhodo40	18.0940	67.4301	LT - B/F
6/7/20	ALS	ALS 55-a	36.4	Rhodo40	18.1023	67.4329	LT - B/F
6/7/20	ALS	ALS 55-b	36.4	Rhodo40	18.1023	67.4329	LT - B/F
7/2/19	ALS	ALS 24-a	50.3	CPSlope50	18.0776	67.4295	LT - B/F

Table 1. Geographic coordinates, depths, survey dates, and benthic habitat classifications for stations sampled during the 2018-20 monitoring survey compatible to those originally sampled during the baseline surveys.

CPRT – Colonized Pavement Reef Top; **CPSlope** – Colonized Pavement Slope; **CPWall** – Colonized Pavement Wall; **Rhod** – Rhodolith bed; **BCR** – Bank Coral Reef; **PCR** – Patch Coral Reef; **ACR** – Aggregate Coral Reef; **DT** – Drift Belt-Transect; **PT** – 3 x 10m Permanent Transect; **LT** – 3 x 10m Line Photo-Transect; **B/F** –Benthic/Fish Survey on 3 x 10m belt-transect; **LDF** - Large Demersal Fishes/Shellfishes

Date	Site	Station	Depth (m)	Benthic Habitat	Latitude Start	Longitude Start	Survey
7/2/19	ALS	ALS 24-b	50.3	CPSlope50	18.0776	67.4295	LT - B/F
7/3/19	ALS	ALS 26-a	47.6	CPSlope50	18.0832	67.4323	LT - B/F
7/3/19	ALS	ALS 26-a	47.6	CPSlope50	18.0832	67.4323	LT - B/F
7/2/19	ALS	ALS 22-a	47.3	CPSlope50	18.0641	67.4205	LT - B/F
7/2/19	ALS	ALS 22-b	47.6	CPSlope50	18.0641	67.4205	LT - B/F
7/3/19	ALS	ALS 28-a	50.3	CPSlope50	18.0878	67.4342	LT - B/F
7/3/19	ALS	ALS 28-b	50.3	CPSlope50	18.0878	67.4342	LT - B/F
10/26/18	ALS	ALS 45	26.7 - 28.9	CPRT25	18.0854	67.4285	DT - LDF
10/26/18	ALS	ALS 46	24.2 - 28.0	CPRT25	18.1071	67.4279	DT - LDF
10/26/18	ALS	ALS 47	24.4 - 28.6	CPRT25	18.0705	67.4206	DT - LDF
10/26/18	ALS	ALS 48	22.1 - 27.8	CPRT25	18.0583	67.4127	DT - LDF
11/30/18	ALS	ALS-49	24.0 - 28.2	CPRT25	18.0171	67.3958	DT - LDF
6/13/19	ALS	ALS-1	30.3 - 33.3	CPRT30	18.0753	67.4276	DT - LDF
1/29/19	ALS	ALS - 8	32.1 - 32.7	CPRT30	18.0636	67.4197	DT - LDF
1/15/19	ALS	ALS-64	31.8 - 32.1	CPRT30	18.0642	67.4201	DT - LDF
1/15/19	ALS	ALS-7	32.1 - 33.0	CPRT30	18.0668	67.4219	DT - LDF
1/29/19	ALS	ALS 3	29.0 - 30.3	CPRT30	18.0930	67.4330	DT - LDF
6/13/19	ALS	ALS-9	36.4 - 39.4	CPSlope40-50	18.0766	67.4285	DT - LDF
1/15/19	ALS	ALS-71	33.3 - 37.3	CPSlope40-50	18.0827	67.4317	DT - LDF
1/15/19	ALS	ALS-69	33.0 - 36.4	CPSlope40-50	18.0741	67.4214	DT - LDF
5/17/19	ALS	ALS-15	37.9 - 40.6	CPSlope40-50	18.0682	67.4231	DT - LDF
5/17/19	ALS	ALS-60	36.4 - 39.4	CPSlope40-50	18.0611	67.4179	DT - LDF
7/23/19	ALS	ALS-23	43.0 - 47.3	Rhod50	18.0639	67.4182	DT - LDF
7/23/19	ALS	ALS-42	44.6 - 50.0	Rhod50	18.0644	67.4189	DT - LDF
7/23/19	ALS	ALS-44	40.6 - 43.9	Rhod50	18.0680	67.4219	DT - LDF
7/23/19	ALS	ALS-54	35.5 - 40.0	Rhod50	18.0994	67.4519	DT - LDF
7/23/19	ALS	ALS-68	37.0 - 41.6	Rhod50	18.0756	67.4259	DT - LDF

Table 1. Geographic coordinates, depths, survey dates, and benthic habitat classifications for stations sampled during the 2018-20 monitoring survey compatible to those originally sampled during the baseline surveys.

CPRT – Colonized Pavement Reef Top; **CPSlope** – Colonized Pavement Slope; **CPWall** – Colonized Pavement Wall; **Rhod** – Rhodolith bed; **BCR** – Bank Coral Reef; **PCR** – Patch Coral Reef; **ACR** – Aggregate Coral Reef; **DT** – Drift Belt-Transect; **PT** – 3 x 10m Permanent Transect; **LT** – 3 x 10m Line Photo-Transect; **B/F** –Benthic/Fish Survey on 3 x 10m belt-transect; **LDF** - Large Demersal Fishes/Shellfishes

Date	Site	Station	Depth (m)	Benthic Habitat	Latitude Start	Longitude Start	Survey
Bajo de Sico (BDS)							
2/29/20	BDS	BDS 25-1	25.8	CPRT25	18.2312	67.4308	LT - B/F
2/29/20	BDS	BDS 25-2	26.1	CPRT25	18.2312	67.4308	LT - B/F
7/23/20	BDS	BDS 25-3	25.2	CPRT25	18.2300	67.4306	LT - B/F
7/23/20	BDS	BDS 25-4	25.8	CPRT25	18.2300	67.4306	LT - B/F
7/23/20	BDS	BDS 25-5	28.5	CPRT25	18.2266	67.4249	LT - B/F
7/23/20	BDS	BDS 25-6	28.5	CPRT25	18.2266	67.4249	LT - B/F
6/12/20	BDS	BDS 30-1	28.2	CPRT 30	18.2279	67.4278	LT - B/F
6/12/20	BDS	BDS 30-2	30.3	CPRT 30	18.2279	67.4278	LT - B/F
6/12/20	BDS	BDS 30-3	35.4	CPRT 30	18.2310	67.4301	LT - B/F
6/12/20	BDS	BDS 30-4	35.4	CPRT 30	18.2310	67.4301	LT - B/F
7/23/20	BDS	BDS 30-5	30.0	CPRT 30	18.2276	67.4262	LT - B/F
7/23/20	BDS	BDS 30-6	30.0	CPRT 30	18.2276	67.4262	LT - B/F
2/29/20	BDS	BDS 40-1	38.8	CPWall40	18.2311	67.4306	LT - B/F
2/29/20	BDS	BDS 40-2	38.8	CPWall40	18.2311	67.4306	LT - B/F
2/29/20	BDS	BDS 40-3	37.9	CPWall40	18.2311	67.4310	LT - B/F
2/29/20	BDS	BDS 40-4	36.4	CPWall40	18.2311	67.4310	LT - B/F
7/23/20	BDS	BDS 40-5	32.0	CPWall40	18.2310	67.4309	LT - B/F
7/23/20	BDS	BDS 40-6	32.0	CPWall40	18.2310	67.4309	LT - B/F
6/12/20	BDS	BDS 50-1	48.8	Rhod50	18.2285	67.4205	LT - B/F
6/12/20	BDS	BDS 50-2	49.1	Rhod50	18.2285	67.4205	LT - B/F
6/12/20	BDS	BDS 50-3	49.1	Rhod50	18.2303	67.4231	LT - B/F
6/12/20	BDS	BDS 50-4	49.1	Rhod50	18.2303	67.4231	LT - B/F
7/23/20	BDS	BDS 50-5	49.4	Rhod50	18.2252	67.4195	LT - B/F
7/23/20	BDS	BDS 50-6	49.7	Rhod50	18.2252	67.4195	LT - B/F
1/31/20	BDS	BDS-4	32.7 - 33.5	CPRT30	18.2270	67.4270	DT - LDF
10/23/19	BDS	BDS-11	30.0 - 33.0	CPRT30	18.2280	67.4258	DT - LDF
10/23/19	BDS	BDS-15	30.0 - 33.0	CPRT30	18.2270	67.4240	DT - LDF
1/31/20	BDS	BDS-3	30.3 - 34.2	CPRT30	18.2271	67.4277	DT - LDF
7/24/20	BDS	BDS-12	23.6 - 31.2	CPRT30	18.2290	67.4270	DT - LDF

Table 1. Geographic coordinates, depths, survey dates, and benthic habitat classifications for stations sampled during the 2018-20 monitoring survey compatible to those originally sampled during the baseline surveys.

CPRT – Colonized Pavement Reef Top; **CPSlope** – Colonized Pavement Slope; **CPWall** – Colonized Pavement Wall; **Rhod** – Rhodolith bed; **BCR** – Bank Coral Reef; **PCR** – Patch Coral Reef; **ACR** – Aggregate Coral Reef; **DT** – Drift Belt-Transect; **PT** – 3 x 10m Permanent Transect; **LT** – 3 x 10m Line Photo-Transect; **B/F** –Benthic/Fish Survey on 3 x 10m belt-transect; **LDF** - Large Demersal Fishes/Shellfishes

Date	Site	Station	Depth (m)	Benthic Habitat	Latitude Start	Longitude Start	Survey
7/24/20	BDS	BDS-9	23.6 - 31.2	CPRT30	18.2259	67.4229	DT - LDF
2/29/20	BDS	BDS-6	36.4 - 30.0	CPRT40	18.2309	67.4298	DT - LDF
7/24/20	BDS	BDS-1	38.0 - 41.2	CPRT40	18.2241	67.4229	DT - LDF
7/24/20	BDS	BDS0-17	37.6 - 40.9	CPRT40	18.2300	67.4300	DT - LDF
6/12/20	BDS	BDS-1	38.2 - 40.0	CPRT40	18.2240	67.4230	DT - LDF
7/24/20	BDS	BDS-18	30.3 - 40.3	CPRT40	18.2280	67.4258	DT - LDF
10/23/19	BDS	BDS-19	45.0 - 50.0	Rhod40-50	18.2240	67.4280	DT - LDF
2/29/20	BDS	BDS-16	41.2 - 36.6	Rhod40-50	18.2291	67.4240	DT - LDF
2/29/20	BDS	BDS-21	48.5 - 45.0	Rhod40-50	18.2230	67.4249	DT - LDF
10/23/19	BDS	BDS-20	35.0 - 40.0	Rhod40-50	18.2241	67.4242	DT - LDF
10/23/19	BDS	BDS-8	35.0 - 40.0	Rhod40-50	18.2291	67.4281	DT - LDF
10/23/19	BDS	BDS-17	35.0 - 40.0	Rhod40-50	18.2300	67.4302	DT - LDF
Tourmaline (TOUR)							
10/21/18	TOUR	T25-1	24.8	ACR-1	18.1656	67.2820	PT - B/F
10/21/18	TOUR	T25-2	24.2	ACR-2	18.1657	67.2820	PT - B/F
10/21/18	TOUR	T25-3	25.1	ACR-3	18.1658	67.2820	PT - B/F
10/21/18	TOUR	T25-4	28.0	ACR-4	18.1658	67.2820	PT - B/F
4/25/19	TOUR	T25-5	28.0	ACR-5	18.1658	67.2819	PT - B/F
3/7/19	TOUR	T9-30	31.8	CPSlope30-50	18.1710	67.3170	LT - B/F
2/13/10	TOUR	T8-40	38.2	CPSlope30-50	18.1767	67.3348	LT - B/F
6/6/19	TOUR	T9-40	38.2	CPSlope30-50	18.1737	67.3170	LT - B/F
6/6/19	TOUR	T2-50	45.4	CPSlope30-50	18.1406	67.4265	LT - B/F
4/25/19	TOUR	T3-50	45.4	CPSlope30-50	18.1550	67.4171	LT - B/F
2/13/19	TOUR	T8-30	31.8	CPSlope30-50	18.1728	67.3347	LT - B/F
6/27/19	TOUR	T6-50	51.2	CPSlope30-50	18.1783	67.3710	LT - B/F
4/25/19	TOUR	T2-30	33.3	CPSlope30-50	18.1399	67.4238	LT - B/F
3/7/19	TOUR	T7-30	31.2	CPSlope30-50	18.1717	67.3524	LT - B/F
6/6/19	TOUR	T7-40	41.2	CPSlope30-50	18.1772	67.3527	LT - B/F
4/25/19	TOUR	T8-50	48.9	CPWall50	18.1765	67.3346	LT - B/F
6/27/19	TOUR	T9-50	47	CPWall50	18.1737	67.3170	LT - B/F

Table 1. Geographic coordinates, depths, survey dates, and benthic habitat classifications for stations sampled during the 2018-20 monitoring survey compatible to those originally sampled during the baseline surveys.

CPRT – Colonized Pavement Reef Top; **CPSlope** – Colonized Pavement Slope; **CPWall** – Colonized Pavement Wall; **Rhod** – Rhodolith bed; **BCR** – Bank Coral Reef; **PCR** – Patch Coral Reef; **ACR** – Aggregate Coral Reef; **DT** – Drift Belt-Transect; **PT** – 3 x 10m Permanent Transect; **LT** – 3 x 10m Line Photo-Transect; **B/F** –Benthic/Fish Survey on 3 x 10m belt-transect; **LDF** - Large Demersal Fishes/Shellfishes

Date	Site	Station	Depth (m)	Benthic Habitat	Latitude Start	Longitude Start	Survey
4/25/19	TOUR	T1-30	33.6	Rhodo30-50	18.1242	67.4315	LT - B/F
4/11/19	TOUR	T4-30	31.8	Rhodo30-50	18.1655	67.3992	DT - LDF
4/10/19	TOUR	T1-40	38.5	Rhodo30-50	18.1242	67.4323	LT - B/F
4/25/19	TOUR	T3-40	39.7	Rhodo30-50	18.1544	67.4164	LT - B/F
4/11/19	TOUR	T4-40	41.2	Rhodo30-50	18.1662	67.4024	DT - LDF
5/2/19	TOUR	T4-50	48.9	Rhodo30-50	18.1656	67.4041	DT - LDF
7/23/19	TOUR	T5-50	48.5	Rhodo30-50	18.1660	67.4038	DT - LDF
6/6/19	TOUR	T-445	48.5	Rhodo30-50	18.12519	67.43227	LT - B/F
10/21/18	TOUR	T7-25	24.2 - 28.0	ACR25	18.1664	67.2763	DT - LDF
3/7/19	TOUR	T8-25	27.0 - 29.6	ACR25	18.1660	67.2808	DT - LDF
10/20/18	TOUR	T1-25	26.0 - 29.6	CPSlope25-30	18.1663	67.3474	DT - LDF
10/20/18	TOUR	T2-25	24.2 - 28.0	CPSlope25-30	18.1667	67.3716	DT - LDF
10/20/18	TOUR	T3-25	27.0 - 30.0	CPSlope25-30	18.1642	67.3898	DT - LDF
10/20/18	TOUR	T4-25	26.0 - 28.7	CPSlope25-30	18.1597	67.4026	DT - LDF
10/20/18	TOUR	T5-25	27.0 - 28.7	CPSlope25-30	18.1368	67.4186	DT - LDF
10/21/18	TOUR	T6-25	23.6 - 27.0	CPSlope25-30	18.1660	67.3247	DT - LDF
5/3/19	TOUR	T8-30	30.0 - 31.8	CPSlope31-40	18.1728	67.3347	DT - LDF
2/13/19	TOUR	T9-30	30.0 - 32.1	CPSlope31-40	18.1709	67.3171	DT - LDF
3/12/19	TOUR	T10 - 30	30.3 - 33.9	CPSlope31-40	18.1692	67.2990	DT - LDF
3/12/19	TOUR	T13-30	30.0 - 33.3	CPSlope31-40	18.1749	67.3653	DT - LDF
5/3/19	TOUR	T21-30	31.0 - 34.8	CPSlope31-40	18.1702	67.2998	DT - LDF
5/3/19	TOUR	T9-40	37.9 - 40.6	CPSlope31-40	18.1736	67.3169	DT - LDF
5/3/19	TOUR	T10-40	36.6 - 38.2	CPSlope31-40	18.1702	67.2991	DT - LDF
3/7/19	TOUR	T14-30	29.0 - 34.0	Rhod30-50	18.1732	67.3815	DT - LDF
5/2/19	TOUR	T2-40	38.8 - 40.6	Rhod30-50	18.1407	67.4267	DT - LDF
4/11/19	TOUR	T4-40	38.2 - 41.2	Rhod30-50	18.1662	67.4024	DT - LDF
5/2/19	TOUR	T4-50	47.2 - 48.9	Rhod30-50	18.1656	67.4041	DT - LDF
4/11/19	TOUR	T4-30	30.0 - 31.8	Rhod30-50	18.1655	67.3992	DT - LDF
5/17/19	TOUR	T6-50	45.5 - 46.6	CPWall-1	18.1780	67.3709	DT - LDF
5/17/19	TOUR	T2-50	47.2 - 50.0	CPWall-2	18.1407	67.4265	DT - LDF

Table 1. Geographic coordinates, depths, survey dates, and benthic habitat classifications for stations sampled during the 2018-20 monitoring survey compatible to those originally sampled during the baseline surveys.

CPRT – Colonized Pavement Reef Top; **CPSlope** – Colonized Pavement Slope; **CPWall** – Colonized Pavement Wall; **Rhod** – Rhodolith bed; **BCR** – Bank Coral Reef; **PCR** – Patch Coral Reef; **ACR** – Aggregate Coral Reef; **DT** – Drift Belt-Transect; **PT** – 3 x 10m Permanent Transect; **LT** – 3 x 10m Line Photo-Transect; **B/F** –Benthic/Fish Survey on 3 x 10m belt-transect; **LDF** - Large Demersal Fishes/Shellfishes

Date	Site	Station	Depth (m)	Benthic Habitat	Latitude Start	Longitude Start	Survey
2/13/19	TOUR	T9-50	45.0 - 48.5	CPWall-3	18.1737	67.3170	DT - LDF
Isla Desecheo (DES)							
11/12/18	DES	DES 25-1	23.8	ACR25	18.3777	67.4835	PT - B/F
11/12/18	DES	DES 25-2	23.8	ACR25	18.3777	67.4835	PT - B/F
11/12/18	DES	DES 25-3	24.1	ACR25	18.3777	67.4835	PT - B/F
11/12/18	DES	DES 25-4	24.4	ACR25	18.3777	67.4835	PT - B/F
11/12/18	DES	DES 25-5	24.7	ACR25	18.3777	67.4835	PT - B/F
1/23/20	DES	DES 30-1	30.3	CPSlope30	18.3775	67.4850	PT - B/F
1/23/20	DES	DES 30-2	30.3	CPSlope30	18.3775	67.4850	PT - B/F
1/23/20	DES	DES 30-3	30.3	CPSlope30	18.3774	67.4850	PT - B/F
2/28/20	DES	DES 30-4	30.3	CPSlope30			PT - B/F
2/28/20	DES	DES 30-5	30.3	CPSlope30			PT - B/F
1/23/20	DES	DES 40-1	39.4	CPSlope40	18.3775	67.4858	PT - B/F
1/23/20	DES	DES 40-2	39.1	CPSlope40	18.3775	67.4857	PT - B/F
1/23/20	DES	DES 40-3	41.5	CPSlope40	18.3774	67.4856	PT - B/F
1/23/20	DES	DES 40-4	39.4	CPSlope40	18.3773	67.4851	PT - B/F
2/28/20	DES	DES 40-5	39.4	CPSlope40			PT - B/F
1/23/20	DES	DES 50-1	48.5	Rhod50	18.3766	67.4855	LT - B/F
1/23/20	DES	DES 50-2	49.0	Rhod50	18.3766	67.4855	LT - B/F
2/28/20	DES	DES 50-3	46.4	Rhod50	18.3771	67.4852	LT - B/F
6/11/20	DES	DES 50-4	47.9	Rhod50	18.3773	67.4862	LT - B/F
6/11/20	DES	DES 50-5	47.9	Rhod50	18.3773	67.4862	LT - B/F
11/6/18	DES	DES S-1	22.1 - 27.3	ACR25-1	18.3767	67.4801	DT - LDF
11/6/18	DES	DES S-2	24.0 - 28.1	ACR25-2	18.3777	67.4836	DT - LDF
11/6/18	DES	DES S-3	21.2 - 25.1	ACR25-3	18.3788	67.4871	DT - LDF
11/6/18	DES	DES S-4	21.2 - 25.1	ACR25-4	18.3815	67.4897	DT - LDF
1/31/20	DES	DES S-5	24.2 – 26.4	CPRT30-40	18.3798	67.4715	DT - LDF
10/16/19	DES	DES-24	30.0 - 33.0	CPRT30-40	18.3773	67.4838	DT - LDF
10/18/19	DES	DES-1A	35.0 - 40.0	CPRT30-40	18.3772	67.4853	DT - LDF
10/14/19	DES	DES-1	35.0 - 40.0	CPRT30-40	18.3781	67.4868	DT - LDF

Table 1. Geographic coordinates, depths, survey dates, and benthic habitat classifications for stations sampled during the 2018-20 monitoring survey compatible to those originally sampled during the baseline surveys.

CPRT – Colonized Pavement Reef Top; **CPSlope** – Colonized Pavement Slope; **CPWall** – Colonized Pavement Wall; **Rhod** – Rhodolith bed; **BCR** – Bank Coral Reef; **PCR** – Patch Coral Reef; **ACR** – Aggregate Coral Reef; **DT** – Drift Belt-Transect; **PT** – 3 x 10m Permanent Transect; **LT** – 3 x 10m Line Photo-Transect; **B/F** –Benthic/Fish Survey on 3 x 10m belt-transect; **LDF** - Large Demersal Fishes/Shellfishes

Date	Site	Station	Depth (m)	Benthic Habitat	Latitude Start	Longitude Start	Survey
10/14/19	DES	DES-6	35.0 - 40.0	CPRT30-40	18.3827	67.4914	DT - LDF
10/18/19	DES	DES-11	30.0 - 33.0	ACR30-40	18.3965	67.4816	DT - LDF
10/14/19	DES	DES-15	30.0 - 33.0	ACR30-40	18.3908	67.4745	DT - LDF
10/14/19	DES	DES-16	30.0 - 33.0	ACR30-40	18.3940	67.4770	DT - LDF
10/16/19	DES	DES-18	30.0 - 33.0	ACR30-40	18.3850	67.4703	DT - LDF
11/12/18	DES	DES 19-2	30.0 - 36.7	ACR30-40	18.3969	67.4799	DT - LDF
10/16/19	DES	DES-10	35.0 - 40.0	ACR30-40	18.3927	67.4750	DT - LDF
10/16/19	DES	DES-9	35.0 - 40.0	ACR30-40	18.3889	67.4724	DT - LDF
1/31/20	DES	DES-14	39.7 - 40.0	ACR30-40	18.3913	67.4728	DT - LDF
10/14/19	DES	DES-3	45.0 - 50.0	Rhod50	18.3775	67.4861	DT - LDF
10/14/19	DES	DES-13	45.0 - 50.0	Rhod50	18.3797	67.4690	DT - LDF
1/31/20	DES	DES-17	45.6 - 48.5	Rhod50	18.3838	67.4687	DT - LDF
10/16/19	DES	DES-21	45.0 – 50.0	Rhod50	18.3783	67.4869	DT - LDF
10/16/19	DES	DES-23	45.0 - 50.0	Rhod50	18.3853	67.4936	DT - LDF
El Seco (SECO)							
6/29/20	SECO	V-12a	22.1	CPRT23-27	18.1252	65.2053	LT - B/F
6/29/20	SECO	V-12b	22.1	CPRT23-27	18.1252	65.2053	LT - B/F
6/29/20	SECO	V-49a	26.1	CPRT23-27	18.1305	65.2033	LT - B/F
6/29/20	SECO	V-49b	26.1	CPRT23-27	18.1305	65.2033	LT - B/F
6/30/20	SECO	V-59a	24.5	CPRT23-27	18.1273	65.1992	LT - B/F
6/30/20	SECO	V-59b	24.2	CPRT23-27	18.1273	65.1992	LT - B/F
6/30/20	SECO	V-18a	33.6	BCR33-40	18.1387	65.1971	LT - B/F
6/30/20	SECO	V-18b	33.6	BCR33-40	18.1387	65.1971	LT - B/F
6/30/20	SECO	V-42a	34.8	BCR33-40	18.1353	65.1961	LT - B/F
6/30/20	SECO	V-42b	36.1	BCR33-40	18.1353	65.1961	LT - B/F
6/30/20	SECO	V-39a	41.2	BCR33-40	18.1307	65.1890	LT - B/F
6/30/20	SECO	V-39b	41.2	BCR33-40	18.1307	65.1890	LT - B/F
6/29/20	SECO	V-52a	37.5	PCR35-40	18.1263	65.1893	LT - B/F
6/29/20	SECO	V-52b	38.5	PCR35-40	18.1263	65.1893	LT - B/F

Table 1. Geographic coordinates, depths, survey dates, and benthic habitat classifications for stations sampled during the 2018-20 monitoring survey compatible to those originally sampled during the baseline surveys.

CPRT – Colonized Pavement Reef Top; **CPSlope** – Colonized Pavement Slope; **CPWall** – Colonized Pavement Wall; **Rhod** – Rhodolith bed; **BCR** – Bank Coral Reef; **PCR** – Patch Coral Reef; **ACR** – Aggregate Coral Reef; **DT** – Drift Belt-Transect; **PT** – 3 x 10m Permanent Transect; **LT** – 3 x 10m Line Photo-Transect; **B/F** –Benthic/Fish Survey on 3 x 10m belt-transect; **LDF** - Large Demersal Fishes/Shellfishes

Date	Site	Station	Depth (m)	Benthic Habitat	Latitude Start	Longitude Start	Survey
6/29/20	SECO	V-4a	40.6	PCR35-40	18.1238	65.1906	LT - B/F
6/29/20	SECO	V-4b	40.9	PCR35-40	18.1238	65.1906	LT - B/F
6/30/20	SECO	V57a	40.3	PCR35-40	18.1251	65.1904	LT - B/F
6/30/20	SECO	V-57b	40.3	PCR35-40	18.1251	65.1904	LT - B/F
6/29/20	SECO	V-64a	48.5	Rhod40-50	18.1234	65.2268	LT - B/F
6/29/20	SECO	V-64b	49.5	Rhod40-50	18.1234	65.2268	LT - B/F
6/29/20	SECO	V-62a	40.9	Rhod40-50	18.1250	65.2192	LT - B/F
6/29/20	SECO	V-62b	40.9	Rhod40-50	18.1250	65.2192	LT - B/F
6/30/20	SECO	V-34a	39.4	Rhod40-50	18.1293	65.2305	LT - B/F
6/30/20	SECO	V-34b	39.4	Rhod40-50	18.1293	65.2305	LT - B/F
7/1/20	SECO	V-59	23.0 - 28.0	CPRT23-28	18.1273	65.1992	DT - LDF
7/1/20	SECO	V-11	22.7 - 24.2	CPRT23-28	18.1300	65.2010	DT - LDF
8/13/20	SECO	V-27	23.0 - 30.3	CPRT23-28	18.1359	65.2011	DT - LDF
8/14/20	SECO	V-68	23.3 - 28.0	CPRT23-28	18.1253	65.2025	DT - LDF
8/13/20	SECO	V-49	24.2 - 27.3	CPRT23-28	18.1341	65.2033	DT - LDF
7/2/20	SECO	V-41	36.0 – 38.4	BCR35-40	18.1326	65.1965	DT - LDF
7/2/20	SECO	V-46	32.4 - 35.8	BCR35-40	18.1399	65.1938	DT - LDF
7/1/20	SECO	V-44	36.4 - 39.4	BCR35-40	18.1373	65.2071	DT - LDF
8/14/20	SECO	V-37	34.5 - 28.2	BCR35-40	18.1282	65.1909	DT - LDF
8/14/20	SECO	V-43	35.8 - 39.4	BCR35-40	18.1374	65.2105	DT - LDF
7/1/20	SECO	V-51	36.4 - 38.8	PCR36-42	18.1279	65.1873	DT - LDF
7/2/20	SECO	V-54	36.3 - 37.9	PCR36-42	18.1312	65.2096	DT - LDF
8/14/20	SECO	V-55	37.3 - 40.0	PCR36-42	18.1417	65.2214	DT - LDF
8/13/20	SECO	V-SPAG	38.8 - 42.4	PCR36-42	18.1238	65.1906	DT - LDF
8/14/20	SECO	V-48	38.2 - 40.0	PCR36-42	18.1362	65.2161	DT - LDF
8/13/20	SECO	V-35	37.9 - 39.4	Rhod40-50	18.1238	65.2331	DT - LDF
7/1/20	SECO	V-65	48.0 - 50.0	Rhod40-50	18.1234	65.2268	DT - LDF
7/1/20	SECO	V-66	47.0 - 50.0	Rhod40-50	18.1248	65.2265	DT - LDF
8/13/20	SECO	V-67	47.0 - 49.4	Rhod40-50	18.1245	65.2299	DT - LDF
8/13/20	SECO	V-61	38.2 - 38.8	Rhod40-50	18.1311	65.2155	DT - LDF

Table 1. Geographic coordinates, depths, survey dates, and benthic habitat classifications for stations sampled during the 2018-20 monitoring survey compatible to those originally sampled during the baseline surveys.

CPRT – Colonized Pavement Reef Top; **CPSlope** – Colonized Pavement Slope; **CPWall** – Colonized Pavement Wall; **Rhod** – Rhodolith bed; **BCR** – Bank Coral Reef; **PCR** – Patch Coral Reef; **ACR** – Aggregate Coral Reef; **DT** – Drift Belt-Transect; **PT** – 3 x 10m Permanent Transect; **LT** – 3 x 10m Line Photo-Transect; **B/F** –Benthic/Fish Survey on 3 x 10m belt-transect; **LDF** - Large Demersal Fishes/Shellfishes

Date	Site	Station	Depth (m)	Benthic Habitat	Latitude Start	Longitude Start	Survey
Boya 4 (B-4)							
1/17/19	BOY4	B4 25-1	23.0	CPSlope25	17.9585	67.3485	PT - B/F
1/17/19	BOY4	B4 25-2	25.1	CPSlope25	17.9585	67.3485	PT - B/F
1/17/19	BOY4	B4 25-3	26.1	CPSlope25	17.9586	67.3486	PT - B/F
1/17/19	BOY4	B4 25-4	26.7	CPSlope25	17.9587	67.3486	PT - B/F
1/17/19	BOY4	B4 25-5	25.0	CPSlope25	17.9589	67.3487	PT - B/F
3/29/19	BOY4	B4 30-1	31.8	CPSlope30	17.9843	67.3602	LT - B/F
3/29/19	BOY4	B4 30-2	30.0	CPSlope30	17.9793	67.3572	LT - B/F
3/29/19	BOY4	B4 30-3	30.3	CPSlope30	17.9748	67.3555	LT - B/F
4/5/19	BOY4	B4 30-4	31.8	CPSlope30	17.9655	67.3528	LT - B/F
4/5/19	BOY4	B4 30-5	30.9	CPSlope30	17.9613	67.3505	LT - B/F
3/29/19	BOY4	B4 40-1	41.2	CPSLope40	17.9849	67.3613	LT - B/F
3/29/19	BOY4	B4 40-2	40.0	CPSLope40	17.9839	67.3603	LT - B/F
3/20/19	BOY4	B4 40-3	39.4	CPSLope40	17.9904	67.3683	LT - B/F
3/20/19	BOY4	B4 40-4	40.0	CPSLope40	17.9871	67.3637	LT - B/F
3/20/19	BOY4	B4 40-5	39.4	CPSLope40	17.9613	67.3507	LT - B/F
3/13/19	BOY4	B4 50-1	49.7	CPSlope50	17.9611	67.3506	LT - B/F
3/13/19	BOY4	B4 50-2	48.8	CPSlope50	17.9871	``67.3637	LT - B/F
3/13/19	BOY4	B4 50-3	48.8	CPSlope50	17.9900	67.3677	LT - B/F
3/13/19	BOY4	B4 50-4	49.7	CPSlope50	17.9909	67.3695	LT - B/F
3/20/19	BOY4	B4 50-5	49.7	CPSlope50	17.9970	67.3808	LT - B/F
11/30/18	BOY4	B4 1-25	26.0 - 29.0	CPSlope25	17.9944	67.3754	DT - LDF
11/30/18	BOY4	B4 2-25	24.2 - 26.7	CPSlope25	17.9995	67.3803	DT - LDF
11/30/18	BOY4	B4 3-25	25.8 - 29.1	CPSlope25	17.9995	67.3840	DT - LDF
11/17/19	BOY4	B4 4-25	24.2 - 31.8	CPSlope25	17.9578	67.3480	DT - LDF
11/17/19	BOY4	B4 5-25	24.5 - 32.0	CPSlope25	17.9655	67.3525	DT - LDF
1/21/19	BOY4	B4 1-30	31.2 - 34.8	CPSlope30	17.9586	67.3487	DT - LDF
1/21/19	BOY4	B4 2-30	30.3 - 35.1	CPSlope30	17.9610	67.3502	DT - LDF
1/21/19	BOY4	B4 3-30	30.3 - 33.9	CPSlope30	17.9655	67.3525	DT - LDF

Table 1. Geographic coordinates, depths, survey dates, and benthic habitat classifications for stations sampled during the 2018-20 monitoring survey compatible to those originally sampled during the baseline surveys.

CPRT – Colonized Pavement Reef Top; **CPSlope** – Colonized Pavement Slope; **CPWall** – Colonized Pavement Wall; **Rhod** – Rhodolith bed; **BCR** – Bank Coral Reef; **PCR** – Patch Coral Reef; **ACR** – Aggregate Coral Reef; **DT** – Drift Belt-Transect; **PT** – 3 x 10m Permanent Transect; **LT** – 3 x 10m Line Photo-Transect; **B/F** –Benthic/Fish Survey on 3 x 10m belt-transect; **LDF** - Large Demersal Fishes/Shellfishes

Date	Site	Station	Depth (m)	Benthic Habitat	Latitude Start	Longitude Start	Survey
1/21/19	BOY4	B4 4-30	30.3 - 34.8	CPSlope30	17.8880	67.3619	DT - LDF
1/29/19	BOY4	B4 5-30	29.1 - 34.2	CPSlope30	17.9977	67.3809	DT - LDF
3/29/19	BOY4	B4 1-40	28.0 - 41.2	CPSlope40	17.9849	67.3613	DT - LDF
3/29/19	BOY4	B4 2-40	38.0 – 40.0	CPSlope40	17.9839	67.3603	DT - LDF
3/20/19	BOY4	B4 3-40	38.0 - 39.4	CPSlope40	17.9904	67.3683	DT - LDF
3/20/19	BOY4	B4 4-40	38.5 - 40.0	CPSlope40	17.9871	67.3637	DT - LDF
3/20/19	BOY4	B4 5-40	38.0 - 39.4	CPSlope40	17.9613	67.3507	DT - LDF
3/13/19	BOY4	B4 1-50	47.0 - 49.7	CPSlope50	17.9611	67.3506	DT - LDF
3/13/19	BOY4	B4 2-50	47.0 - 48.8	CPSlope 50-2	17.9871	67.3637	DT - LDF
3/13/19	BOY4	B4 3-50	47.0 - 48.5	CPSlope 50-3	17.9900	67.3677	DT - LDF
3/13/19	BOY4	B4 4-50	47.0 - 49.7	CPSlope 50-4	17.9909	67.3695	DT - LDF
3/20/19	BOY4	B4 5-50	47.0 - 48.5	CPSlope 50-5	17.9970	67.3808	DT - LDF

Fish/Shellfish Community Characterizations

1. Small Demersal Fishes

Small demersal reef fishes were surveyed by 10m long by 3m wide (30m^2) belt-transects centered over the reference line of transects used for sessile-benthic characterizations. At least five (5) 30m^2 belt-transects were surveyed from each of the main benthic habitats distributed within the 25 – 50m depth range at each site. Each transect was surveyed during five (5) - 10 minutes, depending on the species richness and density. The first minute was used to survey transitory species (parrotfishes, doctorfishes, creole wrasse, jacks, others) that may not remain within transect areas. The next two minutes were used to identify and count species attracted to divers (e. g. wrasses) and that their densities may increase with survey time. The final two (2) – three (3) minutes were used to count territorial species (damselfishes, squirrelfishes, gobies, etc.) that remain within transect areas throughout the entire survey duration. Inevitably, some large demersal fishes invade 10m x 3m belt-transect areas designed to sample small demersal species resulting in over-estimates of their densities. These include (among others) the blackfin snapper (*Lutjanus buccanella*), queen triggerfish (*Balistes vetula*), and nurse sharks (*Ginglymostoma cirratum*). Thus, inferences regarding population densities of these large demersal species were based on the data from drift belt-transects (see next section). The total number of fish individuals of any particular species observed within 3 x 10m "belt- transects" was reported as the density of that species in units of # Ind/30m^2. The mean of all density estimates (for any particular species) from belt-transects surveyed at any given habitat/depth was reported as the species mean density. The sum total of densities by all fish species at any given habitat/depth was reported as the total mean density. The density of any given species across all habitats/depths in a given site was reported as the site mean density.

2. Large Demersal Fishes

Large demersal fishes and shellfishes (spiny lobster and queen conch) were surveyed by a series of drift belt-transects 265m long (mean distance) x 6m wide (mean total survey area: 1,590 m^2). At least five (5) transects were surveyed from each main habitat type within the 25 – 50m depth range at each site. Transect distances were estimated from GPS marks (coordinates) at the point of diver's entry to GPS marks at a point where the divers sank a marker buoy several times, or until signal confirmation was produced from the boat captain by accelerating the engines in neutral. Information on the date, station identification, diver names, time in and out of the water, and distance surveyed was collected by an on-deck support team.

Drift belt-transect surveys were performed close to the bottom in order to discern and provide size estimates (fishes) or measurements of queen conch (*Lobatus gigas*). Therefore, coastal and migratory pelagic species (e. g. jacks, mackerels, dolphinfish, wahoo, tunas, marlins) that swim at mid-water and or at the surface were included in the taxonomic listings of survey stations if detected within transects rectangular areas, but not used for comparative assessments since these sightings were considered fortuitous and not indicative of their real density within a given habitat/depth. Drift belt-transect surveys included all snappers (Lutjanidae), all groupers (Serranidae), queen triggerfish (Balistidae), trunkfishes (Ostraciidae), hogfish (Labridae), great barracuda (Sphyraenidae), mackerels (Scombridae), lionfish (Scorpaenidae), large parrotfishes (*Scarus coelestinus, S, coeruleus, S. guacamaia*), and shellfishes - spiny lobster (*Panulirus argus*), and queen conch (*L. gigas*). Size estimates (in cms) of the fork length (FL) or total length (TL) were recorded for all fish individuals observed within belt-transects. Total shell length measurements of queen conch (*L. gigas*) individuals were collected on-site with a plastic ruler.

The cephalothorax length (CL) of spiny lobsters (*P. argus*) was estimated for individuals observed within belt-transects. Size-frequency distributions of numerically dominant fish/shellfish species were expressed as the percent of total individuals by each size class (in cm).

3. Statistical Analyses

The sampling design of the 2018-20 monitoring survey consisted of a series of at least five (5) replicate samples representative of the main benthic habitats within the 25 – 50m depth range at each site. Benthic data included measurements of percent substrate cover by sessile-benthic categories/species and prevalence data on coral disease infections and bleaching per transect. Fish data sets included the taxonomic composition and density estimates of small demersal fishes from 3m x 10m belt-transects, and the taxonomic composition, density, and size distributions of large demersal fishes and shellfishes (spiny lobster and queen conch) from drift belt-transects at each site. Benthic habitat types were distributed across different depths depending on site and were classified along with a depth code (e. g. CPSlope30-50) for statistical treatments. Samples from similar habitat/depths were used as replicates for comparative analyses of percent cover by benthic categories/species, and fish/shellfish density between habitats/depths per site and survey, and between sites and surveys for any particular habitat/depth.

Data of fish density and percent substrate cover were log N transformed to make data sets more suited for parametric testing. In those particular cases where data sets contained zeros, X +1 log N transformations were applied. One-way analyses of variance (ANOVA) were used to test for differences of percent substrate cover, and fish/shellfish density and species richness between habitats/depths from each site. Variations between surveys were tested by Two-way ANOVA's with replication, including survey year and habitat/depths as sources of variation. When interaction factors in the Two-Way ANOVA procedures were statistically significant ($p < 0.05$) the 95% confidence interval of the mean values were used to determine differences between habitat/depths on any given survey, or between surveys for any given habitat/depth at each site. Statistical significance for null-hypothesis rejection was set at $p < 0.05$.

Variations of the benthic and fish/shellfish community structure between habitat/depths at each site, or between surveys at representative habitats/depths for any given site were analyzed using multivariate statistics (PRIMER software). The Bray-Curtis similarity/dissimilarity index (BC) was used to quantify differences in species populations between surveys, sites and or habitats/depths.

Bray-Curtis dissimilarity = BC_{ij}=1- 2C_{ij} / Si + Sj , where i and j were two different sites; Si was the total number of specimens on site I; Sj was the total number of specimens in site j; Cij was the sum of only the lesser counts for each species found in both sides. Bray-Curtis similarity % = (1 – BC) *100. Euclidean distances based on the Bray-Curtis parameters were used to represent community structure similarities within and between habitats/depth and surveys in non-metric multidimensional plots (nMDS).

Similarity/dissimilarities of benthic populations were based on the relative (%) composition of the main categories (abiotic, benthic algae, cyanobacteria, stony corals, soft corals, and sponges). Similarity/dissimilarities of fish/shellfish populations were based on the relative densities (Ind/m^2) of species assemblages contributing at least 90% of the total individuals in order to disregard differences associated to species represented by only one individual. Data were double-standardized by total and maximum values and square-root transformed to reduce the weight of numerically dominant species in the samples. Average similarities and dissimilarities within and between habitats/depths on each site, as well as species contributions (top 70% cumulative contributions) were produced from SIMPER analyses (PRIMER software).

Fish/shellfish size distributions were plotted as the percent of the total individuals by each size class. Size distribution curves of numerically dominant species were constructed from the composite of individuals at all depths and benthic habitats per site to allow for comparative analyses between sites and between surveys (Kolmogorov-Smirnov).

VIII. Results and Discussion

a. Abrir La Sierra, Cabo Rojo

Physical Description

Abrir La Sierra (ALS), is a shelf-edge reef system located approximately 14.6 NM west off Punta Guaniquilla, Cabo Rojo, on the west coast of Puerto Rico. The reef runs to the north and west of NOAA's Buoy 6. The outer shelf has an initial shelf drop-off at depths of 20 – 25m that extends across 8.5 kms along the north-south axis (Figure 3). The primary drop-off leads to an outer shelf basin at depths ranging from 30 - 48m extending offshore 0.2 - 0.3 km. A continuous hard bottom ridge that rises from the outer shelf basin to depths of 26 – 33m fringes the shelf-edge. The final drop-off at the shelf-edge is abrupt, except at the northern section, where the slope is more gradual.

The mesophotic habitat at ALS has a total area of 3,217 km^2. The largest area within the 30 – 50m depth range corresponds to the 35 – 40m contour, which represents approximately 49% of the total area within the 30 – 50m depth range (Garcia-Sais et al., 2010a). The main benthic habitats within the 30 – 50m depths include a colonized pavement reef top at 25m (CPRT25), and 30m (CPRT30), colonized pavement slope at 40 - 50m (CPSlope40-50), and a rhodolith bed in the outer shelf basin at 40m (Rhod40). A detailed characterization and map of benthic habitats within the 30 – 50m depth range is available from Garcia-Sais et al. (2010a). Location of stations sampled in 2018-20 previously surveyed in the 2008-10 baseline study is shown in Figure 4. Images of the main benthic habitats and associated communities surveyed during 2018-20 are shown in Photo Album 1.

Benthic Community

Depth/habitat related patterns of benthic community structure, 2018-20 survey

The mean percent substrate cover by sessile-benthic categories measured from the main habitats/depths at ALS during 2018-20 are presented in Table 2. Benthic algae were the main category in terms of percent substrate cover at all depths surveyed during 2018-20 with means ranging between 60.76% at CPRT30 and 66.94% at CPSlope50 (Figure 5). Differences of cover by total benthic algae between habitats/depths were statistically insignificant (ANOVA; $p = 0.714$) but marked habitat/depth related variations among the main algal taxonomic components were noted. Turf algae were the dominant component of the CPRT25, representing 63.4% of the mean total benthic algae but declined markedly with depth, down to < 2% at CPSlope50 (Figure 6).

Brown fleshy macroalgae (mostly *Dictyota sp*) represented less than 3.0% at CPRT25 but increased its substrate cover at deeper stations with a maximum contribution of 45.0% of the total at CPSlope40. The encrusting fan alga (*Lobophora sp*.) was the dominant component of benthic algae below 25m, reaching a maximum cover of 44.46%, or 66.4% of the total at CPSlope50. Green calcareous algae (*Halimeda sp*) exhibited a pattern of increasing cover with depth but in relatively low cover (range: 0.20 – 3.06%). Habitat/depth related differences of reef substrate cover by cyanobacteria (blue-green algae) were statistically significant (ANOVA; p= 0.003) associated with higher cover at CPSlope30, Rhod40 and CPSlope40, relative to CPRT25 and CPSlope50 (Figure 5).

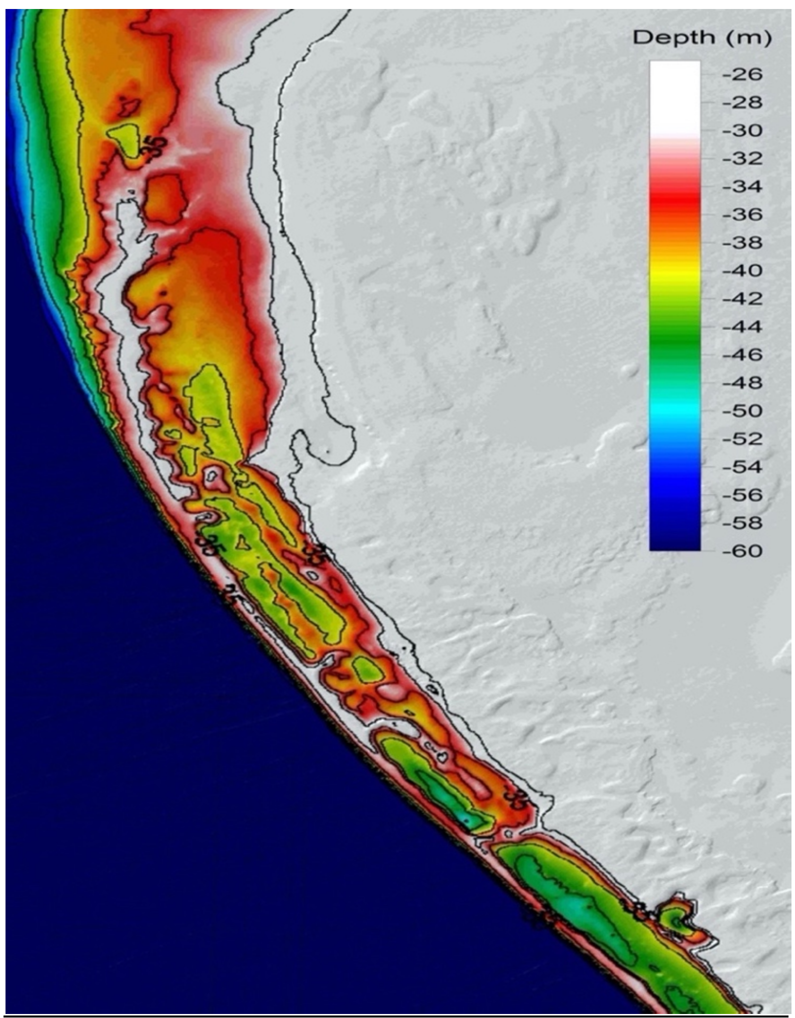

Figure 3. Bathymetry at Abrir La Sierra. (Garcia-Sais et al, 2010). Source data: http://ccma.nos.noaa.gov/ecosystems/coral reef/usvi_nps.html

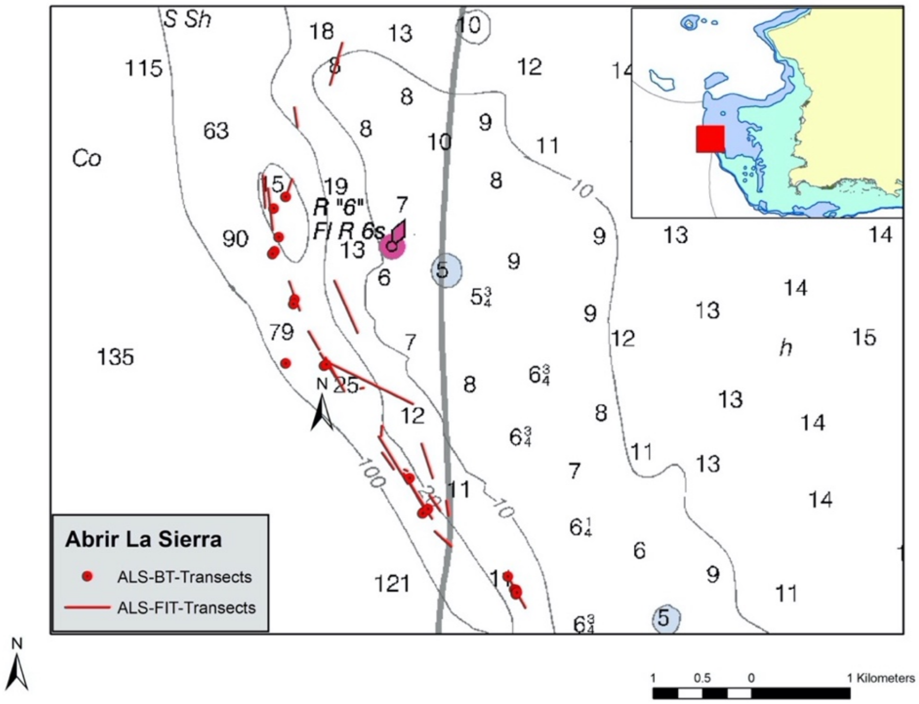

Figure 4. Location of sampling stations at Abrir La Sierra, 2018-20 survey

Stony corals were represented by 18 species within the 25 – 50m depths surveyed during 2018-20 at ALS, with mean substrate cover ranging from a maximum of 6.87% at CPRT30 to a minimum of 0.26% at Rhod40 (Table 2). Statistically significant differences were found (ANOVA; $p < 0.0001$) associated with higher cover at CPRT25 and CPRT30, relative to all other habitats/depths. Stony coral species richness and mean density of colonies declined markedly below 30m, from 15 and 11 species at CPRT25 and CPRT30, respectively, to < 5 from other habitats/depths. Such differences appeared to be related to the higher availability of hard ground, horizontally oriented substrates at CPRT habitats, compared to the steep, sediment rich CPSlope40 and CPSlope50, and the algae dominated rhodolith bed. Habitat/depth related variations of substrate cover by stony coral species were noted. Lettuce coral (*Agaricia agaricites*), mustard-hill coral (*Porites astreoides*) and mountainous star coral (*Orbicella faveolata*) were the dominant species at CPRT25 and CPRT30 but were absent from Rhod40, CPSlope40, and CPSlope50 (Figure 7). Great star coral (*Montastraea cavernosa*) was the dominant species in terms of reef substrate cover at CPRT25 but declined with increasing depth down to Rhod40 and was not observed at CPSlope40 and CPSlope50. Conversely, whitestar sheet coral (*A. lamarki*) increased in cover with depth reaching a peak mean cover of 0.28% at CPSlope50.

Table 2. Mean percent substrate cover by sessile-benthic categories from transects surveyed within the 25 – 50m depth range at Abrir La Sierra during 2018-19.

BENTHIC CATEGORIES	CPRT25	CPRT30	Rhod40	CPSlope40	CPSlope50
Abiotic					
Pavement	13.09	0.49			
Sand	0.48	7.65	11.16	6.95	12.35
Dead Coral					
Rhodolith			0.15	0.46	
Rubble			0.12	0.48	0.09
Total Abiotic	13.57	8.15	11.43	7.88	12.44
Benthic Algae					
Turf (mixed) with sediment	0.54	2.72			
Peyssonnelid (mixed)		1.25	0.59	0.13	0.91
Turf (mixed)	38.43	4.17	3.36	0.38	1.00
Lobophora sp.	20.27	31.09	37.85	26.46	44.46
Jania sp.					
Halimeda spp.	0.20	1.29	2.88	2.30	3.06
Dictyota spp.	1.79	7.92	15.07	9.55	8.85
Padina sp.					
Ramicrusta sp.					
Fleshy macroalgae (mixed)	0.05	11.50	11.21	15.07	7.91
CCA (mixed)	0.20	0.81	0.85	0.57	0.75
Total Benthic Algae	61.48	60.76	71.81	54.46	66.94
Cyanobacteria	5.27	11.71	20.93	20.80	1.32
Hard Coral					
Agaricia agaricites	0.42	0.94			
Agaricia fragilis		0.06			
Agaricia grahamae	0.07	0.39			0.17
Agaricia lamarcki	0.15	0.13		0.21	0.28
Madracis decactis	0.05		0.04	0.04	
Madracis sp.					0.08
Meandrina meandrites	0.33	0.34			
Millepora alcicornis	0.52	0.10	0.09	0.08	
Montastraea cavernosa	1.22	0.21	0.13	0.13	
Mycetophyllia aliciae					
Orbicella faveolata	0.28	1.41			
Orbicella franksi	0.05	2.18			
Porites astreoides	0.79	0.53			
Porites porites	0.20				
Pseudodiploria strigosa	0.23				
Siderastrea siderea	0.43	0.58			
Stephanocoenia intersepta	0.09			0.06	
Unknown coral	0.17				
Total Hard Coral	4.99	6.87	0.26	0.52	0.52
# Coral Colonies/photo frame	3.66	3.02	0.25	0.62	0.34
# Diseased Coral Colonies/photo frame	0.12	0.06	0.00	0.00	0.00
# Antipatharian Colonies/photo frame	0.00	0.00	0.00	0.00	0.04
Octocoral					
Antillogorgia spp.	0.88			0.22	0.04
Briareum asbestinum			0.09	0.09	

Table 2. Mean percent substrate cover by sessile-benthic categories from transects surveyed within the 25 – 50m depth range at Abrir La Sierra during 2018-19.

BENTHIC CATEGORIES	CPRT25	CPRT30	Rhod40	CPSlope40	CPSlope50
Erythropodium caribaeorum	0.04				
Ellisella sp.					
Eunicea spp.	0.26	0.02	0.10	0.24	0.06
Gorgonia ventalina	0.18				
Iciligorgia schrammi	0.15			0.56	0.24
Muricea spp.		0.12		0.06	
Plexaura spp.	0.04				
Plexaurella spp.	0.10				
Pseudoplexaura spp.	0.05				
Ptergorgia sp.					
Unidentified					
Total Soft Corals	1.70	0.14	0.19	1.17	0.33
# Soft Corals/photo frame	2.66	1.28	0.72	8.21	2.55
Sponges					
Agelas clathrodes	1.03	0.92	0.16	0.43	1.54
Agelas citrina	0.27	0.26	0.14	0.13	0.77
Agelas conifera	1.09	1.34	1.06	1.35	2.96
Agelas dispar	0.81	0.32	0.18	0.31	0.04
Agelas fistularis					
Agelas sceptrum	0.06	0.21	0.66	0.70	0.38
Agelas sventres		0.15	0.94	1.31	0.24
Agelas tubulata					
Agelas sp.				0.04	
Aiolochoria crassa	0.05		0.04	0.13	0.23
Amphimedon compressa		0.02	0.18	0.06	0.10
Amphimedon sp.					0.09
Aplysina archeri				0.07	
Aplysina cauliformis	0.22	0.49	0.12	0.05	0.04
Aplysina fistularis	0.05		0.05	0.05	
Aplysina insularis					
Batzella sp.					
Callyspongia armigera		0.03			
Callyspongia ferox					
Cinachyrella kuekenthali			0.02	0.02	
Clathria sp.		0.07			
Cliona caribbaea		0.10			
Clathria faviformis				0.17	
Cliona delitrix					
Cliona varians					
Chondrilla caribensis					
Desmapsamma anchorata	0.13	0.05	0.04		
Ectyoplasia ferox	0.13	0.03	0.05	0.05	0.21
Erylus sp.					
Iotrochota birotulata	0.68		0.07	0.04	
Haliclona sp.					
Halisarca sp.					
Hyrtios cavernosus		0.07	0.60	0.66	0.47
Iotrochota birotulata		0.37	0.26	0.22	
Ircinia felix	0.13		0.10		
Ircinia strobilina	0.24	0.25	0.24	0.22	0.12

Table 2. Mean percent substrate cover by sessile-benthic categories from transects surveyed within the 25 – 50m depth range at Abrir La Sierra during 2018-19.

BENTHIC CATEGORIES	CPRT25	CPRT30	Rhod40	CPSlope40	CPSlope50
Monanchora arbuscula			0.04	0.04	
Mycale laevis	0.06	0.03			
Myrmekioderma gyroderma			0.01	0.13	0.06
Myrmekioderma rea		0.06			
Neofibularia nolitangere					
Neopetrosia proxima		0.19	0.10		0.05
Neopetrosia sp.		0.07	0.02	0.02	
Niphates digitalis					
Niphates erecta				0.04	
Niphates alba			0.04	0.04	0.17
Niphates sp.				0.09	0.08
Oceanapia bartschi			0.04		
Petrosia pellasarca		0.02	0.04	0.10	
Petrosia weinbergi				0.06	0.25
Plakortis spp.	0.06	0.57	0.80	1.17	0.70
Pleraplysilla sp.					0.04
Prosuberites laughlini				0.03	0.39
Scopalina ruetzleri	0.04	0.07			0.19
Smenospongia aurea					
Smenospongia conulosa			0.02	0.35	
Spheciospongia vesparium		0.02	0.04	0.04	
Spirastrella coccinea	0.39	0.06	0.19		0.09
Spirastrella hartmani					
Suberea sp.					0.04
Svenzea zeai	0.30	1.19	0.30	0.52	1.43
Unknown sponges	1.80	1.34	2.40	2.14	3.26
Verongula rigida	0.25				
Verongula sp.			0.04		
Xestospongia muta	5.19	3.24	3.83	3.67	4.51
Total Sponges	13.00	11.54	12.80	14.43	18.42

Soft corals (gorgonians) presented statistically significant habitat/depth related differences of reef substrate cover (ANOVA; p= 0.031). Higher substrate cover was measured at CPRT25 (mean: 1.70%) compared to samplings at deeper stations. Sea plumes (*Antillogorgia spp*.) and sea rods (*Eunicea spp*) were the dominant soft coral taxa at CPRT25, whereas the deep-water gorgonian (*Iciligorgia schrammi*) was the dominant species at CPSlope40 and CPSlope50 (Figure 8). Black coral (antipatharian) colonies were only present within photo-frames at CPSlope50 with a mean cover of 0.04%. The bushy Caribbean black coral (*Antipathes caribbeana*) was the main species present within and outside transects.

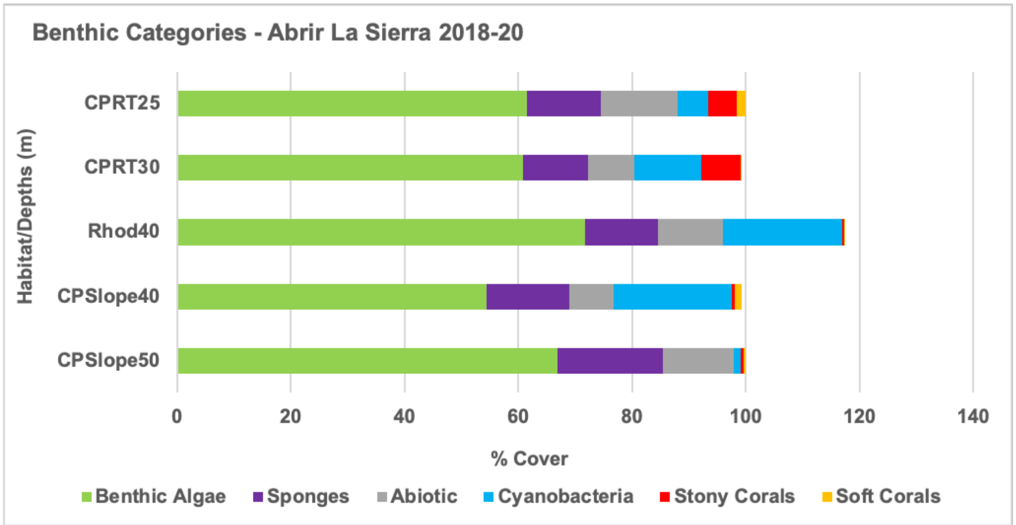

Figure 5. Mean percent substrate cover by benthic categories across the 25 – 50m depth range surveyed at Abrir La Sierra, 2018-20

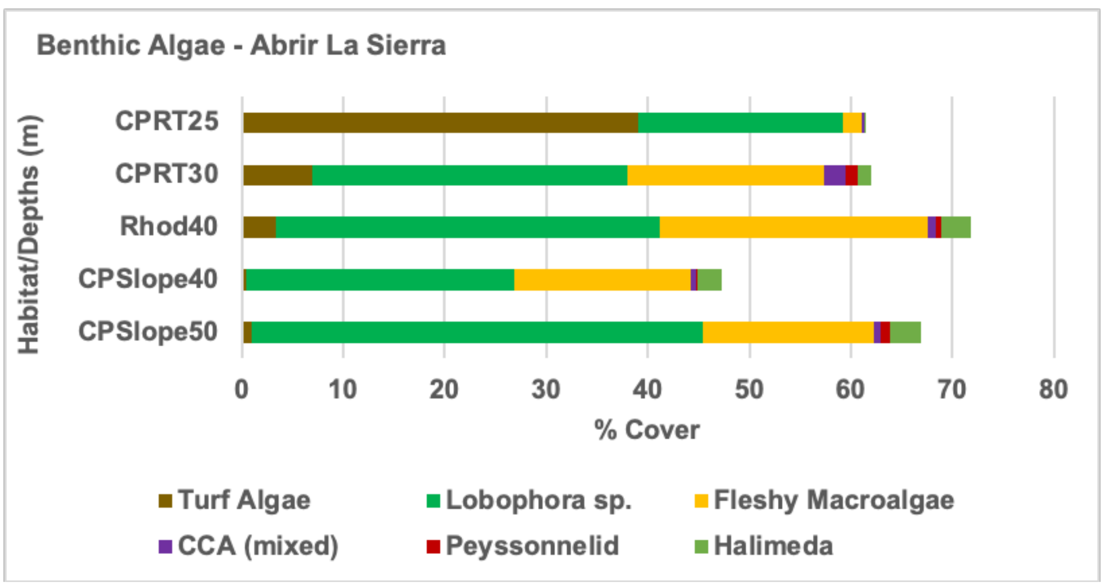

Figure 6. Mean percent substrate cover by benthic algae components across the 25 – 50m depth range surveyed at Abrir La Sierra, 2018-20

A total of 48 sponge species were identified from photo-transects within the 25m – 50m depth range at ALS during 2018-20 with mean substrate cover ranging from 11.54% at CPRT30, and 18.42% at CPSlope50 (Table 2). Habitat/depth related variations of reef substrate cover by total sponges were statistically insignificant (ANOVA; p = 0.124), but a trend of increasing species richness with depth down to 40m (max. 34 spp) was noted. The giant basket sponge

(*Xestospongia muta*) was the dominant species throughout the habitat/depth range surveyed with peak cover at CPRT25 (5.19%). Branching sponges in the *Agelas spp*, complex, including *A. conifera, A. sventres, A. sceptrum,* and *A. clathrodes* were the dominant assemblage at CPRT30 and Rhod40 (Figure 9). Sponges, particularly *X. muta* and *Agelas spp*. were observed to contribute markedly to the topographic relief and structural habitat complexity and thus, played a highly important role as protective habitats for the demersal fish community at mesophotic stations.

Reef substrate cover by total abiotic categories varied between means of 7.88% and 13.57% within the 25 – 50m mesophotic range at ALS during the 2018-20 monitoring survey (Table 2). Differences of substrate cover by abiotic categories between surveyed habitats/depths were statistically insignificant (ANOVA; p= 0.088). Sand cover increased with depth and was the main abiotic component from stations below 25m (Figure X). Extensive sand patches were observed down the outer shelf slope, partially covering sponges, soft corals and another sessile-benthic biota in some areas.

Similarities of benthic community structure at ALS within the 25 – 50m depth range surveyed were influenced by the presence of different benthic habitat types across the depth profile (Figure 10). Colonized pavement reef tops (CPRT) were limited to the 25m and 30m depths, a rhodolith bed prevailed on the outer basin at depths of 36 -40m, whereas colonized pavement slopes (CPSlope) prevailed in the 40m - 50m range. In addition to depth, marked differences of slope influenced the benthic community structure of these habitats. The highest similarities were observed within Rhod40 (88.0%), contributed by the high relative cover of benthic algae, abiotic, and sponges. Similarity was also very high at CPRT25 (87.3%), mostly contributed by stony corals and soft corals (Table 3).

The relatively high cover by benthic algae and sponges was a unifying feature contributing similarity across all habitats/depths surveyed. Conversely, reef substrate cover by stony corals was largely restricted to the horizontally oriented CPRT habitats. The highest dissimilarities of benthic community structure were observed between the CPRT25 and Rhod40 (37.7%), strongly influenced by the higher relative cover of stony corals and soft corals at CPRT25 (Table 4). Dissimilarity was also relatively high between CPRT30 and CPSlope40 (35.8%) driven by the higher cover of cyanobacteria and soft corals from CPSlope40 and the relatively higher cover by stony corals from CPRT30.

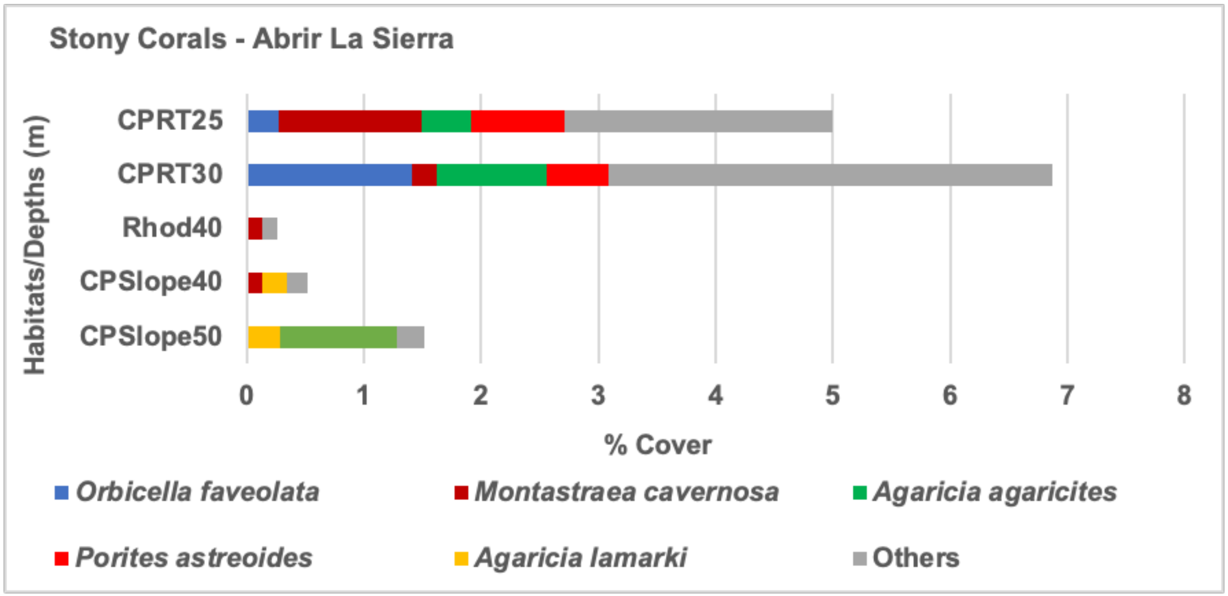

Figure 7. Mean percent substrate cover by stony coral species across the 25 – 50m depth range surveyed at Abrir La Sierra, 2018-20

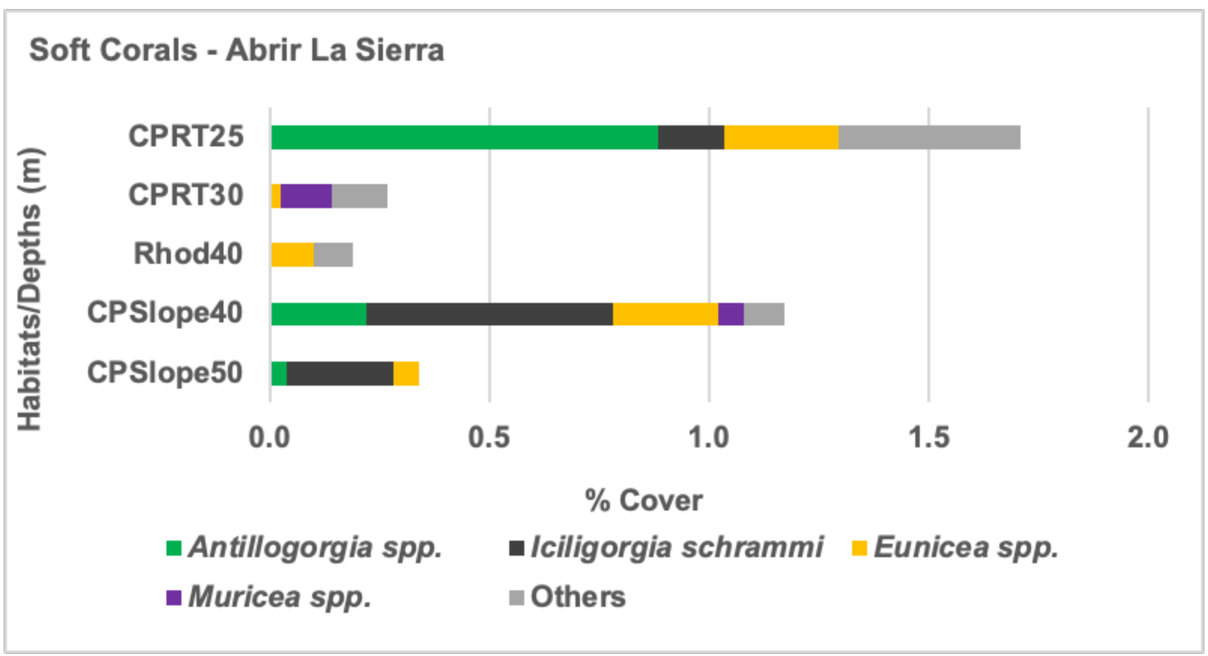

Figure 8. Mean percent substrate cover by soft coral species across the 25 – 50m depth range surveyed at Abrir La Sierra, 2018-20

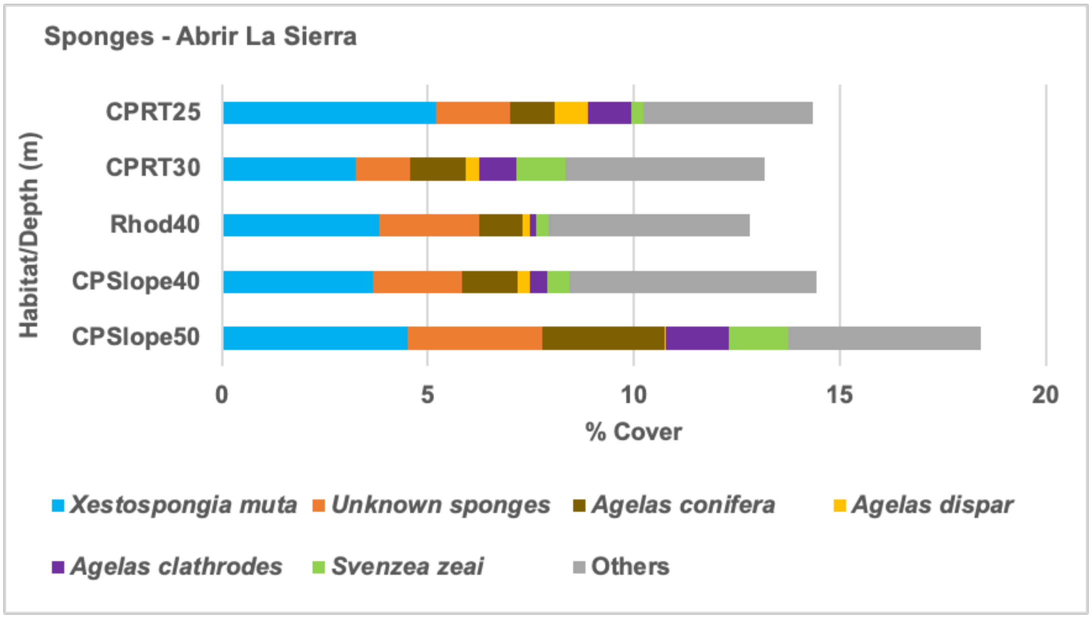

Figure 9. Mean percent substrate cover by sponge species across the 25 – 50m depth range surveyed at Abrir La Sierra, 2018-20

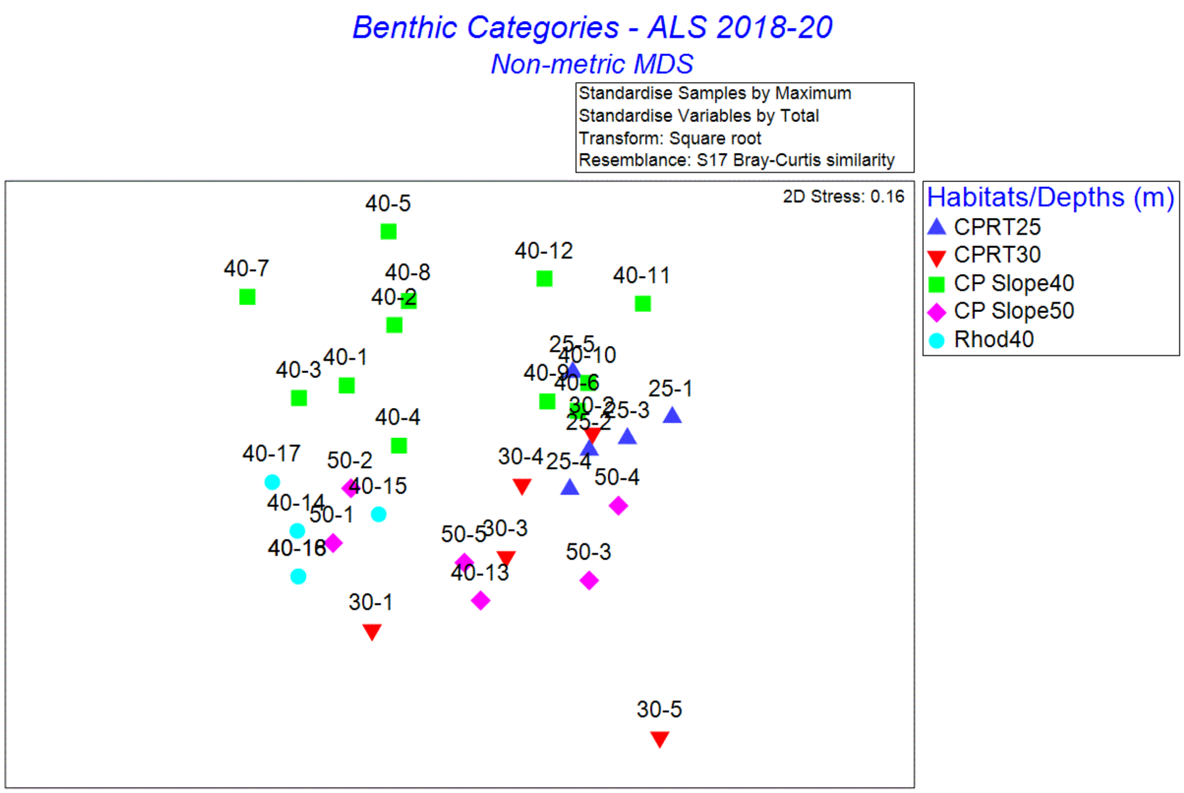

Figure 10. Non-metric multidimensional scaling (nMDS) plot of Bray-Curtis similarities between photo-quadrat samples of sessile-benthic communities surveyed from sub-mesophotic (25m) and upper mesophotic (30 – 50m) habitats/depths at Abrir La Sierra, 2018-20 survey.

Table 3. Similarities of sessile-benthic community structure at the main habitats/depths surveyed from Abrir La Sierra during 2018-20, including contributions of benthic categories to the within habitat similarity.

	CPRT25	CPRT30	Rhodo40	CPSlope40	CPSlope50
Similarity (%)	87.3	71.3	88.0	73.0	76.1
Benthic Categories					
Total Abiotic			31.3		25.0
Total Benthic Algae	17.6	29.0	35.2	25.0	33.2
Cyanobacteria				26.8	
Total Stony Coral	21.7	26.9			
Total Soft Corals	20.3				
Total Sponges	16.3	22.3	18.2	22.9	33.4

Table 4. Dissimilarity matrix between benthic habitats surveyed at Abrir la Sierra during 2018-20, including contributions of benthic categories to the between habitat dissimilarity.

	CPRT25 vs CPRT30	CPRT25 vs CPSlope40	CPRT30 vs CPSlope40	CPRT25 vs CPSlope50	CPRT30 vs CPSlope50	CPSlope40 vs CPSlope50	CPRT25 vs Rhod40	CPRT30 vs Rhod40
Dissimilarity (%)	25.5	30.3	35.8	30.0	30.8	32.8	37.7	34.6
Benthic Categories								
Total Abiotic	13.8				13.7	16.3		18.1
Total Benthic Algae								
Cyanobacteria		22.4	28.7			38.0		26.2
Total Stony Coral	25.1	27.0	31.3	36.4	48.0		35.6	
Total Soft Corals	41.9	30.0	20.4	34.5	17.5	24.6	40.1	23.3
Total Sponges								19.3

Temporal (monitoring) trends of benthic community structure

Variations of the mean percent substrate cover by benthic categories measured from a similar set of 26 sampling stations representative of the main benthic habitats at ALS in the 2008-10 baseline and 2018-20 monitoring survey are shown in Figure 11. Differences of substrate cover between surveys were statistically significant only for soft corals (Two-way ANOVA, $p < 0.0001$, Table 5). Benthic algae, sponges and cyanobacteria prevailed as the main sessile-benthic categories in terms of reef substrate cover at ALS during both surveys. Differences of reef substrate cover by soft corals were related to an 84.6% (site mean) decline, from 3.28% in 2008-10 to 0.51% in 2018-20. Such decline may have been influenced by the surge, scouring, and/or abrasion effects induced by extremely high wave action associated with the pass of Hurricane Maria in September 2017, and/or winter storm Riley in March 2018. Such extreme events may have also played a role in the 56.6% measured increment of abiotic (mostly sand) cover during 2018-20 relative to 2008-10.

Reef substrate cover by total benthic algae exhibited minimal differences between the 2008-10 baseline and the 2018-20 monitoring survey (-0.001%), but major differences in the relative contributions of taxonomic components were noted. Substrate cover by turf algae (mixed assemblage) declined 91.8%, from a mean of 36.4% in 2008-10 to a mean of 3.00% in 2018-20 (ANOVA; $p < 0.0001$). Corresponding increments of cover by encrusting fan alga (*Lobophora sp*), fleshy algae (mostly *Dictyota sp*), and calcareous algae (*Halimeda spp*) were measured (Figure 12). *Lobophora sp*. increased 158.0%, from a mean of 13.80% in 2008-10 to a mean of 35.60% in 2018-20 (ANOVA; $p < 0.0001$). Fleshy algae increased 24.1%, from a mean of 10.80% in 2008-10 to a mean of 13.40% in 2018-20 (ANOVA; $p = 0.241$). *Halimeda spp*. increased 200.0%, from a mean of 0.80 % in 2008-10 to a mean of 2.40% in 2018-20 (ANOVA; $p = 0.0004$). Substrate cover by cyanobacteria also increased by 31.4%, from a mean of 8.64% in 2008-10 to a mean of 11.36% in 2018-20, but the difference was statistically insignificant (ANOVA; $p = 0.910$; Table 5).

The marked variations in the taxonomic components of benthic algae between surveys may be related to several factors including a potentially strong nutrient spike associated with the pass of Hurricane Maria in 2017. Hurricanes are divergent systems and an episode of nutrient upwelling into the surface mixed layer could have been triggered with potential implications to the taxonomic structure of benthic algae within the mesophotic habitats of ALS. Perhaps, such changes of the benthic algae community structure are transitory and in absence of another nutrient enrichment processes the algae community may revert back to the 2008-10 condition characterized by the dominance by turf algae. Similar changes associated with the reduction of reef substrate cover by turf algae and corresponding increments of brown fleshy algae, and/or crustose calcareous algae (Peissonnellidae) have been noted in shallow (neritic) reefs from the PRCRMP monitoring surveys of 2018 and 2019 (Garcia-Sais et al., 2018, 2019) and believed to be related to the effects of hurricanes and/or exceptionally strong winter storms (e. g. Riley - 2018). The 56.6% increment of abiotic (mostly sand) cover measured in 2018-20, relative to 2010 from mesophotic habitats in the 30 – 50m range at ALS may be have been forced by Hurricane Maria in 2017, and/or winter storm Riley in 2018. If so, there is also the possibility that sand cover may have caused significant mortality of the short growing turf algae allowing larger (taller) algae, such as *Lobophora sp*. and/or *Dictyota sp*. to colonize hard ground (pavement) reef substrates previously colonized by turf algae. Changes in the taxonomic composition of benthic algae may have also had potential effects upon the fish and shellfish community structure and productivity due to herbivore algal food preferences and palatability. Of particular interest is the issue regarding increments of reef substrate cover by *Lobophora sp*., since its palatability as food for reef fishes and crabs has been found to vary significantly depending on its growth form, being the "ruffled" type more palatable than the "decumbent" type, which is more common on outer reefs >15m depths (Coen and Tanner, 1989).

Table 5. Temporal variations of reef substrate cover by sessile-benthic categories between the 2008-10 baseline and the 2018-20 monitoring surveys at Abrir la Sierra.

BENTHIC CATEGORIES	Site Mean 2010	Site Mean 2018-20	% Change	ANOVA p-value
Abiotic	6.45	10.11	56.6	0.162
Stony Coral	2.06	1.60	-0.05	0.886
Soft Corals	3.28	0.50	-84.6	< 0.0001*
Sponges	14.04	12.89	-8.2	0.493
Benthic Algae	62.85	62.80	-0.001	0.536
Cyanobacteria	8.64	11.36	31.4	0.910
Turf Algae	36.40	3.00	-91.8	< 0.0001*
Lobophora sp	13.80	35.60	158.0	< 0.0001*
Fleshy Algae	10.80	13.40	24.1	0.153

* statistically significant; ANOVA p< 0.05. Ln (X+1) transformed values

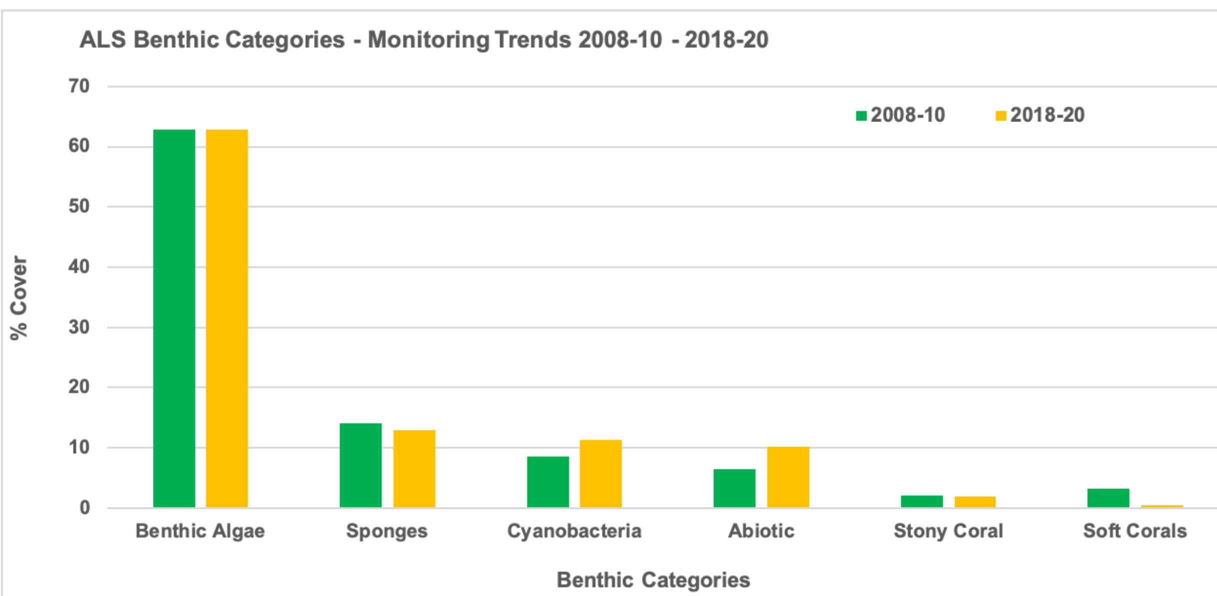

Figure 11. Variations of (study) mean substrate cover by major sessile-benthic categories measured from a similar set of stations within the 30 – 50m mesophotic depth range at Abrir la Sierra during the 2008-10 baseline and the 2018-20 monitoring surveys

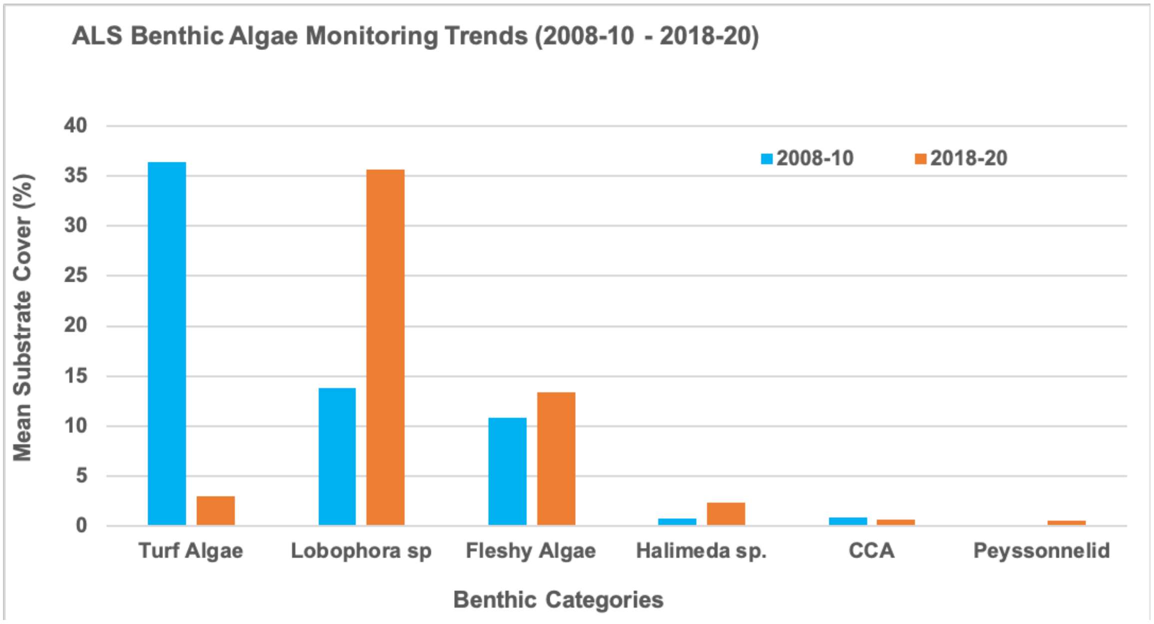

Figure 12. Variations of (study) mean substrate cover by the main taxonomic components of the benthic algae measured from a similar set stations within the 30 – 50m mesophotic depth range at Abrir la Sierra during the 2008-10 baseline and the 2018-20 monitoring surveys

Fish Communities ALS

Small demersal fish species, 2018-20 survey

Depth/habitat related patterns of fish community structure

A total of 60 small demersal fish species were identified from 3m x 10m belt-transects within the 25 – 50m depth range at ALS in the 2018-20 survey (Table 6). Mean density ranged between 191.8 Ind/30m^2 at CPSlope50 and 43.8 Ind/30m^2 at Rhod40. Mean fish species richness varied between 13.4 Spp/30m^2 at CPRT25 and 9.6 Spp/30m^2 at CPSlope50. Statistically significant differences of fish density between habitats/depth were found (ANOVA; p= 0.004) associated with higher densities at CPSlope50 relative to other depths. Density differences from habitats/depths in the 25 – 40m range were within 95% confidence limits.

The higher densities at CPSlope50 were driven by peak densities of sunshine chromis (*Chromis insolata*), school bass (*Schultzea beta*), masked goby (*Coryphopterus personatus*), and creole wrasse (*Clepticus parrae*). Large schooling aggregations of these small fishes were observed associated with sponge-gorgonian bioherms at the outer insular slope in 2018-20. Both *C. insolata* and *S. beta* displayed distinct patterns of increasing density with depth (Figure 13). Conversely, patterns of decreasing density with depth were noted for bicolor damselfish (*Stegastes partitus*), stripped, princess, bucktooth, and redband parrotfishes (*Scarus iserti, S. taeniopterus, Sparisoma radians, S. aurofrenatum*), doctorfish (*Acanthurus chirurgus*), and squirrelfish (*Holocentrus rufus*). Yellowhead wrasse (*Halichoeres garnoti*) and longspine squirrelfish (*Holocentrus rufus*) were present across the entire depth range (25 – 50m) without any distinct depth or habitat-related density pattern. Depth/habitat related differences of fish species richness were not statistically significant (ANOVA; p= 0.279).

Variations of the relative abundance by small demersal fish species surveyed from 3m x 10m belt-transects within the 25 – 50m depth profile at ALS during the 2018-20 survey are displayed in a non-metric multi-dimensional scaling plot (nMDS) based on Bray-Curtis similarities in Figure 14. Benthic habitats were used as discriminatory factor for testing fish community structure similarities since different habitats were sampled across the 40m depth, and CPRT was sampled across the 25 – 30m range. The highest similarity of fish community structure corresponded to CPRT25 (80.8%), largely contributed by an assemblage of neritic reef fishes, including doctorfish (*Acanthurus chirurgus*), coney (*Cephalopholis fulva*), saddled blenny (*Coryphopterus glaucofraenum*), and the princess, bucktooth, and redband parrotfishes (*Scarus taeniopterus, Sparisoma radians, S. aurofrenatum*).

Similarity was also relatively high at Rhod40 (66.0%), contributed by greenbloth parrotfish (*Sparisoma atomarium*), cherubfish (*Centropyge argi*), and bicolor damselfish (*Stegastes partitus*) (Table 7). Blue chromis (*Chromis cyanea*) and red hind (*Epinephelus guttatus*) were the main contributors to similarity at CPRT30, whereas bluehead wrasse (*Thalassoma bifasciatum*) and sunshine chromis (*C. insolata*) were the main species contributing similarity at CPSlope40 and CPSlope50, respectively. CPRT30, CPSlope40, and CPSlope50 exhibited relatively lower similarities (<45%), influenced by the aggregated distributions of numerically dominant species, such as *Thalassoma bifasciatum*, *Clepticus parrae, Chromis cyanea, Schultzea beta, C. insolata*).

Table 6. Taxonomic composition and density of small demersal fishes surveyed from 10 x 3m belt-transects within the 25 – 50 depth range at Abrir La Sierra. 2018-20 survey

Fish Species	CPRT25	CPRT30	Rhod40	CPSlope40	CPSlope50
Chromis insolata		3.80		13.75	70.25
Chromis cyanea	5.00	41.40		9.25	16.13
Stegastes partitus	23.00	10.20	18.20	6.13	3.75
Schultzea beta				3.75	41.50
Halichoeres garnoti	6.40	10.20	4.60	6.13	6.75
Coryphopterus personatus		2.00		1.38	30.63
Clepticus parrae		15.00			11.63
Thalassoma bifasciatum		8.80	2.40	4.88	
Centropyge argi		0.80	7.60	1.50	1.25
Scarus iseri	3.20	1.80		0.38	0.13
Sparisoma atomarium			3.60	0.88	
Acanthurus chirurgus	2.40	1.60			
Holocentrus rufus	1.80	0.80	0.20	0.38	0.75
Scarus taeniopterus	3.00	0.80			0.13
Serranus tigrinus	1.20	1.00	0.80	0.25	
Sparisoma radians	2.80			0.25	
Sparisoma aurofrenatum	1.60	0.20		0.25	0.88
Serranus annularis					2.63
Cephalopholis fulva	1.60			0.38	0.38
Coryphopterus glaucofraenum	1.20	0.60	0.20		
Epinephelus guttatus		1.20		0.25	0.50
Serranus tabacarius			1.20	0.38	
Coryphopterus sp.	1.00		0.20	0.25	
Chromis multilineata		1.20		0.25	
Holocentrus adscensionis			0.40	1.00	
Elacatinus evelynae	1.40				
Acanthurus tractus			0.60	0.63	0.13
Serranus baldwini		0.20	1.00		0.13
Gramma loreto					1.25
Balistes vetula		0.40	0.60	0.25	
Holacanthus tricolor	0.80	0.20			0.13
Xanthichthys ringens				0.88	0.13
Chaetodon capistratus		0.80			
Opistognathus aurifrons			0.40		0.38
Holacanthus ciliaris		0.60		0.13	
Pseudupeneus maculatus		0.60		0.13	
Cephalopholis cruentatus		0.20			0.50
Chaetodon striatus	0.40			0.25	
Myripristis jacobus		0.60			
Neoniphon marianus		0.60			
Halichoeres maculipinna		0.20	0.20	0.13	
Bodianus rufus				0.13	0.38
Chaetodon sedentarius		0.20			0.25
Hypoplectrus puella		0.20			0.25
Pomacanthus paru		0.20		0.25	
Haemulon flavolineatum		0.40			
Malacanthus plumieri		0.20	0.20		
Carangoides ruber			0.40		
Serranus tortugarum			0.40		

Table 6. Taxonomic composition and density of small demersal fishes surveyed from 10 x 3m belt-transects within the 25 – 50 depth range at Abrir La Sierra. 2018-20 survey

Fish Species	CPRT25	CPRT30	Rhod40	CPSlope40	CPSlope50
Canthigaster rostrata			0.20		0.13
Hypoplectrus unicolor		0.20			0.13
Prognathodes aculeatus			0.20		0.13
Paranthias furcifer					0.25
Chaetodon aculeatus		0.20			
Sargocentron coruscum		0.20			
Cryptostomus roseus			0.20		
Apsilus dentatus					0.13
Lutjanus jocu					0.13
Scarus guacamaia					0.13
Cephalopholis cruentatus					
Cantherhines pullus					
Mean Density (Ind/30m^2)	**56.80**	**107.60**	**43.80**	**54.38**	**191.75**
Mean Species Richness (Spp/30m^2)	**13.4**	**13.0**	**10.4**	**10.0**	**9.6**

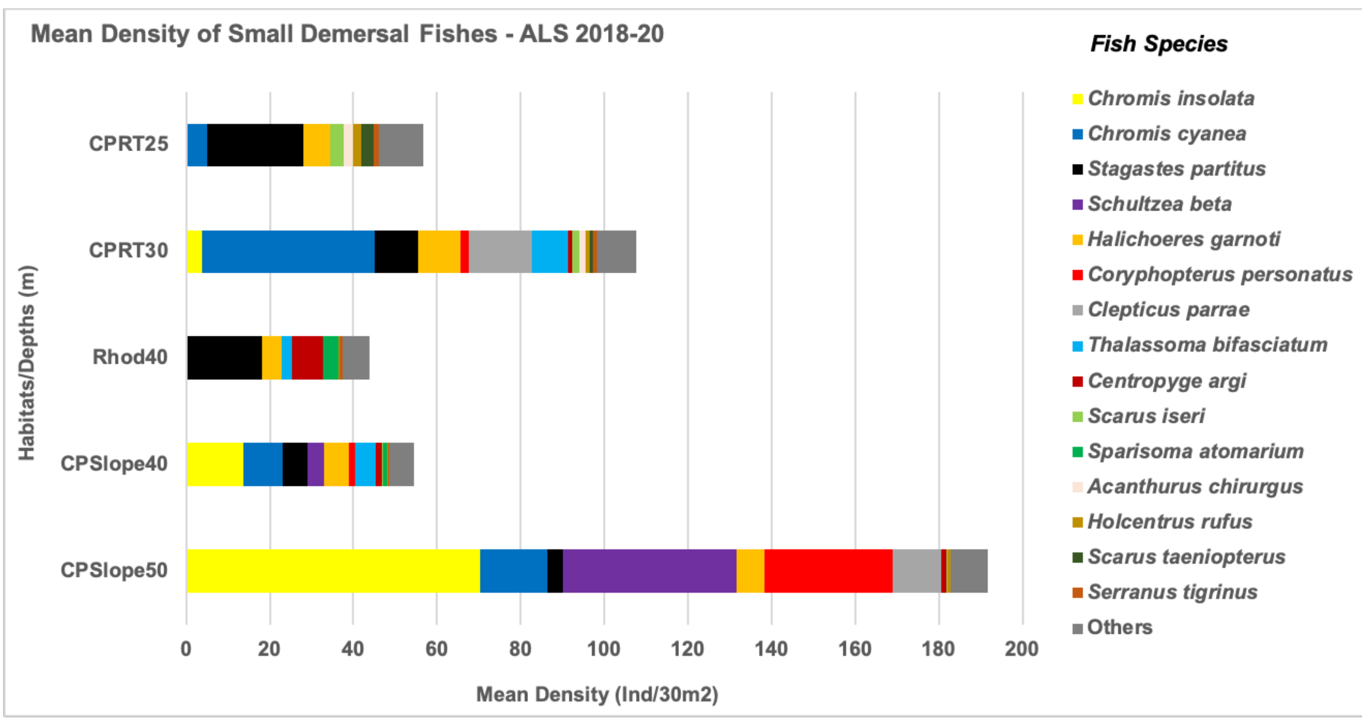

Figure 13. Variations of mean density by small demersal fishes surveyed within 10 x 3m belt-transects within the 25 – 50m depth range at Abrir La Sierra, 2018-20 survey

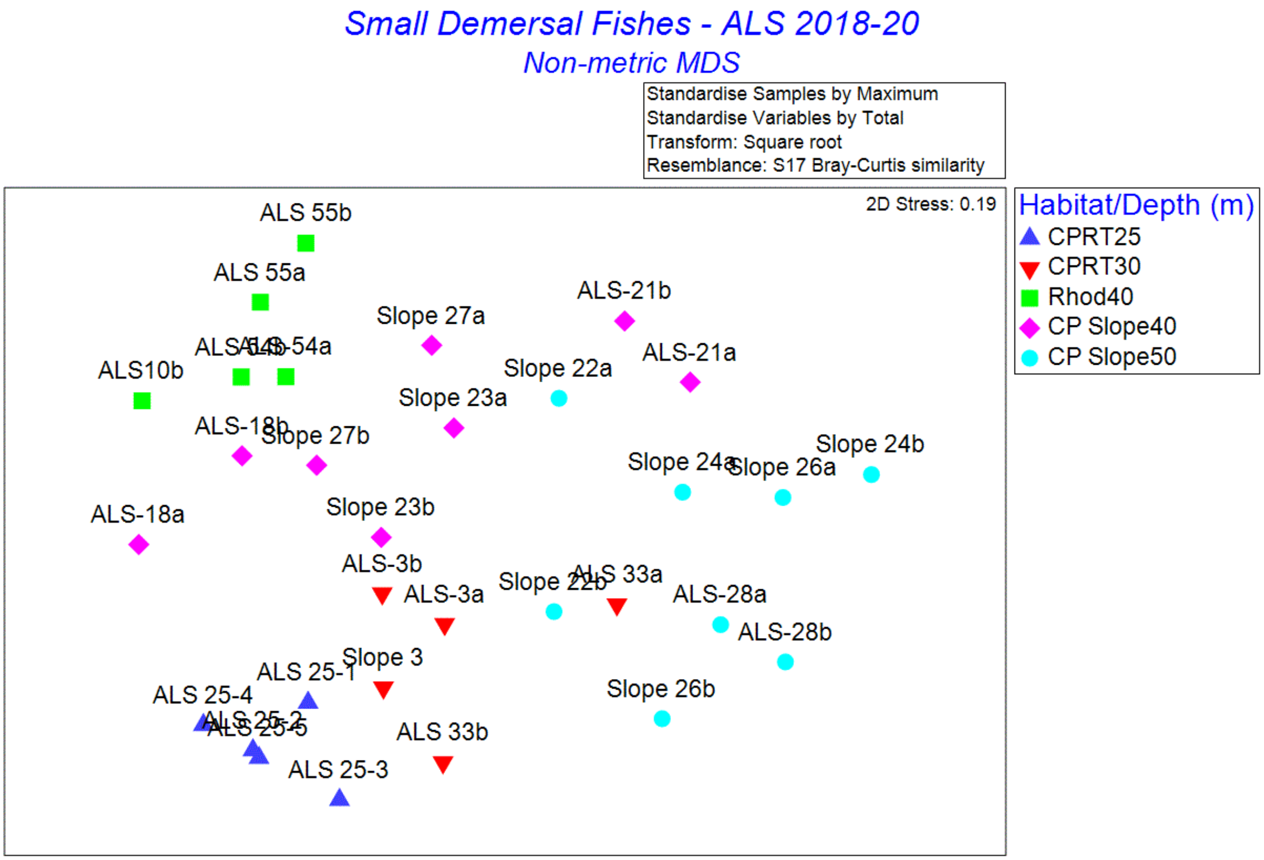

Figure 14. Non-metric multidimensional scaling (nMDS) plot of Bray-Curtis similarities of small demersal fish relative densities within 10m x 3m belt-transects surveyed from mesophotic benthic habitats (25 – 50m) at Abrir La Sierra, 2018-20 survey.

Dissimilarity of small demersal fish community structure between benthic habitats was moderately high (> 64%), indicative of distinctive species assemblages in terms of their relative densities. The highest dissimilarity was observed between habitats at opposite ends of the depth gradient CPRT25 and CPSlope50 (81.2%), influenced by the occurrence of an assemblage of neritic species from CPRT25, such as doctorfish (*Acanthurus chrysurus*), saddled blenny (*Coryphopterus glaucofraenum*), and the princess, redband and bucktooth parrotfishes (*Scarus taeniopterus, Sparisoma aurofrenatum*, *S. radians*) that were not observed, or observed in low densities at CPSlope50 (Table 8). Dissimilarity between CPSlope50 and other habitats (including CPRT25) was mostly associated with the higher relative densities of sunshine and blue chromis (*Chromis insolata, C. cyanea*), school bass (*Schultzea beta*), and masked goby (*Coryphopterus personatus*). These are schooling species, mostly present on CPSlope50 as juveniles associated with branching sponges (*Agelas spp*) and sponge/coral bioherms that were common at the outer insular shelf slope within the 40 – 50m depth range.

Table 7. Similarity matrix (SIMPER) of small demersal fish community structure within habitats/depths surveyed from ALS within the 25 – 50m depth range, with species contributions to similarity at each habitat/depth, 2018-20 survey.

	CPRT25	CPRT30	Rhod40	CP Slope40	CP Slope50
Average Similarity (%)	80.8	43.6	66.0	31.6	41.2
Species Contributions					
Acanthurus chirurgus	12.1				
Coryphopterus glaucofraenum	11.7				
Scarus taeniopterus	11.0				
Cephalopholis fulva	10.1				
Sparisoma radians	9.6				
Sparisoma aurofrenatum	9.2				
Holocentrus rufus	9.2				
Chromis cyanea		27.5		11.3	10.0
Epinephelus gutattus		16.3			
Halichores garnoti		12.3		25	10.3
Thalassoma bifasciatum		10.6		20.5	
Stegastes partitus		7.3	22.6	19.6	
Sparisoma atomarium			30.8		
Centropyge argi			23.1		
Chromis insolata					33.8
Coryphopterus personatus					13.6
Gramma loreto					9.7

Similar coral/sponge microhabitats were observed at the CPRT distributed across the 25 – 30m depth range, but the prevailing species there were the blue chromis (*C. cyanea*), creole wrasse (*Clepticus parrae*), bicolor damselfish (*Stegastes partitus*), yellowhead and bluehead wrasses (*Halichoeres garnoti, Thalassoma bifasciatum*). Bicolor damselfish (*S. partitus*) exhibited a pattern of declining density with depth, and bluehead wrasse (*T. bifasciatum*) was not observed at 50m, suggesting that depth was also a factor influencing small demersal fish community structure within the 25 - 50m depth range surveyed at ALS. Dissimilarity between Rhod40 and other benthic habitats was mostly driven by the relatively higher densities of cherubfish (*Centropyge argi*), and greenbloth parrotfish (*S. atomarium*). Higher relative densities of red hind (*Epinephelus guttatus*), blue chromis (*C. cyanea*), and creole fish (*Clepticus parrae*) separated CPRT30 from other habitats/depths.

Table 8. Dissimilarity matrix (SIMPER) of small demersal fish relative densities at benthic habitats and depths surveyed from Abrir La Sierra, 2018-20 survey.

	CPRT25 vs CPRT30	CPRT25 vs CPSlope40	CPRT25 vs CPSlope50	CPRT25 vs Rhod40	CPRT30 vs CPSlope40	CPRT30 vs CPSlope50	CPRT30 vs Rhod40	CPSlope40 vs Rhod40	CPSlope40 vs CPSlope50
Average Dissimilarity (%)	64.9	75.8	81.2	75.8	67.8	72.6	77.9	64.3	74.7
Species Contributions									
Sparisoma radians	9.8	8.3	8.0	9.0					
Cephalopholis fulva	9.7	7.2		8.9					
Scarus taeniopterus	9.3								
Coryphopterus glaucofraenum	8.8	9.2	8.6	8.3					
Sparisoma aurofrenatum	8.3	7.5	5.4	8.4		4.1			5.0
Epinephelus gutattus	7.0				8.6	8.1	8.8		5.2
Acanthurus chirurgus	6.7	9.3	8.6	9.7	6.8	6.3	6.3		
Scarus iseri	6.3	6.7	6.1		6.6	5.5	5.5		
Holocentrus rufus	5.5	6.7	5.3		5.6			5.1	4.3
Scarus taeniopterus		9.3	8.4	9.7					
Thalassoma bifasciatum		5.8			7.0	5.6		9.2	8.4
Chromis insolata			6.8		4.9	8.6		5.2	7.2
Cephalopholis fulva			6.3						
Coryphopterus personatus			5.3			7.8			7.8
Clepticus parrae					6.9	8.0	6.4		4.6
Serranus tigrinus					6.0		5.4	8.2	
Holocentrus adscensionis					6.0			9.2	5.6
Chromis cyanea					5.3	4.6	9.1	6.4	4.9
Halichores garnoti					4.5			4.5	4.6
Sparisoma atomarium				9.6	4.2		13.0	12.3	
Gramma loreto						7.3			7.4
Schultzea beta						5.6			7.1
Centropyge argi				9.0			11.3	12.3	
Stegastes partitus							5.1		

Temporal Variations of Small Demersal Fish Density and Community Structure, 2008-10/ 2018-20

Density variations of small demersal fishes between the 2008-10 baseline survey and the 2018-20 monitoring survey at ALS were not statistically significant within the 30 – 50m depth range surveyed (Two-way ANOVA, p = 0.491) (Table 9). The largest variation of mean density was related to a 41.4% decline at CPRT30 during the 2018-20 survey, strongly influenced by presence of a large school of mackerel scad (*Decapterus macarellus*) during the 2008-10 survey. This is transitory schooling pelagic species and its presence within the CPRT30 was fortuitous and without any direct implication of change in the small demersal fish community structure. Masked goby (*Coryphopterus personatus*), the numerically dominant species in 2018-10, and peppermint goby (*C. lipernes*) (ranked 6th) evidenced sharp density declines during 2018-20, relative to the 2008-10 baseline survey. The population crash of *C. personatus* after 2017 was previously reported for many neritic reefs in Puerto Rico (Garcia-Sais et al., 2018, 2019) and associated to surge and abrasion effects induced by Hurricanes Irma and Maria in 2017, and/or winter storm Riley in 2018. Peppermint goby is another small demersal species that lives directly over live stony corals and may have been also vulnerable to the extreme oceanographic conditions induced by hurricanes and/or winter storm Riley previous to the 2018-20 survey. The density collapse of *C. personatus* during the 2018-20 relative to the baseline survey (ANOVA; p= 0.023) was also detected at the CPSlope50.

Mean densities by other numerically dominant species, such as sunshine chromis (*Chromis insolata, C. cyanea*), bicolor damselfish (*Stegastes partitus*), yellowhead and bluehead wrasses (*Halichoeres garnoti, Thalassoma bifasciatum*), and cherubfish (*Centropyge argi*) remained stable between surveys (Table 10). Statistically significant density increments at CPRT30 and CPSlope50 were noted for *C. cyanea* (ANOVA, p= 0.001). This is a numerically dominant zooplanktivore species typically observed in schooling aggregations. The increase of its population may respond to higher zooplankton food availability, lower predation pressure, recruitment success variability, migration to deeper, less physically impacted zones, and other density dependent and density independent factors that will require analyses over a broader spatial framework to discern any real pattern. Differences of fish species richness between surveys were statistically insignificant (Two-way ANOVA; p = 0.670; Table 9) indicative of no major changes in the community structure of small demersal fishes within the habitats/depths surveyed.

Table 9. Density and species richness variations of small demersal fishes between the baseline 2008-10 and the 2018-20 monitoring surveys at ALS.

Depth (m)	Benthic Habitat	Mean Density 2008-10	Mean Density 2018-20	% Change	ANOVA p-value Density	Mean Spp. Richness 2008-10	Mean Spp. Richness 2018-20	% Change	ANOVA p-value Spp. Richness
30	CPRT	149.2	107.6	-27.9	0.525	17.70	13.0	-26.6	0.176
36	Rhodo	44.67	43.8	-1.9	0.898	11.50	10.4	-9.6	0.365
40	CPSlope	103.7	54.4	-47.5	0.571	10.80	10	-7.4	0.978
50	CPSlope	201.1	191.8	-4.6	0.957	10.10	9.6	-5.0	0.423

Statistical significance at $p < 0.05$

Table 10. Mean density variations of numerically dominant small demersal fishes between the baseline 2008-10 and the 2018-20 monitoring surveys at ALS.

Numerically Dominant	CPRT30		Rhod40		CPSlope40		CPSlope50	
Small Demersal Fishes	2008-10	2018-20	2008-10	2018-20	2008-10	2018-20	2008-10	2018-20
Centropyge argi	0.0	0.8	12.3	9.2	0.7	1.8	1.2	1.2
Chromis cyanea	3.2	32.2	0.0	0.5	5.8	12.3	1.9	16.1
Chromis insolata	0.0	3.2	0.0	0.0	23.3	18.3	92.1	70.2
Coryphopterus lipernes	20.7	0.0	0.0	0.0	0.0	0.0	0.0	0.0
Coryphopterus personatus	36.7	0.0	0.0	0.0	49.0	1.8	87.4	30.6
Decapterus macarellus	33.3	0.0	0.0	0.0	0.0	0.0	0.0	0.0
Halichoeres garnoti	6.3	6.2	1.2	4.8	7.0	6.3	6.0	6.8
Stegastes partitus	13.5	10.7	13.7	16.5	6.2	6.0	3.4	3.8
Thalassoma bifasciatum	6.0	8.7	1.5	2.5	1.5	4.8	0.0	0.0

Similarities of small demersal fish community structure between the 2008-10 baseline and the 2018-20 monitoring surveys based on the relative densities of the top 20 numerically dominant species within 3m x 10m belt-transects are shown in a multidimensional scaling (nMDS) plot of Bray-Curtis similarities in Figure 15. Higher similarity of community structure between surveys was noted from Rhod40 (88.3%) and CPRT30 (66.3%).

Greenbloth parrotfish (*Sparisoma atomarium*), cherubfish (*Centropyge argi*), bicolor damselfish (*Stegastes partitus*) and tobacco, harlequin and lantern bass (*Serranus tabacarius, S. tigrinus, S. baldwini*) were the main contributors to similarity at Rhod40 with consistently high relative abundance in both surveys. Likewise, numerically dominant species at CPRT30, such as red hind (*Epinephelus guttatus*), bluehead wrasse (*Thalassoma bifasciatum*), and the princess and redband parrotfishes (*Scarus taeniopterus, Sparisoma aurofrenatum*) contributed to the community structure similarity between surveys.

Major differences in the community structure of the small demersal fishes between surveys were evidenced at CPSlope40 and CPSlope50 (Figure 15). Differences from both habitats/depths were influenced by the sharp density decline of masked goby (*Coryphopterus personatus*) during the 2018-20 survey, relative to the 2008-10 baseline survey, and to marked density increments during the 2018-20 survey of numerically dominant species with highly aggregated (patchy) distributions, such as the school bass (*Schultzea beta*), creole wrasse (*Clepticus parrae*) and blue chromis (*Chromis cyanea*).

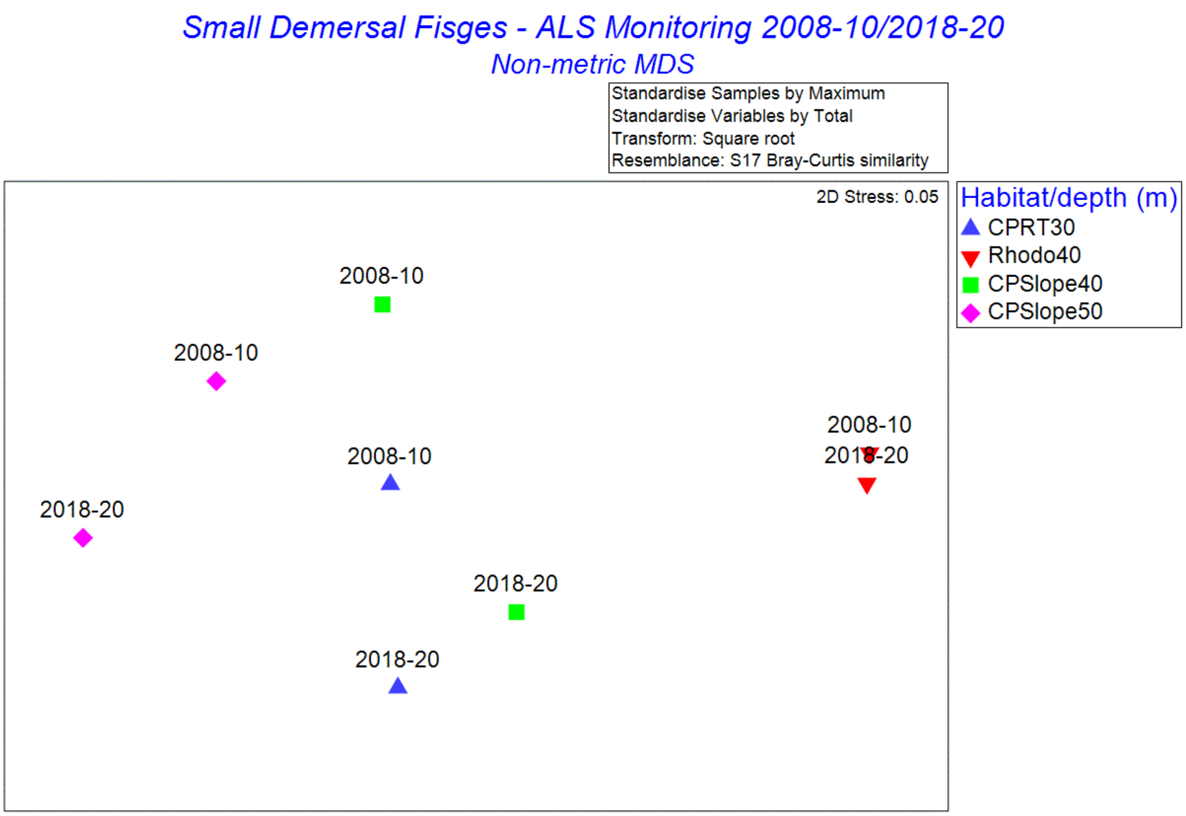

Figure 15. Non-metric multidimensional scaling (nMDS) plot of Bray-Curtis similarities of the relative densities by small demersal fishes surveyed from 10m x 3m belt-transects within mesophotic benthic habitats in the 30 – 50m depth range at Abrir La Sierra during the baseline 2008-10 and the 2018-20 monitoring survey

Large Demersal Fishes and Shellfishes

Depth/habitat related variations of fish density and community structure, 2018-20

Mean densities of large demersal fishes and shellfishes (queen conch and spiny lobster) surveyed by drift belt-transects within the 25 – 50m depth range at ALS during 2018-20 are presented in Table 11. Mean total densities varied between 56.2 Ind/10^3m^2 at Rhod40 and 13.8 Ind/10^3m^2 at CPSlope40-50. Total fish density differences between habitats/depths were not statistically significant (ANOVA; p = 0.149) due to the high variability within replicate samplings but marked depth related patterns were evidenced for several fish and shellfish species (Figure 16). Queen conch (*Lobatus gigas*) was observed from all habitats/depths surveyed but presented a peak mean density at Rhodo40 (28.8 Ind/10^3m^2) that was 27X higher than at any other depth. Although depth related differences of the total fish/shellfish densities were statistically insignificant, the contribution of *L. gigas* to the total fish/shellfish density at Rhodo40 accounted for most of the difference of mean densities between depths.

Density differences of *L. gigas* between depths were not statistically significant (ANOVA; p= 0.059) due to its highly aggregated (patchy) distribution (var/mean= 85.0) that introduced high sampling variability error. Peak densities of *L. gigas* were surveyed from the rhodolith habitat in the deep basin of ALS, where relatively high concentrations were detected in three out of the five drift transects surveyed in the 43 – 50m depth range. Overall, *L. gigas* were observed in eight (8) out of the 20-drift belt-transects surveyed at ALS in 2018-20.

Yellowtail and mutton snappers (*Ocyurus chrysurus, Lutjanus analis*) were observed throughout the 25 – 50m depth range but showed peak densities at CPRT25 and lowest densities at either CPSlope40-50 (Figure X). Differences were not statistically significant because of the high sampling variability produced by the high number of transects with zero individuals and few transects with multiple individuals. For example, *O. chrysurus* and *L. analis* individuals were observed in only eight (8) and five (5) out of the 20 transects surveyed in 2018-20. These are schooling species with patchy distributions but prominent in terms of their mean densities in the composite samplings. One large school of blackfin snapper (*Lutjanus buccanella*) was observed from CPSlope40-50, which appears to be the upper range of its distribution at ALS. More uniform distributions across the depth gradient were observed for queen triggerfish (*Balistes vetula*), red hind (*Epinephelus guttatus*) and coney (*Cephalopholis fulva*) (Figure X).

Contrary to schooling snappers, triggerfish and grouper species appeared to be more territorial and/or solitary within the mesophotic habitats of ALS. All three species were observed in the 20 transects surveyed without statistically significant differences between depths (ANOVA; $p > 0.05$). A total of 12 spiny lobsters (*Panulirus argus*) were observed with a study (all depths) mean density of 0.354 Ind/10^3m^2.

Table 11. Mean densities of large demersal fishes/shellfishes surveyed from drift belt-transects across 25 – 50m depths in Abrir La Sierra, 2018-20 survey.

Habitat/Depths (m)	CPRT25		CPRT30		Rhod40		CPSlope40-50	
Fish Species	**Total Ind**	**Ind/10^{3}m^2**	**Total Ind**	**Ind/10^{3}m^2**	**Total Ind**	**Ind/10^{3}m^2**	**Total Ind**	**Ind/10^{3}m^2**
Acanthostracion polygonia	1	0.170	4	0.350	0	0.000	2	0.217
Balistes vetula	23	2.588	16	1.199	16	5.527	10	0.961
Caranx hippos	4	0.377	0	0.000	0	0.000	0	0.000
Caranx lugubris	0	0.000	3	0.225	0	0.000	0	0.000
Cephalopholis cruentatus	0	0.000	0	0.000	2	0.968	1	0.108
Cephalopholis fulva	70	7.945	58	4.299	18	5.730	47	4.585
Dasyatis americana	0	0.000	0	0.000	1	0.168	0	0.000
Epinephelus guttatus	23	2.373	79	5.632	21	8.819	55	5.260
Elagatis bipinulatus	0	0.000	0	0.000	0	0.000	3	0.259
Epinephelus striatus	0	0.000	1	0.082	0	0.000	2	0.173
Ginglymostoma cirratum	1	0.094	0	0.000	1	0.782	1	0.072
Lachnolaimus maximus	3	0.403	3	0.212	1	0.782	2	0.158
Lactophrys trigonus	5	0.453	0	0.000	0	0.000	0	0.000
Lactophrys triqueter	2	0.134	0	0.000	0	0.000	1	0.125
Lutjanus analis	39	3.708	1	0.109	3	1.135	1	0.125
Lutjanus buccanella	0	0.000	0	0.000	8	1.488	0	0.000
Lutjanus cyanopterus	3	0.353	6	0.493	0	0.000	3	0.269
Lutjanus jocu	0	0.000	1	0.075	0	0.000	1	0.072
Mycteroperca venenosa	0	0.000	2	0.150	0	0.000	4	0.302
Ocyurus chrysurus	49	5.921	18	1.324	2	0.354	1	0.072
Pterois sp.	9	0.866	3	0.173	1	0.782	1	0.072
Scarus guacamaia	0	0.000	0	0.000	0	0.000	2	0.158
Scomberomorus cavalla	0	0.000	0	0.000	0	0.000	1	0.072
Scomberomorus regalis	2	0.259	0	0.000	0	0.000	5	0.360
Sphyraena barracuda	3	0.366	5	0.348	0	0.000	2	0.158
Invertebrates								
Panulirus argus	0	0.000	6	0.366	4	0.870	2	0.180
Lobatus gigas	8	1.065	5	0.543	55	28.825	1	0.086
MEANS	**245**	**27.07**	**211**	**15.58**	**133**	**56.23**	**148**	**13.84**

Temporal variations of large demersal fishes/shellfishes (2012 and 2018-20 surveys)

Large demersal fishes and shellfishes were surveyed during 2011-12 and 2018-20 from a similar set of sampling stations across the 30 – 50m depth range at ALS. Mean density differences for the total large demersal fish/shellfish assemblage were not statistically significant between surveys for any habitat/depth (Two-way ANOVA; $p = 0.394$. Variations of mean density by the numerically dominant fish/shellfish species from the main habitats/depths surveyed during 2011-12 and 2018-20 at ALS are presented in Figure 17. The 66.3% density decline from CPRT30 was mostly influenced by presence of one schoolmaster snapper (*Lutjanus apodus*) schooling aggregation of 150 individuals. The occurrence of such schooling aggregations within drift belt-transects is considered fortuitous, without any ecologically significant implications related to fish density differences between surveys.

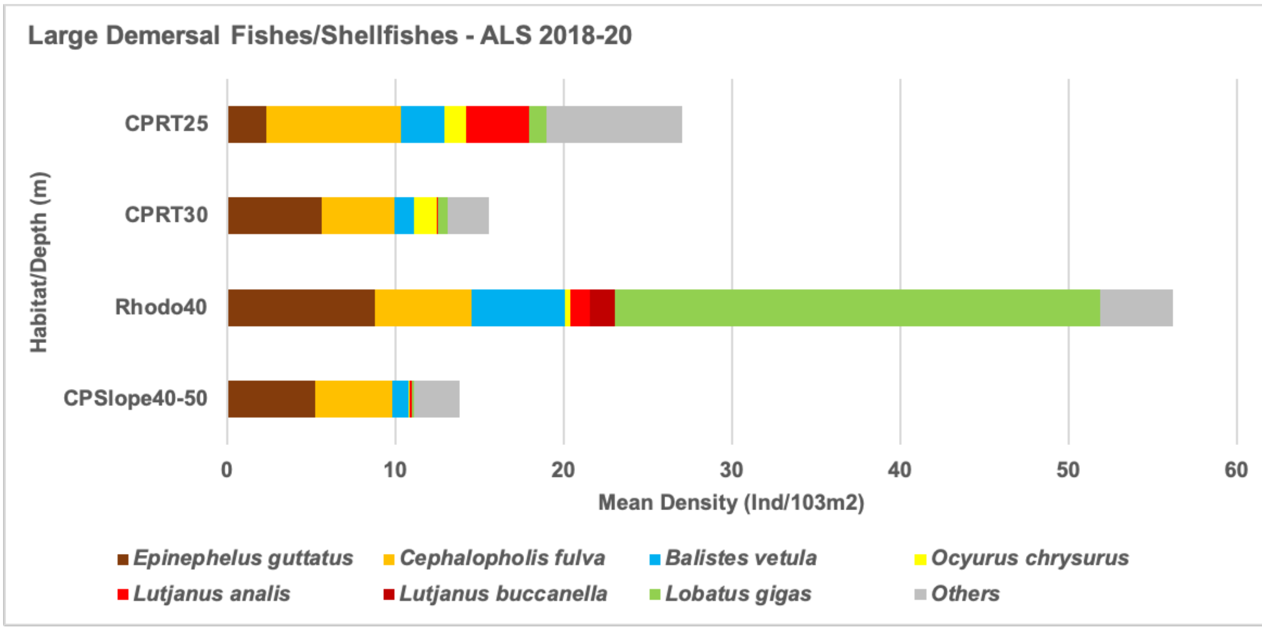

Figure 16. Mean density of large demersal fishes and shellfishes surveyed by drift belt-transects from the 25 – 50m depth range at Abrir La Sierra, 2018-20 survey

A 94.3% decline of mean lionfish (*Pterois sp*) density, from a mean of 3.7 Ind/10^3m^2 in 2011-12 to a mean of 0.2 Ind/10^3m^2 contributed substantially to the density differences between surveys at CPRT30. Conversely, density increments of queen triggerfish (*Balistes vetula*), yellowtail snapper (*Ocyurus chrysurus*), and red hind (*Epinephelus guttatus*) were measured during 2018-20, relative to the 2011-12 baseline survey but differences were statistically insignificant (ANOVA; $p > 0.05$) (Figure 18).

A 28.3% decline of mean total density at CPSlope40-50 during 2018-20 (Figure 17) was influenced by a 98.0% decline of lionfish (*Pterois sp*) density from a mean of 4.6 Ind/10^3m^2 in 2010-11 to a mean of 0.09 Ind/10^3m^2 in 2018-20. Lionfish densities were not influenced by patchily distributed schooling aggregations. On the contrary, *Pterois sp*. appeared to display fairly uniform territorial distributions in 2008-10 (var/mean= 2.3) when individuals were observed from all (10) CPRT30 and CPSlope40-50 stations, compared to only two out of 10 in 2018-20. This may be indicative of a real declining trend of the *Pterois sp*. population within the mesophotic habitats of ALS during this period. Lionfish is an invasive species that may have been facing recruitment failures that are presently affecting their populations. Conversely, density increments of queen triggerfish (*Balistes vetula)* and red hind (*Epinephelus guttatus)* were observed from Rhod40, but differences were statistically insignificant (ANOVA; $p > 0.05$).

The most pronounced differences of large demersal fish/shellfish densities between the 2011-12 and 2018-20 surveys at ALS were noted from Rhod40 (Figure 17). Mean density increased 206.2%, from 14.7 Ind/10^3m^2 in 2011-12 to 45.1 Ind/10^3m^2 in 2018-20 largely contributed by the sharp density increments of queen conch (*Lobatus gigas*), red hind (*Epinephelus guttatus*), and queen triggerfish (*Balistes vetula*). The mean densities of all three species peaked at Rhod40 in 2018-20. Queen conch presented a 213.9% density increment, from 9.2 Ind/10^3m^2 in 2011-12 to 28.8 Ind/10^3m^2 in 2018-20. Differences were not statistically significant due to the high variability associated with patchy distributions (ANOVA; p = 0.639). The marked density increment of *L. gigas* may be related to migration of individuals from other sections of the shelf and slope to the more protected habitat of ALS outer deep basin induced perhaps by extreme conditions associated with the impact of Hurricane Maria in 2017 and/or storm Riley in 2018.

Queen triggerfish (*Balistes vetula*) increased 231.6%, from 1.7 Ind/10^3m^2 in 2011-12 to 5.5 Ind/10^3m^2 at Rhod40-50m in 2018-20. Density increments of *B. vetula* were measured from all benthic habitats at ALS in 2018-20 relative to 2011-12 (Figure 19). Differences between surveys were statistically significant (ANOVA; p = 0.005) for the composite of the 20 samples from similar stations sets between surveys. It's peak density at Rhod40 was probably influenced by the function of this habitat as a prime reproductive site for adult *B. vetula*. As with the increased density trends of queen conch and red hind, the density increment of queen triggerfish must be analyzed in the broader context of neighboring sites within the Cabo Rojo – Mayaguez shelf and slope.

The mean density of spiny lobster (*Panulirus argus*) increased 70.0%, from 0.30 Ind/10^3m^2 in 2011 to 0.51 Ind/10^3m^2 in 2018-20. Differences were not statistically significant because of the high sampling variability. Spiny lobsters were observed from all three main benthic habitats within the 30 – 50m depth range in 2018-20, but only from the CPSlope40-50 in 2011-12 (Figure 20). This result must be evaluated with caution due to the small sample size (N= 19) and examined in the broader context of neighboring sites within the Cabo Rojo – Mayaguez shelf and slope.

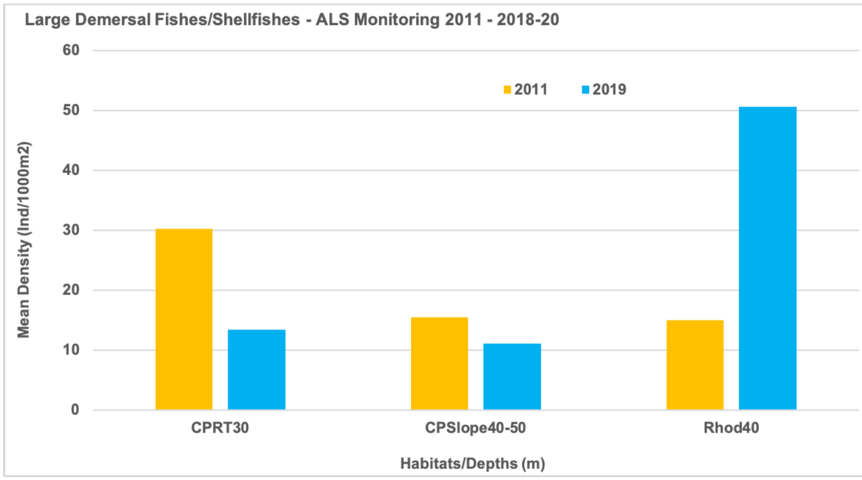

Figure 17. Mean density variations of large demersal fishes/shellfishes surveyed from mesophotic habitats (30 – 50m) between the 2011-12 baseline and the 2018-20 monitoring survey at ALS

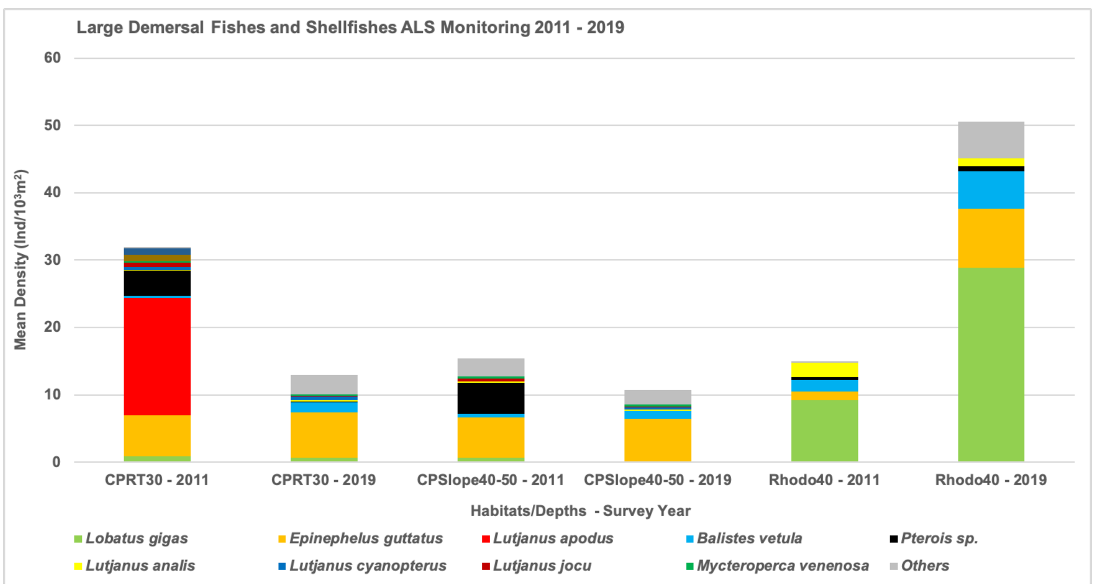

Figure 18. Mean density variations of numerically dominant large demersal fishes/shellfishes surveyed from mesophotic habitats (30 – 50m) between the 2011-12 baseline and the 2018-20 monitoring survey at ALS

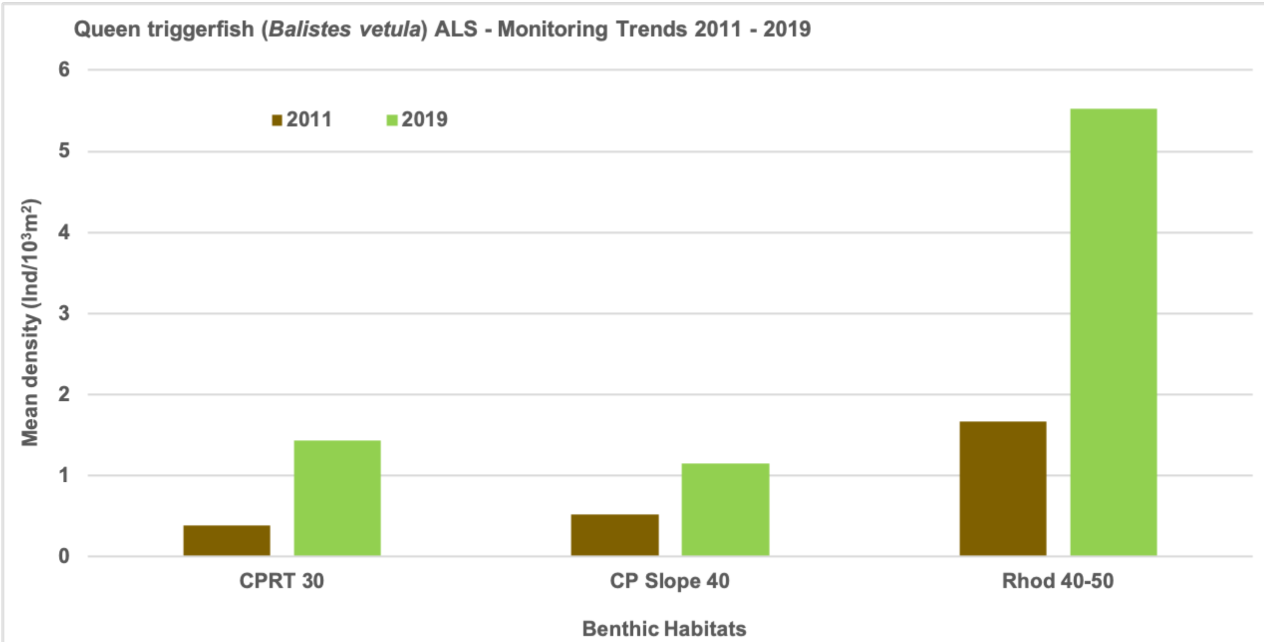

Figure 19. Variations of queen triggerfish (*Balistes vetula*) mean densities between the 2011-12 baseline and the 2018-20 monitoring survey from mesophotic habitats (30 – 50m) at Abrir La Sierra.

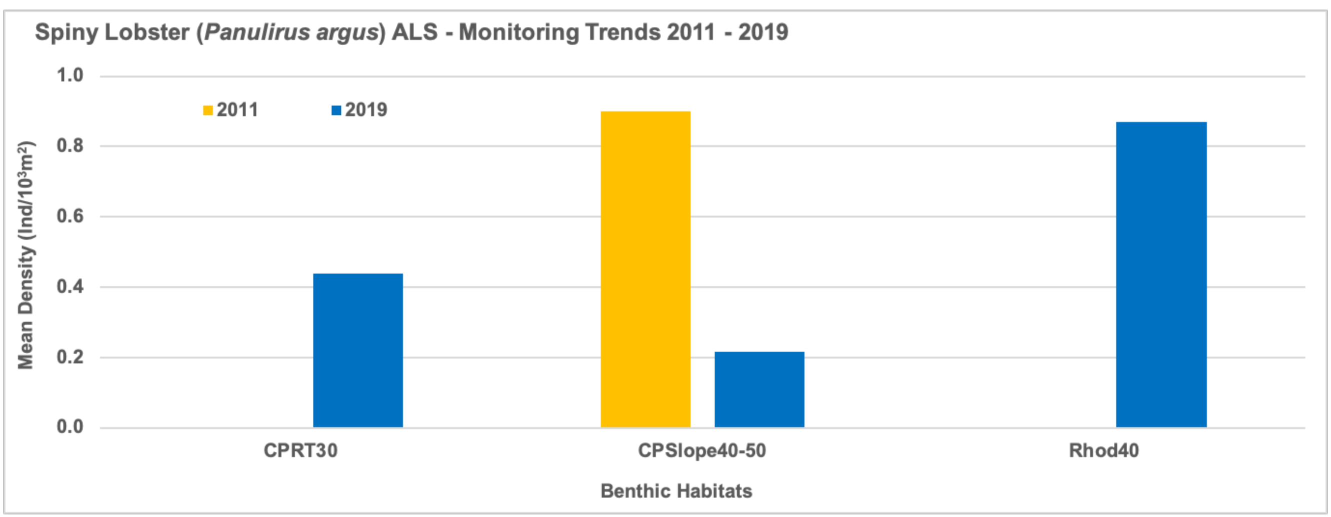

Figure 20. Variations of spiny lobster (*Panulirus argus*) mean densities between the 2011-12 baseline and the 2018-20 monitoring survey from mesophotic habitats (30 – 50m) at Abrir La Sierra

Size distributions of numerically dominant large demersal fish/shellfish species, ALS 2011-12/2018-20 surveys

Red Hind (*Epinephelus guttatus*)

Red hind (*E. guttatus*) was the numerically dominant fish species surveyed by drift belt-transects from mesophotic habitats (30 – 50m) at ALS during 2018-20 with an overall site mean (all benthic habitats and depths) of 5.46 Ind/10^3m^2 and ranked second during 2011-12 with a study mean of 4.45 Ind/10^3m^2. The size frequency distributions based on a total of 268 individuals during both surveys are presented in Figure 21. The main total length (TL) mode was consistent at 31cm during both surveys. The 2018-20 size distribution curve was more skewed toward larger individuals, with a secondary mode of 34cm and an overall higher proportion of 37cm individuals, whereas the secondary mode during 2011-12 was at 28cm. Differences in the size distributions of *E. guttatus* between surveys were not statistically significant (Kolmogorov-Smirnov, $p > 0.10$), but there was a trend towards larger individuals combined with a 22.7% increase of mean density that suggest that the population of *E. guttatus* at ALS may be in a direction of replenishment and growth. *E. guttatus* is a commercially important species under management by both state and federal government administrations and regulations include fishing closures during its seasonal spawning aggregation from December – February.

Size at maturity for *E. guttatus* was reported at 25cm (Froese and Pauly, 2019). Thus, more than 80% of the total individuals observed during both surveys at ALS were adults. The relatively low composition by juveniles may be indicative that mesophotic habitats from ALS are not the prime recruitment habitats for red hind. Recruitment size for *E. guttatus* into mesophotic habitats of ALS was observed at 13cm in 2011-12 and at 10cm in 2018-20. The maximum size of 43cm TL was observed during the 2018-20 survey.

Queen Triggerfish (*Balistes vetula*)

A total of 57 individuals of *B. vetula* were surveyed from mesophotic habitats (30 – 50m) at ALS during the 2011-12 baseline and the 2018-20 monitoring surveys. Site mean densities varied from 0.86 Ind/10^3m^2 in 2011-12 and 2.71 Ind/10^3m^2 in 2018-20. A strong mode at 35cm and another secondary mode at 40cm prevailed during both surveys (Figure 22). Recruitment size into mesophotic habitats was at 25cm in both surveys and the maximum size at 50cm was also consistent during both surveys. A mild trend of higher proportion of smaller individuals was noted in the 2018-20 survey compared with 2010-11, whereas a larger proportion of the larger individuals (> 40cm) resulted from 2011-12. However, the higher proportion of larger individuals resulted from the much smaller sample size in 2011-12 (15) relative to 2018-20 (42). Actually, only three (3) individuals larger than 40cm were observed from both surveys. Differences in the size distribution of *B. vetula* between the 2011-12 and the 2018-20 surveys were not statistically significant (Kolmogorov-Smirnov, $p > 0.10$).

The size at maturity for *Balistes vetula* was reported at 23.5cm (Froese and Pauly, 2019). Thus, all of the *B. vetula* individuals observed from mesophotic habitats at ALS were adults. Queen triggerfish forage at CPRT30 and at CPSlope40-50 habitats, but their preferred residential habitat from ALS was at Rhod40, where they constructed nests with the abundant rhodoliths available. Courtship and nesting defense behaviors were observed from the reproducing adult populations of *B. vetula* at the Rhod40 habitat. The marked increment of density between survey years and the consistent size distribution toward full adult sizes suggest that the *B. vetula* population is healthy and thriving within mesophotic habitats (30 – 50m) of ALS.

Lionfish (*Pterois sp*)

Site mean densities of lionfish (*Pterois sp.*) varied from 2.90 Ind/10^3m^2 in 2011-12 to 0.36 Ind/10^3m^2 in 2018-20. A total of 78 *Pterois sp*. individuals observed from mesophotic habitats in the 30 – 50m depth range at ALS but only five (5) were observed in the 2018-20 survey, all in the 21 – 24 cm (TL) mode. In order to expand the size frequency information of *Pterois sp*. for comparative purposes (between surveys) individuals from the sub-mesophotic CPRT25 stations surveyed in 2018-20 at ALS were included in the size distribution data set. The CPRT25 was not surveyed in 2011-12. The resulting size distributions are shown in Figure 23. The TL mode in 2011-12 was at 21cm, whereas the TL mode in 2018-20 was at 24cm. The 2018-20 size distribution curve was markedly skewed toward larger sizes with consistently higher proportion of individuals larger than 24cm. Differences between the size distributions were not statistically significant due to the small sample size in 2018-20 (N= 14; Kolmogorov-Smirnov; $p > 0.01$).

The size at maturity for *Pterois volitans* has been reported at 23.5cm (Froese and Pauly, 2019) indicative that the lionfish population surveyed within the 25 – 50m depth range at ALS was comprised by juveniles and adults. Juveniles represented 76.7% of the total lionfish population in 2011-12 but declined to 35.7% in 2018-20. The minimum size in 2010-11 was estimated at 10cm, whereas the smallest individual observed during 2018-20 was estimated at 21cm. These data suggest a marked decline of lionfish recruitment into the sub-mesophotic and upper mesophotic habitats of ALS within the 25 – 50m depth range, and that the marked population density decline, as inferred from the 2018-20 survey data may be associated to recruitment failure.

Mutton Snapper (*Lutjanus analis*)

A total of 21 mutton snappers (*Lutjanus analis*) were surveyed within mesophotic habitats in the 30 – 50m range at ALS during 2011-12 and 2018-20. Site means varied from 0.81 Ind/10^3m^2 in 2011-12 to 0.47 Ind/10^3m^2 in 2018-20. The 2011-12 size distribution was skewed toward the larger individuals with a strong mode at 50cm FL, and with 70% of the total individuals at 45cm FL or larger. Conversely, in the 2018-20 survey the main mode was at 20cm FL with a secondary mode at 45cm FL (Figure 24). Differences of the size distributions between surveys were not statistically significant (Kolmogorov-Smirnov, $p > 0.01$) due to the high variability associated with the small sample size (N= 21). The size at maturity of *L. analis* was reported at 28.0cm (Froese and Pauly, 2019), therefore only adults were surveyed in 2011-12, whereas 70% of the individuals surveyed in 2018-20 were juveniles. Evidently, the *L. analis* population at ALS is comprised by both juveniles and adult individuals with a recruitment size at 25cm and reaching a maximum size at 65cm, but further evaluation of its size distribution is limited by the small sample size.

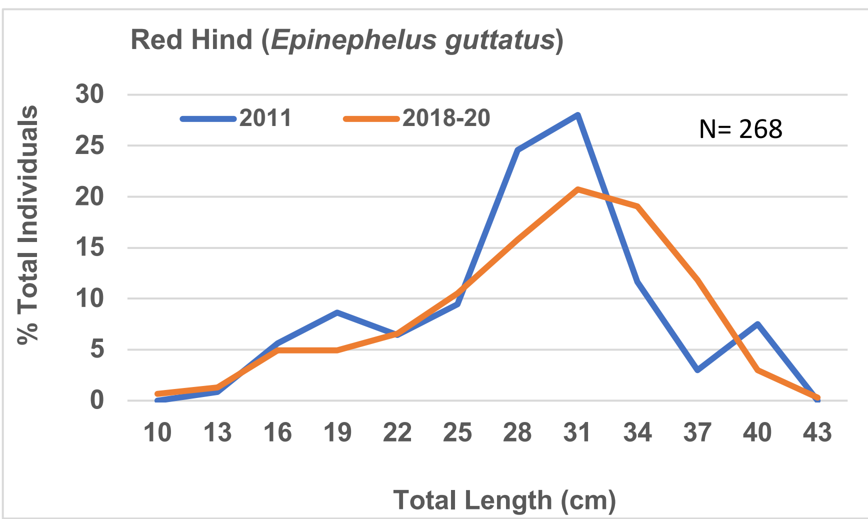

Figure 21. Size-frequency distribution of red hind (*Epinephelus guttatus*) from mesophotic habitats (30 – 50m) depth at Abrir La Sierra (2011-12 and 20198-20 surveys).

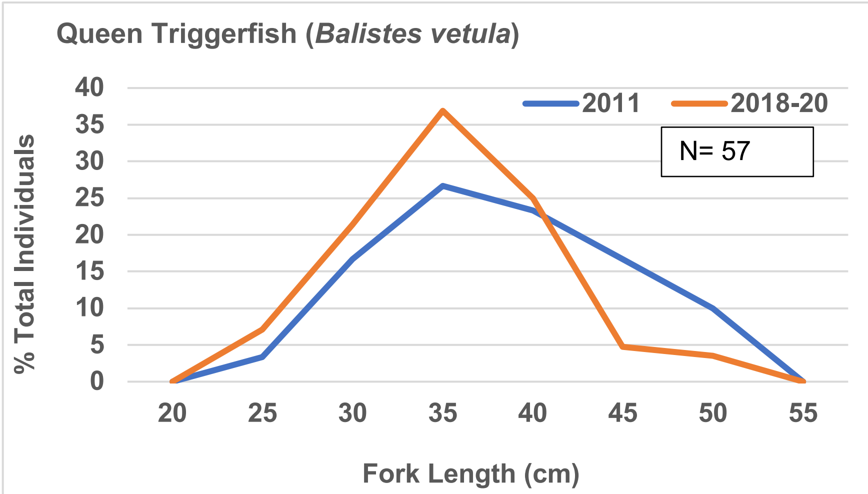

Figure 22. Size-frequency distribution of queen triggerfish (*Balistes vetula*) from mesophotic habitats (30 – 50m) at ALS (2011-12 and 2018-20 surveys)

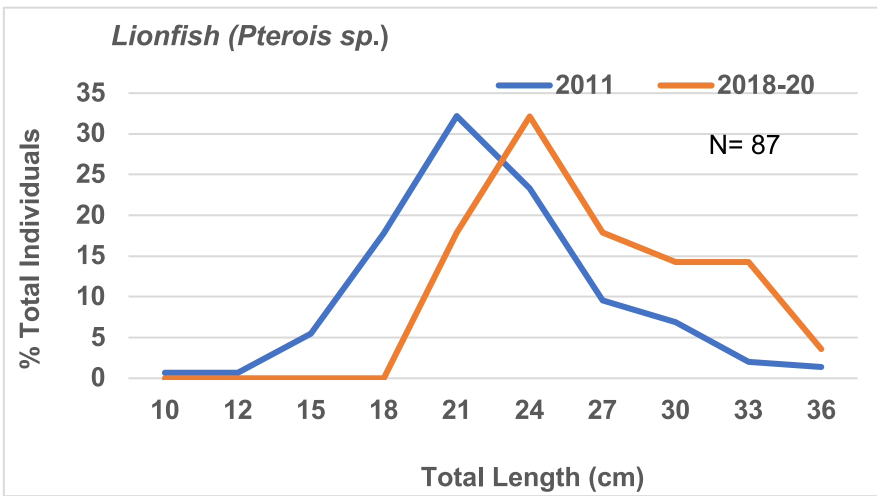

Figure 23. Size-frequency distribution of lionfish (*Pterois sp.*) from sub-mesophotic and mesophotic habitats (25 – 50m) at ALS (2011-12 and 2018-20 surveys)

Coney (*Cephalopholis fulva*)

Coney (*C. fulva*) ranked 2nd among the large demersal fish species surveyed within the 25 – 50m depth range at ALS during 2018-20 with a site mean density of 5.36 Ind/10^{3}m^{2}. Coney was not included in the 2011-12 baseline survey. The size frequency distribution of *C. fulva* presented a strong mode at 22 cm (TL) that represented 22.1% of the total individuals (Figure 25). Secondary modes were noted at 25cm and 19cm, representative of 18.1% and 17.7% of the total population, respectively. Size at maturity of *C. fulva* was reported at 14.7cm (Froese and Pauly, 2019). Thus, approximately 91% of the total individuals observed in the 2018-20 survey were adults. Juvenile individuals were observed to recruit into the 25 – 50m depth range at ALS at a minimum size of 10cm. Given its density and size distribution *C. fulva* is perhaps the grouper with highest biomass within the 25 – 50m depth at ALS.

Cubera Snapper (*Lutjanus cyanopterus*)

A total of 13 cubera snappers (*L. cyanopterus*) were surveyed within mesophotic habitats in the 30 – 50m range at ALS during 2011-12 and 2018-20. Site means varied from 0.16 Ind/10^3m^2 in 2011-12 to 0.31 Ind/10^3m^2 in 2018-20. The size distribution in the 2011-12 survey was comprised by only four (4) individuals in the 50 – 60cm FL range, whereas nine (9) individuals were observed in the 2018-20 survey with a mode at 80cm (Figure 26). Comparative statistics of size distributions between surveys were not performed due to the high variability associated with the small sample size. Despite the limitations imposed by the small sample size, the modal size at 80cm and maximum size of 95cm observed in the 2018-20 survey is indicative that the *L. cyanopterus* population is comprised by very large individuals that represent some of the largest demersal predators within the surveyed depth range at ALS. Given the ciguatera potential of these large individuals it is possible that they may not be presently targeted by comercial fishermen and thus grow to their maximum size.

Spiny Lobster (*Panulirus argus*)

Site mean densities of spiny lobster (*Panulirus argus*) surveyed by drift belt-transects from mesophotic habitats in the 30 – 50m depth range at ALS varied between 0.04 Ind/10^3m^2 in 2011-12 and 0.51 Ind/10^3m^2 in 2018-20. Only one (1) *P. argus* individual was observed in the 2011-12 survey, whereas 16 individuals were observed in the 2018-20 survey. A strong mode at 9cm CL (Cephalothorax Length) and a secondary mode at 11cm CL were noted during the 2018-20 survey, with the largest individuals reaching 16cm CL (Figure 27). The marked population increase and size distribution including very large individuals suggests that the spiny lobster population at ALS has been replenished with large adults that represent important contributions to the spawning stock biomass. This result is based on a small sample size and must be evaluated in a larger spatial context including samplings from adjacent mesophotic habitats within the west coast insular shelf and slope.

Queen Conch (*Lobatus gigas*)

A total of 128 queen conch (*Lobatus gigas*) were observed and measured from drift belt-transects within the 30 – 50m depth range at ALS during the 2011-12 and 2018-20 surveys. Site means varied from 3.60 Ind/$10^3$$m^2$ in 2011 and 7.30 Ind/$10^3$$m^2$ in 2018-20. Size frequency distributions exhibited almost identical curves with a strong primary mode at 24cm (shell length) that represented 42.4% and 38.4% of the total individuals during the 2011-12 and 2018-20 surveys, respectively (Figure 28). A secondary mode that represented 22.9% and 25.9% of the total individuals was noted at 26cm in both surveys. Differences of *L. gigas* size distributions between surveys were not statistically significant (Kolmogorov-Smirnoff; $p > 0.10$). Recruitment into mesophotic habitats was noted at 12cm during both surveys. The 103% increase in mean density of *L. gigas* measured in 2018-20, relative to the 2011-12 survey was associated with an increase of large individuals at the 24cm modal size and larger without any contributions by the smaller size classes. This data suggests that, in absence of recruitment evidence the measured *L. gigas* population increase between surveys resulted from either immigration from adjacent habitats or is an artifact of sampling variability influenced by the patchy (aggregated) distribution. This trend needs to be analyzed in the larger spatial perspective with data from adjacent west coast insular shelf and slope mesophotic habitats.

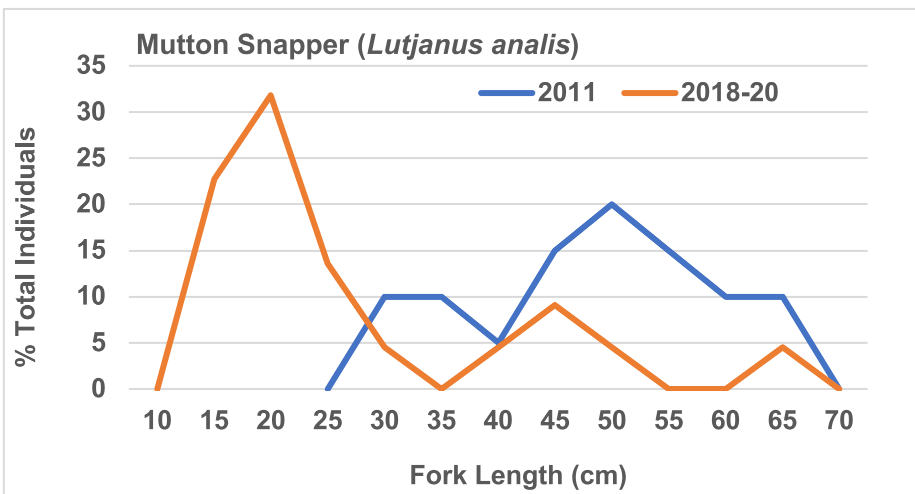

Figure 24. Size-frequency distribution of mutton snapper (*Lutjanus analis*) from mesophotic habitats (30 – 50m) at ALS (2011-12 and 2018-20 surveys)

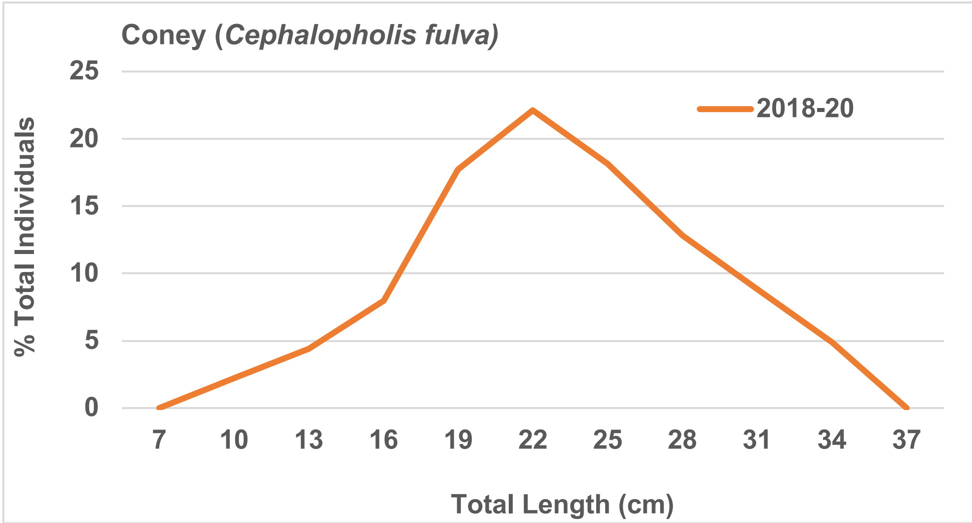

Figure 25. Size-frequency distribution of coney (*Cephalopholis fulva*) from sub-mesophotic and mesophotic habitats (25 – 50m) at ALS, 2018-20 survey

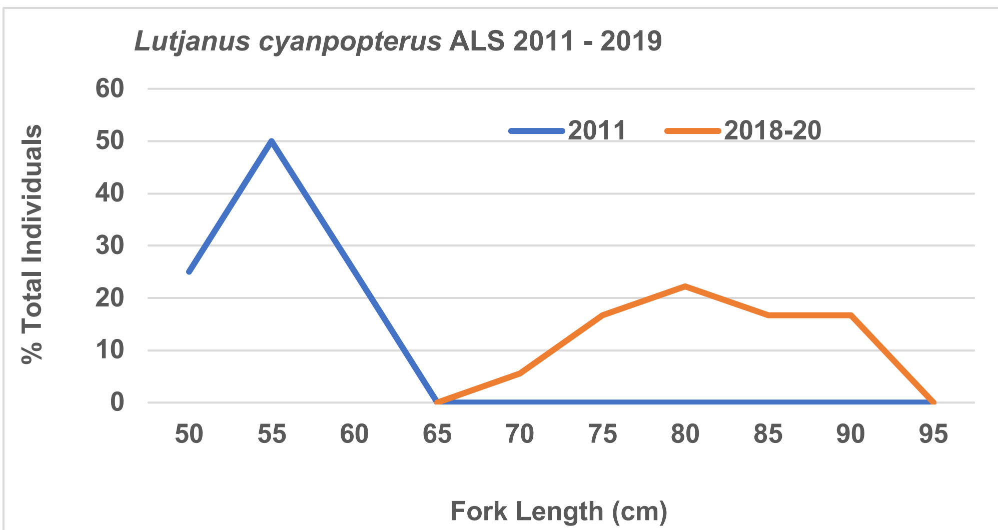

Figure 26. Size-frequency distribution of cubera snapper (*Lutjanus cyanopterus*) from mesophotic habitats (30 – 50m) at ALS (2011-12 and 2018-20 surveys)

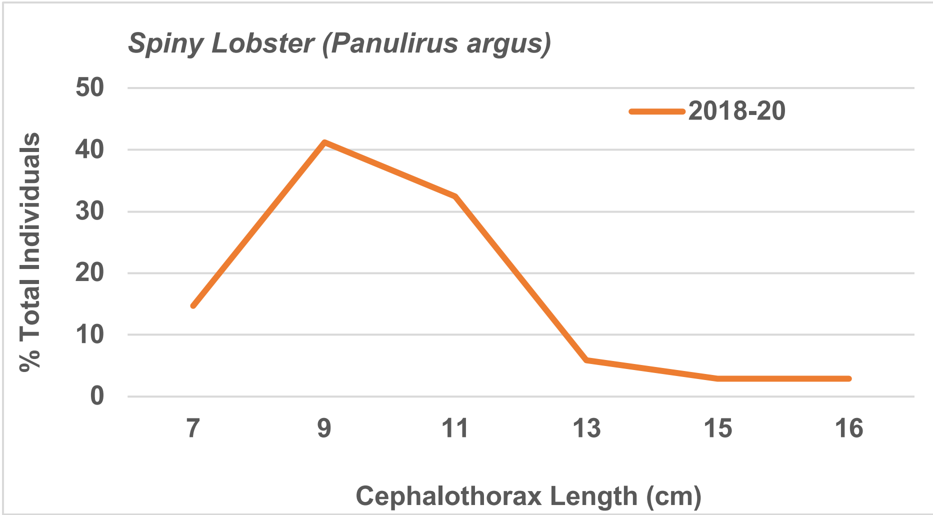

Figure 27. Size-frequency distribution of spiny lobster (*Panulirus argus*) from mesophotic habitats (30 – 50m) at ALS, 2018-20 survey

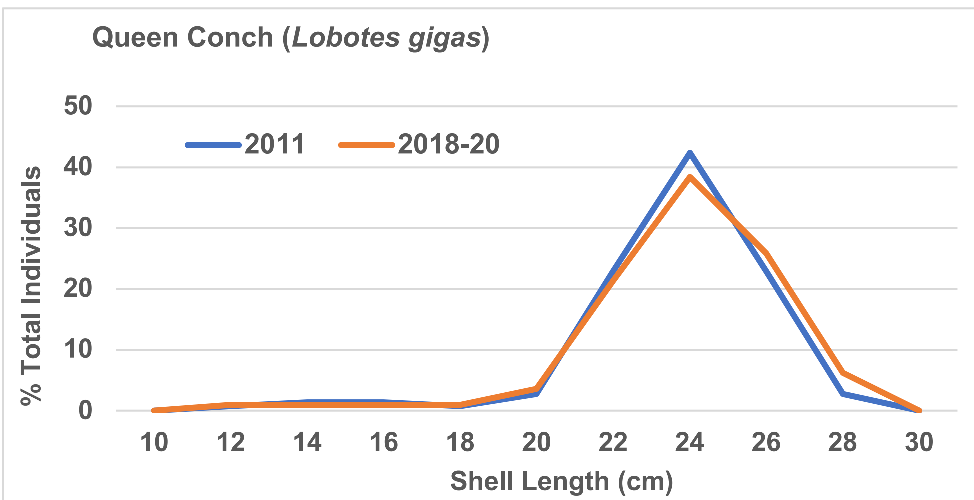

Figure 28. Size-frequency distribution of queen conch (*Lobatus gigas*) from mesophotic habitats (30 – 50m) at ALS (2011-12 and 2018-20 surveys)

Photo Album 1 - ALS
Colonized Pavement Reef Top






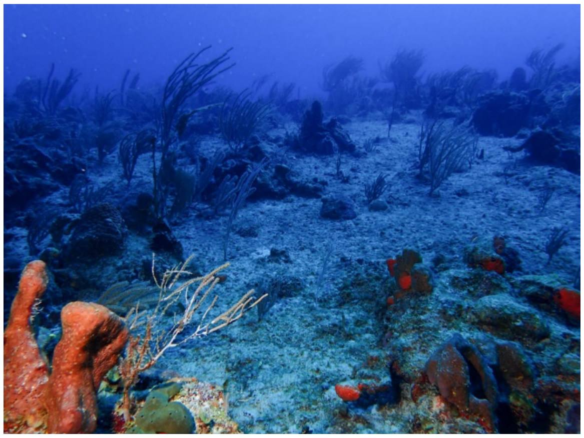

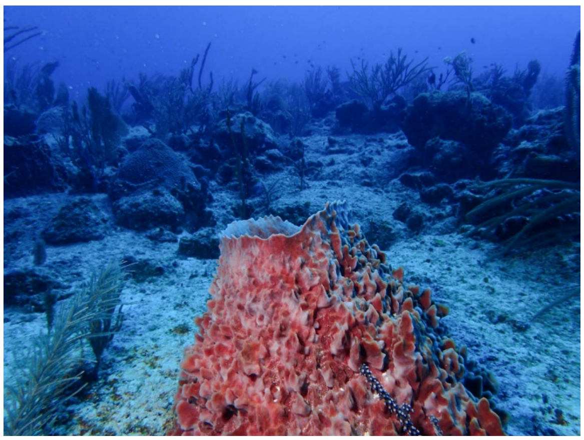

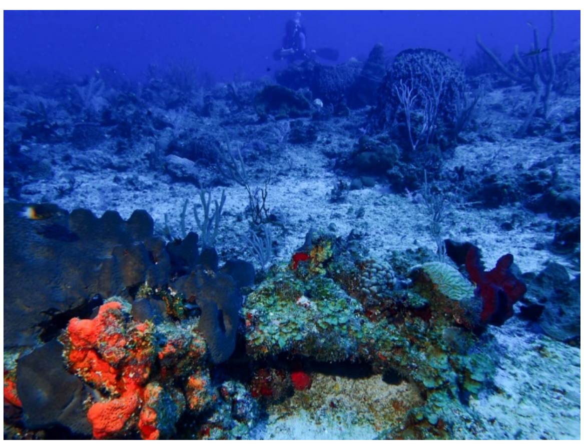






ALS- Colonized Pavement Slope

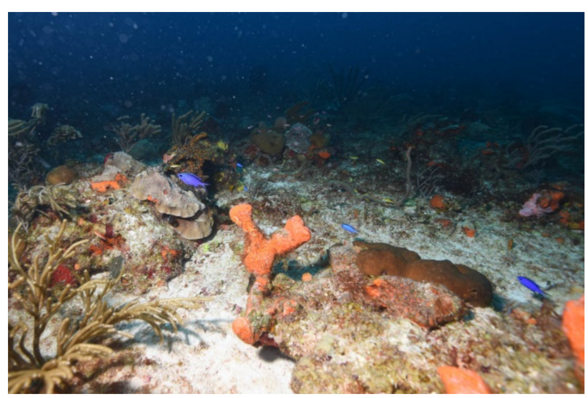


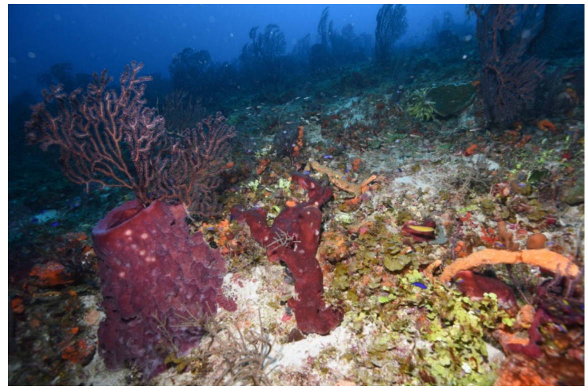



ALS- Rhodolith



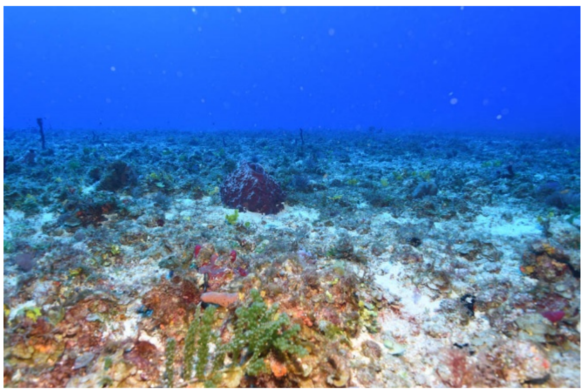
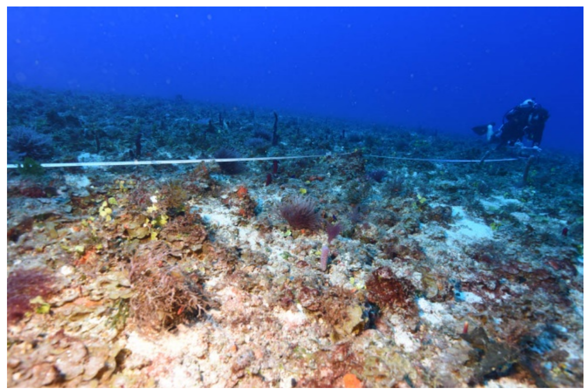
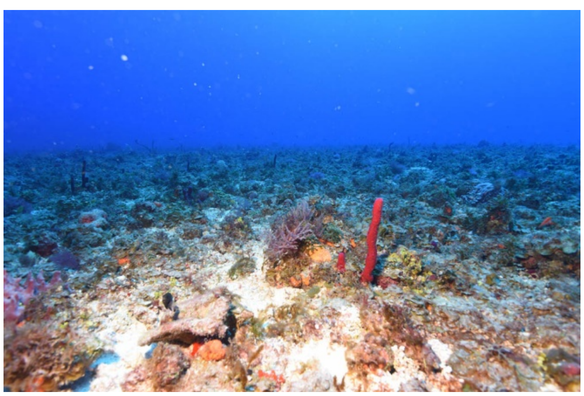


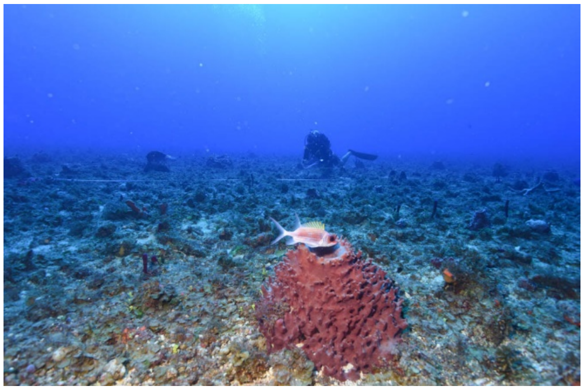

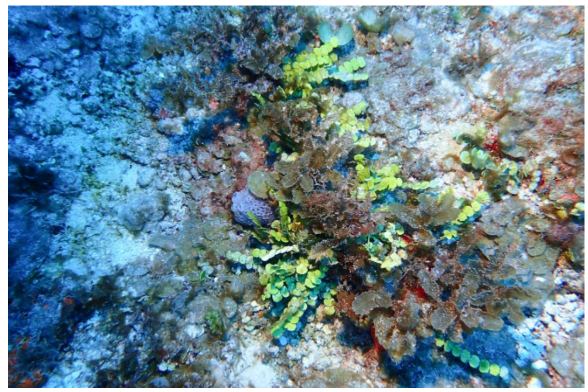

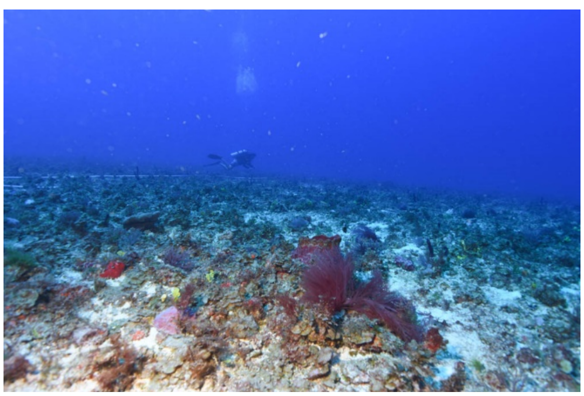

Bajo de Sico

Physical Description

Bajo de Sico (BDS) is located in Mona Passage, about 27 kilometers off Mayagüez in the west coast of Puerto Rico (Figure 29). It is part of the Great Southern Puerto Rico Fault Zone (Glover, 1967; Garrison and Buell, 1971), a submerged section of the Antillean ridge that extends across the entire Mona Passage, connecting Puerto Rico with La Hispaniola. The ridge rises from a depth of approximately 3,500m and includes the islands of Mona, Monito and Desecheo, as well as submerged seamounts that reach depths of less than 100m, such as BDS, Bajo Esponjas and Bajo Pichincho in PR, and Cabo Engaño, partially within Dominican Republic waters. The seamount promontories at BDS rise from a submerged platform that extends out to the north from the insular slope of western Puerto Rico. Reef bathymetry at BDS is characterized by a ridge of rock promontories aligned southeast – northwest which rise from a platform at 45m to a reef top at 25m, and an extensive, mostly flat, homogeneous and gradually sloping shelf that ends as a vertical wall at depths between 90 – 100m reaching down to depths of 200 – 300m at the seamount base. Salient oceanographic features of the water column influencing the reef system include a warm mixed surface water mass with a summer thermocline at a depth of 45 – 50m, strong, persistent northwesterly surface currents, and high-water transparency with 1% light penetration reaching depths of almost 80m (Garcia-Sais et al., 2007).

Benthic habitats at BDS were field verified to a maximum depth of 50m by Garcia-Sais et al., (2007). These include a colonized pavement reef top (CPRT) distributed at depths between 25 – 30m, a colonized pavement vertical wall associated with rock promontories in the 35 – 50m range (CPWall), colonized and uncolonized sections of sand, gravel and rhodoliths at the base of channels separating rock outcrops, and a colonized rhodolith bed (Rhod) surrounding rock promontories below depths of 40m. Benthic habitats beyond 50m have not been field verified, but several video images produced by the R/V Nancy Foster (NOAA, 2007) detected coral growth down to a maximum depth of 90m along the deep shelf platform at BDS. From the multi-beam bathymetry survey of the reef produced aboard the R/V Nancy Foster (NOAA, 2007), the total extension of BDS includes a surface area of approximately 11.1 km^2, of which only 3.6 % is associated with rock promontories (0.4 km^2) and more than 88% corresponds to the deep shelf platform at depths below 50m. The location of benthic and drift transects surveyed during the 2018-20 monitoring event at BDS is shown in Figure 30. Panoramic views of the benthic habitats and photos representative of the main mesophotic communities are shown in Photo Album 2.

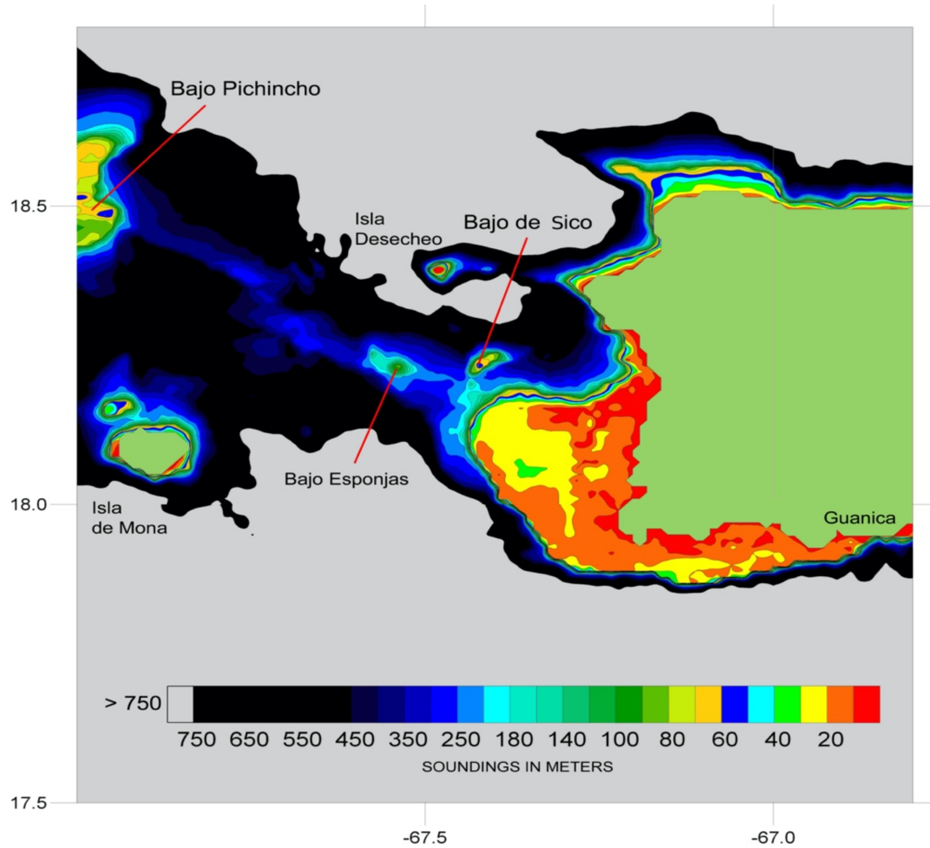

Figure 29. Location of Bajo de Sico on Mona Passage, west coast of Puerto Rico

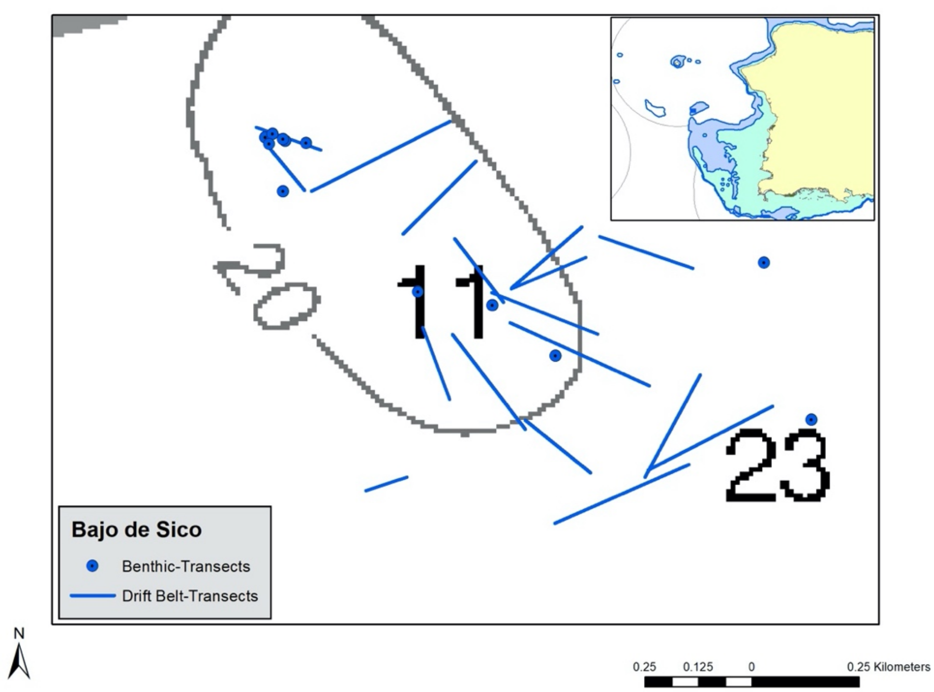

Figure 30. Location of sampling stations at Bajo de Sico, 2018-20 monitoring survey

Benthic Community

Depth/habitat related patterns of benthic community structure, 2018-20 survey

Benthic algae were the main category in terms of percent substrate cover from all habitats/depth surveyed within the 25 – 50m depth range at BDS during the 2018-20 monitoring survey (Table 12). Differences of cover by total benthic algae between habitats/depths were statistically significant (ANOVA; $p< 0.0001$), associated with higher cover at Rhod50 relative to shallower habitats/depths (Figure 31). Such difference was driven by the much higher cover of brown encrusting fan alga (*Lobophora sp.*) (ANOVA; $p < 0.0001$), and also influenced by the higher cover of red Peyssonnelid algae relative to the CPRT25, CPRT30, and CPWall40 (ANOVA; $p < 0.0001$). Conversely, higher substrate cover by turf algae (mixed assemblage) and brown fleshy algae (mostly *Dictyota sp*) were measured from CPRT25 and CPRT30, relative to deeper stations (ANOVA; $p < 0.0001$) (Figure 32). Depth-related factors influencing the composition of algal taxonomic components include the exponential decline of light penetration with depth. Also, a marked reduction of water current velocity with depth (within the surface – 50m range) was measured at BDS (Garcia-Sais et al., 2007), along with the reduced surge and abrasion effects associated with wave action at the reef top. Differences were also noted in relation to the prevailing substrates available for algal growth. Solid rock substrates prevailed on rock promontories in the 25m to 40m range, whereas rhodoliths were the main substrate at 45 - 50m.

A total of 18 stony corals were identified within the 25 – 50m depth gradient surveyed at BDS. Statistically significant differences of substrate cover by stony corals were measured (ANOVA; $p = 0.0012$), associated with higher cover at CPRT25 and CPRT30, relative to CPWall40 and Rhod50 (Figure 33). Substrate cover by stony corals ranged from 10.91% at CPRT25 and 3.02% at CPWall40. Marked habitat/depth-related variations of taxonomic composition by stony corals were noted. Higher cover by lettuce coral (*Agaricia agaricites*), fire coral (*Millepora spp*), and great star coral (*Montastraea cavernosa*) were measured at CPRT25 and CPRT30 (ANOVA; $p < 001$), whereas higher cover by whitestar sheet and scroll corals (*A. lamarki, A. undata*) were measured from Rhod50, relative to shallower habitats/depths (ANOVA; $p < 0.001$) (Figure 33). Soft corals (Octocorallia) and black corals (Antipatharia) were mostly associated with CPWall40. The deep-water gorgonian (*Iciligorgia schrammi*) and sea plumes (*Diodogorgia s*p) were the most prominent soft corals. At least seven black coral species were identified from BDS within the 25 – 50m range at BDS (Garcia-Sais et al., 2007). The bushy black coral (*Antipathes caribbeana*) was the most common at CPWall40 during the 2018-20 survey.

Table 12. Mean percent substrate cover by the main sessile-benthic categories from transects surveyed within the 25 – 50m depth range at Bajo de Sico, 2018-20 survey.

	% Substrate Cover			
BENTHIC CATEGORIES	**CPRT25**	**CPRT30**	**CPWall40**	**Rhod50**
Abiotic				
Sand	2.37	1.87	0.05	0.32
Total Abiotic	**2.37**	**1.87**	**0.05**	**0.32**
Benthic Algae				
Turf (mixed) with sediment		0.11		
Peyssonnelid (mixed)	0.44	2.19	0.94	3.68
Turf (mixed)	14.43	15.01	7.41	5.09
Lobophora sp.	23.30	31.14	27.83	63.84
Halimeda spp.	0.04	0.45	0.04	1.21
Dictyota spp.	5.88	2.81	1.04	
Ramicrusta sp.		0.10		
Fleshy macroalgae (mixed)	0.03	0.32	0.49	
CCA (mixed)	2.30	3.61	2.59	2.81
Total Benthic Algae	**46.40**	**55.72**	**40.33**	**76.63**
Cyanobacteria	**2.17**	**3.12**	**0.05**	**4.20**
Stony Coral				
Agaricia agaricites	3.05	2.20	0.19	0.04
Agaricia fragilis	0.18	0.24	0.09	
Agaricia grahamae	0.28	0.25	0.28	0.33
Agaricia lamarcki	0.04	0.04	0.10	1.05
Agaricia undata	0.03		0.33	0.77
Eusmilia fastigiata	0.07	0.09		0.04
Leptoseris cucullata		0.03	0.04	
Madracis decactis	0.16	0.37	0.10	
Madracis sp.	0.04		0.31	
Meandrina meandrites	0.10	0.71		
Millepora alcicornis	4.00	0.47	0.05	
Montastraea cavernosa	1.06	1.65	0.65	0.07
Orbicella faveolata	0.07	0.95	0.09	0.39
Orbicella franksi		0.14		
Porites astreoides	0.46	1.76	0.05	0.38
Pseudodiploria strigosa	0.23	0.05		
Siderastrea siderea	0.27	0.51	0.05	
Tubastrea aurea	0.89	0.10	0.51	
Unknown coral			0.18	
Total Stony Coral	**10.91**	**9.55**	**3.02**	**3.06**
# Coral Colonies/photo frame	14.27	13.05	7.86	5.05
# Diseased Coral Colonies/photo frame	0.05	0.15	0.02	0.12
# Coral colonies bleached/photo frame	0.08	0.15	0.02	0.08
# Antipatharian Colonies/photo frame	0.04	3.24	3.43	0.15
Black Coral cover	0.00	0.04	0.39	0.0
Octocoral				
Diodogorgia sp.			0.49	
Eunicea spp.			0.28	
Iciligorgia schrammi			0.94	
Unidentified		0.10	0.06	

BENTHIC CATEGORIES	CPRT25	CPRT30	CPWall40	Rhod50
Total Soft Corals	**0.00**	**0.10**	**2.06**	**0.00**
# Soft Corals/photo frame	0.21	0.53	4.52	0.00
Sponges				
Agelas clathrodes	0.46	0.20	0.05	0.18
Agelas citrina	0.19	0.15	0.37	0.60
Agelas conifera	0.28	6.46	12.96	0.20
Agelas dispar	3.68	1.53	0.37	0.08
Agelas sceptrum	0.06	0.04	0.60	0.88
Agelas sventres	3.93	1.19	0.50	0.47
Aiolochoria crassa	0.50	0.25	0.15	0.64
Amphimedon compressa			0.05	0.30
Aplysina archeri				0.25
Aplysina cauliformis	0.11	0.20		3.50
Aplysina sp.				0.06
Aplysina insularis				0.10
Callyspongia ferox			0.26	
Callyspongia plicifera		0.24	0.16	
Cinachyrella kuekenthali			0.30	
Clathria sp.	0.09	0.30	0.06	
Ectyoplasia ferox	0.08		0.06	
Erylus sp.			0.04	
Geodia neptuni			0.23	
Halisarca sp.			0.31	
Hyrtios cavernosus	0.56	0.09	2.15	
Ircinia campana	0.32		0.43	
Ircinia strobilina	1.28	0.23	0.77	
Myrmekioderma gyroderma			0.33	
Myrmekioderma rea	0.03	0.04	0.28	0.10
Neofibularia nolitangere	0.22	0.10		
Neopetrosia proxima			0.45	
Neopetrosia sp.		0.21	0.14	
Niphates erecta	0.03		0.13	
Oceanapia bartschi		0.16	0.78	0.07
Petrosia pellasarca	0.08		0.14	0.17
Plakortis spp.	1.73	2.97	8.82	0.42
Pleraplysilla sp.			0.35	
Prosuberites laughlini	0.16	0.52	0.84	0.03
Scopalina ruetzleri	0.90	0.12	0.55	0.03
Smenospongia aurea			0.20	
Smenospongia conulosa	5.36		0.57	0.19
Spirastrella coccinea	0.36	0.04	1.69	0.07
Spirastrella hartmani		0.08	0.22	
Svenzea zeai	0.80	7.82	2.48	0.25
Unknown sponges	6.05	2.54	9.51	3.32
Verongula reiswigi	0.33		0.09	0.24
Verongula rigida	0.21			0.09
Verongula sp.				0.08
Xestospongia muta	8.47	2.86	4.20	2.53
Total Sponges	**36.24**	**28.34**	**51.56**	**14.83**

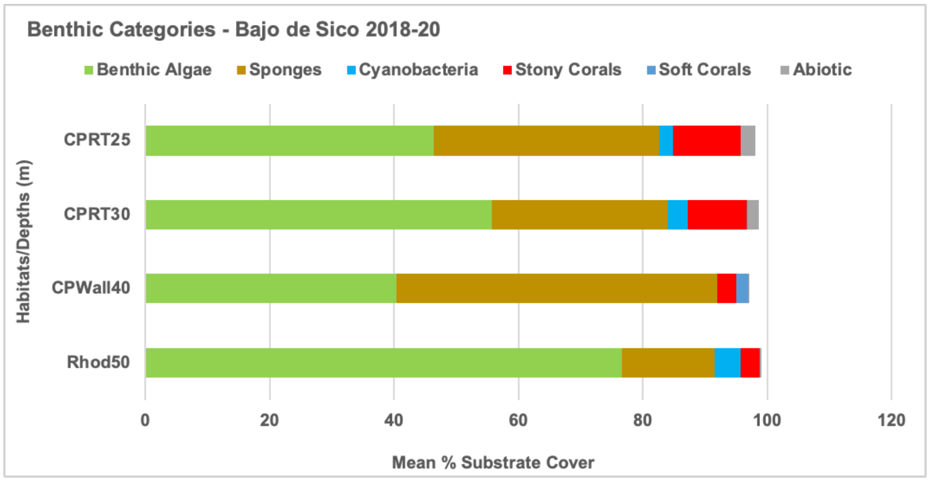

Figure 31. Mean percent substrate cover by benthic categories across the 25 – 50m depth range surveyed at Bajo de Sico, 2018-20

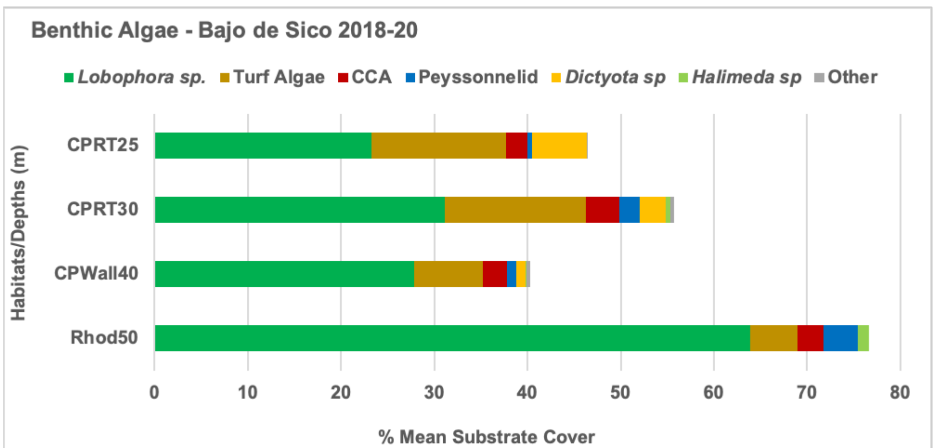

Figure 32. Mean percent substrate cover by benthic algae components across the 25 – 50m depth range surveyed at Bajo de Sico, 2018-20

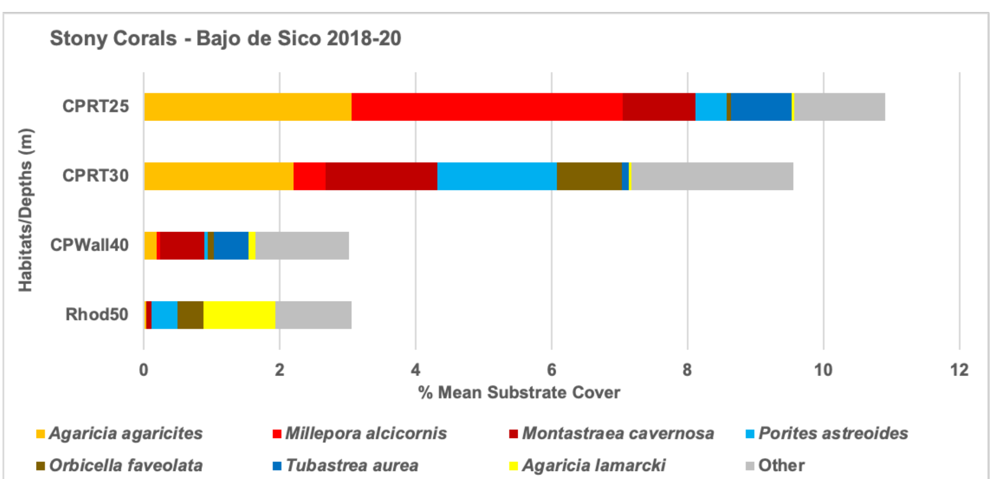

Figure 33. Mean percent substrate cover by stony coral species across the 25 – 50m depth range surveyed at Bajo de Sico, 2018-20

A total of 45 sponge species were identified within photo-transects across the main benthic habitats/depths surveyed at BDS during 2018-20 (Table 12). Mean substrate cover by sponges ranged between 14.83% at Rhod50 and 51.56% at CPWall40. Statistically significant differences were found between habitats/depths associated with higher cover at CPWall40 (ANOVA; $p < 0.0001$). The sponge assemblage at CPWall40 which included 38 species was largely dominated in terms of substrate cover by *Agelas conifera*, *Plakortis sp*. and an assemblage of unidentified sponges, most of which were comprised by small encrusting types growing on the vertically projected seascape of the rock promontory walls (Figure 34). The increased water flow associated with topographically steered currents appeared to favor growth of sponges, soft corals, and black corals at CPWall40, perhaps due to increased contact with zooplankton food and/or lower competition for space with benthic algae which appear to prevail in horizontally oriented substrates due to higher light availability. Lower substrate cover by sponges was measured from Rhod50, where encrusting fan alga (*Lobophora sp*) grows as a carpet over the rhodolith bed limiting colonization by another encrusting biota.

Abiotic cover was minimal at BDS within the depth/habitats surveyed, ranging from 0.05% at CPWall40 and 2.37% at CPRT25. This implies that more than 97% of the hard substrates surveyed on pavement and rhodolith habitats were biologically colonized, with only small sand patches present within these habitats. Most of the abiotic substrates at BDS were associated with sand/rubble channels separating the rock promontories but transects were not performed on these channels during the 2018-20 survey.

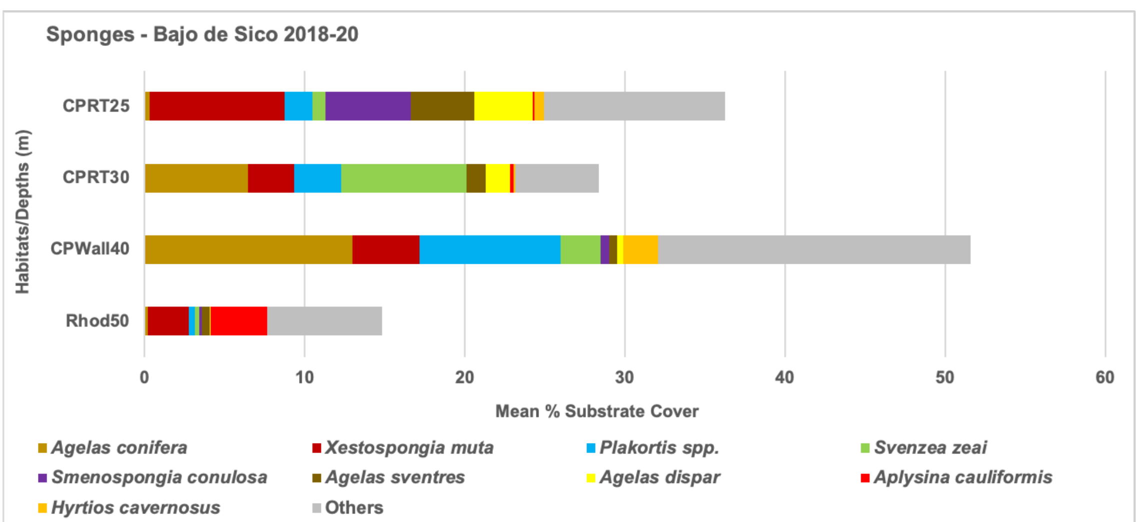

Figure 34. Mean percent substrate cover by sponge species across the 25 – 50m depth range surveyed at Bajo de Sico, 2018-20

Similarities of benthic community structure between surveyed habitats/depths based on the percent cover by the main substrate categories are presented in a non-metric multidimensional scaling (nMDS) plot of Bray-Curtis similarities in Figure 35. The highest average similarity was observed from the CPWall40 (83.8%), mostly contributed by soft corals, sponges, and benthic algae (Table 13). Substrate cover by soft corals, black corals, and sponges peaked at CPWall40 and represented a distinguishing feature of this habitat/depth. Soft corals and black corals, particularly the deep-water gorgonian (*Iciligorgia schrammi*), and the bushy black coral (*Antipathes caribbeana*) were found growing almost exclusively at the side walls of rock promontories (CPWall40), where increased topographically steered current flows enhance contact of benthic zooplanktivores with zooplankton prey. Benthic similarities at CPRT25 (72.9%) and CPRT30 (73.2%) were strongly contributed by stony coral cover, which declined markedly at CPWall40 and Rhod50. Substrate cover by benthic algae, largely comprised by encrusting fan alga (*Lobophora sp*) peaked at Rhod50, and were the main benthic category contributing similarity at this habitat/depth (average: 39.8%).

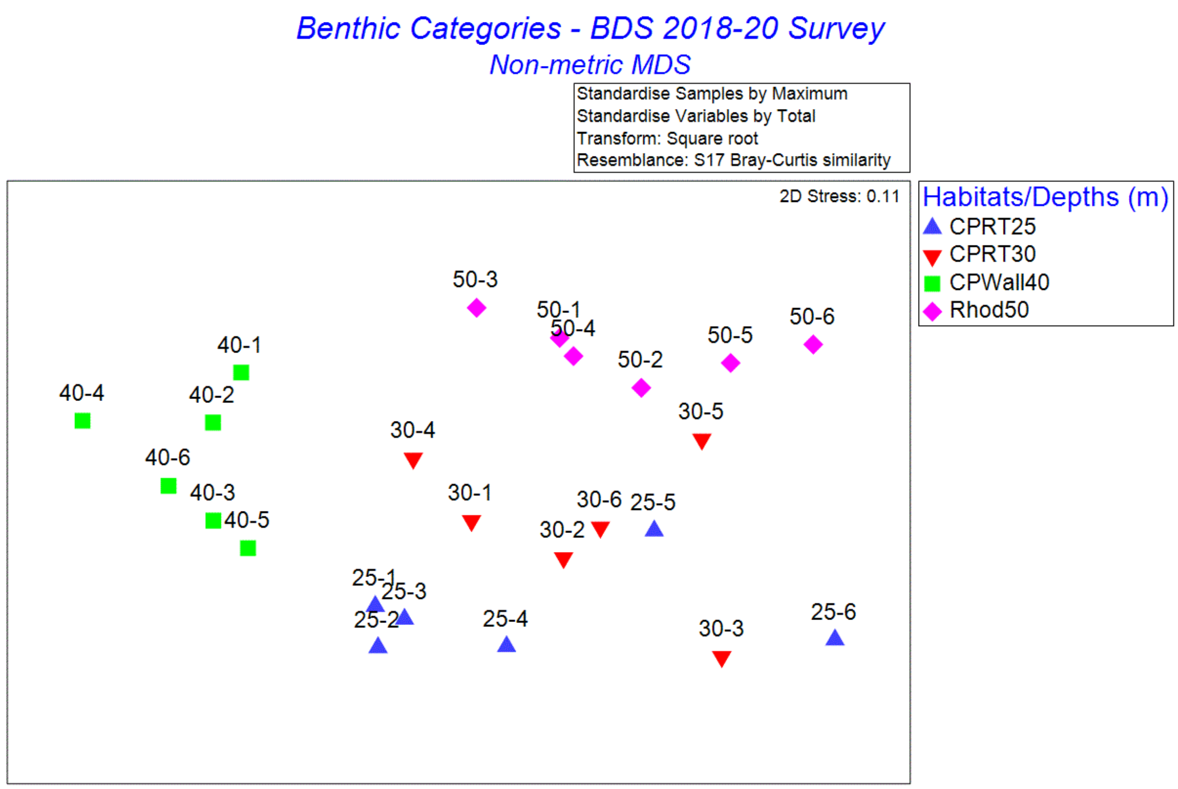

Figure 35. Non-metric multidimensional scaling (nMDS) plot of Bray-Curtis similarities between photo-quadrat samples of sessile-benthic communities surveyed from sub-mesophotic (25m) and upper mesophotic (30 – 50m) depths at Bajo de Sico, 2018-20 survey.

Table 13. Similarity matrix (SIMPER) of sessile-benthic community structure at the main benthic habitats/depths surveyed from Bajo de Sico during 2018-20, including contributions of benthic categories to the within habitat similarity.

	CPRT25	CPRT30	CPWall40	Rhod50
Average Similarity (%)	72.9	73.2	83.8	76.0
Benthic Categories				
Abiotic				
Benthic Algae	28.3	28.6	21.0	39.8
Cyanobacteria				19.6
Stony Corals	36.5	27.3		
Soft Corals			32.0	
Sponges	29.3	22.7	31.4	18.8

Benthic community structure dissimilarity was highest between the CPWall40 and all other habitats (Table 14). Dissimilarities were strongly driven by the higher substrate cover of soft corals at CPWall40 relative to other habitats/depths. Conversely, substrate cover by cyanobacteria, abiotic, and benthic algae were relatively lower at the CPWall40 relative to other habitats/depths. Substrate cover by stony corals was highest at CPRT25 and CPRT30, and represented the main category contributing dissimilarity between these and other benthic habitats/depths. Cyanobacteria was the main substrate category contributing dissimilarity between Rhod50 and all other habitats/depths surveyed at BDS during the 2018-20 monitoring survey.

Table 14. Dissimilarity matrix (SIMPER) between habitats/depths surveyed at Bajo de Sico during 2018-20, including contributions of benthic categories to the between habitat dissimilarity.

	CPRT25	CPRT25	CPRT25	CPRT30	CPRT30	CPWall40
	vs CPRT30	vs CPWall40	vs Rhod50	vs CPWall40	VS Rhod50	vs Rhod50
Average Dissimilarity	27.7	41.6	38.3	43.3	30.3	49.7
Benthic Categories				15.3		
Abiotic	35.0	17.6	22.9		25.8	
Benthic Algae						
Cyanobacteria	36.6		31.1	23.1	28.2	23.1
Stony Corals		16.7	26.2		25.6	
Soft Corals		44.9		38.0		42.7
Sponges						17.4

Temporal (monitoring) variations of benthic community structure, 2006-07/2018-20

Variations of the mean percent substrate cover by benthic categories measured from a similar set of 24 sampling stations representative of the main benthic habitats surveyed at BDS during the 2006-07 baseline and 2018-20 monitoring survey are presented in Figure 36 Differences of substrate cover between surveys were statistically significant for abiotic and soft corals (Two-way ANOVA, $p < 0.0001$) (Table 15). Substrate cover by soft coral declined 91.0%, from a mean of 6.55% in 2006-07 to a mean cover of 0.59% in 2018-20. Such decline is consistent with observations from many neritic reefs around Puerto Rico after the pass of Hurricanes Irma and Maria in September 2017, and winter storm Riley in March 2018 (Garcia-Sais et al, 2018, 2019). Soft corals may have been detached by the scouring and/or abrasion effects induced by extremely high wave and surge action during these extreme events. Substrate cover by black corals also declined between surveys (-73.8%), but due to high sampling variability such effects were statistically insignificant (ANOVA; $p= 0.106$). The 82.8% decline of abiotic cover largely associated with sand may respond also to the turbulent conditions and advective forces acting upon unconsolidated sediments during such storms. Differences of substrate cover by benthic algae between surveys were statistically significant, but differences depended upon habitat/depth (Two-way ANOVA; $p = 0.046$). Differences were largely related to the increase of cover by fleshy algae (mostly *Dictyota sp*.) at CPWall40, and *Lobophora sp*. and at Rhod50.

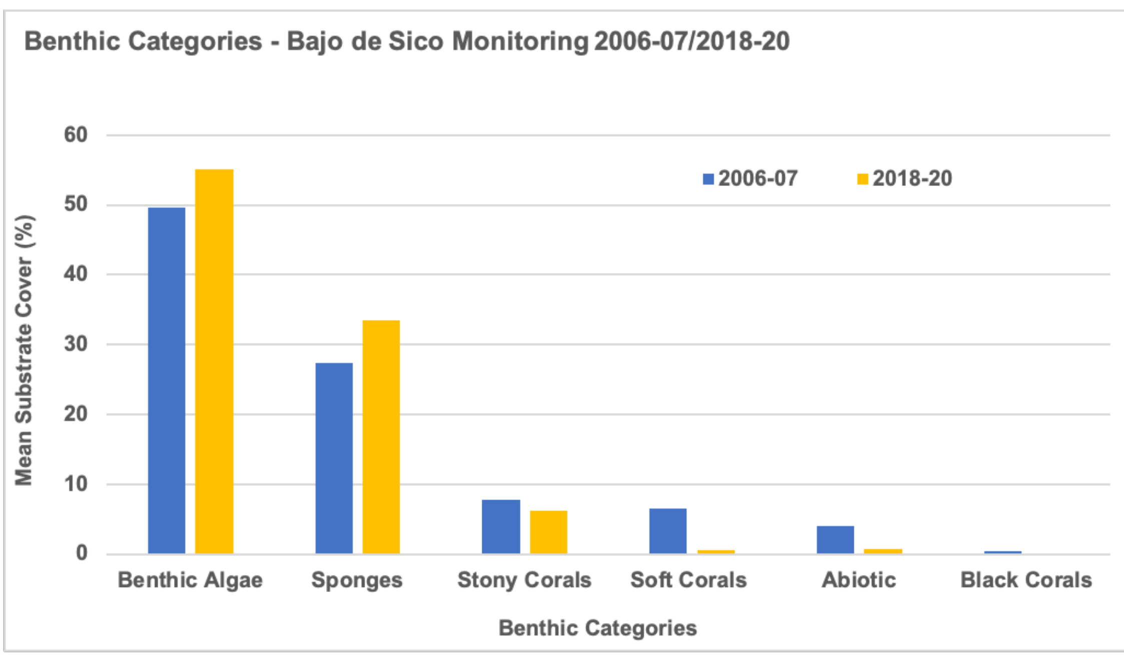

Figure 36. Variations of mean substrate cover by the main sessile-benthic categories measured from a similar set of stations within the 25 – 50m depth range at Bajo de Sico during the 2006-07 baseline and the 2018-20 monitoring surveys

Table 15. Temporal variations of reef substrate cover by sessile-benthic categories between the 2006-07 baseline and the 2018-20 monitoring surveys at Bajo de Sico. Site means include values across all habitats/depths.

Benthic Categories	Site Means 2006-07	Site Means 2018-20	% Change	Two-way ANOVA p-value
Benthic Algae	49.66	55.08	10.9	0.046*
Sponges	27.36	33.51	22.5	0.092
Stony Corals	7.74	6.24	-19.5	0.137
Soft Corals	6.55	0.59	-91.0	< 0.0001*
Abiotic	4.06	0.70	-82.8	< 0.0001*
Black Corals	0.42	0.11	-73.8	0.106

* Statistically significant differences, Alpha level < 0.05

Major differences in the relative contributions of taxonomic components to the total benthic algae assemblage were noted. Substrate cover by fleshy algae increased 2,300.0%, from a site mean (across all habitats/depths) of 0.11% in 2006-07 to a site mean of 2.64% in 2018-20 (ANOVA; p = 0.005). Crustose coralline algae (CCA) increased 350.6%, from a site mean of 1.0 % in 2006-07 to a site mean of 4.7% in 2018-20 (ANOVA; p < 0.0001). Brown encrusting fan-leaf alga (*Lobophora sp.*) increased 23.1%, from a site mean of 29.7% in 2006-07 to a site mean of 36.5% in 2018-20 but differences were statistically insignificant (ANOVA; p = 0.150). Conversely, turf algae declined 39.0%, from a site mean of 17.2% in 2006-07 to a site mean of 10.5% in 2018-20 (ANOVA; p = 0.297). The marked variations in the taxonomic components of benthic algae after 2017 may be related to several factors including a potentially strong nutrient spike associated with the pass of Hurricanes Irma and Maria in 2017. Hurricanes are divergent systems and nutrient upwelling into the surface mixed layer could have been triggered with potential implications to the taxonomic structure of benthic algae within the mesophotic habitats at BDS, as previously reported for neritic reefs in PR (Garcia-Sais et al., 2018, 2019).

Benthic community structure similarities between the 2006-07 baseline and the 2018-20 monitoring survey are presented in a non-metric multidimensional scaling plot (nMDS) of Bray-Curtis similarities based on the site mean percent substrate cover by major substrate categories from the main habitats/depths surveyed (Figure 37). Similarities ranged between 81.7% at Rhod50 and 66.2% at CPWall40 (Table 16). Benthic algae were one of the main contributors to similarity across all habitats and depths, but played a more prominent role at Rhodo50, with a 42.9% contribution to similarity. Stony corals were also highly relevant to the similarity between surveys at CPRT25 and CPRT30. Similarity was relatively lower at the CPWall40 due to the marked decline of cover by soft corals.

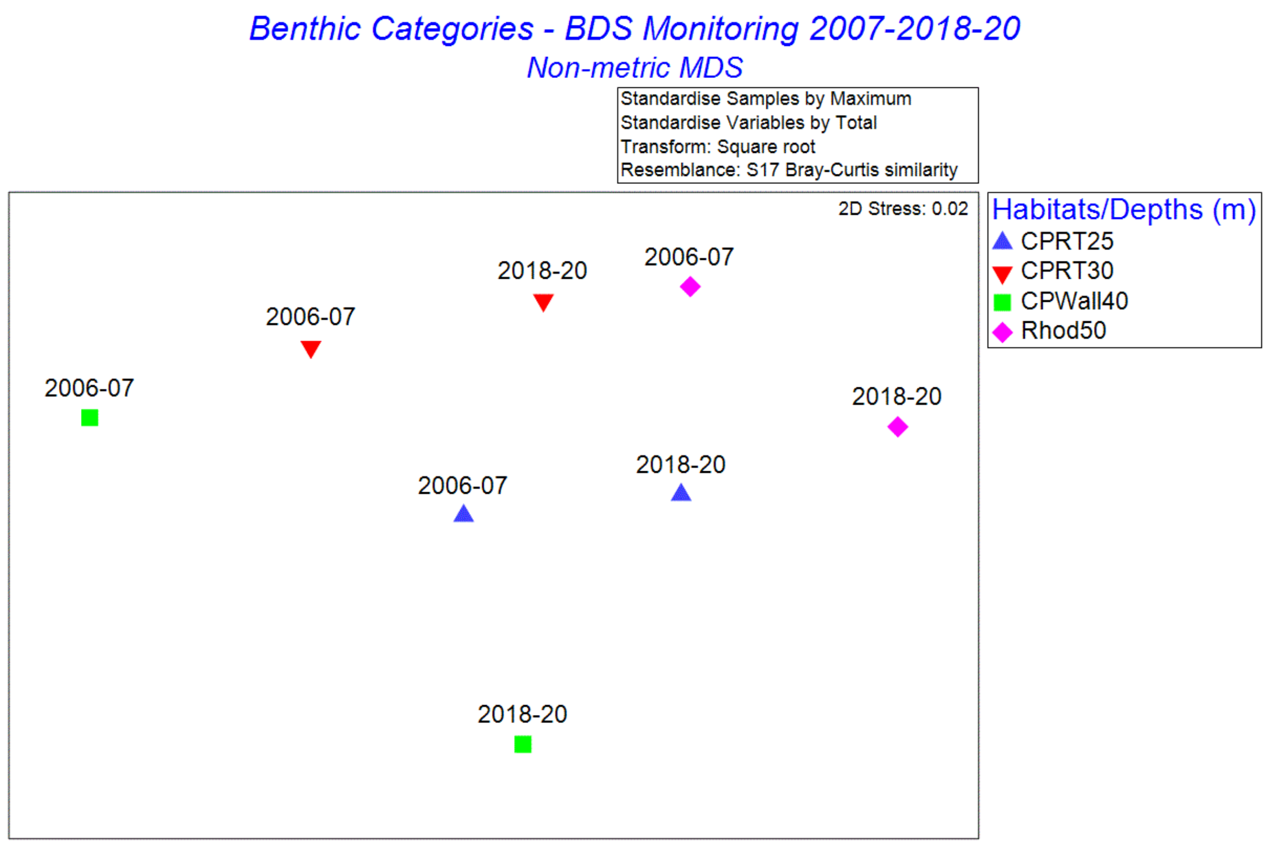

Figure 37. Non-metric multidimensional scaling (nMDS) plot of Bray-Curtis similarities of the percent cover by major substrate categories from the main mesophotic (25 – 50m) habitats and depths surveyed from Bajo de Sico during the 2006-07 baseline and 2018-20 monitoring surveys.

Table 16. Similarity matrix of benthic community structure between the 2006-07 baseline and the 2018-20 monitoring survey based on study mean percent cover by major substrate categories from the main habitats and depths surveyed at Bajo de Sico

	CPRT25	CPRT30	CPWall40	Rhodo50
Average Similarity (%)	76.6	79.0	66.2	81.7
Benthic Categories				
Benthic Algae	32.9	25.5	30.0	42.9
Stony Corals	29.4	26.4		21.8
Soft Corals			18.9	
Sponges	24.6	22.4	35.0	23.4

Fish Community

Small demersal fish species, 2018-20 survey

Depth/habitat related patterns of fish community structure

A total of 59 small demersal fish species were identified from 10m x 3m belt-transects within the 25 – 50m depth range at BDS during the 2018-20 survey (Table 17). Mean density ranged between 85.5 Ind/30m^2 at Rhod50 and 230.0 Ind/30m^2 at CPRT30. Mean fish species richness varied between 8.7 Spp/30m^2 at Rhod50 and 18.5 Spp/30m^2 at CPRT25. Fish density and species richness were both higher at CPRT25 and CPRT30, compared to CPWall40 and Rhod50 (ANOVA; $p< 0.0001$). Differences of density and species richness between CPRT25 and CPRT30, and between CPWall40 and Rhod50 were within 95% confidence limits. The study mean density of the top 10 species represented 86.7% of the total fish density across all habitats/depths surveyed. These included the bicolor damselfish (*Stegastes partitus*), bluehead and yellowhead wrasse (*Thalassoma bifasciatum, Halichoeres garnoti*), brown, blue and sunshine chromis (*Chromis multilineata, C. cyanea, C. insolata*), fairy basslet (*Gramma loreto*), creole wrasse (*Clepticus parrae*), creole fish (*Paranthias furcifer*), and masked goby (*Coryphopterus personatus*).

Habitat/depth related density differences were noted for some of the numerically dominant species (Figure 38). Bicolor damselfish (*Stegastes partitus*) exhibited high habitat plasticity across the entire 25m - 50m range, but its density was statistically lower at CPWall40, compared to other habitats/depths (ANOVA; $p = 0.0006$). CPWall40) was the only vertically oriented habitat surveyed within the 25 – 50m range at BDS. Conversely, densities of fairy basslet (*Gramma loreto*), and creole fish (*Paranthias furcifer*) were significantly higher at CPWall40, compared to other habitats/depths (ANOVA; $p < 0.001$), which may be related to preference by these species for vertically oriented habitats. Densities of bluehead wrasse (*Thalassoma bifasciatum*), and blue and brown chromis (*Chromis cyanea, C. multilineata*) were significantly higher at CPRT25 and CPRT30. Given the significantly higher substrate cover by stony corals at CPRT25 and CPRT30, relative to other habitats surveyed, higher densities of the aforementioned species may be influenced by the higher substrate heterogeneity and structural habitat complexity conferred by the higher stony coral cover. Likewise, the significantly higher fish species richness associated with CPRT25 and CPRT30, relative to the CPWall40 and Rhod50 may have been driven by the higher microhabitat availability and heterogeneity associated with stony coral buildup and substrate cover.

Table 17. Taxonomic composition and mean densities of small demersal fishes surveyed by 3m x 10m belt-transects within the 25 – 50m depth range at Bajo de Sico, 2018-20 survey.

	Mean Density (Ind/30m^2)			
Species	**CPRT25**	**CPRT30**	**CPWall40**	**Rhod50**
Stegastes partitus	47.83	43.83	13.67	46.00
Chromis multilineata	17.17	50.83	7.33	0.00
Thalassoma bifasciatum	30.83	36.00	7.67	4.00
Chromis cyanea	5.50	28.50	2.00	13.17
Gramma loreto	3.00	10.67	28.17	0.00
Clepticus parrae	1.67	34.50	2.83	0.00
Halichoeres garnoti	4.33	4.50	2.17	2.33
Paranthias furcifer	0.67	1.67	8.67	0.50
Coryphopterus personatus	0.00	0.00	8.67	0.00
Chromis insolata	0.00	0.33	3.50	4.50
Centropyge argi	0.00	1.83	0.00	6.17
Kyphosus sp.	1.00	0.00	5.17	0.00
Holocentrus rufus	2.50	1.50	1.33	0.17
Cephalopholis fulva	3.00	0.67	1.17	0.67
Caranx crysos	5.33	0.00	0.00	0.00
Amblycirrhitus pinos	2.17	1.50	0.17	0.33
Bodianus rufus	0.67	1.67	0.67	0.00
Acanthurus tractus	0.67	2.00	0.17	0.00
Halichoeres maculipinna	0.33	1.83	0.00	0.17
Chaetodon capistratus	0.83	0.50	0.83	0.00
Elagatis bipinnulata	2.00	0.00	0.00	0.00
Scarus taeniopterus	0.50	0.50	1.00	0.00
Scarus iseri	1.17	0.00	0.33	0.00
Cephalopholis cruentatus	0.33	1.00	0.17	0.17
Sparisoma aurofrenatum	0.17	0.83	0.17	0.50
Acanthurus coeruleus	1.17	0.33	0.00	0.00
Melichthys niger	1.00	0.33	0.00	0.00
Holacanthus tricolor	0.50	0.67	0.17	0.00
Sparisoma viride	0.33	0.83	0.00	0.00
Canthigaster rostrata	0.33	0.33	0.33	0.00
Acanthurus chirurgus	0.67	0.17	0.00	0.00
Chaetodon striatus	0.33	0.33	0.17	0.17
Sparisoma atomarium	0.00	0.00	0.00	1.00
Elacatinus evelynae	0.50	0.33	0.00	0.00
Epinephelus guttatus	0.33	0.17	0.00	0.33
Serranus baldwini	0.00	0.00	0.00	0.83
Holacanthus ciliaris	0.33	0.17	0.17	0.00
Schultzea beta	0.00	0.00	0.00	0.67
Cantherhines pullus	0.33	0.17	0.00	0.00
Coryphopterus glaucofraenum	0.50	0.00	0.00	0.00
Lactophrys triqueter	0.17	0.17	0.17	0.00
Balistes vetula	0.17	0.17	0.00	0.17
Carangoides ruber	0.00	0.33	0.00	0.00

Table 17. Taxonomic composition and mean densities of small demersal fishes surveyed by 3m x 10m belt-transects within the 25 – 50m depth range at Bajo de Sico, 2018-20 survey.

	Mean Density (Ind/30m^2)			
Species	**CPRT25**	**CPRT30**	**CPWall40**	**Rhod50**
Caranx lugubris	0.17	0.00	0.17	0.00
Prognathodes aculeatus	0.00	0.17	0.17	0.00
Pterois sp.	0.17	0.17	0.00	0.00
Sparisoma radians	0.33	0.00	0.00	0.00
Xanthichthys ringens	0.00	0.33	0.00	0.00
Coryphopterus lipernes	0.00	0.00	0.17	0.17
Lactophrys bicaudalis	0.00	0.00	0.00	0.33
Chaetodon ocellatus	0.00	0.17	0.00	0.00
Epinephelus striatus	0.00	0.00	0.17	0.00
Ginglymostoma cirratum	0.17	0.00	0.00	0.00
Holocentrus adscensionis	0.17	0.00	0.00	0.00
Lutjanus jocu	0.00	0.00	0.17	0.00
Microspathodon chrysurus	0.17	0.00	0.00	0.00
Neoniphon marianus	0.00	0.00	0.17	0.00
Serranus tigrinus	0.17	0.00	0.00	0.00
Lutjanus buccanella	0.00	0.00	0.00	0.17
Mean Density (Ind/30m^2)	**139.7**	**230.0**	**97.8**	**82.5**
Mean Species Richness (# Spp/30m^2)	**18.5**	**18.3**	**11.8**	**8.7**

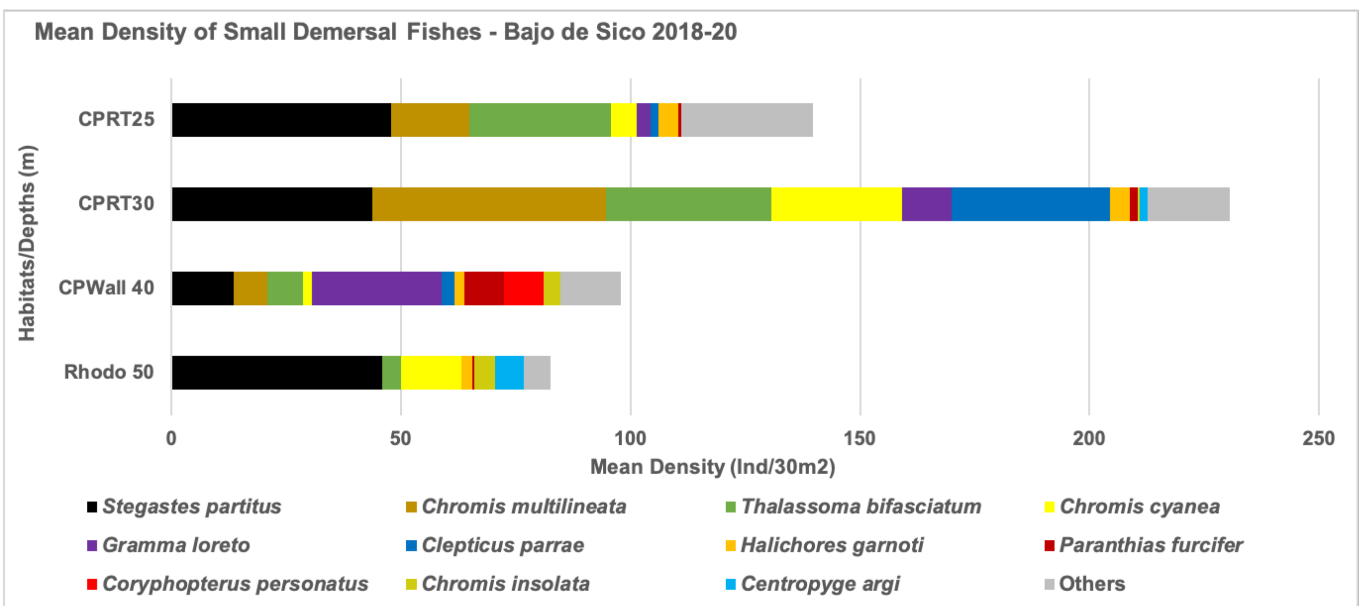

Figure 38. Depth/habitat related variations of mean density by numerically dominant small demersal fishes surveyed within the 25 – 50m depth range at Bajo de Sico, 2018-20 survey.

Small demersal fish community structure similarities between habitats/depths based on the relative densities from belt-transects surveyed within the 25 – 50m depth profile at BDS during the 2018-20 survey are displayed in a non-metric multi-dimensional scaling plot (nMDS) of Bray-Curtis similarities in Figure 39. Benthic habitats were used as discriminatory factor for testing fish community structure similarities since different habitats were sampled across the 25 - 50m depth range. The highest similarity of fish community structure corresponded to the reef top habitats CPRT25 (73.2%) and CPRT30 (69.9%), largely contributed by the coney (*Cephalopholis fulva*), bicolor damselfish (*Stegastes partitus*), longspine squirrelfish (*Holocentrus rufus*), bluehead wrasse (*Thalassoma bifasciatum*), and the blue and brown chromis (*Chromis cyanea, C. multilineata*) (Table 18). Similarity at the CPWall40 (47.9%) was mostly contributed by fairy basslet (*Gramma loreto*), whereas cherubfish (*Centropyge argi*) was the main species contributing similarity at Rhod50. Numerically dominant species distributed across the entire habitat/depth range surveyed, such as *S. partitus* and yellowhead wrasse (*H. garnoti*) contributed markedly to similarity both within and between habitats/depths. An additional nine (9) species were observed within belt-transects throughout the 25m – 50m habitat/depth range surveyed.

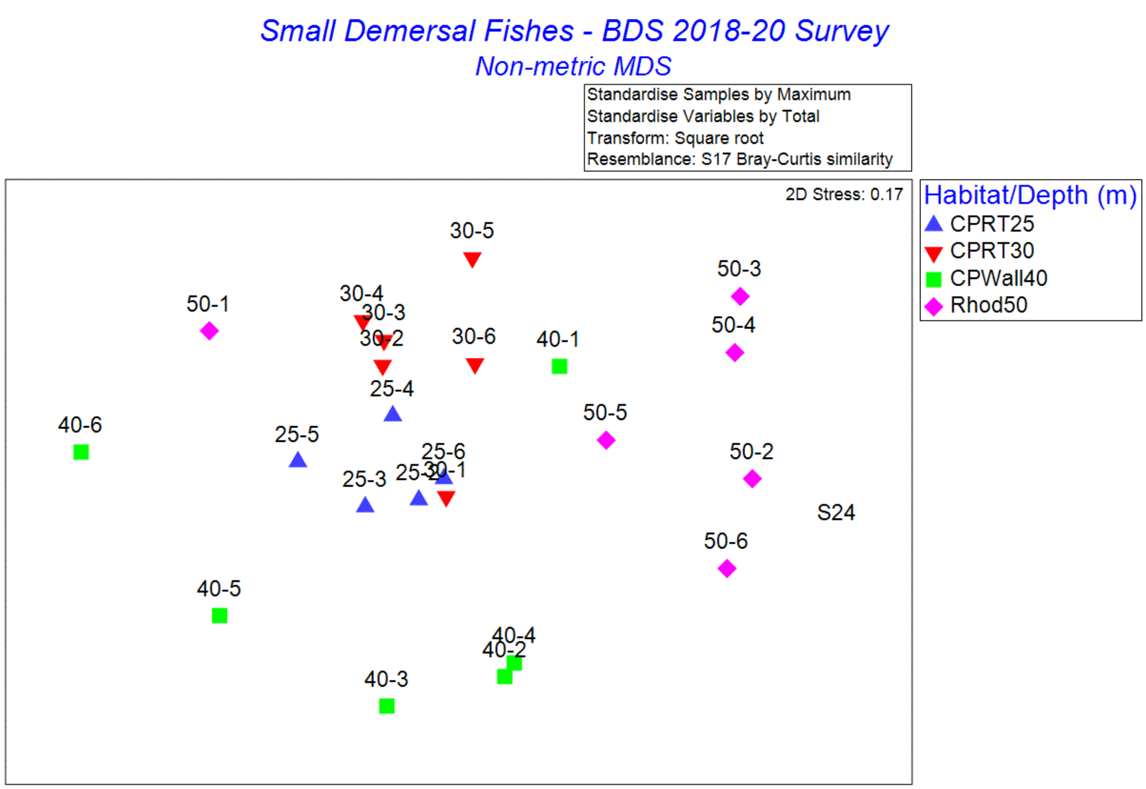

Figure 39. Non-metric multidimensional scaling (nMDS) plot of Bray-Curtis similarities between habitats/depths based on the relative densities of small demersal fishes from 10m x 3m belt-transects surveyed within the 25 – 50m depth profile at Bajo de Sico, 2018-20 survey

Table 18. Similarity matrix of small demersal fish community structure at the main benthic habitats/depths surveyed from Bajo de Sico during 2018-20, including species contributions to the within habitat similarity.

	CPRT25	CPRT30	CPWall40	Rhod50
Average Similarity (%)	73.2	69.9	47.9	61.6
Species Contributions				
Cephalopholis fulva	18.1			
Stegastes partitus	17.8	12.0	15.1	24.2
Thalassoma bifasciatum	17.7	12.0	14.2	
Holocentrus rufus	15.8		9.9	
Halichoeres garnoti	15.2	11.5	12.0	13.1
Chromis multilineata		15.8		
Chromis cyanea		14.0		13.9
Clepticus parrae		12.1		
Gramma loreto			25.9	
Centropyge argi				26.0

Dissimilarity between habitats/depths was highest between the CPWall40 and Rhod50 (60.9%) strongly influenced by the density differences of numerically dominant species, such a fairy basslet (*Gramma loreto*), and cherubfish (*Centropyge argi*). The fairy basslet is adapted to live upside-down in crevices and ledges that are common features of walls (e.g., CPWall40) and other vertically oriented habitats, whereas cherubfish prefers small microhabitats in horizontally oriented habitats, such as rhodolith beds (e.g., Rhod50). Cherubfish was also the main species contributing to the dissimilarity between Rhod50 and all other habitats/depths surveyed (Table 19). Likewise, fairy basslet was one of the main species contributing dissimilarity between the CPWall40 and all other habitats surveyed from BDS within the 25 – 50m depth range. Dissimilarity was lowest between the CPRT25 and CPRT30 (30.6%), mostly contributed by numerically dominant species with highly aggregated distributions, such as creole wrasse (*Clepticus parrae*) and blue chromis (*Chromis cyanea*). Such aggregated distributions introduced high sampling variability error for comparative analyses of fish density between habitats/depths. The low dissimilarity of small demersal fish community structure between CPRT25 and CPRT30 was expected given the continuity and uniformity of the benthic habitat at the rock promontories' reef top, relatively high stony coral cover, and the small depth variation.

Table 19. Dissimilarity matrix (SIMPER) of small demersal fish community structure between habitats/depths surveyed within the 25 – 50m depth range at BDS, 2018-20 survey.

	CPRT25	CPRT25	CPRT25	CPRT30	CPRT30	CPWall40
	vs. CPRT30	vs CPWall40	vs Rhod50	vs CPWall40	vs Rhod50	vs Rhod50
Average Dissimilarity (%)	36.6	49.4	56.1	51.2	54.8	60.9
Species Contributions						
Clepticus parrae	20.3			13.8	14.2	
Cephalopholis fulva	12.5	8.7	7.6			
Chromis cyanea	14.1		10.9	7.4	7.5	8.3
Chromis multilineata	8.8		10.9	9.1	12.8	
Holocentrus rufus	6.7	8.1	11.6	6.9	8.8	8.2
Centropyge argi			18.0		14.4	12.8
Gramma loreto	8.8	14.9		10.1	7.3	12.5
Coryphopterus personatus						7.8
Kyphosus sp.		11.5		9.2		8.4
Paranthias furcifer		8.5		8.0		8.1
Chromis insolata		9.0	10.0	8.1	7.9	9.6
Thalassoma bifasciatum			7.0			

Temporal Variations of Small Demersal Fish Density and Community Structure, 2006-07/ 2018-20

Mean density variations of small demersal fishes between the 2006-07 baseline and the 2018-20 monitoring survey from the main benthic habitats/depths sampled at BDS are shown in Figure 40. Density differences between surveys depended on habitat/depths (Two-Way ANOVA interaction factor; p = 0.05). The largest difference of the total mean density was associated with an 82.2% decline at CPRT25 during the 2018-20 survey relative to 2006-07 (One-way ANOVA; p = 0.023). Differences from other habitats/depths were statistically insignificant (Table 20). Sharp density declines by numerically dominant species, such as the bicolor damselfish (*Stegastes partitus*) and brown chromis (*Chromis multilineata*) were the main drivers of the density difference between surveys at CPRT25 (Figure 41). Density declines by these species at CPRT25 may have been influenced by the turbulent conditions potentially associated with the pas of Hurricanes Irma and Maria in September 2017 and/or winter storm Riley in March 2018 pervious to our monitoring survey at BDS. Density differences of bicolor damselfish and brown chromis at deeper stations were negligible, indicative of no relevant changes to either fish population. Differences of the small demersal fish species richness between surveys were statistically insignificant for all habitats/depths (ANOVA; p > 0.05) indicative of no ecologically relevant changes of small fish community structure between surveys at BDS.

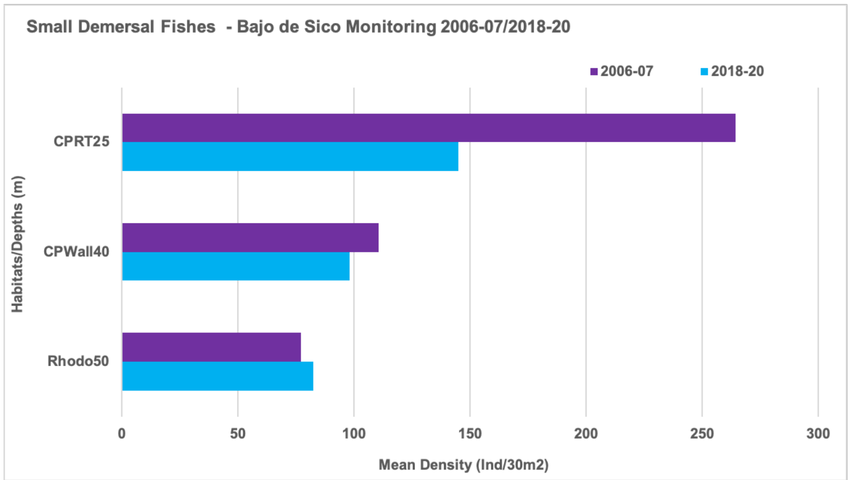

Figure 40. Mean density variations of small demersal fishes between the 2006-07 baseline and the 2018-20 monitoring survey at BDS. Data are means from similar set of stations sampled by 10m x 3m belt-transects at the main habitats/depths.

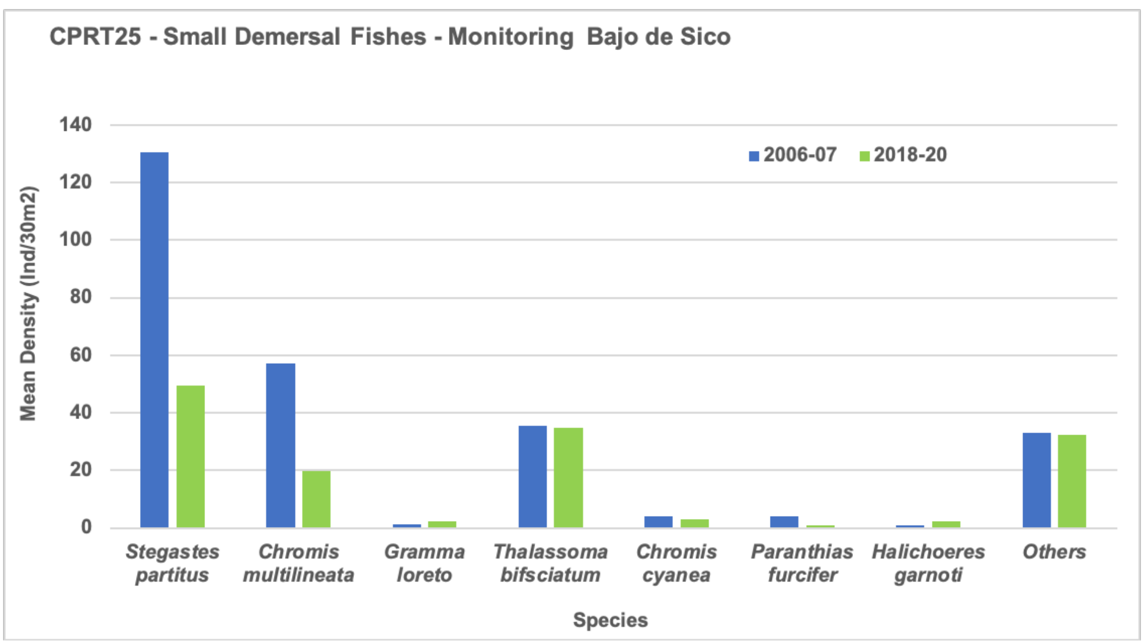

Figure 41. Mean density variations of numerically dominant small demersal fishes between the 2006-07 baseline and the 2018-20 monitoring survey at CPRT25. Data are means from similar set of stations sampled by 10m x 3m belt-transects at CPRT25, BDS.

Table 20. Variations of mean density and species richness of small demersal fishes between the 2006-07 baseline and the 2018-20 monitoring surveys at Bajo de Sico

	Mean Density (Ind/30m2)			One-Way ANOVA	Mean Species Richness (# Spp/30m2)			One-Way ANOVA
Habitat/Depth (m)	2006-07	2018-20	**% Change**	**p-value**	2006-07	2018-20	**% Change**	**p-value**
CPRT25	264.2	145.0	-45.1	**0.023**	20.2	18.0	-10.9	**0.352**
CPWall40	110.5	98.0	-11.3	**0.422**	14.0	11.8	-15.7	**0.086**
Rhod50	77.0	82.5	7.1	**0.741**	8.8	8.7	-1.1	**0.767**

Similarities of small demersal fish community structure between the 2006-07 baseline and the 2018-20 monitoring surveys are shown in a multidimensional scaling (nMDS) plot of Bray-Curtis similarities in Figure 42. High similarities prevailed between surveys for all of the main habitats/depths driven by distinct habitat/depth specific fish assemblages (Table 21). Highest similarity of community structure between surveys was observed at the CPRT25 (78.8%) contributed by a series of typical neritic reef species, including brown chromis (*Chromis multilineata*), red-spotted hawkfish (*Amblycirrhitus pinos*), black durgon (*Melichthys niger*), stripped and princess parrotfishes (*Scarus iseri, S. taeniopterus*), bicolor damselfish (*Stegastes partitus*), bluehead wrasse (*Thalassoma bifasciatum*), blue tang (*Acanthurus coeruleus*), graysbe and coney (*Cephalopholis cruentatus, C. fulva*). Similarity at the CPWall40 was mostly contributed by fairy basslet (*Gramma loreto*), Caribbean puffer (*Canthigaster rostrata*) and sunshine chromis (*C. insolata*), whereas cherubfish (*Centropyge argi*) and blue chromis (*C. cyanea*) were the main contributors to similarity at Rhod50. These data suggest that the community structure of small demersal fishes remained stable between surveys at BDS.

Large Demersal Fishes and Shellfishes

Depth/habitat related variations of fish density and community structure, 2018-20

Mean densities of large demersal fishes and shellfishes (queen conch and spiny lobster) surveyed by drift belt-transects within the 25 – 50m depth range at BDS during 2018-20 are listed in Table 22. Mean densities varied between 24.3 Ind/10^3m^2 at Rhod50 and 35.8 Ind/10^3m^2 at CPRT50. The combined densities of nine (9) fishes and one shellfish represented 91.6% of the total density within transects surveyed across all habitats/depths. Density differences between habitats/depths for the total fish/shellfish assemblage were not statistically significant (One-way ANOVA; p = 0.947) but marked habitat/depths related patterns were noted for some numerically dominant species, such as Coney (*Cephalopholis fulva*), Nassau grouper (*Epinephelus striatus*), lionfish (*Pterois sp.*). and queen triggerfish (*Balistes vetula*) (Figure 43).

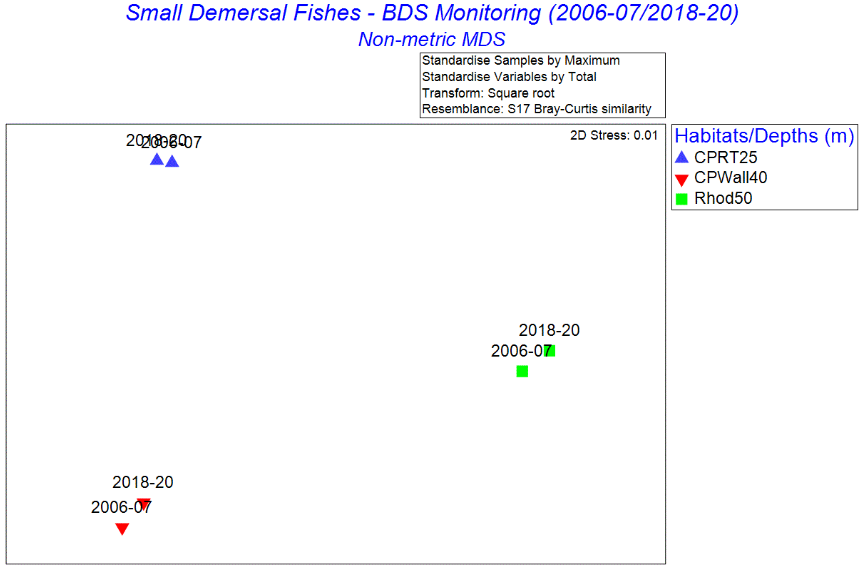

Figure 42. Non-metric multidimensional scaling (nMDS) plot of Bray-Curtis similarities between the 2006-07 baseline and the 2018-20 monitoring survey based on the relative densities of small demersal fishes from the main habitats/depths surveyed from Bajo de Sico.

Table 21. Similarity matrix (SIMPER) of small demersal fish community structure between the 2006-07 baseline and the 2018-20 monitoring surveys at the main habitats/depths from Bajo de Sico.

	CPRT25	CPWall40	Rhod50
Average Similarity (%)	78.8	70.3	67.4
Species			
Chromis multilineata	9.2		
Amblycirrhitus pinos	8.9		7.7
Melichthys niger	8.3		
Scarus iseri	8.3		
Stegastes partitus	7.5		12.4
Thalassoma bifasciatum	7.0		
Cephalopholis cruentatus	6.4	6.7	
Acanthurus coeruleus	6.3		
Scarus taeniopterus	6.3		
Cephalopholis fulva	5.9		
Gramma loreto		10.3	
Canthigaster rostrata		8.2	
Chromis insolata		7.6	
Bodianus rufus		7.2	
Coryphopterus personatus		7.1	
Prognathodes aculeatus		7.1	
Halichores garnoti		6.6	8.6
Cephalopholis fulva		6.4	
Centropyge argi			18.5
Chromis cyanea			15.9

Table 22. Taxonomic composition and mean densities of large demersal fishes and shellfishes surveyed by drift belt-transects across the 25 – 50m depth range at Bajo de Sico, 2018-20 survey

Toal Area Surveyed (m^2)		8,221.35		10,427.29		11,254.63
Depth range (m)	CPRT30		CPRT40		Rhod50	
	8,221.3	MEAN	10,427.29	MEAN	11,254.63	MEAN
Fish Species	Total Ind.	Ind/10^3m^2	Total Ind.	Ind/10^3m^2	Total Ind.	Ind/10^3m^2
Cephalopholis fulva	155	19.38	83	13.53	71	8.61
Epinephelus guttatus	25	3.11	17	2.56	37	4.55
Elagatis bipinnulata	13	2.00	9	1.91	34	4.77
Lutjanus apodus	0	0.00	26	6.34	0	0.00
Balistes vetula	3	0.40	4	0.55	14	1.88
Epinephelus striatus	11	1.47	10	1.86	1	0.10
Pterois sp.	19	2.30	23	4.64	1	0.13
Sphyraena barracuda	4	0.53	0	0.00	5	0.54
Ocyurus chrysurus	2	0.29	3	0.64	6	0.79
Scomberomorus regalis	3	0.30	0	0.00	3	0.49
Cephalopholis cruentatus	5	0.52	1	0.21	0	0.00
Mycteroperca venenosa	3	0.35	1	0.12	2	0.22
Dasyatis americana	1	0.14	2	0.37	1	0.13
Ginglymostoma cirratum	0	0.00	3	0.61	1	0.13
Mycteroperca bonaci	1	0.10	3	0.70	0	0.00
Caranx crysos	0	0.00	2	0.42	0	0.00
Gymnothorax funebris	1	0.16	0	0.00	1	0.13
Lactophrys triqueter	3	0.42	0	0.00	1	0.13
Calamus bajonado	0	0.00	0	0.00	1	0.09
Caranx hippos	0	0.00	1	0.21	0	0.00
Caranx lugubris	0	0.00	1	0.12	0	0.00
Lactophrys trigonus	1	0.15	0	0.00	0	0.00
Lutjanus cyanopterus	1	0.10	0	0.00	1	0.09
Lutjanus jocu	1	0.15	1	0.15	0	0.00
Mycteroperca intersititialis	1	0.10	0	0.00	0	0.00
Mycteroperca tigris	1	0.10	0	0.00	0	0.00
Scarus guacamaia	0	0.00	1	0.24	0	0.00
Scomberomorus cavalla	1	0.14	0	0.00	0	0.00
Sparisoma viride (tpm)	0	0.00	1	0.21	0	0.00
Panulirus argus	1	0.16	1	0.12	1	0.10
Lobatus gigas	9	1.02	2	0.33	14	1.43
Mean Density (Ind/10^3m^2)	**265**	**33.38**	**195**	**35.84**	**195**	**24.33**
Total Individuals	**265**		**195**		**195**	

Mean density of coney (*Cephalopholis fulva*) declined with depth (Figure 43), but differences were statistically insignificant (ANOVA, $p = 0.211$) due to the within habitat/depth sampling variability. Coney was the numerically dominant species surveyed across all habitats/depths, despite a 55.6% density decline between the CPRT30 and the Rhod50. Nassau grouper (*Epinephelus striatus*) and lionfish (*Pterois sp*) both exhibited higher densities at the CPRT30 and CPWall40 than at Rhod50 (ANOVA; $p < 0.05$). These species appeared to prefer the higher rugosity and large crevices and ledges associated with rock promontories that prevailed within the 25 – 40m depths, compared to the mostly flat and homogeneous rhodolith bed habitat in the 45 - 50m range. Conversely, densities of queen triggerfish (*Balistes vetula*) were significantly higher at Rhod50 (ANOVA; $p = 0.005$). The vertical distribution pattern of *B. vetula* was probably more influenced by habitat type than depth, since the rhodolith habitat functions as the courtship and nesting grounds for adult queen triggerfish.

Other relevant habitat/depth related distributions of large demersal fishes/shellfishes at BDS include the peak densities of rainbow runner (*Elagatis bipinnulata*) at Rhod50, and peak density of schoolmaster snapper (*Lutjanus apodus*) at CPWall40. Rainbow runner is a schooling coastal pelagic species that feeds on reef fishes at BDS and is thereby transitional across the entire habitat/depth range surveyed. This is an important forage species for many large coastal and migratory pelagic species that forage at BDS, including wahoo (*Acanthosybium solandri*), king mackerel (*Scomberomorus cavalla*), tunas (*Thunnus spp*), dolphinfish (*Coryphaena hippurus*), and blue and white marlins (*Makaira nigricans, Kajikia albida*).

Large schooling aggregations of schoolmaster snappers (*L. apodus*) have been previously reported from BDS (Garcia-Sais et al, 2007) and appeared to be associated with the rock promontories but have been typically observed at the sides (walls) of the promontories in areas protected from the current. Queen conch (*Lobatus gigas*) was observed throughout the depth range in horizontally projected habitats surveyed at BDS, both at the reef top and sand/rubble channels separating rock promontories of the CPRT30, CPRT40, and at Rhod50.

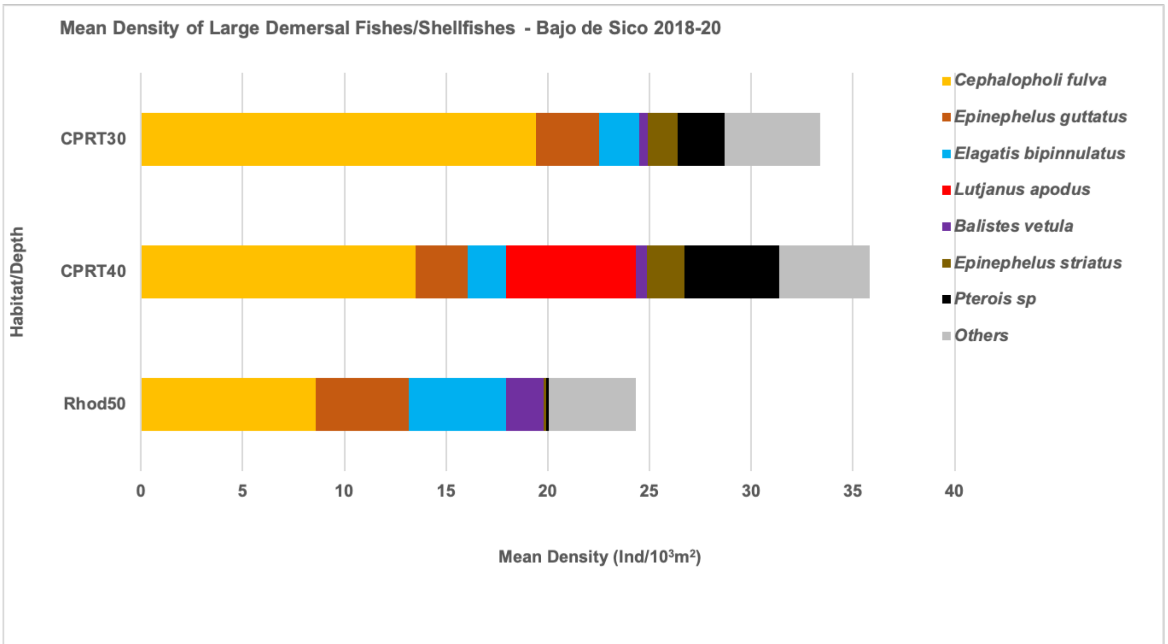

Figure 43. Mean densities of large demersal fishes surveyed by drift belt-transects across the main habitats in the 25 – 50m depth range at Bajo de Sico, 2018-20 survey

Community structure variations of large demersal fish species and shellfishes surveyed within the main benthic habitats in the 25 – 50m depth profile at BDS during the 2018-20 survey are displayed in a non-metric multi-dimensional scaling plot (nMDS) based on Bray-Curtis similarities in Figure 44. Benthic habitats were used as discriminatory factor for testing fish community structure similarities since different habitats were sampled across the depth profile. Similarities between habitats/depths were generally low, indicative of distinctive fish assemblages prevailing at the different habitats/depths surveyed. The highest similarity of fish community structure corresponded to Rhod50 (39.0%), largely contributed by queen triggerfish (*Balistes vetula*), red hind (*Epinephelus guttatus*), and coney (*Cephalopholis fulva*) (Table 23). Both *E. guttatus* and *C. fulva* exhibited high habitat plasticity with relatively high contributions to similarity across all habitats/depths.

Dissimilarity of large demersal fish/shellfish community structure was highest between CPRT40 and Rhod50 (75.4%) largely contributed by the higher densities of lionfish (*Pterois sp*), Nassau grouper (*Epinephelus striatus*), and nurse shark (Ginglymostoma cirratum) at CPWall40, and the higher densities of queen triggerfish (*Balistes vetula*), blue runner (*Elagatis bipinnulata*), and cero mackerel (*Scomberomorus regalis*) at Rhod50. An essentially similar assemblage with additional contributions from queen conch (*Lobatus gigas*) separated CPRT30 from Rhod50 (Table 24).

Dissimilarities between CPRT30 and CPRT40 were mostly contributed by the higher densities of dog snapper (*Lutjanus jocu*) and graysbe (*Cephalopholis cruentatus*) at CPRT30, and higher densities of black grouper (*Mycteroperca bonaci*), nurse shark (*G. cirratum*), and blackjack (*Caranx lugubris*) at CPRT40, but such dissimilarities were based on very small sample sizes (1-2 fish individuals).

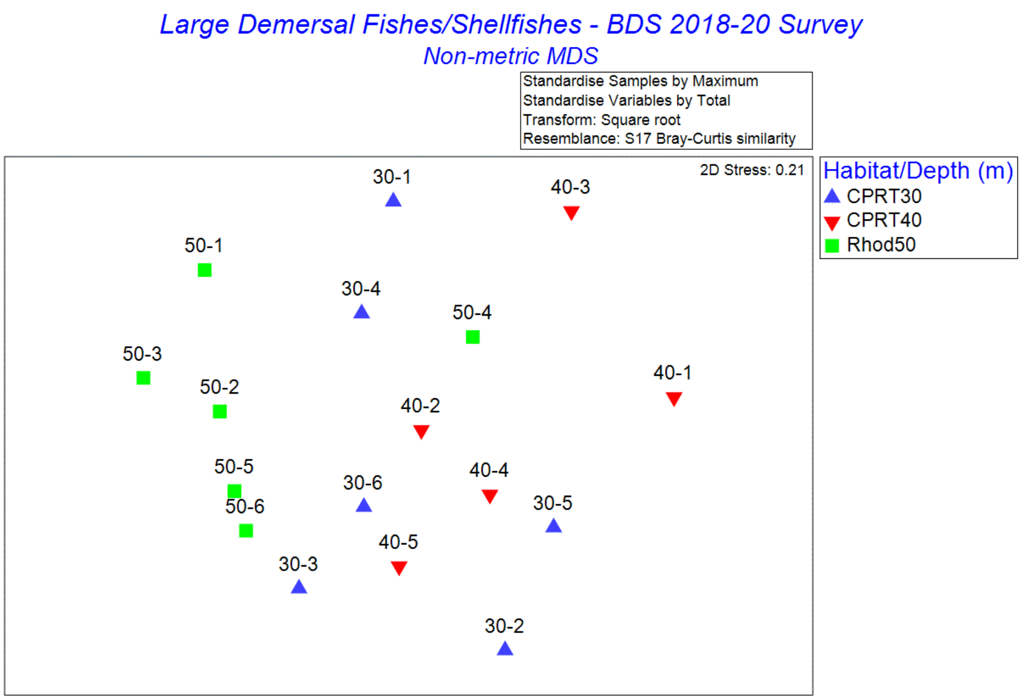

Figure 44. Non-metric multidimensional scaling (nMDS) plot of Bray-Curtis similarities of large demersal fish/shellfish relative densities within drift belt-transects surveyed from mesophotic benthic habitats in the 25 – 50m depth range at Bajo de Sico, 2018-20 survey.

Table 23. Similarity matrix (SIMPER) of large demersal fish community structure between habitats/depths surveyed at Bajo de Sico across the 25 – 50m depth range, with species contributions to similarity within habitats/depths.

	CPRT30	CPRT40	Rhod50
Average Similarity (%)	27.2	27.1	39.0
Species Contributions			
Cephalopholis fulva	28.4	25.0	19.5
Epinephelus striatus	19.4	16.8	
Epinephelus guttatus	16.3	15.7	24.8
Pterois sp.	15.8	24.2	
Balistes vetula			28.2

Table 24. Dissimilarity matrix (SIMPER) of large demersal fish community structure between habitats/depths surveyed at Bajo de Sico across the 25 – 50m depth range, with species contributions to dissimilarity within habitats/depths.

	CPRT30 vs. CPRT40	CPRT30 vs Rhod50	CPRT40 vs Rhod50
Average Dissimilarity (%)	70.7	72.1	75.4
Species Contributions			
Ginglymostoma cirratum	5.2		5.5
Caranx lugubris	4.9		5.0
Cephalopholis cruentatum	4.6		
Lutjanus jocu	5.8		
Dasyatis americana	5.1		
Mycteroperca bonaci	4.2		
Balistes vetula		4.8	5.3
Scomberomorus regalis		4.8	5.8
Elagatis bipinnulata		4.1	5.1
Lobatus gigas		4.2	
Lactophrys triqueter			
Epinephelus striatus		4.0	4.9
Pterois sp.		3.8	6.3

Temporal variations of large demersal fishes/shellfishes between the 2011 baseline and the 2018-20 monitoring survey

Large demersal fishes and shellfishes were surveyed during the 2011 baseline and the 2018-20 monitoring survey from a similar set of 16 sampling stations across the 25 – 50m depth range at BDS. Density differences of the total large demersal fish/shellfish assemblage between surveys were statistically insignificant (Two-way ANOVA; $p = 0.385$), despite a 127.3% and a 38.3% mean density increments from the CPRT30 and CPRT40 during 2018-20 relative to the 2011 baseline survey (Table 25). Density increments by numerically dominant species, such as red hind (*Epinephelus guttatus*), rainbow runner (*Elagatis bipinnulata*), Nassau grouper (*E. striatus*), and lionfish (*Pterois sp*),) contributed markedly to the density increments between surveys at CPRT30 and CPWall40 during 2018-20 (Figures 45 and 46). Density differences between surveys were statistically significant (ANOVA; $p < 0.05$) for *E. guttatus, E. striatus*, and *E. bipinnulata* (Table 26). The mean density contributions from the aforementioned assemblage were partially offset by the mean density reductions during 2018-20 of queen conch (*Lobatus gigas*) throughout the habitat/depth range surveyed, and from the schoolmaster snapper (*Lutjanus apodus*) at CPRT40 and Rhod50 (Figures 46 and 47). Density differences between surveys for *L. gigas* and *L. apodus* were statistically insignificant (ANOVA; $p > 0.05$).

Table 25. Variations of the mean density by the total large demersal fishes/shellfishes surveyed across the main habitats and depths (25 – 50m) during the 2011 baseline and 2018-20 monitoring survey at Bajo de Sico.

Habitat/Depth (m)	2011	2018-20	% Change
CPRT30	6.16	14.00	127.3
CPRT40	16.14	22.32	38.3
Rhod50	16.90	15.87	-6.1

Table 26. Variations of the site mean densities by the numerically dominant fishes/shellfishes surveyed across the main habitats/depths in the 25 – 50m range during the 2011 baseline and 2018-20 monitoring surveys at Bajo de Sico.

	Site Means			ANOVA
Species	**2011**	**2018-20**	**% Change**	**p-value**
Lutjanus apodus	6.68	1.98	-70.4	0.302
Epinephelus guttatus	1.03	3.28	218.9	< 0.001*
Elagatis bipinnulata	0.21	3.14	1380.9	0.019*
Epinephelus striatus	0.42	1.13	166.2	0.046*
Pterois sp.	1.07	2.36	121.5	0.158
Lobatus gigas	1.29	0.63	-51.2	0.361
Balistes vetula	0.42	0.95	128.2	0.059

* Statistically significant at $p < 0.05$

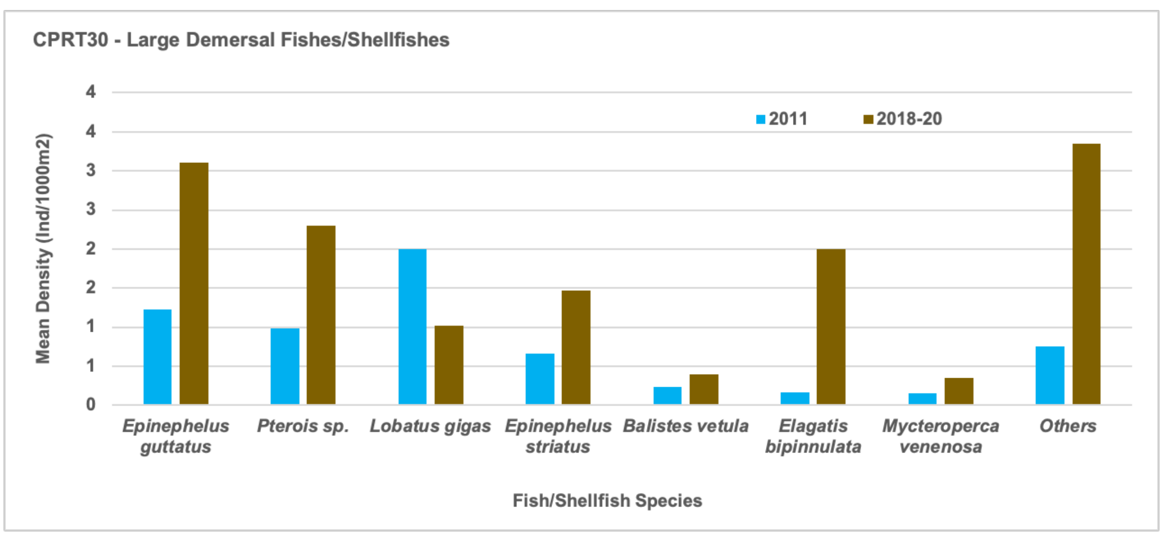

Figure 45. Variations of mean density by large demersal fishes/shellfishes between the 2011 baseline and the 2018-20 monitoring survey at CPRock30, BDS

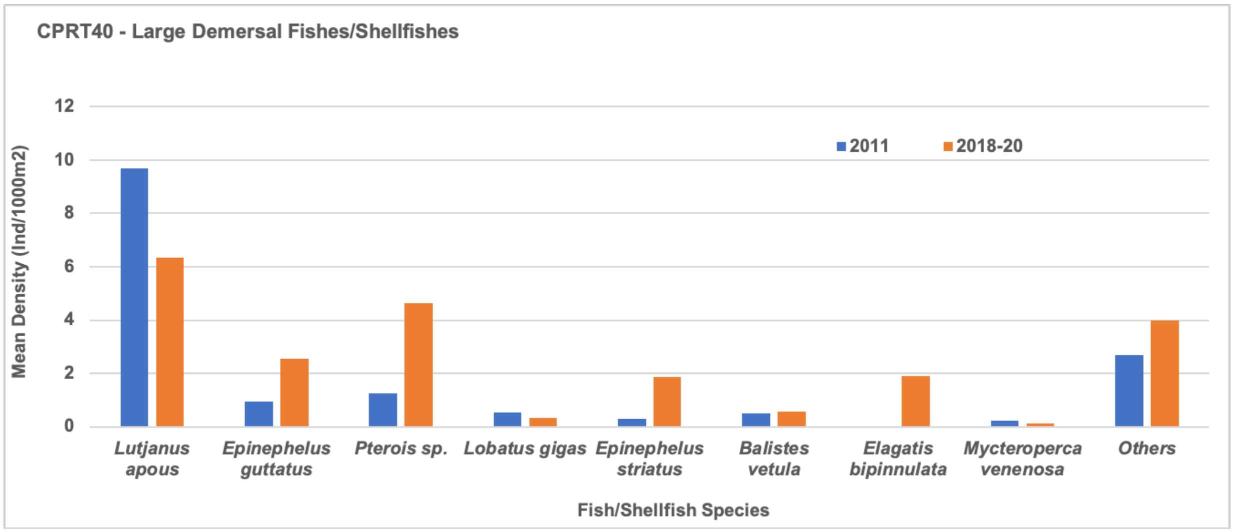

Figure 46 Variations of mean density by large demersal fishes/shellfishes between the 2011 baseline and the 2018-20 monitoring survey at CPRock40, BDS

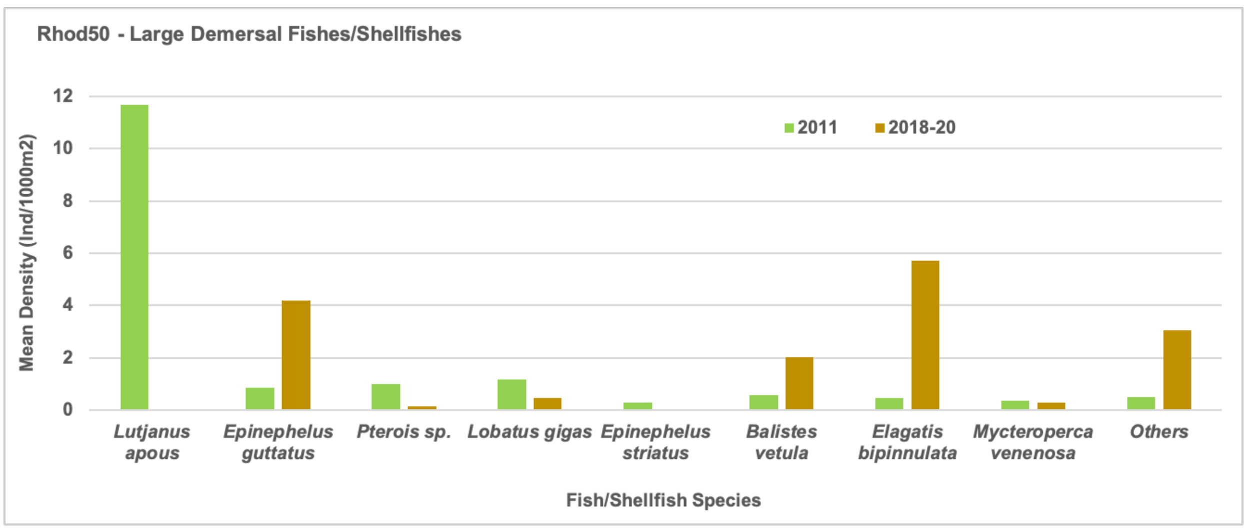

Figure 47. Variations of mean density by large demersal fishes/shellfishes between the 2011 baseline and the 2018-20 monitoring survey at Rhodo50, BDS

Density increments of red hind (*Epinephelus guttatus*) between surveys at BDS appear to be real and consistent with a pattern of increased density across most mesophotic habitats included in the 2018-20 monitoring survey (Garcia-Sais et al, this volume). Such trends of increasing red hind population size may be related to complex socioeconomic issues resulting in the reduction of fishing mortality due to a release of fishing effort. Also, increased awareness and compliance by commercial and recreational fishermen to state and federally regulated seasonal fishing closures directed to the protection of red hind spawning aggregations may be contributing to increased spawning biomass and recruitment. The possibility of increased larval transport and/or adult red hind spillover from prime permanently closed to fishing red hind mesophotic habitats in the USVI, such as the Hind Bank Marine Conservation District and Grammanik Bank, south of St. Thomas, and the Mutton Snapper Bank and Lang Bank, St. Croix, USVI may have contributed to the recuperation trend of the red hind population in the Puertorrican shelf. Density increments of Nassau grouper (*E. striatus*) measured during the 2018-20 survey must be evaluated with caution due to small sample size (total 31 Individuals) but is indicative of a still thriving *E. striatus* population at BDS. Statistically significant density increments between surveys were also detected for rainbow runner (*Elagatis bipinnulata*). This is a coastal pelagic schooling species with a wide distribution range that may be beyond the Puertorrican shelf and thereby, such density fluctuations may have resulted by chance or associated with density independent factors, such as the recruitment dynamics of the population, water current patterns, etc. Whatever the factors influencing such density increments, the occurrence of this species is highly relevant to the trophic dynamics of the large pelagic fish community at BDS.

Size distributions of numerically dominant large demersal fish/shellfish species, BDS 2011 /2018-20 survey

Coney (*Cephalopholis fulva*)

Coney (*C. fulva)* was the most abundant fish species identified within drift belt-transects at BDS with a site mean density of 10.3 Ind/10^3m^2 in 2018-20. Two main modes at 20cm and 22cm (TL), representative of 34.2% of the total individuals were noted from the size distribution based on a sample of 371 individuals (Figure 48). The length at maturity of *C. fulva* was reported at 14.5cm (Froese and Pauly, 2019). Therefore, both size modes were part of the adult population with individuals reaching up to a maximum size of 34cm. The juvenile population represented by individuals smaller than 14cm accounted for only 5.2% of the total, indicative of a population largely comprised by adults. It is possible that juveniles were underestimated due to their semi-cryptic behavior and the high rugosity and habitat complexity of the rock promontories at BDS. Recruitment of coneys into the mesophotic habitats of BDS was observed at 8cm, but smaller individuals were observed within 10m x 3m belt-transects. Coneys were not included in the 2011 survey because they were not considered as a large demersal species but given their relatively high density and commercial value it is now considered as one of the most important grouper species in terms of total biomass within mesophotic habitats of BDS and other mesophotic habitats within the Puertorrican shelf.

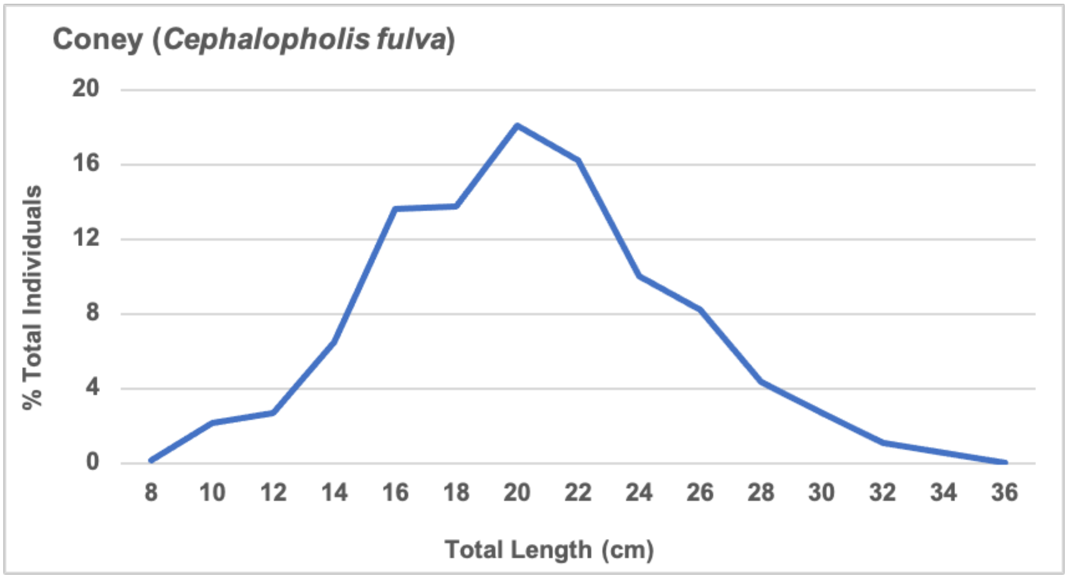

Figure 48. Size distribution of coney (*Cephalopholis fulva*) at Bajo de Sico. 2018-20 survey

Red Hind (*Epinephelus guttatus*)

Red hind (*E. guttatus*) was the second most abundant fish species surveyed by drift belt-transects from mesophotic habitats (25 – 50m) at BDS during 2018-20 with a site mean density (all habitats/depths) of 3.28 Ind/10^3m^2 and ranked third in 2011 with a site mean of 1.03 Ind/10^3m^2. Size frequency distributions based on a total of 144 individuals during both surveys are presented in Figure 49. Two main total length (TL) modes at 32cm and 30cm were consistent during both surveys. The 2011 size distribution curve was more skewed toward larger fishes due to the higher proportion of individuals smaller than 30cm in 2018-20. Differences in the size distributions of *E. guttatus* between surveys were not statistically significant (Kolmogorov-Smirnov, $p > 0.10$), but the increase of smaller sizes in 2018-20 is indicative of active recruitment and population replenishment.

Red hind is a commercially important species under management by both state and federal government administrations and regulations include fishing closures during its seasonal spawning aggregation from December – February. Size at maturity of red hind (*E. guttatus*) was reported at 25cm (Froese and Pauly, 2019). Thus, approximately 15.2% of the population were juveniles in 2011, whereas the juvenile population increased to 28.3% during 2018-20. Recruitment size for *E. guttatus* into mesophotic habitats of BDS was observed at 16cm during both surveys. The maximum size at 43cm TL was also observed during both surveys.

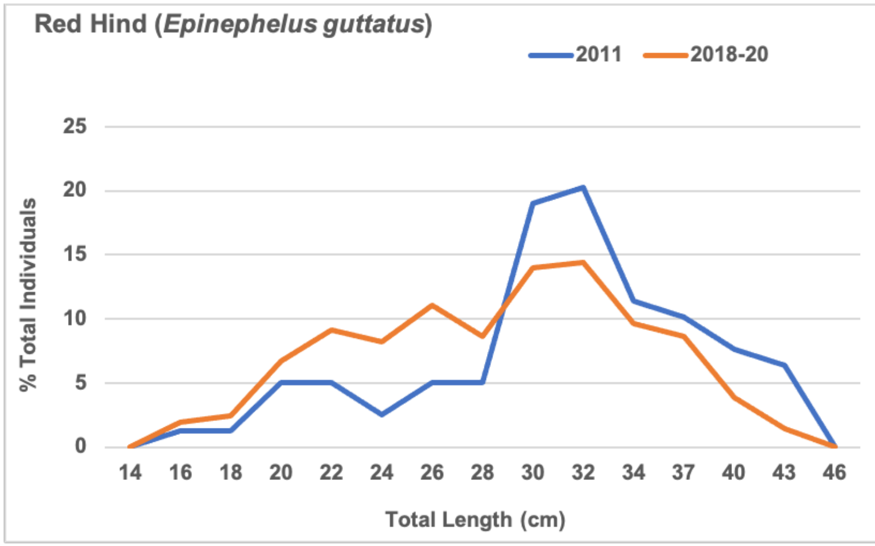

Figure 49. Size distribution of red hind (*Epinephelus guttatus*) during the 2011 baseline and the 2018-20 monitoring surveys at Bajo de Sico

Queen Triggerfish (*Balistes vetula*)

A total of 60 queen triggerfish (*Balistes vetula)* individuals were surveyed from mesophotic habitats (25 – 50m) at BDS during the 2011 baseline and the 2018-20 monitoring surveys. Site mean densities varied from 0.42 Ind/10^3m^2 in 2011 and 0.95 Ind/10^3m^2 in 2018-20. The size distribution of 2011 was more skewed toward larger individuals with a main mode at 46cm and secondary modes at 48cm and 51cm, representative of 50.0% of the total population (Figure 50). A more balanced distribution was observed in 2018-20 with modes at 40cm and 43cm, representative of 39.3% of the total individuals and a much larger proportion of individuals smaller than 40cm. Recruitment size into mesophotic habitats was at 26cm in both surveys. Maximum size was observed at 54cm in 2011 and at 51cm in 2018-20. Differences in the size distribution of *B. vetula* between the 2011 and the 2018-20 surveys were not statistically significant (Kolmogorov-Smirnov, $p > 0.10$). The size at maturity for *Balistes vetula* was reported at 23.5cm (Froese and Pauly, 2019). Thus, all of the *B. vetula* individuals observed from mesophotic habitats at BDS were adults. Queen triggerfish were observed foraging across all habitats/depths surveyed at BDS within the 25 – 50m depth range but were most abundant at rhodolith bed habitats (Rhod50). Courtship and nesting behaviors were observed from reproducing adult populations of *B. vetula* at Rhod50. The marked increment of density between surveys strongly influenced by recruitment of young adults and the consistent size distribution with full adult sizes suggest that the *B. vetula* population is healthy and replenishing within mesophotic habitats of BDS in the 25 – 50m depth range.

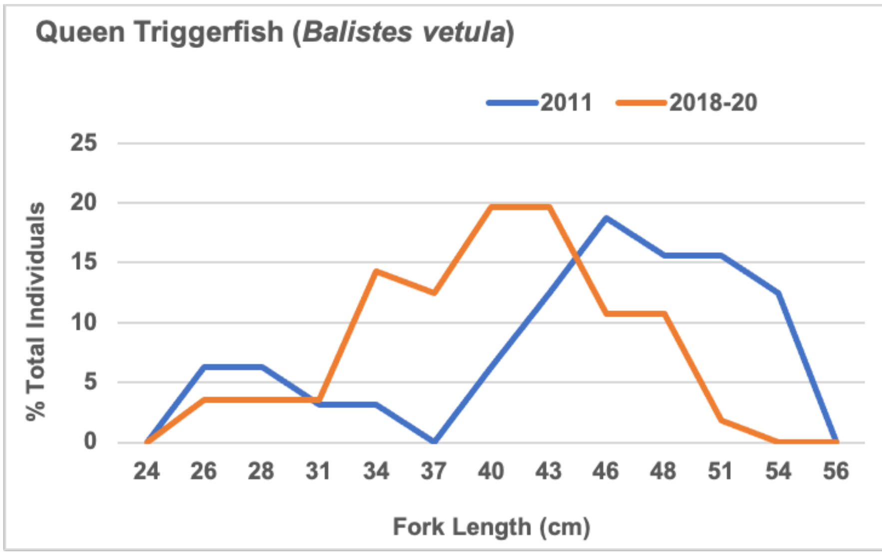

Figure 50. Size distribution of queen triggerfish (*Balistes vetula*) during the 2011 baseline and the 2018-20 monitoring surveys at Bajo de Sico

Lionfish (*Pterois sp*)

A total of 107 *Pterois sp*. individuals were observed from mesophotic habitats in the 25 – 50m depth range at BDS during the 2011 baseline and the 2018-20 monitoring surveys. Site mean densities varied from 1.07 Ind/10^3m^2 in 2011 to 2.36 Ind/10^3m^2 in 2018-20. The size distribution during 2018-20 was strongly skewed toward larger individuals with a main mode at 33cm and a maximum size at 43cm (Figure 51). Individuals larger than 27cm represented 66.7% of the total population in 2018-20. The primary mode in 2011 was at 24cm, with 17.0% of the total individuals larger than 27cm and a maximum size of 33cm. Differences of the size distributions between surveys were statistically significant (Kolmogorov-Smirnov; $p < 0.01$), suggesting growth of the main cohort from 24cm in 2011 to 33cm in 2018-20, but without successful recruitment from smaller size classes.

The size at maturity for *Pterois volitans* has been reported at 23.5cm (Froese and Pauly, 2019) indicative that the lionfish population at BDS was comprised by juveniles and adults in both surveys. Juveniles represented 30.9% of the total lionfish population in 2011, whereas only 10.0% of the population in 2018-20 were juveniles. Despite the increase of lionfish density between surveys, it is evident that this species is experiencing recruitment failure into mesophotic habitats at BDS resulting in a population mostly represented by full adult individuals reaching the maximum size reported for the species at 45.7cm (Froese and Pauly, 2019).

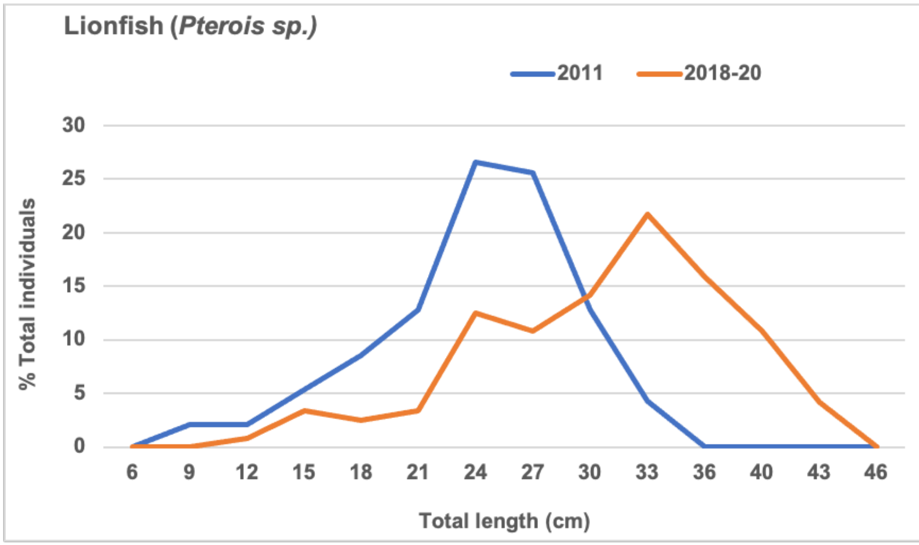

Figure 51. Size distribution of lionfish (*Pterois sp.*) during the 2011 baseline and the 2018-20 monitoring surveys at Bajo de Sico

Nassau Grouper (*Epinephelus striatus*)

A total of 52 Nassau grouper (*Epinephelus striatus*) individuals were identified within mesophotic habitats of BDS in the 25 – 50m depth range during the 2011 baseline and the 2018-20 monitoring surveys. Site means varied from 0.42 Ind/10^3m^2 in 2011 to 1.13 Ind/10^3m^2 in 2018-20. Size frequency distributions for *E. striatus* are presented in Figure 52. The 2011 size distribution was skewed toward the larger individuals with the main mode at 60cm TL. Individuals larger than 60cm represented 64.1% of the total population surveyed in 2011. Modes at 60cm and 65cm prevailed during 2018-20, with 37.5% of individuals larger than 60cm. Differences of size distributions between surveys were not statistically significant (Kolmogorov-Smirnov, $p > 0.10$) due in part to the small sample size.

The size at maturity of Nassau grouper was reported at 48.0cm (Froese and Pauly, 2019), therefore all individuals observed within belt-transects in the 2011 baseline survey were adults, whereas 37.7% of the total individuals the 2018-20 monitoring survey were juveniles. This data is indicative that the 169% increment of *E. striatus* mean density at BDS was largely explained by juvenile recruitment into mesophotic habitats. Additional observations are needed to explain the decline of very large individuals from BDS. It is possible that some of the larger individuals were able to migrate to deeper waters to avoid the turbulent conditions associated with extreme events of wave action associated with the pass of hurricanes in 2017 and winter storm Riley in 2018, or to reach lower temperature waters.

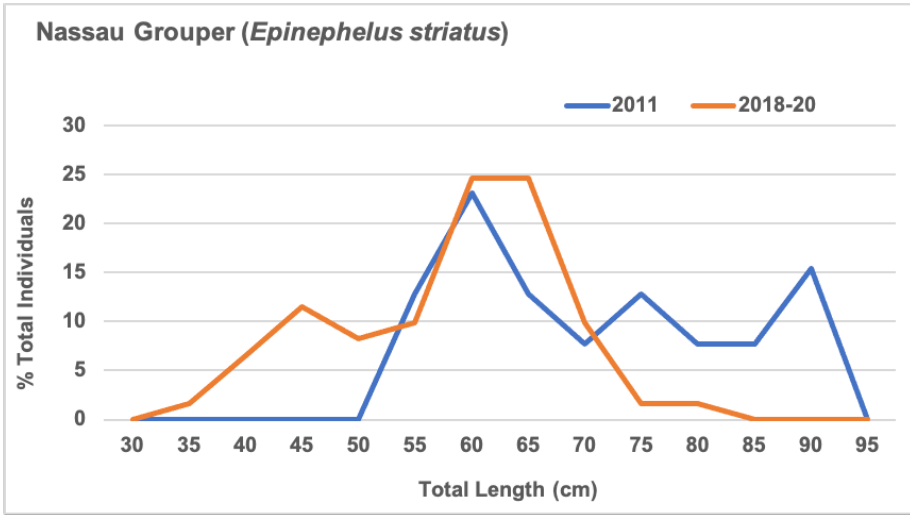

Figure 52. Size distribution of Nassau grouper (*Epinephelus striatus*) during the 2011 baseline and the 2018-20 monitoring surveys at Bajo de Sico

Schoolmaster Snapper (*Lutjanus apodus*)

Schoolmaster (*Lutjanus apodus*) was the numerically dominant large demersal fish species surveyed within drift belt-transects within the 25 – 50m depth range at BDS during the 2011 baseline survey with a site mean density of 6.68 Ind/10^3m^2 and ranked fifth in mean density during the 2018-20 survey with a site mean density of 1.98 Ind/10^3m^2. The size frequency distributions based on a total of 382 individuals during both surveys are presented in Figure 53. Strong primary and secondary modes at 27cm and 30cm FL, representative of 63.1% of the total individuals were observed during 2011, whereas a dominant primary mode at 39cm FL prevailed during 2018-20, representative of approximately 32.6% of the total individuals (Figure 53). The dominant size modes in the 27 – 30cm size classes were associated with a large schooling aggregation of approximately 317 individuals in 2011, with a few larger solitary individuals observed within reef benthic habitats. A much smaller schooling aggregation of 30 individuals was observed during the 2018-20 survey with an additional 19 solitary individuals. Differences in the size frequency distributions between surveys were statistically significant (Kolmogorov-Smirnov, $p < 0.10$) and possibly (at least in part) related to growth of individuals observed during 2011, since individuals smaller than 24cm were not observed during 2011 and may be part of the 39cm primary mode of 2018-20. Maximum size was stable at 45cm during both surveys. Size at maturity of *L. apodus* has been reported as 25cm (Froese and Pauly, 2019). Thus, 81.5% of the total individuals observed during 2011 were adults, whereas 98.9% were adults in 2018-20. Juvenile individuals were observed within drift belt-transects with minimum sizes of 24cm during both surveys.

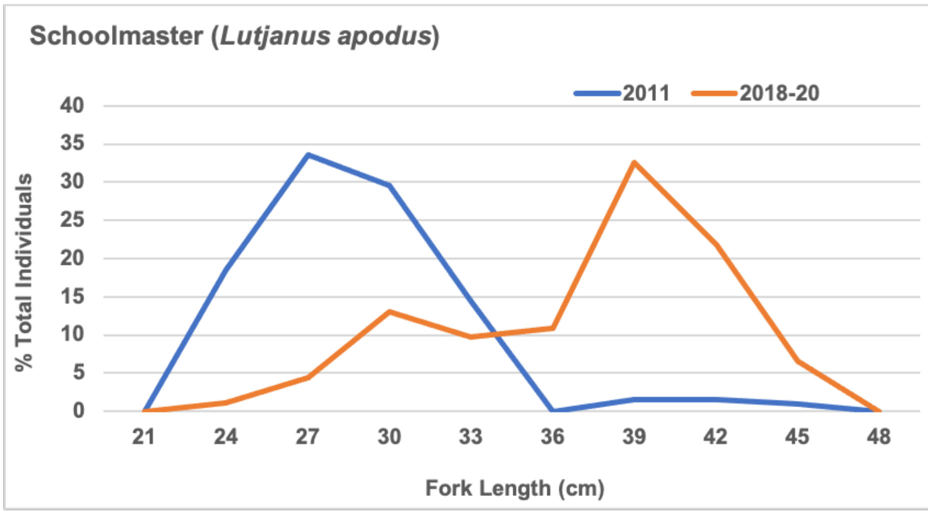

Figure 53. Size distribution of schoolmaster snapper (*Lutjanus apodus*) during the 2011 baseline and the 2018-20 monitoring surveys at Bajo de Sico

Queen Conch (*Lobatus gigas*)

A total of 58 queen conch (*Lobatus gigas*) were observed within drift belt-transects at BDS during the 2011 baseline and the 2018-20 monitoring survey. Site means varied from 1.29 Ind/10^3m^2 in 2011 and 0.63 Ind/10^3m^2 in 2018-20. Size frequency distributions exhibited almost identical curves with a strong primary and secondary modes in the 26cm and 27cm range (shell length) that represented 68.2% and 56.0% of the total individuals during the 2011 and 2018-20 surveys, respectively (Figure 54). Differences of *L. gigas* size distributions between surveys were not statistically significant (Kolmogorov-Smirnoff; $p > 0.10$). Maximum size was measured at 30cm during both surveys. These data are indicative that the queen conch population at BDS is largely comprised by large adults. Individuals smaller than 26cm represented 3% and 12% of the total individuals during the 2011 and 2018-20 surveys, respectively. Recruitment into mesophotic habitats was measured at 22cm.

Spiny Lobster (*Panulirus argus*)

Spiny lobsters (*Panulirus argus*) were rare at BDS during both 2011 and 2018-20 surveys with a total of two (2) individuals observed in 2011, and three (3) individuals observed within drift belt-transects in 2018-20. The size range (cephalothorax length) varied between 10 -12cm in 2011 and between 15 – 17cm in 2018-20. The limited data available suggests that the spiny lobster population at BDS is relatively small and comprised by very large individuals.

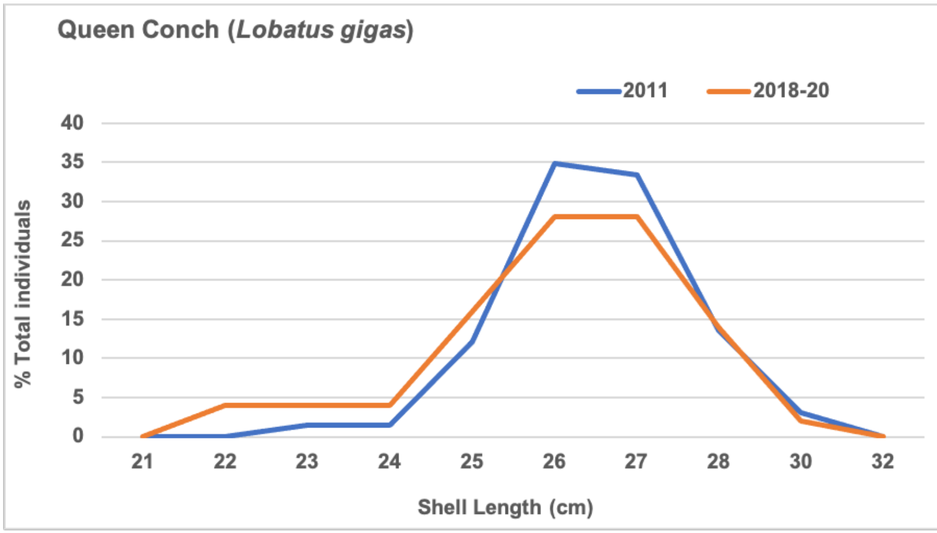

Figure 54. Size distribution of queen conch (*Lobatus gigas*) during the 2011 baseline and the 2018-20 monitoring surveys at Bajo de Sico

Photo Album 2 - BDS

Colonized Pavement Reef Top and Wall

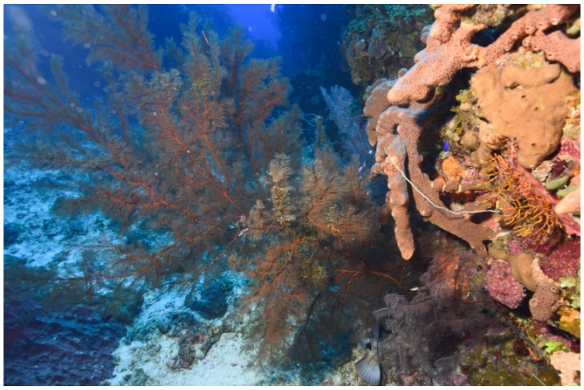

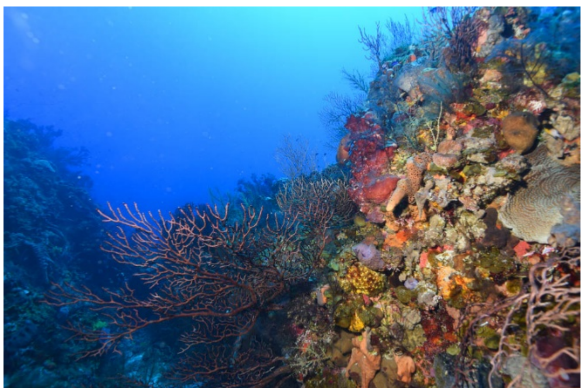

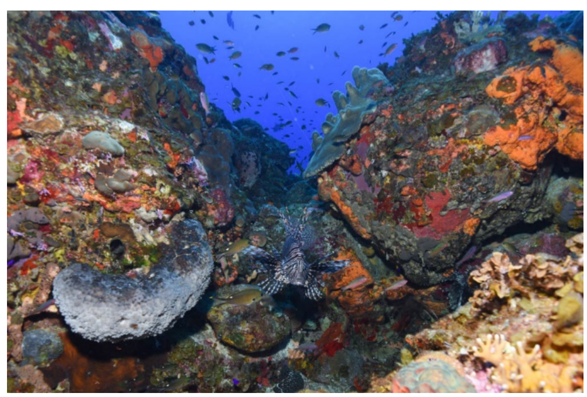






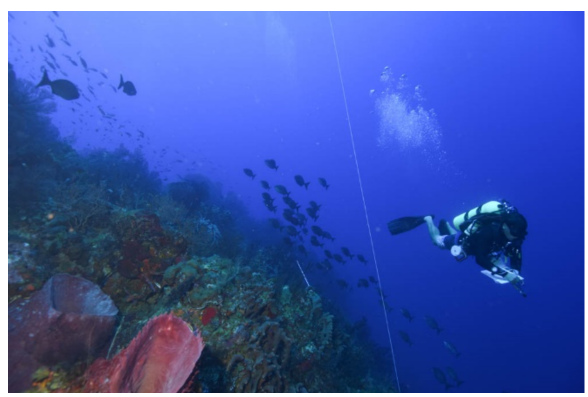

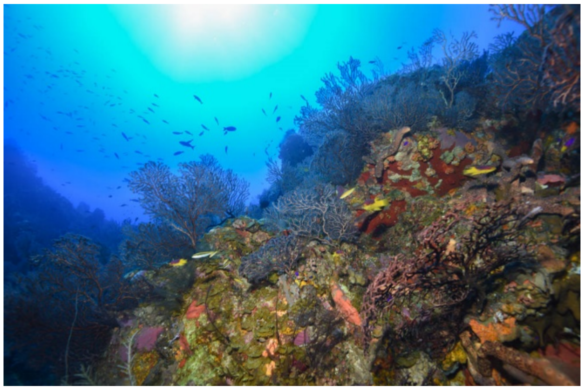

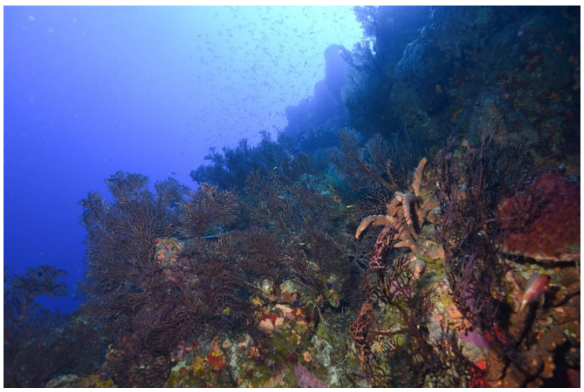




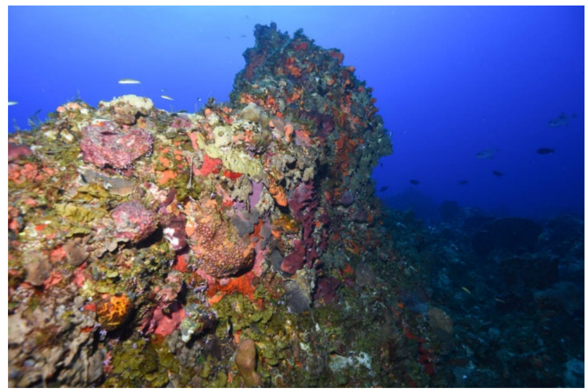

BDS Rhodolith



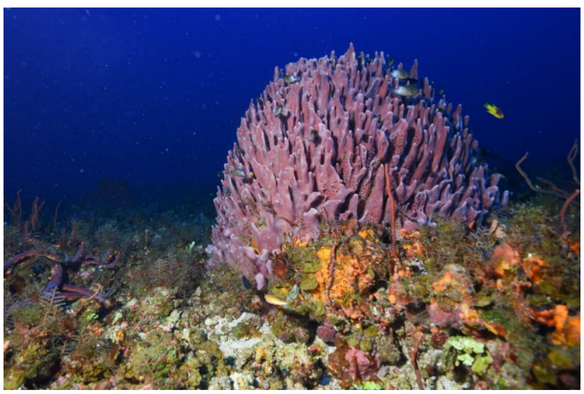
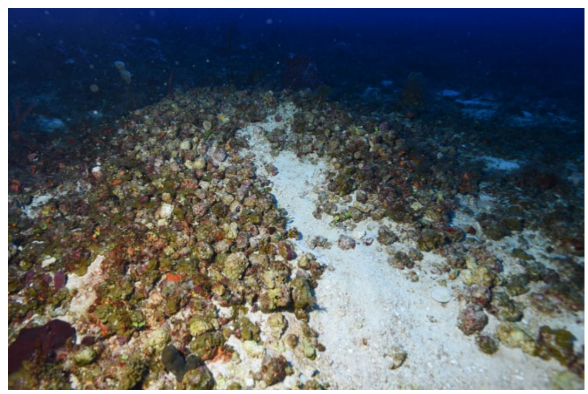

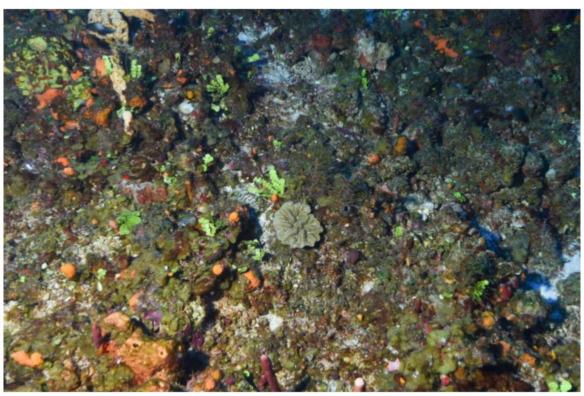

Tourmaline Reef

Physical Description

Tourmaline Reef is located about 15 nautical miles due west of Punta Guanajibo, Cabo Rojo, on the west coast of Puerto Rico. The shelf-edge reef has a horseshoe shape extending approximately 13 nautical miles between Buoy 6 to the southwest and Buoy 8 to the northeast (Figure 55). Because of its partial extension beyond the nine-mile commonwealth jurisdictional limit, Tourmaline Reef is managed both by the Puerto Rico Department of Natural and Environmental Resources (PRDNER) and the Caribbean Fishery Management Council (CFMC). It is seasonally closed to fishing during the spawning aggregation of the red hind (*Epinephelus* guttatus) between January and March. Reef stations within the Tourmaline Reef system were included in the Puerto Rico Coral Reef Monitoring Program (PRCRMP) and monitoring surveys of its coral reef community at depths between 10 – 30m are available from 2000 until present (Garcia-Sais et al., 2019 and references therein). A benthic habitat map (Figure 55) along with baseline quantitative characterizations of the sessile-benthic, fish and shellfish communities associated with mesophotic habitats within the 30 - 50m depth range from the Tourmaline Reef system was prepared by Garcia-Sais et al. (2014).

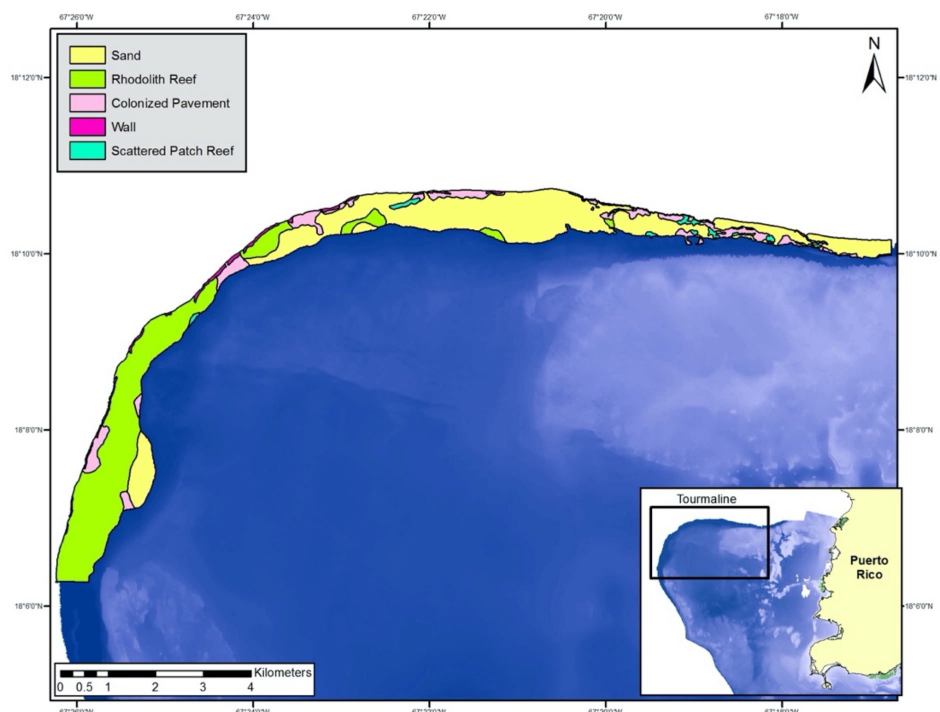

Figure 55. Map of the main benthic habitats distributed within the 30 – 50m mesophotic section of Tourmaline Reef, Mayaguez (from Garcia-Sais et al., 2014).

Five main benthic habitat types were recognized within the 30 – 50 m mesophotic depth range during the baseline survey by Garcia-Sais et al. (2014), these included: 1) sandy substrate; 2) patch coral reef; 3) colonized pavement; 4) rhodolith bed; and 5) slope wall. Sand was the main substrate type in terms of areal cover with approx. 6.7 km^2, or 48.1% of the total mesophotic study area. Rhodolith beds were the most prominent biologically colonized benthic habitat in terms of areal cover with 5.19 km^2, or 37.5% of the total study area within the 30 – 50 m depth range. Coral reef habitats were limited to a relatively small yellow-pencil (*Madracis mirabilis*) patch within the rhodolith bed, representative of 1.9% of the total area.

A total of 20 sampling stations from the baseline study (Garcia-Sais et al., 2014) were revisited during the 2018-20 monitoring survey for measurements of percent cover by benthic categories and fish/shellfish taxonomic composition, density and species richness to allow comparative analyses between surveys (Figure 56). Five additional stations were also surveyed to expand the information on sub-mesophotic habitats, including an aggregate coral reef at 25m depth (ACR25). Representative images of the main benthic habitats and associated communities are included as Photo Album 3.

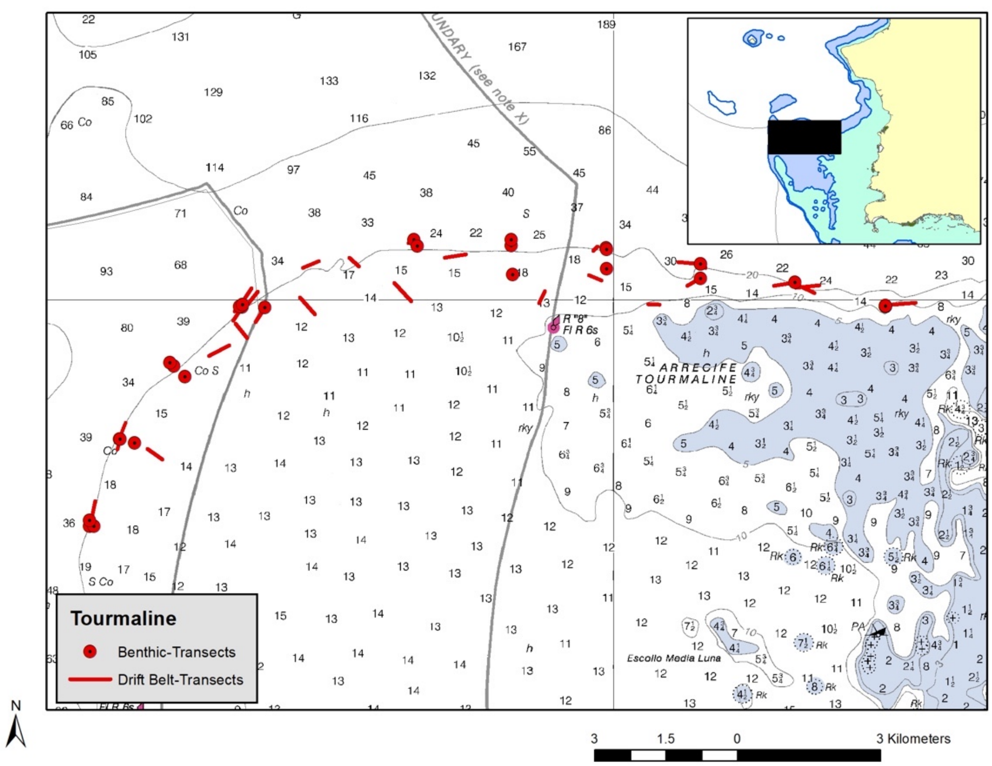

Figure 56. Location of surveyed stations at Tourmaline Reef, 2018-20

Benthic Community

Depth/habitat related patterns of benthic community structure

Colonized pavement, rhodolith beds, and sandy bottom habitats were found intermixed across the 30 – 50 m depth profile surveyed from Tourmaline Reef. Rhodolith (Rhod30-50) bed habitats were more common along the southern (northeast-southwest oriented) insular slope (stations T1 thru T5), whereas colonized pavement (CPSlope30-50; CPWall50), and sandy habitats prevailed along the northern, east-west oriented insular slope section (T6 – T10) (Figure 57). Coral reef habitats (ACR25) were limited to the shelf-edge in the sub-mesophotic 23 - 25m depth range.

The mean percent substrate cover by sessile-benthic categories from all habitats/depths surveyed in 25 - 50m depth range are presented in Table 27. Benthic algae were the main category in terms of percent substrate cover from all habitats/depths, with means ranging between a minimum of 49.27% at ACR25 and a maximum of 72.50% at CPWall50 (Figure 57). Differences between habitats/depths of total benthic algae were statistically insignificant (ANOVA; p= 0.445) but marked depth-related variations were evidenced for turf algae, encrusting fan alga (*Lobophora sp.*), and fleshy macroalgae (ANOVA; p< 0.0001). Substrate cover by turf algae (mixed assemblage) were significantly lower at Rhod30-50 compared to all other habitats/depth surveyed (ANOVA; p = 0.002). Conversely, encrusting fan alga (*Lobophora sp.*) and brown fleshy macroalgae (including *Dictyota sp*), were significantly higher at Rhod30-50, relative to other habitats/depths (ANOVA; p < 0.001) (Figure 58). Crustose coralline algae (CCA mixed assemblage) peaked at CPSlope30-50 with a mean cover of 3.44% but remained below 1% in all other habitats/depth. Likewise, crustose calcareous red algae (Peissonnellidae) peaked at ACR25 with 3.91% but was undetected from CPWall50 and measured below 1% at CPSlope30-50. Small, isolated tufts of green calcareous algae (*Halimeda sp*) were present at all habitats/depths with a maximum mean cover at Rhod30-50 (3.47%).

Habitat/depth related differences of substrate cover by abiotic categories associated with higher cover of sand at CPSlope30-50 and Rhod30-50, relative to other habitats/depths (ANOVA; p = 0.001). The extensive sand cover of mesophotic habitats at Tourmaline Reef was previously reported (García-Sais et al., 2014). Still, the occurrence of partially buried erect sponges and gorgonians noted during the 2018-20 survey is indicative of an underlying biologically colonized hard bottom recently covered by massive sand transport, perhaps associated with the extreme surge action produced by Hurricanes Irma and Maria in September 2017, and/or winter storm Riley in March 2018.

Table 27. Mean percent substrate cover by sessile-benthic categories from depths surveyed at Tourmaline Reef, 2018-20

Benthic Categories	ACR25	Rhodo30-50	CPSlope30-50	CPWall50
Abiotic				
Pavement	0	0.44	0.38	
Sand	3.05	18.99	33.65	
Rhodolith	0.00	9.68	3.32	
Rubble	2.05	0.00	0.58	
Total Abiotic	5.10	29.11	37.93	0.00
Benthic Algae				
Turf (mixed) with sediment	42.12	0.02	18.85	71.62
Peyssonnelid (mixed)	3.91	1.00	0.29	
Turf (mixed)	1.90	3.14	8.79	
Lobophora sp.	0.58	34.77	5.86	
Halimeda spp.	0.04	3.47	1.46	0.18
Dictyota spp.	0.00	13.43	8.42	
Fleshy macroalgae (mixed)	0.00	6.74	4.76	
CCA (mixed)	0.71	0.74	3.44	0.70
Total Benthic Algae	49.27	63.31	51.87	72.50
Cyanobacteria	2.28	2.26	3.34	0.22
Hard Coral				
Agaricia agaricites	1.16	0.05	0.03	
Agaricia fragilis	0.19			
Agaricia grahamae	3.49			
Agaricia lamarcki	0.13			
Leptoseris cucullata	0.10			0.46
Madracis carmabi	0.13			
Madracis decactis	0.48	0.02		
Madracis sp.			0.18	0.23
Meandrina meandrites	0.31		0.03	
Millepora alcicornis	0.09	0.02		
Montastraea cavernosa	1.85	0.02		
Mycetophyllia aliciae	0.32			
Orbicella faveolata	9.17	0.05		
Orbicella franksi	2.69			
Porites astreoides	0.50	0.05	0.08	
Siderastrea siderea	0.75		0.02	
Stephanocoenia intersepta	0.64		0.03	
Tubastrea aurea			0.08	
Unknown coral	1.62			
Total Hard Coral	23.61	0.22	0.44	0.69
# Coral Colonies/photo frame	6.75	0.40	0.55	1.28
# Diseased Coral Colonies/photo frame	0.19	0.00		
# Coral colonies bleached/photo frame	0.00	0.00		
			0.05	
Total Black Corals	0.00	0.15	0.05	9.83
Black Coral cover				
Octocoral				
Antillogorgia spp.	0.07			
Briareum asbestinum	6.79			
Erythropodium caribaeorum	7.90			
Ellisella sp.				0.41
Eunicea spp.	0.04	0.06	0.13	0.23

Table 27. Mean percent substrate cover by sessile-benthic categories from depths surveyed at Tourmaline Reef, 2018-20

Benthic Categories	ACR25	Rhodo30-50	CPSlope30-50	CPWall50
Gorgonia ventalina	0.07			
Iciligorgia schrammi			0.10	0.55
Muricea spp.			0.03	
Plexaura spp.	0.05		0.02	
Pseudoplexaura spp.			0.02	
Ptergorgia sp.		0.05		
Total Soft Corals	14.93	0.11	0.30	1.19
# Soft Corals/photo frame	2.37	0.09	0.34	5.09
Sponges				
Agelas clathrodes	0.05	0.10		
Agelas conifera	1.12			
Agelas sceptrum		0.10		
Agelas sp.		0.02	0.02	
Aiolochoria crassa	0.34	0.39	0.10	
Amphimedon compressa		0.10	0.03	
Aplysina archeri		0.02	0.03	
Aplysina cauliformis	0.04		0.18	
Aplysina fistularis		0.10		
Aplysina insularis	0.05	0.02		
Batzella sp.	0.04			
Callyspongia ferox	0.10			
Clathria sp.		0.05	0.05	
Cliona caribbaea	0.08		0.06	
Cliona varians	0.22			
Chondrilla caribensis		0.02	0.05	
Desmapsamma anchorata				0.23
Erylus sp.			0.02	
Haliclona sp.		0.03		
Halisarca sp.				0.23
Iotrochota birotulata	0.28	0.05	0.12	
Ircinia felix		0.05	0.05	
Ircinia strobilina		0.05	0.24	
Monanchora arbuscula	0.21			
Mycale laevis	0.17			
Myrmekioderma rea		0.04		
Neofibularia nolitangere		0.01		
Neopetrosia proxima	0.04	0.07	0.28	
Niphates digitalis				0.47
Niphates erecta			0.02	
Niphates sp.				0.24
Petrosia pellasarca		0.02	0.05	
Plakortis spp.	0.57	0.42	0.17	0.20
Prosuberites laughlini			0.04	0.23
Scopalina ruetzleri	0.29	0.04		
Smenospongia aurea		0.07		
Smenospongia conulosa			0.02	
Spheciospongia vesparium	0.09		0.06	0.23
Spirastrella coccinea	0.08		0.35	0.22
Spirastrella hartmani			0.12	
Svenzea zeai	0.13			
Unknown sponges	0.67	1.55	2.26	11.83

Table 27. Mean percent substrate cover by sessile-benthic categories from depths surveyed at Tourmaline Reef, 2018-20

Benthic Categories	ACR25	Rhodo30-50	CPSlope30-50	CPWall50
Verongula rigida	0.25	0.20	0.02	
Xestospongia muta		1.15	1.55	
Total Sponges	4.81	4.70	5.89	13.87

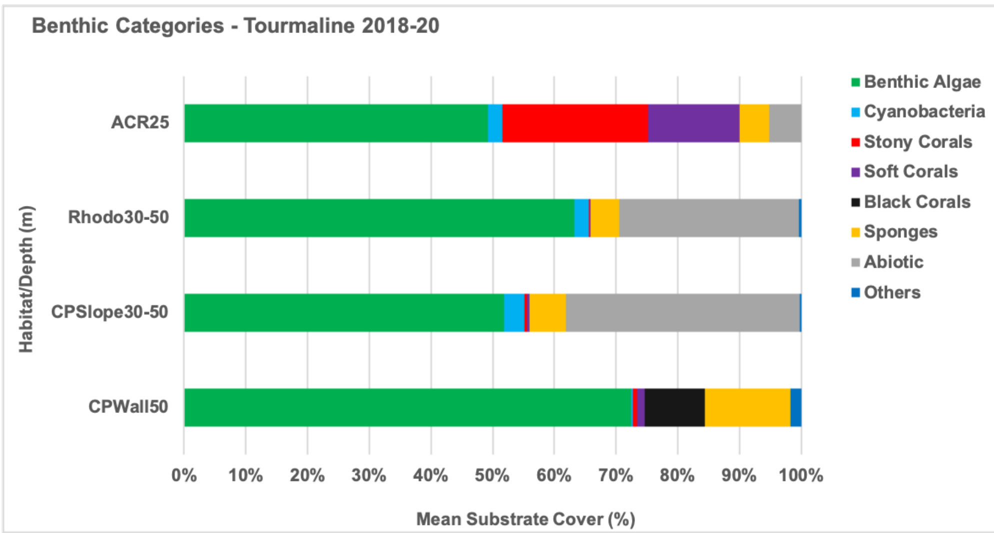

Figure 57. Mean percent substrate cover by the main sessile-benthic categories across The main habitats/depths surveyed at Tourmaline Reef, 2018-20

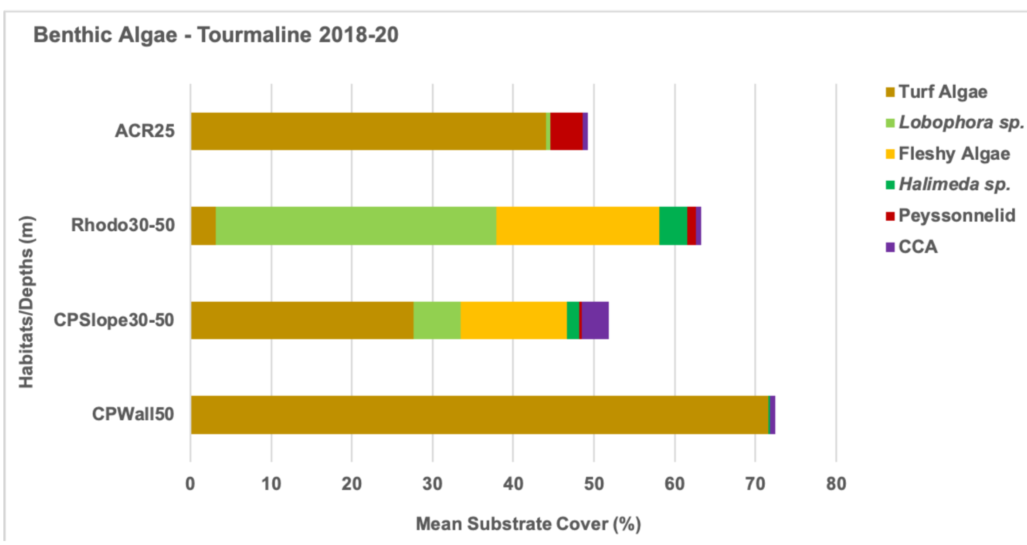

Figure 58. Mean percent substrate cover by benthic algae taxonomic components across main habitats/depths surveyed at Tourmaline Reef, 2018-20

Stony corals were represented by 19 species within the 25 – 50m depths surveyed at Tourmaline Reef (Table 27). Statistically significant variations of substrate cover in relation to habitat/depth were noted, with higher cover at ACR25 relative to all other habitats/depths surveyed (ANOVA, p < 0.0001). The mean reef substrate cover by stony corals varied from a maximum of 23.61% at ACR25 to less than 1% at deeper stations (Figure 59). Stony coral species richness and mean density of colonies also declined markedly between habitats/depths, from 17 species and 6.8 colonies/frame at ACR 25 to a minimum of two (2) species at CPWall50 and 0.55 colonies/frame at CPSlope30-50. The *Orbicella spp*. complex, comprised by mountainous star coral (*O. faveolata*) and boulder star coral (*O. franksi*) were the dominant species assemblage at ACR25 with a combined mean substrate cover of 11.86%, representative of 50.2% of the total cover by stony corals. The *Agaricia spp*. complex, integrated by dimpled lettuce coral (*A. grahamae*), lettuce coral (*A. agaricites*), fragile saucer coral (*A. fragilis*), and whitestar sheet coral (*A. lamarki*) were also prominent at ACR 25 with a combined cover of 5.0%, representative of 21.18% of the total cover by stony corals. Sunray lettuce coral (*Helioseris cucullata*) and maze coral (*Meandrina sp*) were the dominant corals at CPWall50 and CPsSlope30-50 (Figure 59).

Soft corals (gorgonians) exhibited a similar habitat/depth distribution pattern as stony corals with peak substrate cover (14.93%), density of colonies (2.4 colonies/frame), and species richness (6 spp) at ACR25 compared to deeper stations surveyed. Differences of substrate cover by soft corals associated with habitat/depth were statistically significant (ANOVA; p < 0.0001). The encrusting gorgonian (*Erythropodium caribaeorum*) and the corky-sea finger (*Briareum asbestinum*) were the dominant species at ACR 25 with means of 7.90% and 6.79%, respectively. The deep-water gorgonian (*Iciligorgia schrammi*) was the dominant species at CPSlope30-50 and CPWall50. Black coral (antipatharian) colonies were prominent at CPWall50 with a mean cover of 9.83%. The bushy Caribbean black coral (*Antipathes caribbeana*) was the main species present. Large colonies of *A. caribbeana* were observed growing out into the water column from deep crevices and ledges of steep walls of the insular slope in the 40 - 50m depth range.

A total of 41 sponge species were identified from the main mesophotic habitats/depth at Tourmaline Reef with mean substrate cover ranging from 4.70% at Rhod30-50 and 13.83% at CPWall50 (Table 27). Variations of reef substrate cover by total sponges between depths were not statistically significant (ANOVA; p = 0.209). The *Agelas spp*, complex, comprised by *A. conifera* and *A. clathrodes* were the dominant assemblage at ACR25, whereas *Xestospongia muta* was the main species from CPSlope30-50 and Rhod30-50 (Figure 60).

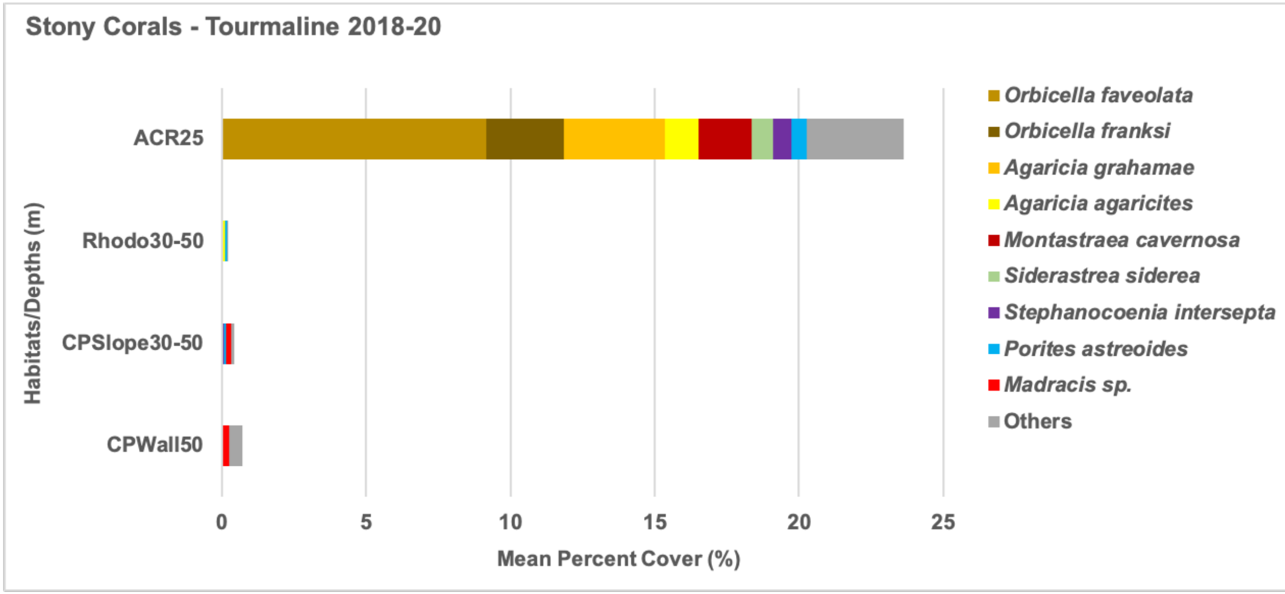

Figure 59. Mean percent substrate cover by stony corals across the main habitats/depths surveyed at Tourmaline Reef, 2018-20

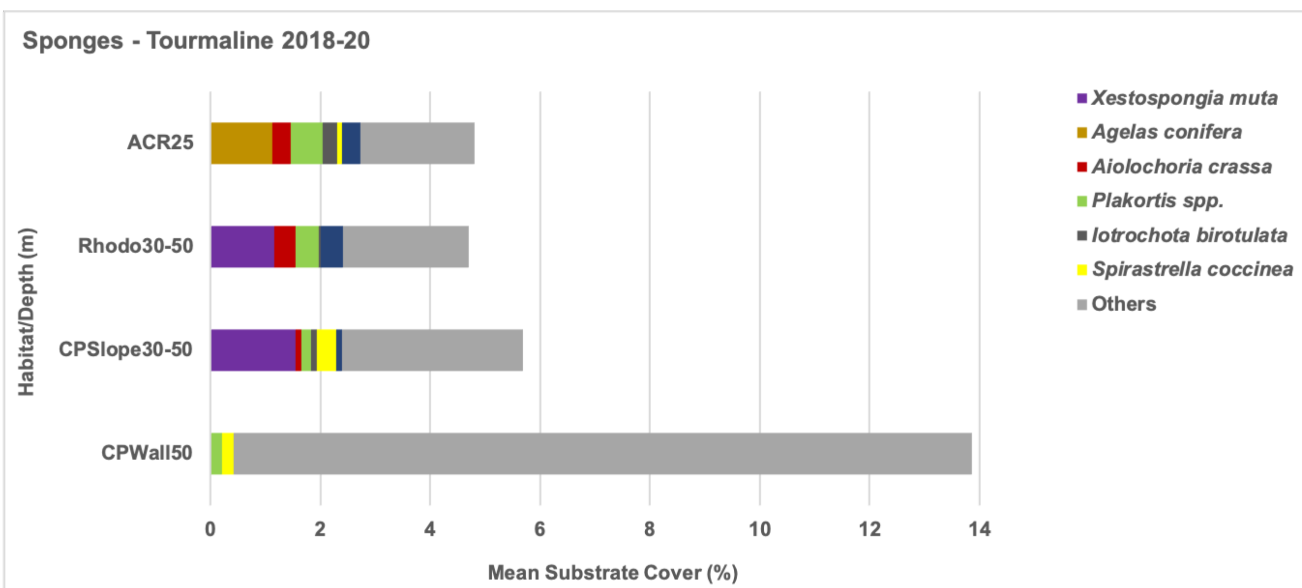

Figure 60. Mean percent substrate cover by sponges across the main habitats/depths surveyed at Tourmaline Reef, 2018-20

Similarities of benthic community structure from the main habitats/depths surveyed within the 25 – 50m depth profile at Tourmaline Reef are shown in a non-metric multidimensional scaling plot (nMDS) based on Bray-Curtis similarities in Figure 61. The highest similarity (88.6%) was observed from coral reef stations of ACR25. Stony corals and soft corals were the main contributors to the within habitat similarity at ACR25 with a cumulative contribution of 59.9% (Table 28). Similarity was moderate at Rhod30-50 (75.0%) and CPWall (72.0%), largely contributed by benthic algae (31.8%) and abiotic (28.7%) at Rhod30-50, and by black corals (46.5%) at CPWall50. The lowest similarity was observed from CPSlope30-50 (60.3%) probably related to the high within habitat/depth variability of slope angles and position relative to wave and current direction. Benthic community structure dissimilarity was highest between CPSlope30-50 and CPWall50 (61.8%) driven by the higher cover by black corals (Antipatharia) at CPWall50 (Table 29). Black corals were the main category contributing dissimilarity between CPWall50 and all other habitats/depths. Likewise, the combined contribution of stony corals and soft corals separated ACR25 from all other habitats/depths, whereas the relatively high abiotic cover separated CPSlope30-50 and Rhod30-50 from other habitats/depths. The relatively high substrate cover by benthic algae contributed to the similarity between all habitats/depths.

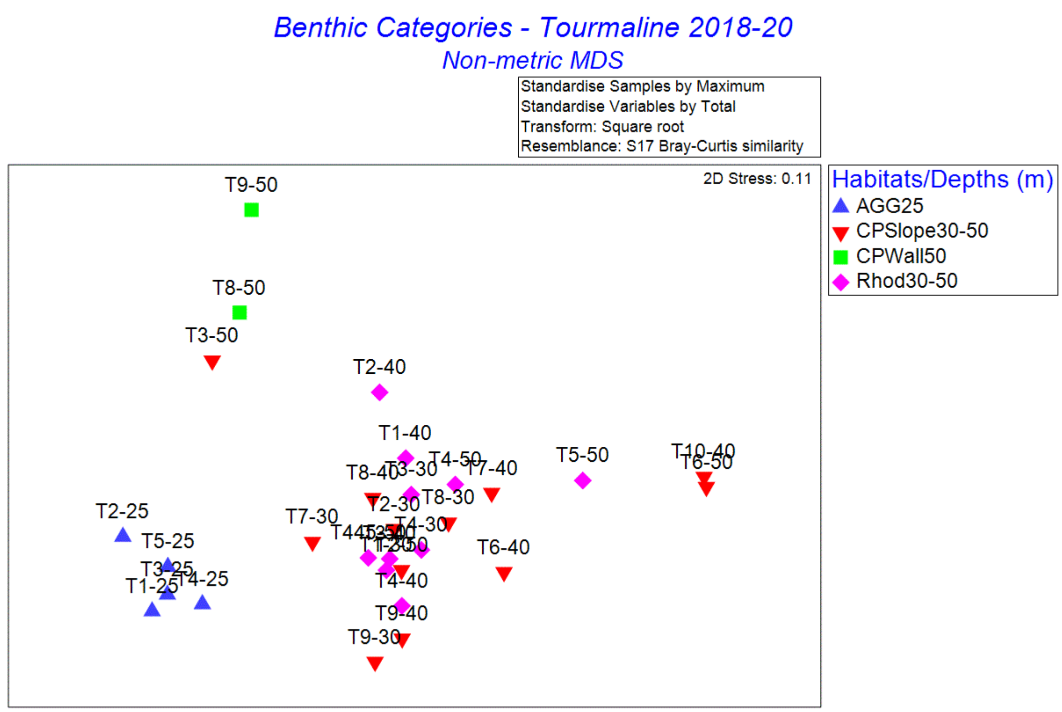

Figure 61. Non-metric multidimensional scaling (nMDS) plot of Bray-Curtis similarities between photo-quadrat samples of sessile-benthic communities surveyed from sub-mesophotic (25m) and upper mesophotic (30 – 50m) depths at Tourmaline Reef, 2018-20 survey

Table 28. Similarity matrix (SIMPER) of sessile-benthic community structure at the main benthic habitats/depths surveyed from Tourmaline Reef, 2018-20 survey

	AGG25	CPSlope30-50	Rhod30-50	CPWall50
Average Similarity (%)	88.6	60.3	75.0	72.0
Benthic Categories				
Abiotic		29.6	28.7	
Benthic Algae	14.9	24.8	31.8	21.7
Cyanobacteria				
Stony Corals	30.1			
Soft Corals	29.8			
Black Corals				46.5
Sponges		26.0	25.4	22.3

Table 29 Dissimilarity matrix (SIMPER) of sessile-benthic community structure between the main benthic habitats/depths surveyed from Tourmaline Reef, 2018-20 survey

	AGG25 vs CPSlope30-50	AGG25 vs CPWall50	AGG25 vs Rhod30-50	CPSlope30-50 vs CPWall50	CPSlope30-50 vs Rhod30-50	Rhod30-50 vs CPWall50
Average Dissimilarity (%)	53.7	60.2	50.6	61.8	32.0	58.0
Benthic Categories						
Abiotic				15.4	22.3	16.3
Benthic Algae					12.9	
Cyanobacteria	10.9			10.6	28.3	9.8
Stony Corals	33.8	23.0	36.4			
Soft Corals	33.3	19.6	36.5			
Black Corals		37.5		50.2		52.0
Sponges					15.0	

Temporal (monitoring) trends of benthic community structure

Differences of percent substrate cover by benthic categories surveyed from mesophotic benthic habitats within the 30 – 50m depth range between the 2012 baseline and the 2018-20 monitoring survey at Tourmaline Reef were statistically insignificant for all major habitats/depths (2-Way ANOVA; $p > 0.05$) (Table 30). The largest differences in terms of percent change were observed for stony corals at Rhod30-50 (287.0%) and CPSlope30-50 (165.0%), but these changes were based on very low substrate cover means (< 1%) and high sampling variability associated with many observations from stations with no coral cover. Stony corals were not a prominent feature of mesophotic habitats surveyed from Tourmaline Reef in neither of the surveys. Increments of cover by benthic algae were measured from the three main habitats/depth surveyed but differences were small and within sampling variability error. Variations of the site mean percent cover of the major benthic categories during both surveys are shown in Figure 62.

Table 30. Temporal variations of the mean percent substrate cover by benthic categories from the main benthic habitats/depths between the 2012 baseline and the 2018-20 monitoring surveys at Tourmaline Reef.

Benthic	**CPSlope30-50**			**CPWall50**			**Rhod30-50**			2-Way ANOVA
Categories	2012	2018-20	% Change	2012	2018-20	% Change	2012	2018-20	% Change	p-value
Abiotic	23.53	37.93	61.22	0.00	0.00	0.00	45.72	29.11	-36.34	0.570
Benthic Algae	49.03	51.87	5.81	71.15	72.50	1.89	38.44	63.31	64.68	0.779
Cyanobacteria	2.54	3.34	31.44	0.00	0.22	0.00	5.43	2.26	-58.46	0.913
Stony Corals	0.17	0.44	165.00	0.35	0.69	95.71	0.06	0.22	287.00	0.244
Black Corals	0.00	0.05		0.00	9.83		0.00	0.15		0.104
Soft Corals	2.34	0.30	-87.30	1.05	1.19	12.86	0.00	0.11	0.00	0.102
Sponges	9.48	5.89	-37.85	16.20	13.87	-14.38	5.04	4.70	-6.93	0.087

2-Way ANOVA p-values are for "survey years" as sources of variation

Benthic community structure similarities between the 2012 baseline and the 2018-20 monitoring survey are presented in a non-metric multidimensional scaling plot (nMDS) of Bray-Curtis similarities based on the study mean percent substrate cover at the main habitats/depths surveyed (Figure 63). Similarities between surveys ranged between 71.9% at CPWall50 and 81.4% at COSlope30-50. Cyanobacteria and abiotic cover were main contributors to similarity between surveys at CPSlope30-50 and Rhod30-50, whereas sponges and benthic algae were the most important contributors to similarity at CPWall50. In general terms, benthic community structure at Tourmaline mesophotic habitats in the 30 – 50m depth range remained without any major change, with benthic algae and abiotic cover as the main categories of reef substrate cover. The increase of substrate cover by benthic algae was mostly from Rhod30-50, associated with increase cover by encrusting fan alga (*Lobophora sp*.) and Y-twig alga (*Dictyota sp*.). A marked increase of cover by black corals was measured from CPWall50 but only two (2) transects were sampled from CPWall50 and inferences from this habitat/depth are limited by small sample size.

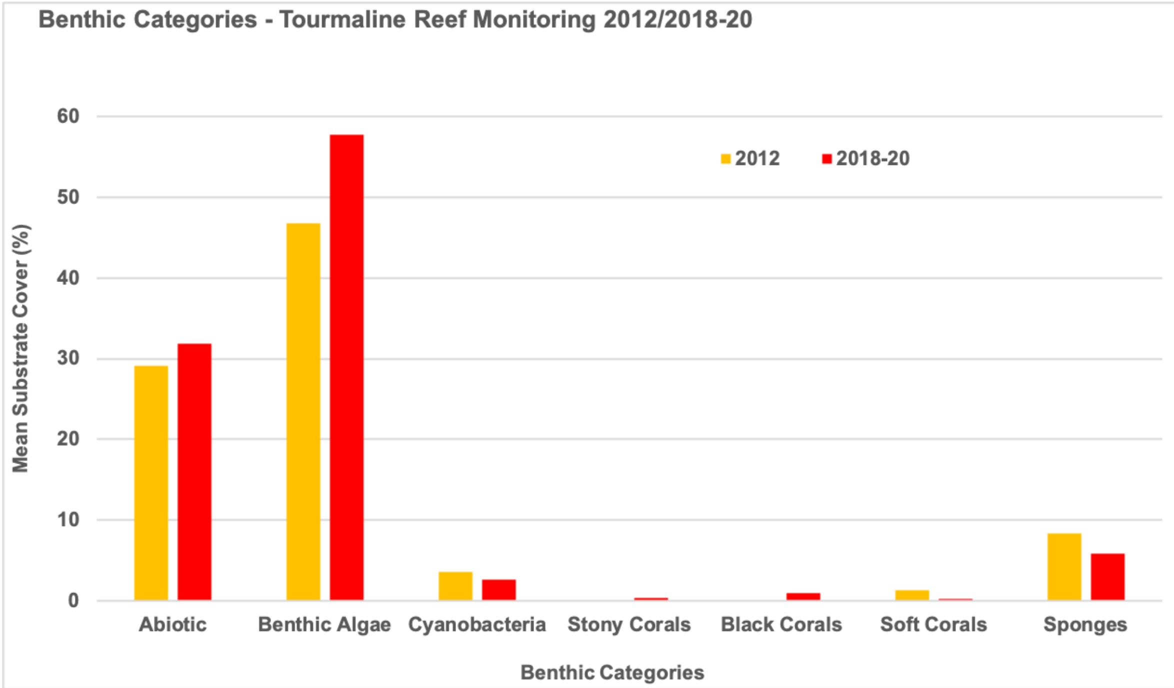

Figure 62. Variations of site mean percent cover by benthic categories from a set of 23 sampling stations within the 30 – 50m mesophotic depth range at Tourmaline Reef during the initial 2012 baseline and the 2018-20 monitoring survey.

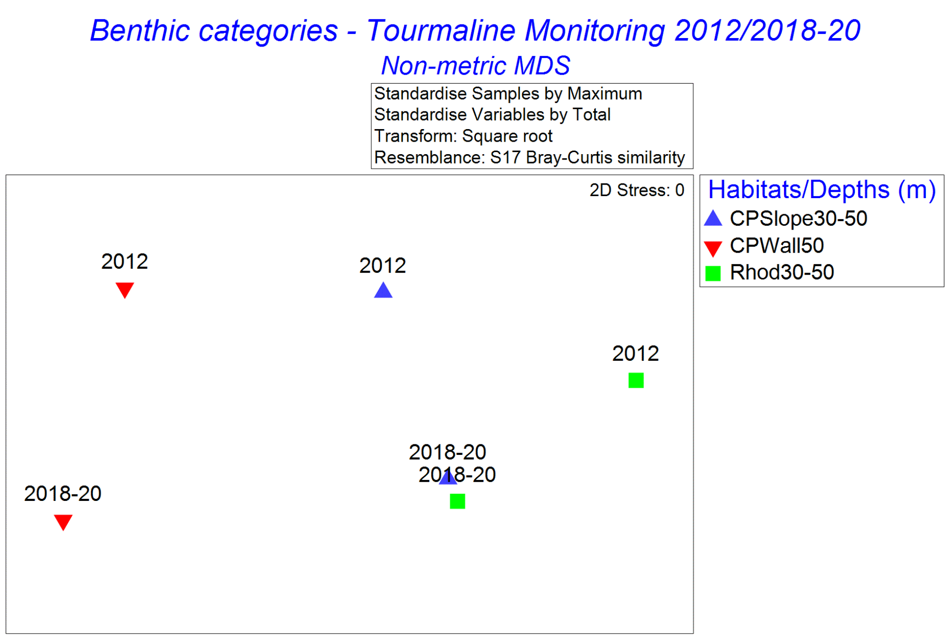

Figure 63. Non-metric multidimensional scaling (nMDS) plot of Bray-Curtis similarities of substrate cover by major substrate categories from the main mesophotic (30 – 50m) habitats and depths surveyed from Tourmaline Reef during the 2012 baseline and 2018-20 monitoring surveys.

Fish Community

Small Demersal Fishes
Habitat/Depth related patterns of density and community structure, 2018-20 survey

A total of 74 small demersal fish species were identified from mesophotic habitats in the 25 – 50m depth range at Tourmaline Reef during the 2018-20 monitoring survey (Table 31). An assemblage of eight species represented 77.0% of the total fish density across all habitats/depths. These included the masked goby (*Coryphopterus personatus*), blue and sunshine chromis (*Chromis cyanea, C. insolata*), fairy basslet (*Gramma loreto*), creole and bluehead wrasse (*Clepticus parrae, Thalassoma bifasciatum*) and bicolor damselfish (*Stegastes partitus*). Fish density and species richness peaked at ACR25 with means of 190.0 Ind/30m^2 and 43 Spp/30m^2 (Figure 64). Differences of fish density between habitats/depths were statistically significant (ANOVA, p< 0.0001) related to the higher density at ACR25 relative to other habitats/depths. Differences of density between other habitats/depths were statistically insignificant. The higher fish density at ACR25 was largely driven by the peak density of masked goby (*Coryphopterus personatus*) (90.2 Ind/30m^2), that represented 47.4% of the total fish density from that habitat/depth. Densities of blue chromis (*Chromis cyanea*), creole wrasse (*Clepticus parrae*), peppermint goby (*C. lipernes*) bluehead wrasse (*Thalassoma bifasciatum*), tomtate (*Haemulon aurolineatum*), black bar soldierfish (*Myripristis jacobus*), princess and redband parrotfish (*Scarus taeniopterus, Sparisoma aurofrenatum*) and another 26 species also reached their highest densities at ACR25 which contributed to the fish density differences between depths (Figure 64).

Differences of fish species richness between depths were statistically significant (ANOVA; p< 0.0001) related to the higher richness at ACR25 compared to other habitats/depths. Mean fish species richness declined more than 2-fold between the maximum at ACR25 (mean: 19.6 Spp/30m^2) and deeper mesophotic stations surveyed (< 9.0 Spp/30m^2). Differences of species richness between habitats surveyed below 25m were not statistically significant (ANOVA; p > 0.05). The higher density and species richness at ACR25 were influenced by the higher rugosity, live coral cover, and overall structural complexity (microhabitat heterogeneity) available from the coral reef habitat at ACR25. Habitat/depth related density distribution patterns were detected for several numerically dominant species. Densities of sunshine chromis (*Chromis insolata*) and fairy basslet (*Gramma loreto*) were significantly higher at CPWall50 (ANOVA; p < 0.001). Fairy basslet was also present from all transects surveyed at ACR25 but appeared to have stronger preference for vertically oriented habitats (such as walls) down to the maximum depth surveyed (e. g. 50m).

Table 31. Taxonomic composition and mean density of small demersal fishes from 10 x 3 m belt-transects surveyed within the 25 – 50 m depth range at Tourmaline Reef, 2018-20 survey

Species	ACR25	Rhod30-50	CPSlope30-50	CPWall50
Acanthurus chirurgus	0.00	1.00	0.20	
Acanthurus coeruleus	0.40	0.13		1.00
Acanthurus tractus		0.13	0.10	
Anisotremus virginicus	0.60		0.10	
Aulostomus maculatus	0.20			
Balistes vetula	0.00	1.25	0.50	
Bodianus rufus	0.20			
Canthigaster rostrata	1.80		0.50	
Carangoides ruber	0.20			
Caranx lugubris			0.20	
Carcharhinus perezi				0.50
Centropyge argi	0.00	1.50	0.90	
Cephalopholis cruentatus	1.20		0.10	
Cephalopholis fulva	0.60	0.63	0.10	1.00
Chaetodon capistratus	0.80		0.20	1.00
Chaetodon sedentarius				0.50
Chromis cyanea	24.00	0.38	0.20	
Chromis insolata	0.80	0.25	0.90	12.50
Chromis multilineata	0.20			
Clepticus parrae	17.60			
Coryphopterus glaucofraenum		0.13		
Coryphopterus lipernes	11.20			
Coryphopterus personatus	90.20		0.20	
Coryphopterus sp.		0.50	0.30	
Cryptostomus roseus			0.50	
Dactylopterus volitans			0.10	
Elacatinus evelynae	0.60			
Epinephelus guttatus		0.25	0.10	
Equetus punctatus			0.10	
Gramma loreto	4.40		2.20	17.50
Haemulon aurolineatum	4.80			
Halichoeres bivittatus			0.30	
Halichoeres cynocephalus			0.10	
Halichoeres garnoti	0.40	2.88	2.90	
Holacanthus ciliaris				2.00
Holacanthus tricolor	0.40	0.13	0.10	
Holocentrus adscensionis	0.00	1.75	0.90	
Holocentrus rufus	0.20	0.13	0.30	
Lachnolaimus maximus	0.20	0.13	0.10	
Lutjanus analis			0.10	0.50
Lutjanus buccanella	0.00	1.38	0.00	
Lutjanus jocu				0.50
Lutjanus mahogoni	0.20			
Lutjanus synagris	0.60			
Malacanthus plumieri		0.13		
Malacoctenus triangulatus			0.10	
Mulloidichthys martinicus	0.60			
Myripristis jacobus	3.00			

Table 31. Taxonomic composition and mean density of small demersal fishes from 10 x 3 m belt-transects surveyed within the 25 – 50 m depth range at Tourmaline Reef, 2018-20 survey

Species	**ACR25**	**Rhod30-50**	**CPSlope30-50**	**CPWall50**
Neoniphon marianus	0.40			
Ocyurus chrysurus	1.20		0.30	1.50
Opistognathus aurifrons		0.13		
Paranthias furcifer	0.20			
Pomacanthus arcuatus	0.40	0.38	0.10	
Pomacanthus paru		0.13		
Prognathodes aculeatus	0.20			
Pterois sp.	0.20		0.1	
Sargocentron coruscum	0.20			
Scarus iseri	*2.60*			
Scarus taeniopterus	2.80			
Scorpaena plumieri		0.13		
Serranus annularis		0.13		
Serranus baldwini			0.6	
Serranus tabacarius	0.00	1.38	0.30	
Serranus tigrinus	0.00	0.50	0.80	
Sparisoma atomarium		0.38		
Sparisoma aurofrenatum	1.20	0.13	0.10	
Sparisoma radians		0.13		
Sparisoma viride	*0.20*			
Sphyraena barracuda	0.20			
Stegastes leucostictus	*0.60*			
Stegastes partitus	2.60	6.88	4.50	2.00
Stegastes variabilis	1.20			
Thalassoma bifasciatum	10.40	0.75	1.70	
Xanthichthys ringens		0.13		
Total Ind	190.00	23.75	20.90	40.5
Total Spp	19.6	8.6	6.7	7.5

Sunshine chromis were observed across all habitats/depths. It's higher densities at CPWall may be related to the higher availability of protective habitats and lower predation pressure on recruitment juveniles observed to be abundant at CPWall50. The higher densities of blue chromis at ACR25 (ANOVA; p = 0.003) suggests a potential zonation of *Chromis* species associated with depth. Bluehead wrasse (*Thalassoma bifasciatum*) was present within belt-transects at Rhod30-50 and CPSlope 30-50 but exhibited significantly higher densities at ACR25 (ANOVA; p < 0.0001). An assemblage of 12 species were only observed from 40 and/or 50m depth stations, whereas another 30 species were only identified from 25m and 30m stations, suggesting potential depth and or habitat related distribution patterns (Table 32). Elucidation of such patterns will require larger replicated samplings of different depths within a common habitat and of different habitats within a common depth.

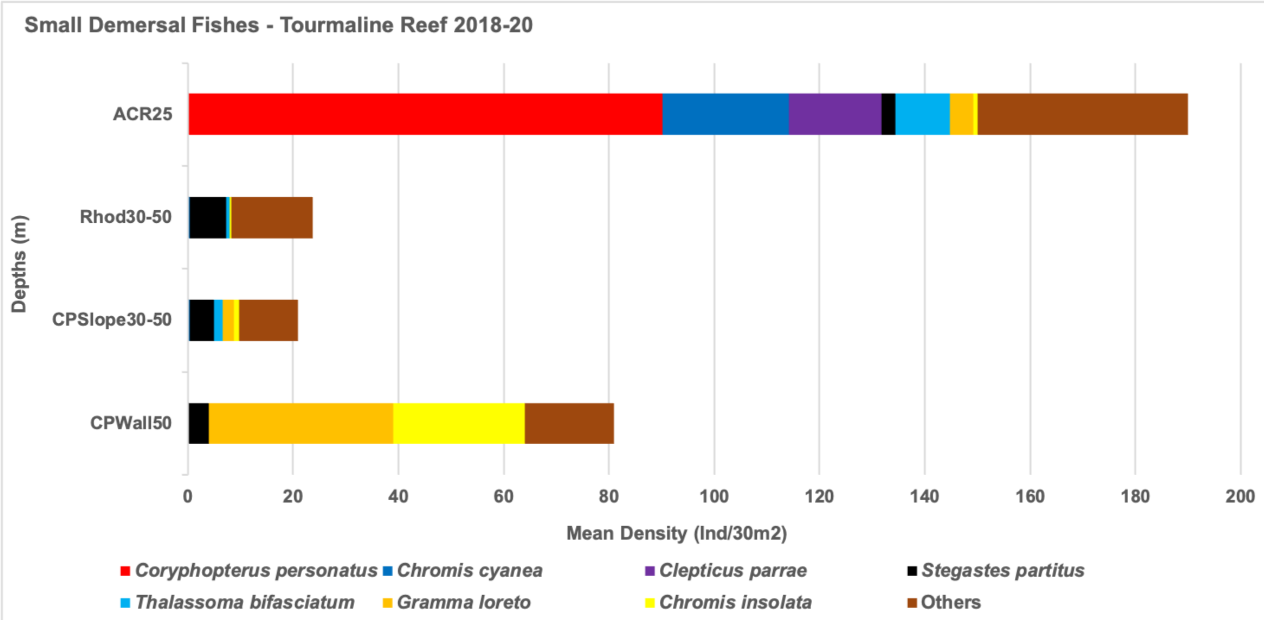

Figure 64. Variations of mean density by small demersal fishes (Ind/30m^2) across the main habitats/depths surveyed from Tourmaline Reef. Data are means from 10 x 3m belt-transects, 2018-20 survey.

Variations of the relative densities of the small demersal fish species surveyed from 10m x 3m belt-transects within the main benthic habitats in the 25 – 50m depth range at Tourmaline Reef are displayed in a non-metric multi-dimensional scaling plot (nMDS) based on Bray-Curtis similarities in Figure 65. Benthic habitats were used as a discriminatory factor for testing fish community structure similarities since different habitats were sampled on similar depths within the 25 – 50m profile. Similarities were moderately low across all habitats/depth driven by the high variability of relative densities and/or presence/absence of numerically dominant species within habitat/depths. The lowest similarities were noted from CPSlope30-50 (17.8%) and Rhodo30-50 (40.9%), influenced by the patchy occurrence of fairy basslet (*Gramma loreto*), bluehead wrasse (*Thalassoma bifasciatum*), and sunshine chromis (*Chromis insolata*) at CPSlope30-50, and of cherubfish (*Centropyge argi*), yellowhead wrasse (*Halichoeres garnoti*) and bicolor damselfish (*Stegastes partitus*) at Rhod30-50. Similarity was highest at ACR25 (65.7%), largely contributed by masked and peppermint gobies (*Coryphopterus personatus, C. lipernes*), black bar soldierfish (*Myripristis jacobus*), and tomtate (*Haemulon aurolineatum*) (Table 32). Fairy basslet (*Gramma loreto*), and the sunshine chromis (*Chromis insolata*) were the main contributors to similarity within CPWall stations.

Fish community structure dissimilarities between habitats/depths were high across all pairwise comparisons, indicative of distinctive species assemblages despite the inherent variability associated with patchy distributions of numerically dominant species. The highest dissimilarities of fish assemblages were observed between ACR25 and other habitats/depths, and between the CPWall and other habitats/depths (Table 33). The main species contributions to dissimilarities between ACR25 and other stations included black bar soldierfish (*Myripristis jacobus*), peppermint and masked gobies (*Coryphopterus lipernes, C. personatus*), princess parrotfish (*Scarus taeniopterus*), tomtate (*Haemulon aurolineatum*), bluehead wrasse (*Thalassoma bifasciatum*). The higher relative densities of fairy basslet (*Grama loreto*) and sunshine chromis (*Chromis insolata*) was the main distinctive species assemblage separating CPWall50 from other habitats/depths surveyed. Rhodo30-50 was characterized by relatively higher densities of tobaccofish (*Serranus tabacarius*), queen triggerfish (*Balistes vetula*) and yellowhead wrasse (*Halichoeres garnoti*), whereas higher relative densities of yellowtail snapper (*Ocyurus chrysurus*), four-eye butterflyfish (*Chaetodon capistratus*), coney (*Cephalopholis fulva*) and harlequin bass (*Serranus tabacarius*) distinguished CPSlope from other habitats/depths during 2018-20 at Tourmaline Reef.

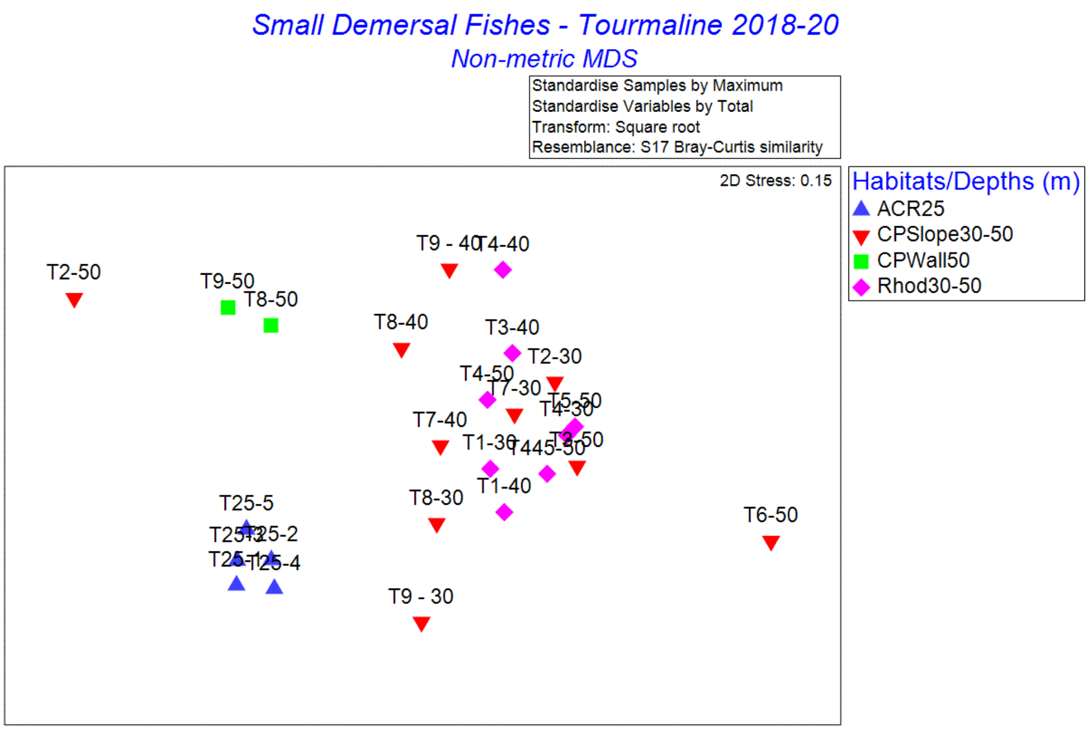

Figure 65. Non-metric multidimensional scaling (nMDS) plot of Bray-Curtis similarities of small demersal fish community structure characterized by their relative densities within 10m x 3m belt-transects surveyed from mesophotic benthic habitats (25 – 50m) at Tourmaline Reef during 2019.

Table 32. Similarity matrix (SIMPER) of small demersal fish community structure surveyed from benthic habitats within the 25 – 50m depth range at Tourmaline Reef, with species contributions to similarity, 2018-20 survey.

	ACR25	CPSlope30-50	CPWall50	Rhod30-50
Average Similarity (%)	65.7	17.8	51.1	40.9
Coryphopterus personatus	17.2			
Coryphopterus lipernes	15.8			
Myripristis jacobus	15.5			
Haemulon aurolineautum	14.1			
Scarus taeniopterus	7.1			
Thalassoma bifasciatum	6.3			
Stegastes partitus		38.6		30.8
Halichores garnoti		20.0		15.2
Serranus tigrinus		10.4		
Balistes vetula		9.3		21.8
Gramma loreto			61.1	
Chromis insolata			38.9	
Serranus tabacarius				12.2

Table 33. Dissimilarity matrix (SIMPER) of small demersal fish community structure surveyed from benthic habitats within the 25 – 50m depth range at Tourmaline Reef, with species contributions to dissimilarity, 2018-20 survey.

	ACR25 vs CPSlope30-50	ACR25 vs CPWall50	ACR25 vs Rhod30-50	CPSlope30-50 vs CPWall50	CPSlope30-50 vs Rhod30-50	CPWall50 vs Rhod30-50
Average Dissimilarity (%)	91.6	89.3	93.9	85.3	71.8	91.8
Myripristis jacobus	9.5	9.5	8.4			
Coryphopterus lipernes	9.4	9.4	8.4			
Haemulon aurolineautum	9.0	9.1	8			
Coryphopterus personatus	8.7	9.2	8.1			
Scarus taeniopterus	7.0	7.0	6.2			
Chromis cyanea	4.8	4.9	4.3			
Canthigaster rostrata	4.6					
Thalassoma bifasciatum	4.1		3.6		6.3	
Scarus iseri	4.0		3.7			
Sparisoma aurofrenatum	3.9		3.5			
Clepticus parrae	3.7					
Stegastes partitus	3.4		4.4	5.6		6.0
Chromis insolata		9.2		16.0		12.7
Gramma loreto		9.1		18.3		16.5
Ocyurus chrysurus		4.6		9.4		6.7
Chaetodon capistratus				8.3		5.8
Cephalopholis fulva				7.0		5.6
Serranus tigrinus				5.7	8	
Balistes vetula			4.8		8.1	7.5
Serranus tabacarius			4.3		9.5	6.9
Halichores garnoti					7.1	6.2
Holocentrus adscensionis					6.7	
Centropyge argi					6.6	
Cephalopholis fulva					6.3	
Canthigaster rostrata					5.3	

Temporal (monitoring) trends of small demersal fish density and community structure

Variations of mean densities by the small demersal fish community between the 2012 baseline and the 2018-20 monitoring survey from the main benthic habitats/depths surveyed in Tourmaline Reef are shown in Figure 66. Density differences between surveys were not statistically significant (ANOVA, $p > 0.05$) for any habitat/depth (Table 34). Differences between surveys were strongly influenced by schooling aggregations of numerically dominant species, such as blackfin snapper (*Lutjanus buccanella*), sunshine chromis (*Chromis insolata*), and fairy basslet (*Gramma loreto*) but due to the high sampling variability associated with aggregated (patchy) distributions differences between surveys were statistically insignificant. Density differences between surveys of the numerically dominant fish species are shown in Table 35. Differences were large for many species but due to the high sampling variability associated with patchy distributions were statistically significant only for blackfin snapper (*Lutjanus buccanella*) (ANOVA; $p = 0.029$). Blackfin snapper is attracted to divers and thereby its densities are largely overestimated by 10m x 3m belt-transects, and thus its density variations must by analyzed from the larger area drift belt-transects designed for density estimates of large demersal fishes.

Variations of small demersal fish species richness between surveys were statistically significant only at Rhod30-50 (ANOVA; $p = 0.008$), associated with a 36.4% increase during 2018-20. The increase of species richness was related to an assemblage of 12 species represented by only one individual, including several shallow water (neritic) reef species, such as bucktooth and redband parrotfishes (*Sparisoma radians, S. aurofrenatum*), doctorfish (*Acanthurus chirurgus),* harlequin bass (*Serranus tigrinus*)*,* and saddled goby (*Coryphopterus glaucofraenum*). Penetration of these species into deeper waters may be a response to temperature stress and/or physical disturbances associated with strong wave action on shallower habitats.

Small demersal fish community structure similarities between surveys based on the relative densities of the numerically dominant species (top 90% density) are shown in a multidimensional scaling plot of Bray-Curtis similarities in Figure 67. Similarities between surveys were generally low from all benthic habitats/depths, ranging from a maximum of 45% at CPSlope30-50 to a minimum of 32.4% at Rhod30-50 (Table 36). Masked goby (*Coryphopterus personatus*), Yellowhead wrasse (Halichoeres garnoti), bicolor damselfish (*Stegastes partitus*), and lionfish (*Pterois sp*) were the main species contributing similarity between surveys at CPSlope30-50. Bicolor damselfish (*S. partitus*) was also the main species contributing similarity at CPWall50.

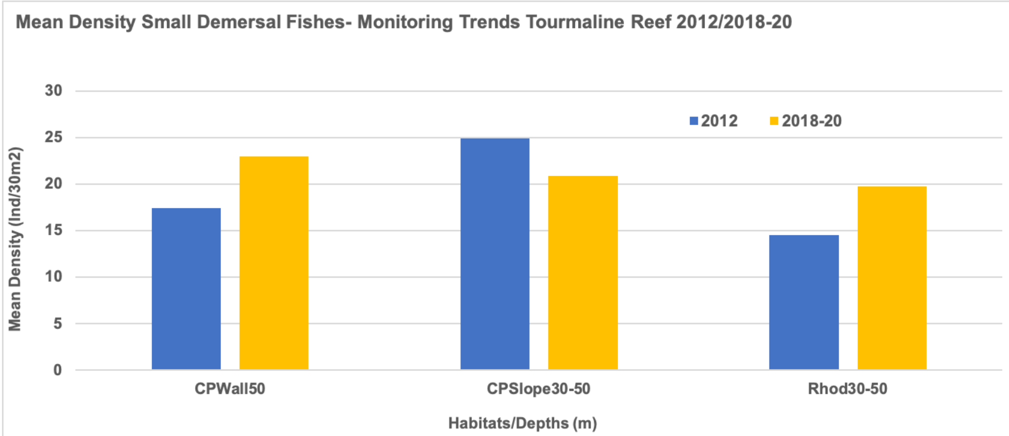

Figure 66. Mean density variations by small demersal fishes between the 2012 baseline and the 2018-20 monitoring survey at the main habitats/depth surveyed from Tourmaline Reef.

Table 34. Variations of mean density and species richness of small demersal fishes between the 2012 baseline and the 2018-20 monitoring surveys at Tourmaline Reef

	Mean Density (Ind/30m2)			ANOVA	Mean Spp. Richness (Spp/30m2)			ANOVA
Habitats/depths (m)	2012	2018-20	**% Change**	**p-value**	2012	2018-20	**% Change**	**p-value**
CPSlope30-50	24.9	20.89	-16.10	0.928	6.7	6.89	2.83	0.836
Rhod30-50	14.5	19.75	36.21	0.383	5.5	7.5	36.40	0.008*
CPWall50	17.4	23	32.18	0.194	2.6	7.8	200.00	0.352
Statistically significant differences at p < 0.05								

Table 35. Variations of site mean densities by numerically dominant small demersal fishes sampled from mesophotic habitats in the 30 – 50m depth range at Tourmaline Reef during the 2012 baseline and the 2018-20 monitoring survey.

				ANOVA
Fish Species	**2012**	**2018-20**	**% Change**	**p-value**
Stegastes partitus	5.07	5.13	1.18	0.589
Chromis insolata	4.33	1.67	-61.43	0.916
Lutjanus buccanella	5.00	0.00	-100.00	0.029*
Halichoeres garnoti	1.47	2.60	76.87	0.579
Coryphopterus personatus	1.07	0.13	-87.85	0.573
Holocentrus rufus	0.67	0.20	-70.15	0.055
Pterois sp.	0.67	0.07	-89.55	0.357
Gramma loreto	0.73	3.80	420.55	0.363
Thalassoma bifasciatum	0.53	1.33	150.94	0.299
Cephalopholis fulva	0.67	0.27	-59.70	0.292
Statistically significant at p < 0.05				

The relatively low similarity between surveys of small demersal fish community structure was influenced by the high variability of the numerically dominant species within all three main habitats/depths during both surveys, perhaps with the exception of bicolor damselfish (*Stegastes partitus*). For example, sunshine chromis was the numerically dominant species at CPSlope30-50 in 2012 but was not observed within transects in 2018-20. Conversely, it was the second numerically dominant species at Rhod30-50 in 2018-20 but was not observed within belt-transects in 2012. Sunshine chromis exhibited highly aggregated (patchy) distributions across the entire 30 – 50m depth range in Tourmaline Reef. Likewise, blackfin snapper (*Lutjanus buccanella*) was the numerically dominant species within belt-transects at Rhod30-50 in 2012 but was not observed at Rhod30-50 in 2018-20. Nevertheless, the densities of blackfin snapper are overestimated by small belt-transects because the species is attracted to divers and enters transect areas in large schools, with marked effects on the relative densities of the small demersal fish community at any given habitat/depth.

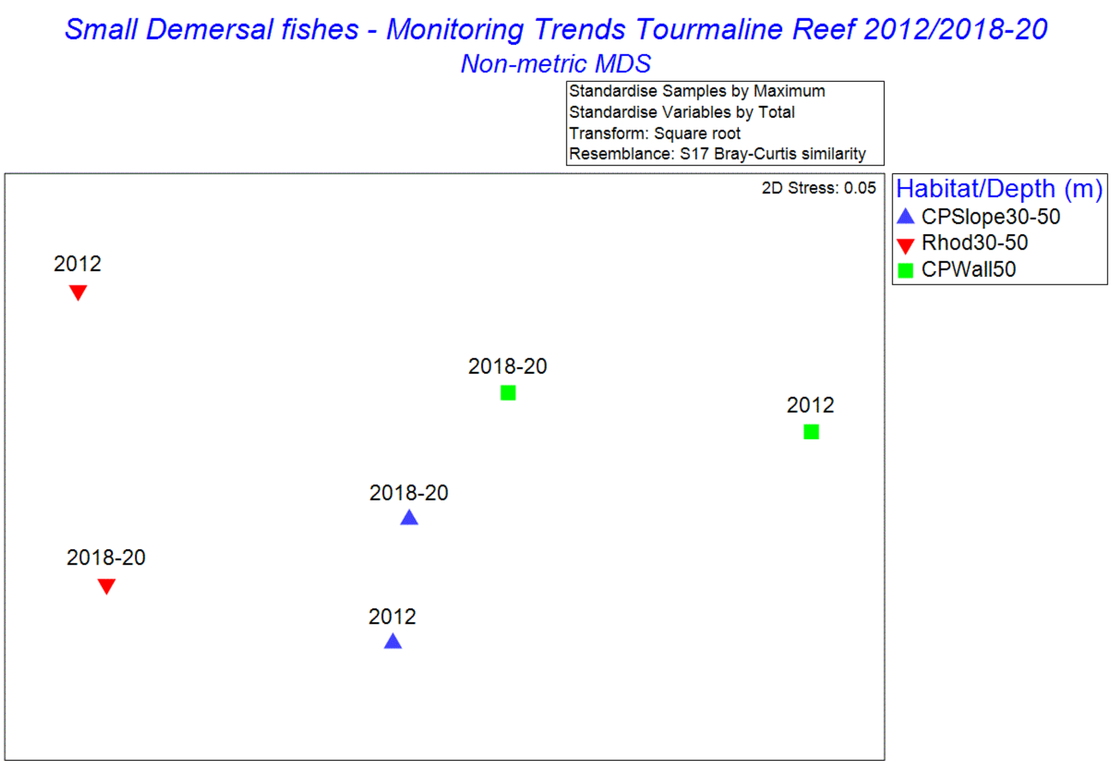

Figure 67. Multidimensional scaling plot of Bray-Curtis similarities of small demersal fish densities between the 2012 baseline and the 2018-20 monitoring surveys at the main habitats/depths surveyed within the 30 – 50m range at Tourmaline Reef.

Table 36. Similarity (SIMPER) matrix of small demersal fish community structure between the 2012 baseline and the 2018-20 monitoring surveys, with species contributions to similarity.

	CPSlope30-50	Rhod30-50	CPWall50
Average Similarity (%)	45.5	32.4	34.5
Fish Species			
Coryphopterus personatus	12.8		
Halichores garnoti	12.1		30.2
Stegastes partitus	11.8		48.9
Pterois sp.	11.7		
Chaetodon capistratus	10.9		
Centropyge argi	9.6		
Holocentrus rufus	9.5		
Holacanthus ciliaris		44.7	
Cephalopholis fulva		39.48	

Community structure of large demersal fishes and shellfishes

Depth/habitat related patterns of density and community structure

A total of 29 large demersal fishes and two shellfish species (queen conch and spiny lobster) were identified from drift belt-transects across the 25 – 50m depth range in Tourmaline Reef during the 2018-20 monitoring survey. Mean densities varied between 7.34 Ind/10^3m^2 at CPSlope25-40 and 31.27 at ACR25 Ind/10^3m$^{2.}$ (Table 37). The combined mean densities of seven species represented 66.0% of the total density of large demersal fishes and shellfishes across the habitats/depths surveyed. These included the blackfin, schoolmaster and lane snappers (*Lutjanus buccanella, L. apodus, L. synagris*), coney (*Cephalopholis fulva*), queen conch (*Lobatus gigas*), queen triggerfish (*Balistes vetula*), and red hind (*Epinephelus guttatus*). Density differences between habitats/depths were not statistically significant (ANOVA; $p = 0.285$) but marked habitat/depth related distribution patterns for numerically dominant species were noted (Figure 68. Densities of lane and yellowtail snappers (*L. synagris, Ocyurus chrysurus*) were higher at ACR25 than at all other habitats/depths (ANOVA; $p < 0.0001$). Conversely, density of queen triggerfish (*B. vetula*) was lower at ACR25 than at any other habitat/depth and higher at Rhod30-50 than at other habitats/depths (ANOVA; $p = 0.0007$). Densities of queen conch (*L. gigas*) were significantly higher at Rhod30-50 and at CPSlope25-30 than at other habitats/depths (ANOVA; $p = 0.008$). Coneys (*C. fulva*), hogfish (*Lachnolaimus maximus*), and mutton snapper (*L. analis*) were observed within drift belt-transects from all habitats/depths within the 25 – 50m depth profile at Tourmaline Reef during the 2018-20 monitoring survey. A total of 18 spiny lobsters (*Panulirus argus*) were all surveyed from CPSlope25-30 and CPSlope31-40 with mean densities of 0.74 and 0.66 Ind/10^3m^2, respectively, and a site mean density of 0.32 Ind/10^3m^2 across all habitats/depths.

Table 37. Taxonomic composition and mean density of large demersal fishes and shellfishes surveyed by drift belt-transects across the main benthic habitats/depths within the 25 – 50m depth range in Tourmaline Reef, 2018-19 survey.

Habitats/Depths (m)	ACR25		CPSlope25-30		CPSlope31-40		Rhod30-50		CPWall50	
Species	Ind	Ind/1000m2	Ind	Ind/1000m2	Ind	Ind/1000m2	Ind	Ind/1000m2	Ind	Ind/1000m2
Fishes										
Lutjanus apodus	2	1.00		0.00	32	1.77	50	4.71		0.00
Lutjanus buccanella		0.00		0.00	52	3.21	1	0.09	28	11.37
Cephalopholis fulva	4	1.99	11	1.18	40	2.59	9	0.89	11	2.16
Balistes vetula		0.00	22	1.83	9	0.57	22	2.33	5	1.54
Lutjanus synagris	35	12.05		0.00	4	0.22		0.00		0.00
Epinephelus guttatus	2	0.40	8	0.68	12	0.79	8	0.80		0.00
Ocyurus chrysurus	21	8.37	3	0.22	2	0.11	2	0.22		0.00
Sphyraena barracuda	3	0.60	2	0.14	23	1.40		0.00		0.00
Lutjanus cyanopterus	1	0.20		0.00		0.00	5	0.47	12	1.80
Lutjanus analis	4	0.80	1	0.08	6	0.38	4	0.38	2	0.83
Cephalopholis cruentatus		0.00		0.00	15	0.82		0.00		0.00
Pterois sp.		0.00		0.00	8	0.49		0.00	6	2.01
Acanthostracion polygonia		0.00	1	0.07	2	0.12	9	0.98		0
Lachnolaimus maximus	2	0.70	1	0.11	6	0.35	1	0.09	1	0.43
Lutjanus jocu		0.00		0.00		0.00	3	0.28	7	1.05
Lactophrys triqueter	3	0.60		0.00	4	0.26		0.00		0.00
Lutjanus mahogoni	6	2.99		0.00	1	0.05		0.00		0.00
Lactophrys trigonus		0.00	3	0.23		0.00	2	0.22	1	0.41
Euthynnus alletteratus		0.00	5	0.36		0.00		0.00		0.00
Caranx lugubris		0.00		0.00		0.00		0.00	3	0.45
Seriola rivoliana		0.00		0.00	2	0.12		0.00	1	0.43
Ginglymostoma cirratum	2	0.70		0.00		0.00		0.00		0.00
Lutjanus griseus	2	0.40		0.00		0.00		0.00		0.00
Scomberomorus cavalla		0.00	2	0.14		0.00		0.00		0.00
Carcharhinus perezi		0.00		0.00		0.00	1	0.11		0.00
Mycteroperca bonaci	1	0.50		0.00		0.00		0.00		0.00
Mycteroperca intersititialis		0.00		0.00		0.00		0.00	1	0.41
Shellfishes										
Lobatus gigas		0.00	19	1.55		0.08	23	2.38		0.00
Panulirus argus		0.00	9	0.74	9	0.66		0.00		0.00
Totals	88	**31.27**	59	**5.04**	218	**13.26**	117	**11.57**	78	**22.88**
Others: *C. hippos, C. latus*										

Community structure similarities based on the relative densities of large demersal fishes/shellfishes from the main benthic habitats/depths surveyed within the 25 – 50m depth range in Tourmaline Reef during the 2018-20 monitoring survey are presented in a multidimensional scatter diagram of Bray-Curtis similarities in Figure 69. Similarities were generally low (18.3 – 50.2%) due to the aggregated distributions of the numerically dominant species introducing high sampling variability to the within habitat/depth similarities.

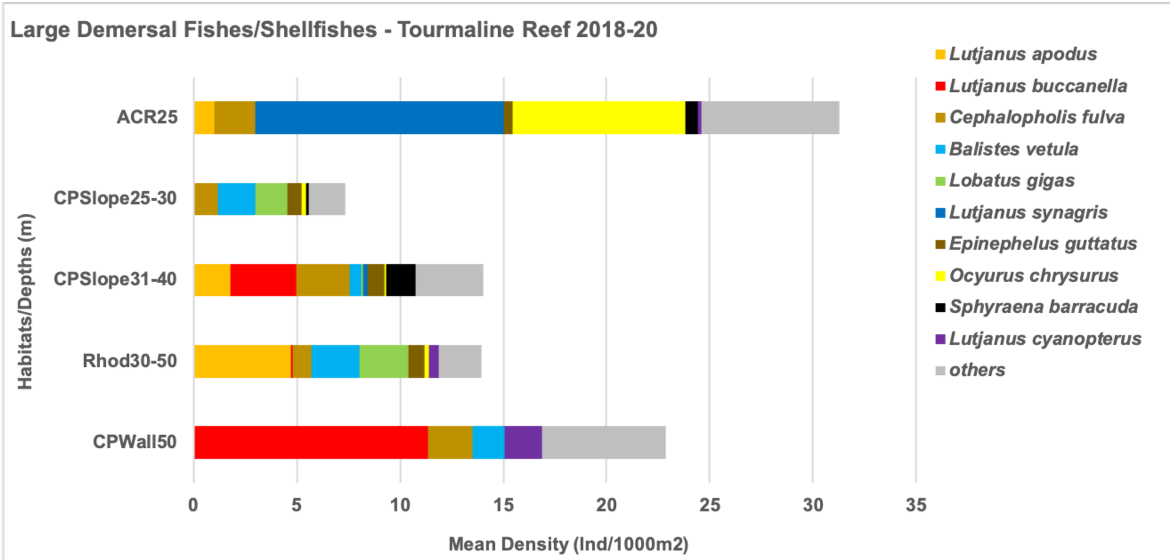

Figure 68. Variations of mean density by large demersal fishes/shellfishes across the main benthic habitats/depths surveyed by drift belt-transects within the 25 - 50m depth range at Tourmaline Reef, 2018-19. Each bar represents the total density at each depth with the mean density contributions of the main species to the total density.

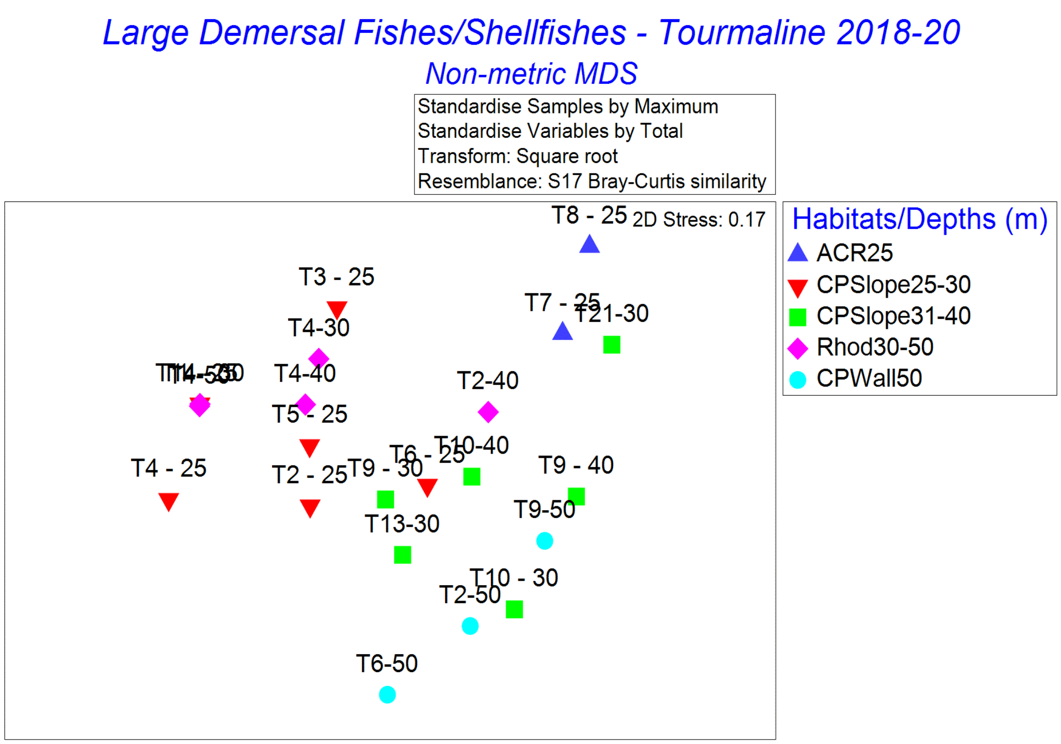

Figure 69. Non-metric multidimensional scaling plot of Bray-Curtis similarities based on the relative densities (top 90% of species) of large demersal fishes/shellfishes surveyed by drift belt-transects from the main benthic habitats/depths in the 25 – 50m depth range at Tourmaline Reef, 2018-20 survey

ACR25 presented the highest similarity (50.2%) largely contributed by lane and yellowtail snappers (*Lutjanus synagris, Ocyurus chrysurus*) (Table 38). These snappers were observed in schooling aggregations and ranked as the top two species in terms of density at ACR25. Lane snappers were observed close to the bottom at the sand-reef interface. Yellowtail snappers were observed over the reef reaching midwater. Community structure variability at ACR25 was related to density inconsistencies within belt-transects of other schooling species, such as mahogany and schoolmaster snappers (*L. mahogoni, L. apodus*), and coney (*Cephalopholis fulva*). The coral reef section at ACR25 was relatively small and was surveyed by two drift-belt-transects. Thus, results from this habitat/depth must be analyzed with caution due to the low sample size.

Queen conch (*Lobatus gigas*) and queen triggerfish (*Balistes vetula*) were the main species contributing similarity at Rhod30-50 (Table 38). The rhodolith habitat is horizontally oriented and of high benthic algal cover making it an ideal habitat for a benthic herbivore such as the queen conch (*L. gigas*). The rhodolith habitat functions as a mating and nesting site for both adult queen conch and queen triggerfishes (*B. vetula*), which use the rhodolith nodules in nest construction. High variability at Rhod30-50 was introduced by schooling aggregations of blackfin and schoolmaster snappers (*Lutjanus buccanella, L. apodus*), each species observed within one out of the six belt-transects surveyed at Rhod30-50.

High relative densities of queen triggerfish (*Balistes vetula*) and spiny lobster (*Panulirus argus*) were the main contributors to large demersal fish/shellfish community structure similarity at CPSlope25-30 (Table 38). The queen triggerfish population at CPSlope25-30 is abundant and individuals were observed from all six (6) belt-transects surveyed from this habitat/depth. Spiny lobsters (*P. argus*) were observed in eight out of the 12 transects surveyed from CPSlope25-30 and CPSlope31-40, occupying small crevices/holes in pavement sections surrounded by sand. Relatively high densities of coney (*Cephalopholis fulva*), lionfish (*Pterois sp.*), mutton snapper (*Lutjanus analis*), and red hind (*Epinephelus guttatus*) were the main contributors (along with *P. argus*) to community structure similarity at CPSlope31-40) (Table 38). Schooling aggregations of blackfin snapper and schoolmaster snappers (*L. buccanella, L. apodus*) and great barracuda (*Sphyraena barracuda*) introduced high variability to the within habitat/depth similarity at CPSlope31-40. Similarity at CPWall was very low (18.3%) due to the high variability introduced by schooling aggregations of blackfin and cubera snappers (*L. buccanella, L. cyanopterus*) observed within one of the three drift belt-transects surveyed from this habitat/depth. Thus, results from this habitat/depth must be interpreted with caution due to the small sample size.

Table 38. Similarity matrix (SIMPER) of large demersal fish/shellfish community structure based on relative densities from the main habitats/depths surveyed within the 25 – 50m depth range at Tourmaline Reef, with species contributions to similarity, 2018-20 survey.

	ACR25	CPSlope25-30	CPSlope31-40	Rhod30-50	CPWall50
Average Similarity (%)	**50.2**	**37.5**	**36.4**	**45.4**	**18.3**
Species Contributions					
Lutjanus synagris	50.3				
Ocyurus chrysurus	30.4				
Balistes vetula		59.3		40.0	36.1
Panulirus argus		16.5	10.0		
Cephalopholis fulva			26.8		
Pterois sp.			16.4		31.0
Lutjanus analis			11.2		19.2
Epinephelus guttatus			9.5		
Lobatus gigas				42.6	

Dissimilarities of large demersal fish/shellfish community structure between the main habitats/depth surveyed during 2018-20 are shown in Table 39. Dissimilarities were highest between ACR25 and other habitats/depths, largely contributed by the higher relative densities of lane, mahogany and yellowtail snappers (*Lutjanus synagris, L. mahogoni, Ocyurus chrysurus*) at ACR25. The higher relative densities of queen conch (*Lobatus gigas*) and queen triggerfish (*Balistes vetula*) contributed markedly to dissimilarities between Rhod30-50 and other habitats/depths, whereas spiny lobster (*Panulirus argus*) distinguished CPSlope25-30 and CPSlope31-40 from other habitats/depths. The higher relative densities of lionfish (*Pterois sp*), hogfish (*Lachnolaimus maximus*), and blackfin and cubera snappers (*L. buccanella, L. cyanopterus*) were the main contributors to dissimilarity between CPWall50 and other habitats/depths (Table 39).

The relatively high dissimilarities between habitats/depths across the 25 – 50m depth range surveyed from Tourmaline Reef during 2018-20 is indicative of distinct species-habitat assemblages that may have been influenced by a series of factors, including microhabitat and food availability, depth, slope, water temperature, predation pressure, ontogenetic and/or reproductive behavior (including spawning aggregations), recruitment supply, fishing mortality, and/or physical forcing factors associated with wave action, surge (scouring), and sand movements and abrasion.

Table 39. Dissimilarity matrix (SIMPER) of large demersal fish/shellfish community structure based on relative densities from the main habitats/depths surveyed within the 25 – 50m depth range at Tourmaline Reef, with species contributions to similarity, 2018-20 survey.

Habitats/Depths (m)	**ACR25 vs CPSlope25-30**	**ACR25 vs CPSlope31-40**	**ACR25 vs Rhod30-50**	**ACR25 vs CPWall50**	**CPSlope25-30 vs CPSlope31-40**	**CPSlope25-30 vs Rhod30-50**	**CPSlope25-30 vs CPWall50**	**CPSlope31-40 vs Rhod30-50**	**CPSlope31-40 vs CPWall50**	**Rhod30-50 vs CPWall50**
Average Dissimilarity (%)	**89.1**	**79.6**	**88.7**	**87.9**	**74.8**	**58.4**	**85.2**	**80.1**	**70.4**	**84.8**
Species Contributions										
Lutjanus synagris	19.3	16.4	19.4	18.7						
Ocyurus chrysurus	13.1	12.1	12.8	13.7						
Lutjanus mahogoni	13.0	11.6	12.6	12.4						
Lutjanus cyanopterus				9.2			12.9		11.1	13.2
Balistes vetula	8.1		7.6							
Lachnolaimus maximus	6.9		6.8	7.5			8.3		8.7	7.5
Sphyraena barracuda	6.5									
Lutjanus analis	5.6	5.9			9.2		7.8	8.2	8.4	7.5
Cephalopholis fulva		5.8			9.4	8.3		8.40	7.80	
Panulirus argus		5.8			8.7	12.5	8.0	8.2	8.8	
Pterois sp.				8.7	8.5		13.8	7.7	10.5	13.3
Lutjanus buccanella					8.5		12.2		11.2	11.6
Epinephelus guttatus					8.4	11.6		6.7	7.9	
Lobatus gigas			8.6			15.8	8.2	9.7		13.6
Acanthostracion polygonia			6.0			14.8		8.1		8.7
Lutjanus apodus						7.4		6.4		

Temporal Variations of Large Demersal Fish/Shellfish Densities and Community Structure Between the 2012 baseline and the 2018-20 Monitoring Survey

Variations of mean densities by large demersal fishes and shellfishes (queen conch and spiny lobster) surveyed by drift belt-transects between the 2012 baseline and the 2018-20 monitoring survey are summarized in Table 40. Total fish density varied between a maximum of 181.7 Ind/10^3m^2 at the CP Wall during 2012, and a minimum of 8.6 Ind/10^3m^2 at Rhod30-50 during the 2018-20 survey (Figure 70). Total fish/shellfish density differences between surveys were statistically insignificant for all habitats/depths (ANOVA; $p > 0.05$). The largest variation was an 88.6% decline of mean density from CPWall50 during 2018-20, associated with an 8-fold density decline of dog snapper (*Lutjanus jocu*). Such variation was related to the presence of a dog snapper spawning aggregation of approx. 240 large adult individuals observed within the survey area of one drift belt-transect at CPWall50 during the baseline survey in June 2012. Schooling aggregations unrelated to spawning from other habitats/depths were also noted for blackfin, mutton, schoolmaster, lane, mahogany, and cubera snappers (*L. buccanella, L. analis, L. apodus, L. synagris, L. mahogoni, L. cyanopterus*). Schooling aggregations strongly influenced the total density estimates for particular habitats/depths, but the highly aggregated (patchy) distributions resulted in high (within habitat/depth) sampling variability and thereby introduced high uncertainty associated to density means of the large demersal fish assemblage from each habitat/depth.

Table 40. Temporal variations of large demersal fish/shellfish densities from the main benthic habitats/depths surveyed within the 30 – 50m depth range at Tourmaline Reef during the 2012 baseline and the 2018-20 monitoring survey.

Large Demersal	Mean Densities (Ind/1000m2)			ANOVA
Fish/Shellfish	**2012**	**2018-20**	**% Change**	**p-value**
Total Assemblage				
CPSlope30-50	11.00	20.71	88.25	0.0744
Rhod30-50	22.00	8.62	-60.82	0.0626
CPWall50	181.67	20.71	-88.60	0.569
Fish Species				
Balistes vetula	1.56	1.29	-17.7	0.386
Epinephelus guttatus	0.73	0.74	1.1	0.953
Lachnolaimus maximus	0.31	0.30	-5.6	0.768
Lutjanus analis	0.94	0.53	-99.3	0.507
Lutjanus apodus	0.00	1.67		0.123
Lutjanus buccanella	0.21	4.70	2154.3	0.04*
Lutjanus jocu	27.40	0.29	-99.0	0.394
Pterois sp	1.04	0.65	-37.2	0.441
Shellfishes				
Lobatus gigas	6.46	1.94	-70.0	0.202
Panulirus argus	0.21	0.91	338.7	0.202
* Statistically significant at $p < 0.05$ (One-way ANOVA)				

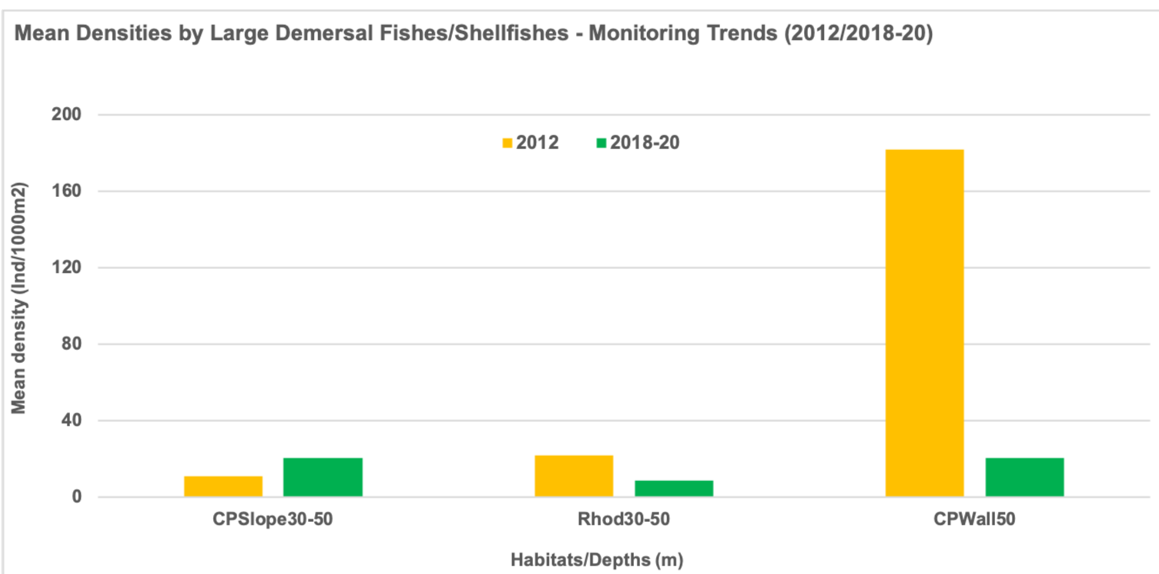

Figure 70. Mean density variations large demersal fish/shellfishes surveyed from the main benthic habitats/depths within the 30 – 50m depth range at Tourmaline Reef during the 2012 baseline and the 2018-20 monitoring survey.

Site mean density of queen conch (*Lobatus gigas*) declined 70.0% between the 2012 baseline and the 2018-20 monitoring survey. Differences were not statistically significant (ANOVA; p = 0.202) due to the high variability associated with the aggregated (patchy) distribution and the relatively high frequency of 0 sightings from drift belt-transect samplings in both surveys. Queen conch individuals were observed in nine (9) out of the 15 samplings from CPSlope30-50 and Rhod30-50 in 2012, and from six (6) out of the 15 samplings from the same stations in 2018-20. As would be expected, *L. gigas* were not observed at the CPWall50 due to the vertical substrate inclination. Many dead *L. gigas* with unbroken shells were observed in the 2018-20 survey. This may be indicative of exposure to a severe stress leading to non-fishery related mortality. Extreme surge and abrasion associated with the pass of Hurricane Maria in 2017 and/or winter storm Riley in 2018 may have been causal factors of such conditions. Conversely, mean densities of spiny lobster (*Panulirus argus*) increased by +338.7% during 2018-20, relative to 2012, from two (2) individuals in 2018-20 to nine (9) individuals in 2018-20. The difference was statistically insignificant (ANOVA; p = 0.202) due to the high variability introduced by the relatively large number of transect samplings with 0 individuals.

Six snappers (Lutjanidae), including the blackfin, cubera, mutton, lane, schoolmaster, and mahogany (*Lutjanus buccanella, L. cyanopterus, L. analis, L. synagris, L. apodus, L. mahogoni*) were the numerically dominant large demersal fish assemblages from all habitats/depths surveyed within the 25 – 50m depth range at Tourmaline during both surveys. Density differences between surveys were only statistically significant for *L. buccanella* (ANOVA; p = 0.04). Habitats in the 40-50m depth range appeared to be the shallow frontier of blackfin snapper foraging grounds and despite the apparent increase of density this result is not considered to provide an assessment of change for this population. Certainly, there is a healthy population of blackfin snapper associated with the upper insular slope at Tourmaline Reef and schools of juveniles and small adults were attracted to divers during drift transect surveys. Cubera and dog snappers (*L. cyanopterus, L. jocu*) represented some of the top predators of the reef system and were abundant at the CPWall50 during both surveys. Lane, mahogany, and schoolmaster snappers (*L. synagris, L. mahogoni, L. apodus*) appeared to prefer the high rugosity and high coral cover of the aggregated coral reef habitat at ACR25. Mean densities of red hind (*Epinephelus guttatus*), queen triggerfish (*Balistes vetula*), and hogfish (*Lachnolaimus maximus*) remained virtually constant between surveys from mesophotic habitats in the 30 -50m depth range at Tourmaline Reef suggesting that these populations have remained stable during this period.

Temporal differences (between surveys) of the large demersal fish and shellfish community structure analyzed by the relative contributions of species to the total density from mesophotic benthic habitats surveyed across the 30 – 50m depth range are presented in a multidimensional scaling plot of Bray-Curtis similarities in Figure 71. The highest similarities between surveys were observed from the CPSlope30-50 (63.7%), largely contributed by hogfish (*Lachnolaimus maximus*), yellowtail and mutton snapper (*Ocyurus chrysurus*, *Lutjanus analis*), and red hind (*Epinephelus guttatus*) (Table 41). Similarity between surveys at Rhod30-50 (43.2%) was largely contributed by queen conch (*Lobatus gigas*), queen triggerfish (*Balistes vetula*), and mutton snapper (*Lutjanus analis*). Red hinds were observed in six (6) out of the 10-drift belt-transects surveyed at the CPSlope during both surveys. Queen conch and queen triggerfish were observed in four (4) transects during 2012, and in three (3) and seven (7) transects during 2018-20, respectively. Queen conch (*Lobatus gigas*), queen triggerfish (*Balistes vetula*), and cubera snapper (*Lutjanus cyanopterus*) were the main contributors to similarities between surveys at the Rhod30-50. Queen conch were observed in four (4) out of the five (5) belt-transects at Rhod30-50 habitat during both surveys, but a very large aggregation of 40 Ind/10^3m^3, representative of 41.4% of the total individuals surveyed in 2012 had a marked effect in terms of community structure by driving differences in the rank order of densities between survey years, from first (1^{st}) in 2012, to third (3^{rd}) in 2018-20. Queen triggerfish (*B. vetula*) was observed in all five (5) drift-transects in 2018-20 and in three (3) drift belt-transects in 2012. Resident adult, actively reproducing populations were observed during both surveys. Cubera (*L. cyanopterus*) and mutton snappers (*L. analis*) appear to be transitional predators that forage at the rhodolith habitat.

The lowest similarities between surveys of the large demersal fish/shellfish community structure were observed from CPWall50 (26.6%). Similarities between surveys were mostly contributed by dog snapper and mutton snappers (*Lutjanus jocu, L. analis*), and queen triggerfish (*Balistes vetula*). Dog snapper was observed in both 2012 and 2018-20 surveys at CPWall50, but its density was two orders of magnitude higher (146.1 Ind/10^3m^2) in 2012 (rank 1) versus 2018-20 (1.05 Ind/10^3m^2 - rank 5). Differences were associated with a spawning aggregation of more than 200 individuals during June 14, 2012 driving the large separation of similarities between survey years at CPWall50 (Figure 71). The relatively low similarity between surveys at the CPWall50 was also influenced by another schooling aggregation of blackfin snapper (*L. buccanella*) observed during 2018-20. Given the fact that only three drift belt-transect samplings were performed at CPWall50, temporal patterns about large demersal fish/shellfish community structure from this habitat/depth must be analyzed with caution due to the small sample size.

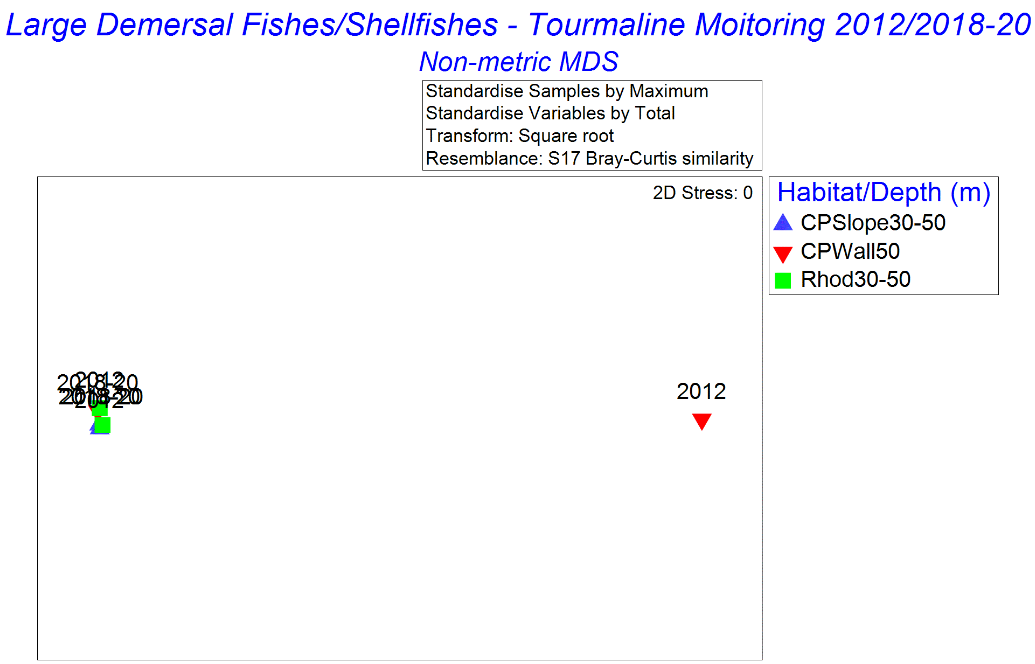

Figure 71. Multidimensional scaling plot based on Bray-Curtis similarities of the relative densities of large demersal fishes and shellfishes surveyed from drift belt-transects during the 2012 baseline and the 2018-20 monitoring surveys at mesophotic benthic habitats within the 30 – 50m depth range in Tourmaline Reef.

Table 41. Similarity matrix (SIMPER) of large demersal fish community structure between the 2012 baseline and the 2018-20 monitoring survey at mesophotic benthic habitats surveyed across the 30 – 50m depth range in Tourmaline Reef.

Habitats/Depths (m)	CPSlope30-50	Rhod30-50	CPWall50
Average Similarity (%)	63.7	43.2	26.6
Fish/Shellfish Species Contributions			
Lachnolaimus maximus	11.7		
Ocyurus chrysurus	11.1		
Lutjanus analis	11.0	24.5	13.4
Epinephelus guttatus	10.4		
Panulirus argus	9.9		
Lobatus gigas	9.6	28.1	
Lutjanus jocu			45.4
Balistes vetula		25.7	19.0

Size distributions of numerically dominant large demersal fish/shellfish species, 2012 – 2018-20 surveys

Dog Snapper (*Lutjanus jocu*)

Dog snapper (*L. jocu*) was the numerically dominant species from drift belt-transect surveyed within the 30 – 50m depth range during 2012 at Tourmaline Reef with a site mean density of 48.7 Ind/10^3m^2 and ranked fifth in 2018-20 with a site mean density of 1.05 Ind/10^3m^2. Statistically significant differences of the size distributions between the 2012 baseline and the 2018-20 monitoring surveys were found (Kolmogorov-Smirnoff; $p < 0.01$). Size distributions in 2012 were strongly influenced by a spawning aggregation of approximately 240 individuals with a strong mode in the 50 – 55cm FL size classes, and a maximum size of 70cm FL (Figure 72). The size distribution was skewed towards larger individuals with a mode at 70 - 75cm FL and maximum size of 80cm FL in 2018-20. Evidently, the spawning aggregation was an important factor influencing the size distributions between surveys. It also provided a key inference about the spawning stock biomass of *L. jocu* corresponding to at least 240 individuals in 2012. It is uncertain if the aggregation included only individuals from Tourmaline Reef, or if it also included individuals from adjacent shelf regions.

If the mean density of *L. jocu* from mesophotic habitats (30 – 50m depth) surveyed from Tourmaline Reef in 2018-20 (0.035 Ind/10^3m^2) is multiplied by the total mesophotic area (excluding sand habitats) within the 30 - 50m depth (7,180 x 10^3m^2) (Garcia-Sais et al., 2014) the total population estimate for *L. jocu* in 2018-20 would be 253 individuals, very similar to the spawning aggregation estimate of 240 individuals in 2012, suggesting that the aggregation was from a localized population within Tourmaline Reef, not from the entire southwest shelf region, and that the population numbers have remained more or less stable during the seven year survey interval at this reef system. All *L. jocu* surveyed in 2012 and 2018-20 were larger than the minimum size at maturity of 31 cm (Froese and Pauly, 2019), indicative of an adult population.

Mutton Snapper (***Lutjanus analis***)

Mutton snapper (*L. analis*) ranked fifth in terms of site mean density within drift belt-transects in 2012 (0.91 Ind/10^3m^2) and ranked 12th in 2018-20 with a site mean density of (0.51 Ind/10^3m^2). Size distribution differences of *Lutjanus analis* between the 2012 and the 2018-20 surveys were statistically significant (Kolmogorov-Smirnoff; $p < 0.01$). The results must be interpreted with caution because they were based on a small sample size (N = 40). During both survey years, *L.*

analis presented a primary mode of 42cm FL (Figure 73). In 2012, *L. analis* exhibited a secondary mode of 51cm and a tertiary mode of 60cm, whereas the 2018-20 survey included a secondary mode of 48cm and a maximum FL of 57cm. The main difference was supported by the group of 60cm individuals in 2012 not observed during 2018-20. These results will be analyzed in the broader context of adjacent sites in the west coast in order to establish if such size distribution differences represent a real trend or an artifact of sampling variability influenced by the small sample size. The size at maturity of *L. analis* has been reported as 31cm FL (Froese and Pauly, 2019). Therefore, all of the individuals observed within mesophotic habitats at Tourmaline Reef were adult individuals.

Blackfin snapper (*Lutjanus buccanella*)

Blackfin snapper (*L. buccanella*) was the numerically dominant species from drift belt-transects surveyed within the 30 – 50m depth range at Tourmaline Reef during 2018-20 with a mean density of 5.52 Ind/10^3m^2 and ranked 12th with a mean density of 0.11 Ind/10^3m^2 in 2012. Size differences between surveys were not statistically significant (Kolmogorov-Smirnoff; $p > 0.10$). *L. buccanella* is a schooling species and in most instances, schools were comprised by individuals of similar sizes. In 2012, size modes in the 25 – 30cm FL prevailed, whereas 20 – 25cm size modes prevailed in 2018-20 (Figure 74). Maximum sizes of 35 and 40cm were observed during 2018-20 and 2012, respectively. Since the size at maturity of *L. buccanella* is reported at 31cm FL, most of the individuals observed during both survey years were juveniles. Adult *L. buccanella* are typically found deeper down the insular slope.

Cubera Snapper (*Lutjanus cyanopterus*)

Cubera snapper (*L. cyanopterus*) ranked 4th in terms of site mean density within drift belt-transects in 2012 (1.63 Ind/10^3m^2) and ranked 10th with a site mean density of 0.54 Ind/10^3m^2 in 2018-20. *L. cyanopterus* was the largest species observed among snappers (Lutjanidae) from Tourmaline Reef in both survey years with maximum sizes reaching up to 120cm FL and 110cm FL in 2012 and 2018-20, respectively. Size distribution differences between survey years were statistically insignificant (Kolmogorov-Smirnoff; $p > 0.10$). More than 60% of the 88 individuals observed during both surveys were distributed within the 80 - 100cm FL size classes (Figure 75). Size at maturity information for *L. cyanopterus* is presently unavailable but given the skewed distribution towards very large sizes it appears that mostly an adult population was observed from mesophotic habitats in Tourmaline Reef. Cubera snappers have been reported to a max size of 160cm FL and are common to 90cm (Froese and Pauly, 2019).

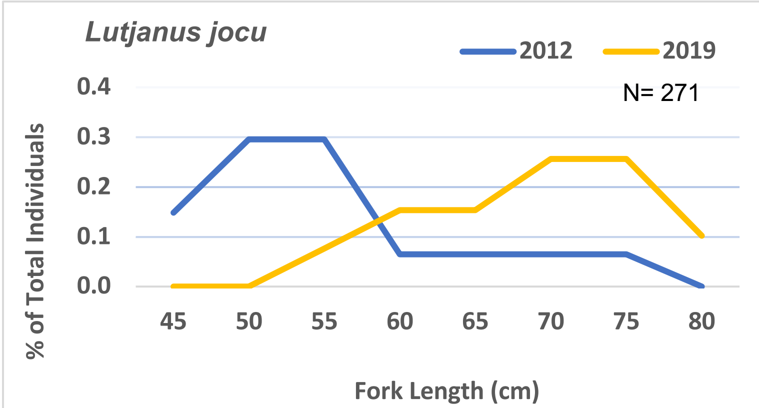

Figure 72. Size-frequency distribution of dog snapper (*Lutjanus jocu*) from mesophotic habitats in the 30 – 50m depth range in Tourmaline Reef (2012 and 2018-20 surveys).

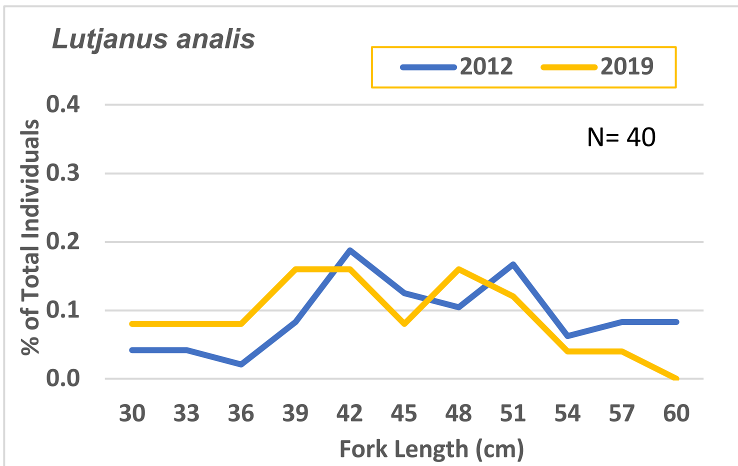

Figure 73. Size-frequency distribution of mutton snapper (*Lutjanus analis*) from mesophotic habitats in the 30 – 50m depth range in Tourmaline Reef (2012 and 2018-20 surveys).

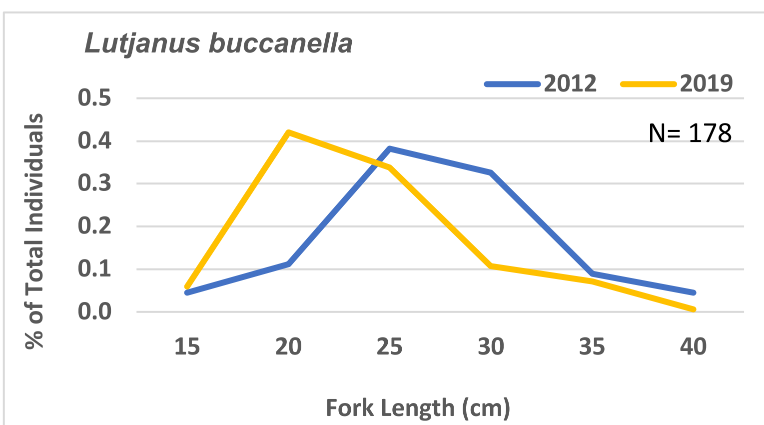

Figure 74. Size-frequency distribution of blackfin snapper (*Lutjanus buccanella*) from mesophotic habitats in the 30 – 50m depth range in Tourmaline Reef (2012 and 2018-20 surveys).

Red Hind (*Epinephelus guttatus*)

Red hind (*E. guttatus*) ranked 5th in terms of site mean density within drift belt-transects in 2012 (0.56 Ind/10^3m^2) and ranked 6th with a site mean density of 0.87 Ind/10^3m^2 in 2018-20. It was the most abundant grouper (Serranidae) surveyed during both years from Tourmaline Reef. Size distributions of *E. guttatus* from the 2012 and 2018-20 surveys within the 30 – 50m depth range were not statistically different (Kolmogorov-Smirnoff; $p > 0.10$). Two main total length (TL) modes at 21cm and at 30cm were evident from the 2012 and the 2018-20 surveys (Figure 76). The length at maturity of *E. guttatus* was reported at 25cm TL, and the maximum length at 76 cm (Froese and Pauly, 2019). Therefore, the smaller size mode observed corresponds to a juvenile cohort (15 – 24cm TL) distributed throughout all benthic habitats and depths surveyed. The juvenile cohort represented 41.0% and 34% of the total population within drift belt-transects during 2012 and 2018-20, respectively. The mode at 30 cm TL corresponded to an adult population that included individuals up to a maximum length of 42 and 39 cm TL observed in samplings during 2012 and 2018-20, respectively.

Coney (*Cephalopholis fulva*)

Coneys (*C. fulva)* were the 3rd most abundant fish species identified within drift belt-transect surveys in 2018-20 with a site mean density of 2.17 Ind/10^3m^2. Two main TL modes at 16cm and at 25 cm were evidenced from the size distribution of 2018-20, based on a sample of 69 individuals (Figure 77). The length at maturity of *C. fulva* was reported at 14.5cm (Froese and Pauly, 2019). Therefore, both of the size modes were part of the adult population with individuals reaching up to a maximum size of 37cm. The juvenile population of *C. fulva*, represented by individuals smaller than 14cm accounted for 9.6% of the total observed within drift belt-transects in 2018-20. Coneys were not included in the 2012 survey because they were not considered as a large demersal species but given their relatively much higher density compared to larger grouper species it appears to be at present the most important grouper in terms of total biomass within mesophotic habitats of Tourmaline Reef.

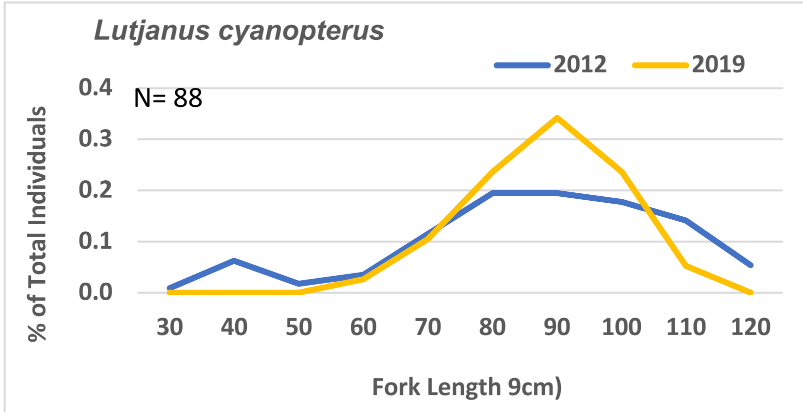

Figure 75. Size-frequency distribution of cubera snapper (*Lutjanus cyanopterus*) from mesophotic habitats in the 30 – 50m depth range in Tourmaline Reef (2012 and 2018-20 surveys).

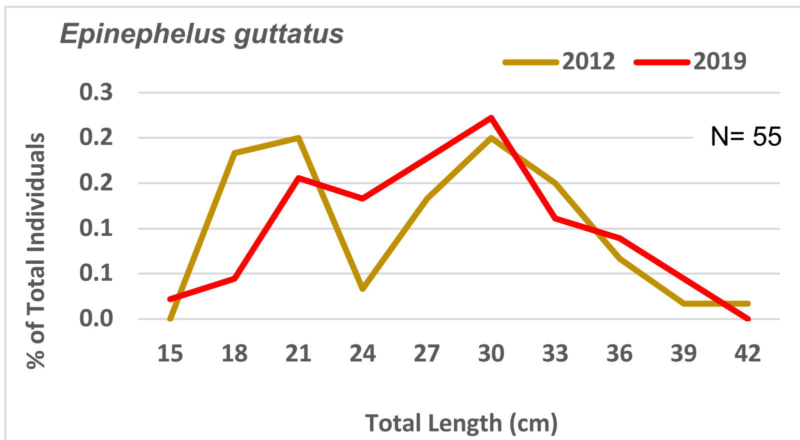

Figure 76. Size-frequency distribution of red hind (*Epinephelus guttatus*) from mesophotic habitats in the 30 – 50m depth range in Tourmaline Reef (2012 and 2018-20 surveys).

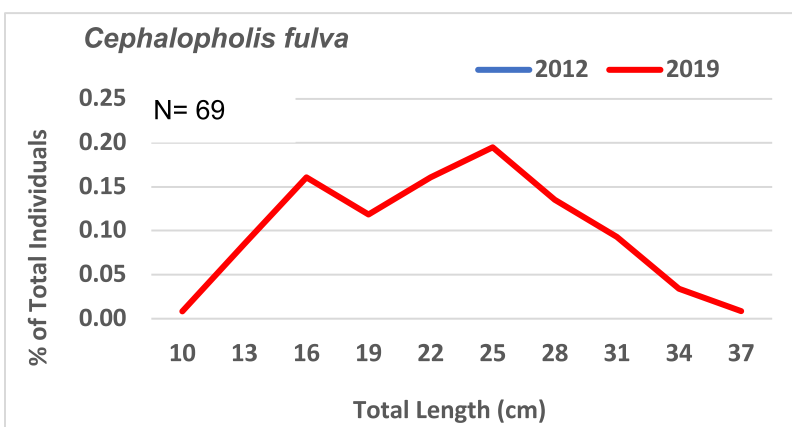

Figure 77. Size-frequency distribution of coney (*Cephalopholis fulva*) from mesophotic habitats in the 30 – 50m depth range in Tourmaline Reef (2012 and 2018-20 surveys).

Queen Triggerfish (*Balistes vetula*)

Queen triggerfish (*B. vetula*) ranked as the 3rd most abundant fish species within drift belt-transects in both the 2012 and 2018-20 surveys with site mean densities of 1.87 Ind/10^3m^2 and 1.43 Ind/10^3m^2 in 2012 and 2018-20, respectively. Individuals of *B. vetula* were observed from all benthic habitats and depths surveyed at Tourmaline Reef during both survey years. Differences of size distributions of *B. vetula* in the 2012 and 2018-20 surveys were statistically insignificant (Kolmogorov-Smirnoff; $p > 0.10$).

Two principal FL modes at 31cm and 34cm were recognized in 2012 and 2018-20, respectively (Figure 78). Approximately 50% of the total populations surveyed in both years were included within those size modes producing size distributions markedly skewed to the smaller sizes within the observed range. Size at maturity of *B. vetula* was reported at 25.5cm (Froese and Pauly, 2019). So, the entire *B. vetula* population surveyed from mesophotic habitats at Tourmaline Reef during both survey years consisted only of adults, but mostly of young adults. It is possible that the prominence of strong size classes close to the size at maturity are associated with the function of mesophotic habitats as recruitment sites for reproductively active individuals. Queen triggerfish reproductive activities involving courtship and defense of nesting sites were observed from rhodolith benthic habitats down to the maximum depth surveyed of 50m. Maximum FL sizes were observed at 48cm and 46cm in 2012 and 2018-20, respectively.

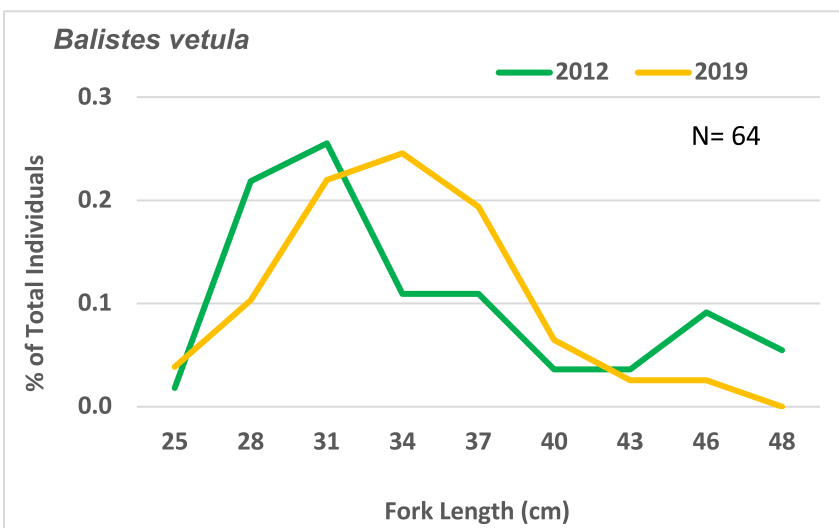

Figure 78. Size-frequency distribution of queen triggerfish (*Balistes vetula*) from mesophotic habitats in the 30 – 50m depth range in Tourmaline Reef (2012 and 2018-20 surveys).

Lionfish (*Pterois sp.*)

Site mean densities of lionfish (*Pterois sp.*) surveyed by drift belt-transects within the 30 – 50m mesophotic depth range in Tourmaline Reef varied between 0.56 Ind/$10^3$$m^2$ in 2012 (rank 4^{th} tie) and 0.64 Ind/$10^3$$m^2$ in 2018-20 (rank 8^{th}). Strong TL modes were evidenced at 24cm in 2012 (30% of total individuals) and at 30cm in 2018-20 (25% of total individuals) (Figure 79). Size distribution differences were not statistically significant (Kolmogorov-Smirnoff; $p > 0.10$), despite the marked size increment between survey years. More than 90% of the total individuals in 2012 were larger than the reported length at maturity of 16.0cm TL (Froese and Pauly, 2019) for *P. volitans*, whereas all individuals in 2018-20 fell into the adult size classes. Maximum lengths were at 33cm in 2012 (3.2% of the total individuals) and 36cm in 2018-20 (7.6% of the total individuals). The size distribution of *P. volitans* evidenced that mostly adults' individuals were present within the 30 – 50m depth range in Tourmaline Reef with what appears to be a marked trend toward larger sizes in 2018-20. Also, the pronounced skewness of the 2018-20 size distribution suggests lack or paucity of recruitment into adult size classes within this depth range.

Queen Conch (*Lobatus gigas*)

A total of 133 queen conch (*L. gigas*) were included in the 2012 baseline and 2018-20 monitoring survey of mesophotic habitats within the 30 – 50m depth range in Tourmaline Reef with site mean densities of 5.77 Ind/$10^3$$m^2$ in 2012 and 1.30 Ind/$10^3$$m^2$ in 2018-20. Size frequency distributions exhibited a primary mode at 23cm (shell length) and a secondary mode at 21cm during both survey years. Individuals within these size modes represented 75% and 59% of the total population in 2012 and 2018-20, respectively (Figure 80). The size distribution in 2018-20 was more skewed towards larger sizes influenced by a tertiary mode at 25cm representative of 25% of the total individuals. Maximum sizes up to 27cm were observed during both surveys. Recruitment into mesophotic habitats was noted at 19cm in both survey years. Differences of *L. gigas* size distributions between survey years were not statistically significant (Kolmogorov-Smirnoff; $p > 0.10$).

The high similarity of *L. gigas* size distributions between the 2012 and 2018-20 surveys suggests that the 4.4-fold decline of the population measured in 2018-20 was unrelated to recruitment failure, nor fishing mortality. In fact, a comparatively larger queen conch population was observed in 2018-20, whereas the recruitment size remained the same. The population decline was observed across all sizes which coincides with the findings of unbroken empty shells of various sizes within sampling areas.

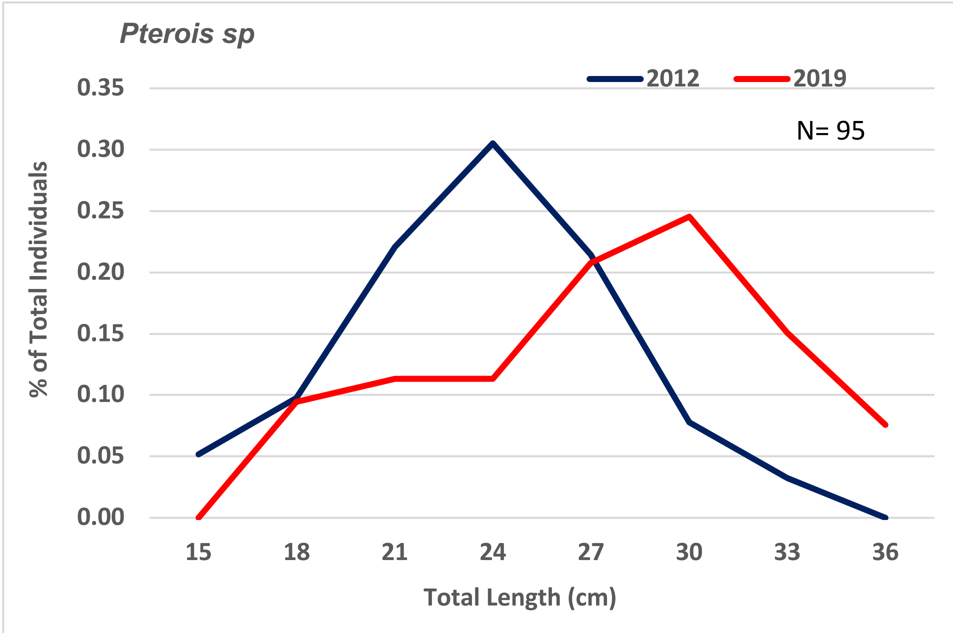

Figure 79. Size-frequency distribution of lionfish (*Pterois sp.*) from mesophotic habitats in the 30 – 50m depth range in Tourmaline Reef (2012 and 2018-20 surveys).

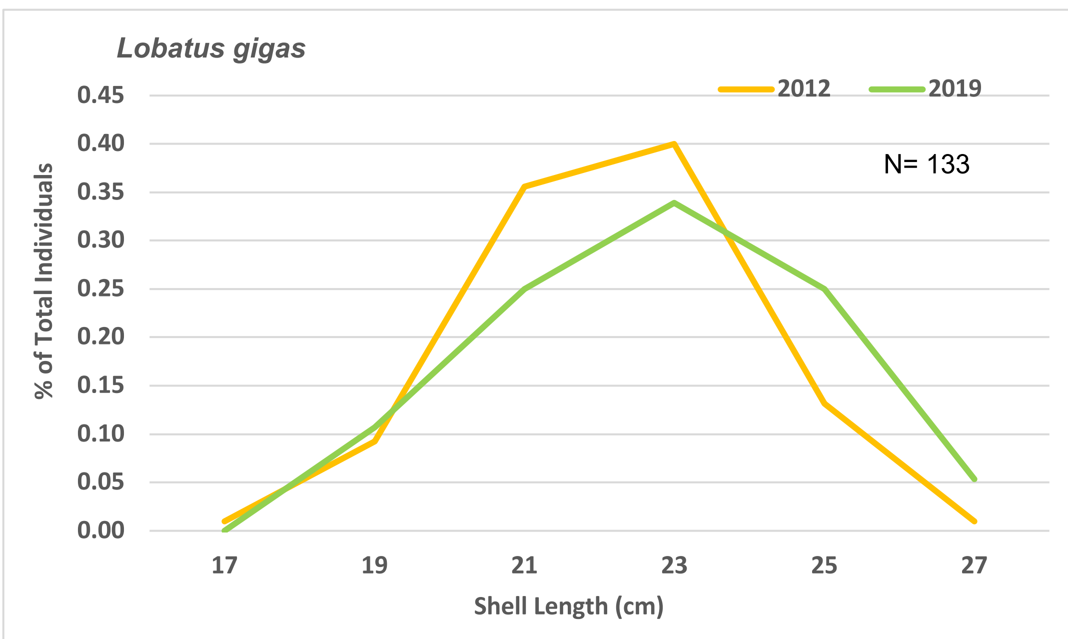

Figure 80. Size-frequency distribution of queen conch (*Lobatus gigas*) from mesophotic habitats in the 30 – 50m depth range in Tourmaline Reef (2012 and 2018-20 surveys).

Spiny Lobster (*Panulirus argus*)

Site mean densities of spiny lobsters (*P. argus*) from mesophotic habitats within the 30 – 50m depth range surveyed by drift belt-transects in Tourmaline Reef varied between 0.11 Ind/10^3m^2 in 2012 and 0.49 Ind/10^3m^2 in 2018-20. Strong cephalothorax length (CL) modes were noted at 8cm in 2012 (33.3% of total individuals) and at 7cm in 2018-20 (31.6% of total individuals) (Figure 81). These modes represent the population recruitment size classes (cohorts) into mesophotic habitats of Tourmaline Reef. Size distribution differences of *P. argus* between survey years were not statistically significant (Kolmogorov-Smirnoff; $p > 0.10$), but evidently a higher proportion of individuals 10cm and larger were observed in 2018-20 (52.7%), relative to 2012 (13.4%).

The higher proportion of larger *P. argus* individuals and the 3.4-fold increase of the mean population density within drift belt-transects in 2018-20 may be related to a release of fishing pressure. This trend needs to be examined in the context of a larger sample size including more mesophotic survey sites because of the high uncertainty associated with the small sample size from Tourmaline Reef.

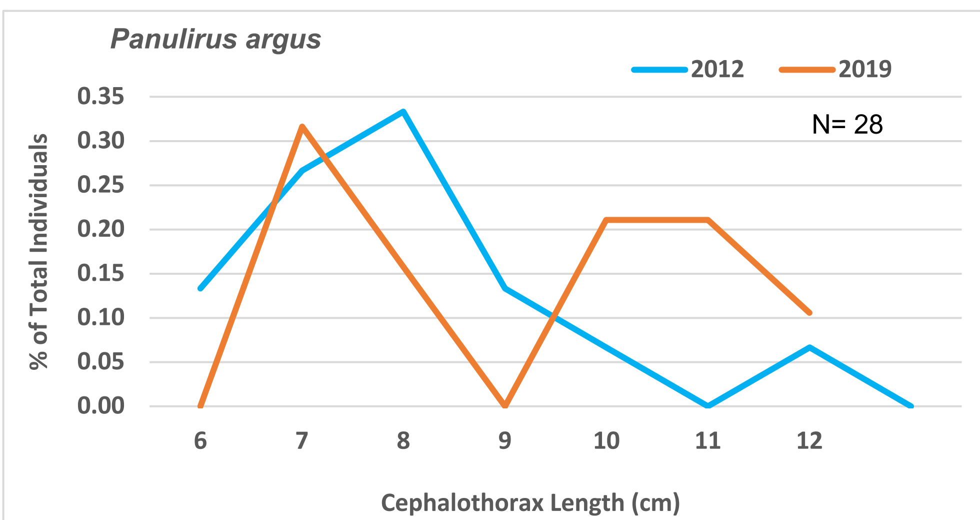

Figure 81. Size-frequency distribution of spiny lobster (*Panulirus argus*) from mesophotic habitats in the 30 – 50m depth range of Tourmaline Reef (2012 and 2018-20 surveys).

Photo Album 3 – Tourmaline Reef

Aggregate Coral Reef - TOUR



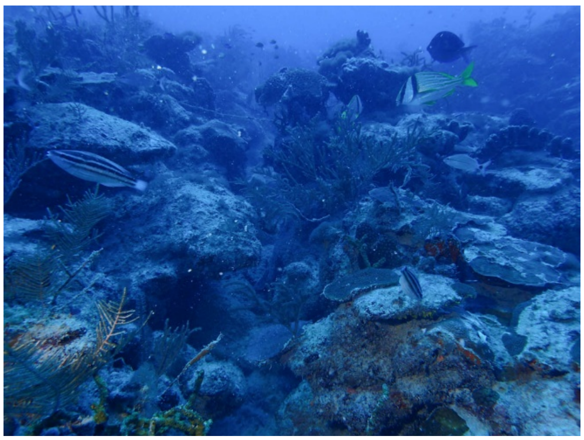


Colonized Pavement Reef Top - TOUR

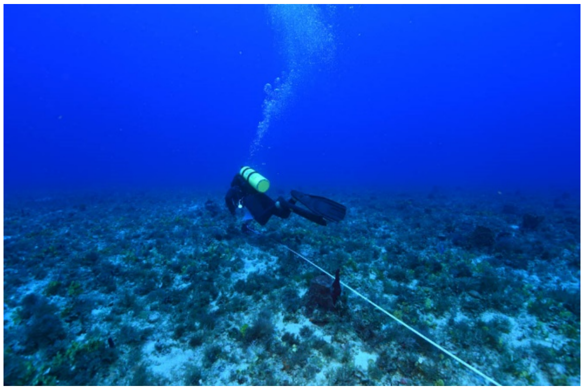

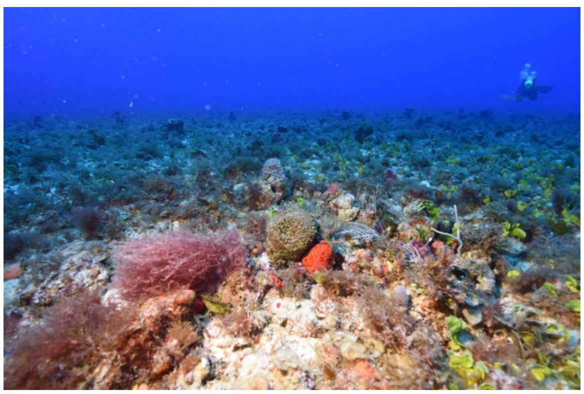

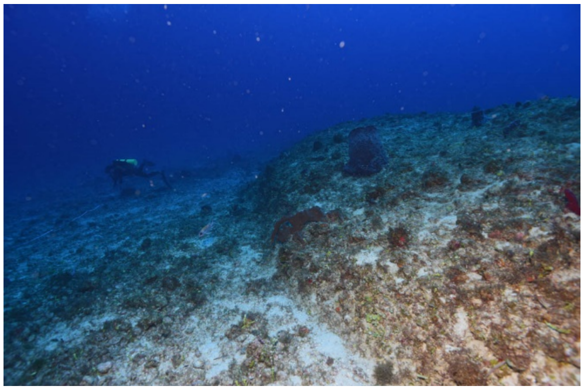

Isla Desecheo – Physical Description

Desecheo is an oceanic island located in Mona Passage, about nine nautical miles off Rincón, northwest coast of Puerto Rico. The emergent section of the island is about 1.6 km long by 1.4 km wide. Its submerged shelf, down to a depth of 100m is approximately 5 km long along its most extensive northeast to southwest axis. Surrounding depths range between 400 - 900m, increasing abruptly to the north, where the southwestern edge of the Puerto Rico Trench is found. A rocky shoreline fringes the entire island, except for two small sandy beach coves on the west and southwest coast (Puerto Botes and Puerto Canoas). A fishing closure of 0.5 miles around the island's shoreline is in effect year-round.

A map of mesophotic benthic habitats is presently unavailable for Isla Desecheo, but drift dive surveys performed around the island within the 30 – 50m depth range have identified coral reef habitats in the 30 – 40m depth range along the western insular shelf and slope sections, and also associated with patch coral reefs on the north and northeast shelf sections (Garcia-Sais et al., 2012). Colonized pavement habitats prevail along the shelf-edge and upper insular slope in mostly flat seascapes and associated with rocky outcrops. Coralline sand deposits with scattered rocks and rubble cover extensive areas of the shelf and slope. Rhodolith habitats variably colonized by benthic algae, sponges, corals and other encrusting biota were found and characterized below a depth of 40m off the western and southwestern shelf sections extending down the insular slope of Isla Desecheo (Garcia-Sais et al., 2005, 2012).

The 2018-20 monitoring survey of sessile-benthic substrate categories and small demersal fishes was based on a set of 15 sampling stations previously surveyed during the 2005 baseline characterization (Garcia-Sais et al., 2005), and an additional set of five stations to provide a baseline characterization of sub-mesophotic communities at a depth of 25-28m. A total of 16 drift belt-transect surveys for monitoring of the large demersal fish/shellfish community were performed on previously occupied stations during a fishery independent survey by Garcia-Sais et al. (2012). The location of sampling stations for benthic and fish characterizations of sub-mesophotic (25m) and mesophotic (30 – 50m) habitats at Isla Desecheo during the 2018-20 survey is shown in Figure 82. Images of the mesophotic communities at Isla Desecheo are shown in Photo Album 4.

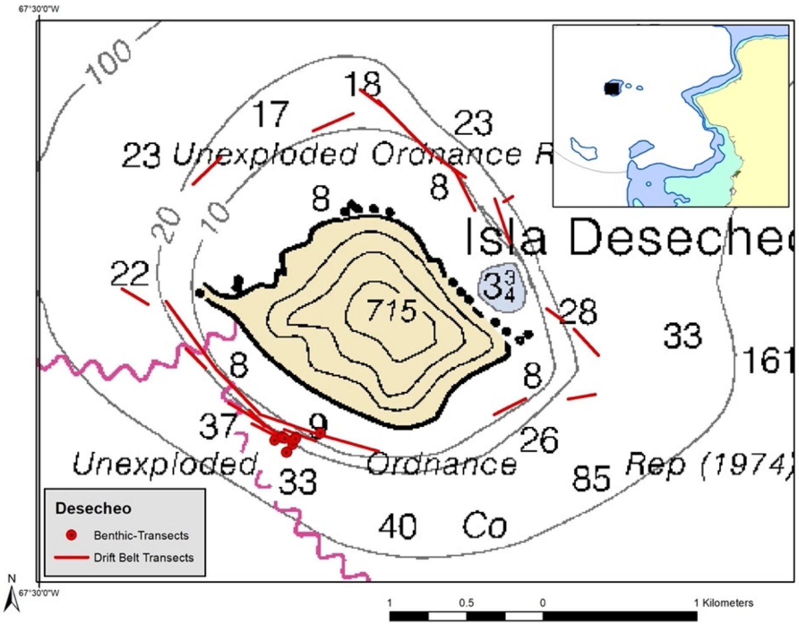

Figure 82. Location of sampling stations at Isla Desecheo, 2018-19 survey

Benthic Community

Depth/habitat related patterns of benthic community structure

The mean percent substrate cover by sessile-benthic categories at the main benthic habitats/depths surveyed within the 25 – 50m depth range from Isla Desecheo during 2018-20 are presented in Table 42. Benthic algae were the main category in terms of percent substrate cover at all habitats/depths with means ranging between a minimum of 50.19% at CPSlope40 and a maximum of 69.42% at CPSlope30 (Figure 83). Differences of total benthic algae between habitats/depths were statistically insignificant (ANOVA; p = 0.158) but marked depth-related variations among the main algal taxonomic components were noted. Brown fleshy macroalgae, *Dictyota sp* was the dominant component at ACR25, representing 58.6% of the mean total benthic algae (Figure 84). A similar pattern of decreasing substrate cover with depth was noted for the crustose calcareous Peyssonnelid macroalgae. Conversely, encrusting fan alga (*Lobophora sp*.) was dominant at habitats/depths below ACR25, with a maximum contribution of 91.02% at Rhod50. Red crustose coralline algae (CCA, mixed assemblage) exhibited a pattern of increasing substrate cover with depth with maximum cover of 2.55%, representative of 4.4% of the total benthic algae at Rhod50. Turf algae (mixed assemblage) were present from all habitats/depths surveyed with a maximum mean cover of 19.76%, or of 28.5% of the total benthic algae at CPSlope30. Small patches of cyanobacteria (blue-green algae) were observed from all habitats/depths surveyed with low substrate cover (< 1.2%).

Table 42. Mean substrate cover by benthic categories from the main habitats/depths surveyed across the 25 – 50m depth range from Isla Desecheo. 2018-20 survey.

BENTHIC CATEGORIES	ACR25	CPSlope30	CPSlope40	Rhod50
Abiotic				
Pavement	1.10			
Sand	1.64	8.25	14.92	4.42
Rubble			0.42	
Total Abiotic	**2.74**	**8.25**	**15.35**	**4.42**
Benthic Algae				
Turf (mixed) with sediment		16.65	3.96	
Peyssonnelid (mixed)	4.48	1.77	1.53	0.326
Turf (mixed)	6.82	3.11	2.62	2.772
Lobophora sp.	11.79	39.48	39.44	56.85
Jania sp.	0.13			
Halimeda spp.	0.09			0.172
Dictyota spp.	37.11	8.23	2.29	0.642
Padina sp.	0.30			
Ramicrusta sp.	0.04			
Fleshy macroalgae (mixed)				0.334
CCA (mixed)	2.55	0.19	0.36	0.816
Total Benthic Algae	**63.31**	**69.42**	**50.19**	**61.91**
Cyanobacteria	**0.13**	**1.15**	**0.19**	**4.29**
Stony Coral				
Agaricia agaricites	4.27	0.77	0.58	
Agaricia fragilis	0.05	0.07	0.35	0.08
Agaricia grahamae		0.27	0.21	0.684
Agaricia lamarcki		0.12	0.89	7.948
Colpophyllia natans	0.75	0.25		
Dendrogyra cylindrus	0.05			
Diploria labyrinthiformis	0.09			
Eusmilia fastigiata	1.45	0.07	0.11	
Leptoseris cucullata			0.05	
Madracis decactis	0.09	0.05	0.36	
Meandrina meandrites	0.55	0.30	0.82	0.148
Millepora alcicornis	0.04			
Montastraea cavernosa	0.04	0.87	0.71	0.25
Mycetophyllia aliciae	0.09			
Mycetophyllia lamarckiana	0.13			
Orbicella annularis	1.10			
Orbicella faveolata	18.58	3.68	6.95	1.046
Orbicella franksi	0.93	0.56	0.19	
Porites astreoides	1.53	0.87	0.21	0.93
Porites furcata	0.04			
Porites porites	0.40	0.30		
Pseudodiploria strigosa		0.28		
Siderastrea siderea	0.24	0.75		
Unknown coral		0.07	0.05	0.15
Total Stony Coral	**30.43**	**9.26**	**11.48**	**11.23**

# Coral Colonies/photo frame	**5.38**	**14.45**	**6.95**	**13.62**
# Diseased Coral Colonies/photo frame	**0.89**	**0.31**	**0.54**	**0.29**
# Bleached Coral Colonies/photo frame	**0.00**	**0.96**	**0.29**	**3.62**
Octocoral				
Erythropodium caribaeorum	0.08			
Total Soft Corals	**0.08**	**0.00**	**0.00**	**0.00**
# Soft Corals/photo frame	**0.00**	**0.04**	**0.28**	**0.04**
Sponges				
Agelas clathrodes	0.57	2.28	0.91	4.324
Agelas citrina	1.03	0.56	2.96	1.526
Agelas conifera	0.98	2.80	5.37	3.488
Agelas dispar	0.10	0.30	1.35	0.244
Agelas sceptrum		0.65	1.26	0.804
Agelas sventres		0.88	1.74	1.34
Agelas sp.		0.24		
Aiolochoria crassa		0.21		0.57
Aplysina cauliformis		0.10		0.088
Aplysina fistularis		0.10	0.05	0.072
Cliona caribbaea			0.05	
Cribochalina vasculum			0.08	
Iotrochota birotulata	0.04			
Ircinia felix				0.1
Ircinia strobilina				0.1
Myrmekioderma gyroderma				0.088
Neofibularia nolitangere				0.3
Neopetrosia proxima	0.13	0.59	1.06	0.78
Neopetrosia sp.		0.18	0.06	0.232
Oceanapia bartschi				0.318
Petrosia pellasarca		0.21		0.55
Plakortis spp.			0.18	
Prosuberites laughlini		0.09	0.17	0.088
Scopalina ruetzleri	0.04			
Smenospongia aurea	0.04			
Suberea sp.			0.11	
Svenzea zeai	0.17	0.86	6.86	0.652
Unknown sponge		0.70	0.36	1.834
Verongula reiswigi				0.088
Verongula rigida			0.178	0.226
Xestospongia muta		1.05	0.06	0.36
Total Sponges	**3.11**	**11.79**	**22.80**	**18.17**

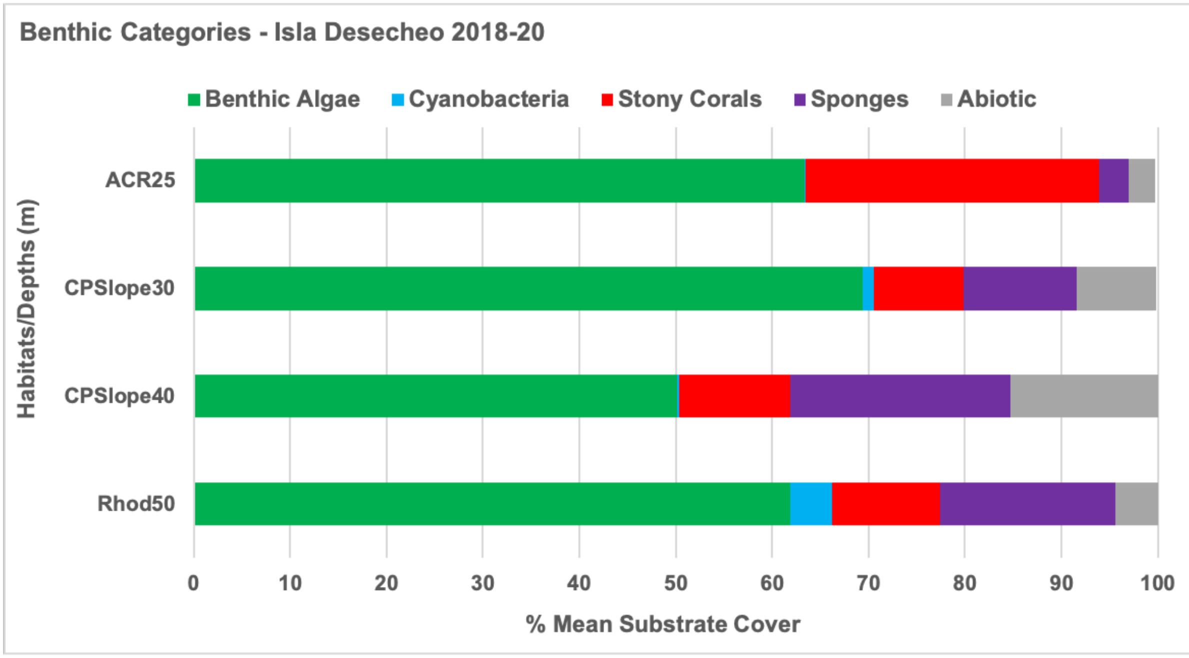

Figure 83. Mean percent cover by sessile-benthic categories from the main habitats/depths surveyed across the 25 – 50m depth range surveyed in Isla Desecheo. 2018-20 survey.

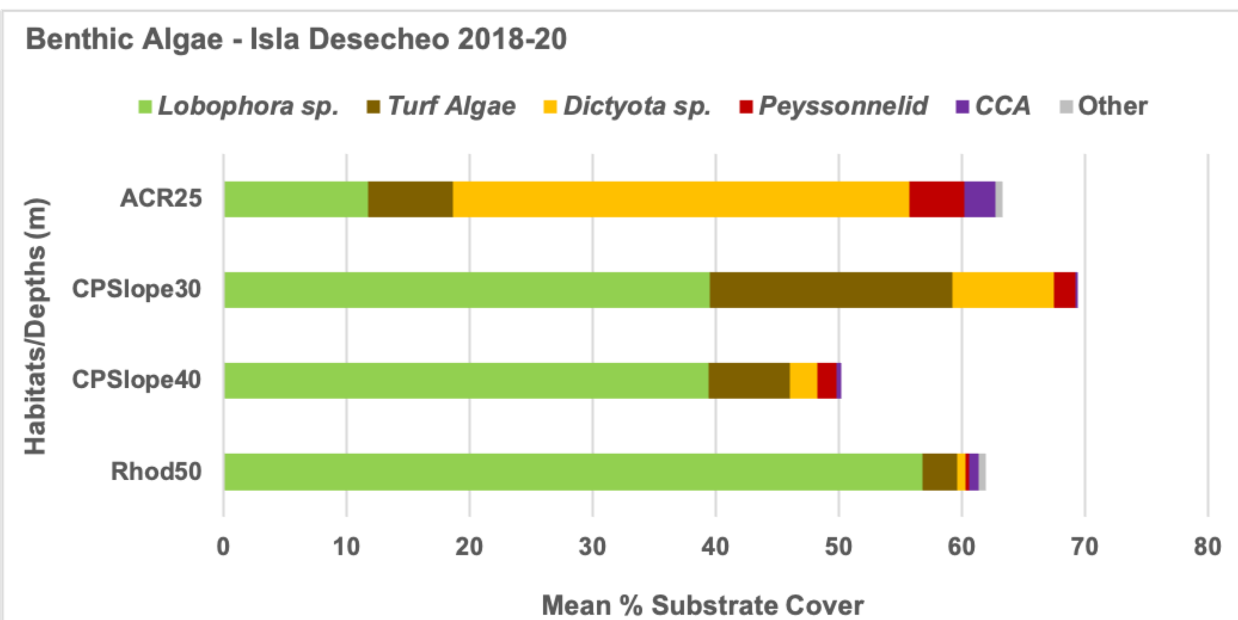

Figure 84. Mean percent cover by benthic algae from the main habitats/depths surveyed across the 25 – 50m depth range surveyed in Isla Desecheo. 2018-20 survey.

A total of 24 species of stony corals were identified from the main habitats/depths surveyed within the 25 – 50m range at Isla Desecheo during 2018-20 with mean substrate cover ranging from a maximum of 30.43% at ACR25 to a minimum of 9.26% at CPSlope30 (Table 42). Differences of substrate cover by stony corals in relation to habitat/depth were statistically insignificant (ANOVA; p = 0.111) due to the high sampling variability (within habitat/depths) but marked vertical distribution patterns were observed for major coral taxonomic components. Mountainous star coral (*Orbicella faveolata*) was identified from photo-transects at all habitats/depths surveyed but presented peak cover at ACR25, with a mean of 18.58%, representative of 61.1% of the total cover by stony corals at ACR25, and minimum cover at Rhod50 (Figure 85). Lettuce coral (*Agaricia agaricites*) also presented a well-defined pattern of decreasing substrate cover with depth with a maximum mean of 4.27% at ACR25, and 0% at Rhod50. Conversely, a pattern of increasing cover with depth was noted for whitestar sheet coral (*A. lamarki*) with peak mean cover of 13.08% at Rhod50 and 0% at ACR25 (Figure 85). Mustard-hill coral (*Porites astreoides*) and great star coral (*Montastraea cavernosa*) were observed within photo-transects throughout the habitat/depth range without any clear pattern of habitat/depth related variation.

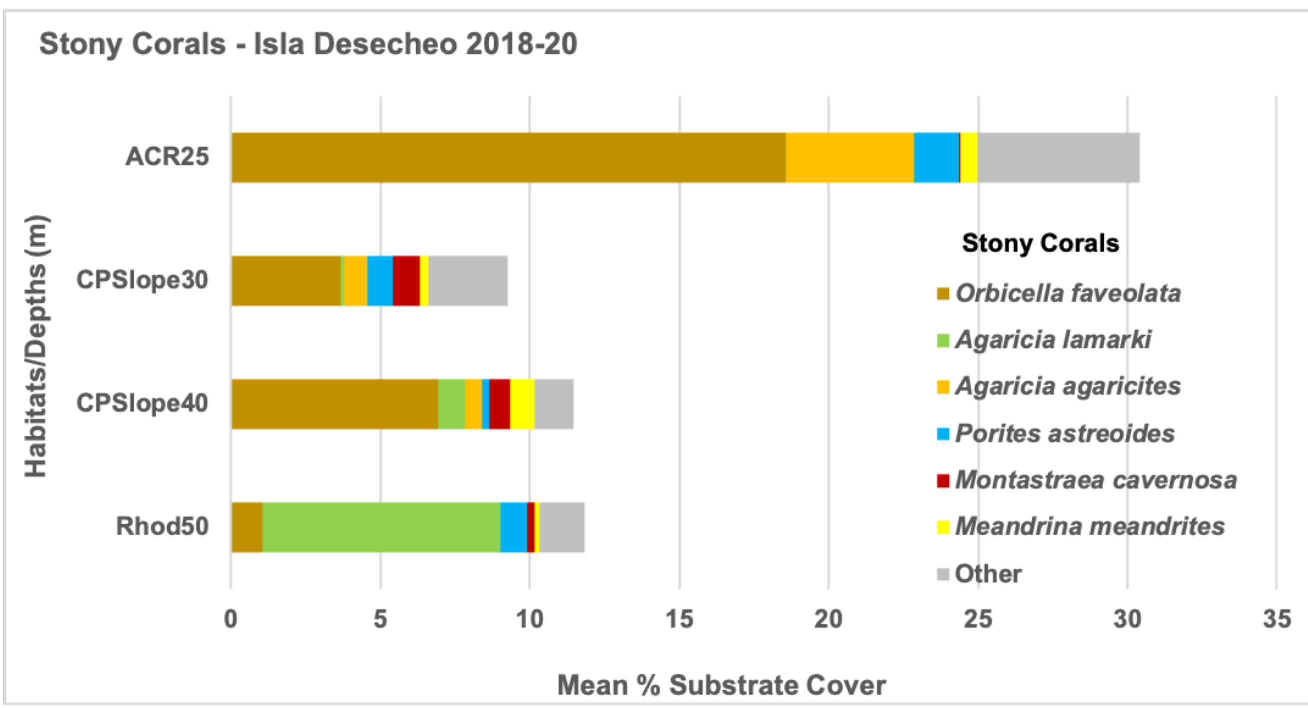

Figure 85. Mean percent substrate cover by stony corals from the main habitats/depths surveyed across the 25 – 50m depth range surveyed in Isla Desecheo. 2018-20 survey.

Diseased coral colonies were observed from all habitats/depths across the 25 – 50m depth range surveyed at Isla Desecheo during 2018-20. Disease prevalence was highest at ACR25 with a mean of 16.6% and lowest at Rhod50 with a mean of 2.12% (Table 42). The most affected species included *Orbicella faveolata, Porites astreoides, Agaricia lamarki,* and *Meandrina meandrites*. Partially bleached coral colonies were observed within habitats in the 30 – 50m depth range. Coral bleaching prevalence varied from a maximum of 26.6% at Rhod50 to a minimum of 0 at ACR25. Bleaching prevalence of coral colonies was highest for *A. lamarki* and *O. faveolata*. The contrasting pattern of bleaching prevalence between ACR25 and stations surveyed in the 30 – 50m depth range was related to the survey date. Benthic transects at ACR25 were surveyed on November 2018, whereas benthic transects at 30 – 50 m were surveyed between January and February 2020. A coral bleaching event was affecting PR corals since October 2019. These observations of coral bleaching down to 50m represent the deepest reports of coral bleaching during the 2019-20 bleaching event in PR.

A total of 27 species of sponges were identified within the main habitats surveyed in the 25 – 50m depth range from Isla Desecheo with mean substrate cover ranging from 22.80% at CPSlope40 and 3.11% at ACR25 (Table 42). Differences of substrate cover in relation to habitat/depth were significant (ANOVA; $p < 0.0001$), associated with lower cover at ACR25, relative to all other habitats/depths. In part, this pattern of lower sponge cover at ACR25 may be related to the higher cover by stony corals in the horizontally oriented seascape of the island shelf. Six sponge species were observed across the entire 25 – 50m habitat/depth range. These included *Svenzea zeai, Neopetrosia proxima, Agelas clathrodes, A, conifera, A. citrina* and *A. dispar*. Their mean combined substrate cover across all depths surveyed (9.89%) represented 70.4% of the total cover by sponges. The three dominant species in terms of substrate cover, *A. conifera, A. citrina* and *S. zeai* presented peak cover at CPSlope40 (Figure 86).

Similarities of benthic community structure from the main benthic habitats/depths surveyed at Isla Desecheo during 2018-20 are displayed in a non-metric multidimensional scaling plot in Figure 87. The highest similarities were observed within CPSlope40 (83.0%), mostly contributed by consistently high cover of sponges and abiotic categories. ACR25 ranked second in similarity (77.5%) with stony corals as the main contributor to similarity (Table 43). The relatively high cover by benthic algae was a unifying feature contributing similarity across depths and habitats. Conversely, reef substrate cover by stony corals was largely restricted to horizontally oriented habitats, such as ACR25 and Rhod50.

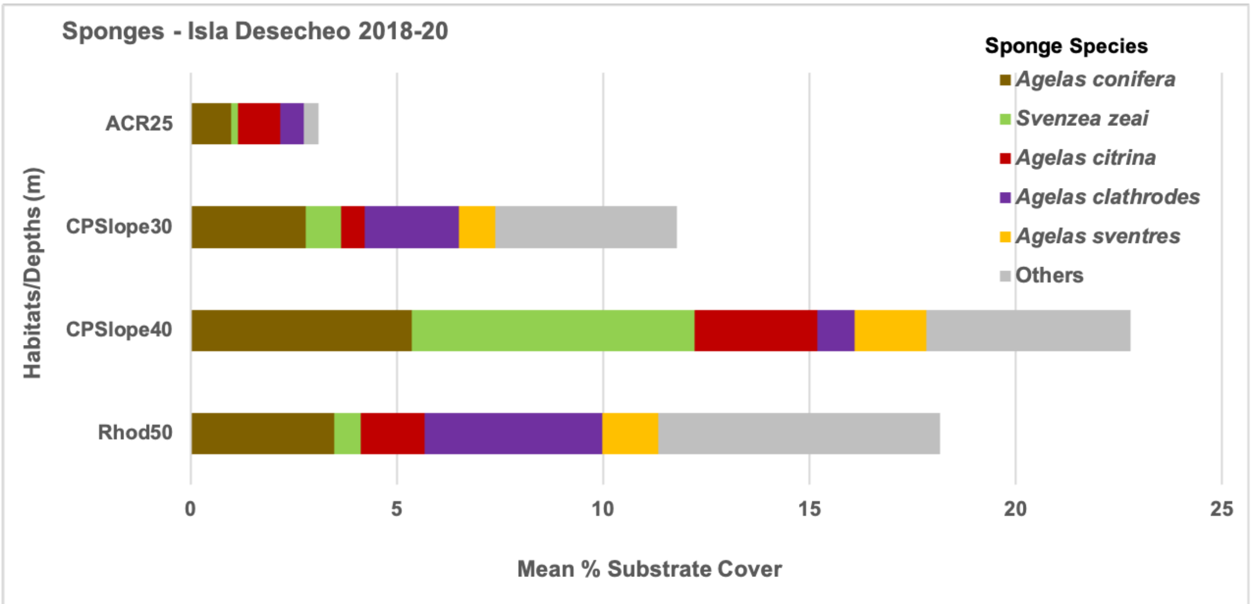

Figure 86. Mean percent cover by sponges from the main habitats/depths surveyed across the 25 – 50m depth range surveyed in Isla Desecheo. 2018-20 survey.

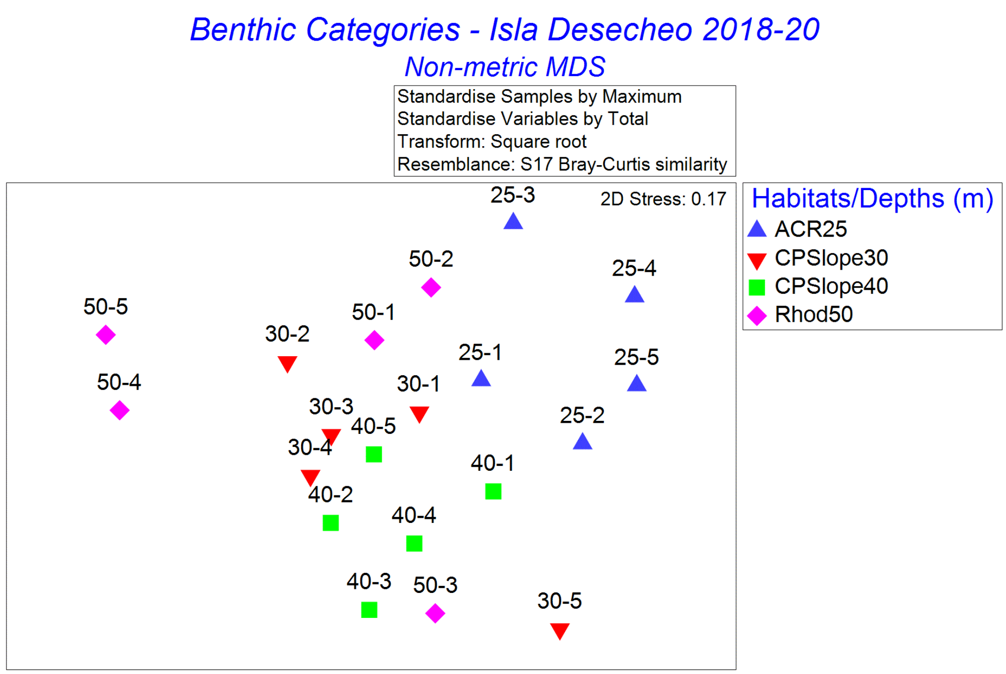

Figure 87. Non-metric multidimensional scaling (nMDS) plot of Bray-Curtis similarities between photo-quadrat samples of sessile-benthic communities surveyed from sub-mesophotic (25m) and upper mesophotic (30 – 50m) depths at Isla Desecheo, in 2018-20.

Table 43. Similarity matrix (SIMPER) of sessile-benthic community structure from the main benthic habitats/depths surveyed from Isla Desecheo in 2018-20, including contributions of benthic categories to the within habitat similarity.

Benthic Habitats	ACR25	CPSlope30	CPSlope40	Rhod50
Average Similarity (%)	77.5	77.3	85.6	68.9
Benthic Categories				
Abiotic		16.1	26.8	
Benthic Algae	36.6	32.5	23.8	31.3
Cyanobacteria				16.9
Stony Corals	39.4			
Sponges		24.2	28.1	31.2

Benthic community structure dissimilarities between the main benthic habitats/depth surveyed within the 25 – 50m depth range at Isla Desecheo during the 2028-20 monitoring survey are presented in Table 44. The highest dissimilarities were observed between the ACR25 and CPSlope30 (36.3%). Dissimilarity was largely contributed by the much higher substrate cover of cyanobacteria at CPSlope30, and the relatively higher cover of stony corals at ACR25 (Table 45). Dissimilarity between ACR25 and CPSlope40 (35.6%) was influenced by the relatively higher cover by abiotic categories (mostly sand) at CPSlope40 and the relatively higher cover by stony corals at ACR25.

Table 44. Dissimilarity matrix (SIMPER) of sessile-benthic community structure between the main benthic habitats/depths surveyed at Isla Desecheo in 2018-20, including contributions of benthic categories to the between habitat/depth dissimilarity.

Benthic Habitats	ACR25 vs CPSlope30	ACR25 vs CPSlope 40	ACR25 vs Rhod50	CP Slope30 vs CPSlope 40	CP Slope30 vs Rhod50	CP Slope40 vs Rhod50
Average Disimilarity (%)	29.9	32.2	38.3	23.8	27	30.2
Benthic Categories						
Abiotic	23.6	37.2		34.6	21.6	29.7
Benthic Algae						
Cyanobacteria	27.0		37.7	27.0	44.0	39.0
Stony Corals	28.8		24.9		22.9	20.2
Sponges		35.3	22.3	24.9		

Temporal (monitoring) variations of benthic community structure

Variations of substrate cover by benthic categories between the 2004-05 and the 2018-20 surveys at the main benthic habitats/depths surveyed within the 30 – 50m depth range at Isla Desecheo are presented in Figures 88 - 90. Statistically significant differences were noted for benthic algae, abiotic categories, and sponges (Two-way ANOVA; $p < 0.05$) but differences between surveys depended on habitats/depths. The main pattern was an increase of cover by benthic algae measured in the 2018-20 survey that was statistically significant at CPSlope30 and CPSlope40 (ANOVA; $p < 0.01$). Mean cover by benthic algae increased 67.2% at CPSlope30 and 41.4% at CPSlope40, largely influenced by substrate cover increases of brown fleshy macroalgae (*Dictyota sp.*), and encrusting fan alga (*Lobophora sp*). A corresponding decline of 67.6% of abiotic cover was measured at CPSlope30 in the 2018-20 survey (ANOVA; $p = 0.010$). Sand transport across the outer shelf and slope is a highly dynamic process and may have accounted for the variations of cover by benthic algae and abiotic categories. It is also possible that increments of cover by benthic algae could have been influenced by nutrient enrichment associated with upwelling during the pass of Hurricane Maria in late 2017, as previously noted for neritic reefs during this period (Garcia-Sais et al., 2018, 2019).

Increments of cover by benthic algae were also accompanied by reductions of cover by sponges from all habitats/depths, with statistically significant differences associated with a 31.1% decline at Rhod50 (ANOVA $p = 0.012$). The giant barrel sponge (*Xestospongia muta*) was the main species that declined in cover between surveys (mean: -37.2%). Dead *X. muta* skeletons still standing and others showing advanced necrosis were observed during the 2018 - 20 survey. Such disease-related losses may have accounted in part for the declines of sponge cover between surveys. Declines of sponge abundance and diversity associated with disease outbreaks were reported for the Caribbean region in 2005 (Fenner, 2005; Wulf, 2005; Angermeier et al., 2012) including losses of *X. muta* in Panama associated with a high prevalence of "white spot disease".

Stony coral community structure remained stable between surveys at all habitats/depths (ANOVA; $p > 0.05$). *Orbicella spp*. (mostly *O. faveolata*) were the dominant species at CPSlope30 and CPSlope40, whereas *Agaricia spp*. were the dominant assemblage at Rhod50 in both surveys. Increments of the total cover by stony corals between surveys were more prominent at Rhod50, largely influenced by an 61.7% increase in cover by *Agaricia spp*., but differences between surveys were statistically insignificant (ANOVA; $p > 0.05$).

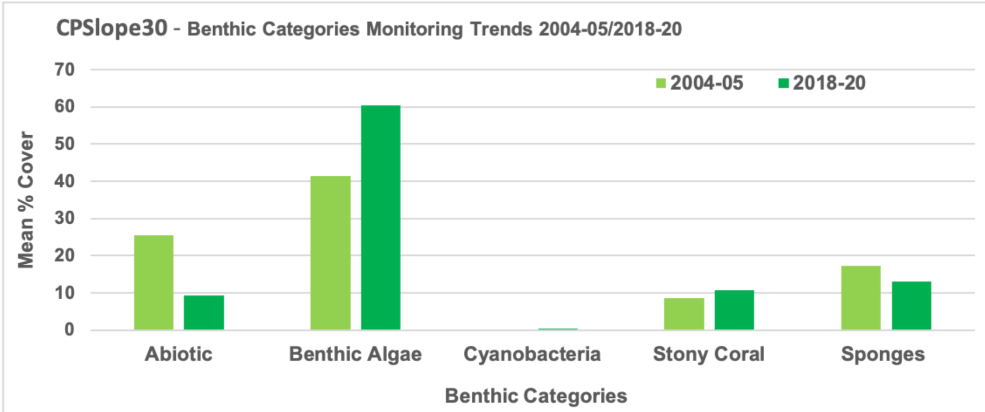

Figure 88. Variations of mean % substrate cover by sessile-benthic categories between the 2004-05 baseline and the 2018-20 monitoring survey at CPSlope30, Isla Desecheo

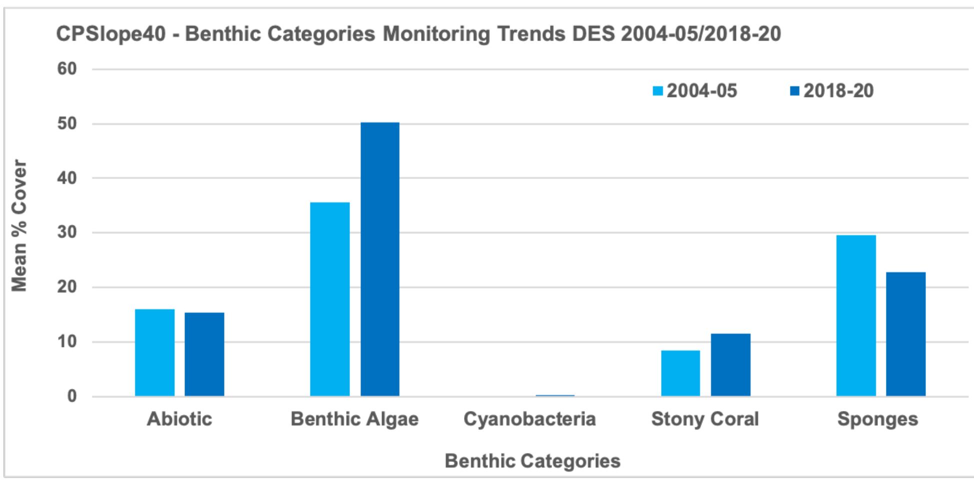

Figure 89. Variations of mean % substrate cover by sessile-benthic categories between the 2004-05 baseline and the 2018-20 monitoring survey at CPSlope40, Isla Desecheo

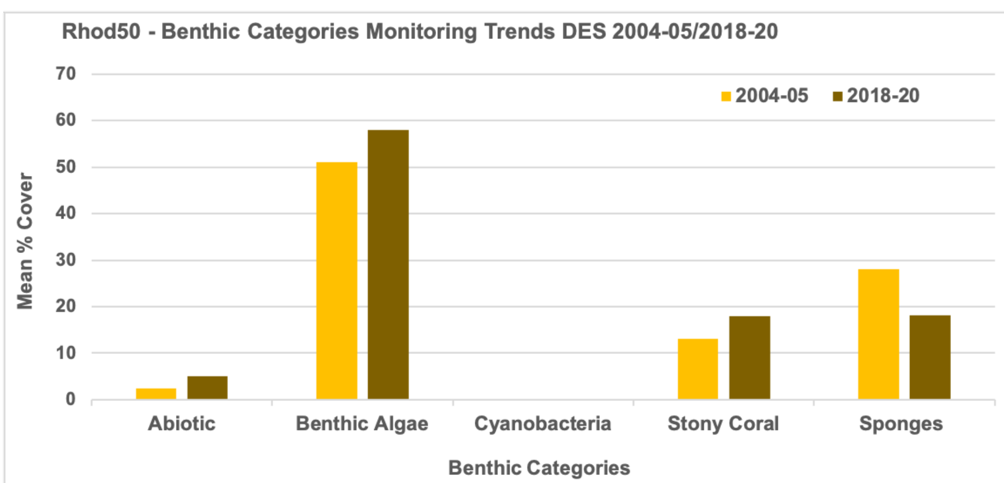

Figure 90. Variations of mean % substrate cover by sessile-benthic categories between the 2004-05 baseline and the 2018-20 monitoring survey at Rhod50, Isla Desecheo

Fish Community Structure

Small demersal fish species

A total of 57 small demersal fish species were identified from 10m x 3m belt-transects within the 25 – 50m depth range during the 2018-20 survey at Isla Desecheo (Table 45). Mean density varied between 173.2 Ind/30m^2 at ACR25 and 84.3 Ind/30m^2 at Rhod50. Fish density differences related to habitats/depths were not statistically significant (ANOVA; p= 0.178). The five (5) numerically dominant species, representative of 61.1% of the total fish density were distributed across the entire 25 – 50m depth range without any distinct habitat/depth related density distribution pattern (Figure 91). The assemblage included the creole wrasse (*Clepticus parrae*), blue chromis (*Chromis cyanea*), bicolor damselfish (*Stegastes partitus*), bluehead wrasse (*Thalassoma bifasciatum*), and masked goby (*Coryphopterus personatus*). Numerically dominant species with distinct habitat/depth related distributions included the sunshine chromis (*C. insolata*) and fairy basslet (*Gramma loreto*). Sunshine chromis were observed from all habitat/depths below 30m with peak density at CPSlope40, whereas fairy basslet was among the top five numerically dominant species of habitats in the 25 – 40m depth range but was not observed at Rhod50.

Habitat/depth plasticity and ontogenetic habitat transitions appeared to play an important role in the distributions of small demersal fish densities across the depth range surveyed from Isla Desecheo during 2018-20. A large proportion of the adult creole wrasse (*C. parrae*) and blue chromis (*C. cyanea*) population were observed from ACR25 and CPSlope30, whereas most of their populations at CPSlope40 and Rhod50 were comprised by swarms of early juvenile stages associated with sponge-coral bioherms at those habitats/depths. Bluehead wrasse (*T. bifasciatum*) is a well-known neritic coral reef species and showed a density peak at ACR25 (34.6 Ind/30m^2). It's distribution as a numerically dominant species at Rhod50 appeared to be related to the high substrate cover by stony corals at Rhod50. The distribution of cherubfish (*Centropyge argi*) peaked at Rhod (3.3 Ind/30m^2) probably influenced by the high availability of microhabitats associated with rhodolith deposits. Conversely, fairy basslet (*G. loreto*) has a strong preference for high relief, even vertically distributed habitats that were unavailable at Rhod50. Likewise, peak densities of sunshine chromis (*Stegastes insolata*) were noted from the colonized pavement slope CP Slope40, but it was not observed at Rhod50. Preference of zooplanktivores, such as *G. loreto* and *C. insolata* for vertically oriented habitats, such as slopes and walls may be influenced by the higher flux of zooplankton food associated with slopes and walls due to topographically steered current flows.

Table 45. Mean densities of small demersal fishes surveyed from 10m x 3m belt-transects across the 25 – 50m range at Isla Desecheo, 2018 – 20 survey.

Species	Mean ACR25	Mean CPSlope30	Mean CPSlope40	Mean Rhod50
Clepticus parrae	18.6	25.0	23.0	16.7
Chromis cyanea	33.8	14.4	17.8	6.7
Stegastes partitus	12.2	13.2	6.2	24.3
Thalassoma bifasciatum	34.6	10.0	1.0	8.7
Coryphopterus personatus	16.6	1.0	12.6	6.7
Gramma loreto	13.4	6.8	15.0	
Halichoeres garnoti	8.0	12.0	4.6	1.7
Kyphosus sp.	8.2	6.0	9.4	
Chromis insolata		1.8	15.0	3.0
Coryphopterus lipernes	5.4	1.4	4.2	1.3
Holocentrus rufus	1.4	0.8	3.0	2.0
Scarus taeniopterus	2.8	2.4	0.6	0.7
Sparisoma aurofrenatum	1.4	1.6	0.6	1.7
Lutjanus apodus	0.6		4.2	
Centropyge argi		0.4		3.3
Cephalopholis fulva	0.2	1.0	0.8	1.3
Elacatinus evelynae	0.6	1.2	1.4	
Sparisoma viride	2.2	0.2	0.4	
Cephalopholis cruentatus	1.8		1.0	
Stegastes planifrons	2.8			
Chaetodon capistratus	0.8	0.4	0.8	0.7
Chromis multilineata		0.4	2.2	
Canthigaster rostrata	1.6	0.2	0.6	
Acanthurus coeruleus	1.2	0.6	0.2	
Prognathodes aculeatus	0.8	0.2	0.8	
Pterois sp.	0.6	0.2	1.0	
Scarus iseri		1.0	0.8	
Epinephelus guttatus	0.2	0.2	0.6	0.7
Serranus tigrinus		0.4	0.2	1.0
Xanthichthys ringens		0.6	1.0	
Ginglymostoma cirratum	0.2	0.4	0.6	0.3
Echeneis neucratoides			0.6	0.7
Neoniphon marianus	0.4		0.6	
Sparisoma atomarium				1.0
Holocentrus adscensionis	0.8			
Bodianus rufus	0.4			0.3
Amblycirrhitus pinos				0.7
Holacanthus tricolor		0.2	0.4	
Caranx hippos			0.6	
Coryphopterus sp.		0.6		
Sparisoma radians			0.6	
Caranx crysos			0.4	
Microspathodon chrysurus	0.2	0.2		

Table 45. Mean densities of small demersal fishes surveyed from 10m x 3m belt-transects across the 25 – 50m range at Isla Desecheo, 2018 – 20 survey.

Species	Mean ACR25	Mean CPSlope30	Mean CPSlope40	Mean Rhod50
Myripristis jacobus	0.2		0.2	
Caranx lugubris				0.3
Scomberomorus regalis				0.3
Sphyraena barracuda				0.3
Acanthostracion polygonius	0.2	0.0	0.0	0.0
Anisotremus virginicus			0.2	
Carangoides ruber	0.2			
Epinephelus striatus	0.2			
Gymnothorax funebris			0.2	
Haemulon flavolineatum			0.2	
Lactophrys triqueter	0.2			
Lutjanus jocu	0.2			
Melichthys niger	0.2			
Paranthias furcifer			0.2	
Total Individuals	**173.2**	**104.8**	**133.8**	**84.3**
Total Species	**19.6**	**14.4**	**20.0**	**13.0**

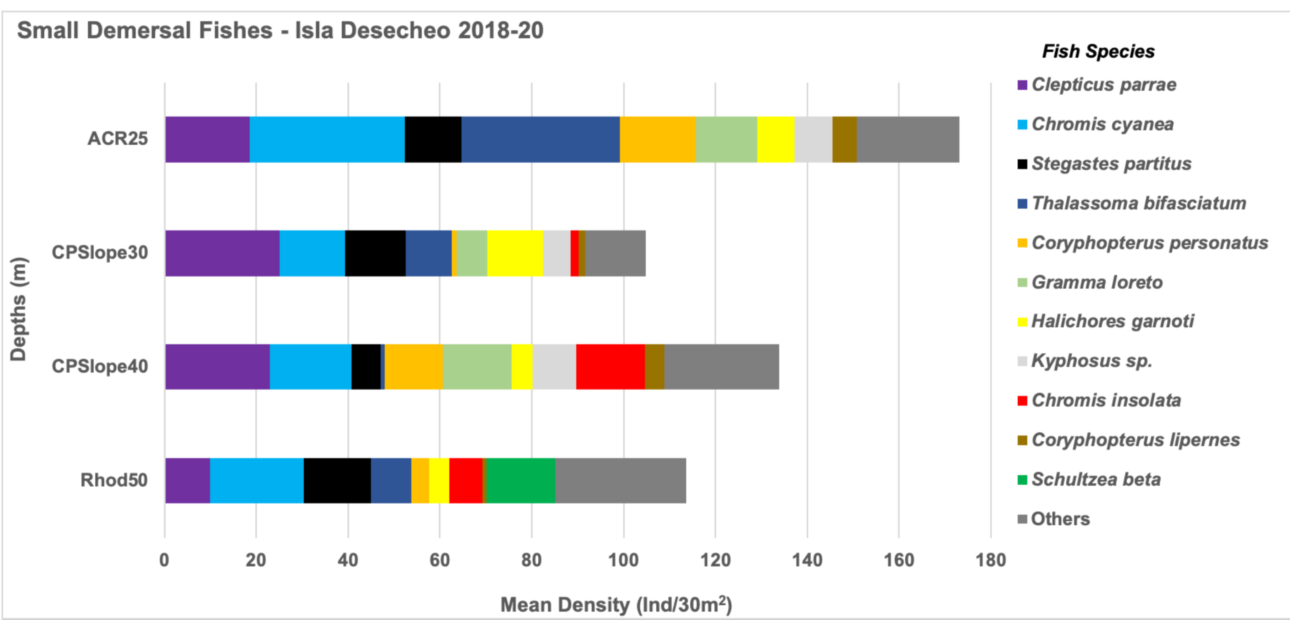

Figure 91. Variations of mean density by small demersal fishes surveyed from the main benthic habitats/depths in the 25 – 50m depth range at Isla Desecheo. 2018-20 survey.

Fish species richness varied between 20.0 Spp/30m^2 at CPSlope40 and 13.0 Spp/30m^2 at Rhod50. Differences between habitats/depths were statistically significant (ANOVA; $p = 0.0002$), associated with higher number of species at ACR25 and CPSlope40, compared to those at CPSlope30 and Rhod50. The coral reef habitat at ACR25 was characterized by very high live stony coral cover (mean: 30.43%) associated with large coral colonies of mountainous star coral (*Orbicella faveolata*) that provided high topographic relief and habitat complexity, producing high availability of protective microhabitats and ecological niches for a diverse fish community. Stony coral cover was relatively also high at Rhod50 (mean: 17.48%), but lettuce corals (*Agaricia spp.*) were the prevailing coral species there. Lettuce corals were observed growing close to the substrate and did not produce the massive aggregated structures of *O. faveolata* at ACR25. The relatively high fish species richness at CPSlope40 was an interesting finding, probably related to its condition as a physiographic interface between the slope pavement and the sandy corridor that leads to the rhodolith habitat of the western shelf of Isla Desecheo. The CPSlope40 transects were set at the base of the slope, where the more horizontally oriented seascape allowed growth of large *Orbicella faveolata* colonies. The combination of *O. faveolata* growth along with branching sponges (*Agelas spp*) provided for massive and complex structures where a highly diverse fish community was concentrated.

Community structure similarities of small demersal fish species from the main habitats/depths based on the relative densities within 10m x 3m belt-transects surveyed at Isla Desecheo are displayed in a non-metric multi-dimensional scaling plot (nMDS) of Bray-Curtis similarities in Figure 92. The highest similarity was from ACR25 (61.8%), contributed by an assemblage of neritic coral reef species, such as bluehead wrasse (*Thalassoma bifasciatum*), blue tang (*Acanthurus coeruleus*), blue chromis (*Chromis cyanea*), fairy basslet (*Gramma loreto*), yellowhead wrasse (*Halichoeres garnoti*), and peppermint goby (*Coryphopterus lipernes*) (Table 46). These species were present in at least four out of the five transects surveyed at ACR25 and exhibited fairly uniform distributions within such habitat/depth. Similarities at CPSlope30 were mostly contributed by yellowhead wrasse, princess parrotfish (*Scarus taeniopterus*), and bicolor damselfish (*Stegastes partitus*). Likewise, similarities within CPSlope40 were contributed by another unique assemblage comprised mostly by sunshine and blue chromis (*C. insolata, C. cyanea*), squirrelfish (*Holocentrus rufus*), and masked goby (*C. personatus*). Cherubfish (*Centropyge argi*), greenbloth parrotfish (*Sparisoma atomarium*), and bicolor damselfish (*S. partitus*) were the main species contributing similarity of small demersal fish community structure at Rhod50 (Table 46).

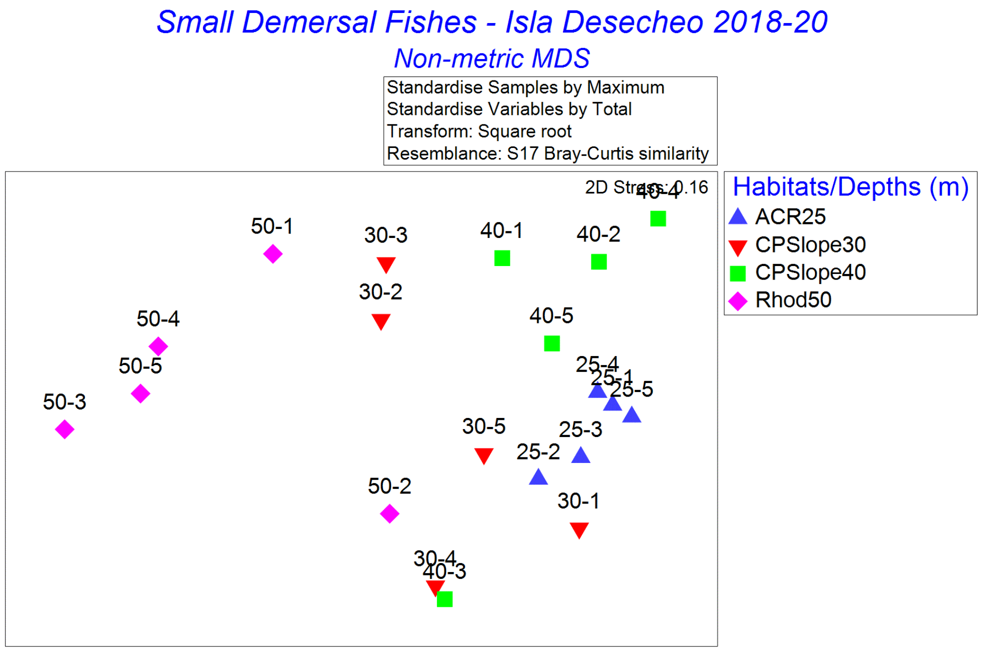

Figure 92. Non-metric multidimensional scaling plot (NMDS) of Bray-Curtis similarities based on the relative densities of small demersal fishes surveyed within the main benthic habitats surveyed within the 25 – 50m depth range at Isla Desecheo, 2018-20 survey.

Table 46. Similarity matrix (SIMPER) of the small demersal fish community structure within the main habitats/depths surveyed at Isla Desecheo within the 25 – 50m depth range, with species contributions to similarity at each benthic habitat, 2018-20 survey

	ACR25	CPSlope30	CPSlope40	Rhod50
Average Similarity (%)	61.8	45.0	46.3	46.2
Species				
Thalassoma bifasciatum	10.9	5.8		9.5
Acanthurus coeruleus	9.4	5.5		
Coryphopterus lipernes	6.9			
Sparisoma viride	6.7			
Cephalopholis cruentatus	6.7		7.7	
Gramma loreto	7.4	8.0	10.4	
Chromis cyanea	7.5	10.7	8.8	
Halichores garnoti	6.9	17.3	8.3	
Scarus taeniopterus		14.6		
Stegastes partitus		11.5		15.9
Chromis insolata			13.3	
Chromis multilineata			7.4	
Holocentrus rufus			10.9	
Centropyge argi				19.4
Sparisoma atomarium				17.6
Serranus tigrinus				10.4

Small demersal fish community structure dissimilarities between the main habitats/depths surveyed from Isla Desecheo in 2018-20 are presented in Table 47. Dissimilarities were generally low due to the marked habitat/depth plasticity exhibited by the seven (7) numerically dominant species, including the creole, bluehead, and yellowhead wrasses (*Clepticus parrae, Thalassoma bifasciatum, Halichoeres garnoti*), bicolor damselfish (*Stegastes partitus*), fairy basslet (*Gramma loreto*), and masked goby (*Coryphopterus personatus*). These species were observed within belt-transects from all habitat/depths. The highest dissimilarities were noted between Rhod50 and all other habitats/depths, driven by the higher relative densities of cherubfish (*Centropyge argi*), and greenblotch parrotfish (*Sparisoma atomarium*) at Rhod50 compared to other habitats/depths. The higher relative densities of three-spot damselfish (*Stegastes planifrons*) and stoplight parrotfish (*S. viride*) separated ACR25 from other habitats/depths, whereas sunshine and brown chromis (*Chromis insolata, C. cyanea*) distinguished CPSlope40 from other habitats/depths.

Table 47. Dissimilarity matrix (SIMPER) of small demersal fish community structure between the main habitats/depths surveyed at Isla Desecheo within the 25 – 50m depth range, with species contributions to dissimilarity at each habitat/depth, 2018-20 survey

Benthic Habitats	Rhod50 vs ACR25	Rhod50 vs SCSlope40	Rhod50 vs SCSlope30	CP Slope30 vs CPSlope40	ACR25 vs CPSlope40	ACR25 vs CPSlope30
Average Dissimilarity (%)	73.6	72.2	66.1	59.8	56.1	53.5
Fish Species						
Centropyge argi	5.3	5.8	5.6			
Sparisoma atomarium	5.3	5.7	6.0			
Stegastes planifrons	4.8				4.3	4.5
Sparisoma viride	4.2					3.6
Serranus tigrinus		4.2	4.0			
Canthigaster rostrata						3.4
Sparisoma aurofrenatum						2.7
Chromis insolata				3.3	4.0	
Chromis multilineata		4.4		4.0	3.7	
Thalassoma bifasciatum				3.4	3.6	
Scarus taeniopterus			4.3	3.3		

Temporal Variations of Small Demersal Fish Density and Community Structure – Monitoring Trends 2004-05 vs 2018-20 Surveys

Variations of mean densities and species richness by small demersal fishes between the 2004-05 baseline and the 2018-20 monitoring survey from the main mesophotic habitats/depths surveyed within the 30 – 50m depth range at Isla Desecheo are presented in Figures 93 and 94. Density differences between surveys were statistically significant for samplings at CPSlope30

(ANOVA; p = 0.045) associated with a 36.6% decline during the 2018-20 survey, relative to the baseline (Figure 93). Another 33.8% mean density reduction resulted from samplings at CPSlope40 during 2018-20 but the difference was not statistically significant (ANOVA; p = 0.113). Differences of species richness between surveys were statistically significant at CPSlope30 (ANOVA; p = 0.00029), associated with a 59.7% decline, and at CPSlope40 associated with a 36.5% decline during the 2018-20 survey, relative to the 2004-05 baseline (Figure 94). Density and species richness differences at Rhod50 were statistically insignificant (ANOVA; p = 0.735).

Density differences between surveys at CPSlope30 were strongly influenced by reductions of numerically dominant species, such as the blue and brown chromis (*Chromis cyanea, C. multilineata*), bicolor damselfish (*Stegastes partitus*), bridled goby (*Coryphopterus glaucofraenum*), fairy basslet (*Gramma loreto*), and sharknose goby (*Elacatinus evelynae*). The assemblage included both water column schooling species, such as *Chromis spp*. and territorial species in close contact with the substrate, such as *S. partitus*, *C. glaucofraenum*, and *G. loreto*. The generalized decline of small demersal fish species, including some numerically dominant populations may be related to a significant change or degradation of the benthic habitat.

Relevant benthic habitat differences were noted between the 2004-05 and 2018-20 surveys within CPSlope30 and CPSlope40, including a 67.2% increment of benthic algae (mostly *Dictyota sp.* and *Lobophora sp.*), a 67.7% decline of sand cover, and 31.6% decline of cover by sponges. The increment of substrate cover by benthic algae over sand at CPSlope30 and CPSlope40 may explain the density declines of bicolor damselfish (*S. partitus*) and bridled goby (*C. glaucofraenum* from those depths (Figures 95 and 96). *Bicolor damselfish* (*S. partitus*) typically maintain territories devoid of fleshy and/or encrusting algae, and bridled goby (*C. glaucofraenum*) lives over sand - away from benthic algae. The decline of cover by sponges was associated with a reduction of cover by habitat forming species, such as *Xestospongia muta* and *Agelas spp*. These are important contributors to the reef topographic relief and their decline imply a reduction of protective habitats for small and/or juvenile fish stages, particularly *Chromis spp*., among others. The decline of cover by sponges was measured across the 30 – 50m depth gradient at Isla Desecheo, correlated with a density decline of *Chromis spp*. across the same depth range.

Superimposed upon these habitat changes are the potential deleterious effects of the pass of Hurricane Maria in 2017 and winter storm Riley in 2018 over small fish populations that may still be in process of recuperation. A generalized decline of mean density and species richness was reported for the majority of the reef stations surveyed in the Puerto Rico Coral Reef Monitoring Program (Garcia-Sais et al., 2018, 2019), including the three stations monitored from Isla Desecheo at 30m, 20m and 15m depths. The surge effects associated with wave action were intense enough to cause structural breakup of massive coral colonies down to 30m depths at the coral reef system off Puerto Canoas (CANO30), Isla Desecheo.

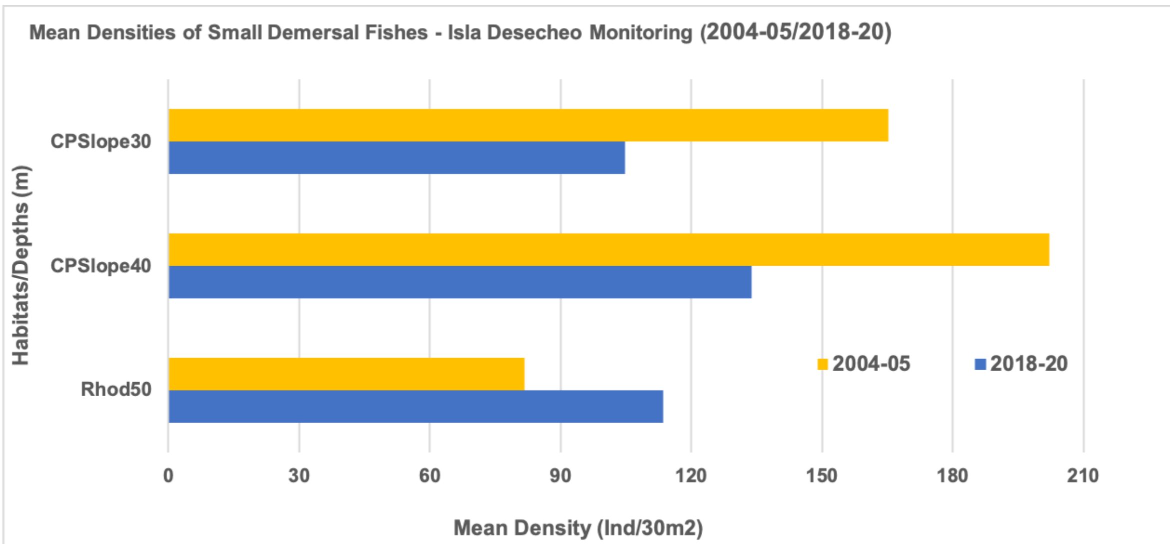

Figure 93. Variations of mean density between the 2004-05 baseline and the 2018-20 monitoring survey by small demersal fishes surveyed by 10 x 3m belt-transects within the main habitats/depths in the 30 – 50m depth range at Isla Desecheo.

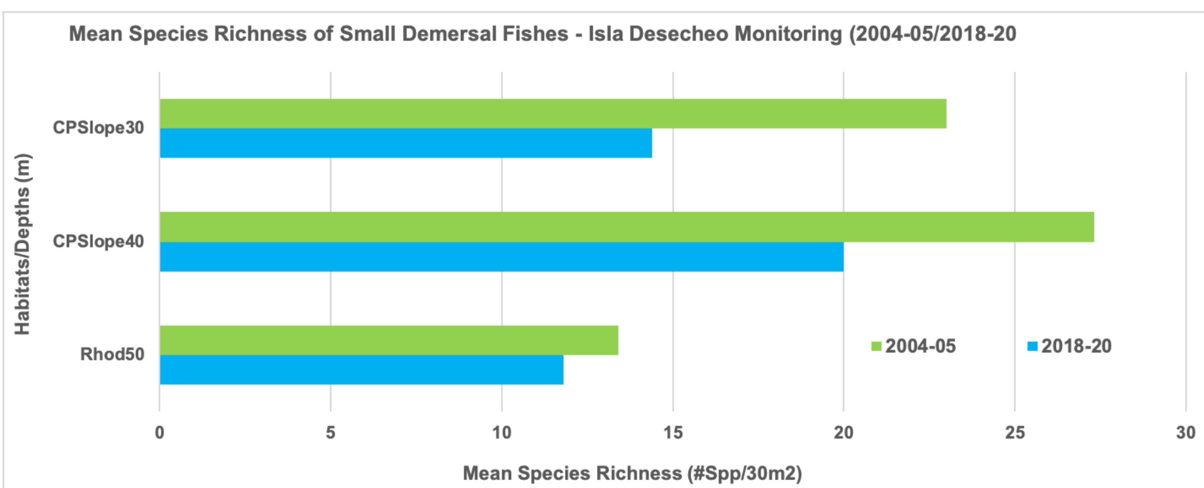

Figure 94. Variations of mean species richness between the 2004-05 baseline and the 2018-20 monitoring survey by small demersal fishes surveyed by 10 x 3m belt-transects within the main habitats/depths in the 30 – 50m depth range at Isla Desecheo.

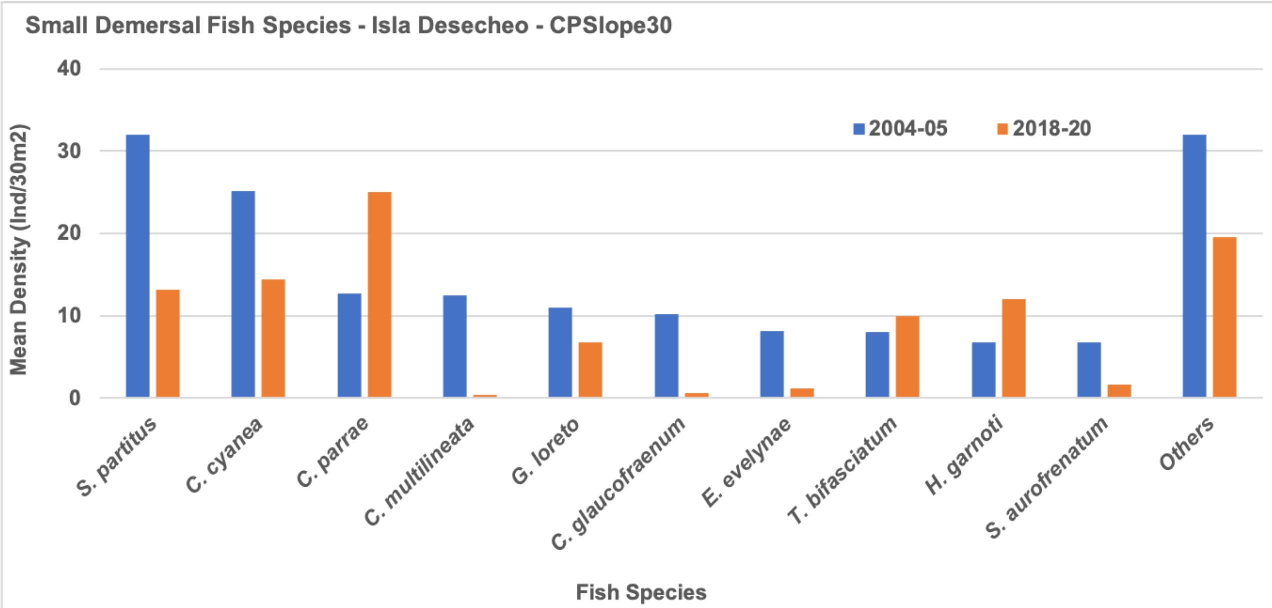

Figure 95. Variations of mean density by small demersal fishes between the 2004-05 baseline and the 2018-20 monitoring survey at Isla Desecheo – CPSlope30

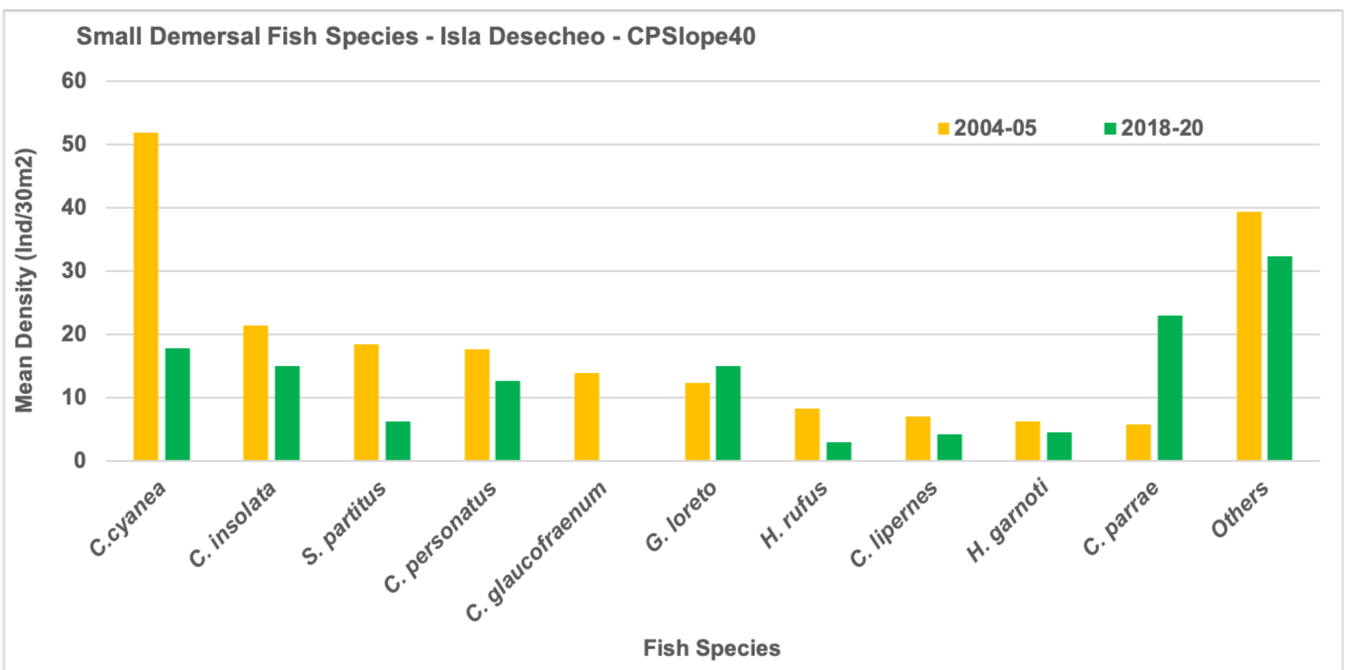

Figure 96. Variations of mean density by small demersal fishes between the 2004-05 baseline and the 2018-20 monitoring survey at Isla Desecheo – CPSlope40

Similarities of small demersal fish community structure between the 2004-05 baseline and the 2018-20 monitoring surveys based on the relative densities of the 14 numerically dominant species surveyed within 3m x 10m belt-transects are shown in a multidimensional scaling plot of Bray-Curtis similarities in Figure 97. The highest similarity (shortest distance) was observed from CPSlope40 (75.15%) mostly contributed by longspine squirrelfish (*Holocentrus rufus*), and numerically dominant species, such as blue and sunshine chromis (*C. cyanea, C. insolata*), fairy basslet (*Gramma loreto*), and peppermint goby (*Coryphopterus lipernes*) (Table 48). Despite the marked density differences of *C. cyanea* between surveys its rank order of density remained high between surveys at CPSlope40. Larger discrepancies of the relative densities by small demersal fish species were observed at CPSlope30 and Rhod50. Bridled goby (*C. glaucofraenum*) ranked 6th in mean density during the 2004-05 baseline survey but declined to 13th during 2018-20 at CPSlope30. Creole wrasse (*Clepticus parrae*) ranked 2nd at Rhod50 in 2018-20 but was not observed within transects during the 2004-05 survey influencing the relatively low similarities from those habitats/depths.

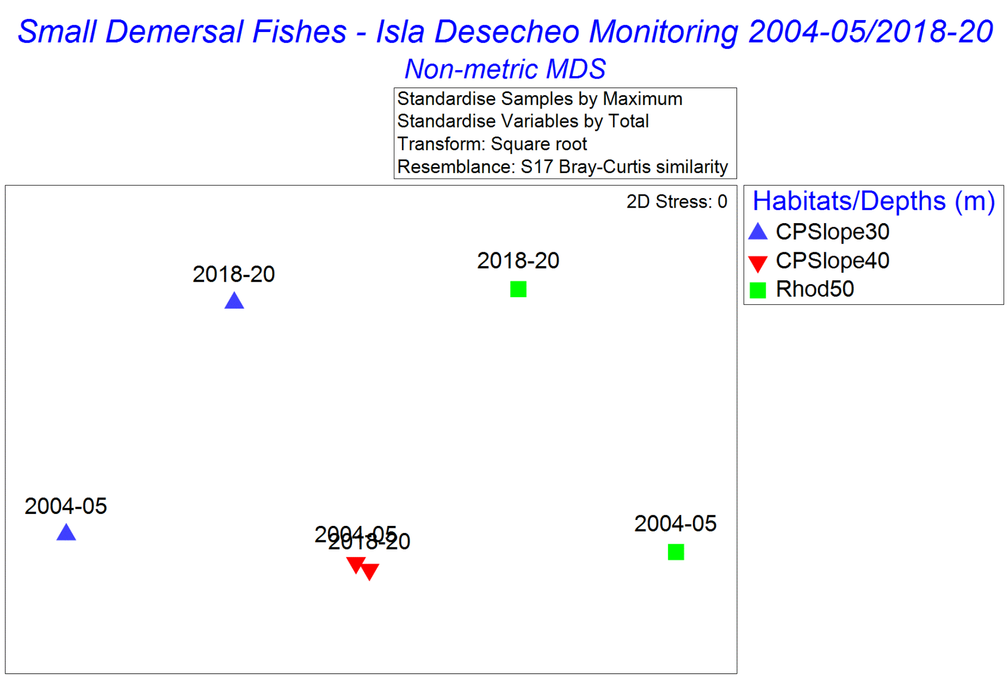

Figure 97. Non-metric multidimensional scaling (nMDS) plot of Bray-Curtis similarities based on the relative densities of small demersal fishes surveyed from 10m x 3m belt-transects within mesophotic benthic habitats in the 30 – 50m depth range at Isla Desecheo during 2004-05 and 2018-20

Table 48. Similarity matrix (SIMPER) of relative densities by small demersal fishes from the main mesophotic habitats/depths surveyed at Isla Desecheo between the 2004-05 baseline and the 2018-20 monitoring survey.

	CPSlope30	CPSlope40	Rhod50
Average Similarity (%)	**70.8**	**75.5**	**65.7**
Species Contributions			
Thalassoma bifasciatum	11.4		12.0
Halichoeres garnoti	10.8	7.7	8.9
Gramma loreto	10.5	9.4	
Sparisoma aurofrenatum	9.9		
Clepticus parrae	9.2		
Chromis cyanea	9.0		
Stegastes partitus	8.8		21.8
Elacatinus evelynae	8.2	8.9	
Holocentrus rufus		13.3	
Chromis insolata		12.0	14.2
Chromis cyanea		10.0	14.2
Coryphopterus lipernes		9.1	

Large Demersal Fishes and Shellfishes

Habitat/depth related variations of density and community structure, 2018-20 Survey

Mean densities of large demersal fishes and shellfishes (queen conch and spiny lobster) surveyed by drift belt-transects within the 25 – 50m depth range at Isla Desecheo during 2018-20 are presented in Table 49. Mean densities varied between 49.8 Ind/10^3m^2 at ACR25 and 33.2 Ind/10^3m^2 at Rhod50. Density differences between habitats/depths of the total large demersal fish/shellfish assemblage were not statistically significant (ANOVA; $p = 0.384$). The top seven numerically dominant species were observed across all benthic habitats/depths within the surveyed range. These included the coney (*Cephalopholis fulva*), schoolmaster snapper (*Lutjanus apodus*), queen conch (*Lobatus gigas*), red hind (*Epinephelus guttatus*), lionfish (*Pterois sp.*), graysbe (*Cephalopholis cruentata*), queen triggerfish (*Balistes vetula*) and great barracuda (*Sphyraena barracuda*) (Figure 98). Habitat/depth related density differences for the aforementioned assemblage were all statistically insignificant (ANOVA; $p > 0.05$). Among the numerically dominant species, habitat/depth related differences were only significant for yellowtail snapper (*Ocyurus chrysurus*), associated with higher densities at ACR25 and CPRT30-40 relative to other habitats/depths (ANOVA; $p = 0.027$).

Table 49. Mean densities of large demersal fishes/shellfishes surveyed from drift belt-transects at the main habitats/depths in the 25 – 50m depth range at Isla Desecheo, 2018-20 survey

Surveyed Area (m2)		9,460.9		10,644.5		7,118.2		5,929.2
Habitat/Depth (m)	**ACR25**		**ACR30-40**		**CPRT30-40**		**Rhod50**	
Fish/Shellfish Species	Total Ind	**Ind/1000m2**	Total Ind	**Ind/1000m2**	Total Ind	**Ind/1000m2**	Total Ind	**Ind/1000m2**
Cephalopholis fulva	161	16.32	186	22.31	73	12.46	49	9.62
Lutjanus apodus	103	11.11	12	1.43	21	3.48	101	14.79
Epinephelus guttatus	23	2.37	42	6.25	32	5.29	9	1.61
Pterois sp.	39	4.29	20	1.88	16	3.03	4	0.84
Cephalopholis cruentatus	20	2.16	6	0.90	10	1.40	1	0.15
Lutjanus mahogoni	12	1.16	9	0.45	21	2.38		
Ocyurus chrysurus	17	1.99			8	1.37		
Balistes vetula	6	0.58	13	1.82	4	0.69	3	0.55
Sphyraena barracuda	6	0.68	2	0.43	2	0.35	3	0.57
Lactophrys triqueter			4	0.34	7	1.02	3	0.58
Caranx crysos	1	0.11	4	0.45	3	0.73	1	0.17
Lutjanus cyanopterus	7	0.77			1	0.16	1	0.20
Epinephelus striatus	3	0.33	5	0.46			1	0.21
Sparisoma viride (tpm)			5	0.64	1	0.15		
Ginglymostoma cirratum	2	0.24	2	0.12	2	0.41	4	0.74
Acanthostracion polygonia	2	0.23	2	0.10	2	0.33	1	0.21
Caranx ruber					4	0.59		
Lactophrys bicaudalis			2	0.31	1	0.15		
Mycteroperca venenosa	1	0.09			2	0.35	1	0.15
Mycteroperca bonaci					2	0.44		
Caranx lugubris			3	0.21				
Scomberomorus regalis	1	0.11	1	0.05			2	0.43
Sparisoma rubripinne			2	0.14				
Dasyatis americana			2	0.12			3	0.60
Seriola rivoliana	1	0.11						
Gymnothorax funebris	1	0.11						
Scarus vetula	1	0.11						
Scomberomorus cavalla	1	0.11						
Trachinotus falcatus			1	0.10				
Lactophrys trigonus			1	0.05				
Mycteroperca intersititialis			1	0.05				
Lutjanus jocu								
Mycteroperca tigris							1	0.20
Invertebrates			0					
Lobatus gigas	55	6.26	57	8.95	21	3.66	10	1.59
Panulirus argus	3	0.33	4	0.39	2	0.44		
Sea Turtles								
Eretmochelys imbricata	2	0.20						
Totals	468	**49.77**	386	**47.95**	235	**38.88**	198	**33.22**

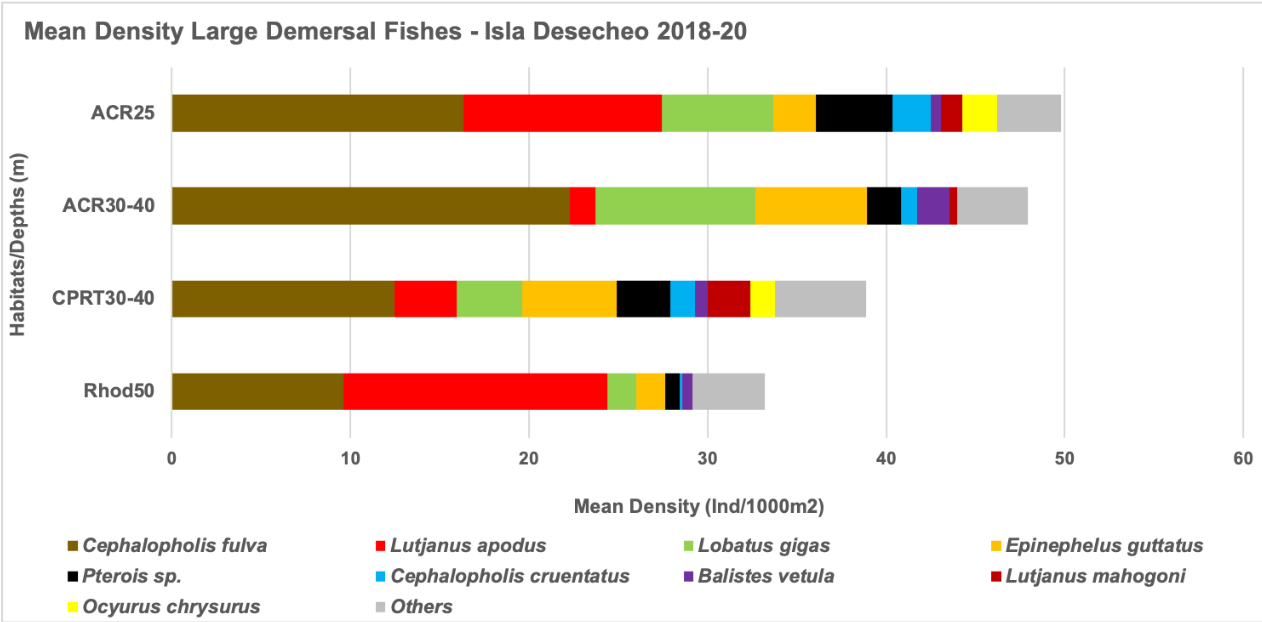

Figure 98. Variations of mean density by numerically dominant fishes and shellfishes surveyed by drift belt-transects across the main benthic habitats in the 25 – 50m depth range at Isla Desecheo. 2018-20 survey.

Coney (*Cephalopholis fulva*) was the numerically dominant species among the large demersal fish/shellfish assemblage in terms of site mean density (across all habitats/depths). It was the dominant species from all habitats/depths except from Rhod50 where it ranked 2nd after schoolmaster snapper (*Lutjanus apodus*). Site mean density of coney (51.09 Ind/10^3m^2) was 3.7-fold higher than that of red hind (*E. guttatus*) which ranked 3rd overall among the large demersal fishes. The graysbe (*C. cruentata*) was also distributed across all habitats/depths and ranked 5th in density. Thus, three out of the five numerically dominant large demersal fish species surveyed from sub-mesophotic and upper mesophotic habitats in Isla Desecheo were groupers (Serranidae). In addition, nine Nassau (*E. striatus*), four yellowfin (*Mycteroperca venenosa*), two black (*M. bonaci*), and one yellowmouth grouper (*M. interstitialis*) were observed within drift belt-transects in the 25 – 50m depth range.

Queen conch (*Lobatus gigas*) ranked 2nd overall (large demersal fish/shellfish) in terms of site mean density (18.9 Ind/10^3m^2). The highest densities were observed from ACR30-40 (8.95 Ind/10^3m^2) and ACR25 6.26 Ind/10^3m^2). Differences were statistically insignificant (ANOVA; p = 0.426) due to the highly aggregated (patchy) distribution and many transects with 0 individuals. Mean densities of red hind (*Epinephelus guttatus*) and queen triggerfish (*Balistes vetula*) also peaked at ACR30-40. The prevailing habitat at ACR30-40 was a mixed seascape of aggregated coral reef and coral reef patches surrounded by coralline sand, coral rubble, rhodoliths, and sponge colonized pavement. Peak density of schoolmaster snapper (*Lutjanus apodus*) at Rhod50 was related to a large schooling aggregation of approx. 100 individuals. Density differences between habitats/depths were statistically insignificant due to the high sampling variability associated with its aggregated distribution. Likewise, peak density of yellowtail snapper (*Ocyurus chrysurus*) at ACR25 was also related to one school of 17 individuals, representative of 56.0% of the total observed. A total of nine (9) spiny lobsters (*Panulirus argus*) were observed from habitats in the 25 – 40m depth range during the 2018-20 survey.

Similarities of large demersal fish/shellfishes within the main habitats/depths surveyed in the 25 – 50m range during the 2018-20 survey at Isla Desecheo based on the relative densities of the 15 numerically dominant fish/shellfish species (top 95% density) are displayed in a multidimensional scaling plot of Bray-Curtis similarities in Figure 99. Similarities within benthic habitats/depths were generally low (28.3% - 48.4%) due to the high variability introduced by aggregated distributions of numerically dominant species and the high habitat plasticity exhibited by most numerically dominant fish/shellfish populations. Habitat/depth plasticity was probably influenced by the relatively small benthic habitat dimensions around the island and high physical connectivity between the various habitat types within a relatively small depth range. Similarity was highest at ACR25 (48.4%) mostly contributed by graysbe, coney, and red hind groupers (*Cephalopholis cruentatus, C. fulva, Epinephelus guttatus*), schoolmaster snapper (*Lutjanus apodus*), and lionfish (*Pterois sp.*) (Table 50). Both coney and red hind were prominent contributors to similarity from all habitats/depths surveyed.

Average dissimilarities of large demersal fish/shellfish relative densities between habitats/depths were generally low due to the widespread penetration of numerically dominant species (coney, queen snapper, red hind, lionfish, queen triggerfish) across the entire habitat/depth range surveyed. Dissimilarities were highest between Rhod50 and all other habitats/depths largely influenced by species present in relatively low density, such as nurse shark (*Ginglymostoma cirratum*) and smooth trunkfish (*Lactophrys triqueter*). Likewise, the higher relative densities of Nassau grouper (*Epinephelus striatus*) largely contributed to dissimilarities between CPRT30 and all other habitats/depths (Table 51). Densities of queen conch (*Lobatus gigas*) were higher at CPRT30 and ACR30-40, contributing to dissimilarities between these and other mesophotic habitats/depths surveyed in 2018-20 from Isla Desecheo.

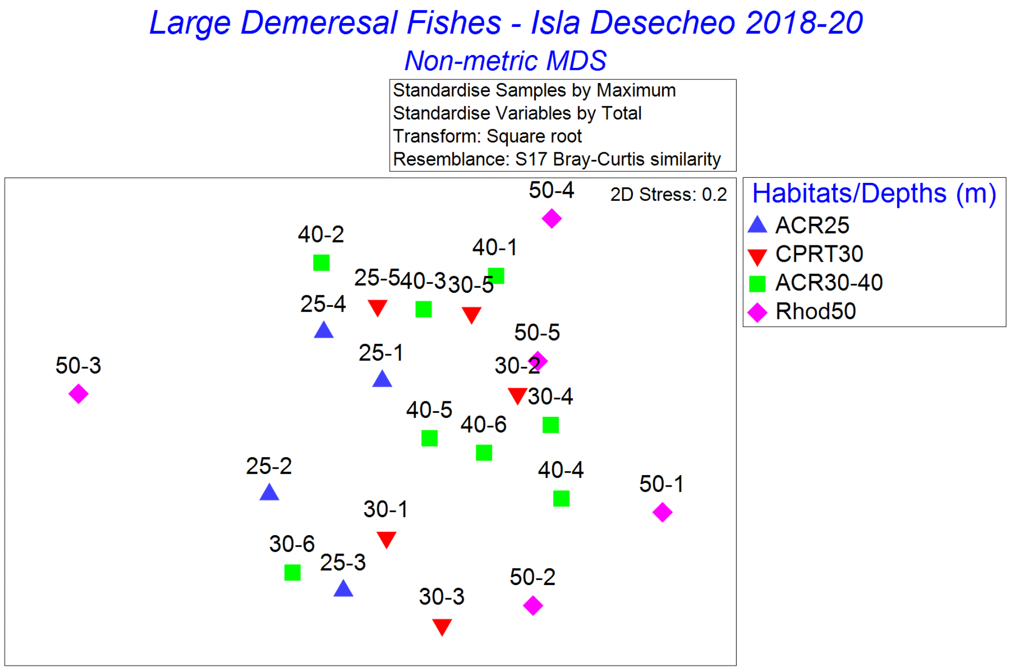

Figure 99. Non-metric multidimensional scaling (nMDS) plot of Bray-Curtis similarities based on the relative densities of large demersal fishes/shellfishes surveyed from the main benthic habitats/depths in the 25– 50m depth range at Isla Desecheo, 2018-20 survey

Table 50. Similarity matrix (SIMPER) of relative densities by large demersal fishes/shellfishes from the main mesophotic habitats/depths surveyed at Isla Desecheo, 2018-20 survey

Habitats/Depths (m)	ACR25	CPRT30	ACR30-40	Rhod50
Average Similarity (%)	48.4	43.6	47.1	28.3
Species Contributions				
Cephalopholis cruentatus	20.0	9.3		
Lutjanus apodus	19.0			
Cephalopholis fulva	15.8	22.2	23.9	30.6
Pterois sp.	13.6		8.9	
Epinephelus guttatus	10.0	22.5	10.7	20.4
Balistes vetula		15.4	20.2	
Lobatus gigas		9.1	13.5	
Lactophrys triqueter				13.8
Ginglymostoma cirratum				13.5

Table 51. Dissimilarity matrix (SIMPER) based on relative density differences by large demersal fish/shellfishes from the main habitats/depths surveyed within the 30 – 50m depth range at Isla Desecheo, 2018-20 survey.

	ACR25 vs	ACR25 vs	ACR25 vs	CPRT30 vs	CPRT30 vs	ACR30-40 vs
Habitats/Depths (m)	**CPRT30**	**ACR30-40**	**Rhod50**	**ACR30-40**	**Rhod50**	**Rhod50**
Average Dissimilarity (%)	54.9	52.6	66.1	52.3	62.0	62.2
Species Contributions						
Lutjanus mahogoni	10.7				9.2	
Lutjanus apodus	10.2	9.5	10.1		6.7	7.9
Epinephelus striatus	8.6		6.2	9.2	9.1	
Ocyurus chrysurus	8.1	9.6	7.4			
Cephalopholis cruentatus	7.6	8.8	10.7	9.0		
Pterois sp.	7.4	6.7	7.5	7.5		6.9
Panulirus argus	7.3	8.1				7.6
Lactophrys triqueter	7.3		6.7	8.6	8.8	8.3
Lobatus gigas	6.8	7.8	7.0	6.1	8.3	8.7
Sphyraena barracuda		7.5	7.9		7.2	7.9
Balistes vetula		7.4		5.9	8.1	9.9
Epinephelus striatus		6.5				
Ginglymostoma cirratum			8.1		9.2	9.1
Lutjanus mahogoni				9.9		

Temporal Variations of Large Demersal Fishes/Shellfishes Between Survey Years 2011-12/ 2018-20

Large demersal fishes and shellfishes were surveyed during 2011-12 and 2018-20 from a similar set of 15 sampling stations across the 30 – 50m depth range at Isla Desecheo. Density differences between surveys of the total large demersal fish/shellfish assemblage were not statistically significant for any habitat/depth (ANOVA; $p > 0.05$) (Table 52). The largest density difference was a 226.1% increment during 2018-20 at Rhod50, driven by a schooling aggregation of schoolmaster snapper (*Lutjanus apodus*) in 2018-20. Density variations of *L. apodus*, both in magnitude and direction associated with schooling aggregations were observed from all habitats/depths (Figures 100 – 102), indicative of no ecologically meaningful implications of the observed changes from any particular habitat/depth. Density differences of *L. apodus* across all habitats/depths were statistically insignificant (Two-way ANOVA; $p = 0.676$) due to the high variability introduced by the patchy distributions and transects with 0 individuals.

Marked density increments of queen conch (*Lobatus gigas*), were evidenced from all habitats/depths during the 2018-20 survey relative to the 2011-12 baseline (Figures 100 - 102).

The site mean density of *L. gigas* increased by 195.1% in the 2018-20 survey but differences were statistically insignificant (ANOVA; p = 0.069) due to the highly patchy distribution. For example, 45.7% of the total density of *L. gigas* in 2018-20 was contributed by individuals observed from one drift belt-transect at ACR30-40. No individuals of *L. gigas* were observed from that same station during the 2011-12 baseline survey, indicative of the high mobility of the population across benthic habitats/depths in Isla Desecheo.

Red hind (*Epinephelus guttatus*) and queen triggerfish (*Balistes vetula*) presented site mean density increments of 55.9% and 140.0% during the 2018-20 survey (Table 52). Differences between surveys were statistically insignificant (ANOVA; p > 0.05) but may be indicative of recuperation trends in the populations of these commercially targeted species. Conversely. a sharp decline of lionfish densities was observed across all habitats/depth during the 2018-20 survey relative to the mean densities of 2011 (Figures 100 – 102). The site mean density declined 49.7% between surveys but differences were statistically insignificant (ANOVA; p = 0.353).

Table 52. Mean density variations of the numerically dominant large demersal fish/shellfish assemblage between the 2011 baseline and the 2018-20 monitoring surveys from the main habitats/depths surveyed in the 30 – 50m depth range at Isla Desecheo.

	Site Means			**Anova**
Habitat/Depth	**2011**	**2018-20**	**% Change**	**p-value**
CPRT30-40	51.23	22.11	-56.8	0.7790
ACR30-40	27.97	25.39	-9.2	0.7820
Rhod50	8.28	27.00	226.1	0.1660
Fish				
Balistes vetula	0.48	1.15	140.0	0.1265
Epinephelus guttatus	3.01	4.70	55.9	0.3295
Epinephelus striatus	0.38	0.26	-30.4	0.3241
Lutjanus apodus	17.31	5.71	-67.0	0.6764
Pterois sp	3.80	1.91	-49.7	0.3529
Sphyraena barracuda	0.55	0.45	-18.1	0.5806
Shellfish				
Lobatus gigas	1.84	5.44	195.1	0.0690
Panulirus argus	0.47	0.29	-36.8	0.2053

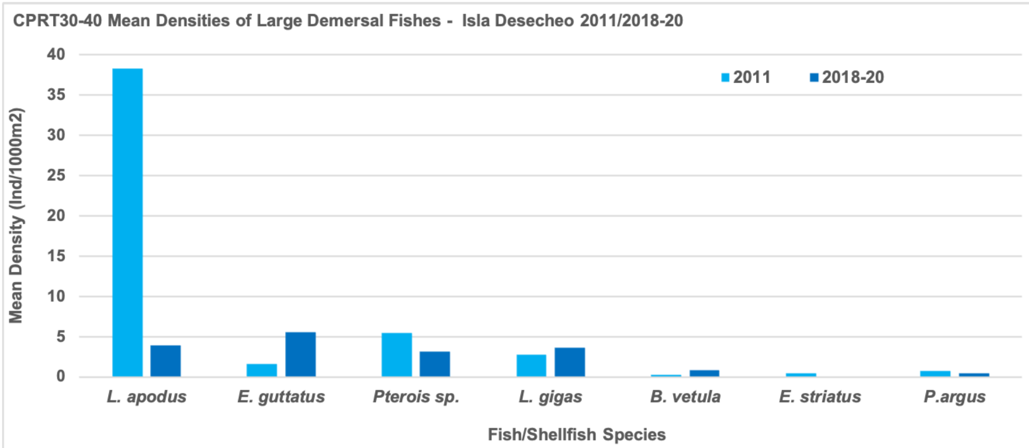

Figure 100. Mean density variations of numerically dominant fish/shellfish between the 2011 baseline and the 2018-20 monitoring survey at CPRT30-40, Isla Desecheo.

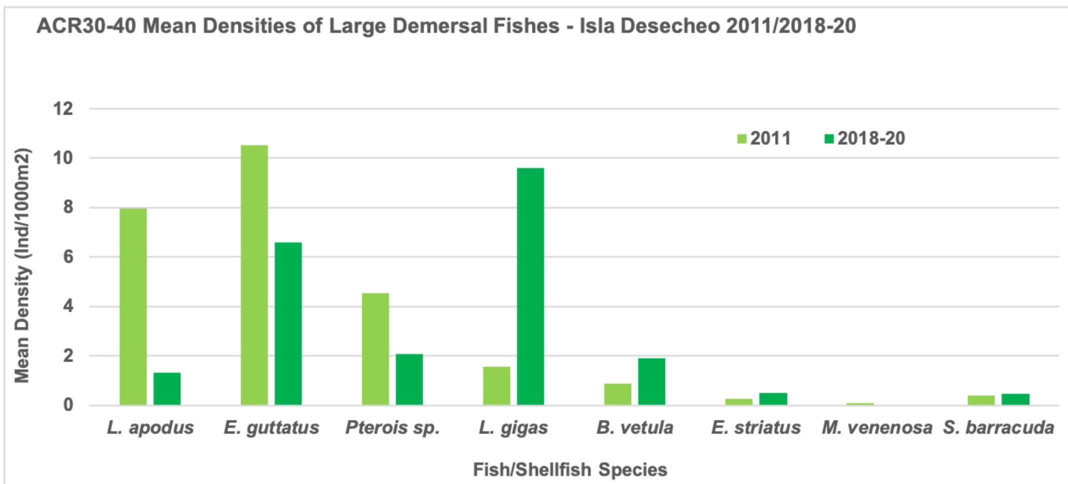

Figure 101 Mean density variations of numerically dominant fish/shellfish between the 2011 baseline and the 2018-20 monitoring survey at ACR30-40, Isla Desecheo.

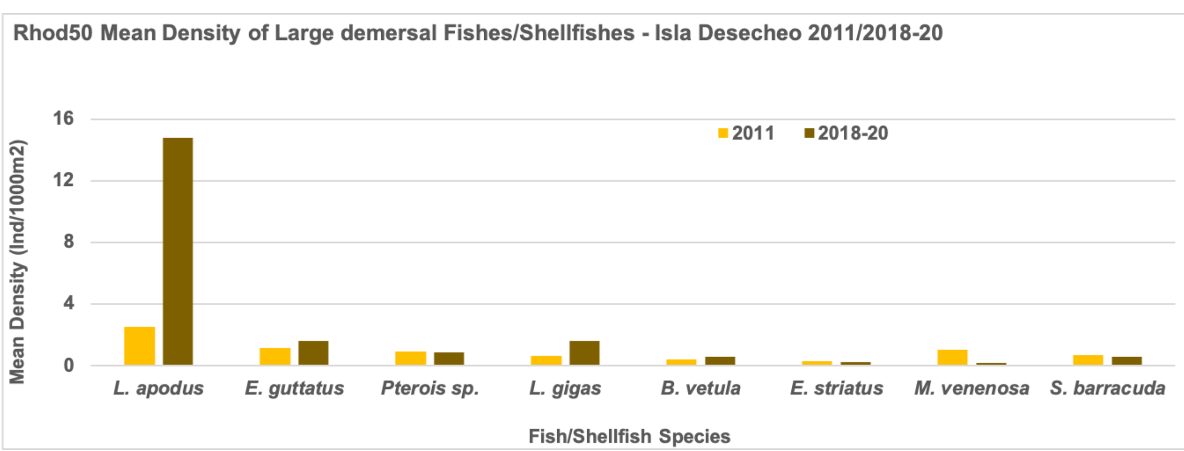

Figure 102. Mean density variations of numerically dominant fish/shellfish between the 2011 baseline and the 2018-20 monitoring survey at Rhod50, Isla Desecheo.

Temporal variations of the large demersal fish/shellfish community structure between the 2011-12 baseline and the 2018-20 monitoring survey, based on the relative densities of the numerically dominant species (>95% total densities on each survey) are presented in a non-metric multidimensional scaling plot of Bray-Curtis similarities in Figure 103. Similarities between surveys were relatively low (49.8% - 54.7%) influenced by habitat/depth density inconsistencies of numerically dominant species, such as schoolmaster snapper (*Lutjanus apodus*) and queen conch (*Lobatus gigas*). Similarity was highest at ACR30-40 (54.7%) contributed by relatively high densities of lionfish (*Pterois sp*), queen triggerfish (*Balistes vetula*), and Nassau grouper (*Epinephelus striatus*) (Table 53). Similarity at CPRT30-40 and Rhod50 was mostly contributed by schoolmaster snapper (*L. apodus*), and other species present in very low densities, such as great barracuda (*Sphyraena barracuda*), yellowfin grouper (*Mycteroperca venenosa*), and spiny lobster (*Panulirus argus*).

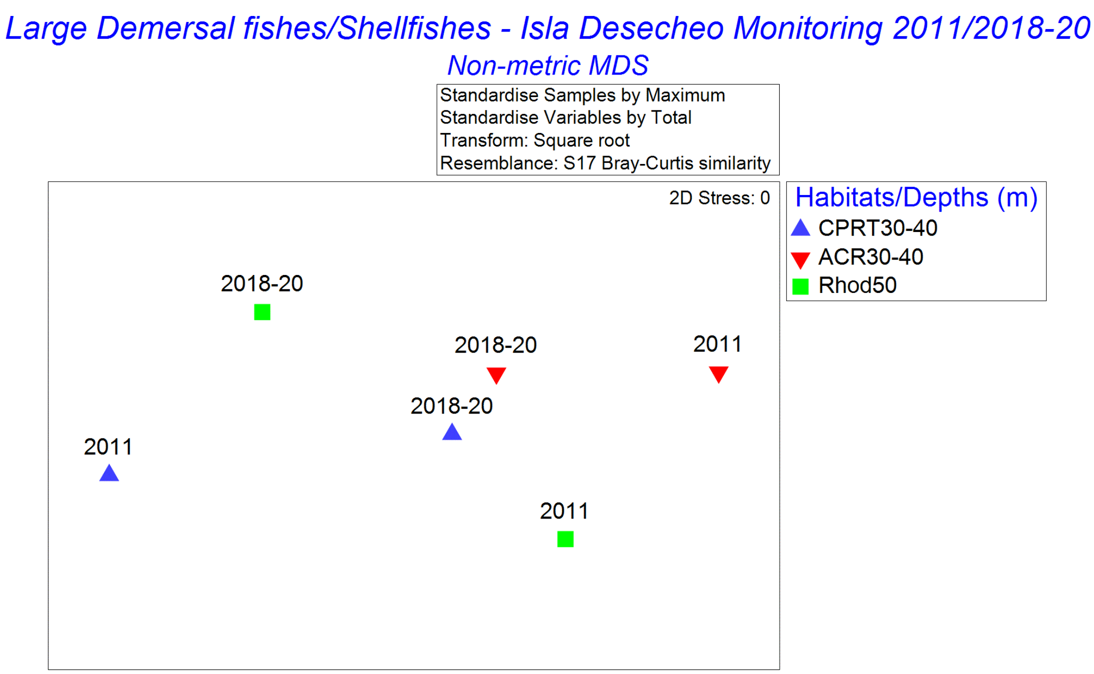

Figure 103. Non-metric multidimensional scaling (nMDS) plot of Bray-Curtis similarities of relative densities by large demersal fishes/shellfishes surveyed from drift belt-transects in the 30 – 50m depth range at Isla Desecheo during the 2004-05 baseline and the 2018-20 monitoring survey

Table 53. Similarity matrix (SIMPER) based on the relative densities of large demersal fishes/shellfishes between the 2011 baseline and the 2018-20 monitoring surveys at the main benthic habitats/depths surveyed in Isla Desecheo.

	CPRT30-40	ACR30-40	Rhod50
Average Similarity (%)	**49.8**	**54.7**	**49.5**
Species Contributions			
Lutjanus apodus	23.2		23.6
Pterois sp.	16.5	12.2	
Panulirus argus	12.8		
Mycteroperca venenosa	12.2		
Sphyraena barracuda	12.1	10	14.8
Epinephelus guttatus		16	
Balistes vetula		12.8	12.4
Epinephelus striatus		12	12.8
Lactophrys trigonus		9.8	
Lobatus gigas			11.1

Size Distributions of Numerically Dominant Large Demersal Fishes/Shellfishes, 2011-12/2018-20

Coney (*Cephalopholis fulva*)

Coneys (*C. fulva)* were the most abundant fish species identified within drift belt-transect surveys in 2018-20 with a mean site density of 16.10 Ind/10^3m^2. One main TL mode at 19cm was observed from the size distribution of the 2018-20 survey based on a sample of 244 individuals (Figure 104). Coneys were not included in the 2011 survey because they were not considered as a large demersal species but were included in the 2018-20 survey given their relatively high density compared to other larger groupers species. The length at maturity of *C. fulva* was reported at 14.5cm (Froese and Pauly, 2019). Therefore, approximately 90% of the coney population observed within drift belt-transects from mesophotic habitats at Isla Desecheo were adults.

Red Hind (*Epinephelus guttatus*)

Red hind (*E. guttatus*) ranked 2nd in terms of site mean density within drift belt-transects in 2011-12 (5.14 Ind/10^3m^2) and ranked 3^{trd} with a site mean density of 4.81 Ind/10^3m^2 in 2018-20. Size distributions of *E. guttatus* from the 2012 and 2018-20 surveys within the 30 – 50m depth range at Isla Desecheo, based on a total of 171 individuals were not statistically different (Kolmogorov-Smirnoff; p > 0.10). Two main total length (TL) modes at 34cm and at 31cm, representative of 58.3% and 51.0% of the total individuals during the 2011-12 and 2018-20 surveys, respectively were evident from the size distributions (Figure 105). The length at maturity of *E. guttatus* was reported at 25cm TL (Froese and Pauly, 2019). Therefore, more than 90% of the total individuals during both surveys were adults. The recruitment size into mesophotic habitats at Isla Desecheo were estimated at 16cm and 19cm during 2011-12 and 2018-20, respectively.

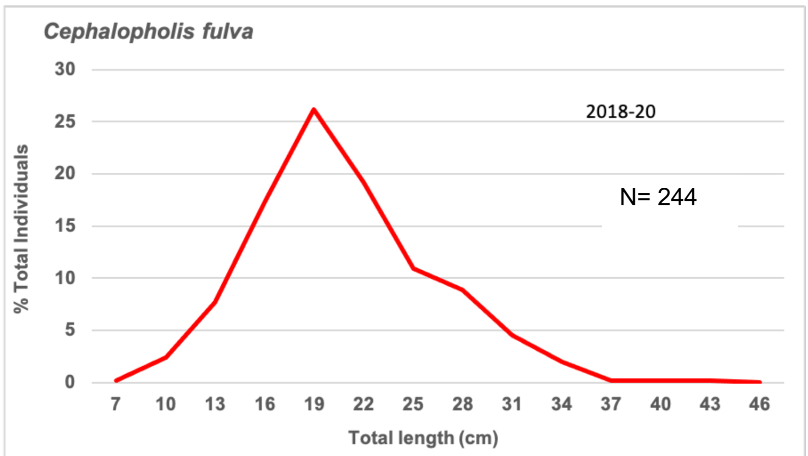

Figure 104. Size-frequency distribution of coney (*Cephalopholis fulva*) from mesophotic habitats in the 25 – 50m depth range at Isla Desecheo (2011-12 and 2018-20 surveys).

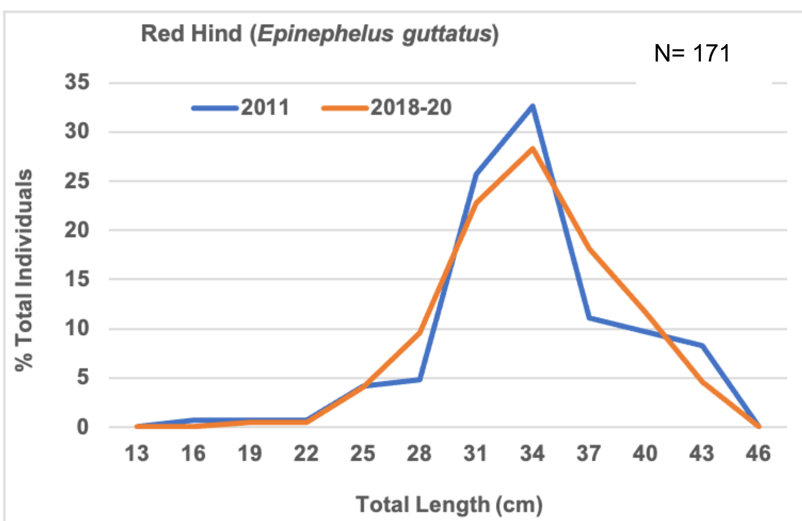

Figure 105. Size-frequency distribution of red hind (*Epinephelus guttatus*) from mesophotic habitats in the 30 – 50m depth range at Isla Desecheo (2011-12 and 2018-20 surveys).

Queen Triggerfish (*Balistes vetula*)

Queen triggerfish (*Balistes vetula*) ranked as the 7th most abundant fish/shellfish species surveyed within drift belt-transects in 2011-12 and 5th in 2018-20 with site mean densities of 0.54 Ind/10^3m^2 and 1.19 Ind/10^3m^2, respectively. Individuals of *B. vetula* were observed from all benthic habitats/depths surveyed at Isla Desecheo during both surveys. Size distributions based on a total of 35 individuals are shown in Figure 106. The size distribution in 2011-12 was strongly skewed towards the larger size classes with a main mode at 40cm and a secondary mode at 43cm, representative of 75.0% of the total individuals. A more balanced size distribution influenced by the presence of smaller individuals was observed in 2018-20 with a main mode at 37cm and a secondary mode at 34cm, representative of 48.0% of the total individuals. Differences of size distributions of *B. vetula* between the 2011-12 and 2018-20 surveys were statistically insignificant (Kolmogorov-Smirnoff; $p > 0.10$).

Size at maturity of queen triggerfish was reported at 25.5cm (Froese and Pauly, 2019). So, the entire *B. vetula* population surveyed from mesophotic habitats at Isla Desecheo during both surveys consisted only of adults. Queen triggerfish reproductive activities involving courtship and defense of nesting sites were observed from rhodolith benthic habitats down to the maximum depth surveyed of 50m. Maximum FL sizes were observed at 46cm in both surveys.

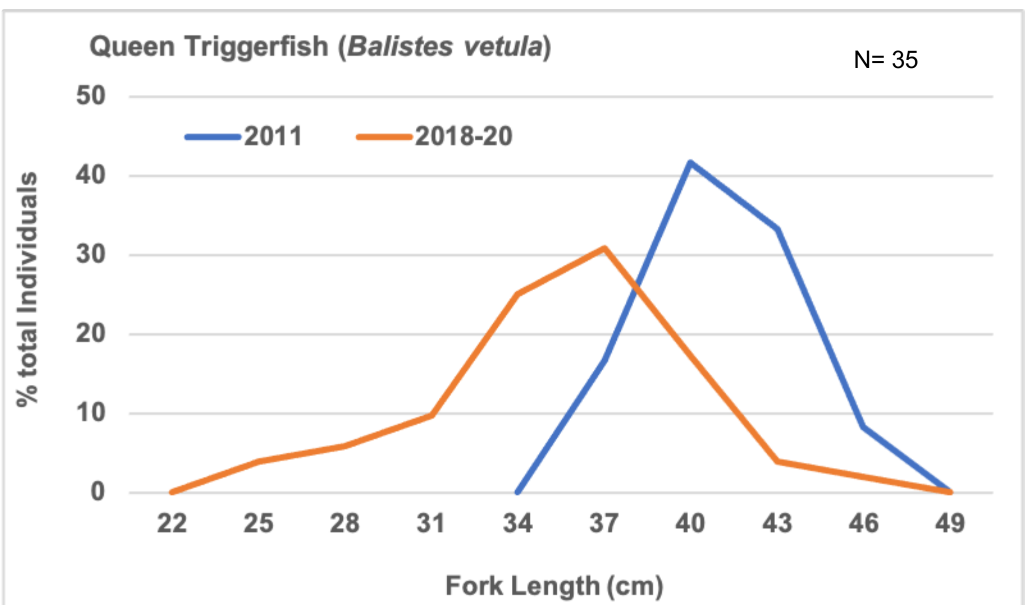

Figure 106. Size-frequency distribution of queen triggerfish (*Balistes vetula*) from mesophotic habitats in the 30 – 50m depth range at Isla Desecheo (2011-12 and 2018-20 surveys).

Lionfish (*Pterois sp.*)

Lionfish (*Pterois sp.*) ranked 3rd during 2011 and 4th during 2018-20 surveys with site mean densities of 3.74 Ind/10^3m^2 and 2.03 Ind/10^3m^2, respectively. Size distributions, based on a total of 141 individuals are shown in Figure 107. The 2011 distribution was characterized by a wide distribution of size classes with a main mode at 28 cm (TL), representative of only 9.6% of the total individuals and a secondary mode at 19cm, representative to 6.7% of the total. Conversely, the size distribution during 2018-20 was more skewed towards larger individuals, with a main mode at 34cm, representative of 20.9% of the total individuals and a secondary mode at 31cm, representative of 17.1% of the total. Size distribution differences were not statistically significant (Kolmogorov-Smirnoff; $p > 0.10$), despite the marked size increment between survey years.

The reported length at maturity of lionfish (*Pterois volitans*) is 16.0cm TL (Froese and Pauly, 2019) Therefore, more than 96% of the lionfish populations surveyed from mesophotic habitats during both surveys at Isla Desecheo were adults. The pronounced skewness of the 2018-20 size distribution toward larger size classes suggests growth in size of the 2011-12 population and paucity of recruitment between surveys. Maximum lengths were at 34cm in 2011-12 (1.9% of the total individuals) and 40cm in 2018-20 (8.9% of the total individuals).

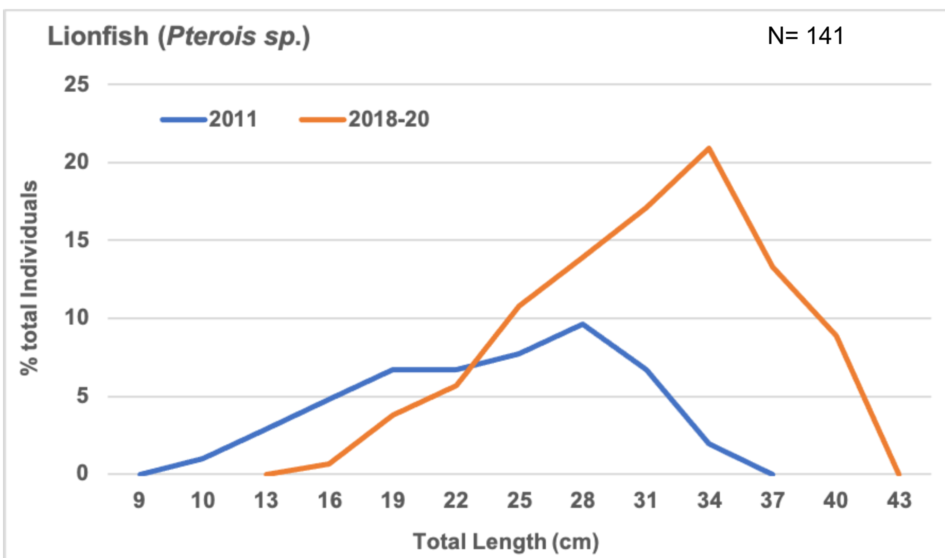

Figure 107. Size-frequency distribution of lionfish (*Pterois sp.*) from mesophotic habitats in the 30 – 50m depth range at Isla Desecheo (2011-12 and 2018-20 surveys).

Schoolmaster Snapper (*Lutjanus apodus*)

Schoolmaster snapper (*Lutjanus apodus*) was the numerically dominant large demersal fish/shellfish species surveyed from mesophotic habitats in the 30 – 50m depth range at Isla Desecheo with site means of 15.27 Ind/10^3m^2 during 2011-12 and 6.04 Ind/10^3m^2 in 2018-20. The size distribution during 2011-12 was characterized by a highly dominant mode in the 31 – 34 cm (FL) range, representative of 68.5% of the total individuals. Such distribution was associated with one large schooling aggregation of approximately 300 individuals of similar size. The 2018-20 size distribution was more balanced with a primary mode at 28cm and a secondary mode at 31cm, representative of 45.0% of the total individuals (Figure 108). Differences of size distributions between surveys were statistically insignificant (Kolmogorov-Smirnoff; $p > 0.10$). Size at maturity of *L. apodus* has been reported at 25cm (Froese and Pauly, 2019). Thus, more than 95% of the total population surveyed during both surveys were adults. Juvenile individuals were observed within drift belt-transects with minimum sizes of 16cm in 2011-12 and 19cm in 2018-20

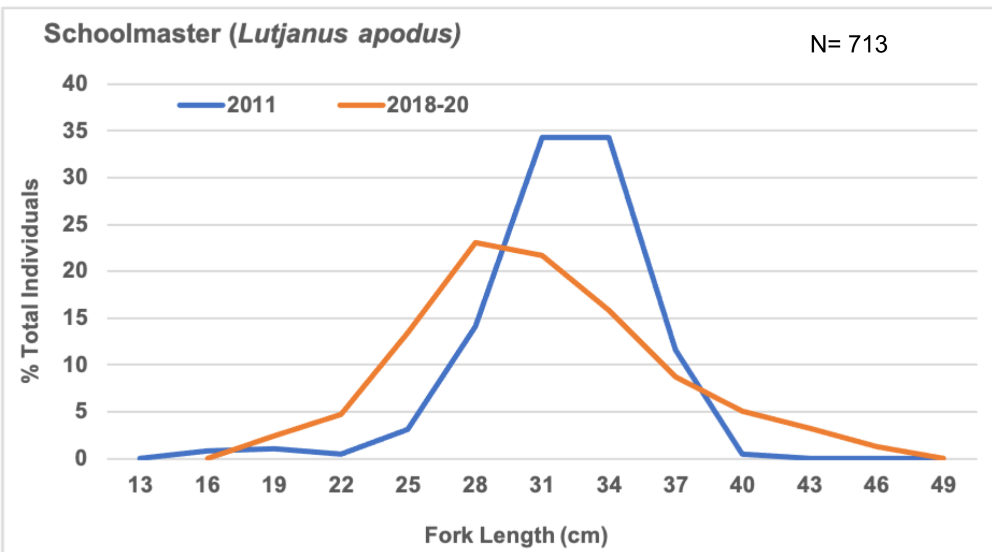

Figure 108. Size-frequency distribution of schoolmaster (*Lutjanus apodus)* from mesophotic habitats in the 30 – 50m depth range at Isla Desecheo (2011-12 and 2018-20 surveys).

Queen Conch (*Lobotes gigas*)

Queen conch (*Lobatus gigas*) ranked 4th among large demersal fishes/shellfishes in terms of its site mean density of 1.63 Ind/10^3m^2 during the 2011-12 baseline survey and ranked 2nd in 2018-20 with a site mean of 5.50 Ind/10^3m^2. The size distributions of queen conch during both surveys based on a total of 161 individuals are presented in Figure 109. Size distribution were similar with a main mode at 26cm representative of 41.7% and 42.3% of the total individuals surveyed within drift belt-transects in 2011-12 and 2018-20. Differences of *L. gigas* size distributions between surveys were not statistically significant (Kolmogorov-Smirnoff; $p > 0.10$). The main difference was associated with the presence of a few individuals smaller than 20cm in 2011-12, representative of approx. 6.0% of the total population that were not observed in 2018-20. Maximum sizes up to 28cm and 30cm were measured in 2011-12 and 2018-20, respectively.

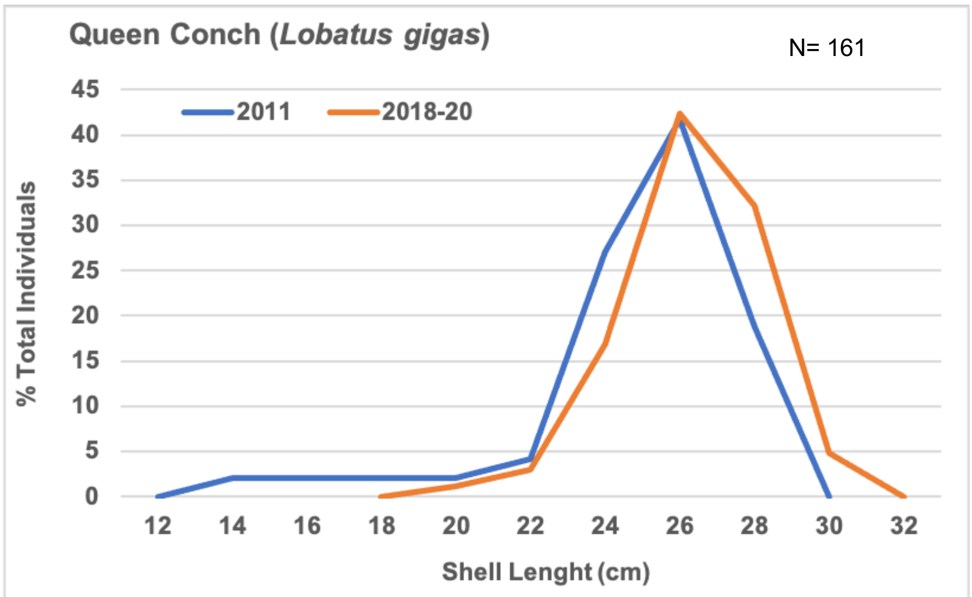

Figure 109. Size-frequency distribution of queen conch (*Lobatus gigas)* from mesophotic habitats in the 30 – 50m depth range at Isla Desecheo (2011-12 and 2018-20 surveys).

Spiny Lobster (*Panulirus argus*)

Mean density of spiny lobsters (*Panulirus argus*) from mesophotic habitats within the 30 – 50m depth range surveyed by drift belt-transects in Isla Desecheo varied between 0.41 Ind/$10^3$$m^2$ in 2011-12 (rank 8^{th}) and 0.31 Ind/$10^3$$m^2$ in 2018-20 (rank 10^{th}). Size distributions based on a total of 12 individuals are shown in Figure 110. The main size mode in 2011-12 was of 20cm (CL), whereas in 2018-20 was of 12cm. Size distribution differences of *P. argus* between survey years were not statistically significant (Kolmogorov-Smirnoff; $p > 0.10$) due to the very small sample size but suggest that mesophotic habitats of Isla Desecheo function as residential/foraging areas of very large spiny lobsters. Using 9cm (3.5 inches) as an adult size for spiny lobsters, more than 90% of the lobsters observed within drift belt-transects during both surveys were adults.

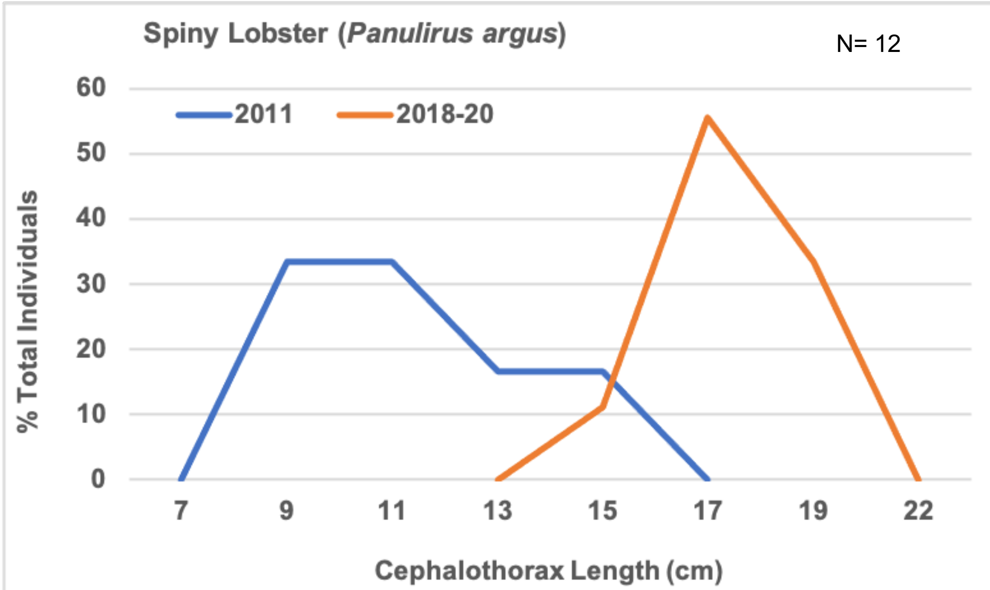

Figure 110. Size-frequency distribution of spiny lobster (*Panulirus argus)* from mesophotic habitats in the 30 – 50m depth range at Isla Desecheo (2011-12 and 2018-20 surveys).

Photo Album 4 – DES
Aggregate Coral Reef - DES

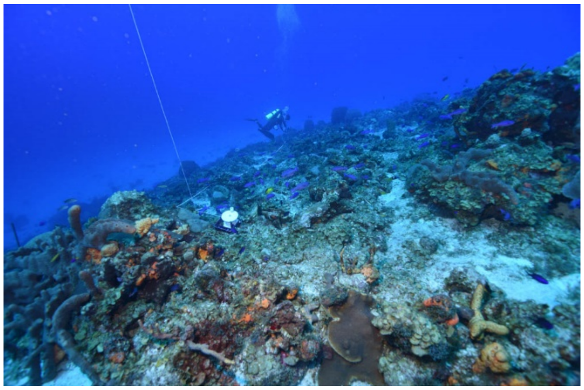







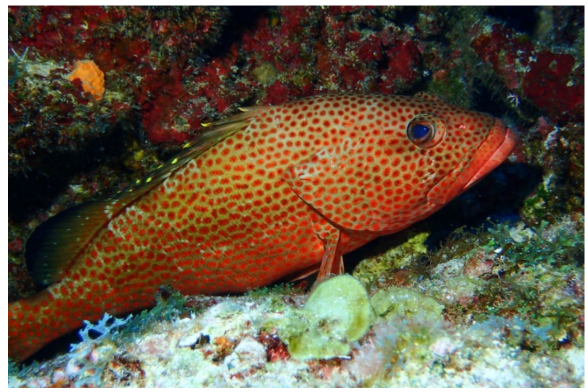

Colonized Pavement Slope (CPSlope) - DES

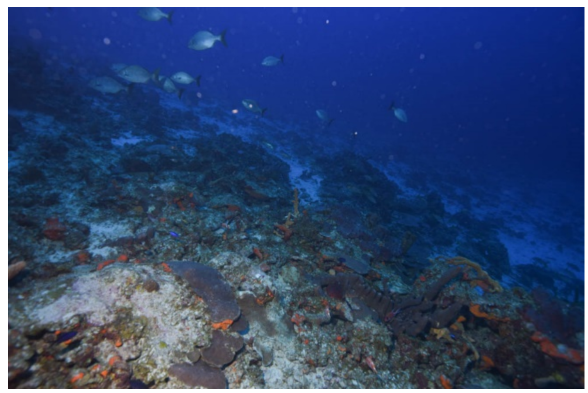

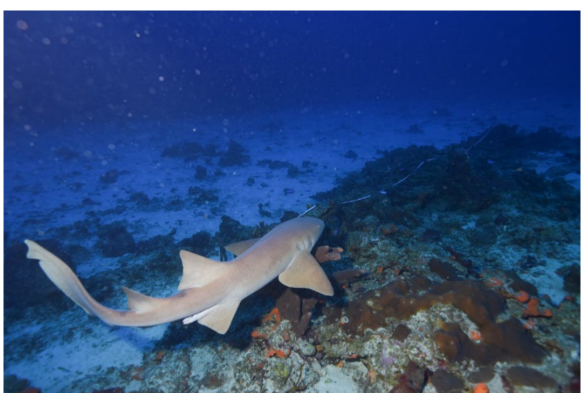

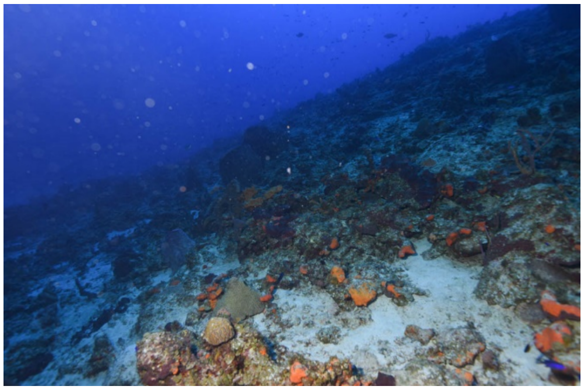
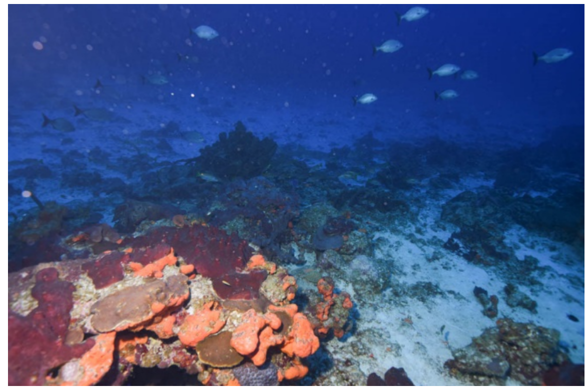



Rhodolith (Rhod50)

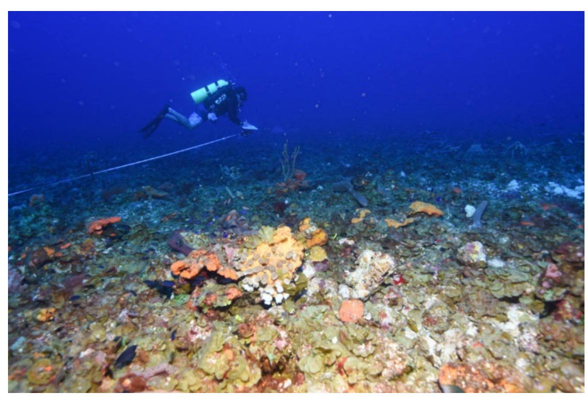

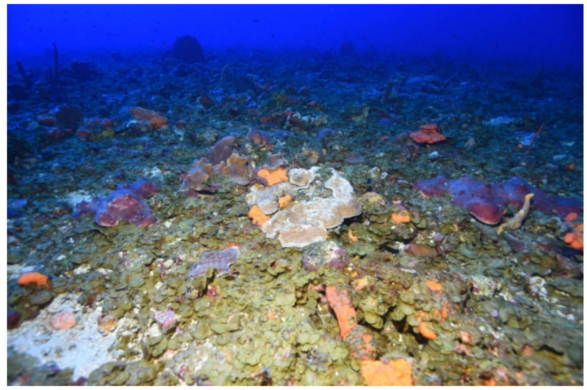

El Seco Reef

Physical Description

"El Seco" is a submerged promontory that rises from a deep outer shelf basin at the southeastern tip of the Vieques shelf, approximately 6 km off Punta del Este. The promontory with an elliptical shape runs along a north-south axis and rises from the basin at depths of 33 – 36m to a mostly flat colonized pavement reef top (CPRT) at depths of 23 – 28m (Figure 111). Mesophotic reef habitats are distributed all around "El Seco" promontory within the deep outer shelf of southeastern Vieques. Depth increases towards the shelf-edge to the east and south of the promontory, and decreases towards the north, where an extensive mesophotic bank coral reef (BCR) system was found and characterized (Garcia-Sais et al, 2011). The BCR ends in a series of patch coral reef (PCR) spurs separated by coralline sand and coral rubble pools at depths between 40 – 45 m. The deepest sections of the shelf basin at depths between 45 – 50m were found associated with a mostly flat and homogeneous bed of rhodolith nodules (Rhodo) to the west and south of the promontory. Exceptionally clear waters prevail at "El Seco" with underwater visibility generally exceeding the 30 - 40m range.

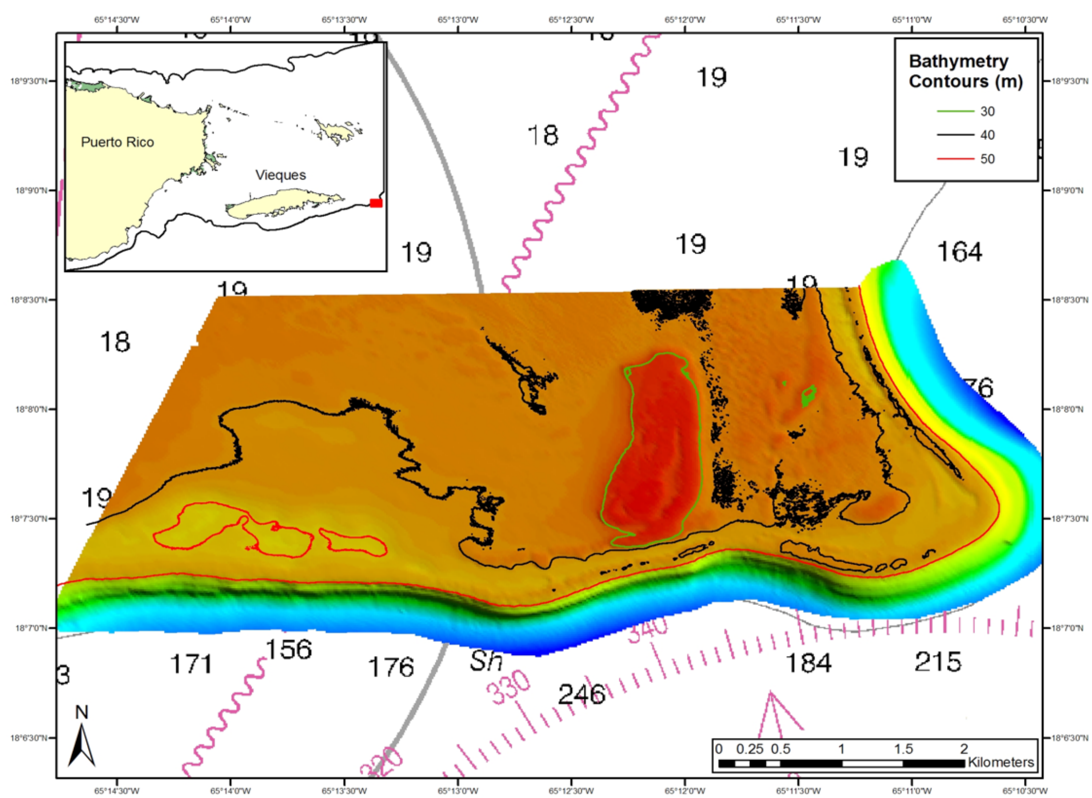

Figure 111. Multibeam bathymetry map of El Seco Reef system at the southeastern boundary of the Vieques Island shelf. Multibeam data from NOAA Biogeography Team.

A benthic habitat map of the southeastern tip of the Vieques shelf surrounding El Seco Reef, along with a baseline characterization of the predominant sessile-benthic and fish/shellfish populations associated with the main benthic habitats was prepared by Garcia-Sais et al. (2011). The CPRT habitat associated with the El Seco promontory was estimated to cover a surface area of approximately 1.6 km^2, or 14.0 % of the surveyed area. The CPRT was described as a highly heterogeneous seafloor with extensive areas of low-relief hard bottom colonized by turf algae and interspersed basket sponges, and the occurrence of rocky outcrops and low ridges colonized by scleractinian corals, gorgonians and another reef biota. There are also sections of flat uncolonized hard bottom covered by sand, coral rubble, and rhodolith nodules.

The BCR habitat is an impressive continuous (aggregated) formation of scleractinian corals, mostly boulder star corals, *Orbicella spp* growing at depths of 33 – 41 m (110 – 135') throughout the northern and northeastern sections of the study area (Garcia-Sais et al., 2011). The total surface area of the BCR was estimated as of 4.6 km^2, or 30% of the total surveyed area (Figure 112). The areal extension of the BCR habitat to the north of the study area remains undescribed. At a depth of approximately 40m, extending down to 45m the BCR breaks down to a discontinuous formation of patch coral reefs (PCR) separated by coralline sand/coral rubble channels and pools covering an estimated surface area of 1.5 km^2, or 10.0 % of the surveyed area. Within sections of the PCR habitat the spawning aggregation site of tiger grouper (*Mycteroperca tigris*) was reported (Sadovy et al., 1994. Matos-Caraballo et al. 2006). A mostly flat, homogeneous benthic habitat (Rhodo) characterized by the predominance of algal rhodoliths was reported along the entire western section of the study area at depths between 35 – 50 m (Garcia-Sais et al., 2011). Algal rhodoliths were observed to be colonized by benthic algae, scleractinian corals, sponges and another encrusting reef biota. The areal extension of Rhodo habitat was estimated at 7.1 km^2, or 48.6 % of the surveyed area.

A total of 24 sampling stations previously included in the 2011 baseline characterization of the sessile-benthic and small demersal fish communities from the main benthic habitats at El Seco (Garcia-Sais et al., 2011) were revisited during the 2018-20 monitoring survey (Figure 113). An additional 20 drift belt-transect stations for characterization of large demersal fishes and shellfishes (spiny lobster and queen conch) were included as baseline characterizations of this reef community component that was not included in the baseline survey by Garcia-Sais et al. (2011). Representative images of the main benthic habitats and associated communities are shown in Photo Album 5.

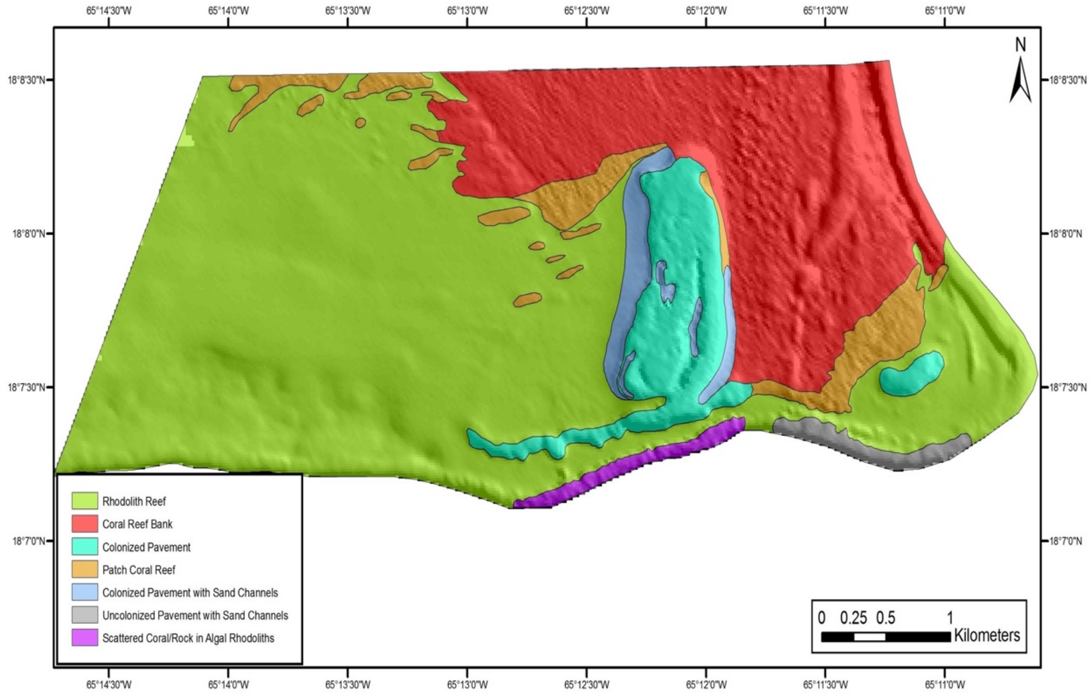

Figure 112. Map of mesophotic benthic habitats within the 25 – 50m depth range at El Seco Reef, southeast Vieques (from Garcia-Sais et al., 2012)

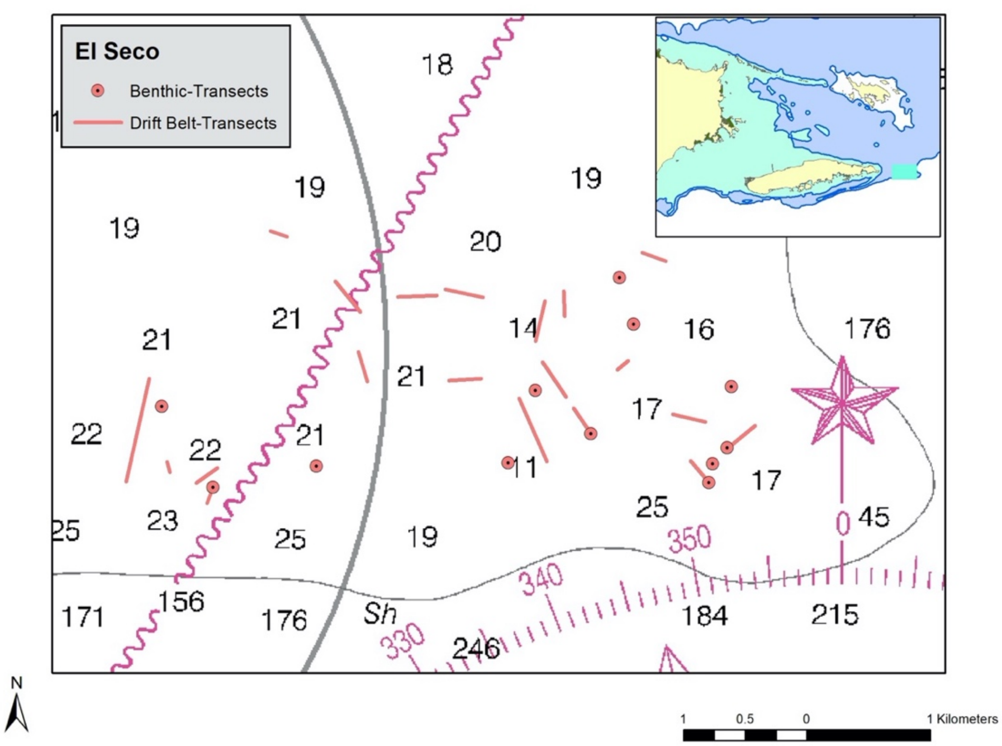

Figure 113. Location of sampling stations at El Seco Reef, 2018-20 monitoring survey

Benthic Community

Depth/habitat related patterns of benthic community structure, 2018-20 survey

Benthic algae were the main category in terms of substrate cover at all habitats/depths with means ranging between a minimum of 67.77% at BCR35-40 and a maximum of 91.55% at CPRT23-30 during the 2018-20 survey (Figure 114). Habitat/depth related differences of substrate cover by total benthic algae were statistically significant (ANOVA; p= 0.0016), associated to the lower cover at BCR35-40 compared to other habitats/depths. Marked habitat/depth related variations among the main algal taxonomic components were noted. The encrusting fan alga (*Lobophora sp.*) was the dominant benthic alga from all habitats/depths with mean substrate cover ranging between 38.20% at CPRT23-30 and 64.39% at Rhod40-50. *Lobophora sp*. and fleshy algae (mostly *Dictyota sp*) exhibited a pattern of increasing cover with depth. Conversely, substrate cover by turf algae, *Ramicrusta sp*., and crustose coralline algae (CCA), declined with depth (Figure 115). Patches of cyanobacteria (blue-green algae) were observed from all habitats/depths surveyed without any statistically significant differences of substrate cover (ANOVA; p = 0.275).

A total of 16 stony corals, including one hydrocoral (*Millepora alcicornis*) were identified from the main habitats/depths surveyed at El Seco Reef during the 2018-20 survey (Table 54). Mean substrate cover varied between 0.28% at Rhod40-50 and 26.95% at BCR35-40. Habitat/depth related differences of substrate cover by stony corals were statistically significant (ANOVA; p < 0.0001), associated with higher cover at BCR35-40 and PCR36-42 compared to other habitats/depths, and higher cover at CPRT23-30 relative to Rhod40-50. The highest substrate cover by stony corals was measured from BCR35-40, driven by peak cover of mountainous/boulder star coral complex (*Orbicella faveolata* and *O. franksi*). Mustard-hill coral (*Porites astreoides*) was present within photo-transects across all habitat/depths with peak cover at PCR36-42. (Figure 116). Lettuce corals (*Agaricia lamarki, A. agaricites,* and *A. grahamae*) were also prominent at BCR35-40 and PCR36-42. Diseased and/or recently dead coral colonies were observed from all habitat/depths surveyed at El Seco Reef in 2018-20. Very high disease prevalence was measured at Rhod40-50 (15.5%), BCR35-40 (15.3%), and PCR 12.3%). The most affected species included *Orbicella faveolata/franksi, Montastraea cavernosa, Porites astreoides, Agaricia lamarcki, A. agaricites,* and *Siderastrea siderea*. Recently dead coral colonies were observed at CPRT23-30, BCR35-40, and PCR36-42. Many dead standing coral colonies, particularly *Dendrogyra cilindrus*, *O. faveolata/franksi*, and *S. siderea* were observed completely overgrown by *Ramicrusta sp*. at CPRT23-30.

Table 54. Percent substrate cover by sessile-benthic categories from the main habitats/depths surveyed at El Seco Reef, 2018-20 survey

BENTHIC CATEGORIES	CPRT23-30	BCR35-40	PCR 36-42	Rhod40-50
Abiotic				
Sand	2.70	0.67	3.37	6.29
Dead Coral	0.04	0.29	0.87	
Rubble	0.17			0.19
Total Abiotic	2.90	0.97	4.24	6.48
Benthic Algae				
Peyssonnelid (mixed)	0.80	6.76	9.93	3.46
Turf Algae (mixed)	32.27	9.37	7.62	8.37
Lobophora sp.	38.20	40.62	54.55	64.39
Halimeda spp.	0.12	0.08		7.70
Dictyota spp.	0.49	0.32	0.45	2.35
Ramicrusta sp.	14.83	7.40	5.85	0.55
Fleshy macroalgae (mixed)	0.08	0.48	0.43	1.33
CCA (mixed)	4.77	2.76	2.09	1.05
Total Benthic Algae	91.55	67.77	80.91	89.20
Cyanobacteria	1.23	3.17	1.30	1.69
Stony Coral				
Agaricia agaricites	0.15	0.29	0.67	
Agaricia fragilis		0.17		
Agaricia grahamae		0.26	0.63	
Agaricia lamarcki		1.23	0.79	
Diploria labyrinthiformis		0.15		
Madracis decactis			0.04	0.05
Millepora alcicornis	0.07	0.06		
Montastraea cavernosa		0.03		
Orbicella faveolata/franksi (complex)	0.04	23.24	9.07	0.17
Porites astreoides	0.34	0.78	1.58	0.07
Porites furcata	0.07			
Porites porites	0.08	0.26		
Pseudodiploria strigosa	0.04			
Siderastrea siderea	0.26	0.30	0.11	
Stephanocoenia intersepta	0.04	0.18		
Total Stony Coral	1.10	26.95	12.88	0.28
# Coral Colonies/photo frame	1.30	15.26	8.78	0.45
# Diseased Coral Colonies/photo frame	0.04	2.34	1.08	0.07
# Coral colonies bleached/photo frame	0.00	0.00	0.00	0.00
# Antipatharian Colonies/photo frame	0.00	0.00	0.00	0.00
Octocoral				
Antillogorgia spp.	0.08			
Erythropodium caribaeorum	0.64	0.10	0.08	
Gorgonia ventalina	0.09			
Pseudoplexaura spp.	0.09			
Total Soft Corals	0.89	0.10	0.08	0.00

Table 54. Percent substrate cover by sessile-benthic categories from the main habitats/depths surveyed at El Seco Reef, 2018-20 survey

BENTHIC CATEGORIES	CPRT23-30	BCR35-40	PCR 36-42	Rhod40-50
# Soft Corals/photo frame	1.62	0.07	0.11	0.02
Sponges				
Agelas sventres	0.08			
Aiolochoria crassa		0.07	0.12	
Amphimedon compressa	0.15			
Aplysina cauliformis	0.20	0.06	0.08	
Aplysina fistularis	0.58			
Aplysina insularis	0.04			
Cinachyrella kuekenthali	0.04			
Cliona tenuis		0.13		
Ircinia strobilina	0.81	0.06		0.14
Mycale laevis			0.04	0.09
Neopetrosia proxima	0.18			
Plakortis spp.		0.17	0.06	0.09
Scopalina ruetzleri	0.18			
Unknown sponges	0.22	0.10	0.17	0.53
Verongula gigantea			0.12	
Xestospongia muta	0.24			0.98
Total Sponges	2.71	0.57	0.60	2.05

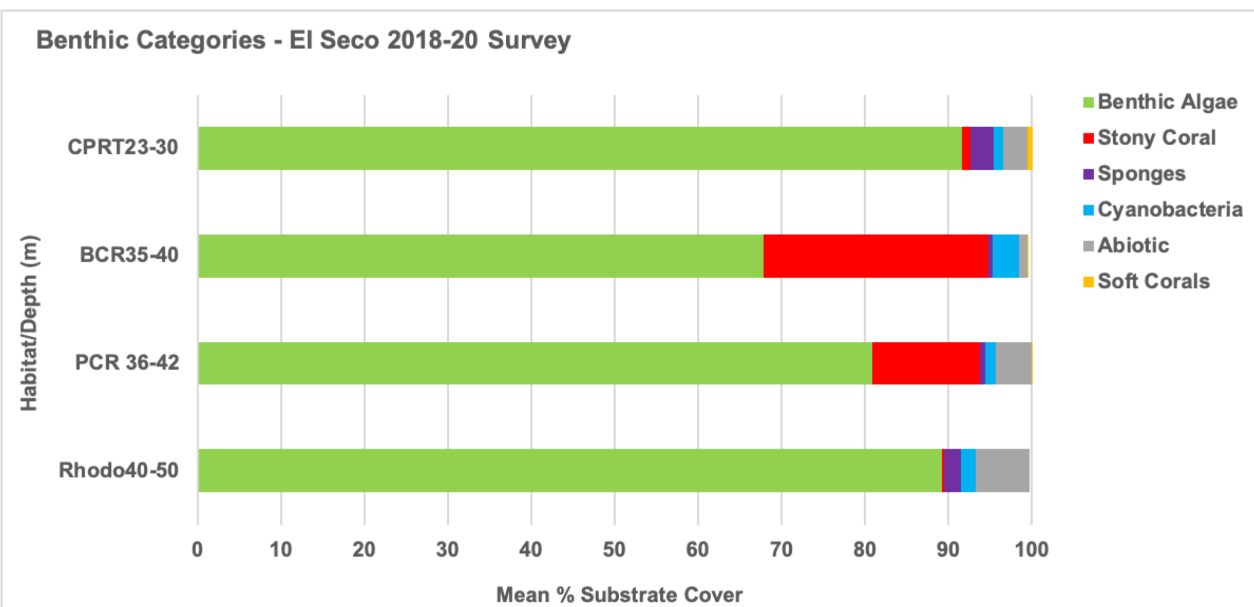

Figure 114. Variations of percent substrate cover by the main sessile-benthic categories from the main habitats/depths surveyed within the 23-50m profile at El Seco Reef, 2018-20 survey.

Soft corals (gorgonians) were not prominent within mesophotic habitats surveyed within the 23 – 50m depth profile at El Seco during the 2018-20 survey. Peak cover was measured from CPRT23-30 (0.89%) and included a total of four species. The encrusting gorgonian (*Erythropodium caribaeorum*) was the dominant species in terms of reef substrate cover with a mean of 0.64% at CPRT23-30 (Table 54). Likewise, sponges were present with relatively low substrate cover at the habitats/depths surveyed. A total of 15 species of sponges were identified with mean substrate cover ranging between 0.57% at BCR35-40 and 2.71% at CPRT23-30 (Table 52). Differences of reef substrate cover by sponges in relation to habitat/depth were statistically significant (ANOVA; $p < 0.0017$), associated with higher cover at CPRT35-40 and Rhod40-50, relative to BCR35-40 and PCR40-50. *Ircinia strobilina* and *Aplysina fistularis* were the dominant species at CPRT23-30, whereas *Xestospongia muta* was the dominant at Rhod40-50 (Table 52).

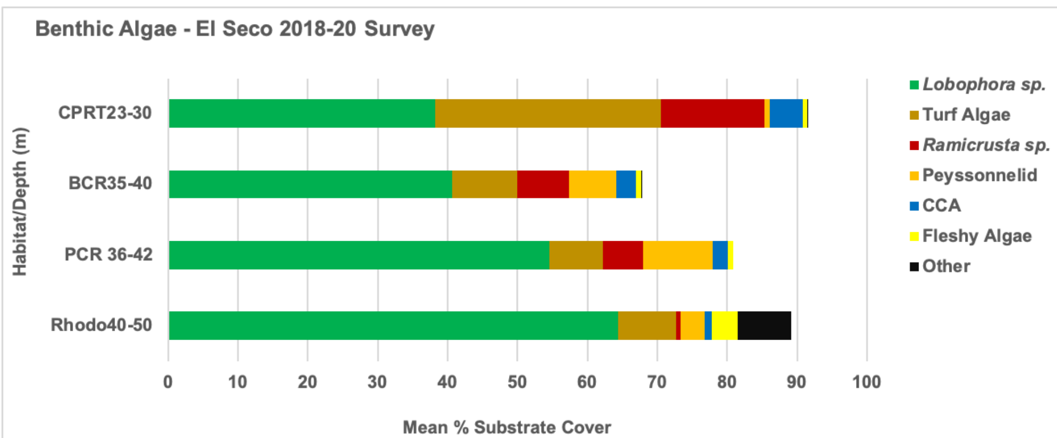

Figure 115. Variations of percent substrate cover by benthic algal taxonomic components from the main habitats/depths surveyed within the 23-50m profile at El Seco Reef, 2018-20 survey.

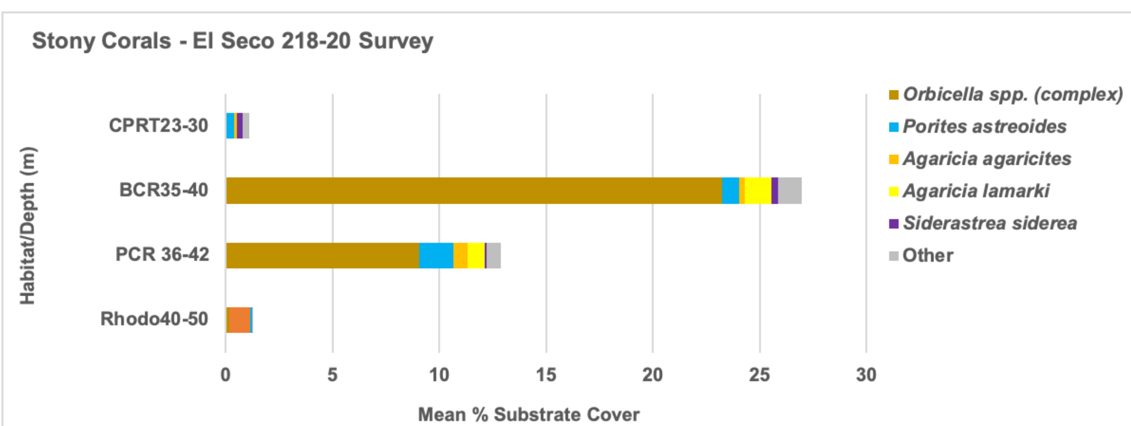

Figure 116. Variations of percent substrate cover by stony corals from the main habitats/depths surveyed within the 23-50m profile at El Seco Reef, 2018-20 survey.

Similarities of benthic community structure based on the percent substrate cover from the main habitats/depths surveyed across the 23 – 50m depth range at El Seco during 2018-20 are presented in a multidimensional scaling plot (NMDS) of Bray-Curtis similarities in Figure 117. The highest similarities were observed within Rhod40-50 (87.4%), mostly contributed by the relatively high substrate cover by sponges, benthic algae, and abiotic categories. Coral reef stations (BCR35-40 and PCR36-42) ranked second and third in similarity with 71.8% and 70.4%, respectively. Stony corals, benthic algae, and cyanobacteria were the main contributors to similarity at BCR35-40, whereas benthic algae, stony corals, and abiotic categories were the main contributors at PCR36-40 (Table 55). The relatively high cover by benthic algae was a unifying feature contributing similarity across all habitats/depths surveyed.

Dissimilarity between habitats/depth was highest between CPRT23-30 and BCR35-40 (45.1%), largely influenced by the much higher cover of stony corals at BCR35-40 and the relatively higher cover of soft corals at CPRT23-30. The relatively higher cover by stony corals was the main factor differentiating BCR35-40 and PCR36-42 from all other habitats/depths. whereas soft corals differentiated CPRT23-30 from all other habitats/depths. The relatively high substrate cover by sponges and abiotic categories differentiated Rhod40-50 from all other habitats/depths (Table 56).

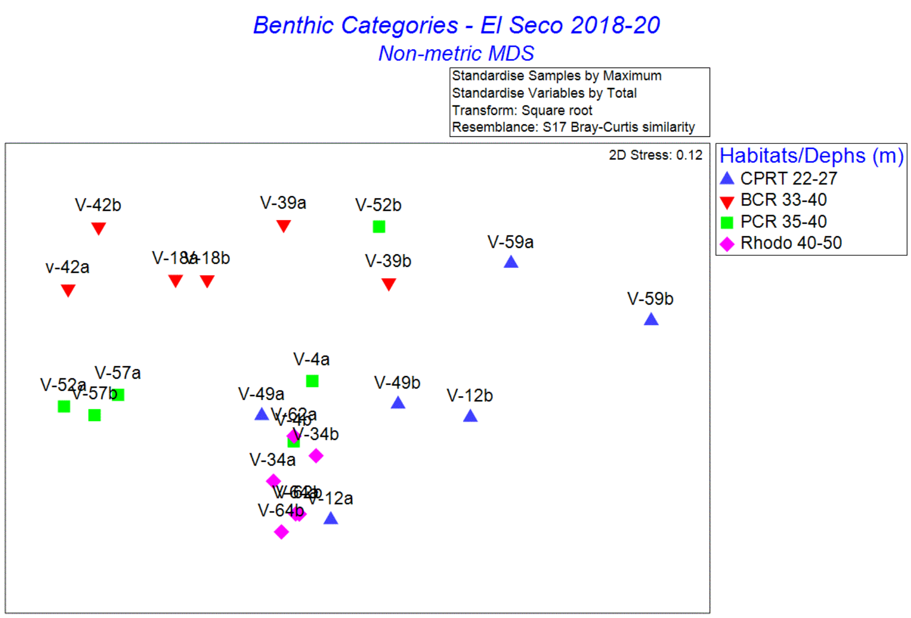

Figure 117. Non-metric multidimensional scaling (nMDS) plot of Bray-Curtis similarities of reef substrate cover by benthic categories surveyed from the main habitats/depth across the 23-50m depth profile at El Seco Reef system, 2018-20 survey.

Table 55. Similarity matrix (SIMPER) of reef substrate cover by benthic categories surveyed from the main habitats/depth across the 23-50m depth profile at El Seco Reef, 2018-20 survey.

Habitat/Depth (m)	CPRT 23-27	BCR 33-40	PCR 35-40	Rhodo 40-50
Average Similarity (%)	73.5	76.0	81.0	78.8
Benthic Categories				
Abiotic	16.4		22.9	30.6
Benthic Algae	22.5	21.6	24.5	28.4
Cyanobacteria		21.5	14.2	
Stony Coral		27.3	19.5	
Soft Corals	26.2			
Sponges	18.0			20.0

Table 56. Dissimilarity matrix (SIMPER) of reef substrate by benthic categories between the main habitats/depths surveyed across a 23-50m depth profile at El Seco Reef, 2018-20 survey.

	CPRT 23-27 vs BCR 33-40	CPRT 23-27 vs PCR 35-40	CPRT 23-27 vs Rhodo 40-50	BCR 33-40 vs PCR 35-40	BCR 33-40 vs Rhodo 40-50	PCR 35-40 vs Rhodo 40-50
Average Dissimilarity (%)	45.07	40.3	31.3	32.4	40.2	30.4
Category Contributions						
Stony Corals	27.9	17.9		26.2	38.4	31.7
Soft Corals	27.4	33.0	44.0			
Cyanobacteria	18.5		14.8	25.6	20.1	
Abiotic			20.6	18.8	19.1	18.5
Sponges		23.5				28.4

Temporal (monitoring) trends of benthic community structure

Variations of the percent reef substrate cover by benthic categories between the 2011 baseline and the 2018-20 monitoring survey were tested by two-way ANOVA procedures with habitats/depths and survey years as sources of variation in a balanced 24 samples per survey matrix, with six (6) replicate samples at four (4) main habitats/depths per survey. Statistically significant differences (Two-way ANOVA; $p < 0.05$) were noted between habitat/depths and survey years for abiotic, benthic algae, cyanobacteria, stony corals, soft corals, and sponges (Table 57). Soft corals, sponges, cyanobacteria, and abiotic categories represented relatively minor components of reef substrate cover at El Seco during both survey years. Therefore, even though variations were relatively high in terms of the percent change between surveys, absolute changes of the mean percent cover were small (Figures 118 – 121).

Table 57. Variations of the percent substrate cover by benthic categories and two-way ANOVA testing for differences between habitats/depths and survey years (2010 vs 2018-20)

	Study Means (% Cover)			Two-way ANOVA p-values	
Benthic Categories	**2010**	**2018-20**	**% Change**	**Habitats/depths**	**Survey Years**
Abiotic	5.28	3.65	-30.9	< 0.0001	0.0338
Benthic Algae	64.68	82.36	27.3	< 0.0001	< 0.0001
Cyanobacteria	4.15	1.85	-55.5	0.0158	0.0062
Stony Corals	18.37	10.30	-43.9	< 0.0001	< 0.0001
Soft Corals	0.75	0.27	-64.6	< 0.0001	0.0092
Sponges	5.07	1.48	-70.8	< 0.0001	< 0.0001

Note: study means include % cover values from all habitats/depths (24 samples)

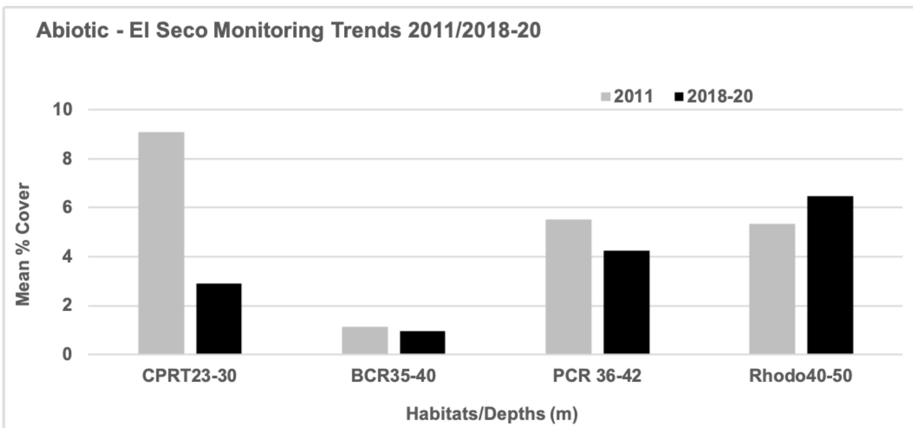

Figure 118. Temporal variations of mean substrate cover by total abiotic categories from the main mesophotic habitats/depths surveyed during the 2010 baseline and the 2018-20 monitoring surveys at El Seco Reef.

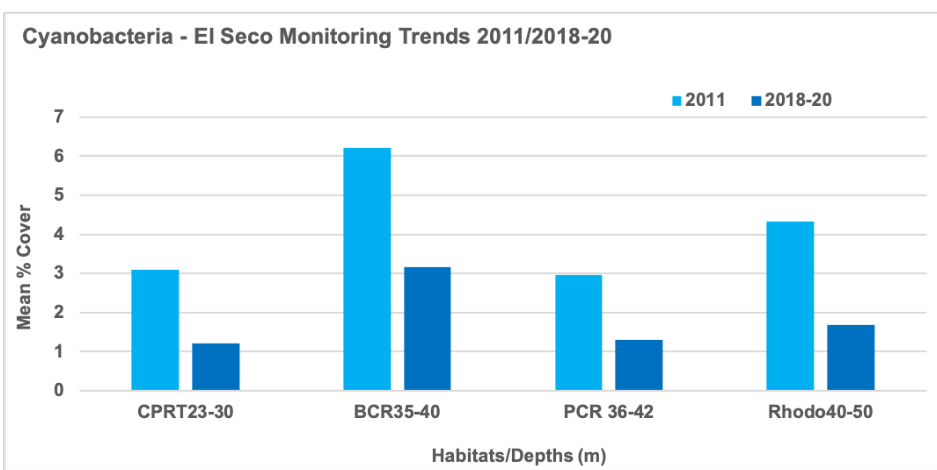

Figure 119. Temporal variations of mean substrate cover by cyanobacteria from the main mesophotic habitats/depths surveyed during the 2010 baseline and the 2018-20 monitoring surveys at El Seco Reef

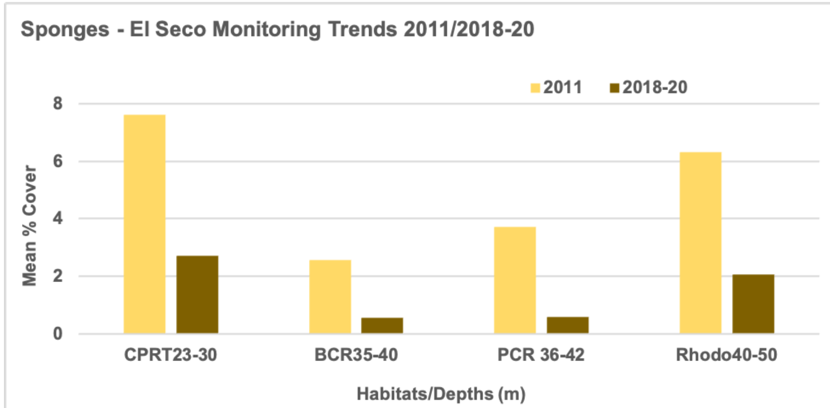

Figure 120. Temporal variations of mean substrate cover by sponges from the main mesophotic habitats/depths surveyed during the 2010 baseline and the 2018-20 monitoring surveys at El Seco Reef system

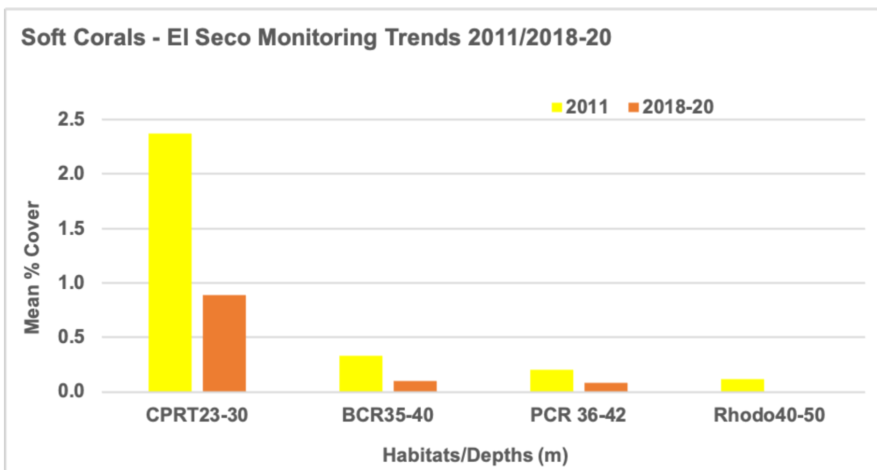

Figure 121. Temporal variations of mean substrate cover by soft corals from the main mesophotic habitats/depths surveyed during the 2010 baseline and the 2018-20 monitoring surveys at El Seco Reef system

More ecologically relevant variations of substrate cover by benthic categories between surveys were related to a 27.3% increase of benthic algae and a 43.9% decline of substrate cover by stony corals (Two-way ANOVA; $p < 0.0001$; Table 57). Turf algae were the dominant benthic algal component in 2011, representative of 58.2% of the total cover by benthic algae. During 2018-20, turf algae declined by 61.7%. The increase of cover by benthic algae during 2018-20 was driven by a 133.8% increase of encrusting fan alga (*Lobophora sp*.), and the proliferation of red crustose calcareous algae (Peissonnellidae), from 0% in 2011 to 12.4% in 2018-20 (Figures 120 – 121). Substrate cover by *Ramicrusta sp*., (site mean: 7.16%) represented more than half of the total cover by Peyssonnelid algae.

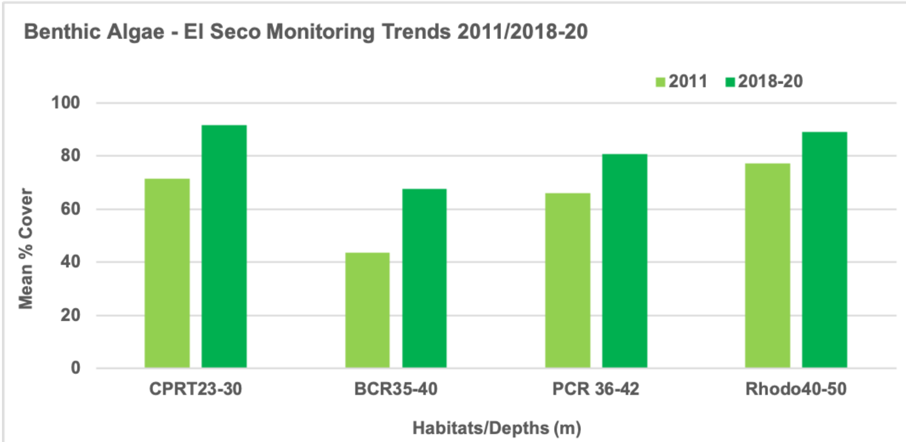

Figure 122. Temporal variations of mean substrate cover by total benthic algae from the main mesophotic habitats/depths surveyed during the 2010 baseline and the 2018-20 monitoring surveys at El Seco Reef.

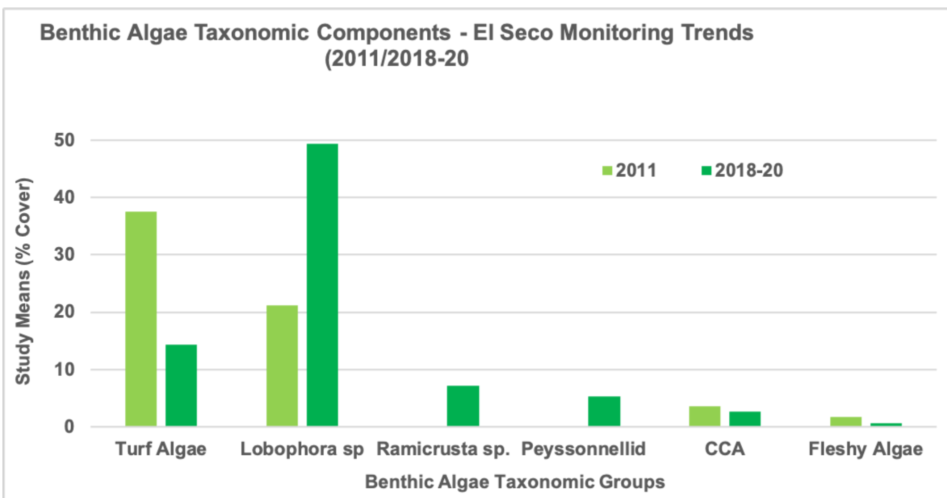

Figure 123. Temporal variations of mean substrate cover by benthic algae taxonomic groups from mesophotic habitats/depths surveyed during the 2010 baseline and the 2018-20 monitoring surveys at El Seco Reef

The structural (taxonomic) shifts of algal assemblages were associated with an increase of substrate cover by *Lobophora sp*. and Peyssonnelid algae over turf algae. This has been observed across many neritic and upper mesophotic reef stations included in the PRCRMP over the last decade, including a more extensive progression of Peyssonnelid algae on the east coast, relative to the west coast reefs during the last 3-5 years (Garcia-Sais et al., 2019; Williams and Garcia-Sais 2020, and references therein). These trends are consistent with other reports from the Caribbean, where Peyssonnelid algal crusts become the dominant substrate category (Edmunds et al, 2019).

The decline of reef substrate cover by stony corals measured during the 2018-20 monitoring survey resulted from reductions across all habitats/depths (Figure 124). The passing of hurricanes Irma and Maria in September 2017, and winter storm Riley in March 2018 may have been an important factor for the decline of live coral cover, particularly at the CPRT23-30 habitat/depth. The scouring, sand abrasion, and mechanical damage to coral colonies associated with extreme wave and surge action produced by such extraordinary storms represent a potential factor of stony coral mortality. Dead coral colonies are appropriate surfaces for colonization by both the encrusting fan alga (*Lobophora sp.*) and Peyssonnelid algae (e. g. *Ramicrusta sp*) and mat have facilitated the measured increments of reef substrate cover by both algal components.

Mortality of stony coral colonies from mesophotic habitats at EL Seco may have also been influenced by coral bleaching, which is a known precursor of disease infections in corals (Weil et al. 2004, Miller et al. 2009, Williams et al. 2019). Coral bleaching was observed from September 2019 thru February 2020 throughout the Puertorrican shelf but was particularly intense at east coast neritic and sub-mesophotic reefs (Garcia-Sais, personal observations). Coral bleaching was observed down to 50m (165') at Isla Desecheo and down to 40m at Bajo de Sico (Garcia-Sais et al., personal observations). Monitoring work at El Seco was performed during June and July 2020, leaving a window of 4 - 10 months for coral mortality and colonization by benthic algae to materialize before our survey observations.

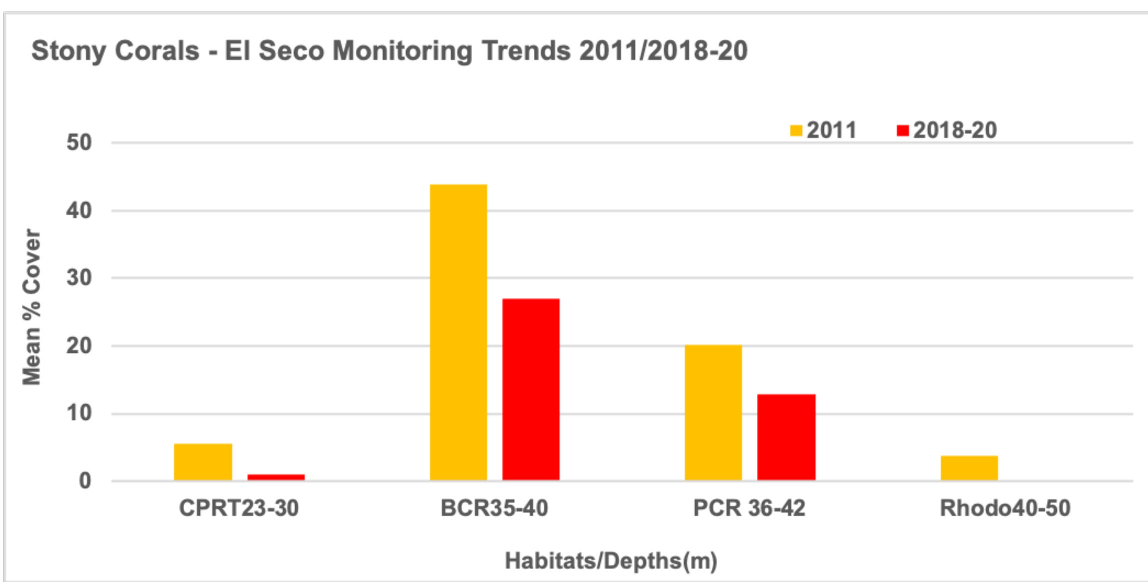

Figure 124. Temporal variations of mean substrate cover by stony corals from the main mesophotic habitats/depths surveyed during the 2011 baseline and the 2018-20 monitoring surveys at El Seco Reef

Another scenario that may explain the coral losses measured at El Seco during the 2018-20 survey is related to a potential Stony Coral Tissue Loss Disease (SCTLD) infection outbreak. SCTLD was first reported in southeastern Florida in 2014, and since then has spread throughout the Caribbean. In Puerto Rico, SCTLD was first reported on shallow-water coral reefs of Isla de Culebra at the end of November 2019 (Weil et al. 2019), and of lately it has been reported for reefs in Isla de Vieques, Fajardo, and San Juan. The gross morphological features of SCTLD include lesions at the middle and within the colony tissue (Florida Department of Environmental Protection 2018). Such lesions were common in many *Orbicella* spp. and *Agaricia* spp. colonies from station V-18 and V-37, consistent with infection by SCTLD. Photos of infected coral colonies from these stations were sent to several coral disease authorities (Judith Lang, Karen Neely, and Marilyn Brandt) and they have expressed positive diagnostics of SCTLD infections from these photos. The implications of such observations, if applicable, may have serious ecological repercussions given the magnitude of coral development at El Seco and the highly transmissible nature of this disease that can kill coral tissue at a rate of 3-4cm/day (Weil et al. 2019).

Fish Community

Small demersal fish species, 2018-20 survey

Depth/habitat related patterns of fish community structure

A total of 68 small demersal fish species were identified from 10m x 3m belt-transects within the 23 – 50m depth range at El Seco Reef during the 2018-20 survey (Table 58). Mean density ranged between 26.7 Ind/30m^2 at Rhod50 and 77.5 Ind/30m^2 at PCR35-40. Mean fish species richness varied between 7.0 Spp/30m^2 at Rhod50 and 18.0 Spp/30m^2 at PCR35-40. Statistically significant differences between depths were found both for fish density (ANOVA; $p = 0.0015$) and species richness (ANOVA; $p < 0.0001$). Fish density was higher at PCR35-40 than at Rhod50, but differences of density and species richness between other habitats/depth surveyed were within 95% confidence intervals. Lower species richness was observed at Rhod50 relative to shallower habitats/depths surveyed. The study mean density of the top nine (9) species represented 77.9% of the total fish density across all habitats/depths. These included the masked goby (*Coryphopterus personatus*), bluehead and yellowhead wrasse (*Thalassoma bifasciatum, Halichoeres garnoti*), bicolor damselfish (*Stegastes partitus*), blue chromis (*Chromis cyanea*), creole wrasse (*Clepticus parrae*), princess parrotfish (*Scarus taeniopterus*), cherubfish (*Centropyge argi*), and ocean surgeonfish (*Acanthurus tractus*).

Table 58. Taxonomic composition and mean density of small demersal fishes at the main benthic habitats and depths surveyed at El Seco, 2018-20 survey

Habitat/depth (m) Species	CPRT 23-27 MEAN	BCR33-40 MEAN	PCR 5-40 MEAN	Rhod40-50 MEAN
Coryphopterus personatus		25.00	12.67	
Thalassoma bifasciatum	20.33	3.33	5.67	0.33
Stegastes partitus	5.67	3.33	8.50	11.00
Clepticus parrae		0.17	15.83	
Chromis cyanea	3.17	3.00	4.83	1.17
Halichoeres garnoti	6.33	0.50	2.00	0.50
Scarus taeniopterus		2.67	3.50	
Centropyge argi	0.50			5.33
Carangoides ruber			4.50	
Acanthurus tractus	1.50	0.67	2.00	0.17
Coryphopterus glaucofraenum	3.67			
Sparisoma aurofrenatum	0.33	1.50	1.17	
Chromis multilineata	1.00	0.83	0.83	
Myripristis jacobus		0.83	1.83	
Sparisoma viride	0.17	1.00	1.50	
Scarus iseri		2.33	0.17	
Ocyurus chrysurus	1.00	0.50	0.83	
Holocentrus rufus	1.17	0.33	0.67	
Sparisoma atomarium				2.17
Cephalopholis fulva	1.33	0.17	0.33	0.17
Acanthurus chirurgus	1.33		0.50	
Chaetodon capistratus	0.33	0.67	0.83	
Chromis insolata				1.83
Gramma loreto		1.50	0.33	
Acanthurus coeruleus	0.33	0.67	0.67	
Epinephelus guttatus	0.67	0.50	0.33	
Prognathodes aculeatus		0.33	0.83	0.17
Serranus tabacarius				1.33
Elacatinus evelynae		1.00	0.17	
Haemulon flavolineatum		0.33	0.83	
Serranus baldwini				1.17
Serranus tortugarum	0.67			0.50
Scarus vetula	0.17	0.83		
Balistes vetula	0.67			0.17
Canthigaster rostrata		0.50	0.33	
Holacanthus tricolor	0.17	0.17	0.50	
Melichthys niger	0.17	0.17	0.50	
Bodianus rufus		0.17	0.50	
Chaetodon sedentarius			0.67	
Coryphopterus lipernes		0.67		
Pterois sp.	0.33	0.17	0.17	
Calamus pennatula	0.50			
Chaetodon striatus	0.17		0.33	
Haemulon sciurus		0.17	0.33	
Hypoplectrus chlorurus		0.50		

Table 58. Taxonomic composition and mean density of small demersal fishes at the main benthic habitats and depths surveyed at El Seco, 2018-20 survey

Habitat/depth (m) Species	**CPRT 23-27 MEAN**	**BCR33-40 MEAN**	**PCR 5-40 MEAN**	**Rhod40-50 MEAN**
Lutjanus apodus		0.17	0.33	
Opistognathus aurifrons	0.50			
Pseudupeneus maculatus		0.33	0.17	
Amblycirrhitus pinos	0.17			0.17
Cephalopholis cruentatus	0.17		0.17	
Haemulon plumieri			0.33	
Hypoplectrus sp.			0.33	
Neoniphon marianus		0.33		
Pomacanthus arcuatus			0.33	
Serranus tigrinus				0.33
Anisotremus virginicus			0.17	
Cantherhines pullus	0.17			
Elagatis bipinnulata			0.17	
Holacanthus ciliaris	0.17			
Lachnolaimus maximus			0.17	
Liopropoma rubre		0.17		
Lutjanus jocu		0.17		
Paranthias furcifer			0.17	
Pomacanthus paru			0.17	
Scomberomorus regalis			0.17	
Serranus sp.				0.17
Sphyraena barracuda			0.17	
Mean Density (Ind/30m^2)	**52.83**	**55.67**	**77.50**	**26.67**
Mean Spp Richness (Spp/30m^2)	**12.8**	**15.2**	**18.0**	**7.0**

Differences of fish density appeared to be strongly related with benthic habitat/depth preferences by numerically dominant species. Masked goby (*Coryphopterus personatus*), creole fish (*Clepticus parrae*), and princess parrotfish (*Scarus taeniopterus*) exhibited significantly higher densities (ANOVA; $p < 0.05$) at coral reef habitats (BCR33-40 and PCR 35-40) relative to shallower and deeper habitats surveyed (Figure 125). Cherubfish (*Centropyge argi*) and greenblotch parrotfish (*Sparisoma atomarium*) were only present at Rhod40-50 (ANOVA; p < 05), even though the depth distribution of Rhod40-50 overlapped with PCR35-40. Bicolor damselfish (*Stegastes partitus*), bluehead and yellowhead wrasse (*Thalassoma bifasciatum, Halichoeres garnoti*) exhibited higher habitat plasticity with individuals observed within belt-transects across all habitats/depths, but densities of both wrasses were significantly higher at CPRT23-27 (ANOVA; $p < 0.05$) than at other benthic habitats. Conversely, *S. partitus* showed higher density at Rhod40-50 (ANOVA; $p = 0.0104$) relative to other habitats/depths (Figure 125). Blue chromis

(*Chromis cyanea*) was observed across all habitats/depths with peak density at PCR40-50 (4.83 Ind/30m^2) and minimum density at Rhod40-50 (1.17 Ind/30m^2), but differences were statistically insignificant due to high within habitat/depth sampling variability.

Small demersal fish community structure similarities between habitats and depths based on the relative densities from 3m x 10m belt-transects surveyed within the 22 – 50m depth profile at El Seco Reef during the 2018-20 survey are displayed in a non-metric multi-dimensional scaling plot (nMDS) of Bray-Curtis similarities in Figure 126. Benthic habitats were used as discriminatory factor for testing fish community structure similarities since different habitats were sampled across the 22 - 50m depth range, and also overlapping similar depths. In general, similarities were low (<55%), due to relatively low fish densities and high sampling variability within habitats/depths. Similarity was highest at Rhod40-50 (54.6%) and CPRT23-27 (53.4%). An assemblage of species that are typical of horizontally oriented habitats with abundant sand and rubble, including the cherubfish (*Centropyge argi*), and the tobaccofish and lantern bass (*Serranus tabacarius, S. baldwini*) were the main contributions to similarity at Rhod40-50 (Table 59). Neritic reef fishes, including the blue and yellowhead wrasses (*Thalassoma bifasciatum, Halichoeres garnoti)*, masked goby (*Coryphopterus personatus*), longspine squirrelfish (*Holocentrus rufus*), and coney (*Cephalopholis fulva*) were the main contributors to similarity at CPRT22-27. Species typical of neritic coral reef habitats, such as the stoplight, redband and princess parrotfish (*Sparisoma viride, S. aurofrenatum, Scarus taeniopterus*) were the main assemblage contributing similarity at BCR33-40, whereas creole wrasse (*Clepticus parrae*), and bicolor damselfish (*Stegastes partitus*) were the main contributors to similarity at the PCR35-40.

Dissimilarity of small demersal fish community structure between habitats/depths was highest (> 85%) between Rhod40-50 and all other habitats/depths surveyed at El Seco within the 23 – 50m depth range (Table 60). An assemblage of species that were numerically dominant at Rhod40-50, but absent or present in very few transect samples at other habitats were the main drivers of dissimilarity. These included the cherubfish (*Centropyge argi*), tobaccofish and lantern bass (*Serranus tabacarius, S. baldwini*), greenblotch parrotfish (*Sparisoma atomarium*), and sunshine chromis (*Chromis insolata*). Dissimilarity was lowest between the BCR33-40 and PCR35-40 (64.2%), both of which share the high cover and topographic relief associated with stony corals. The main species contributing dissimilarity between BCR33-40 and PCR35-40 and other habitats included fairy basslet (*Gramma loreto*), masked goby (*Coryphopterus personatus*), creole fish (*Clepticus parrae*), and princess parrotfish (*Scarus taeniopterus*).

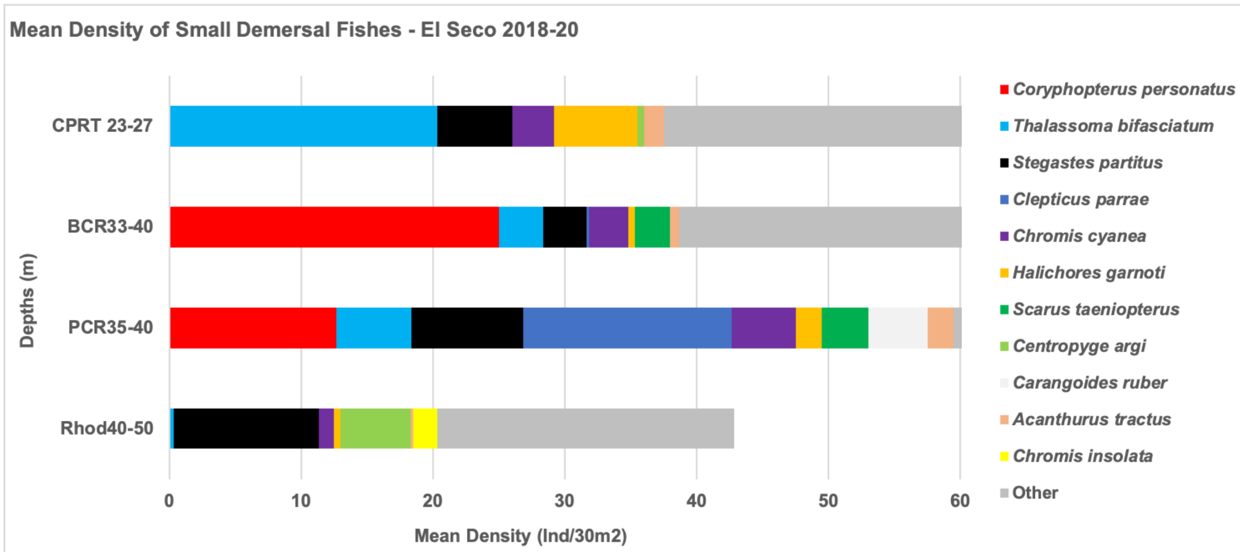

Figure 125. Depth/habitat related variations of mean density by the numerically dominant small demersal fishes surveyed within the 22 – 50m depth range at El Seco Reef, 2018-20 survey.

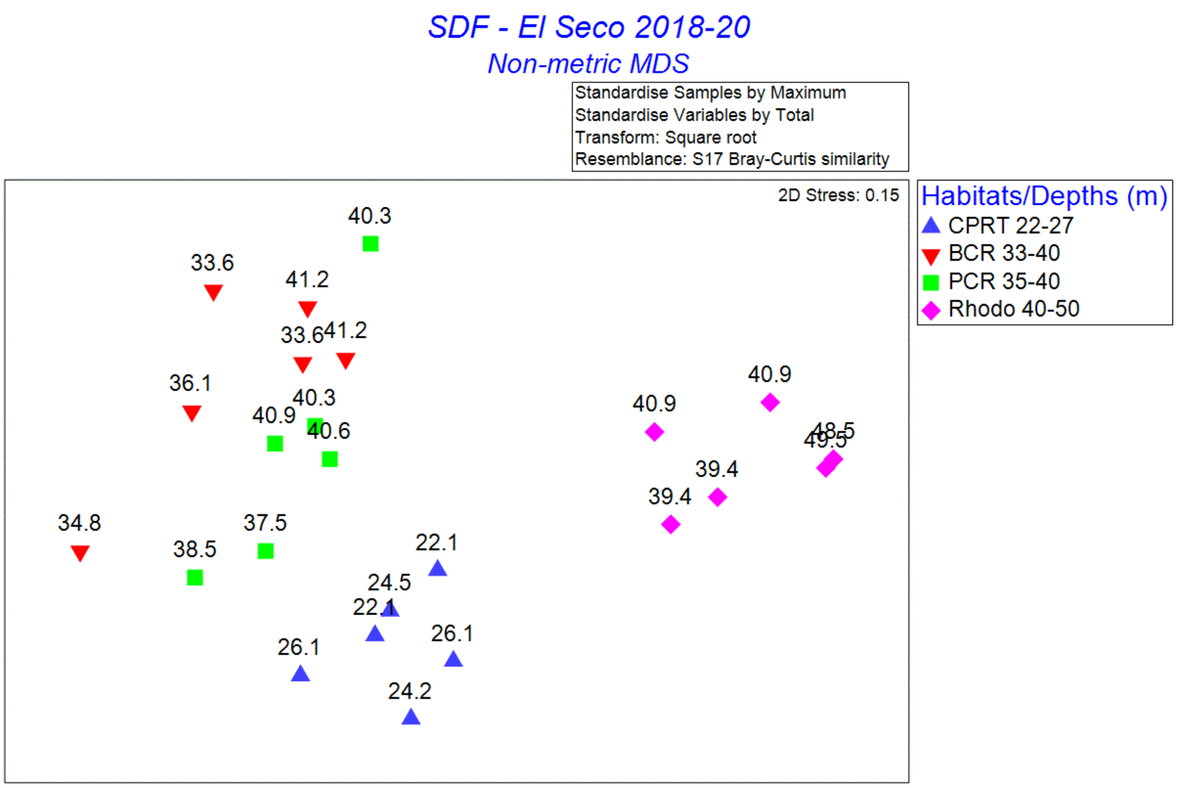

Figure 126. Non-metric multidimensional scaling (nMDS) plot of Bray-Curtis similarities between habitats and depths based on the relative densities from 10m x 3m belt-transects surveyed within the 22 – 50m depth profile at El Seco, 2018-20 survey

Table 59. Similarity matrix (SIMPER) of small demersal fish community structure at the main benthic habitats/depths surveyed from El Seco Reef during 2018-20

	CPRT 22-27	BCR 33-40	PCR 35-40	Rhodo 40-50
Average Similarity (%)	53.4	37.7	36.5	54.6
Species Contributions				
Thalassoma bifasciatum	19.4			
Coryphopterus personatus	19.0	26.1	12.7	
Holocentrus rufus	12.5		6.7	
Cephalopholis fulva	10.6			
Halichoeres garnoti	9.9			
Sparisoma viride		10.8	5.2	
Scarus taeniopterus		9.0		
Gramma loreto		7.6		
Sparisoma aurofrenatum		6.6	4.8	
Chromis cyanea		6.4		
Myripristis jacobus		6.1		
Clepticus parrae			13.2	
Stegastes partitus			11.2	21.5
Prognathodes aculeatus			8.5	
Ocyurus chrysurus			5.2	
Haemulon flavolineatum			4.7	
Centropyge argi				27.1
Serranus tabacarius				19.1
Serranus baldwini				17.9

Table 60. Dissimilarity matrix of small demersal fish community structure between habitats/depths surveyed within the 22 – 50m depth range at El Seco Reef, 2018-20 survey.

	CPRT 22-27 vs BCR 33-40	CPRT 22-27 vs PCR 35-40	CPRT 22-27 vs Rhodo 40-50	BCR 33-40 vs PCR 35-40	BCR 33-40 vs Rhodo 40-50	PCR 35-40 vs Rhodo 40-50
Average Dissimilarity (%)	78.4	73.4	86.4	64.2	93.0	90.2
Species Contributions						
Coryphopterus glaucofraenum	7.9	8.1	8.4			
Coryphopterus personatus	6.6	4.6			6.4	4.2
Cephalopholis fulva	5.3	5.0	5.7			
Acanthurus chirurgus	4.9	4.7	5.2			
Gramma loreto	4.8			5.1		
Halichoeres garnoti	4.8	4.6	5.1			
Holocentrus rufus	4.6		5.7			
Thalassoma bifasciatum	4.3	4.3	6.3			
Epinephelus guttatus	4.2					
Scarus taeniopterus	4.2			4.7	4.2	
Clepticus parrae		6.8		7.4		6.3
Carangoides ruber		4.9		5.4		4.6
Prognathodes aculeatus		4.8		5.2		4.4
Haemulon flavolineatum				5.3		3.8
Myripristis jacobus				4.9		
Elacatinus evelynae				4.7	4.0	
Scarus iseri				4.5		
Acanthurus coeruleus				4.4		
Centropyge argi			7.9		7.7	7.6
Serranus tabacarius			7.5		6.8	6.7
Serranus baldwini			7.5		6.8	6.7
Sparisoma atomarium			6.4		5.8	5.7
Chromis insolata			4.7		4.2	4.2
Sparisoma viride					4.6	3.3

Temporal (monitoring) variations of benthic community structure by small demersal fishes

Variations of the mean density and species richness by small demersal fishes surveyed from a similar set of 24 sampling stations representative of the main benthic habitats at El Seco Reef during the 2011 baseline and 2018-20 monitoring survey are presented in Figures 127 and 128. Statistically significant differences between surveys were associated with increased densities at PCR35-40 and Rhod40-50 during 2018-20 (ANOVA; $p< 0.05$) and increased species richness at Rhod40-50 (ANOVA; $p < 0.0001$) relative to the 2011 baseline survey (Table 61).

Increased densities by several numerically dominant species, such as bicolor damselfish (*Stegastes partitus*), bluehead and yellowhead wrasses (*Thalassoma bifasciatum, Halichoeres garnoti*) and creole wrasse (*Clepticus parrae*) were the main drivers of the increased densities of small demersal fishes observed during 2018-20. Likewise, increased densities by bicolor damselfish (*S. partitus*), cherubfish (*Centropyge argi*), greenblotch parrotfish (*Sparisoma atomarium*), and lantern bass (*Serranus baldwini*) strongly influenced the increased densities at Rhod40-50. Such density increments were not consistent across all habitats/depths surveyed during 2018-20, suggesting that density differences may be an artifact of sampling variability and not indicative of a real change in the status of these populations. For example, densities of bicolor damselfish (*S. partitus*) and creole wrasse (*C. parrae*) declined sharply during 2018-20 at the CPRT23-27 and BCR33-40, respectively. Creole wrasse and bluehead wrasse were numerically dominant species that displayed highly aggregated distributions. Such patchiness conveyed high sampling variability influencing spatial and temporal density fluctuations at the community level.

PCR35-40 and Rhod40-50 were the deeper habitats surveyed and it is possible that small demersal fishes may have migrated to deeper reef sections to avoid the highly turbulent conditions that must have prevailed during and after the pass of hurricanes Irma and Maria in September 2017 and winter storm Riley in March 2018, before our monitoring survey at El Seco. Still, another possibility related with lower temperatures near the thermocline at 45-50m may have influenced migrations of small demersal fishes to deeper habitats. Such migration of small demersal fishes towards deeper habitats may have influenced the 61.5% increase of species richness at Rhod40-50 during the 2018-20 relative to the 2011 baseline survey (Table 61).

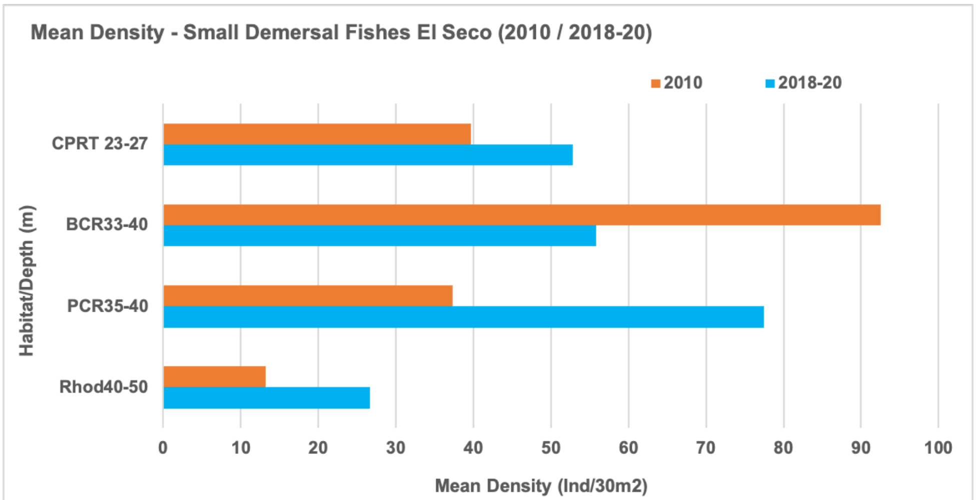

Figure 127. Temporal variations of mean density by small demersal fishes surveyed from the main benthic habitats within the 22 – 50m depth range at El Seco Reef during the 2010 baseline and the 2018-20 monitoring survey

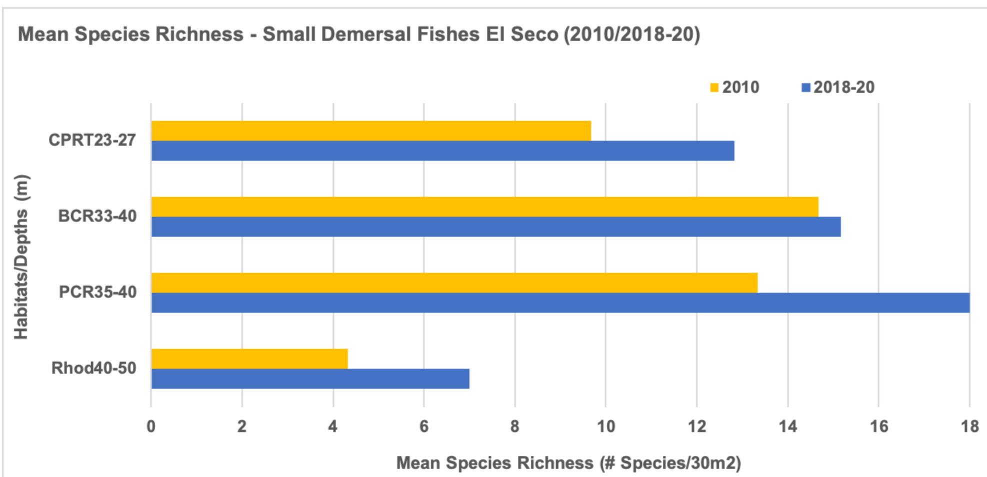

Figure 128. Temporal variations of mean species richness by small demersal fishes surveyed from the main benthic habitats within the 22 – 50m depth range at El Seco Reef during the 2010 baseline and the 2018-20 monitoring survey

Table 61. Temporal variations of mean density and species richness of small demersal fishes surveyed from the main benthic habitats within the 22 – 50m depth range at El Seco Reef during the 2010 baseline and the 2018-20 monitoring survey

	Mean Density (Ind/30m2)			ANOVA	Mean Species Richness (# Species/30m2)			ANOVA
Habitats/Depths (m	2010	2018-20	% Change	p-value	2010	2018-20	% Change	p-value
CPRT23-27	39.67	52.83	33.19	0.416	9.67	12.83	32.76	0.136
BCR33-40	92.50	55.83	-39.64	0.412	14.67	15.17	3.41	0.675
PCR35-40	37.33	77.50	107.59	0.011	13.33	18.00	35.00	0.061
Rhod40-50	13.17	26.67	102.53	0.021	4.33	7.00	61.54	< 0.0001

Similarities of small demersal fish community structure between the 2011 baseline and the 2018-20 monitoring surveys based on the relative densities of the top 25 numerically dominant species representative of more than 90% of the total fish densities in both surveys are shown in a multidimensional scaling (nMDS) plot of Bray-Curtis similarities in Figure 129. Moderate to high similarities (53.2 – 70.0%) prevailed between surveys for the main habitats/depths influenced by distinct habitat/depth specific fish assemblages and the high dissimilarity between the CPRT23-27 and the Rhod40-50 compared to other habitats surveyed (Table 62). Highest similarities of fish community structure between surveys were observed at the BCR33-40 (70.0%) and PCR35-40 (68.5%) contributed by a series of typical coral reef species associated with tridimensional habitats with high rugosity and/or high live coral cover, including the fairy basslet (*Gramma loreto*), masked and peppermint gobies (*Coryphopterus personatus, C. lipernes*), french grunt (*Haemulon flavolineatum*), black-bar soldierfish (*Myripristis jacobus*), longjaw squirrelfish (*Neoniphon marianus*), longsnout butterflyfish (*Prognathodes aculeatus*), and the princess and redband parrotfishes (*Scarus taeniopterus, Sparisoma aurofrenatum*), among others (Table 62).

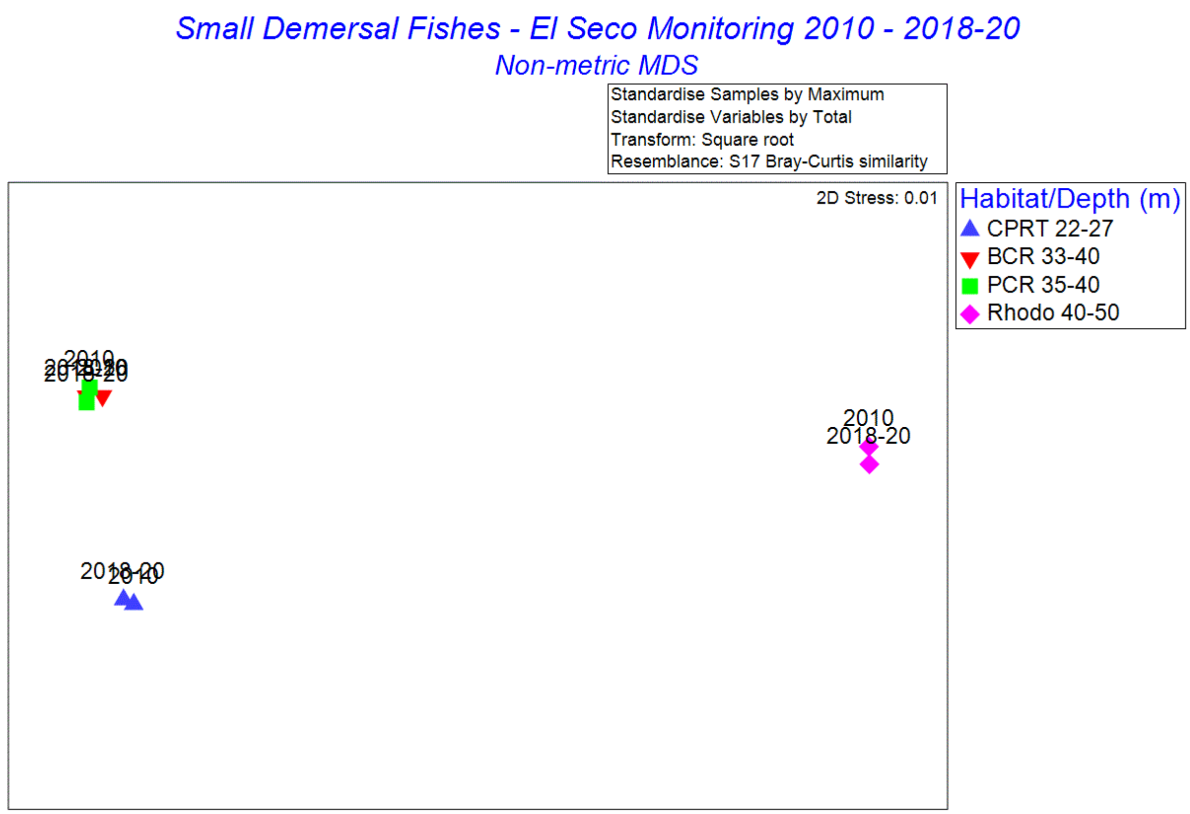

Figure 129. Non-metric multidimensional scaling (nMDS) plot of Bray-Curtis similarities between the 2010 baseline and the 2018-20 monitoring survey of mean densities by small demersal fishes from the main habitats/depths surveyed within the 22 – 50m range at El Seco Reef.

An assemblage of fish species with preferences for small abundant microhabitats in horizontally oriented seascapes were the main contributors to similarity at Rhod40-50. These included the cherubfish (*Centropyge argi*), sunshine chromis (*Chromis cyanea*), and the chalk and lantern bass (*Serranus tortugarum, S. baldwini*). Similarity was lowest at CPRT23-27 (53.2%) contributed by an assemblage of species that were distributed across several or all habitats/depths surveyed. These included the bluehead and yellowhead wrasses (*Thalassoma bifasciatum, Halichoeres garnoti*), coney (*Cephalopholis fulva*), red hind (*Epinephelus guttatus*), doctorfish (*Acanthurus chirurgus*), and four-eye butterflyfish (*Chaetodon capistratus*).

Table 62. Similarity matrix (SIMPER) of small demersal fish community structure between the 2011 baseline and the 2018-20 monitoring surveys at the main habitats/depths from El Seco Reef. Similarities are based on the relative densities of the top 25 numerically dominant species representative of >90% of the total fish density on both surveys.

	CPRT23-27	**BCR33-40**	**PCR35-40**	**Rhod40-50**
Average Similarity (%)	53.2	70.0	68.5	62.4
Species Contributions				
Acanthurus chirurgus	14.4			
Thalassoma bifasciatum	13.9			
Holocentrus rufus	9.2			
Chaetodon capistratus	7.7	4.4		
Cephalopholis fulva	7.5			
Halichores garnoti	7.4			
Epinephelus gutattus	7.4	5.3		
Holacanthus tricolor	6.8		5.1	
Coryphopterus lipernes		8.6		
Scarus iseri		6.0		
Coryphopterus personatus		6.0	4.2	
Gramma loreto		6.0		
Neoniphon marianus		5.5		
Scarus taeniopterus		5.3	4.4	
Myripristis jacobus		4.3	4.8	
Canthigaster rostrata		4.2		
Haemulon flavolineatum			5.4	
Clepticus parrae			5.1	
Sparisoma aurofrenatum			4.9	
Prognathodes aculeatus			4.7	
Centropyge argi				18.2
Chromis insolata				15.1
Serranus tortugarum				14.1
Stegastes partitus				14.0
Serranus baldwini				12.6

Large Demersal Fishes and Shellfishes

Depth/habitat related variations of fish density and community structure, 2018-20

Mean densities of large demersal fishes and shellfishes (queen conch and spiny lobster) surveyed by drift belt-transects within the 23 – 50m depth range at El Seco Reef system during 2018-20 are listed in Table 63. Mean densities varied between 15.7 Ind/10^3m^2 at Rhod40-50 and 56.6 Ind/10^3m^2 at BCR35-40. The combined densities of nine fishes and one shellfish represented 90.4% of the total density within transects surveyed across all habitats/depths. These included the schoolmaster, cubera and yellowtail snappers (*Lutjanus apodus, L. cyanopterus, Ocyurus chrysurus*), coney (*Cephalopholis fulva*), red hind (*Epinephelus guttatus*), lionfish (*Pterois sp*), smooth trunkfish (*Lactophrys triqueter*), queen triggerfish (*Balistes vetula*), and queen conch (*Lobatus gigas*).

Table 63. Taxonomic composition and mean density of large demersal fish/shellfish species identified within drift belt-transects at the main benthic habitats/depth surveyed from El Seco, 2018-20 survey.

Total Area (m2)	8,587.2	Mean	6,954.7	Mean	6,733.7	Mean	5,425.5	Mean
Habitat/Depth (m)	**CPRT 23-30**	**Density**	**BCR 35-40**	**Density**	**PCR 36-42**	**Density**	**Rhodo 40-50**	**Density**
Species	**# Ind.**	**(Ind/10^3m2)**	**# Ind.**	**(Ind/10^3m2)**	**# Ind.**	**(Ind/10^3m2)**	**# Ind.**	**(Ind/10^3m2)**
Lutjanus apodus	18	2.26	309	38.18	62	9.73	0	0.00
Lutjanus cyanopterus	1	0.10	14	2.09	83	11.10	0	0.00
Cephalopholis fulva	39	3.83	4	0.52	24	3.79	23	3.95
Lobatus gigas	6	0.82	0	0.00	20	2.70	53	6.86
Lactophrys triqueter	2	0.21	31	3.97	45	7.36	0	0.00
Pterois sp.	12	1.38	27	3.83	27	4.31	0	0.00
Epinephelus guttatus	39	4.64	6	1.12	13	1.94	7	1.04
Ocyurus chrysurus	11	1.15	23	3.86	14	1.87	0	0.00
Balistes vetula	22	2.40	0	0.00	3	0.40	2	0.39
Lutjanus mahogoni	16	1.55	1	0.12	4	0.63	0	0.00
Lutjanus jocu	0	0.00	17	2.10	3	0.49	0	0.00
Ginglymostoma cirratum	2	0.27	1	0.13	5	0.78	1	0.31
Lutjanus analis	0	0.00	0	0.00	7	0.94	2	0.57
Lachnolaimus maximus	4	0.51	0	0.00	4	0.52	0	0.00
Seriola rivoliana	0	0.00	0	0.00	1	0.13	7	1.76
Sphyraena barracuda	2	0.21	1	0.26	3	0.39	0	0.00
Panulirus argus	2	0.21	0	0.00	0	0.00	2	0.45
Acanthostracion polygonia	0	0.00	1	0.12	0	0.00	2	0.26
Cephalopholis cruentatus	1	0.14	1	0.12	1	0.14	0	0.00
Scomberomorus regalis	2	0.21	1	0.11	0	0.00	0	0.00
Epinephelus striatus	2	0.32	0	0.00	0	0.00	0	0.00
Carcharhinus perezi	0	0.00	1	0.11	0	0.00	0	0.00
Lactophrys bicaudalis	0	0.00	0	0.00	0	0.00	1	0.12
Lutjanus griseus	0	0.00	0	0.00	1	0.16	0	0.00
Total Individuals	**181**		**438**		**320**		**100**	
Mean Density (Ind/10^3m^3)		**20.21**		**56.65**		**47.37**		**15.71**

Statistically significant density differences between habitats/depths for the total fish/shellfish assemblage (ANOVA; p = 0.0.037) were associated with higher densities at PCR36-42, compared to CPRT23-30 and Rhod40-50 (Figure 130). Peak density was observed from BCR35-40, but density differences relative to other habitats/depths were not statistically significant due to the high sampling variability introduced by species distributed in schooling aggregations at BCR35-40, particularly the schoolmaster and dog snappers (*Lutjanus apodus, L. jocu*), and the smooth trunkfish (*Lactophrys triqueter*). Although no evident reproductive behavior was observed from schooling aggregations at BCR35-40, these were comprised only by large adult individuals. An active spawning aggregation of *L. jocu* was previously reported during the 2011 baseline survey at PCR35-40 (Garcia-Sais et al., 2011). Aggregations involving courtship and distinct reproductive coloration were also reported for *L. triqueter* during the 2011 baseline survey. Thus, it is possible that schooling aggregations of the aforementioned species observed in 2018-20 at the BCR35-40 represent residential components of the spawning aggregations that have been previously observed and reported at PCR36-42 from El Seco Reef (Garcia-Sais et al., 2011).

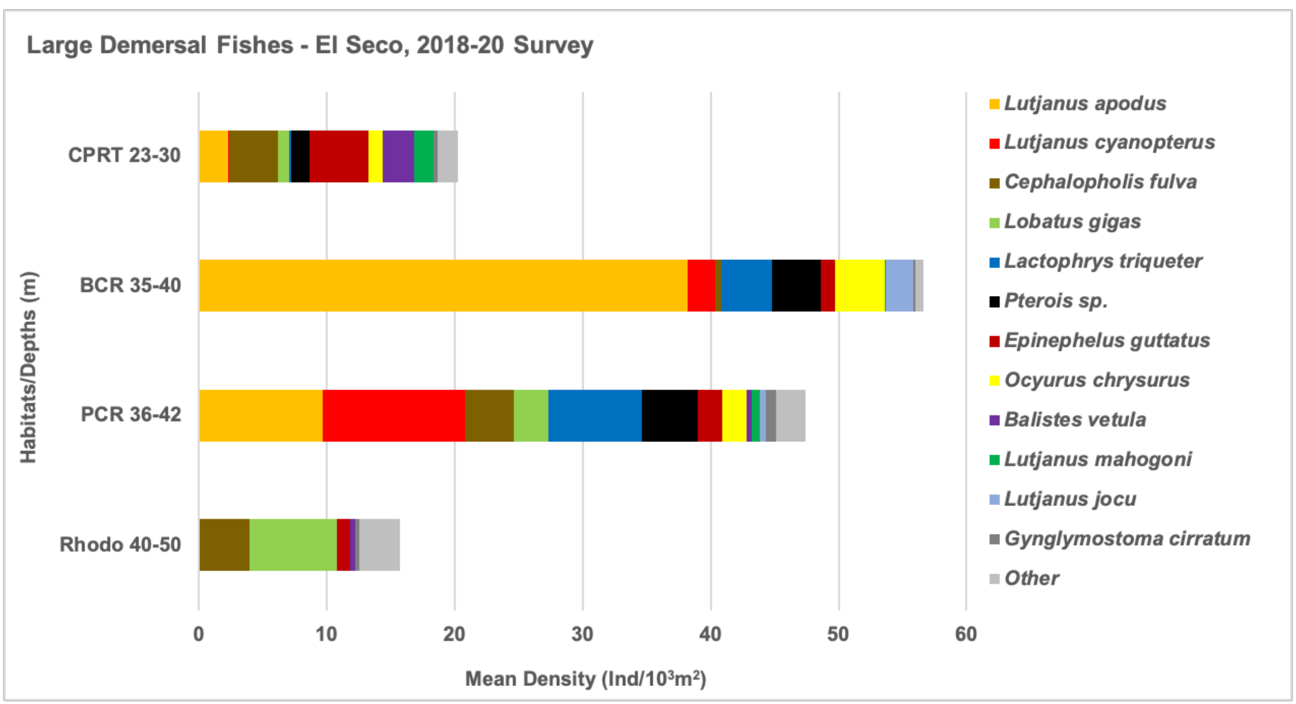

Figure 130. Mean densities of large demersal fishes surveyed by drift belt-transects across the 23 – 50m depth range at El Seco Reef, 2018-20 survey

A reproductively active aggregation of cubera snappers (*Lutjanus cyanopterus*) was observed at PCR36-42 during the 2018-20 monitoring survey, influencing the higher densities of large demersal fishes at this habitat/depth. The aggregation was comprised of approximately 70 large adult individuals that displayed courtship behavior with distinct reproductive coloration. Upward swimming by females followed by males was not observed, but sperm release by one male in the vicinity of females was evidenced. The aggregation was detected on July 1, 2020 and was re-visited on July 2, 2020 for photographic documentation. Location of *L. cyanopterus* aggregation was located near to previously reported spawning aggregations of dog snapper (*L. jocu*) at El Seco (Garcia-Sais et al., 2011).

Distinct habitat/depth related density distribution patterns were observed for some of the numerically dominant large demersal fish/shellfish populations. Approximately 80% of the total schoolmasters (*Lutjanus apodus*) were observed from BCR35-40, but differences were not statistically significant (ANOVA; p= 0.184) due to the high within habitat/depth sampling variability. Red hind (*Epinephelus guttatus*) and coney (*Cephalopholis fulva*) were observed across all habitats/depths surveyed, but densities of *E. guttatus* were significantly higher at CPRT23-30 (ANOVA; p = 0.009), and densities of *C. fulva* were significantly lower at BCR35-40, relative to other habitats/depths (ANOVA; p = 0.016). Both of these grouper species appeared to prefer low relief, horizontally oriented habitats with sparse coral heads, basket sponges, and abundant sand/coral rubble interphases, rather than more topographically structured reef habitats.

Queen conch (*Lobatus gigas*) was observed across the entire depth profile surveyed at El Seco but not observed from BCR35-40. This may be related to the virtual lack of flat substrates in the highly complex (tridimensional) structure of the bank coral reef habitat. Peak densities of *L. gigas* were observed from the Rhod40-50 (6.86 Ind/10^3m^2) where benthic algae were substantially higher than at BCR35-40, but differences between habitat/depth were statistically insignificant (ANOVA; p = 0.328) due to the high sampling variability associated with the aggregated distribution. Cubera snappers (*Lutjanus cyanopterus*) and smooth trunkfishes (*Lactophrys triqueter*) were observed in peak densities at PCR36-42, but differences were statistically insignificant (ANOVA; p > 0.05) due to the high sampling variability associated with the spatially patchy distributions influenced by schooling aggregations.

Community structure similarities of large demersal fish species and shellfishes based on the relative densities at the main habitats/depths surveyed within the 23 – 50m depth profile at El

Seco during the 2018-20 survey are displayed in a non-metric multi-dimensional scaling plot (nMDS) based on Bray-Curtis similarities in Figure 131. Benthic habitats were used as discriminatory factor for testing fish community structure similarities since different habitats were sampled across similar depths and the similar habitats were distributed across different depths. Similarities between habitats/depths were generally low, indicative of distinctive fish assemblages prevailing at the different habitats/depths surveyed. The highest similarity of fish community structure was from PCR36-42 (39.1%) largely contributed by schoolmaster and dog snapper (*Lutjanus apodus, L. jocu*), lionfish (*Pterois sp*), smooth trunkfish (*Lactophrys triqueter*), nurse shark (*Ginglymostoma cirratum*), and coney (*Cephalopholis fulva*). Lowest similarity was observed from Rhod40-50 (21.5%) contributed largely by queen conch (*Lobatus gigas*) and mutton snapper (*Lutjanus apodus*) (Table 64).

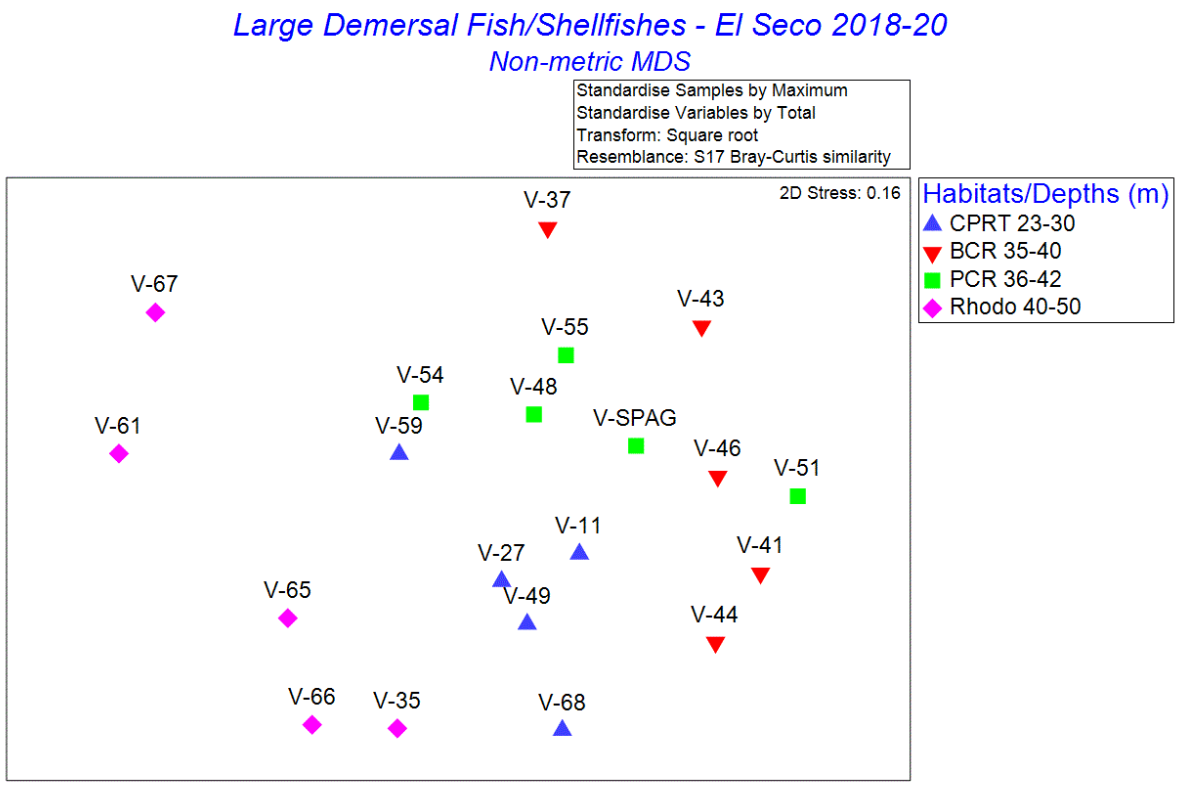

Figure 131. Non-metric multidimensional scaling (nMDS) plot of Bray-Curtis similarities of the relative densities of large demersal fishes surveyed by drift belt-transects from the main habitats/depths within the 23 – 50m range at El Seco Reef, 2018-20 survey.

Table 64. Similarity matrix (SIMPER) of large demersal fishes/shellfishes' relative densities at the main benthic habitats/depths surveyed from El Seco Reef during 2018-20, including species contributions to the within habitat/depth similarity.

	CPRT23-30	BCR35-40	PCR36-42	Rhod40-50
Average Similarity (%)	36.8	31.6	39.1	21.5
Species Contributions				
Epinephelus guttatus	28.2			
Cephalopholis fulva	22.0			39.9
Balistes vetula	18.7			
Pterois sp.	6.6	28.4	15.2	
Ocyurus chrysurus		31.2		
Lutjanus cyanopterus		26.4		
Lutjanus apodus			16.0	
Lutjanus jocu			11.9	
Lactophrys triqueter			10.9	
Ginglymostoma cirratum			9.6	
Cephalopholis fulva			9.5	
Lobatus gigas				26.7
Lutjanus analis				12.9

Dissimilarity of large demersal fish/shellfish community structure was highest between Rhodo40-50 and all other habitats/depths, particularly between Rhodo40-50 and coral reef habitats (BCR35-40 and PCR36-42). Differences were mostly contributed by the higher densities of queen conch (*Lobatus gigas*), mutton snapper (*Lutjanus analis*), coney (*Cephalopholis fulva*), and nurse shark (*Ginglymostoma cirratum*) at Rhodo40-50, compared to other habitats/depths surveyed (Table 65). Dissimilarities between CPRT22-27 and other habitats/depths were also relatively high, driven by the relatively higher densities of queen triggerfish (*Balistes vetula*), red hind (*Epinephelus guttatus*), mahogani snapper (*L. mahogoni*), and hogfish (*Lachnolaimus maximus*).

Coral reef habitats (BCR35-40 and PCR36-42) exhibited the lowest dissimilarity between habitats/depths (67.1%) and were dissimilar from other habitats/depths by the higher relative density of yellowtail, schoolmaster and cubera snappers (*Ocyurus chrysurus, L. apodus, L. cyanopterus*), lionfish (*Pterois sp*), and smooth trunkfish (*Lactophrys triqueter*). Dissimilarities between BCR35-40 and PCR36-42 were mostly contributed by the higher relative densities of dog, schoolmaster, and yellowtail snappers (*L. jocu, L. apodus, O. chrysurus*) at BCR35-40, and the higher densities of cubera snapper (*L. cyanopterus*), and smooth trunkfish (*L. triqueter*) at PCR36-42.

Table 65. Dissimilarity matrix (SIMPER) of large demersal fish/shellfish relative densities between habitats/depths surveyed within the 23 – 50m depth range at El Seco Reef, 2018-20 survey.

	CPRT 23-30	CPRT 23-30	CPRT 23-30	BCR 35-40	BCR 35-40	PCR 36-42
	vs BCR 35-40	vs PCR 36-42	vs Rhodo 40-50	vs PCR 36-42	vs Rhodo 40-50	vs Rhodo 40-50
Average Dissimilarity (%)	76.1	69.4	79.0	67.1	94.0	85.7
Species Contributions						
Balistes vetula	9.2	7.8	7.4			
Epinephelus guttatus	7.0	6.0	6.9	4.2		
Ocyurus chrysurus	6.6			8.2	9.2	
Lutjanus mahogoni	6.4					
Lutjanus cyanopterus	6.0			9.1	7.6	6.5
Cephalopholis fulva	6.0				7.1	
Lachnolaimus maximus	5.9	6.4	5.8			
Scomberomorus regalis	5.4					
Lutjanus jocu		7.3		9.2		7.6
Lactophrys triqueter		6.6		8.6	4.3	6.9
Lutjanus mahogoni		6.5	6.2			
Panulirus argus			7.3			
Acanthostracion polygonia			6.9		7.8	
Lobatus gigas			6.8		7.8	6.5
Lutjanus analis			6.7		7.6	7.2
Ginglymostoma cirratum			5.9	4.5	5.2	6.5
Pterois sp.				4.7	7.6	5.8
Panulirus argus					5.1	4.5
Lutjanus apodus				7.3		7.1

Size distributions of numerically dominant large demersal fish/shellfish species, BDS 2011 /2018-20 survey

Schoolmaster Snapper (*Lutjanus apodus*)

Schoolmaster (*L. apodus*) was the numerically dominant large demersal fish species surveyed by drift belt-transects within the 23 – 50m depth range at El Seco Reef system during 2018-20 with a site mean density of 14.04 Ind/$10^3$$m^2$. Individuals were observed in the CPRT23-27, BCR35-40, and PCR36-42 habitats with a mean peak density of 38.18 Ind/$10^3$$m^2$ at the BCR35-40. The size frequency distribution based on a total of 389 individuals is presented in Figure 132. Strong primary and secondary modes at 32cm and 35cm FL, representative of 41.7% of the total individuals were observed during 2018-20. Modes in the 29 – 38cm size classes were largely associated with a schooling aggregation of approximately 307 individuals. Such unusually large aggregation of adult individuals may be indicative of reproductive behavior, particularly since it was observed in the vicinity of a known spawning aggregation site of other snappers at El Seco (e. g. *L. jocu*; *L. cyanopterus*; Garcia-Sais et al. 2011; this volume). A few larger and smaller individuals were observed solitary or in smaller schools within reef benthic habitats. Size at maturity of *L. apodus* has been reported at 25cm (Froese and Pauly, 2019). Thus, 96.7%% of the total individuals observed during 2018-20 were adults. Maximum size was observed at 47cm. Juvenile individuals were observed within drift belt-transects with minimum sizes of 15cm.

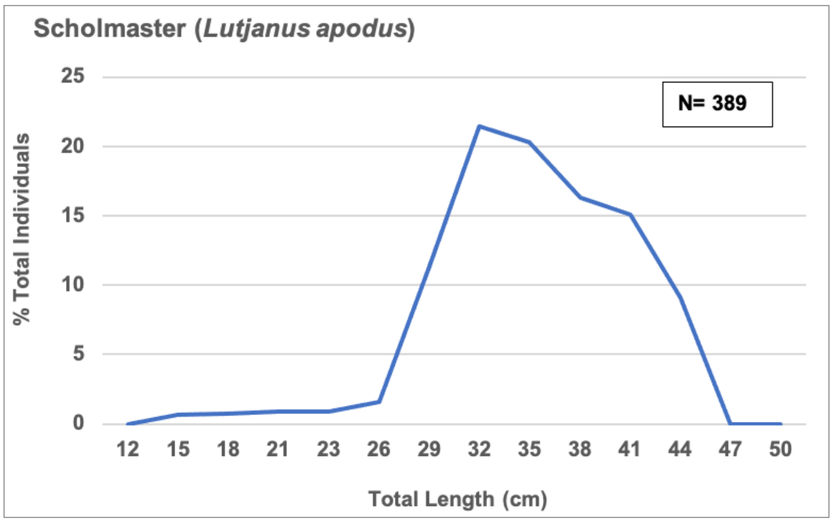

Figure 132. Size distribution of schoolmaster snapper (*Lutjanus apodus*) at El Seco Reef, 2018-20 survey.

Cubera Snapper (*Lutjanus cyanopterus*)

Cubera snappers (*L. cyanopterus*) ranked as the second most abundant large demersal fish surveyed from benthic habitats at El Seco Reef system during the 2018-20 survey with a site mean density (across all habitats and depths) of 3.54 Ind/10^3m^2. Individuals were observed in the CPRT23-27, BCR35-40, and PCR36-42 habitats with a mean peak density of 11.10 Ind/10^3m^2 at the PCR36-42. The size frequency distribution based on a total of 98 individuals is presented in Figure 133. Strong primary and secondary modes were observed at 70cm and 65cm FL, representative of 37.2% of the total individuals observed during 2018-20. Modes in the 65 – 95cm size classes were mostly associated with a spawning aggregation of approximately 70 individuals observed from PCR36-42 during July 1-2, 2020. Courtship behavior and reproductive coloration were noticed, as well as ripe males releasing eggs in the vicinity of females. Upward migration of females followed by males was not observed. Adult solitary individuals were also observed in transit within the PCR36-42 and BCR35-40 habitats in the vicinity of the main aggregation site.

Thus, it is possible that the aggregation was in progress and not fully developed by the time of our survey. Information of size at maturity for *L. cyanopterus* is presently unavailable, but individuals smaller than 60cm FL represented less than 5.0% of the total individuals observed. Since individuals of 65cm were observed associated with the spawning aggregation it is highly probable that all individuals observed within mesophotic habitats at El Seco during 2018-20 were adults. Maximum size was observed at 95cm.

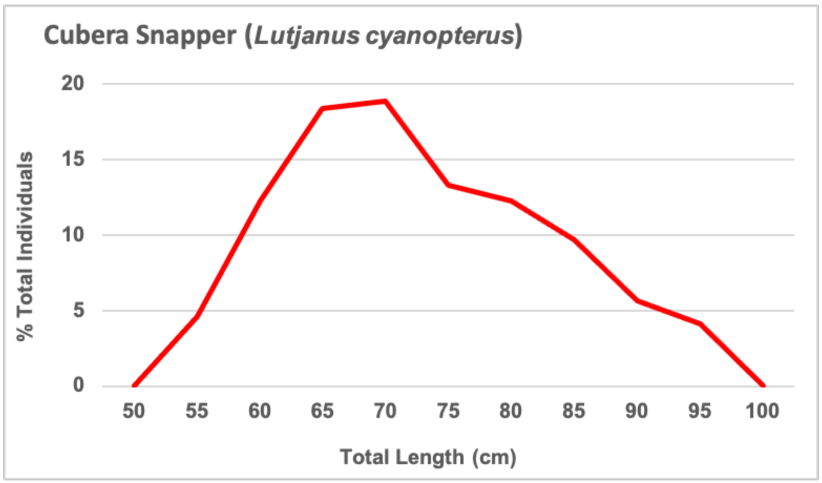

Figure 133. Size distribution of cubera snapper (*Lutjanus cyanopterus*) at El Seco Reef, 2018-20 survey.

Coney (*Cephalopholis fulva*)

Coney (*C. fulva)* was the third abundant fish species identified within drift belt-transects at El Seco Reef system with a site mean density of 3.25 Ind/10^3m^2 in 2018-20. Individuals were observed from all benthic habitats surveyed with a mean peak density of 3.95 Ind/10^3m^2 at Rhodo40-50. The size frequency distribution based on a total of 88 individuals is presented in Figure 134. Two main modes at 20cm and 23cm (TL), representative of 38.1% of the total individuals were noted from the size distribution. The length at maturity of *C. fulva* was reported at 14.5cm (Froese and Pauly, 2019). Therefore, both size modes were part of the adult population with individuals reaching up to a maximum size of 32cm. The juvenile population represented by individuals smaller than 14cm accounted for only 2.3% of the total, indicative of a population largely comprised by adults. Recruitment of coneys into the mesophotic habitats of El Seco was observed at 8cm.

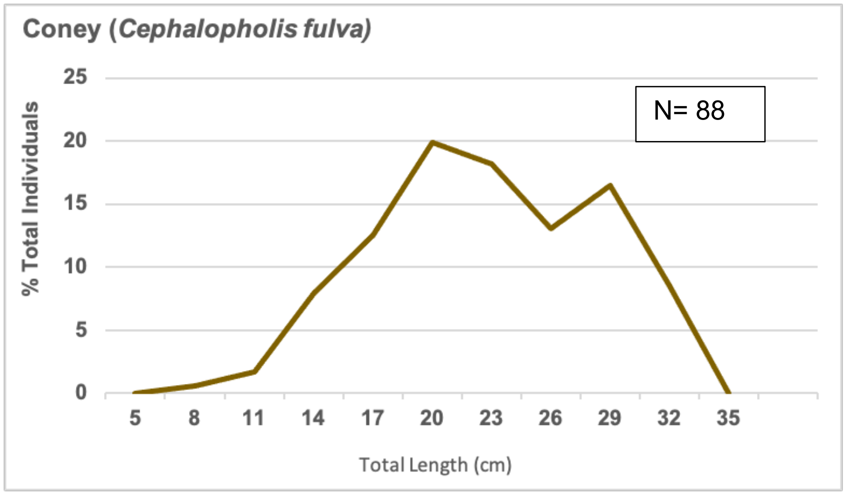

Figure 134 Size distribution of coney (*Cephalopholis fulva*) at El Seco Reef, 2018-20 survey.

Queen Conch (*Lobatus gigas*)

Queen conch (*L. gigas*) ranked as the most abundant shellfish surveyed from mesophotic habitats at El Seco Reef system within the 23 – 50m depth range and was the fourth most abundant species among the large demersal fish/shellfish community with a site mean density of 2.85 Ind/10^3m^2. Peak density was observed from Rhodo40-50 with a mean of 6.86 Ind/10^3m^2. A total of 78 queen conch were observed within drift belt-transects during the 2018-20 survey. Size (shell length) frequency distributions exhibited a very distinct mode of 25cm, representative of 37.8% of the total individuals (Figure 135). Individuals in the size range of 23 – 27cm represented 85.2% of the total observed population within belt-transects. Maximum size was measured at 27cm. These data are indicative that the queen conch population surveyed from El Seco Reef system was largely skewed towards the larger size classes comprised by adults.

A large aggregation of queen conch was observed from Rhodo40-50 engaged in what appeared to be reproductive behavior. A total of 50 individuals were observed in a relatively small section of the rhodolith habitat. Many individuals were observed distributed in pairs or small groups suggesting nesting and egg fertilization activities. Similar observations evidencing nesting and production of egg sacs within the rhodolith habitat were previously reported by Garcia-Sais et al (2012) from a queen conch population on the outer shelf terrace at a depth of 40m in Abrir la Sierra.

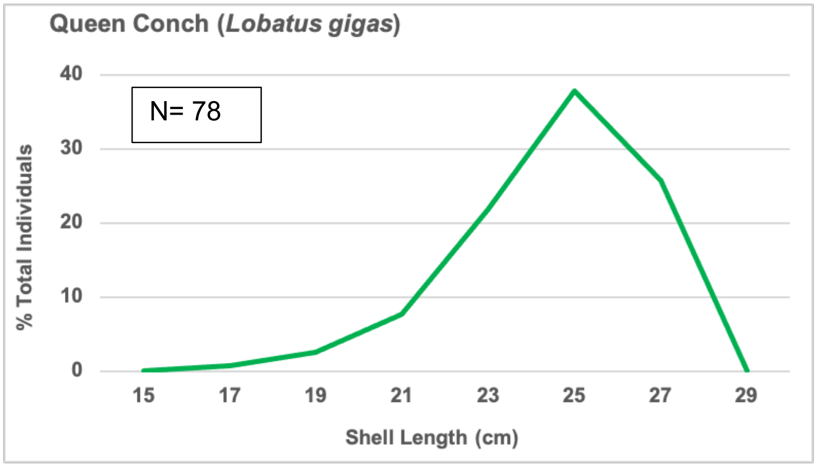

Figure 135. Size distribution of queen conch (*Lobatus gigas*) at El Seco Reef, 2018-20 survey.

Smooth Trunkfish (*Lactophrys triqueter*)

Smooth trunkfish (L. triqueter) was the fifth most abundant fish/shellfish species identified within drift belt-transects from the main mesophotic habitats at El Seco Reef system with a site mean density of 2.82 Ind/10^3m^2 in 2018-20. Individuals were observed in the CPRT23-27, BCR35-40, and PCR36-42 habitats with a peak density of 7.36 Ind/10^3m^2 at the PCR36-42. The size frequency distribution based on a total of 78 individuals is presented in Figure 136. Two main modes at 18cm and 20cm (TL), representative of 52.5% of the total individuals were noted from the size distribution. Information on the length at maturity of *L. triqueter* is presently unavailable, but individuals 16cm and larger, representative of 91.8% of the total population observed within drift belt-transects were probably adults. Individuals in such size range were previously observed to be engaged in what appeared to be reproductive activity at a multi-species spawning site at the edge of the bank coral reef of El Seco (Garcia-Sais et al., 2011). Recruitment of smooth trunkfish into the mesophotic habitats of El Seco was observed at 12cm. Smooth trunkfish (*Lactophrys triqueter*) were observed in small schools of seven (7), 12, 18 and 24 individuals that represented 78.2% of the total individuals surveyed within drift belt-transects. It is uncertain if these schools represent potential spawning aggregations, but *L. triqueter* is more often observed within neritic coral reef habitats as solitary individuals (Garcia-Sais et al., 2018, 2019, and references therein). Given the proximity of these schools to a known multi-species spawning aggregation site at the edge of the El Seco bank coral reef it is possible that reproductive behavior was the driver for such aggregations.

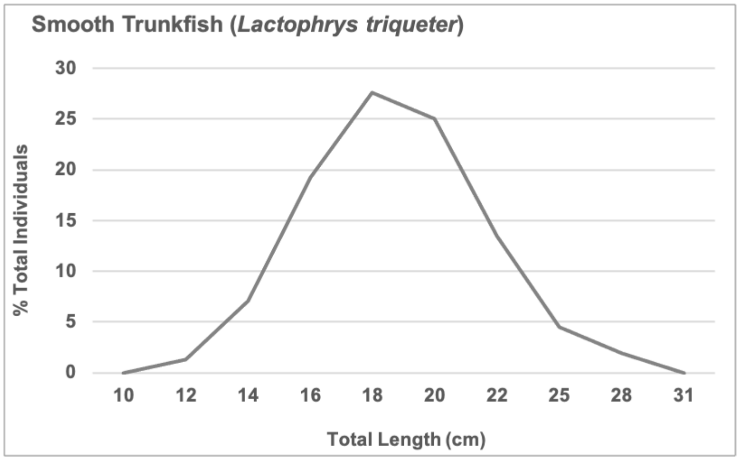

Figure 136. Size distribution of smooth trunkfish (*Lactophrys triqueter*) at El Seco Reef, 2018-20 survey.

Lionfish (*Pterois sp*)

Lionfish (*Pterois sp.*) ranked as the sixth (6th) most abundant large demersal fish surveyed from benthic habitats at El Seco Reef system during the 2018-20 survey with a site mean density of 2.38 Ind/10^3m^2. Individuals were observed in the CPRT23-27, BCR35-40, and PCR36-42 habitats with a mean peak density of 4.31 Ind/10^3m^2 at the PCR36-42. The size frequency distribution based on a total of 78 individuals was strongly skewed towards the larger individuals (Figure 137), with strong modes at 30cm and 27cm (TL). Individuals 27cm and larger represented 75.7% of the total population. The maximum size observed was 39cm. Size at maturity for *Pterois volitans* has been reported at 23.5cm (Froese and Pauly, 2019). Individuals larger than 23.5cm represented 90.4% of the total surveyed within mesophotic habitats at El Seco, indicative of a population largely comprised by adults.

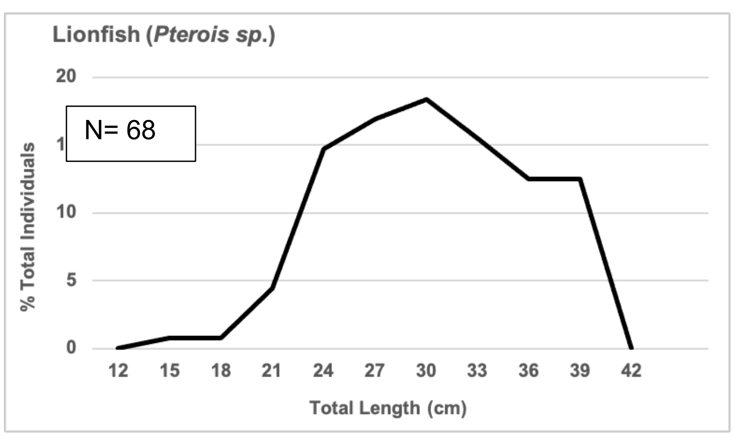

Figure 137. Size distribution of lionfish (*Pterois sp.*) at El Seco Reef, 2018-20 survey

Red Hind (*Epinephelus guttatus*)

Red hind (*E. guttatus*) ranked as the seventh (7th) most abundant large demersal fish surveyed from benthic habitats at El Seco Reef system during the 2018-20 survey with a site mean density of 2.35 Ind/10^{3}m^2. Individuals were observed from all habitats/depth surveyed with a mean peak density of 4.64 Ind/10^{3}m^2 at the CPRT23-30. The size frequency distribution based on a total of 63 individuals is presented in Figure 138. Modal size was at 29cm, with 60.3% of the total population distributed within the 26 – 32cm range. A secondary mode of 44cm individuals was observed, with maximum size reaching 47cm. The two modes may represent two highly successful recruitment events.

The red hind is a commercially important species under management by both state and federal government administrations and regulations include fishing closures during its seasonal spawning aggregation from December – February. Size at maturity of red hind (*E. guttatus*) was reported at 25cm (Froese and Pauly, 2019). Thus, approximately 92.9% of the population surveyed were adults. Recruitment size for *E. guttatus* into mesophotic habitats of El Seco was observed at 20cm.

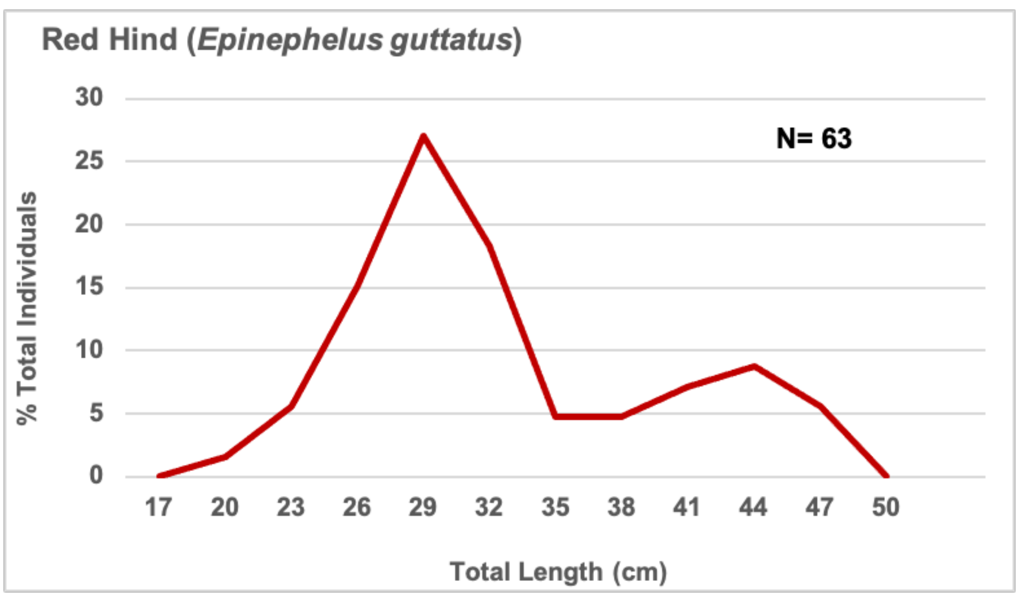

Figure 138. Size distribution of red hind (*Epinephelus guttatus*) at El Seco Reef, 2018-20 survey.

Queen Triggerfish (*Balistes vetula*)

A total of 22 queen triggerfish (*Balistes vetula)* were surveyed from mesophotic habitats of El Seco Reef system within the 23 – 50m depth range during the 2018-20 survey. Queen triggerfishes were observed within drift belt-transects from the CPRT23-30, PCR36-40 and Rhodo40-50 with a site mean density of 0.97 Ind/10^3m^2. Peak density was observed from the CPRT23-30 (2.40 Ind/10^3m^2). The size distribution of *B. vetula* was skewed towards the larger individuals with two main modes at 35cm and 30cm (FL) (Figure 139), representative of 59.1% of the total population. Maximum size was visually estimated at 45cm (FL). The size at maturity for *Balistes vetula* was reported at 23.5cm (Froese and Pauly, 2019). Thus, all of the *B. vetula* individuals observed from mesophotic habitats at El Seco were adults.

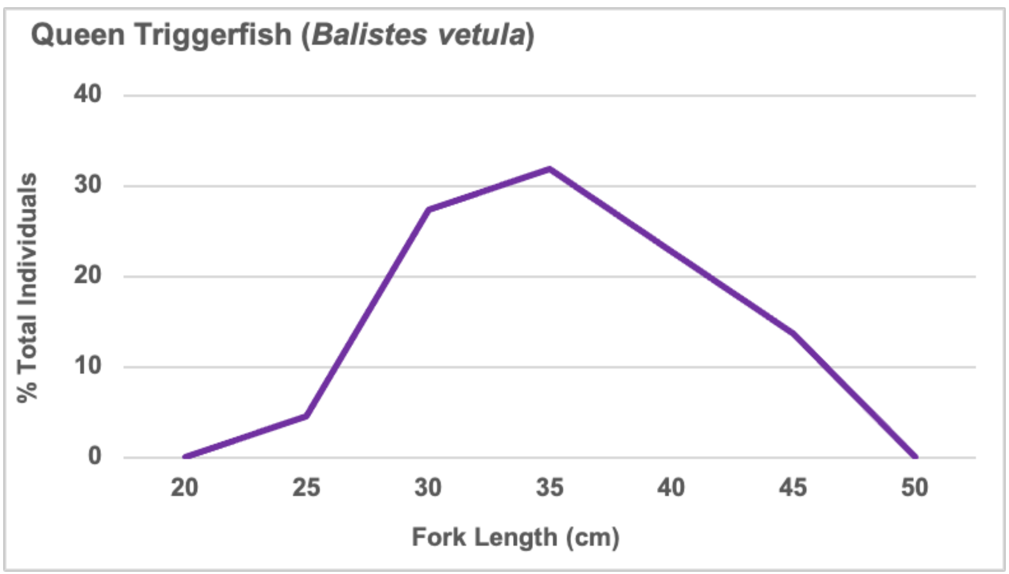

Figure 139. Size distribution of queen triggerfish (*Balistes vetula*) at El Seco Reef, 2018-20 survey.

Photo Album 5 – SECO
Seco – Colonized Pavement Reef Top (CPRT)

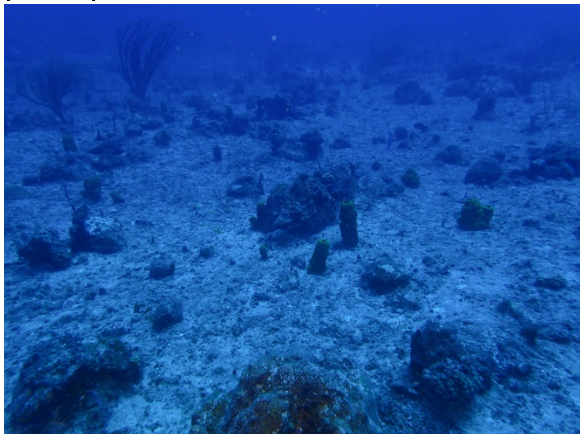
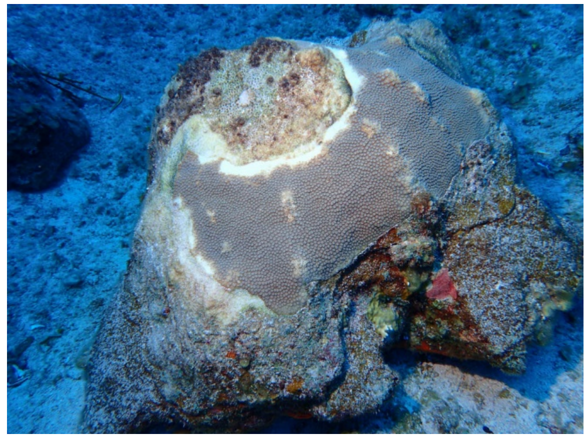
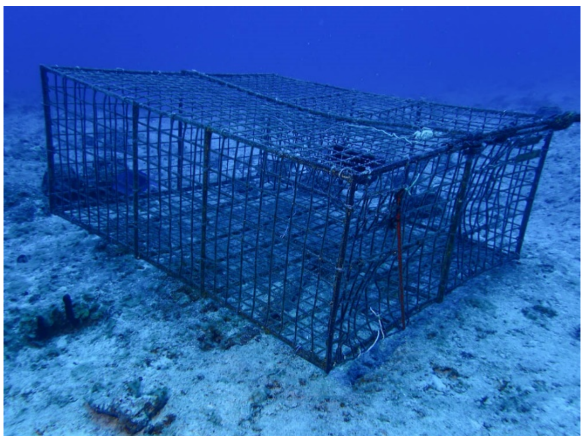
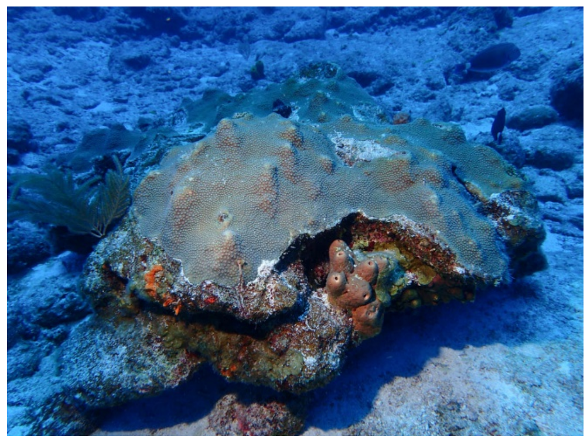
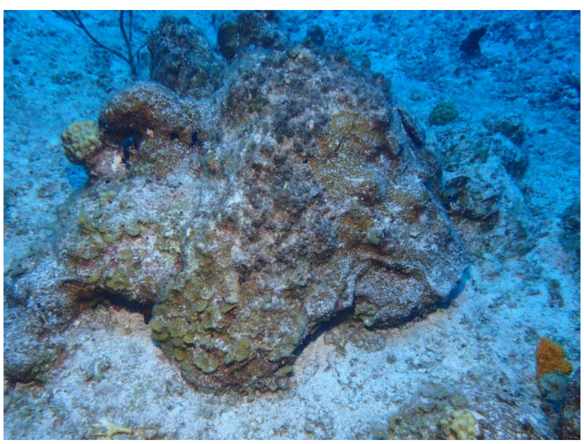
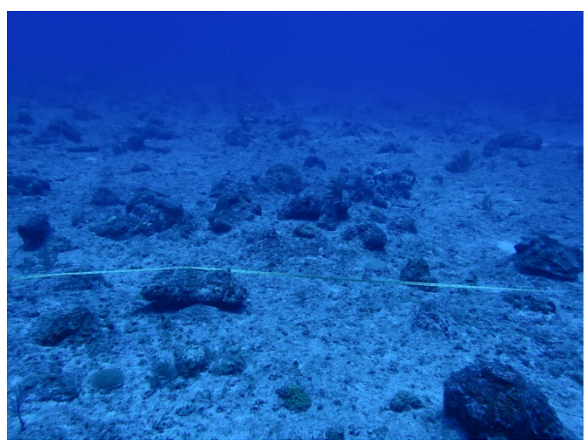

Bank Coral Reef (BCR) - SECO

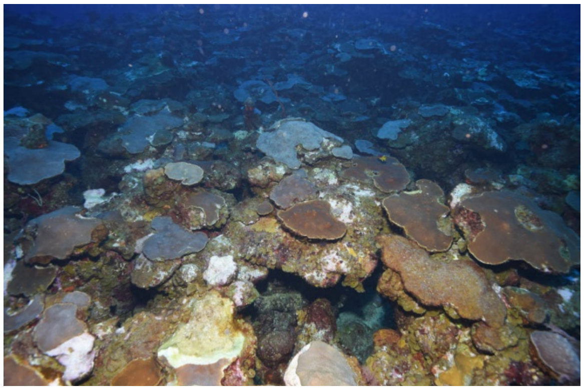
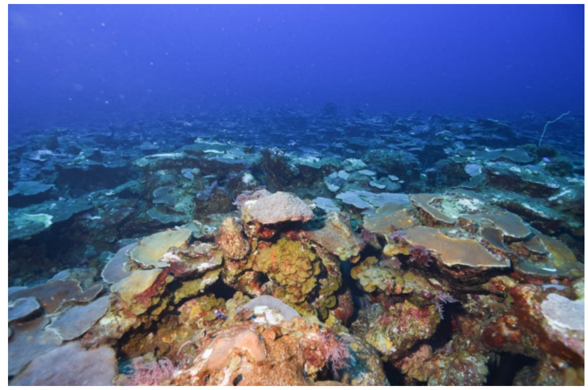
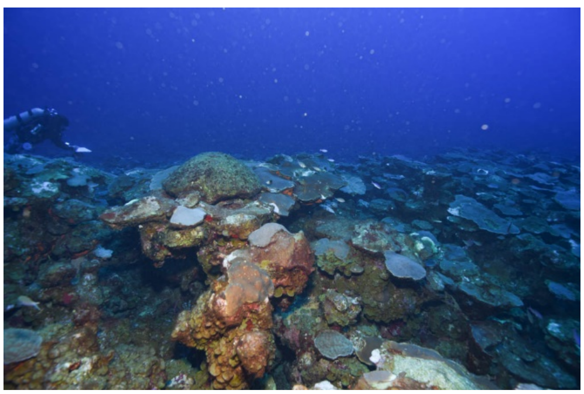

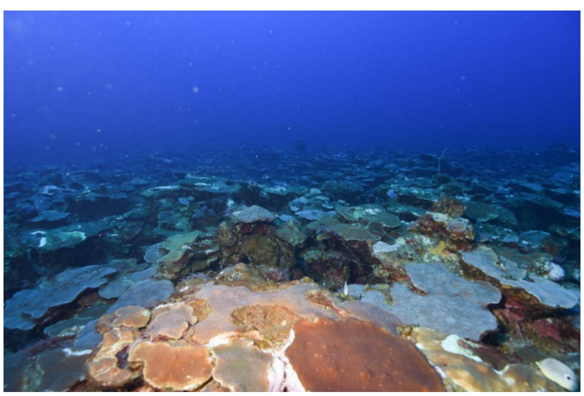


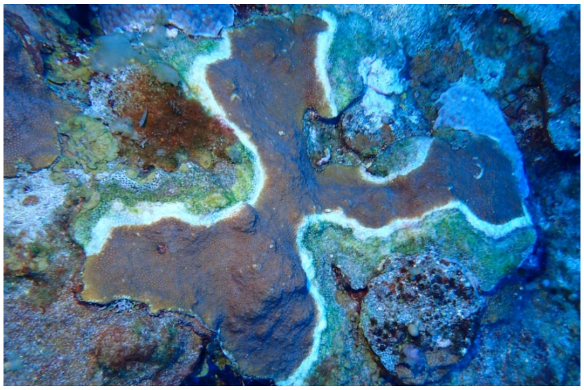

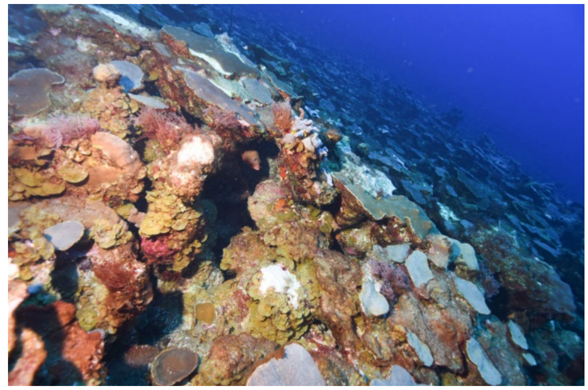

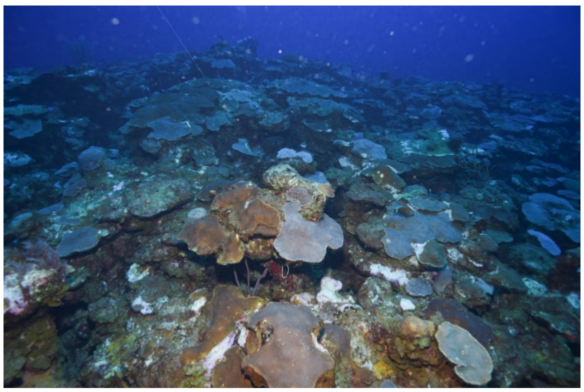

Patch Coral Reef (PCR) - SECO

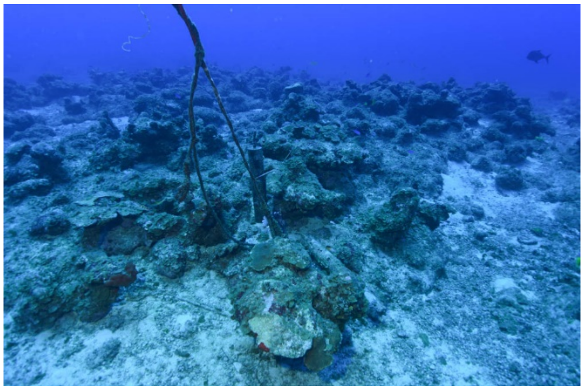

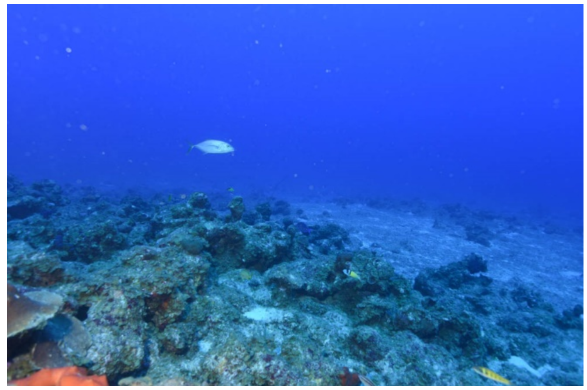

Rhodolith (Rhod) - SECO

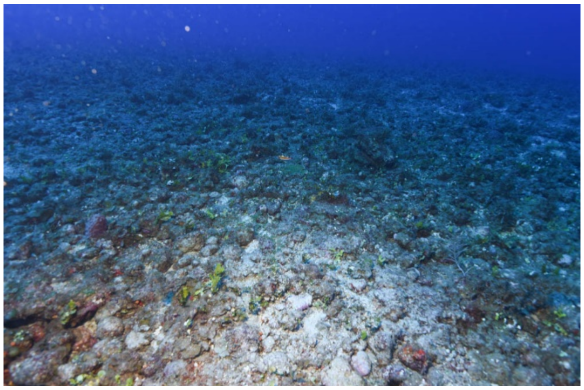
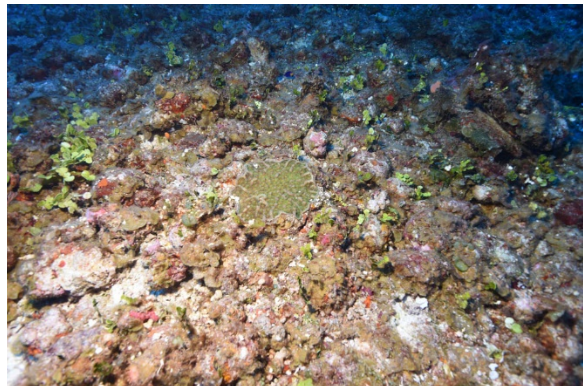

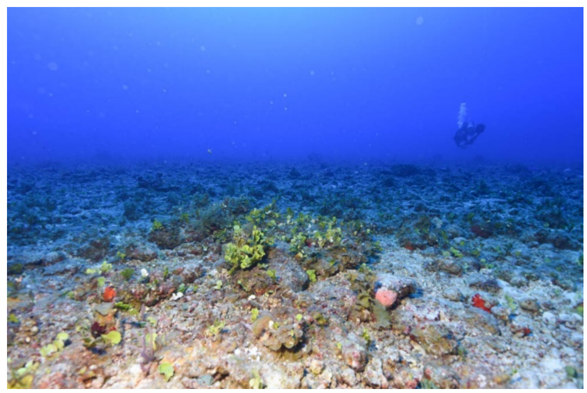
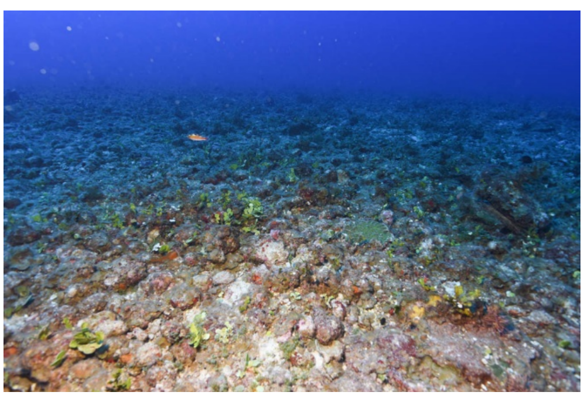
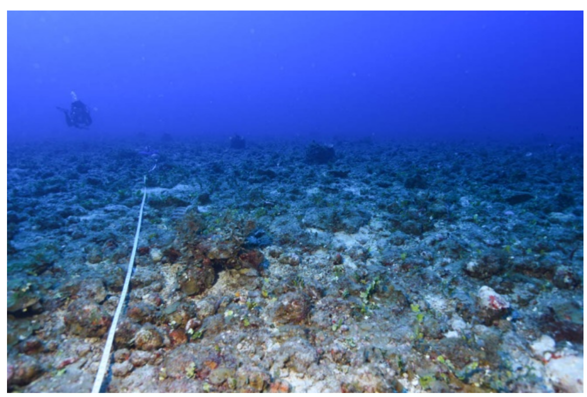

Boya 4

Study Site - Physical Description

Boya 4 is a shelf-edge marker buoy located approximately 11 nautical miles off Punta Guaniquilla in Cabo Rojo. A well-defined spur and groove coral reef formation fringes the shelf-edge at depths from 15.0 – 18.0m. The shelf-edge at 18.0m is abrupt, leading to a steep insular slope with a dominant angle of 60 - 70 degrees. Crevices and slope wall undercuts were noted along the 37 - 40m depth contour suggesting previous exposure of this slope section to breaking waves or other physical erosive forces. A series of small rises, or mini terraces were irregularly distributed down the slope, but were more consistently observed below 40m. Despite the highly steep and abrupt slope, substantial unconsolidated sediments, mostly fine coralline sands covered the seafloor, except for sections where the wall was completely vertical, and the hard ground or pavement was exposed. A mild (0.1 – 0.3 knots) topographically steered (northwesterly) current flow prevailed throughout the 24 – 50m depth range at Boya 4 during the 2018-20 survey.

This study represents a baseline quantitative survey of the sub-mesophotic and upper range mesophotic benthic and fish/shellfish community of Boya 4, with most observations produced between November 2018 and May 2019. The location and types of transect surveys are shown in Figure 140. Individual transect information including survey dates, depths, geographical coordinates and habitat classifications are included in Table 1. A photographic exhibit of the shelf-edge and upper insular shelf reef community at Boya 4 is presented in Photo Album 6.

Benthic Community

Habitat/depth related patterns of sessile-benthic community structure

A colonized pavement benthic habitat prevailed across the 25 – 50m depth profile down the insular slope at Boya 4. The mean substrate cover by sessile-benthic categories from photo-transects surveyed at the 25, 30, 40 and 50m depth contours on the insular slope are presented in Table 66. Benthic algae were the dominant substrate cover category across the entire depth profile, ranging from a minimum of 57.18% at CPSlope25 to a maximum of 68.78% at CPSlope30 (Figure 141). Variations of the percent substrate cover by total benthic algae between depths were statistically insignificant (ANOVA, $p = 0.127$) but marked vertical patterns were evidenced for various algal components. Fleshy macroalgae (mixed assemblage including *Dictyota sp.*) exhibited an increasing pattern of substrate cover with depth, representing 42.8% and 57.8% of the total cover by benthic algae at CPSlope40 and CPSlope50, respectively (Figure 143).

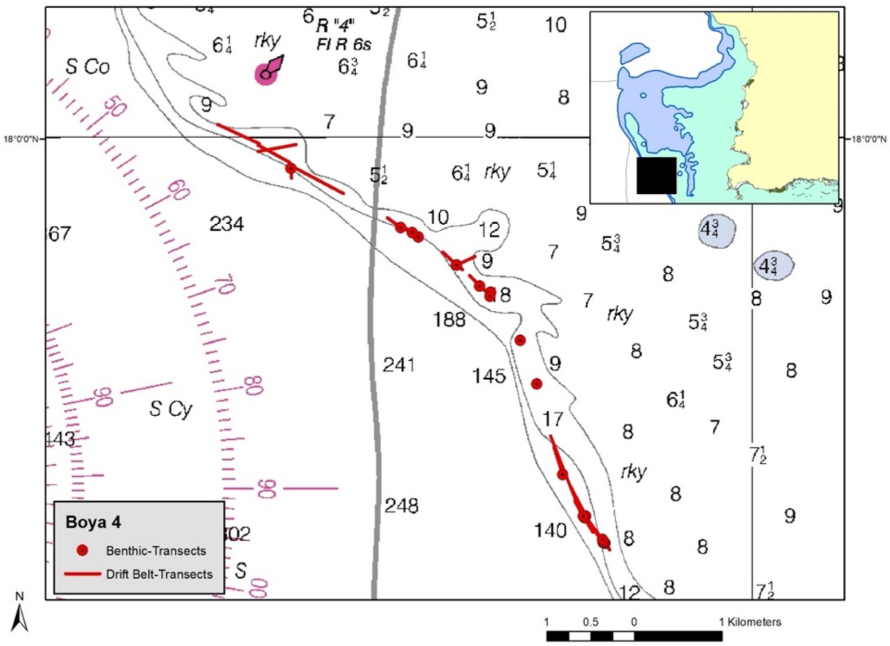

Figure 140. Location of benthic transects and drift belt- transect stations surveyed at Boya 4, 2018-20.

The encrusting fan alga (*Lobophora sp.*) and turf algae (mixed assemblage) were the dominant components at CPSlope25 and CPSlope30, with relatively lower cover at CPSlpoe50 and CPSlope40. Mean substrate cover by *Lobophora sp*. and turf algae both peaked at CPSlope30, representing 39.5% and 31.4% of the total cover by benthic algae, respectively. Crustose coralline algae (CCA - mixed assemblage) and green calcareous algae (*Halimeda spp.*) were observed throughout the depth range surveyed but with low substrate cover relative to other algal components. Substrate cover by cyanobacteria, or blue-green algae ranged between 1.22 % at CPSlope25 and 0% at SPSlope50, exhibiting a pattern of declining cover with depth.

Sponges represented by 33 species were the dominant invertebrate category in terms of substrate cover across the entire depth range. Mean cover varied between 16.98% at CPSlope25 and 12.80% at CPSlope50 (Table 66). Differences of cover between depths were not statistically significant (ANOVA; $p = 0.671$). A declining pattern of species richness with depth was noted, with 25 species identified at CPSlope25 and 11 species at CPSlope50. *Agelas conifera* was the dominant species in terms of substrate cover across the habitat/depth range, with *A. sceptrum*, *Plakortis spp*. and *Xestospongia muta* also prominent, particularly at CPSlope40 and CPSlope50 (Figure 144).

Table 66. Taxonomic composition and mean substrate cover (%) by sessile-benthic and abiotic categories measured from 10m-long photo-transects at Boya 4, 2018-20 survey

BOYA 4	BENTHIC CATEGORIES	CPSlope25	CPSlope30	CPSlope40	CPSlope50
Abiotic					
	Pavement	10.72	0.00	0.00	0.12
	Sand	2.48	9.96	21.78	25.28
	Dead Coral	0.11			
	Rubble		0.26	0.57	
	Total Abiotic	13.31	10.21	22.35	25.40
Benthic Algae					
	Turf (mixed) with sediment	0.76			
	Peyssonnelid (mixed)	2.22	1.90	4.03	1.24
	Turf (mixed)	14.12	21.62	10.32	2.94
	Lobophora variegatus	24.96	27.23	15.99	17.19
	Halimeda spp.	0.75	1.31	3.79	2.89
	Dictyota spp.	9.13	9.94	13.84	5.78
	Fleshy macroalgae (mixed)	2.13	6.62	11.75	27.37
	CCA (mixed)	3.11		0.06	
	Total Benthic Algae	57.18	68.78	59.79	57.42
	Cyanobacteria	1.22	0.69	0.32	0.00
Hard Coral					
	Agaricia agaricites	3.74	0.67	0.06	0.25
	Agaricia fragilis	0.15			
	Agaricia grahamae	0.51	0.72	0.20	0.99
	Agaricia lamarcki	1.52	3.33	1.95	2.02
	Diploria labyrinthiformis	0.05			
	Leptoseris cucullata	0.05			
	Madracis decactis	0.14		0.05	
	Madracis sp.		0.05		
	Meandrina meandrites	0.36			
	Millepora alcicornis	0.83	0.08		
	Montastraea cavernosa	0.59	0.14		
	Mycetophyllia aliciae	0.09			
	Orbicella faveolata	0.95	0.50	0.23	
	Orbicella franksi	0.60	0.10		0.69
	Porites astreoides	0.54			
	Siderastrea siderea	0.65	0.05		0.15
	Stephanocoenia intersepta	0.20	0.05		
	Unknown coral		0.15	0.07	0.46
	Total Hard Coral	10.95	5.85	2.55	4.55
# Coral colonies/photo frame		5.90	3.41	1.31	1.54
# Diseased coral colonies/photo frame		0.16		0.10	
# Antipatharia colonies/photo frame		0.00	0.00	0.08	0.23
Soft Corals					
	Antillogorgia spp.	0.79			
	Erythropodium caribaeorum	0.86	0.45	0.06	
	Eunicea spp.	0.24	0.05		

Table 66. Taxonomic composition and mean substrate cover (%) by sessile-benthic and abiotic categories measured from 10m-long photo-transects at Boya 4, 2018-20 survey

BOYA 4

BENTHIC CATEGORIES	CPSlope25	CPSlope30	CPSlope40	CPSlope50
Gorgonia ventalina	0.11			
Plexaura spp.				0.50
Unidentified		0.05		
Total Soft Corals	2.01	0.55	0.06	0.50
# Soft coral colonies/photo frame	7.81	3.13	2.46	7.24
Sponges				
Agelas clathrodes	0.42	0.54	0.64	
Agelas citrina		0.13		0.09
Agelas conifera	2.93	4.47	4.95	3.83
Agelas dispar	0.23	0.28	0.07	
Agelas sceptrum		0.70	1.34	1.84
Agelas sventres	0.59			
Agelas tubulata	0.09			
Aiolochroia crassa	0.44	0.42	0.52	0.57
Aplysina archeri		0.24	0.10	
Aplysina cauliformis	0.05			
Aplysina fistularis				0.16
Callyspongia ferox			0.12	
Cliona caribbaea	0.84			
Cliona delitrix		0.13		
Desmapsamma anchorata			0.13	
Ectyoplasia ferox	0.11			
Iotrochota birotulata	0.84	0.42		
Hyrtios cavernosus		0.19		
Ircinia felix	0.15			
Ircinia strobilina	0.34	0.10	0.19	
Monanchora arbuscula	0.08			
Neopetrosia proxima	0.14			
Niphates erecta	0.04			
Petrosia pellasarca	0.35	0.75		0.13
Plakortis spp.	2.32	1.31	1.22	1.21
Pleraplysilla sp.	0.03			
Prosuberites laughlini	0.03	0.08		
Scopalina ruetzleri	0.33		0.06	
Smenospongia conulosa	0.04			
Spheciospongia vesparium	0.36	0.06		
Spirastrella coccinea	0.12	0.09	0.09	0.25
Svenzea zeai	1.20	0.52	0.71	0.63
Unknown sponge	4.90	3.19	3.19	3.08
Xestospongia muta		0.31	1.59	1.02
Total Sponges	16.98	13.93	14.93	12.80

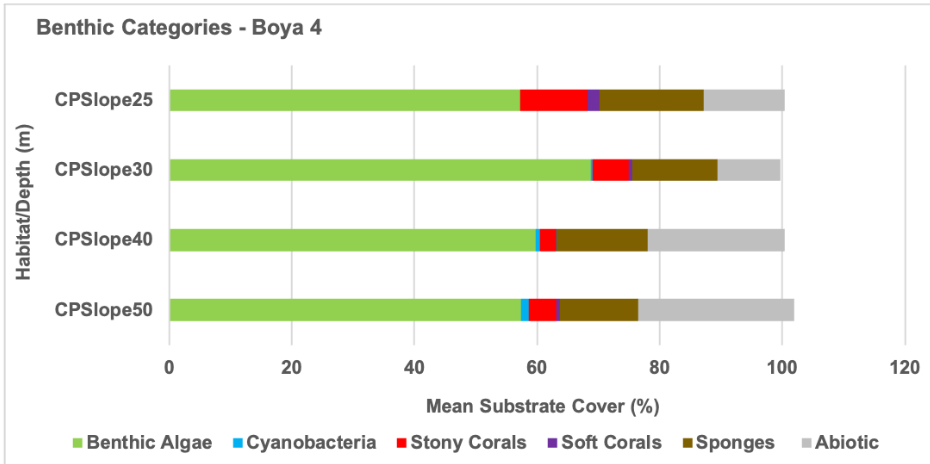

Figure 141. Depth related variations of mean percent substrate cover by the main sessile-benthic categories at Boya 4, 2018-20 survey.

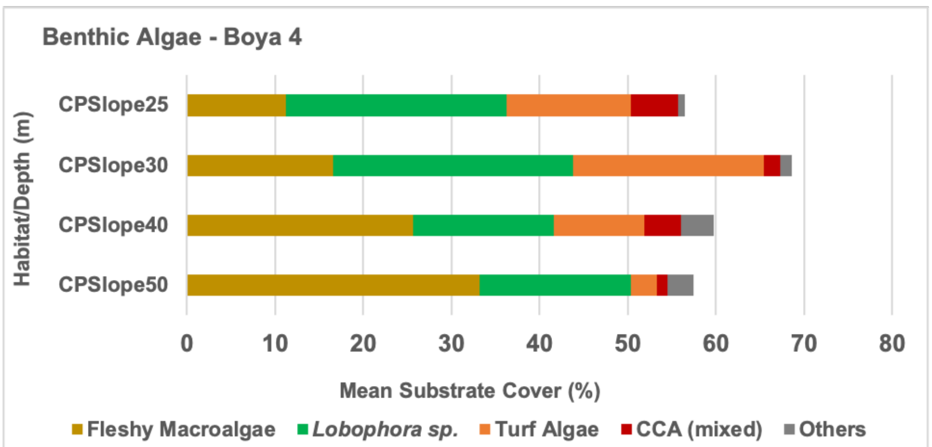

Figure 142. Depth related variations of the mean percent substrate cover by benthic algae at Boya 4, 2018-20 survey.

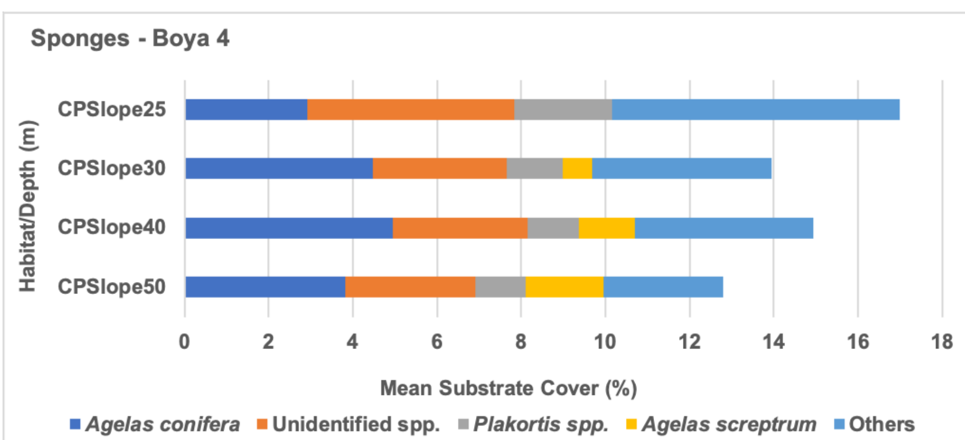

Figure 143. Depth related variations of the mean percent substrate cover by sponges at Boya 4, 2018-20 survey.

Stony corals were represented by 17 species of scleractinians and one hydrocoral (*Millepora alcicornis*), with the higher number of species (15) and mean substrate cover (10.95%) measured from sub-mesophotic stations at CPSlope25 (Table 66). Depth-related differences of substrate cover by stony corals were statistically significant (ANOVA; p = 0.017), with higher cover at CPSlope25 relative to deeper stations. A decreasing pattern of stony coral cover was measured down to CPSlope40, disrupted by increasing cover at CPSlope50. Lettuce corals, comprised by *Agaricia lamarki, A. grahamae* and *A. agaricites* was dominant throughout the entire depth range with *A. agaricites* the main species in terms of substrate cover at CPSslope25, and *A. lamarki* dominant at CPSlope30 thru CPSlope50 (Figure 144). Soft corals (gorgonians) were present throughout the habitat/depth range surveyed at Boya 4 with relatively low substrate cover (max 2.01%). The encrusting gorgonian (*Erythropodium caribaeorum*) was the main species contributing substrate cover across CPSlope25 thru CPSlope40, whereas *Plexaura spp*. were dominant at CPSlope50. Substrate cover by soft corals was higher at CPSlope25 than at all other habitats/depths (ANOVA, p < 0.001). Bushy and wire black coral (*Antipathes caribbeana, Stichopathes lutkeni*) were observed growing out of crevices and slope undercuts throughout the depth range surveyed but were more prominent at CPSlope40 and CPSlope50.

Abiotic categories (mostly sand) exhibited a pattern of increasing substrate cover with depth (Figure 145). Sand transport down the insular slope was substantial and appeared to be an important factor influencing biological community structure by restricting attachment of sessile-benthic biota. It is unclear if the observed magnitude of sand deposition was influenced by hurricane effects during late 2017. Higher sand accumulation was observed at the deeper 40 – 50m sections, perhaps related to the rise or decreasing slope angle.

Variations of the sessile-benthic community structure within the 25 – 50m depth profile surveyed at Boya 4 are displayed in a non-metric multi-dimensional scaling plot (nMDS) based on Bray-Curtis similarities in Figure 146. Colonized pavement prevailed as the dominant benthic habitat type down the insular slope, influencing relatively high similarities of benthic community structure across the depth gradient. The highest similarity of benthic components among samples within the same depth contour was observed from CPSlope25 (83.3%), strongly influenced by the contributions of stony and soft corals (Table 67), which exhibited higher substrate cover at CPSlope25 compared to other depths. The lowest similarities were noted from CPSlope50 (73.0%) and CPSlope40 (74.0%), where abiotic, benthic algae, and sponges were the main contributors to similarity.

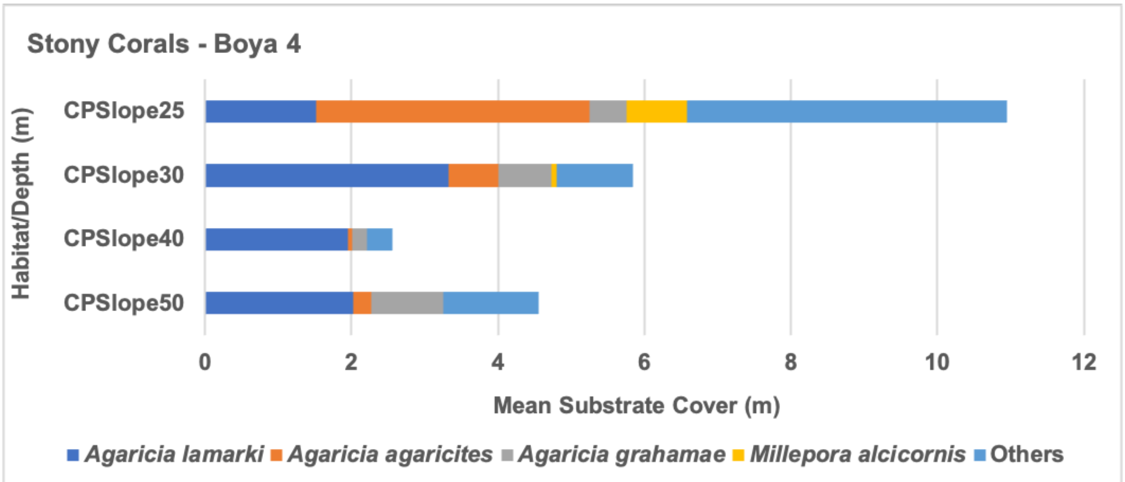

Figure 144. Depth related variations of the mean percent substrate cover by stony corals at Boya 4, 2018-20 survey.

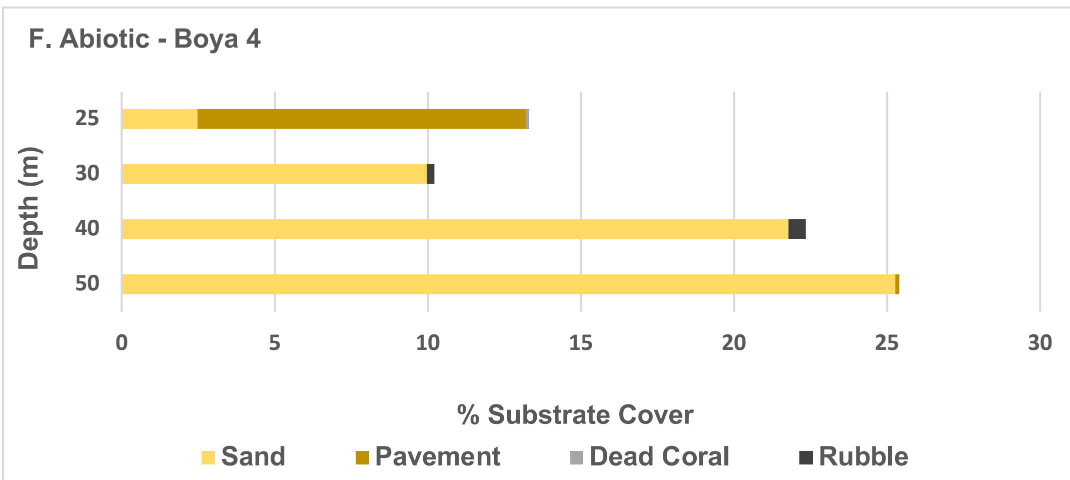

Figure 145. Depth related variations of the mean percent substrate cover by abiotic categories at Boya 4, 2018-20 survey.

The highest dissimilarities of benthic community structure were observed between CPSlope25 and CPSlope50 (33.8%), and also between CPSlope25 and CPSlope40 (29.9%). The main contributors to dissimilarities were the relatively higher substrate cover by stony corals, soft corals and cyanobacteria at CPSlope25 relative to CPSlope40 and CPSlope50, and the higher cover by black corals and abiotic categories (mostly sand) at CPSlope50. Conversely, the relatively uniform distribution of total benthic algae and sponges contributed strongly to similarity of benthic community structure across the habitat/depth range surveyed at Boya 4.

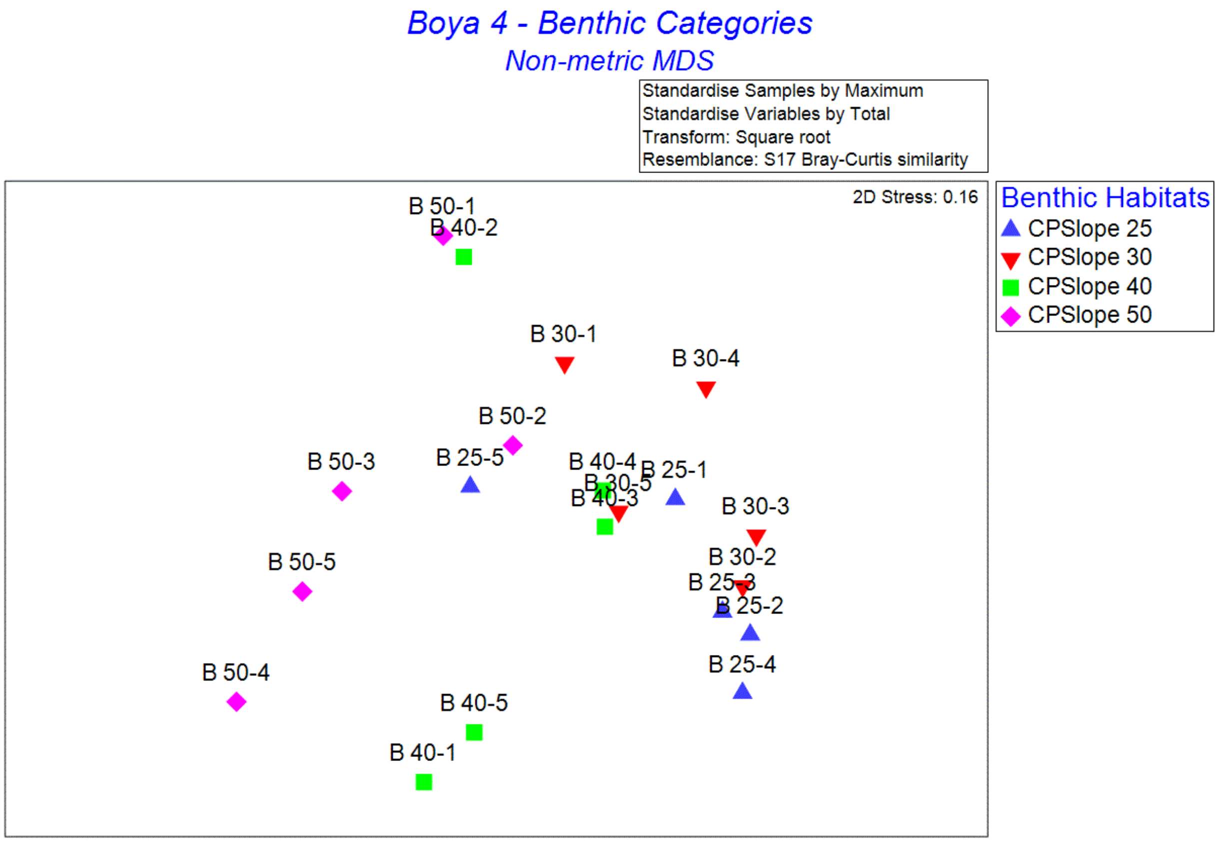

Figure 146. Non-metric multidimensional scaling (nMDS) plot of Bray-Curtis similarities based on the percent substrate cover by sessile-benthic categories surveyed across the 25 – 50m depth profile at Boya 4, 2018-20 survey.

Table 67. Similarity matrix (SIMPER) of sessile-benthic community structure from the main benthic habitats surveyed across the 25 – 50m depth at Boya 4, with contributions of sessile-benthic categories to similarity percentages, 2018-20 survey.

Benthic Habitat/Depths	**CPSlope 25**	**CPSlope 30**	**CPSlope 40**	**CPSlope 50**
Average Similarity (%)	83.3	81.9	74.0	73.0
Benthic Categories				
Stony Corals	22.9	17.1		14.7
Soft Corals	20.4	14.7	12.9	
Benthic Algae	17.6	24.5	24.8	23.0
Sponges	15.8	18.0	21.7	19.2
Cyanobacteria				
Abiotic			23.4	23.7

Fish Community

Small Demersal Fishes

Habitat/depth related variations of density and community structure

A total of 54 species of small demersal fishes were identified within the 25 – 50m depth range at Boya 4 (Table 68). Fish density and species richness peaked at CPSlope25 with means of 196.6 Ind/30m^2 and 18.2 Spp/30m^2. Differences of fish density between depths were statistically significant, associated with higher density at CPSlope25 compared to other habitats/depths (ANOVA, $p < 0.0001$). The higher fish density at CPSlope25 was strongly driven by peak densities of creole wrasse (*Clepticus parrae*) within the depth range surveyed (Figure 147). The mean density of *C. parrae* at CPSlope25 (122.4 Ind/30m^2) represented 62.2% of the total fish density from that habitat/depth. Densities of blue chromis (*Chromis cyanea*), bluehead wrasse (*Thalassoma bifasciatum*), princess and redband parrotfishes (*Scarus taeniopterus, Sparisoma aurofrenatum*), bicolor and cocoa damselfishes (*Stegastes partitus, S. variabilis*), and masked goby (*Coryphopterus personatus*) also peaked at CPSlope25 and contributed markedly to fish density differences between habitats/depths. Conversely, an increasing pattern of fish density with depth was evident for sunshine chromis (*Chromis insolata*) (Figure 147). Fish species richness within belt-transects declined with depth (Table 68). Differences were statistically significant (ANOVA, $p= 0.00014$) associated with higher species richness at CPSlope25 compared to other habitats/depths. Mean fish species richness declined 54.9% between the maximum at CPSlope25 (18.20 Spp/30m^2) and the minimum at CPSlope50 (8.20 Spp/30m^2).

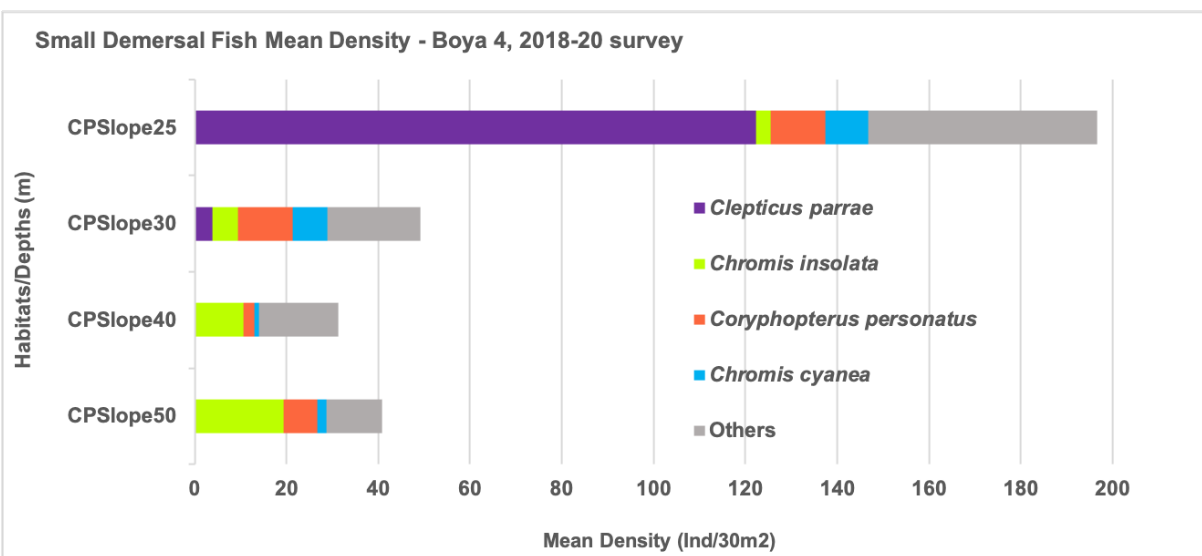

Figure 147. Depth related variations of mean density by small demersal fishes across the 25 – 50m depth range surveyed at Boya 4, 2018-20 survey

Table 68. Taxonomic composition and mean density of small demersal fish species surveyed within 10m x 3 belt-transects at Boya 4, 2018-20 survey

Fish Species	**CPSlope25**	**CPSlope30**	**CPSlope40**	**CPSlope50**
Acanthostracion polygonius		0.20		
Acanthurus coeruleus		0.40		
Acanthurus tractus	1.00			
Anisotremus virginicus	0.20	0.20		
Aulostomus maculatus	0.20	0.20		
Balistes vetula	0.40		0.20	
Bodianus rufus				
Canthigaster rostrata	1.20	0.40	0.20	0.40
Carangoides ruber		0.60		
Caranx hippos				1.00
Caranx lugubris	0.40			
Centropyge argi	0.20			0.20
Cephalopholis cruentatus	1.00	0.20	0.40	0.60
Cephalopholis fulva		0.20		
Chaetodon capistratus		0.20		0.20
Chromis cyanea	9.40	7.60	1.00	2.00
Chromis insolata	3.00	5.60	10.60	19.40
Chromis multilineata	0.20			
Clepticus parrae	122.40	3.80		
Coryphopterus glaucofraenum		0.20		
Coryphopterus lipernes	0.80	1.00		
Coryphopterus personatus	12.00	12.00	2.40	7.40
Epinephelus guttatus		0.20		
Gymnothorax moringa			0.40	
Ginglymostoma cirratum				
Gramma loreto	2.00	3.60	4.60	1.80
Halichoeres garnoti	4.40	2.80	4.80	4.20
Halichoeres maculipinna		0.40		
Holacanthus ciliaris			0.20	0.20
Holacanthus tricolor				0.20
Holocentrus rufus	0.40	0.20	0.20	
Hypoplectrus puella	0.20			
Hypoplectrus unicolor			0.20	
Liopropoma rubre			0.20	
Lutjanus apodus	0.20			0.20
Melichthys niger	2			
Myripristis jacobus	1.2	0.4		0.4
Neoniphon marianus	0.2	0.2	0.6	0.8
Ocyurus chrysurus	2.2	0.6	0.2	

Table 68. Taxonomic composition and mean density of small demersal fish species surveyed within 10m x 3 belt-transects at Boya 4, 2018-20 survey

Fish Species	CPSlope25	CPSlope30	CPSlope40	CPSlope50
Paranthias furcifer			0.6	
Prognathodes aculeatus	0.6	0.40	0.60	0.40
Pseudupeneus maculatus	0.2			
Pterois sp.			0.4	0.2
Scarus taeniopterus	9.6	2.2		
Serranus baldwini				0.4
Sparisoma aurofrenatum	4.8	1.4	0.6	0.2
Sparisoma radians		0.4		
Sparisoma viride	0.2			
Sphyraena barracuda	0.2			
Stegastes leucostictus		0.8	0.6	
Stegastes partitus	5.6	2	1.4	0.4
Stegastes variabilis	1.6			
Thalassoma bifasciatum	8.6	0.8	0.8	
Xanthichthys ringens				0.2
Mean Density (Ind/30m^2)	**196.6**	**49.2**	**31.2**	**40.8**
Mean Species Richness (Spp/30m2)	**33**	**30**	**22**	**21**

Variations of the relative densities of small demersal fish species surveyed from 10m x 3m belt-transects within the 25 – 50m depths at Boya 4 are displayed in a non-metric multi-dimensional scaling plot (nMDS) of Bray-Curtis similarities in Figure 148. Fish community structure similarities within habitats/depths were relatively low across the entire depth range surveyed. The highest similarity was observed from CPSlope25 (45.8%), influenced by contributions of the numerically dominant species, creole wrasse (*Clepticus parrae*), and other shallow-water reef species, including the cocoa damselfish (*Stegastes variabilis*), black durgon (*Melichthys niger*), and princess parrotfish (*Scarus taeniopterus*) (Table 69). Samples in the 30 – 50m depth range exhibited even lower within habitat/depth similarities ranging between 25.5 at CPSlope30 and 28.8% at CPSlope40. The relatively low within habitat/depth similarities of small demersal fish relative densities was strongly influenced by the highly aggregated (patchy) distributions of the numerically dominant fishes from all depths surveyed, including the creole wrasse (*C. parrae*), sunshine and blue chromis (*Chromis insolata, C. cyanea*), and masked goby (*Coryphopterus personatus*).

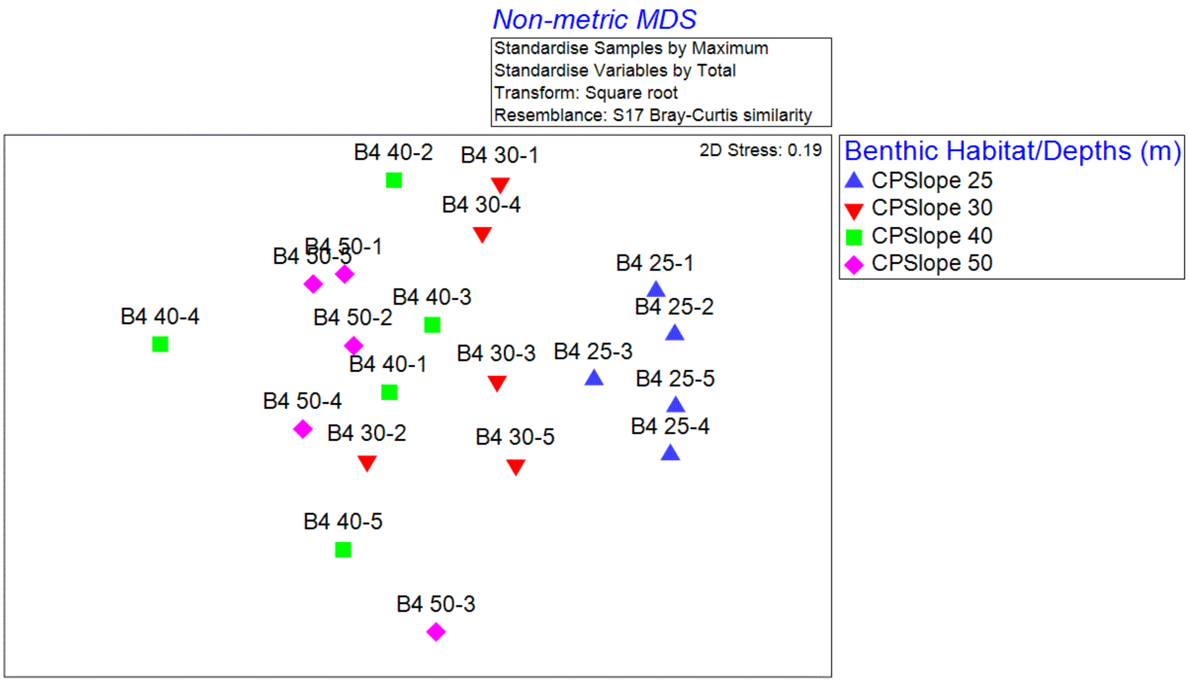

Figure 148. Non-metric multidimensional scaling (nMDS) plot of Bray-Curtis similarities based on the relative densities of small demersal fishes surveyed from 10m x 3m belt-transects across the 25 – 50m depth range at Boya 4, 2018-20 survey

Table 69. Similarity matrix (SIMPER) of small demersal fish community structure from the main habitats/depths surveyed across the 25 – 50m rang at Boya 4, with species contributions to similarity percentages, 2018-20 survey.

Habitats/Depths (m)	**CPSlope25**	**CPSlope30**	**CPSlope40**	**CPSlope50**
Average Similarity (%)	45.8	25.5	28.8	26.4
Species				
Clepticus parrae	17.5			
Stegastes variabilis	15.6			
Melichthys niger	10.6			
Scarus taeniopterus	9.0			
Chromis cyanea		21.5		13.3
Gramma loreto		13.5	22.5	
Chromis insolata		11.3	23.1	27.8
Halichoeres garnoti		11.1	19.1	19.5
Coryphopterus personatus				21.8
Stegastes partitus			10.2	

Dissimilarities of small demersal fish community structure were highest between CPSlope25 and CPSlope50 (85.5%), and also between CPSlope25 and CPSlope40 (85.2%). The main species contributions to dissimilarities between CPSlope25 and deeper stations were from an assemblage of shallow water (neritic) reef fishes that although not numerically dominant at CPSlope25 were not observed deeper than CPSlope30. These included the cocoa damselfish (*Stegastes variabilis*), black durgon (*Melichthys niger*), five-band surgeonfish (*Acanthurus tractus*), and peppermint goby (*Coryphopterus lipernes*), among others (Table 70).

Table 70. Dissimilarity matrix (SIMPER) of small demersal fish community structure between the main habitats/depths surveyed across the 25 – 50m rang at Boya 4, with species contributions to dissimilarity percentages, 2018-20 survey.

Habitats/Depths	CPSlope25 vs CPSlope30	CPSlope25 vs CPSlope40	CPSlope25 vs CPSlope50	CPSlope30 vs CPSlope40	CPSlope30 vs CPSlope50	CPSlope40 vs CPSlope50
Average Dissimilarity (%)	78.4	85.2	85.5	74.6	78.8	72.6
Fish Species						
Stegastes variabilis	5.5	5.9	6.6			
Melichthys niger	4.8	5.2	5.7			
Acanthurus tractus	4.2	5.1	5.0			
Coryphopterus lipernes	3.3	4.5		3.6		
Clepticus parrae			5.8			
Scarus taeniopterus			5.0		3.1	
Stegastes leucostictus				3.6	3.3	
Stegastes partitus				3.5	3.3	
Cephalopholis fulva				3.4		
Chromis cyanea					3.1	
Pterois sp.						5.2
Neoniphon marianus						5.2
Gramma loreto						4.6
Cephalopholis cruentatus						4.5

Large Demersal Fishes and Shellfishes 2018-20 Survey

Depth/habitat related patterns of density and community structure

The taxonomic composition and mean densities of large demersal fishes and shellfishes surveyed by drift dive belt-transects across the 25 – 50 m depth range at Boya 4 are presented in Table 71. The yellowtail snapper (*Ocyurus chrysurus*) was the numerically dominant species throughout the habitat/depth range, representing 84.2% of the total fish density (Figure 149). Peak density of *O. chrysurus* was observed at CPSlope50 (94.5 Ind/10^3m^2), but a distinct vertical distribution pattern was not evident within the depth profile surveyed (ANOVA; p = 0.999). Yellowtail snappers were observed in dense aggregations essentially parallel to the slope with individuals making frequent incursions towards the slope benthos. A total of 2,462 *O. chrysurus* individuals were observed within belt-transect areas, but densities at the aggregation were much higher than those here reported because most of the aggregation was off the slope wall and therefore out of transect areas. Fish movements towards the slope appeared related to feeding and no signs of reproductive behavior were noted.

Also prominent at Boya 4 within the 25 – 50m depth range were the lionfish (*Pterois sp.*), lane and schoolmaster snappers (*Lutjanus synagris, L. apodus*), and red hind (*Epinephelus guttatus*). The aforementioned species were observed with mean densities in the 1.0 - 1.5 Ind/10^3m^2 range across the 25 – 50m depth profile without any statistically significant habitat/depth related distribution patterns (ANOVA; $p > 0.05$). Small groupers, such as the graysbe (*Cephalopholis cruentata*), and coney (*C. fulva*), queen triggerfish (*Balistes vetula*), and great barracuda (*Sphyraena barracuda*) were also common at the upper slope of Boya 4. Lionfishes (*Pterois sp.*) were surveyed in essentially similar densities within the CPSlope30 – CPSlope50 range but were not observed at CPSlope25. Such distribution may have been influenced by the availability of their preferred habitat consisting of deep crevices and ledges within the deeper section of the insular slope surveyed. Their prevalence at the upper insular slope of Boya 4 support the status of lionfish as one of the main small demersal predators of mesophotic habitats.

Schools of lane snappers (*Lutjanus synagris*) were observed at CPSlope30 and CPSlope50, resulting in a study mean density of 1.40 Ind/10^3m^2. The schools were observed in transit, not associated with any particular slope benthic habitat. It is possible that lane snappers use the shallow neritic reef as their residential habitat and undertake foraging excursions down the upper slope section. Schoolmaster snappers (*L. apodus*) were represented by total of 44 individuals observed across the 25 – 50m depth range with a mean density of 1.37 Ind/10^3m^2. A distinct pattern of decreasing density with depth was observed with a mean peak density at CPSlope25 (1.9 Ind/10^3m^2), and the lowest at CPSlope50 (0.48 Ind/10^3m^2). Schoolmasters were observed in small aggregations associated with coral heads and other substrate irregularities, and as solitary individuals in transit close to the seafloor. Other snappers of commercial value observed in relatively lower densities included the cubera, dog, mutton and mahogoni snappers (*L. cyanopterus, L. jocu, L. analis, L. mahogany*).

Spiny lobster (*Panulirus argus*) presented significantly higher densities at CPSlope40, relative to other habitats/depths surveyed from Boya 4 during the 2018-20 survey (ANOVA; $p = 0.0077$). Differences were associated with the higher availability of protective habitats at CPSlope40.

Table 71. Taxonomic composition and mean densities of large demersal fishes/shellfishes identified within drift belt-transects surveyed from the 25 – 50m depth range at Boya 4, 2018-20 survey

Habitat/Depth (m)	**CPSlope25**		**CPSlope30**		**CPSlope40**		**CPSlope50**	
Area Surveyed (m2)		12,357		7,916		5,474		6,285
Fish/Shellfish Species	# Ind.	Ind/10^3m^2	# Ind.	Ind/10^3m^2	# Ind.	Ind/10^3m^2	# Ind.	Ind/10^3m^2
Acanthostracion polygonia	2	0.162			1	0.183	2	0.318
Alectis ciliaris			2	0.253				
Balistes vetula	8	0.647	7	0.884	7	1.279	4	0.636
Carcharhinus perezi							1	0.159
Cephalopholis cruentatus	12	0.971	8	1.011	10	1.827		
Cephalopholis fulva	7	0.566	10	1.263	2	0.365	4	0.636
Dasyatis americana			1	0.126				
Epinephelus guttatus	8	0.647	17	2.148	6	1.096	3	0.477
Ginglymostoma cirratum	4	0.324					1	0.159
Gymnothorax funebris	1	0.081	2	0.253	1	0.183		
Gymnothorax moringa	2	0.162	2	0.253				
Lachnolaimus maximus					3	0.548	1	0.159
Lactophrys triqueter	1	0.081	4	0.505			1	0.159
Lutjanus mahogoni	1	0.081	1	0.126	1	0.183	1	0.159
Lutjanus analis							5	0.796
Lutjanus apodus	24	1.942	10	1.263	7	1.279	3	0.477
Lutjanus synagris			15	1.895			30	4.773
Lutjanus cyanopterus	4	0.324	3	0.379	1	0.183	2	0.318
Lutjanus jocu	2	0.162			1	0.183	4	0.636
Mycteroperca bonaci			1	0.126	1	0.183		
Mycteroperca venenosa	4	0.324					3	0.477
Ocyurus chrysurus	1085	87.804	333	42.067	450	82.207	594	94.511
Pterois sp.	54	4.370	23	2.906	7	1.279	16	2.546
Scomberomorus regalis	4	0.324						
Seriola rivoliana					1	0.183		
Sphyraena barracuda	9	0.728	5	0.632	4	0.731	6	0.955
Invertebrates								
Panulirus argus	2	0.162	3	0.379	9	1.644	5	0.796
Totals	1,234	**99.86**	447	**56.47**	512	**93.53**	686	**109.15**
Others*: Caranx crysos, C. latus*								

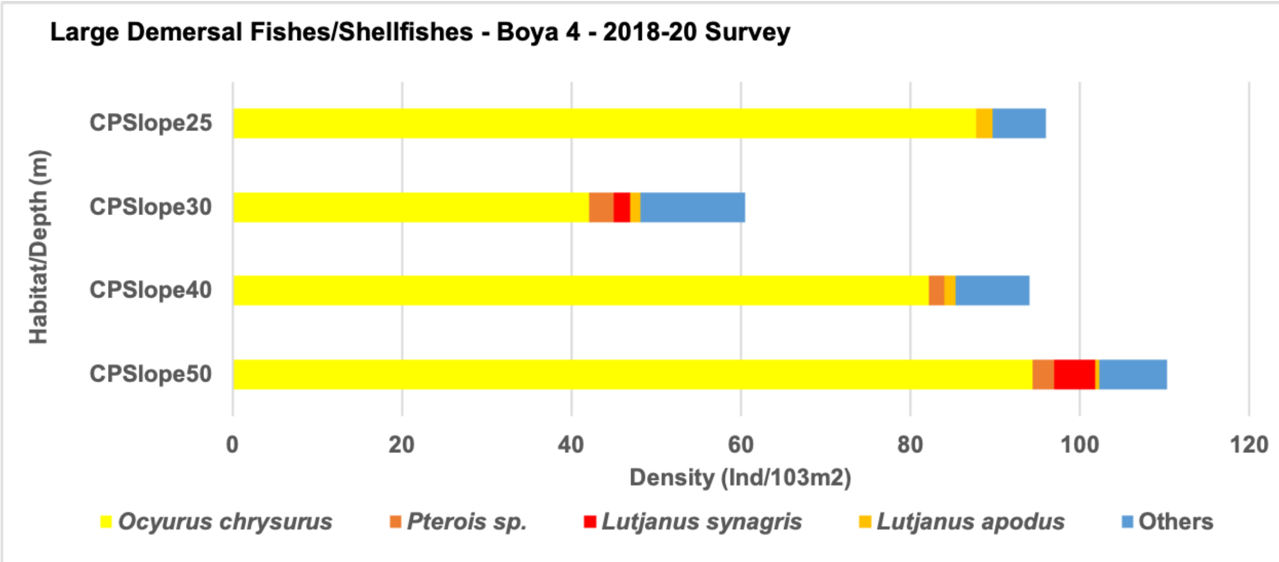

Figure 149. Variations of mean density (Ind/$10^3 m^2$) by commercially important fishes across the 25 – 50m depth profile at Boya 4. Data are means from drift dive belt-transect surveys. 2018-20 survey

Variations of the relative densities of large demersal fish species surveyed from drift belt-transects across the 25 – 50m depth at Boya 4 are displayed in a non-metric multi-dimensional scaling plot (nMDS) of Bray-Curtis similarities in Figure 150. Fish community structure similarities within habitats/depths were relatively low across the entire depth range surveyed despite relatively high contributions of yellowtail snapper (*Ocyurus chrysurus*) to similarity on all habitats/depths. The highest similarity was observed from CPSlope40 (39.3%), contributed by *O. chrysurus*, schoolmaster (*Lutjanus apodus*), great barracuda (*Sphyraena barracuda*), lionfish (*Pterois sp.*), and yellowfin grouper (*Mycteroperca venenosa*) (Table 72). CPSlope50 presented the lowest similarity within habitat/depths (26.2%), mostly contributed by *O. chrysurus*, lionfish, and spiny lobster (*Panulirus argus*).

Average dissimilarity of large fish/shellfish community structure between habitats/depths was highest between CPSlope50 and all other habitat/depths (range: 66.3 – 69.4%). Differences were driven by the relatively higher densities of lane and mutton snappers (*Lutjanus synagris, L. analis*) and great barracuda (*Sphyraena barracuda*), and the relatively lower densities of graysbe, coney (*Cephalopholis cruentatus, C. fulva*), and red hind (*Epinephelus guttatus*) at CPSlope50, compared to other habitats/depths (Table 73).

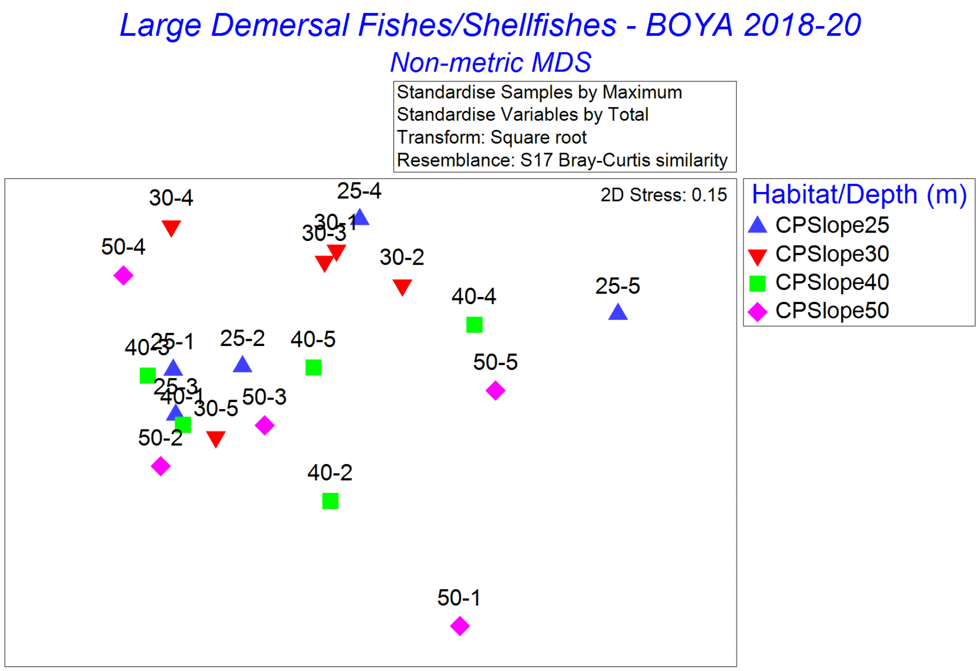

Figure 150. Non-metric multidimensional scaling (nMDS) plot of Bray-Curtis similarities based on the relative densities of large demersal fishes surveyed from 10m x 3m belt-transects across the 25 – 50m depth range at Boya 4, 2018-20 survey

Table 72. Similarity matrix (SIMPER) of large demersal fish/shellfish community structure from the main habitats/depths surveyed across the 25 – 50m rang at Boya 4, with species contributions to similarity percentages, 2018-20 survey.

Habitat/Depth (m)	CPSlope25	CPSlope30	CPSlope40	CPSlope50
Average Similarity (%)	36.4	38.1	39.3	26.2
Fish/Shellfish Spp.				
Ocyurus chrysurus	30.5	34.6	39.8	47.9
Lutjanus apodus	13.7			
Sphyraena barracuda	11.2			
Pterois sp.	11.2	14.4		11.2
Mycteroperca venenosa	8.8			
Balistes vetula		15.1	10.7	
Epinephelus guttatus		13.1		
Panulirus argus			18.5	12.1
Cephalopholis cruentatus			7.4	

Table 73. Dissimilarity matrix (SIMPER) of large demersal fish/shellfish community structure between the main habitats/depths surveyed across the 25 – 50m rang at Boya 4, with species contributions to dissimilarity percentages, 2018-20 survey.

	CPSlope25 vs	CPSlope25 vs	CPSlope25 vs	CPSlope30 vs	CPSlope30 vs	CPSlope40 vs
Habitat/Depths (m)	CPSlope30	CPSlope40	CPSlope50	CPSlope40	CPSlope50	CPSlope50
Average Dissimilarity (%)	60.9	59.9	66.9	60.2	69.4	66.3
Fish/Shellfish Spp.						
Epinephelus guttatus	11.3	8.7		12.4	9.4	
Lutjanus cyanopterus	10.1			8.3	6.2	
Lutjanus apodus	8.8	7.5	7.8	9.6	8.3	
Mycteroperca venenosa	8.6	10.3	8.4			
Lutjanus synagris	8.5			9.7	10.1	7.0
Pterois sp.	7.9	7.6	6.5	9.4	7.0	7.7
Sphyraena barracuda	7.8	10.6	7.4			7.8
Lactophrys triqueter	7.7			7.6	6.7	
Panulirus argus		10.8	8.0	9.8	7.3	10.1
Cephalopholis cruentatus		10.5		9.4		7.3
Cephalopholis fulva		7.9	7.9		6.7	7.8
Lutjanus jocu			8.4			7.4
Lutjanus analis			6.8		6.2	7.4
Balistes vetula					7.6	8.3

Size-frequency Distributions of Large Demersal Fishes

Yellowtail Snapper (*Ocyurus chrysurus*)

A total of 2,535 *O. chrysurus* individuals in the size range of 15 – 38cm FL were observed within drift belt-transects from the insular slope of Boya 4 at depths from 25 – 50m during the 2018-20 survey. Dominant modes of 25cm and 28cm were representative of approximately 65.7% of the total individuals observed within belt-transects Figure 151. The reported length at maturity of *O. chrysurus* at 15cm (Froese and Pauly, 2019) is indicative that most of the individuals were young adults, suggesting that the observed aggregations may not be related to reproductive behavior. The largest specimens were visually estimated in the 36 – 38cm FL size class, which is less than the maximum size at 83.6cm FL reported for the species (Froese and Pauly, 2019).

Lionfish (*Pterois sp.*)

A total of 100 lionfish individuals were observed within belt-transects with a prominent size mode in the 31cm (TL) and a secondary mode in the 34cm TL class (Figure 152). A small cohort in the 18 – 21 cm range included the smallest individuals observed. Still, all individuals were larger than the reported length at maturity of 16cm (Froese and Pauly, 2019). The lack of juvenile lionfishes (*Pterois sp*) may be indicative of recruitment failure within the mesophotic range surveyed at Boya 4. The largest specimens were visually estimated at the maximum size reported of 38 – 40cm TL (Froese and Pauly, 2019).

Schoolmaster Snapper (*Lutjanus apodus*)

A total of 47 *L. apodus* individuals were observed from the insular slope at Boya 4 within the 25 – 50m depth range during the 2018-20 survey. The population included individuals in the size range between 19 – 46 cm (FL) with a main mode at 31cm FL and a secondary mode at 34cm (Figure 153). Using 25 cm as the reported length at maturity (Froese and Pauly, 2019), the *L. apodus* population is comprised by both adult (approx. 80%) and juvenile (approx. 20%) individuals.

Red Hind (*Epinephelus guttatus*)

Red hinds (*E. guttatus*) were present across the 25 – 50m depth profile with a site mean density of 1.06 Ind/10^3m^2. Peak density was observed at CPSlope30 (2.15 Ind/10^3m^2) and the lowest density from CPSlope50 (0.48 Ind/10^3m^2). The size distribution of the red hind population at Boya 4 was strongly skewed towards the larger adult sizes with modes of 31cm and 37cm (TL) (Figure 154). Approximately 15% of the total *E. guttatus* individuals were smaller than the reported length at maturity of 25cm (Froese and Pauly, 2019). Red hind spawning aggregations were not observed at Boya 4, but ripe individuals were noted during the December 2018 and January 2019 surveys.

Queen triggerfish (*Balistes vetula*)

Queen triggerfish (*B. vetula*) were observed throughout the 25 – 50m depth range with a mean density of 0.81 Ind/10^3m^2 (Table 155). Density differences between habitats/depths were not evident (Figure 156). More than 90% of all individuals (16/17) were larger than the reported length at maturity (23.5 cm FL) (Froese and Pauly, 2019). The population size distribution was markedly skewed toward the larger size classes with modes at 31 cm and 37cm FL, and maximum observed size at 46cm FL.

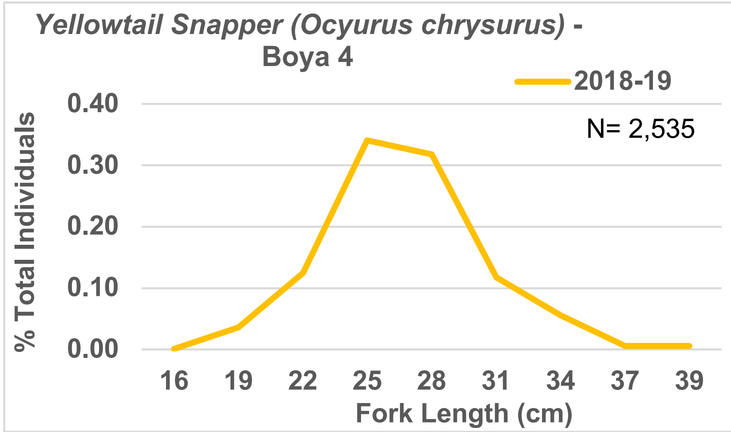

Figure 151. Size distribution of yellowtail snapper (*Ocyurus chrysurus*) within the 25 – 50m depth range at Boya 4, 2018-19 survey

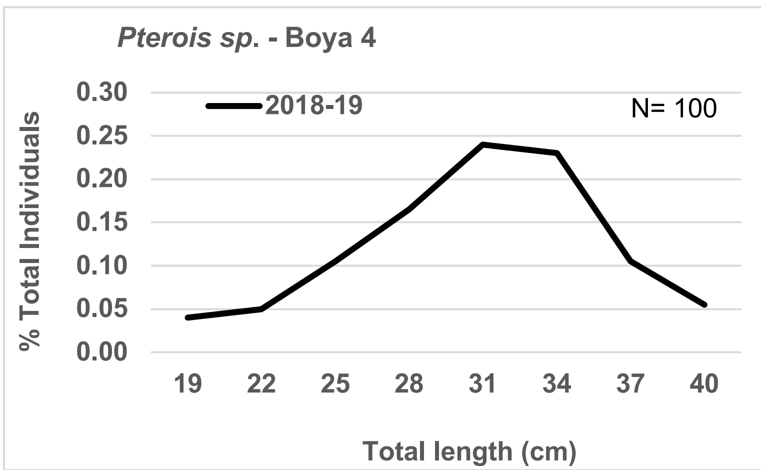

Figure 152. Size distribution of lionfish (*Pterois sp.*) within the 25 – 50m depth range at Boya 4, 2018-19 survey

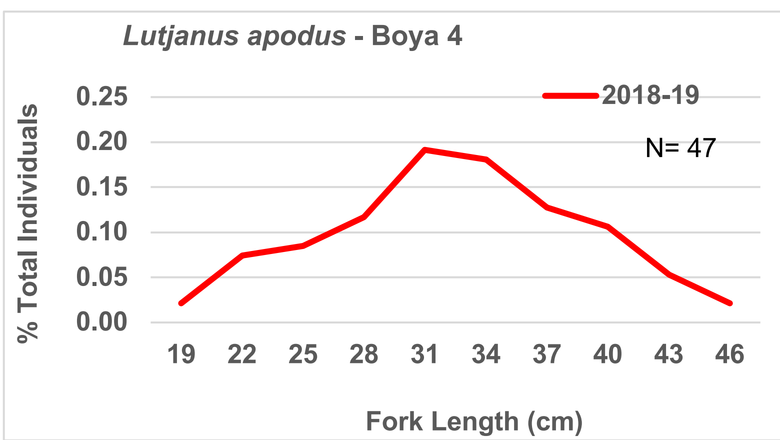

Figure 153. Size distribution of schoolmaster (*Lutjanus apodus*) within the 25 – 50m depth range at Boya 4, 2018-19 survey

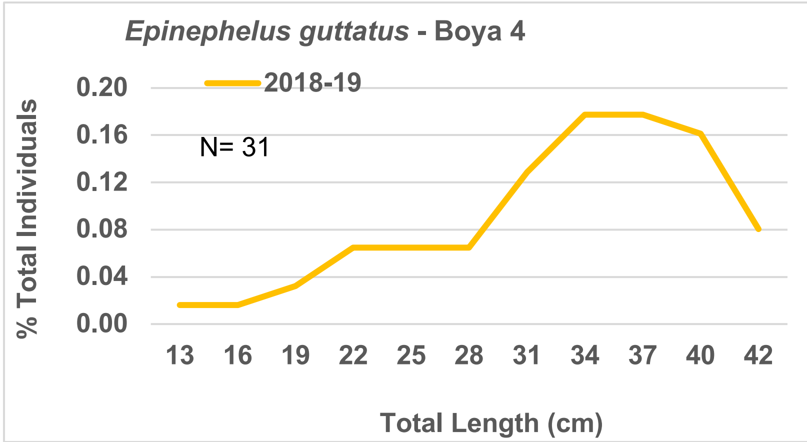

Figure 154. Size distribution of red hind (*Epinephelus guttatus*) within the 25 – 50m depth range at Boya 4, 2018-19 survey

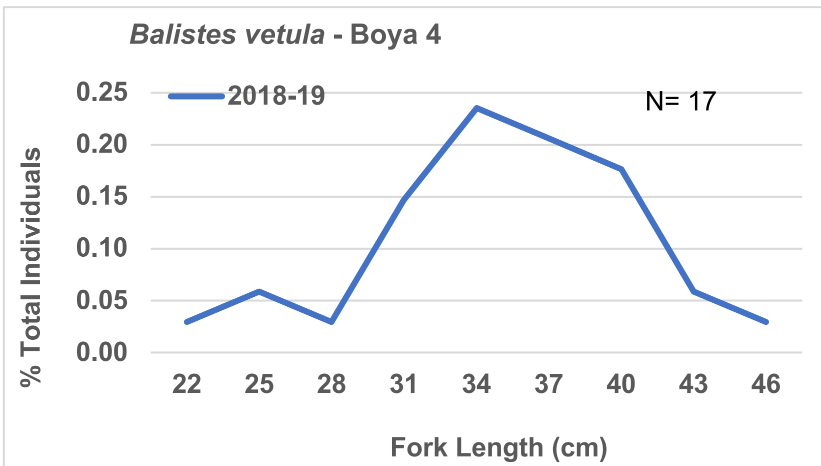

Figure 155. Size distribution of queen triggerfish (*Balistes vetula*) within the 25 – 50m depth range at Boya 4, 2018-19 survey

Coney (*Cephalopholis fulva*), Graysbe (*C. cruentatus*) and other groupers

The smaller groupers, such as the coney (*Cephalopholis fulva*) and graysbe (*C. cruentata*) were also present throughout the 25 – 50m depth profile with site mean densities of 0.72 Ind/10^3m^2 and 0.94 Ind/10^3m^2, respectively. Distinct habitat/depth related density distribution patterns were not evident for any of the two species, except that *C. cruentata* was not observed from CPSlope50. Both populations were largely comprised by adult individuals. Yellowfin and black groupers (*Mycteroperca venenosa, M. bonaci*) were observed in relatively low numbers (2 and 7, respectively) with mean densities of 0.22 Ind/10^3m^2 and 0.06 Ind/10^3m^2, respectively (Table 69).

Only adult individuals (52 – 70 cm TL) from the aforementioned species were observed within the 25 -50m range at Boya 4 during the 2018-19 survey.

Great barracuda (*Sphyraena barracuda*)

A total of 24 great barracuda (*Sphyraena barracuda*) individuals were observed throughout the 25 – 50m depth profile with a site mean density of 0.75 Ind/10^3m^2. Distinct vertical density distribution patterns were not evident. Great barracudas were often observed near the surface and followed divers all the way to the bottom across the survey areas of the insular slope. The population size distribution was dominated by adult individuals in the 60 – 100 cm FL range, with a mode at 70 cm FL.

Spiny lobsters (*Panulirus argus*)

Spiny lobsters (*P. argus*) were present throughout the 25 – 50m depth profile at the Boya 4 insular slope with a site mean density of 0.59 Ind/10^3m^2. Peak density was noted at CPSlope40 (1.64 Ind/10^3m^2), probably influenced by the occurrence of abundant crevices and ledges along that depth contour. The population size distribution was characterized by a dominant mode at 10cm carapace length (CL) and maximum size up to 18 cm CL (Figure 156).

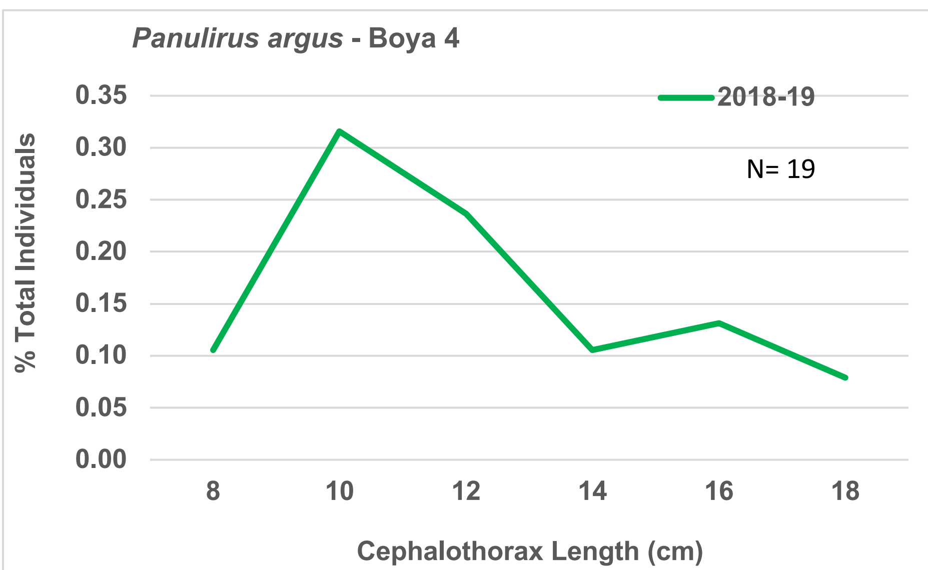

Figure 156. Size distribution of spiny lobster (*Panulirus argus*) within the 20 – 50m depth range at Boya 4, 2018-19 survey

Photo Album 6
Colonized Pavement Slope – (CPSlope) BOYA

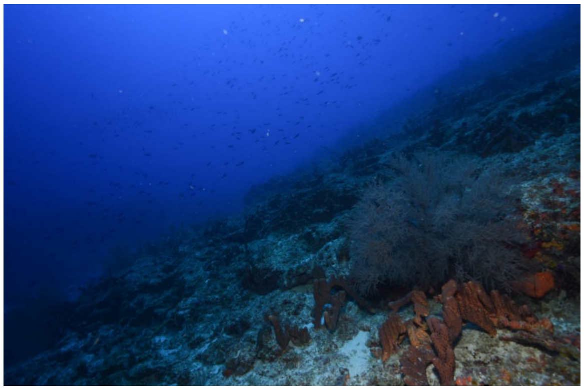



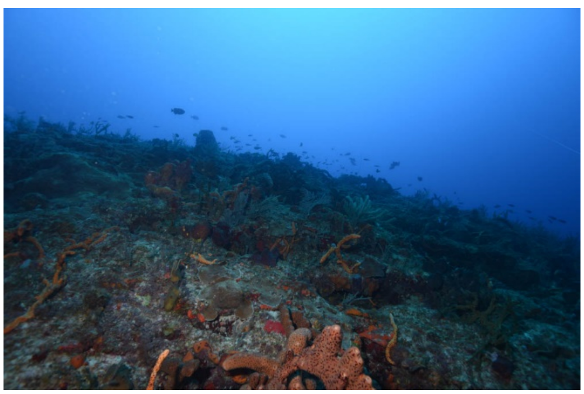


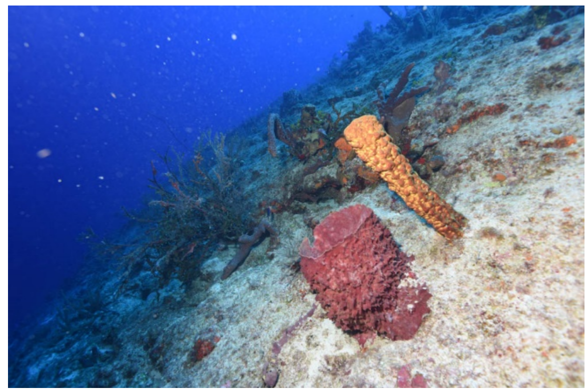

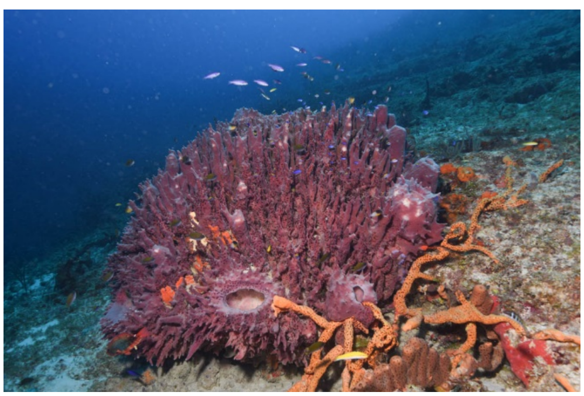

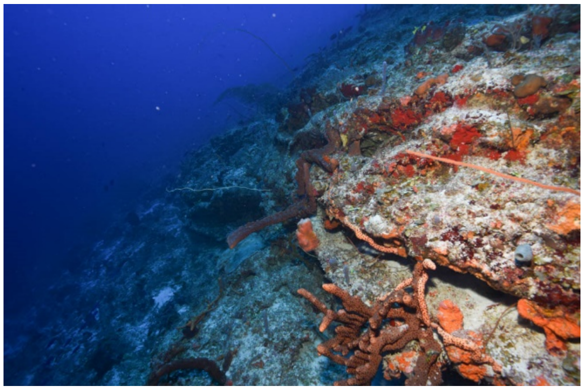

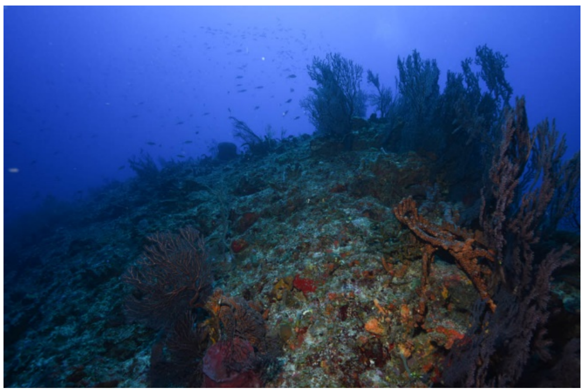

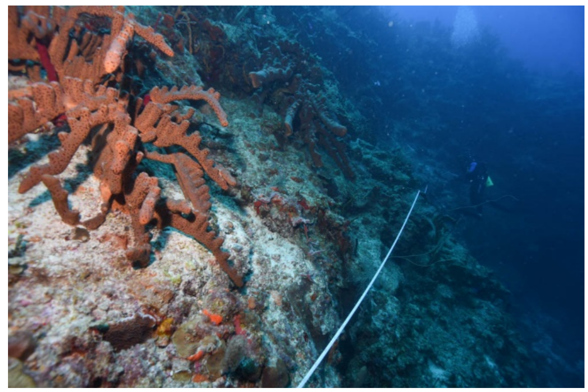

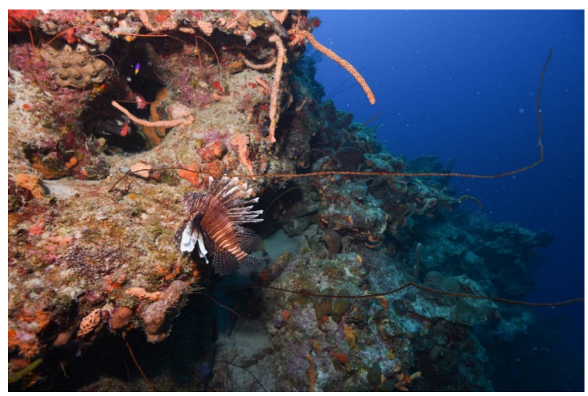

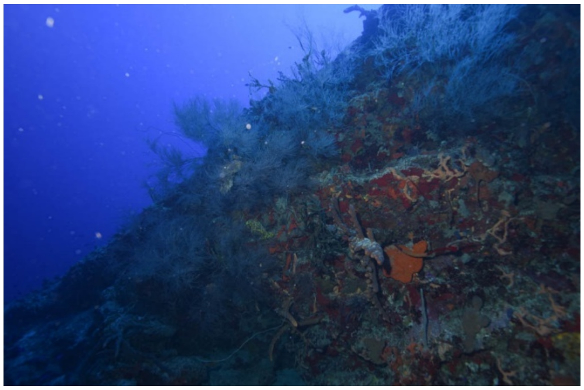

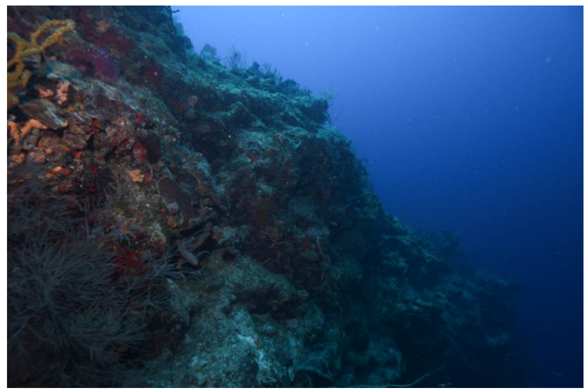

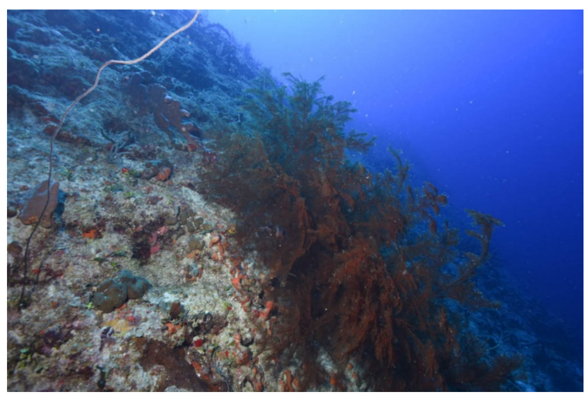

Broad-scale Spatial Patterns of Numerically Dominant Large Demersal Fishes/Shellfishes, 2018-20 Survey

The community structure of large demersal fishes/shellfishes surveyed from mesophotic habitats in the 25 – 50m depth range during 2018-20 was characterized by the presence of numerically dominant populations. An assemblage of nine species (seven fishes and two shellfishes) represented more than 90% of the total individuals observed within drift belt-transects from all sites. Figures 157 – 159 show the broad scale distribution of the numerically dominant groupers (Serranidae), snappers (Lutjanidae), and shellfishes (spiny lobster and queen conch) across all sites surveyed during 2018-20. Statistically significant density differences between sites were found for all seven numerically dominant fish species and for spiny lobster (*Panulirus argus*) (One-way ANOVA; $p < 05$). Density differences between sites of queen conch (*Lobatus gigas*) were also very pronounced but masked by the high sampling variability associated with patchy distributions (ANOVA; $p = 0.077$). The yellowtail snapper (*Ocyurus chrysurus*) presented the highest mean density across all surveyed sites (study mean: 13.92 Ind/10^3m^2). Statistically significant differences (ANOVA; $p < 0.0001$) were associated with the higher densities at BOYA relative to all other sites (Figure 161). Yellowtail snappers were observed within drift belt-transects from all sites, but the site mean density at BOYA (77.69 Ind/10^3m^2) was at least one order of magnitude higher than at any other site. A colonized pavement slope habitat (CPSlope) prevailed across the entire 25 – 50m depth profile at BOYA and density variations of *O. chrysurus* associated with depth were statistically insignificant (ANOVA; $p > 0.05$).

Yellowtail snappers formed a linear (curtain shaped) aggregation roughly parallel to the steep insular slope at BOYA making frequent incursions to the benthos in what appeared to be feeding excursions. Reproductive behavior was not observed. It is uncertain if the high density of *O. chrysurus* at BOYA is a seasonal phenomenon, or if such high aggregation of fishes prevails year-round since our surveys were performed mostly between January through March 2019. The steep slope morphometry at BOYA may be enhancing topographically steered flows (water current patterns) that increase the flux of zooplankton across the face of the slope influencing the concentration of zooplanktivores that may be highly relevant in what appears to be a mostly pelagic food web supporting yellowtail snappers. On the other hand, statistically significant differences (ANOVA; $p < 0.0001$) associated with lower densities of red hind (*Epinephelus guttatus*), coney (*Cephalopholis fulva*), queen triggerfish (*Balistes vetula*), and queen conch (*Lobatus gigas*) were evidenced from BOYA relative to adjacent sites (Figures 162 – 163).

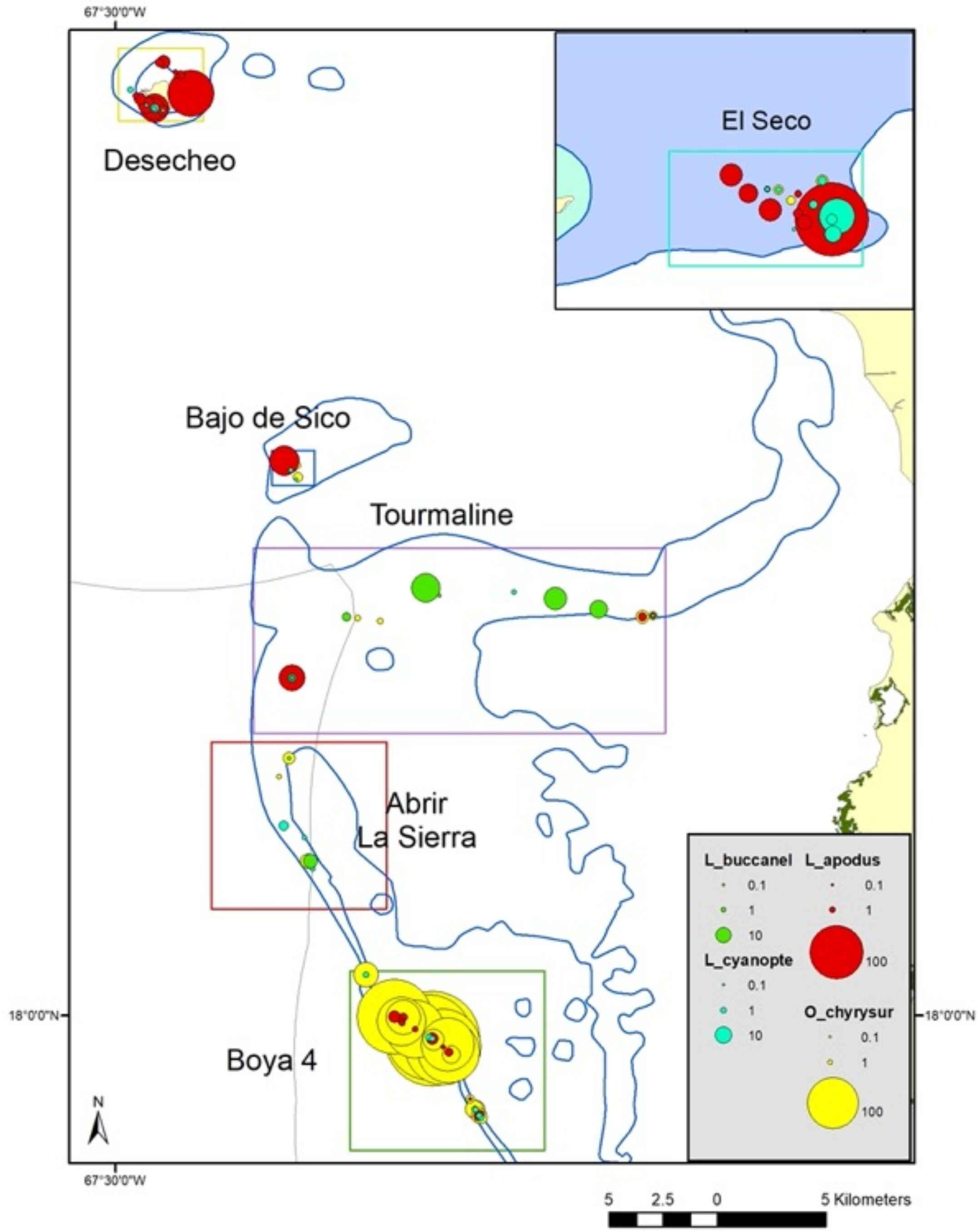

Figure 157. Broad-scale spatial density distribution of numerically dominant snappers (Lutjanidae) from mesophotic habitats at sites surveyed in the west coast and Isla de Vieques (El Seco) during 2018-20.

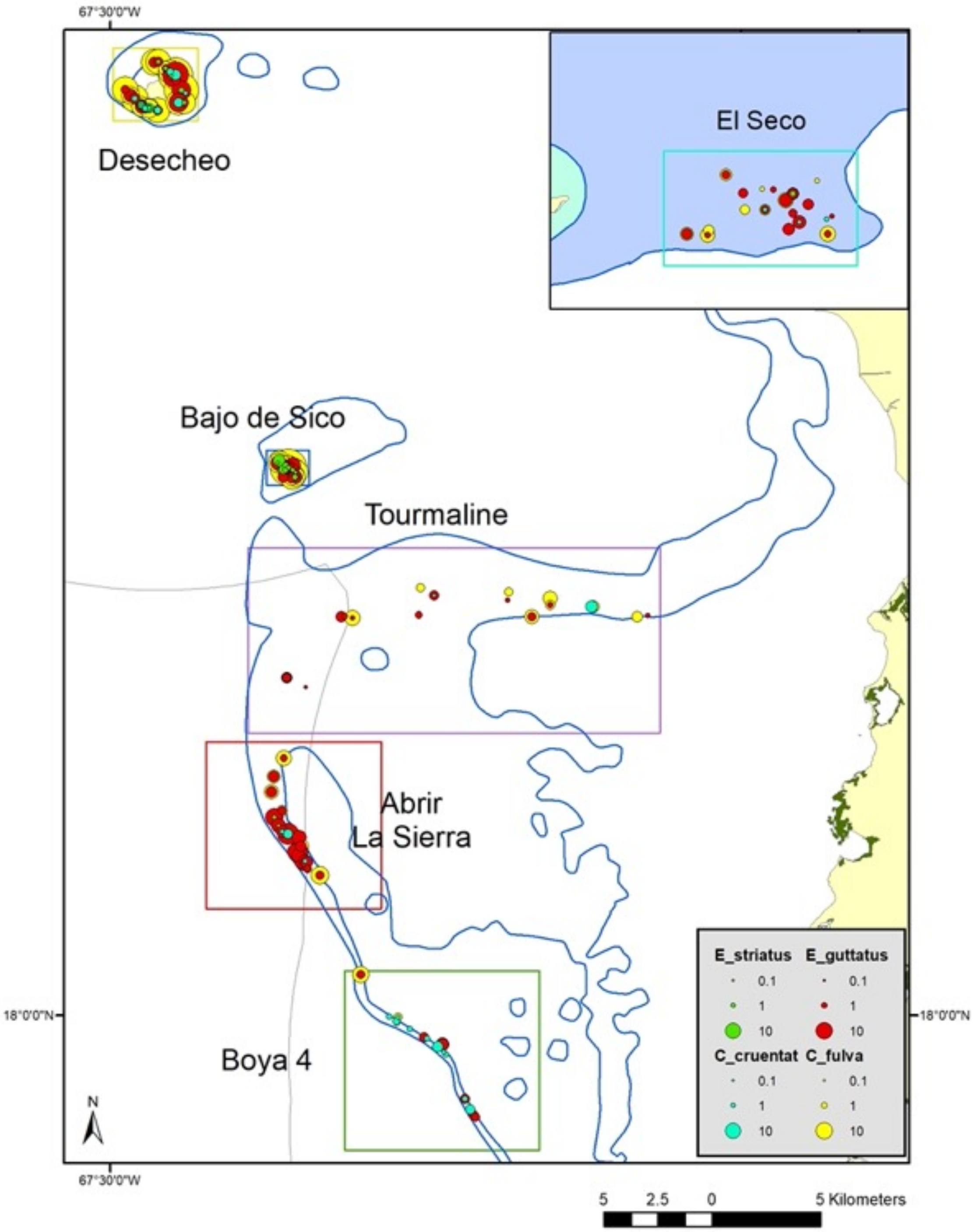

Figure 158. Broad-scale spatial density distribution of numerically dominant groupers (Serranidae) from mesophotic habitats at sites surveyed in the west coast and Isla de Vieques (El Seco) during 2018-20.

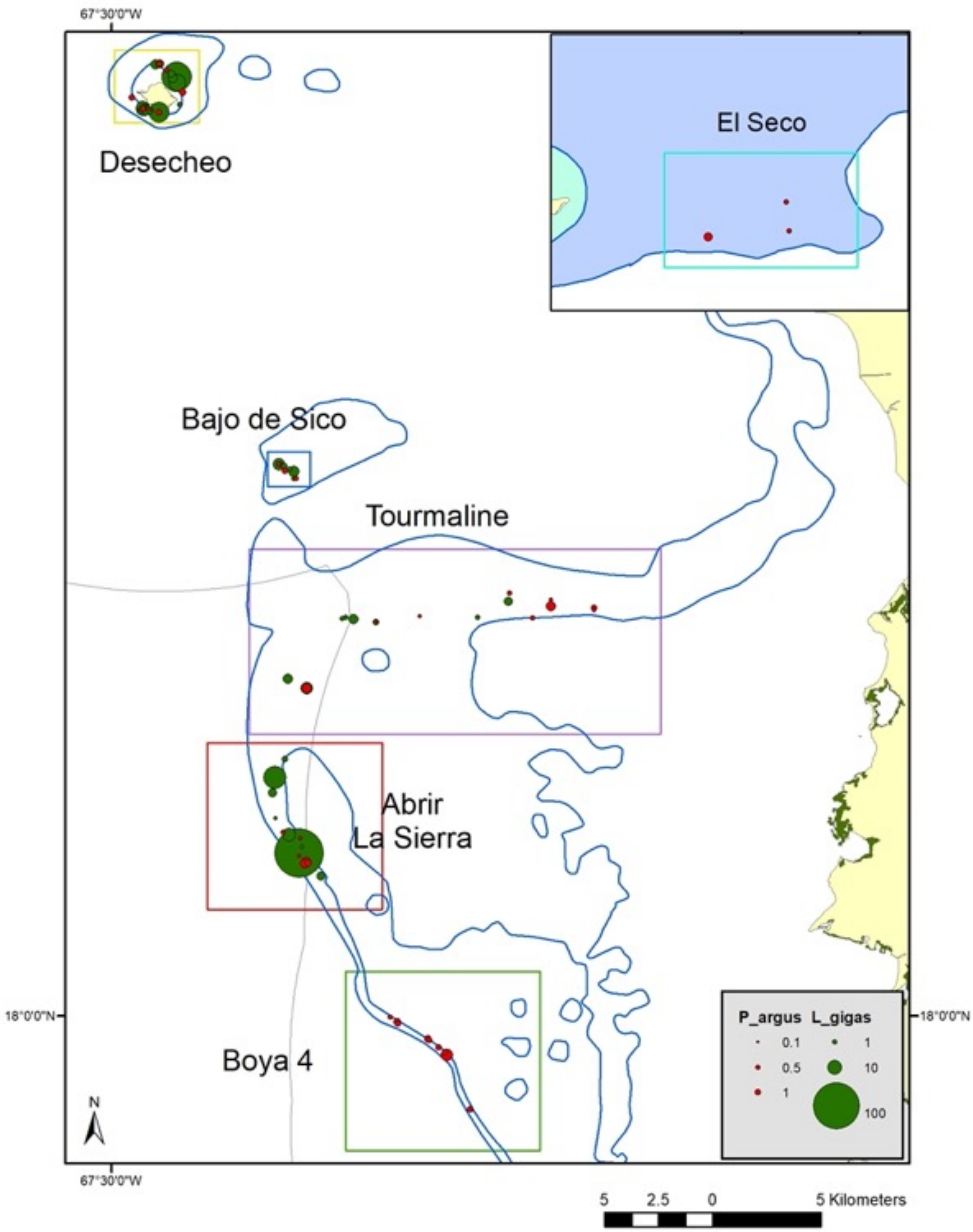

Figure 159. Broad-scale spatial density distribution of spiny lobster (*Panulirus argus*) and queen conch (*Lobatus gigas*) from mesophotic habitats at sites surveyed in the west coast and Isla de Vieques (El Seco) during 2018-20.

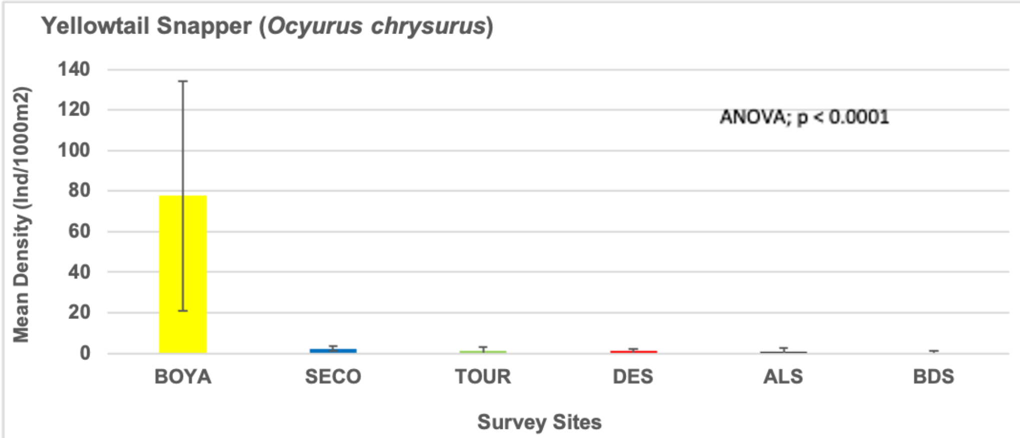

Figure 160. Mean density variations of yellowtail snapper (*Ocyurus chrysurus*) from mesophotic habitats in the 25 – 50m depth range at sites surveyed in the west coast and Isla de Vieques (El Seco) during 2018-20. Error bars are 95% confidence limits.

Red hinds (*Epinephelus guttatus*) and coneys (*Cephalopholis fulva*) exhibited high plasticity with distributions across all benthic habitats, depths, and sites within the 25 – 50m range, except those associated with steep slopes and or walls (BOYA, TOUR). Significantly higher densities of red hind were observed from ALS relative to all other sites, except DES, and from DES, BDS, and SECO relative to BOYA and TOUR (ANOVA; $p < 0.0001$) (Figure 161). Densities of red hind peaked at colonized pavement reef tops (CPRT) of ALS, DES, BDS and SECO, all characterized by horizontally oriented platforms colonized by sponges, corals, turf algae, and moderate amounts of sand cover. Coneys were the second most abundant large demersal fish species surveyed within drift belt-transects with a study mean of 11.4 Ind/10^3m^2. Density of coneys was higher at DES than at any other site (ANOVA; $p < 0.0001$) (Figure 162), influenced perhaps by the availability of preferred horizontally oriented habitats, such as ACR25 and CPRT30-40.

Densities of queen triggerfish (*Balistes vetula*) were higher at ALS and TOUR than at DES and BOYA (ANOVA; $p < 0.0001$) (Figure 163). Peak densities of queen triggerfish were associated with horizontally oriented habitats, particularly rhodolith beds (Rhod) and CPRT's, both of which are lacking at BOYA within the surveyed depth range. The lower densities at DES and BDS, relative to ALS and TOUR may be related to the higher intra-shelf connectivity with neritic nursery habitats. All queen triggerfish observed from mesophotic habitats were adults that use the rhodolith bed habitat for mating and nesting functions. Thus, replenishment of such adult populations may be limited by the deep oceanic barriers separating DES and BDS from neritic nurseries. Likewise, such lack of direct intra-shelf connectivity may be the main driver for the absence of hogfish (*Lachnolaimus maximus*) from DES and BDS.

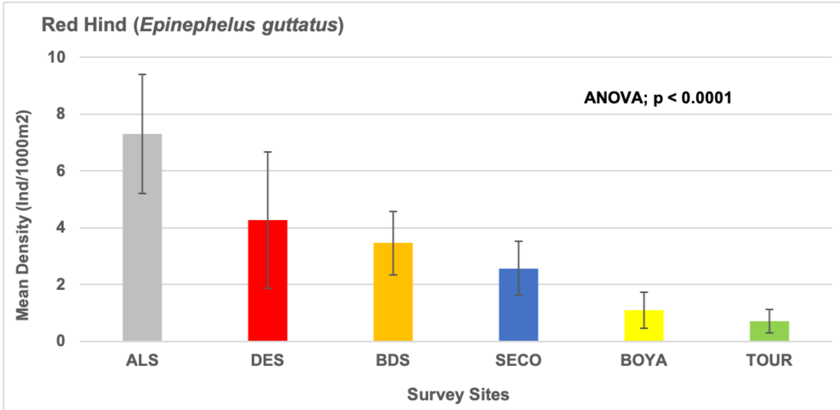

Figure 161. Mean density variations of red hind (*Epinephelus guttatus*) from mesophotic habitats in the 25 – 50m depth range at sites surveyed in the west coast and Isla de Vieques (El Seco) during 2018-20. Error bars are 95% confidence limits.

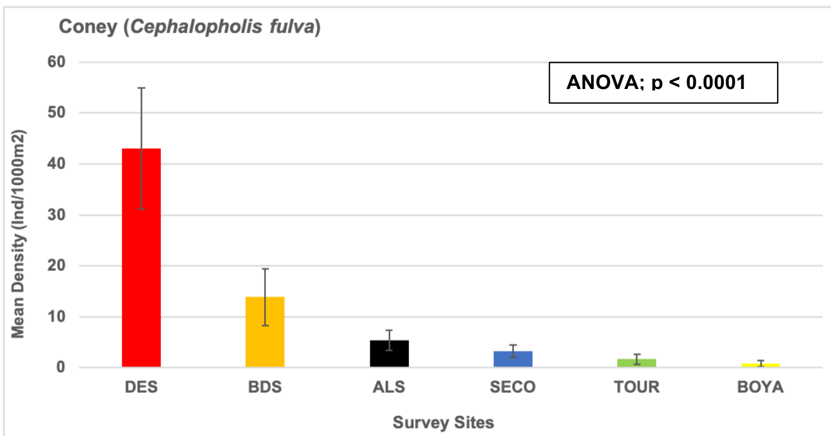

Figure 162. Mean density variations of coney (*Cephalopholis fulva*) from mesophotic habitats in the 25 – 50m depth range at sites surveyed in the west coast and Isla de Vieques (El Seco) during 2018-20. Error bars are 95% confidence limits.

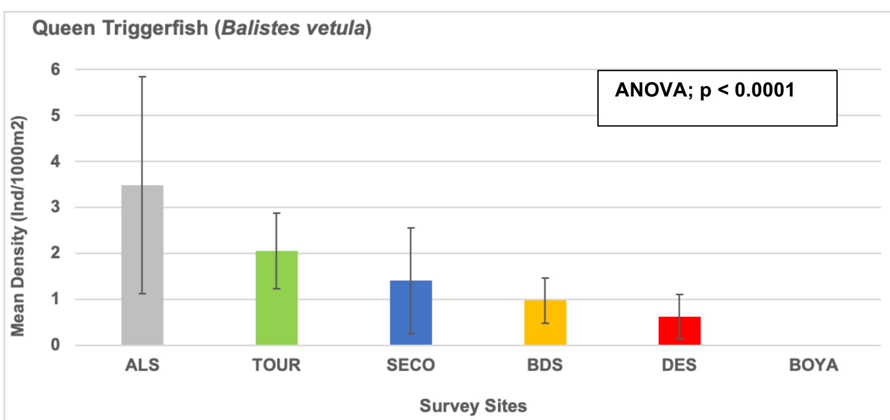

Figure 163. Mean density variations of queen triggerfish (*Balistes vetula*) from mesophotic habitats in the 25 – 50m depth range at sites surveyed in the west coast and Isla de Vieques (El Seco) during 2018-20. Error bars are 95% confidence limits.

Schoolmaster snapper (*Lutjanus apodus*) was a numerically dominant large demersal species from all sites, except ALS, probably due to the overall lack of high relief habitats at ALS. Mean site density was higher at SECO, but the within site variability was so high that statistically significant differences were only related to the higher densities at DES and Boya, relative to ALS (ANOVA; $p < 0.0001$) (Figure 164). Densities at SECO were driven by several schooling aggregations and solitary individuals observed from high rugosity coral reef habitats at BCR35-40 and PCR36-42. Conversely, minimum densities were evidenced from essentially flat rhodolith (Rhod) beds across all sites. Schoolmaster exhibited highly aggregated distributions, with variance to mean ratios of 39:1 (mean from all sites - excluding Rhod habitats). Schooling aggregations consisted mostly of young adults across all sites without any clear indicators of reproductive behavior, except at SECO where one large school of only adults was observed in the vicinity of a multispecies spawning aggregation site within the PCR36-42 habitat. A similar spatial density pattern was noted for cubera snapper (*Lutjanus cyanopterus*) with higher densities at SECO than at any other site (ANOVA; $p = 0.021$) (Figure 165). Peak density (45.3 Ind/10^3m^2) was observed from PCR36-42 associated with a spawning aggregation of 73 large adult individuals displaying clear signs of reproductive behavior, including distinctive coloration and milt release. Cubera snappers were observed within transects in another seven out of the 15 stations from non-rhodolith habitats at SECO with higher prevalence at PCR36-42 and BCR35-40.

Higher density of blackfin snapper (*Lutjanus buccanella*) was observed from TOUR, compared to all other sites (ANOVA; $p < 0.0001$) (Figure 166), driven by peak densities at CPWall50 (11.4 Ind/10^3m^2) and CPSlope31-40 (3.2 Ind/10^3m^2). Blackfin snappers were not observed from habitats shallower than 40m (e. g. ACR25, CPSlope25-30), nor from the rhodolith habitat (Rhod30-50) at TOUR. Such pattern suggests that both slope inclination, morphometry, and depth influenced its distribution. Blackfin snapper appeared to be a slope species with a habitat range much deeper than our survey depth at 50m, but schooling aggregations penetrated shallower depths within the slope habitat as a forage strategy. Differences between sites were probably related to the distribution of habitats surveyed within the 25 – 50m range at the different sites. For example, deep slope habitats were not prominent and not surveyed at SECO, and slope habitats at DES were discontinuous with deeper sections of the slope as they were interrupted by an essentially flat rhodolith bed in the 40 – 50m range. Interestingly, blackfin snappers were not observed from west coast slope sites at ALS and BOYA, nor from mesophotic habitats at BDS. It is possible that slope features below our maximum 50m survey depth are relevant in determining the occurrence of blackfin snappers within the 30 – 50m depth range at the insular slope.

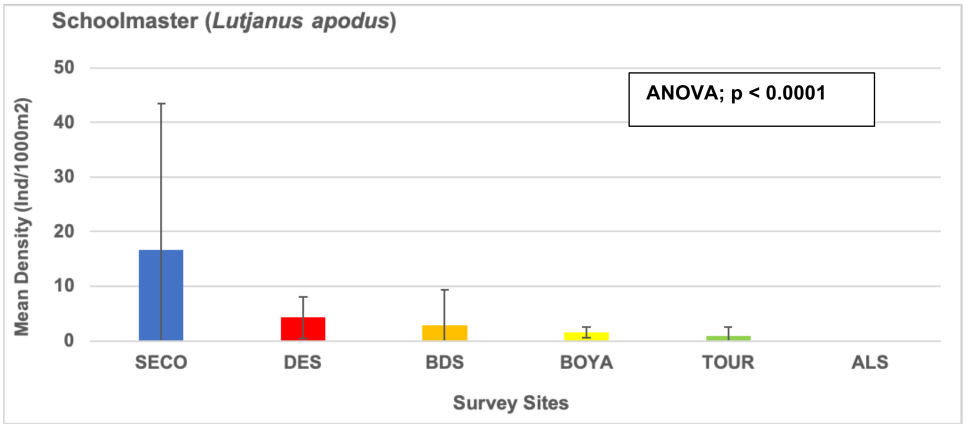

Figure 164. Mean density variations of schoolmaster (*Lutjanus apodus*) from mesophotic habitats in the 25 – 50m depth range at sites surveyed in the west coast and Isla de Vieques (El Seco) during 2018-20. Error bars are 95% confidence limits.

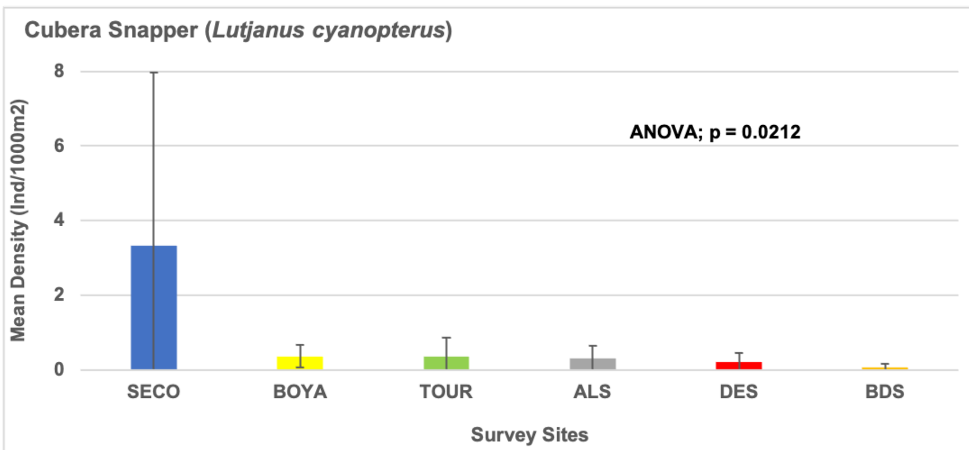

Figure 165. Mean density variations of cubera snapper (*Lutjanus cyanopterus*) from mesophotic habitats in the 25 – 50m depth range at sites surveyed in the west coast and Isla de Vieques (El Seco) during 2018-20. Error bars are 95% confidence limits.

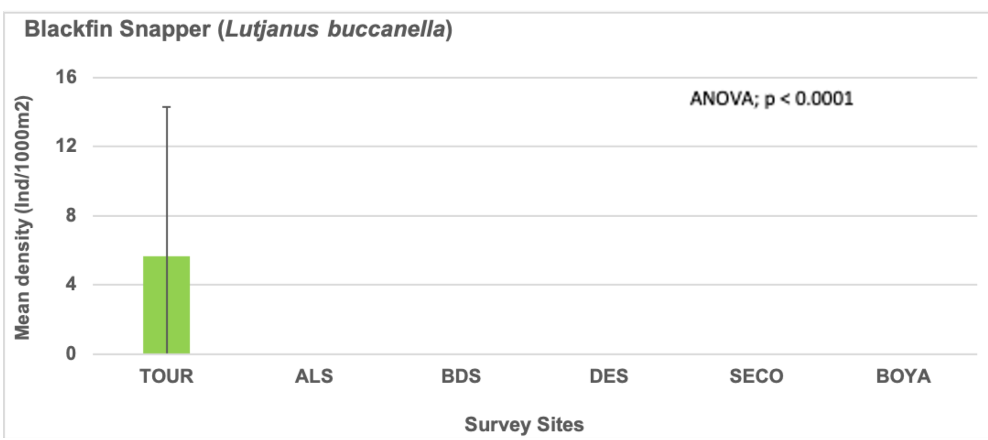

Figure 166. Mean density variations of blackfin snapper (*Lutjanus buccanella*) from preferred mesophotic habitats (CPSlope 40-50 + CPWall50) in the 25 – 50m depth range at sites surveyed in the west coast and Isla de Vieques (El Seco) during 2018-20. Error bars are 95% confidence limits.

The spatial distribution of queen conch (*Lobatus gigas*) from mesophotic habitats surveyed by drift belt-transects within the 25 – 50m depth range at sites in the west coast and Isla de Vieques (SECO) during 2018-20 is shown in Figure 167. The site density mean from preferred habitats (Rhodo + CPRT only) at ALS was at least 375% higher than at any other site surveyed but differences were statistically insignificant (ANOVA; p= 0.077) due to the high sampling variability imposed by its aggregated (patchy) distribution (var/mean = 10.8). High concentrations of *L. gigas* were observed at ALS mostly from Rhod40 (94.0%). This site is known to function as a mating and nesting site for adult queen conch which use the rhodolith nodules to construct a nest where they attach egg sacks (Garcia-Sais et al., 2012). Given the high availability of benthic algae, rhodolith beds also represent prime grazing grounds for queen conch. Given the high sampling variability it is not possible to demonstrate depth preferences of queen conch from surveyed sites, but all of the large aggregations were observed in the 35 – 40m range, and very few individuals were observed deeper than 40m from all sites. Differences in the composition of benthic algae, pelagic larval dispersal and recruitment dynamics may have played an important role in the observed density distribution of queen conch between surveyed sites. The rhodolith bed habitat at ALS is located within an outer shelf basin protected by two slope walls. This may have served as a sheltered environment during the passing of Hurricanes Irma and Maria in 2017 and/or winter storm Riley in 2018, before our survey, influencing the higher densities of queen conch at ALS.

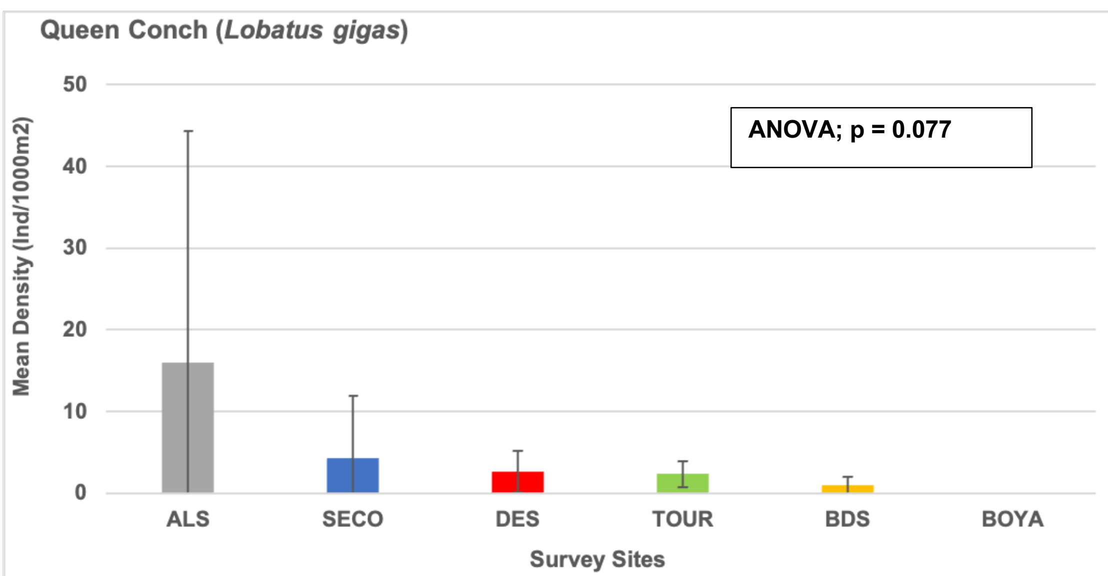

Figure 167. Mean density variations of queen conch (*Lobatus gigas*) from preferred mesophotic habitats (Rhod + CPRT) in the 25 – 50m depth range at sites surveyed in the west coast and Isla de Vieques (El Seco) during 2018-20. Error bars are 95% confidence limits.

Spiny lobsters (*Panulirus argus*) were observed from all sites, benthic habitats, and depths surveyed with higher site densities at TOUR and BOYA, relative to other sites (ANOVA; p = 0.027) (Figure 168). Most of the spiny lobsters at TOUR were observed from the CPSlope habitat in the 25 – 40m depth range, an environment of low topographic relief hard bottom and sand. Lobsters were associated with small coral heads and crevices within the pavement surrounded by sand. At BOYA, spiny lobsters were found inhabiting crevices and ledges particularly from CPSlope30 and CPSlope40. Only one spiny lobster was observed from rhodolith habitats at BDS and none were observed from the BCR nor PCR habitats at SECO.

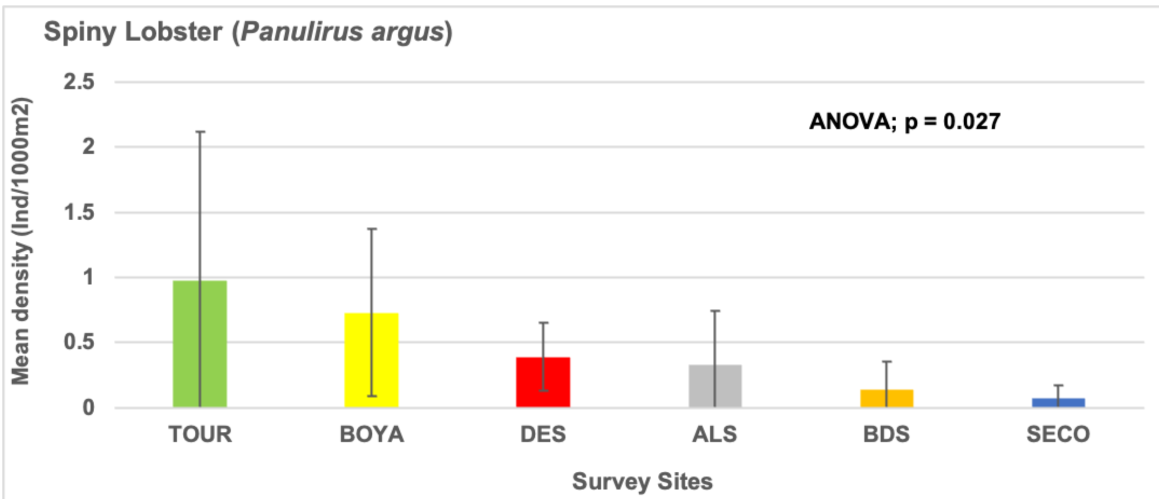

Figure 168. Mean density variations of spiny lobster (*Panulirus argus*) from preferred mesophotic habitats (no Rhodo) in the 25 – 50m depth range at sites surveyed in the west coast and Isla de Vieques (El Seco) during 2018-20. Error bars are 95% confidence limits.

Broad-scale spatial distribution patterns of large demersal fishes and shellfishes were pronounced even between adjacent sites surveyed in the west coast outer shelf and slope. At such spatial scales, differences appeared related to adaptations and/or preferences of numerically dominant species for habitats with particular slope inclination, morphometry, reef rugosity, and depth. In general, groupers (Serranidae), queen triggerfish (*Balistes vetula*), and queen conch (*Lobatus gigas*) prevailed in horizontally oriented habitats, whereas snappers (Lutjanidae) were more associated with steep slopes and high rugosity reef habitats.

Direct intra-shelf connectivity with nursery habitats appeared to be an important driver of broad-scale spatial distributions of large demersal fishes and shellfishes. Perhaps with the exception of schoolmaster (*Lutjanus apodus*), snappers (Lutjanidae) were more abundant from mesophotic habitats within the main insular slope (ALS, TOUR, BOYA, SECO) than at DES and BDS, separated from mainland neritic habitats by deep oceanic channels. Snapper nursery habitats include submerged mangrove roots, seagrass beds, and shallow coral reefs, which are not directly connected with the mesophotic habitats at the oceanic island of DES, nor at the BDS seamount. A similar argument can be raised for hogfish (*Lachnolaimus maximus*), which appeared to be more associated with the mainland shelf sub-mesophotic habitats at 25m than at either BDS or DES. Conversely, groupers (Serranidae) in general were more abundant at DES and BDS than from mainland sites, perhaps with the exception of red hinds (*Epinephelus guttatus*) at ALS. Groupers are known to undertake offshore larval development and relatively longer pelagic larval duration than snappers (Leis and Miller, 1976; Leis, 1982; Brothers et al., 1983; Ramirez-Mella and Garcia-Sais, 2003). Such extended pelagic larval adaptations may favor recruitment into offshore sites, such as oceanic islands and seamounts.

Conclusions

1) Benthic algae were the dominant sessile-benthic category in terms of substrate cover from all mesophotic habitats, depths, and sites surveyed during the baseline characterizations and the 2018-20 monitoring survey.
2) Statistically significant depth/habitat related patterns were detected from the main taxonomic algal components during the 2018-20 survey. Turf algae was dominant at colonized pavement reef tops (CPRT) in the upper 25 – 30m range surveyed but declined with depth. Conversely, encrusting fan alga, *Lobophora sp*., and y-twig alga, *Dictyota sp*., increased substrate cover with depth, representing the dominant components at rhodolith (Rhodo) bed habitats typically found within the 40 – 50m range at most sites.
3) Differences of cover by benthic algae between surveys were statistically insignificant but marked variations and dominance phase shifts were evidenced for different algal taxonomic components within the total assemblage. Reef substrate cover by *Lobophora sp*., fleshy algae (mostly *Dictyota sp*), and crustose Peyssonnelid red algae (including *Ramicrusta sp*.) increased during the 2018-20 survey at all surveyed sites. Corresponding declines of cover by turf algae were measured. The sharp increment of cover by *Ramicrusta sp*. at SECO was associated with a significant decline of substrate cover by stony corals, particularly from the CPRT habitat prevailing in the 22 - 28m depth range.
4) Increased nutrient availability, contributed by upwelling and/or sediment resuspension associated with hurricane activity are proposed as potential drivers of the increased reef substrate cover by *Lobophora sp*. and fleshy algae. Turf algae may have been also affected by large-scale sand movements induced by hurricanes across the outer shelf and slope.
5) The increased cover by *Ramicrusta sp*. at SECO coincided with the proliferation of this alga throughout the east coast neritic reefs but was facilitated at SECO by the availability of new hard substrates for colonization upon stony coral mortality at the CPRT habitat.
6) Statistically significant habitat/depth related distribution patterns of substrate cover by stony corals were evident from all sites except BOYA during the 2018-20 survey. Higher cover was associated with habitats (ACR and CPRT) within the sub-mesophotic 22 – 28m depth range, compared to other habitats/depths from all sites except SECO, where high coral cover BCR and PCR habitats were distributed deeper within the 30 – 40m depth range.
7) Habitat/depth related distribution patterns were noted for stony coral species during the 2018-20 survey. Higher cover by the *Orbicella faveolata/franksi* complex was associated

with ACR and CPRT habitats in the 22 – 28m depth range, whereas lettuce corals *Agaricia lamarki, A. grahamae, A. undata* prevailed at the Rhodo habitat in the 40 – 50m depth range. Mustard-hill coral (*Porites astreoides*) was ubiquitous throughout the surveyed habitat/depth range. Black corals, particularly the bushy black coral, *Antipathes caribbeana* were mostly associated with the deeper sections of colonized pavement slope (CPSlope) and wall (CPWall) habitats in the 40 – 50m range.

8) Reef substrate cover by stony corals remained stable between the baseline and the 2018-20 monitoring survey at all sites, except at SECO, where statistically significant declines of substrate cover were measured from all habitats and depths. Mechanical damage associated with hurricane activity, coral bleaching, and coral disease outbreak(s) (including SCTLD) were proposed as potentially important drivers of the measured stony coral loss at SECO during 2018-20. Statistically significant reductions of cover by soft corals (gorgonians) were also measured from the CPRT habitat at SECO, perhaps also influenced by hurricane-related mechanical damage, surge and sand abrasion effects.
9) A total of 132 fish species and two shellfishes (queen conch and spiny lobster) were identified from belt-transects within the 22 – 50m depth range at sites surveyed during 2018-20. The community structure of small demersal fishes was characterized by the numerical dominance of a relatively small assemblage of species, many of which exhibited highly aggregated distributions associated with schooling behavior (e.g. *Clepticus parrae, Chromis cyanea, C. multilineata, C. insolata, Coryphopterus personatus, Thalassoma bifasciatum, Schultzea beta, Lutjanus buccanella, L. apodus*), and others with more uniform distributions (e.g. *Stegastes partitus, Centropyge argi, Halichoeres garnoti, Cephalopholis fulva*).
10) Strong habitat/depth related affinities of small demersal fishes were detected and contributed both to community structure similarities within habitats/depths and to dissimilarities between the different habitats/depths surveyed across the 22 – 50m depth gradient.
11) Habitat plasticity across the entire 25 – 50m depth range was exhibited by an assemblage of small demersal fishes, including some numerically dominant species, such as bicolor damselfish (*S. partitus*), bluehead and yellowhead wrasse (*T. bifasciatum, H. garnoti*), coney (*C. fulva*), and red hind (*E. guttatus*). This assemblage contributed to the similarity of community structure between habitats/depths from most surveyed sites.
12) Density differences of small demersal fishes between surveys depended on habitat/depths but were mostly influenced by the high sampling variability introduced by

the aggregated distributions of numerically dominant species. Of particular relevance was the statistically significant density decline between surveys of masked goby (*Coryphopterus personatus*), a numerically dominant species from coral reef habitats in baseline surveys. It is suggested that this species was highly vulnerable to the surge and sand abrasion effects of hurricanes and winter storms during 2017-18 and still unable to replenish its populations to the pre-hurricane status.

13) Large demersal fishes and shellfishes surveyed by drift belt-transects during 2018-20 included a total assemblage of 7,079 fish individuals, 277 queen conch (*Lobatus gigas*), and 40 spiny lobsters (*Panulirus argus*).

14) Species specific habitat/depth related density differences of large demersal fishes depended on site. Some of the most prominent patterns included higher densities of queen triggerfish (*B. vetula*) from rhodolith habitats at ALS, BDS, and TOUR, higher densities of red hind (*E. guttatus*) from CPRT and rhodolith habitats at ALS and SECO, higher densities of yellowtail snapper (*O. chrysurus*) at ACR25 habitats of DES and TOUR, and higher densities of queen conch from rhodolith (*L. gigas*) habitats at ALS and TOUR.

15) Habitat/depth affinities by numerically dominant large demersal fishes/shellfishes appeared to be related to habitat slope, reef morphology, and depth. Red hind (*E. guttatus*), coney (*C. fulva*), queen triggerfish (*B. vetula*), and queen conch (*L. gigas*) were mostly distributed on horizontally oriented seascapes with scattered coral colonies, sponges, coral rubble, and sand, such as CPRT's and Rhodo beds. Yellowtail, schoolmaster, cubera, and blackfin snappers (*O. chrysurus, L. apodus, L. cyanopterus, L. buccanella*) were mostly associated with vertically oriented habitats, such as colonized pavement slopes (CPSLope) and colonized pavement walls (CPWall). Horizontally oriented, high rugosity habitats with high coral cover, mostly devoid of sandy substrates, such as BCR and ACR appear to be residential and foraging habitats for coney, red hind, and Nassau groupers (*C. fulva, E. guttatus, E. striatus*), lionfish (*Pterois sp*.), and mahogany, lane, cubera, schoolmaster, and yellowtail snappers (*L. mahogoni, L. synagris, L. cyanopterus, L. apodus, O. chrysurus*).

16) The patch coral reef (PCR) habitat from SECO, previously known as a multi-species fish spawning aggregation site (FSA) was observed to function as the FSA site also for cubera snapper (*L. cyanopterus*) during the 2018-20 survey.

17) Superimposed on observed habitat preferences, depth appears to be a significant factor influencing community structure of some of the large demersal species within the 22 – 50m range. Marked depth-related differences were noted for blackfin snapper (*L.*

buccanella), coney (*C. fulva*), and queen conch (*Lobatus gigas*). Blackfin snappers were mostly observed from CPSlopes and CPWalls below 40m depths. Conversely, densities of coneys and queen conch were consistently lower below 40m from most habitats and sites surveyed.

18) Analyses of density differences by large demersal fishes/shellfishes between surveys were influenced by the high variability within and between habitats/depth for any given site introduced by the aggregated distributions of numerically dominant populations, including species observed within drift belt-transects in spawning aggregations (e. g. *Lutjanus jocu, L. cyanopterus*), and what appeared to be large feeding aggregations (*O. chrysurus*).
19) Statistically significant density increments of red hind and Nassau groupers (*Epinephelus guttatus, E. striatus*), queen triggerfish (*Balistes vetula*), and spiny lobster (*Panulirus argus*) were noted from preferred habitats in most surveyed sites. Sharp density increments of queen conch (*Lobatus gigas*) were observed from ALS and DES, whereas equivalent declines were observed from TOUR and in less magnitude at BDS. Density increments of red hind, queen triggerfish and spiny lobster appeared to be real and supported by both increments in recruitment and maximum size of individuals.
20) Recuperation of fish/shellfish populations may be related to a release of fishing effort influenced perhaps, by a reduction of demand associated with the economic slow-down prevailing in PR since 2006, destruction of fishing gear and infrastructure related to impact by hurricanes, and/or increased awareness and compliance by fishermen to seasonal and areal fishing closures.
21) Direct intra-shelf connectivity with nursery habitats appeared to be an important driver of broad-scale spatial distributions of large demersal fishes and shellfishes. Perhaps with the exception of schoolmaster (*Lutjanus apodus*), snappers (Lutjanidae) were more abundant from mesophotic habitats within the main insular slope (ALS, TOUR, BOYA, SECO) than at DES and BDS, separated from mainland neritic habitats by deep oceanic channels. A similar argument can be raised for hogfish (*Lachnolaimus maximus*), which appeared to be more associated with the mainland shelf sub-mesophotic habitats at 25m than at either BDS or DES. Conversely, groupers (Serranidae) in general were more abundant at DES and BDS than from mainland sites, perhaps with the exception of red hind (*Epinephelus guttatus*) at ALS. Groupers are known to undertake offshore larval development and display relatively longer pelagic larval durations than snappers. Such extended pelagic larval adaptations may favor recruitment into offshore sites, such as oceanic islands and seamounts.

Literature Cited

Aguilar-Perera, A. 2006. Disappearance of a Nassau grouper spawning aggregation off the southern Mexican Caribbean coast. *Marine Ecology Progress Series* 327: 289-296.

Aguilar-Perera, A. and Aguilar-Davila, W. 1996. A spawning aggregation of Nassau grouper *Epinephelus striatus* (Pisces: Serranidae) in the Mexican Caribbean. Env. Biol. Fish., 45: 351-361.

Appeldoorn, R., Ballantine, D., Bejarano, I., Carlo, M/, Nemeth, M., Otero, E., Pagan, F., Ruiz, H., Schizas, N., Sherman, C. and Weil, E. 2016. Mesophotic coral ecosystems under anthropogenic stress: a case study at Ponce, Puerto Rico. Coral Reefs, 35:63-75. https://doi.org/10.1007/s00338-015-1360-5

Appeldoorn et al. 2016. La Parguera, Puerto Rico. In: Baker, E.K., Puglise, K.A. and Harris, P.T. (Eds). Mesophotic coral ecosystems — A lifeboat for coral reefs? The United Nations Environment Programme and GRID-Arendal, Nairobi and Arendal, 98 p.

Armstrong, R. A., Singh, H., Torres, J., Nemeth, R. S., Can, A., Roman, C., Eustice, R., Riggs, L. and Garcia-Moliner, G. 2006. Characterizing the deep insular shelf coral reef habitat of the Hind Bank marine conservation district (US Virgin Islands) using the Seabed autonomous underwater vehicle. Continental Shelf Res 26:194–205

Armstrong, R.A., Singh, H., Rivero-Calle, S., and Gilbes, F. 2009. Monitoring Coral Reefs in Optically Deep Waters. Proceedings of 11th International Coral Reef Symposium, Ft. Lauderdale, Florida, July 2008, 593-597

Angermeier, H., Glockner, V., Pawlik, J. R. and Lindquist, N. L. 2012. Sponge white patch disease effecting the Caribbean sponge Amphimedon compressa. Dis. Aquat. Org., 99: 93-102

Bak, R. P., Nieuwland, M. and Meester, E. H. W. G. 2005. Coral reef crisis in deep and shallow reefs: 30 years of constancy and change in reefs of Curacao and Bonaire. Coral Reefs, 24: 475-479

Bak, R. P. M. and Nieuwland, G. 1995. Long-term change in coral communities along depth gradients over leeward reefs in the Netherlands Antilles. Bull. Mar. Sci., 56 (2): 609-619

Bak, R. P. M. and Luckhurst, B. 1980. Constancy and change in coral reef habitats along depth gradients at Curacao. Oecologia (Bert.) 47: 145-155

Bakker, D. M., van Duyt, F. C., Bak, R. P. M., Nugues, M. M., Nieuwland, G. and Meesters, E. 2017. 40 years of benthic community change on the Caribbean reefs of Curacao and Bonaire: the rise of slimy cyanobacterial mats. Coral Reefs, DOI 10.1007/s00338-016-1534-9

Bannerot, S. P., Fox, Jr. W. W. and Powers, J. E. 1987. Reproductive strategies and the management of snappers and groupers in the Gulf of Mexico and Caribbean. In: J. J. Polovina and S. Ralston (eds.). Tropical snappers and groupers: biology and fisheries management. Westview Press, Boulder, Colorado. Pp. 561-603

Beets, J. and Friedlander, A. 1992. Stock analysis and management strategies for red hind, *Epinephelus guttatus*, in the U.S. Virgin Islands. Proc. Gulf. Carib. Fisheries Inst., 42: 66-79

Beets, J. and Friedlander, A. 1999. Evaluation of a conservation strategy: a spawning aggregation closure for red hind (*Epinephelus guttatus*), in the U. S. Virgin Islands. Envir. Biol. Fish., ***55***:91-98.

Bejarano, I., Appeldoorn, R. S. and Nemeth, M. 2014. Fishes associated with mesophotic coral ecosystems in La Parguera, Puerto Rico. Coral Reefs, 33 (2): 313-328

Bejarano, I., Nemeth, M. and Appeldoorn, R. 2010. Use of mixed-gas rebreathers to assess fish assemblages in mesophotic coral ecosystems (MCE) off La Parguera shelf-edge, Puerto Rico. Proc. 63rd Gulf. Carib. Fisheries Inst., San Juan, P. R. 131-133.

Biggs, C. R. and Nemeth, R. S. 2014. Timing, size and duration of a Dog (*Lutjanus jocu*) and Cubera Snapper (*Lutjanus cyanopterus*) Spawning Aggregation in the U. S. Virgin Islands. Proc. 67th Gulf Carib. Fish. Inst. November 3 – 7, Barbados. 240 –

Bongaerts, P., Ridgway, T., Sampayo, E. M. & Hoegh-Guldberg. 2010. O. Assessing the ‘deep reef refugia’ hypothesis: focus on Caribbean reefs. *Coral Reefs* **29**, 309–327, https://doi.org/10.1007/s00338-009-0581-x (2010)

Bongaerts, P. et. al. 2017. Deep reefs are not universal refuges: reseeding potential varies among coral species. *Sci. Adv.* **3**, e1602373, https://doi.org/10.1126/sciadv.1602373 (2017)

Brothers, E. B., Williams, D. McB. and Sale, P. 1983. Lengths of larval life in twelve families of fishes at “One Tree lagoon”, Great Barrier Reef, Australia. Mar. Biol. 76:319-324

CFMC (Caribbean Fishery Management Council). 2005. Comprehensive amendment to the fishery management plans (FMPs) of the U.S. Caribbean to address required provisions of the Magnuson-Stevens Fishery Conservation and Management Act (Sustainable Fisheries Act Amendment). Caribbean Fishery Management Council, San Juan, Puerto Rico. 533 pp + Appendices.

Claro, R. and Lindeman, K.C. 2003. Spawning aggregation sites of snapper and grouper species (Lutjanidae and Serranidae) on the insular shelf of Cuba. *Gulf and Caribbean Research* 14:91-106

Coen, L. D. and Tanner, C. E. 1989. Morphological variation and differential susceptibility to herbivory in the tropical brown alga Lobophora variegata. Mar. Ecol. Prog. Ser., 54: 287-298

Colin, P. L. 1974. Observations and collections of deep reef fishes off the coasts of Jamaica and Honduras. Mar. Biol., 24 (1): 29-38

Colin, P. L. 1976. Observations of deep reef fishes in the Tongue-of-the-Ocean, Bahamas. Bull. Mar. Sci., 26: 603-605

Eckert, R.J., Studivan, M.S. & Voss, J.D. 2019. Populations of the coral species *Montastraea cavernosa* on the Belize Barrier Reef lack vertical connectivity. *Sci Rep* **9,** 7200 (2019). https://doi.org/10.1038/s41598-019-43479-x

Fenner, D. 2005. Disease threatens Caribbean sponges: Report and identification guide. https. //www. Academia.edu/3317546

Froese, R., and Pauly, D. 2019. Fishbase. http://www.fishbase.org

Edmunds, P., Zimmerman, S. A. and Bramanti, L. 2019. A spatially aggressive Peyssonnelid algal crust (PAC) threatens shallow coral reefs in St. John, US Virgin Islands. Coral reefs, DOI: 10.1007/s00338-019-01846-0

Esteves-Amador, R. F. 2013. Short-term changes to the coral reef community structure following the regional coral bleaching event of 2005. Ph. D. Dissertation, U. Puerto Rico, Mayaguez, 90p.

García-Sais, J. R., Williams, S. M., Sabater-Clavell, J. and Carlo, M. 2019. Puerto Rico Coral Reef Monitoring Program: 2019 Survey. NA17NOS4820037 CRCP State and territorial Coral Reef Conservation Cooperative Agreement. DNER, San Juan, 283p.

García-Sais, J. R., Williams, S. M., Sabater-Clavell, J. and Carlo, M. 2018a. Puerto Rico Coral Reef Monitoring Program: 2017-2018 Survey. FY 17-18 CRCP State and territorial Coral Reef Conservation Cooperative Agreement. NA17NOS4820037. DNER, San Juan, 260p.

García-Sais, J. R., Williams, S. M., Sabater, J., and Garcia-Moliner, G. 2018.b Characterization of benthic habitats associated with deep-water snapper fishing grounds of Desecheo Ridge and other seamounts of the west coast of Puerto Rico. Final Report submitted to the CFMC, 113p

García-Sais, J. R., Williams, S. M., Sabater-Clavell, J. and Carlo, M. 2017. Monitoring of coral reef communities from natural reserves in Puerto Rico: 2017. Final report submitted to DNER/NOAA, San Juan, 311p.

García-Sais, J. R. 2015. Characterization of Deep Reef Benthic Habitats of Queen Snapper in Mona Passage, Puerto Rico. Final Report submitted to the CFMC, 77p

García-Sais, J. R., Williams, S. M., Sabater-Clavell, J., Esteves, R. and Carlo, M. 2014. Mesophotic benthic habitats and associated coral reef communities at Lang Bank, St, Croix, USVI. Final Report submitted to the CFMC/NOAA. 124 p

García-Sais, J. R., Williams, S. M., Sabater-Clavell, J., Esteves, R. and Carlo, M. 2013. Characterization of benthic habitats and associated coral reef communities at Tourmaline Reef, Puerto Rico. Final Report submitted to the CFMC/NOAA. 69 p

García-Sais, J. R., Sabater-Clavell, J., Esteves, R. and Carlo, M. Fishery Independent survey of commercially exploited fish and shellfish populations from mesophotic reefs within the Puertorrican EEZ. Final Report submitted to the CFMC/NOAA. 93 p

García-Sais, J. R., Sabater-Clavell, J., Esteves, R., Capella, J. and Carlo, M. 2011. Characterization of benthic habitats and associated coral reef communities at El Seco, southeast Vieques, Puerto Rico. Final Report submitted to the CFMC/NOAA. 102 p

García-Sais, J. R., Castro, R., Sabater, J., Williams, S. M. and Carlo, M. 2010a. Characterization of benthic habitats and associated reef communities at Abrir La Sierra, Puerto Rico. Final Report submitted to the CFMC/NOAA. 115 p.

García-Sais, J. R. 2010b. Reef habitats and associated sessile-benthic and fish assemblages across a euphotic-mesophotic depth gradient in Isla Desecheo, Puerto Rico, Coral reefs 29: 277-288.

García-Sais, J. R., Castro, R., Sabater, J. and Carlo, M. 2007. Characterization of benthic habitats and associated reef communities at Bajo de Sico Seamount, Mona Passage, Puerto Rico. Final Report submitted to the CFMC/NOAA. 91 p.

García-Sais, J. R., Castro, R., Sabater, J., Esteves, R. and Carlo, M. 2006. Monitoring of coral reef communities at Isla Desecheo, Rincon, Mayaguez Bay, Guánica, Ponce and Isla Caja de Muerto, Puerto Rico, 2006. Final Report submitted to the Department of Natural and Environmental Resources (DNER). U. S. Coral Reef Monitoring Program, NOAA, 145p.

García-Sais, J. R., Castro, R., Sabater, J. and Carlo, M. 2005. Inventory and atlas of corals and coral reefs from the U. S. Caribbean EEZ (Puerto Rico and the United States Virgin Islands). Final Report submitted to the CFMC/NOAA. 215 p.

Garrison, L. E. and Buell, W. 1971. Sea floor structure of the Eastern Greater Antilles. Symposium on Investigations and Resources of the Caribbean and Adjacent Regions. UNESCO, Paris, 1971, 241-245

Glover, L. 1967. Geology of the Coamo area, Puerto Rico with comments on Greater Antillean volcanic arc-trench phenomena. U. S. Geological Survey Open File report. 329p.

Glynn, P. W. 1996. Coral reef bleaching: facts, hypotheses and implications. *Glob. Chang. Biol.* **2**, 495–509, https://doi.org/10.1111/j.1365-2486.1996.tb00063.x (1996)

Goldberg, W. M. 1983. Cay Sal Bank, Bahamas: a biologically impoverished, physically controlled environment. Atoll Research Bulletin, No. 271: 1-24

Goreau, T. F. 1959. The ecology of Jamaican reefs. I. Species composition and zonation. Ecology, 40: 67-90

Goreau, T. F. and Goreau, N. I. 1973. The ecology of Jamaican coral reefs. II. Geomorphology, zonation, and sedimentary phases. Bull. Mar. Sci., 23: 399-464

Grigg, R. W. 2006. Depth limit for reef building corals in the ‘Au‘au Channel, S.E. Hawaii. Coral Reefs, **25**:77-84

Hernández-Delgado E. A., Toledo, C., Claudio, H. J., Lassus, J., Lucking, M. A., Fonseca, J., Hall, K., Rafols, S. J., Horta, H. and Sabat, A. M. 2006. Spatial and taxonomic patterns of coral bleaching and mortality in Puerto Rico during year 2005. In: NOAA-NESDIS-CRWP. NOAA. U. S. Virgin Islands, St. Croix, USA.

Hernández-Delgado E. A., González-Ramos, C. M. and Alejandro-Camis. C. M. 2014. Large-scale coral recruitment patterns on Mona Island, Puerto Rico: evidence of a transitional community trajectory after massive coral bleaching and mortality. Revista de Biología Tropical. On-line version ISSN 0034-7744. 13p.

James, N. P. and Ginsburg, R. N. 1973. *The seaward margin of Belize barrier and atoll reefs* (Blackwell Scientific, 1979).

Kadison, E., Brandt, M., Nemeth, R., Martens, J., Blondeau, J., and Smith, T. 2017. Abundance of commercially important reef fish indicated different level of over-exploitation across shelves of the U. S. Virgin Islands. PLoS One 12(7): e0180063

Kojis, B. L. and Quinn, N. J. 2011. Validation of a spawning aggregation of mutton snapper and characterization of the benthic habitats and fish in the Mutton Snapper Bank seasonal closed area, St. Croix, U. S. Virgin Islands. Final Report submitted to the Caribbean Fishery Management Council. NOAA NA08NMF4410463. 211p.

Leis, J. M. 1982. Nearshore distributional gradients of larval fish (15 taxa) and planktonic crustaceans (6 taxa) in Hawaii. Mar. Biol. 72: 89-97

Leis, J. M. and M. Miller. 1976. Offshore distributional patterns of Hawaiian fish larvae. Mar. Biol. 36: 359-367

Lesser, M. P., Slattery, M. & Leichter, J. J. 2009. Ecology of mesophotic coral reefs. *J. Exp. Mar. Bio. Ecol.* **375**, 1–8, https://doi.org/10.1016/j.jembe.2009.05.009 (2009).

Luckhurst, B.E. 1996. Trends in commercial fishery landings of groupers and snappers in Bermuda from 1975 to 1992 and associated fishery management issues. [Tendencias en los desembarques de la pesqueria commercial de meros y pargos en Bermuda, de 1975 a 1992 y aspectos asociados al manejo de la pesqueria. pp. 277-288. In: F. Arreguin-Sánchex, J.L. Munro, M.C. Balgos and D. Pauly (eds.) *Biology, Fisheries and Culture of Tropical Groupers and Snappers*. ICLARM Conference Proceedings 48, 449p.

Marshak, A. R. 2007a. Evaluation of seasonal closures of red hind, Epinephelus guttatus (Pisces: Serranidae), spawning aggregations to fishing off the west coast of Puerto Rico, using fishery-dependent and independent time series data. M.S. Thesis, University of Puerto Rico, Department of Marine Sciences. 84p.

Marshack, A. 2007. Spatial and ontogenetic patterns of the Queen Conch, *Strombus gigas* along the west coast of Puerto Rico. Report to the CFMC/NMFS/NOAA

Matos-Caraballo, D. 2012. Puerto Rico/NMFS Cooperative Fisheries Statistics Program, April 2007 – September 2012. NA07NMF4340039. Final Report to the National Marine Fishery Service. Department of Natural and Environmental Resources. 67

Matos-Caraballo, D. And W. Padilla.2001. Description of the tiger grouper (*Mycteroperca tigris*) fishery of Vieques, Puerto Rico. Proc. Gulf Carib. Fish. Inst. 48: 143-153

Menza, C., M. Kendall, C. Rogers, and J. Miller. 2007. A deep reef in deep trouble. Continental Shelf Research. 27: 2224-2230.

Miller, J., Muller, E., Rogers, C., Waara, R., Atkinson, A., Whelan, K. R. T., Patterson, M. and Witcher, B. 2009. Coral disease following massive bleaching in 2005 causes 60% decline in coral cover on reefs in the US Virgin Islands. Coral Reefs, 28: 925–937

Morris, J. A. and Atkins., J. L. 2009. Feeding ecology of invasive lionfish (Pterois volitans) in the Bahaman archipelago. Environ. Biol. Fish., 86: 389-398.

Mourier, J., Maynard, J., Parravicini, V., Ballesta, L., Clua, E., Domeier, M. L. and Planes, S. 2016. Extreme inverted trophic pyramid of reef sharks supported by spawning groupers. Curr. Biol., 26(15): 2011-2016, DOI 10.1016/j.cub.2016.05.058

Munro, J. L. 1983. The biology, ecology and bionomics of the hinds and groupers, Serranidae, In J. L. Munro (editor). Caribbean Coral Reef Fishery resources. Pp 59-81, ICLARM Stud. Rev. 7, Manila

Nemeth, R. S. 2005. Population characteristics of a recovering US Virgin Islands red hind spawning aggregation following protection. Mar. Ecol. Prog. ser., 286: 81-97

Nemeth, R. S., Blondeau, J., Herzlieb, S. and Kadison, E. 2007. Spatial and temporal patterns of movement and migration at spawning aggregations of red hind, Epinephelus guttatus, in the U. S. Virgin Islands. Environ. Biol. Fish., 78: 365-381

Nemeth, R. S., Herzlieb, S. and Blondeau, J. 2006a. Comparison of two seasonal closures for protecting red hind spawning aggregations in the US Virgin Islands. In: Proceedings of the 10th International Coral Reef Conference, Okinawa, Japan **4**:1306-1313.

Nemeth, R. S., Kadison, E., Herzlieb, S., Blondeau, J. and Whiteman, A. 2006b. Status of a yellowfin (*Mycteroperca venenosa*) grouper spawning aggregation in the US Virgin Islands with notes on other species. Proc. 57th Gulf Carib Fish Inst. 57:543-558.

Nemeth, R. S, Kadison, E. S. 2020. Status of the Nassau grouper on the Grammanik Bank FSA. Presentation to the CFMC. San Juan, 2020.

Nelson, W. R. and Appeldoorn, R. S. 1985. Cruise Report R/V Seward Johnson. A submersible survey of the continental slope of Puerto Rico and the U. S. Virgin Islands. Report submitted to NOAA, NMFS, SEFC, Mississippi Laboratories. University of Puerto Rico, Department of Marine Sciences. 76 p.

NOAA. 2018. Status of Puerto Rico's coral reefs in the aftermath of Hurricanes Irma and Maria. Assessment Report submitted by NOAA to the FEMA Natural and Cultural Resources Recovery Support Function. 37p.

NOAA 2007. National Centers for Coastal Ocean Science: NOAA ESRI Geotiff – 5m Bathymetry around Bajo de Sico, Puerto Rico, Project NF-07-06, 2007, UTM 19 NAD 83

Olsen, D. A. and LaPlace, J. A. 1978. A study of Virgin Islands grouper fishery based on a breeding aggregation. Proc. Gulf and Carib. Fisheries Inst., 31: 130-144.

Olson, J. C., Appeldoorn, R.S., Scharer-Umpierre, M. T. and Cruz-Mota, J. J. 2019. Recovery when you are on your own: Slow population responses in an isolated marine reserve. PLOS ONE. Doi.org/10.1371/journal.pone.0223102

Pyle, R. L., Boland, R., Bolick H., Bowen, B. W., Bradley, C. J., Kane, C., Kosaki, R. K., Langston, R., Longenecker, K., Montgomery, A., Parrish, F. A., Popp, B. N., Rooney, J., Smith, C. M., Wagner, D. and Spalding, H. L. 2016. A comprehensive investigation of mesophotic coral ecosystems in the Hawaiian Archipelago. *PeerJ* 4:e2475 https://doi.org/10.7717/peerj.2475

Pyle, R. L. 1996. The twilight zone*.* Nat. Hist. Mag., 105: 59-62

Pyle, R. L. 1999. Mixed-gas, closed-circuit rebreather use for identification of new reef fish species from 200–500 fsw*.* In: Hamilton RW, Pence DF, Kesling DE, eds. Assessment and feasibility of technical diving operations for scientific exploration. Nahant: A. Acad. of U. Sci., 53-65

Pyle R. L. 2000. Assessing undiscovered fish biodiversity on deep coral reefs using advanced self-contained diving technology*.* Mar. Tech. Soc. J., 34: 82-91

Ramirez-Mella, J. T. and Garcia-Sais, J. R. 2003. Offshore dispersal of Caribbean reef fish larvae: how far is it? Bull. Mar. Sci., 72(3): 997-1017

Rhodes, K. L. 2019. Grouper (Epinephelidae) spawning aggregations affect activity space of grey reef sharks, *Carcharhinus amblychynchos*, in Pohnpei, Micronesia. PLos One, 14(8): e0221589

Ruiz, H., Scharer, M., Nemeth, R. and Tuohy, E. 2018. Sustainability and recovery of groupers in Puerto Rico and the U. S. Virgin Islands. Final report submitted to NOAA/NMFS NA15NMF427034. 28p.

Ruiz, H., Ballantine, D. L. and Sabater, J. 2017. Continued spread of the seagrass Halophila stipulacea in the Caribbean: Documentation in Puerto Rico and the British Virgin Islands. Gulf and Carib, Res., 28, SC 5-7. DOI 10. 18785/gor2801.05

Rützler, K. and Macintyre, I. G. The habitat distribution and community structure of the barrier reef complex at Carrie Bow Cay, Belize. In: *The Atlantic Barrier Reef Ecosystem at Carrie Bow Cay*, *Belize*, *I: Structure and Communities* (eds Rützler, K. & Macintyre, I. G.) 9–45 (Smithsonian Institution Press, 1982)

Sala, E., Ballesteros, E. and Starr, R. M. 2001. Rapid decline of Nassau grouper spawning aggregation in Belize: fishery management and conservation needs. Fisheries, 26: 10, 23-30, DOI: 101577/1548-8446(2001)

Sadovy, I. 1995. The case of disappearing grouper *Epinephelus striatus*, the Nassau grouper, in the Western Atlantic. Proc. Gulf Carib. Fish. Inst. 45:

Sadovy, I. 1990. Grouper stocks of the Western Central Atlantic: the need for management and management needs. Proc. Gulf Carib. Fish. Inst. 43: 43-64

Sadovy, I. and Eklund, A. M. 1999. Synopsis of biological data on the Nassau grouper, Epinephelus striatus (Bloch, 1792), and the jewfish, E. itajara (Lichtenstein, 1822). NOAA Technical Report NMFS 146. 1-65

Sadovy de Mitcheson, I., Cornish, A., Domeier, M., Colin, P. L. and Lindeman, C. 2008. A global baseline for spawning aggregations of reef fishes. Conservat. Biol., 22 (5): 1233-1244

Sadovy, Y., Colin, P. L. and Domeier, M. L. 1994. Aggregation and spawning in the tiger grouper, Mycteroperca tigris (Pisces: Serranidae). Copeia 1994: 511-516

Sadovy, I. and Figuerola, M. 1992. The status of the red hind fishery in Puerto Rico and St. Thomas as determined by yield-per-recruit analysis. Proc. Gulf Carib. Fish. Inst. 42: 23-38

Scharer-Umpierre, M. T., Matos-Molina, D., Appeldoorn, R., Bejarano, I., Hernández-Delgado, E. A., Nemeth, R. S., Nemeth, M. I., Valdéz-Pizzini, M. and Smith, T. B. 2014. Advances in Marine Biology, 69: 130 – 149

Scharer, M. 2012. Sound production and reproductive behavior of yellowfin grouper, *Mycteroperca venenosa* (Serranidae) at a spawning aggregation. Copeia. Doi: 10.1643/ce-10-151

Scharer, M. 2010. Protecting a multi-species spawning aggregation at Mona Island, Puerto Rico. https://www.academia.edu/2690076

Sherman, C., Nemeth, M., Ruiz, H., Bejarano, I., Appeldoorn, R. S., Pagan, F., Sharer, M. and Weil, E. (2010) Geomorphology and benthic cover of mesophotic coral ecosystems of the upper insular slope of southwest Puerto Rico. Coral Reefs, 29:347–360.

Singh, H., Armstrong, R., Gilbes, F., Eustice, R., Roman, C., Pizarro, O. and Torres, J. 2004. Imaging coral I: Imaging coral habitats with the Seabed AUV. Subsurface Sensing Technologies and Applications. 5 (1): 25-42.

Smith, T. B., Ennis, R. S., Kadison, E., Weinstein, D. W., Jossart, J., Gyory, J. and Henderson, L. 2015. The United States Virgin Islands Territorial Coral Reef Monitoring Program: Year 15 Annual Report. Technical report. Mesophotic.org

Smith, T. B, Blondeau, J., Nemeth, R. S., Pittman, S. J., Calnan, J. M., Kadison, E. and Gass, J. 2010. Benthic structure and cryptic mortality in a Caribbean mesophotic coral reef bank system, the Hind Bank Marine Conservation District, U.S. Virgin Islands. Coral Reefs, 29: 289-308

Toledo-Hernandez, X., Velez-Zuazo, C. P., Ruiz-Diaz, A. R., Patricio, P., Mage, Navarro, M., Sabat, A. M., Betancourt, R., and Papa, R. 2014. Population ecology and genetics of the invasive lionfish in Puerto Rico. Aquatic Invasions, 9 (2): 227-237

Waterhouse, L., Heppell, S. A., Pattengill-Semmens, C. V., McCoy, C., Bush, P. ., Johnson, B. C. and Semmens, B. X. 2020. Recovery of critically endangered Nassau grouper (Epinephelus striatus) in the Cayman Islands following targeted conservation actions. Proc. Natl. Acad. Sci. U. S. A. 117 (3): 1587-1595

Weil, E. 2004. Coral Reef Diseases in the Wider Caribbean. In Coral Health and Diseases (E. Rosenberg, and Y. Loya, Eds): 35-68. Springer-Verlag. New York.

Weil, E., Hernandez-Delgado, E. A., Gonzalez, M., Williams, S., Suleiman-Ramos, S., Figuerola, M. and Metz-Estrella, T. 2019. Spread of the new coral disease "SCTLD" into the Caribbean: implications for Puerto Rico. Reef Encounter, 34: 39-43

Weil, E., Croquer, A. and Urreiztieta, I. 2009. Temporal variability and impact of coral diseases and bleaching in La Parguera, Puerto Rico from 2003 – 2007. Caribbean Journal of Science, 45:221-246.

Williams, S. M. and Garcia-Sais, J. R. 2020. A potential new threat on the coral reefs of Puerto Rico: The recent emergence of *Ramicrusta sp.* Marine Ecology, DOI.org/10.1111maec.12592

Wulff, J. L. 2005. Rapid diversity and abundance decline in a Caribbean coral reef sponge community. Biological Conservation. 127: 167-176